INSECT PHYSIOLOGICAL RESPONSES TO NATURAL AND SYNTHETIC XENOBIOTICS

EDITED BY: Ran Wang, József Fail and Qingjun Wu

PUBLISHED IN: Frontiers in Physiology

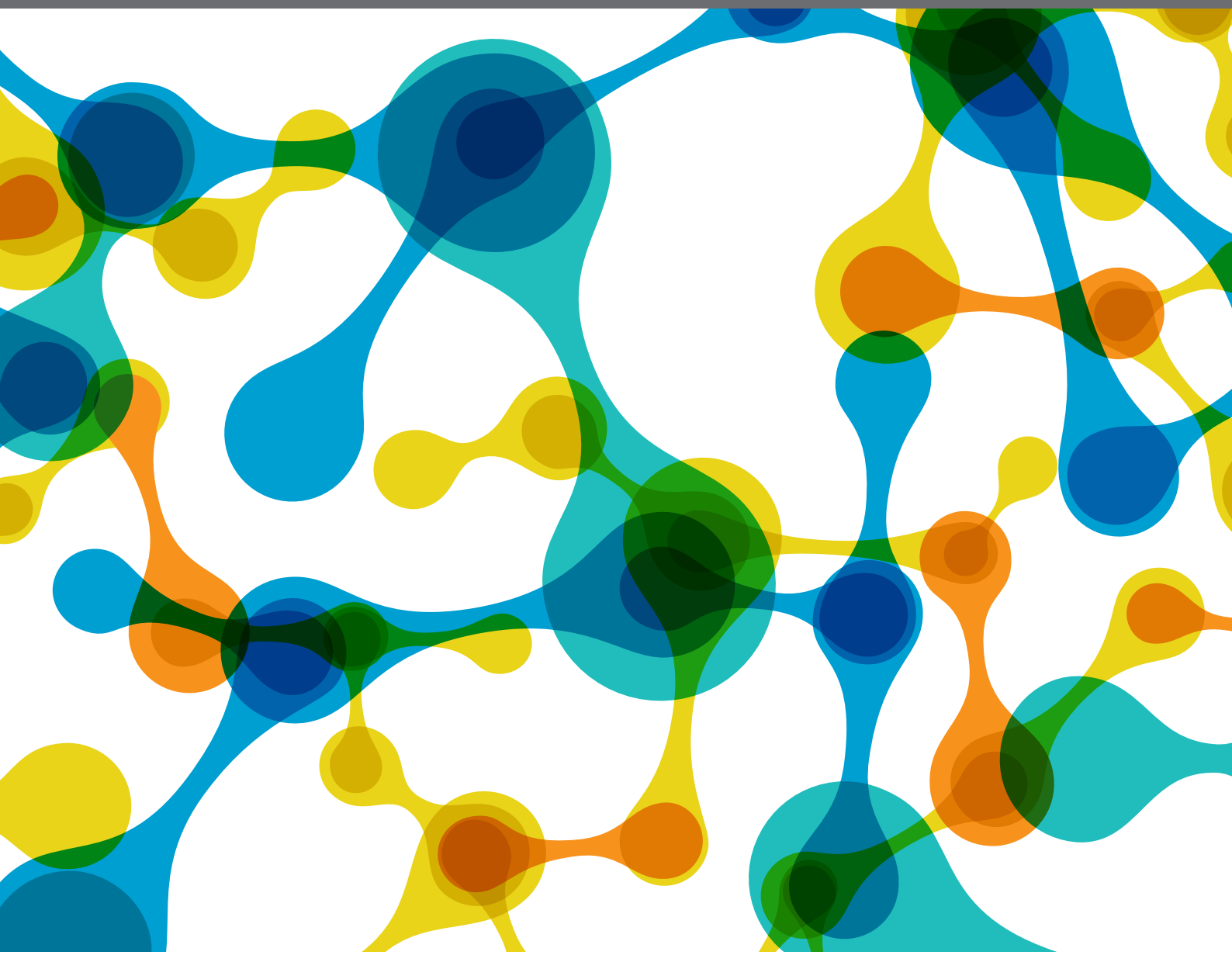

frontiers Research Topics

frontiers

ISSN 1664-8714
ISBN 978-2-88976-912-4
DOI 10.3389/978-2-88976-912-4

About Frontiers

Frontiers is more than just an open-access publisher of scholarly articles: it is a pioneering approach to the world of academia, radically improving the way scholarly research is managed. The grand vision of Frontiers is a world where all people have an equal opportunity to seek, share and generate knowledge. Frontiers provides immediate and permanent online open access to all its publications, but this alone is not enough to realize our grand goals.

Frontiers Journal Series

The Frontiers Journal Series is a multi-tier and interdisciplinary set of open-access, online journals, promising a paradigm shift from the current review, selection and dissemination processes in academic publishing. All Frontiers journals are driven by researchers for researchers; therefore, they constitute a service to the scholarly community. At the same time, the Frontiers Journal Series operates on a revolutionary invention, the tiered publishing system, initially addressing specific communities of scholars, and gradually climbing up to broader public understanding, thus serving the interests of the lay society, too.

Dedication to Quality

Each Frontiers article is a landmark of the highest quality, thanks to genuinely collaborative interactions between authors and review editors, who include some of the world's best academicians. Research must be certified by peers before entering a stream of knowledge that may eventually reach the public - and shape society; therefore, Frontiers only applies the most rigorous and unbiased reviews.
Frontiers revolutionizes research publishing by freely delivering the most outstanding research, evaluated with no bias from both the academic and social point of view. By applying the most advanced information technologies, Frontiers is catapulting scholarly publishing into a new generation.

What are Frontiers Research Topics?

Frontiers Research Topics are very popular trademarks of the Frontiers Journals Series: they are collections of at least ten articles, all centered on a particular subject. With their unique mix of varied contributions from Original Research to Review Articles, Frontiers Research Topics unify the most influential researchers, the latest key findings and historical advances in a hot research area! Find out more on how to host your own Frontiers Research Topic or contribute to one as an author by contacting the Frontiers Editorial Office: frontiersin.org/about/contact

INSECT PHYSIOLOGICAL RESPONSES TO NATURAL AND SYNTHETIC XENOBIOTICS

Topic Editors:
Ran Wang, Beijing Academy of Agriculture and Forestry Sciences, China
József Fail, Hungarian University of Agriculture and Life Sciences, Hungary
Qingjun Wu, Insititute of Vegetables and Flowers, Chinese Academy of Agricultural Sciences, China

Citation: Wang, R., Fail, J., Wu, Q., eds. (2022). Insect Physiological Responses to Natural and Synthetic Xenobiotics. Lausanne: Frontiers Media SA.
doi: 10.3389/978-2-88976-912-4

Table of Contents

frontiers in Physiology

ORIGINAL RESEARCH
published: 30 September 2021
doi: 10.3389/fphys.2021.739800

Integrated Microbiome–Metabolome Analysis Reveals Stage-Dependent Alterations in Bacterial Degradation of Aromatics in *Leptinotarsa decemlineata*

Wei-Nan Kang[1], *Lin Jin*[1], *Hong-Yu Ma*[2] *and Guo-Qing Li*[1]*

[1] *Education Ministry Key Laboratory of Integrated Management of Crop Diseases and Pests, College of Plant Protection, Nanjing Agricultural University, Nanjing, China,* [2] *Public Laboratory Platform, College of Plant Protection, Nanjing Agricultural University, Nanjing, China*

To avoid potential harm during pupation, the Colorado potato beetle *Leptinotarsa decemlineata* lives in two different habitats throughout its developmental excursion, with the larva and adult settling on potato plants and the pupa in soil. Potato plants and agricultural soil contain a specific subset of aromatics. In the present study, we intended to determine whether the stage-specific bacterial flora plays a role in the catabolism of aromatics in *L. decemlineata*. Kyoto Encyclopedia of Genes and Genomes (KEGG) pathway analysis of the operational taxonomic units (OTUs) obtained by sequencing of culture-independent 16S rRNA region enriched a group of bacterial genes involved in the elimination of mono- and polycyclic aromatics at the pupal stage compared with those at the larval and adult periods. Consistently, metabolome analysis revealed that dozens of monoaromatics such as styrene, benzoates, and phenols, polycyclic aromatics, for instance, naphthalene and steroids, were more abundant in the pupal sample. Moreover, a total of seven active pathways were uncovered in the pupal specimen. These ways were associated with the biodegradation of benzoate, 4-methoxybenzoate, fluorobenzoates, styrene, vanillin, benzamide, and naphthalene. In addition, the metabolomic profiles and the catabolism abilities were significantly different in the pupae where their bacteria were removed by a mixture of three antibiotics. Therefore, our data suggested the stage-dependent alterations in bacterial breakdown of aromatics in *L. decemlineata*.

Keywords: ***Leptinotarsa decemlineata*, stage-specific bacteria, habitat, aromatics, biodegradation**

OPEN ACCESS

Edited by:
Ran Wang,
Beijing Academy of Agricultural and Forestry Sciences, China

Reviewed by:
Wenwu Zhou,
Zhejiang University, China
Hong-xing Xu,
Shaanxi Normal University, China

***Correspondence:**
Guo-Qing Li
ligq@njau.edu.cn

Specialty section:
This article was submitted to Invertebrate Physiology, a section of the journal Frontiers in Physiology

Received: *12 July 2021*
Accepted: *16 August 2021*
Published: *30 September 2021*

Citation:
Kang W-N, Jin L, Ma H-Y and Li G-Q (2021) Integrated Microbiome–Metabolome Analysis Reveals Stage-Dependent Alterations in Bacterial Degradation of Aromatics in Leptinotarsa decemlineata. Front. Physiol. 12:739800. doi: 10.3389/fphys.2021.739800

INTRODUCTION

For holometabolous insect species, sessile pupae are defenseless against potentially harmful factors such as pathogen infection, parasitism, predation, and desiccation. Consequently, a lot of Holometabolans leave their host plants and pupate in soil, an adaptation termed as ontogenetic niche shift (ONS). For example, the final instar larval period of the Colorado potato beetle *Leptinotarsa decemlineata* is divided into two subphases, the feeding and wandering stages. Whereas, a feeding beetle continuously gnaws potato foliage, a wandering larva typically undergoes an ONS to pupate in the soil (Meng et al., 2019). Obviously, a *L. decemlineata* beetle lives in two

different habitats throughout its developmental excursion, with the larva and adult settling on potato plants and the pupa in soil.

In the present paper, we focused on a serious challenge for *L. decemlineata*: degrading excessive aromatics derived from potato plants and agricultural soil. In potato plants, the metabolism of three aromatic amino acids (i.e., tyrosine, phenylalanine, and tryptophan) can produce large number of monoaromatics. These monoaromatics can be used to biosynthesize structurally complex substances. For instance, catecholamines, derived from tyrosine and phenylalanine, can be used to produce betalains, alkaloids, melanins, and hydroxycinnamic acid amides (Gandia-Herrero and Garcia-Carmona, 2013; Kostyn et al., 2020). To improve soil quality and increase crop yield, the plant residues, such as straws and stubbles after harvest, organic fertilizers, for example, manure and human excreta, and other organic landfills, are often applied to agricultural fields. These additives generate a variety of organic compounds incorporated into agricultural soil (Kumar and Goh, 2000; Hanselman et al., 2003; Kjaer et al., 2007). Among these organic pollutants are monoaromatics, for instance, benzene, toluene, ethylbenzene, xylene (collectively known as BTEX), styrene, and phenol and polycyclic aromatics such as naphthalene, dioxin, and steroids (Chen et al., 2017; Steinmetz et al., 2019).

Some aromatics are toxic, antinutritive, or/and repellent at high concentrations (Ceja-Navarro et al., 2015; Hammer and Bowers, 2015; Vilanova et al., 2016; Berasategui et al., 2017). Specifically, catecholamines are toxic and can pose a threat to cellular components (Kostyn et al., 2020). Moreover, quinones can lead to the formation of quinoprotein by a reaction between dopaquinone and the sulfhydryl groups of proteins and cause negative effects such as enzyme deactivation, mitochondrial dysfunction, DNA fragmentation, and apoptosis (Mushtaq et al., 2013; Kostyn et al., 2020). Furthermore, dopa may be incorporated into proteins *via* mimicking tyrosine or phenylalanine in the respective tRNA synthesis (Rodgers and Shiozawa, 2008), or serves as a deterrent to herbivores (Fürstenberg-Hägg et al., 2013; Kostyn et al., 2020). Therefore, these aromatics may adversely affect *L. decemlineata* when accumulated to high concentrations in the body.

It is well-known that insects have evolved different mechanisms to circumvent deleterious effects from the environment (Berasategui et al., 2017). One of the strategies is enlisting the cooperation of bacteria (Lesperance and Broderick, 2020). These bacteria dramatically change during development (Chen et al., 2016; Kang et al., 2021). For instance, a shift of microbial flora coupled with ONS has been documented in *L. decemlineata*, where a total of 18 bacteria genera are specifically distributed in pupae. In contrast, a subset of bacteria genera has larger populations in larvae and adults than those in pupae (Kang et al., 2021). Accordingly, we hypothesized that the stage-specific bacteria flora forms different symbiotic interplays with *L. decemlineata* to biodegrade stage-dependent aromatics from potato plant and agricultural soil, respectively.

The objective of our study was to test the hypothesis. First, we found that a group of bacterial genes involved in the catabolism of monoaromatics and polycyclic aromatics were abundantly expressed at the pupal stages. Second, we evaluated the metabolome profiles in the fourth-instar larvae, pupae, and adults by ultra-performance liquid chromatography–quadrupole–time of flight mass spectrometry (UPLC-Q-TOF MS). We identified stage-specific aromatic biomarkers and active pathways. Finally, we removed bacteria in the pupae by a mixture of three antibiotics, and compared the metabolome profiles between control and treated pupae. Our results revealed stage-dependent alterations in the bacterial breakdown of aromatics in *L. decemlineata*. We argue that the larvae and adults rely on two routes to deal with excessive aromatics, namely, bacterial biodegradation and intestinal excretion. In contrast, the pupae mainly depend on bacteria to catabolize aromatics since the alimentary canal is not well-developed.

METHODS AND MATERIALS

Insect Rearing and Sampling

The *L. decemlineata* beetles were routinely reared using a previously described method (Meng et al., 2019). Briefly, the beetles were maintained in an insectary at 28°C, under a 16:8 h (light/dark) photoperiod, and 50–60% relative humidity using potato foliage at the vegetative growth or young tuber stages to assure sufficient nutrition. At this feeding protocol, the larvae progressed the first-, second-, penultimate-, and final-instar stages with approximate periods of 2, 2, 2, and 4 days, respectively. On reaching full size, the final larval instars stopped feeding, dropped to the ground, burrowed to the soil, and entered the prepupal stage. The prepupae spent ∼3 days to pupate. The pupae lasted about 5 days and the adults emerged.

All solvents used for UPLC-Q-TOF-MS analysis were of analytical or HPLC grade and purchased from Sigma-Aldrich Co., Ltd. (Shanghai, China).

The detailed procedure of sample preparation for UPLC-Q-TOF-MS was as follows: ten (5 males and 5 females) 2-day-old fourth-instar larvae, ten 4-day-old pupae, and ten 5-day-old adults were collected as a replicate. The collection continued for three consecutive generations to generate three biologically independent replicates. The specimens were individually weighed and then crushed in a pre-chilled mortar using a pellet pestle. Each sample was lyophilized, added with 1 ml of methanol/water (7:3, v/v), vortexed, and sonicated twice on ice for 30 min. Then the metabolite was incubated at −20°C for 1 h and centrifuged at 13,000 rpm at 4°C for 15 min. The supernatant was lyophilized and stored at −80°C.

Analysis for Operational Taxonomic Units Data From High-Throughput Sequencing of 16S rRNA Genes

Functional prediction was carried out based on the operational taxonomic units (OTU) data downloaded from the NCBI Sequence Read Archive (SRA) database (Accession Number: PRJNA613266) (Kang et al., 2021). The OTU data were obtained by high-throughput sequencing of 16S rRNA genes from three biologically independent collections from three consecutive generations. Each collection included ten 2-day-old fourth-instar larvae, ten 4-day-old pupae, and ten 5-day-old adults with the sex

ratio of 1:1 (5 males and 5 females). The PICRUSt algorithm was used to infer the functions of the bacterial communities through the Kyoto Encyclopedia of Genes and Genomes (KEGG) database (Kanehisa et al., 2012).

Analysis Conditions of UPLC/Q-TOF-MS

The supernatant was reconstituted with 500 μl of methanol, vortexed, and centrifuged at 20,000 rpm at 4°C for 20 min. Then the supernatant was filtered through a 0.22 μm (nylon) syringe filter and analyzed by UPLC-Q-TOF-MS system (Waters). Each sample was analyzed six times (i.e., 2 μl aliquot of each sample was injected six times).

Since the retention times or even elution order in analytical system may vary during the UPLC-Q-TOF-MS analysis, it is necessary to monitor the system consistency. In this study, a 60 μl mixture of the control (30 μl) and treatment samples (30 μl) was used as a quality control (QC) sample for method validation. A QC sample ran four times prior to beginning the whole sample list. Moreover, a QC sample was run every six samples during the analytical run.

The analysis was performed on an HSS T3 column (2.1 × 100 mm, 1.8 μm; Waters Acquity), using an ACQUITY UPLC I-Class PLUS System (Waters) coupled with a Xevo® G2-XS QT of High-Definition Mass Spectrometer (Waters). Mobile phase A was water and mobile phase B was 0.1% formic acid acetonitrile solution. The gradient elution procedure was set as follows: 0–1 min, 0–2% B; 1–2 min, 2–25% B; 2–4 min, 25–60% B; 4–7.5 min, 60–90% B; 7.5–9.5 min, 90–99% B; 9.5–12.5 min, 99% B; 12.5–13 min, 99–2% B; and 13–16 min, 2% B. The flow rate was 0.4 ml/min, and the column temperatures were held constant at 45°C.

Each sample was detected by positive and negative ion modes using an electrospray ionization mass spectrometer (ESI-MS). The product ion scan was acquired using the first- and second-level mass spectrometry data acquisition method based on the Photodiode Array (PDA) detector.

The ESI conditions were as follows: nitrogen was used as cone gas and desolvation gas at a flow rate of 50 and 800 l/h, respectively. The source temperature was 120°C and desolvation gas temperature was 450°C. Quality scanning range was set *m*/*z* 50–1,200. In positive ion mode, capillary, cone, and extraction cone voltages were 3.0 kV, 40 V, and 5.0 V, respectively. In negative ion mode, capillary, cone, and extraction cone voltages were 2.0 kV, 40 V, and 5.0 V, respectively. MS data were acquired in full-scan mode from 100 to 1,000 Da.

Data Processing and Statistical Analysis of UPLC/Q-TOF-MS Data

The raw data detected by UPLC-Q-TOF-MS were loaded on the commercial metabolites database Progenesis QI (Waters Corporation, Milford, USA) for peak detection, alignment, and normalization, as well as the main information, such as the mass, retention time, and intensity of the peaks in each chromatogram. The metabolites were identified by comparing their retention times, *m*/*z* values, and MS fragmentation patterns with those of commercial standard compounds. Fragmentation patterns collected in online databases, such as MycompoundID (http://www.mycompoundid.org), MassBank (http://www.massbank.jp), ChemSpider database (www.chemspider.com), and METLIN (http://metlin.scripps.edu) were also considered, especially when no authentic standard compounds were available.

Before multidimensional statistical analysis, the data were processed: the missing values of the original data >50% were excluded. The processed data were then imported into SIMCA-P14.1 software (Umetrics, Umea, Sweden) for pattern recognition, and Pareto scaling was used to preprocess the data for principal component analysis (PCA) and orthogonal PLS-DA analysis (OPLS-DA). According to the Variable Importance for the Projection (VIP) obtained by the OPLS-DA model and Max Fold Change (MFC) from Progenesis QI, the influence intensity and explanatory ability of each metabolite on the classification and discrimination of each group of samples were evaluated, and the biologically significant differential metabolites were mined. The larger the VIP and MFC values, the greater the contribution of the metabolite in the differentiation of the sample, and the variable with VIP > 1 and MFC > 2 was generally considered to have a significant difference. In the experiment, based on the screening criteria of VIP > 1 and MFC > 2, the substances between the groups were initially screened. Next, the univariate statistical analysis was used to verify whether the selected metabolites had significant differences. Ions meeting VIP > 1, MFC > 2, and $0.05 < p < 0.1$ were considered differential metabolites; VIP > 1, MFC > 2, and $p < 0.05$ were regarded as significantly different metabolites.

To highlight differential biomarker role, the resulting significant differential metabolites were analyzed in KEGG (http://www.kegg.jp) to resolve the topological trait of metabolic pathways.

Antibiotics Exposure and Examination of Bacteria in Resultant Beetles

The same method was used to expose the larvae to an antibiotic mixture (Löfmark et al., 2010; Xia et al., 2020). Briefly, a mixture containing three antibiotics (1 mg/ml ciprofloxacin, 1 mg/ml levofloxacin, and 2 mg/ml metronidazole) in 1% Tween 20 aqueous solution was used to immerse potato foliage. Tween 20 in sterile water (1%) was set as the control group. Ten newly ecdysed fourth-instar larvae were confined in a Petri dish (9 cm diameter and 1.5 cm height) containing five treated leaves. The larvae were allowed to feed on the treated leaves until they reached the prepupal stage. The foliage was replaced with freshly treated ones each day.

The total microbial DNAs were individually extracted from 4-day-old pupae having fed on the antibiotic mixture or control solution as larvae, using E.Z.N.A.® Tissue DNA Kit (Omega). The removal of bacteria was examined using a pair of universal primers, the forward primer 5′-TCCTACGGGAGGCAGCAGT-3′ and reverse primer 5′-GGACTACCAGGGTATCTATCCTGTT-3′, of 16S rDNA from the Domain Bacteria (Nadkarni et al., 2002; Silkie and Nelson, 2009). Quantitative DNA measurements were performed by real-time quantitative reverse transcription PCR (qRT-PCR) in technical triplicate. Relative expression level of 16S rDNA was

calculated by the $2^{-\Delta\Delta CT}$ method, using the geometric mean of two internal control genes (*LdRP4* and *LdARF1*) (Shi et al., 2013) for normalization.

To further examine the removal of bacteria, the dissected guts from newly emerged adults in control and treatment groups were homogenized. The supernatants separated by centrifugation at 500 g were spread on a plate culture medium (Luria–Bertani) after diluting for 10 times. The dishes were inoculated at 30°C for 17 h and then the bacterial spots were detected.

The metabolites in control and bacteria-removed pupae were tested using UPLC-Q-TOF-MS system and the data were analyzed using the method described above.

Statistical Analysis

Using SPSS for Windows (Chicago, IL, USA), one-way analysis of variance (ANOVA) with a Tukey–Kramer test, or Student's *t*-test was performed to determine significant difference between average values (±SD). Results were considered statistically significant when $p < 0.05$.

RESULTS

Functional Analysis of Bacteria

The OTUs of bacteria obtained by PCR amplification and sequencing of culture-independent 16S rRNA (Kang et al., 2021) were analyzed using KEGG enrichment analysis. At KEGG level 1, metabolism was the most active one, especially in the pupa group (**Figure 1A**). The highly expressed genes associated with the catabolism of aromatic compounds (at KEGG level 3) were observed in the pupa group, followed by those in the larvae, and the levels were lower in the adult collection. One-way ANOVA revealed that a statistical significant difference was present between pupa and adult groups ($p < 0.05$) (**Figure 1B**).

Correspondingly, the actively expressed genes (at KEGG level 3) involved in the degradation of benzoate, aminobenzoate, styrene, toluene, xylene, nitrotoluene, ethylbenzene, bisphenol, fluorobenzoate, naphthalene, dioxin, steroid, polycyclic aromatic hydrocarbon, caprolactam, atrazine, furfural, chloroalkane, chloroalkene, chlorocyclohexane, and chlorobenzene were significantly richer in the pupa group than those in the larva and adult collections (**Figure 1C**).

Potential Biomarkers of Aromatic Compounds

To obtain comprehensive information on the metabolome, small molecule metabolites in the larval, pupal, and adult samples were analyzed by UPLC-Q-TOF-MS. A preliminary analysis of all samples was performed by PCA. The larva and adult groups were biased compared with the pupa collection in both positive and negative ion maps, whereas the larva and adult groups were overlapped (**Figures 2A,B**).

By OPLS-DA model, 43 potential aromatic biomarkers were screened in positive ion mode. Out of them, a subset of 39 was greater in the pupal specimen compared with those in the larval sample, while another subset of 40 was more in the pupal specimen than those in the adult group (**Table 1**). A total of 11 potential aromatic biomarkers were obtained in negative ion mode. Among them, subsets of 9 and 8 were greater in the pupal sample than those in the larva and adult groups, respectively (**Table 2**).

Active Pathway in Pupae

Biological pathway analysis revealed that five active pathways were involved in the metabolism of aromatics in pupae compared with those in the larva/adult groups. These ways contained the catabolism of styrene, naphthalene, fluorobenzoate, aminobenzoate, and benzoate, respectively (**Figures 2C,D**).

Enrichment of Xenobiotics in Aposymbiontic Pupa

Feeding a mixture of three antibiotics by the fourth-instar larvae almost completely removed culturable aerobic bacteria (**Figure 3B** vs. **Figure 3A**), and all other bacteria (**Figure 3C**) in the resultant pupae. In the PCA graphs, the aposymbiontic groups were biased compared with the control groups in both positive and negative ion maps (**Figures 3D,E**).

In both positive and negative ion modes, the differences in xenobiotic biomarkers between control and aposymbiontic pupal samples included a great number of aromatic compounds (**Tables 3**, **4**).

Metabolic pathway analysis revealed that a total of seven active pathways were enriched in either control or aposymbiontic pupal samples (**Figures 3F,G**). These ways were involved in the degradation of styrene, naphthalene, benzoate, fluorobenzoate, aminobenzoate, xylene, and dioxin.

Metabolism Pathways

Identified metabolites and biological pathways were imported into the KEGG (http://www.kegg.jp/) to find interactions. Among networks for catabolism of aromatics, benzoates, 4-methoxybenzoate, vanillin, and benzamide were finally transferred into succinyl-CoA and acetyl-CoA, which were completely degraded to CO_2 through tricarboxylic acid cycle (**Figures 4A,B,E**). Fluorobenzoates, for instance, 3-fluorobenzoate and 4-fluorobenzoate, were finally converted to 2-fluoro-cis, cis-muconate, 3-fluoro-cis, cis-muconate, and 4-fluoromuconolactone (**Figure 4F**). Styrene was oxidized to phenylacetic acid (**Figure 4D**). In contrast, the degradation of (2-naphthyl)methanol (naphthalene) was only partially annotated by KEGG (**Figure 4C**).

Comparison of metabolite enrichment between control and aposymbiontic pupal samples revealed that 4-methoxybenzoate (**Figure 4A**), vanillin (**Figure 4B**), (2-naphthyl)methanol (**Figure 4C**), styrene oxide, and phenylacetaldehyde (**Figure 4D**) were higher in the control group. These findings indicated that the soil aromatic precursors could be actively converted into these compounds by pupa bacteria. Conversely, benzoate, styrene, and 3,4-dihydroxybenzoate were accumulated in the aposymbiontic pupal group (**Figures 4A,B,E**). These results suggested that pupa bacteria were associated with the catabolism of the three chemicals. In contrast, the contents of 3-fluorocatechol and 4-fluorocatechol in control group were similar to those in the aposymbiontic pupal group (**Figure 4F**). These data implied that pupae may metabolize fluorobenzoates.

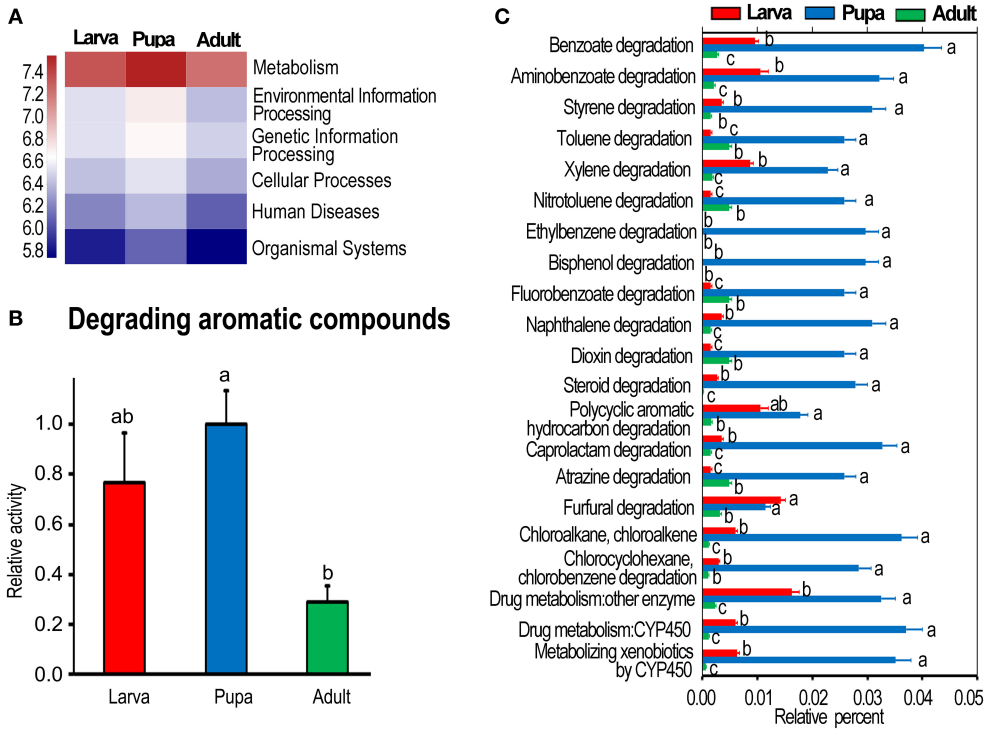

FIGURE 1 | Kyoto Encyclopedia of Genes and Genomes (KEGG) analysis of bacterial flora in *Leptinotarsa decemlineata*. **(A)** Shows whole metabolism activities at KEGG level 1. The relative activities in **(B)** are the ratios of relative percentages in larvae and adults relative to that in the pupae, which is set as 1. **(C)** Displays the relative activity (percentage) of individual aromatics in the larvae, pupae, and adults at the third KEGG level. The columns represent averages with vertical lines indicating SE. Different letters indicate a significant difference at p-value < 0.05 using analysis of variance with the Tukey–Kramer test.

DISCUSSION

To the best of our knowledge, the stage-dependent alterations in the biodegradation of aromatics by the stage-specific bacteria flora in insects have not been well-explored. In the present study, PCA analysis of UPLC-Q-TOF-MS data revealed that the larva and adult groups were biased compared with the pupa collection in both positive and negative ion maps (**Figure 2**). The shift indicates that the metabolites in the pupa group differ from those in the larva and adult groups. In accordance with the indication, the habitat in which the larvae and adults live is different from that of pupae, with the larva and adult settling on potato plants and the pupa in soil (Meng et al., 2019).

The Pupae Mainly Rely on Bacteria to Biodegrade Aromatics

Incorporation of plant residues and organic fertilizers into soil brings about some secondary chemicals, e.g., alkaloids, terpenoids, cardenolides, glucosinolates, and oxalates (Zhang et al., 2020), and their metabolites such as monoaromatics (e.g., BTEX and phenol) and polycyclic aromatics (e.g., naphthalene, dioxin, and steroids) (Chen et al., 2017; Steinmetz et al., 2019). These compounds often exert deleterious effects to soil-dwelling pupae when accumulated to high concentrations within the bodies. Insects are hypothesized to specify their microbial community compositions to degrade these substances to avoid intoxication, if suitable ecological conditions are satisfied (Zhang et al., 2020). However, the experimental evidence to support the hypothesis is very limited.

In the present study, we analyzed the bacterial OTU data (Kang et al., 2021) by KEGG and found that a subset of bacterial genes was abundantly expressed at the pupal stage. These genes were associated with the catabolism of aromatics (**Figure 1**). Consistently, metabolomic analysis displayed that dozens of monoaromatics, polycyclic aromatics, and steroids were richer in the pupal sample than those in the larval and adult specimens (**Tables 1**, **2**).

According to the identified metabolites and biological pathways, a total of seven active ways were enriched. These active pathways are mainly involved in the degradation of various benzoates and their precursors, which include benzoate, 4-methoxybenzoate, 3-fluorobenzoate, 4-fluorobenzoate, vanillin (aminobenzoate), and benzamide (**Figure 4**). Most of these benzoates were finally transferred into succinyl-CoA and acetyl-CoA, which were completely degraded to CO_2 through tricarboxylic acid cycle. Similarly, *Dechloromonas* sp. strains RCB and JJ can completely break down aromatic compounds into CO_2, coupled with the reduction of nitrate (Coates et al., 2001). *Dechloromonas* belongs to proteobacteria. Among the 18 pupa-specific genera identified (Kang et al., 2021), *Escherichia_Shigella*,

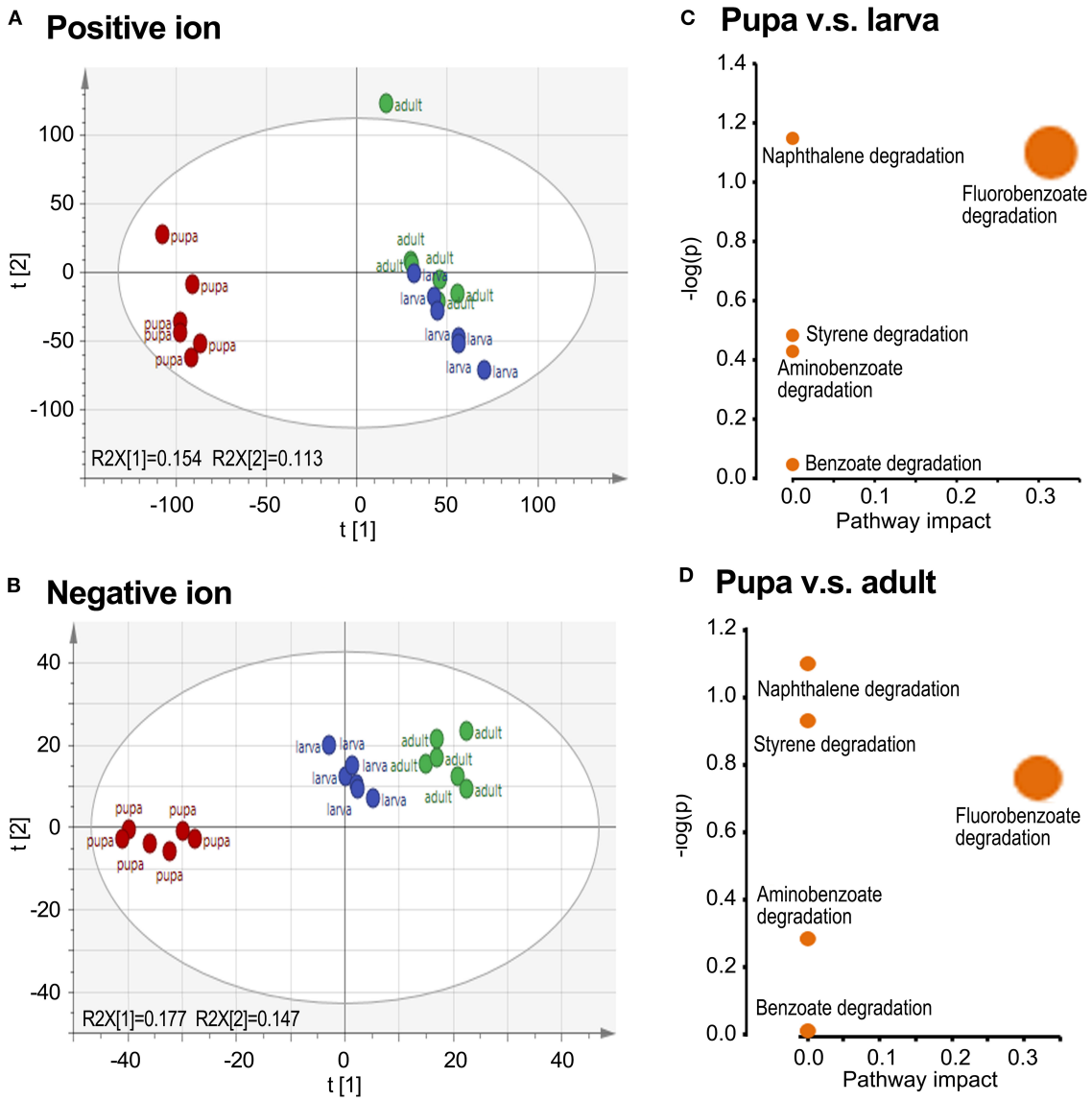

FIGURE 2 | Grouping comparison of metabolomics in larvae, pupae, and adults in *L. decemlineata*. The ultra-performance liquid chromatography–quadrupole–time of flight mass spectrometry (UPLC-Q-TOF-MS) data were analyzed by principal component analysis (PCA). Positive and negative ion mode PCA score maps **(A,B)** and pathway enrichment analyses **(C,D)** of larva, pupa, and adult groups are shown. Different colors in the **(A,B)** represented different groups and each point represented a sample.

Acinetobacter, *Pseudomonas*, *Lysobacter*, and *Stenotrophomonas* are also proteobacteria. One or several genera listed above may be responsible for the catabolism of the benzoates in *L. decemlineata* pupae.

Specifically, we uncovered that pupa bacteria were involved in the aerobic degradation of styrene to phenylacetic acid in *L. decemlineata* (**Figure 4**). In agreement with our result, the way in other documented results involves epoxidation of the vinyl side chain, followed by isomerization of the epoxy styrene to form phenylacetaldehyde. This compound is subsequently oxidized to phenylacetic acid through the action of either an NAD^+- or phenazine methosulfate-dependent dehydrogenase (O'Connor and Dobson, 1996; O'Leary et al., 2002). Conversion of styrene to phenylacetic acid has been documented in various bacterial strains; examples include *Pseudomonas putida* CA-3 (O'Connor et al., 1995), *P. fuorescens* ST (Marconi et al., 1996), *Pseudomonas* sp. VLB120 (Panke et al., 1999), *Pseudomonas* sp. Y2 (Utkin et al., 1991; Velasco et al., 1998), *Xanthobacter* sp. 124X (Hartmans et al., 1989), and *Xanthobacter* sp. S5 (Hartmans et al., 1990). *Pseudomonas* is among the 18 pupa-specific genera identified recently (Kang et al., 2021), and the genus may be responsible for the catabolism of styrene in *L. decemlineata* pupae.

At present, polycyclic aromatic hydrocarbons produced by all vertebrates as well as some invertebrates have been considered

TABLE 1 | Differential xenobiotics with higher levels in pupae v.s. larvae/adults in positive ion mode.

KEGG CID	Metabolites	P/L	P/A	VIP(P/L)	P(P/L)	VIP(P/A)	P(P/A)
C00755	Vanillin	↑	↑	2.2	<0.01	2.1	<0.01
C02519	4-Methoxybenzoate	↑	↑	2.2	<0.01	2.1	<0.01
C16472	3-Fluorocatechol	↑	↑	4.4	<0.01	5.2	<0.01
C16473	4-Fluorocatechol	↑	↑	4.4	<0.01	5.2	<0.01
C14110	4-Hydroxymethylcatechol	↑	↑	2.2	<0.01	2.1	<0.01
C02909	(2-Naphthyl)methanol	↑	↑	4.7	<0.01	4.8	<0.01
NA	2-Methoxynaphthalene	↑	↑	4.7	<0.01	4.8	<0.01
C14790	1-Naphthylamine		↑			3.3	<0.01
C00601	Phenylacetaldehyde	↑	↑	2.4	<0.01	2.5	<0.01
C04043	3,4-Dihydroxyphenylacetaldehyde	↑	↑	2.2	<0.01	2.1	<0.01
C02505	2-Phenylacetamide		↑			2.0	<0.01
C02083	Styrene oxide	↑	↑	2.4	<0.01	1.5	<0.01
C05627	4-Hydroxystyrene	↑	↑	2.4	<0.01	1.5	<0.01
C06758	4-Methylbenzaldehyde	↑	↑	2.4	<0.01	1.5	<0.01
C07209	3-Methylbenzaldehyde	↑	↑	2.4	<0.01	1.5	<0.01
C07214	2-Methylbenzaldehyde	↑	↑	2.4	<0.01	1.5	<0.01
C02519	p-Anisic acid	↑	↑	2.2	<0.01	2.1	<0.01
C07113	Acetophenone	↑	↑	2.4	<0.01	1.5	<0.01
C03663	2′,4′-Dihydroxyacetophenone	↑	↑	2.2	<0.01	2.1	<0.01
C10675	3′,4′-Dihydroxyacetophenone	↑	↑	2.2	<0.01	2.1	<0.01
C13635	2,4′-Dihydroxyacetophenone	↑	↑	2.2	<0.01	2.1	<0.01
C15513	Benzyl acetate		↑			2.0	<0.01
NA	4-Hydroxy-3-methylbenzoic acid	↑	↑	2.2	<0.01	2.1	<0.01
C10804	2-(Hydroxymethyl)benzoic acid	↑	↑	2.2	<0.01	2.1	<0.01
C02181	Phenoxyacetic acid	↑	↑	2.2	<0.01	2.1	<0.01
NA	3-Cresotinic acid	↑	↑	2.2	<0.01	2.1	<0.01
C14103	4-Methylsalicylate	↑	↑	2.2	<0.01	2.1	<0.01
D07721	Chlophedianol	↑		1.2	<0.01		
NA	Hericenone A	↑	↑	2.5	<0.01	2.4	<0.01
C07311	Stanozolol	↑	↑	3.4	<0.01	3.6	<0.01
C10794	Ginkgoic acid	↑	↑	3.2	<0.01	4.8	<0.01
NA	Methyl-[10]-shogaol	↑	↑	3.2	<0.01	4.8	<0.01
C07420	Pentamidine	↑	↑	1.6	<0.01	1.5	<0.01
C08157	Testosterone enanthate	↑	↑	1.2	<0.01	1.2	<0.01
NA	Pregnanetriol	↑	↑	3.7	<0.01	3.9	<0.01
C14606	11-Hydroxyandrosterone	↑		1.1	0.0145		
NA	Saponin H	↑	↑	1.5	<0.01	1.4	<0.01
NA	Assamsaponin D	↑	↑	1.5	<0.01	1.4	<0.01
NA	2,3-Dihydrobenzofuran	↑	↑	2.4	<0.01	2.5	<0.01
C11168	Tetrabenazine	↑	↑	1.6	<0.01	1.5	<0.01
C12508	Nateglinide	↑	↑	1.6	<0.01	1.5	<0.01
NA	Eremopetasinorol	↑		1.7	<0.01		
NA	Chloropanaxydiol	↑		1.0	<0.01		

P/L, pupal group vs. larval group; P/A, pupal group v.s. adult group; ↑, upregulation.

one of the most important environmental problems (Xiong et al., 2019; Chiang et al., 2020). In this study, we discovered that the polycyclic aromatic hydrocarbon (2-naphthyl)methanol (naphthalene) can be biodegraded by pupa-specific bacteria in *L. decemlineata* (**Figure 4**). It has been reported that naphthalene can be catabolized by *P. fluorescens* AH-40 (Mawad et al., 2020), *P. putida* BS3701 (Pozdnyakova-Filatova et al., 2020), and *Stenotrophomonas* sp. S1VKR-26 (Patel and Patel, 2020). Naphthalene is converted *via* salicylate and catechol to the intermediates of tricarboxylic acid cycle in *P. putida* PpG1 (Yen and Gunsalus, 1982), catalyzed by four key enzymes, namely, naphthalene 1,2-dioxygenase, salicylate hydroxylase, catechol 2,3-dioxygenase, and catechol 1,2-dioxygenase (Izmalkova et al., 2006). In this survey, we determined that 3- and 4-fluorocatechol,

TABLE 2 | Differential xenobiotics with higher levels in pupae v.s. larvae/adults in negative ion mode.

KEGG CID	Metabolites	P/L	P/A	VIP(P/L)	P(P/L)	VIP(P/A)	P(P/A)
NA	4-Hydroxybenzylamine		↑			1.2	<0.01
C10770	5-(8-Pentadecenyl)-1,3-benzenediol	↑	↑	1.3	<0.01	1.9	0.016
C03719	Phenylacetothiohydroximate	↑	↑	1.8	<0.01	1.7	<0.01
C08158	Testosterone propionate	↑	↑	5.9	<0.01	5.3	<0.01
C14643	Medrysone	↑	↑	5.9	<0.01	5.3	<0.01
C08185	Triamcinolone hexacetonide	↑	↑	1.7	0.02	1.6	0.02
C07119	Medroxyprogesterone		↑			5.3	<0.01
C01780	Aldosterone	↑		1.0	<0.01		
C18039	Aldosterone hemiacetal	↑		1.0	<0.01		
C19873	26-Hydroxycastasterone		↑			1.7	<0.01
C19326	p-Anisidine	↑	↑	1.5	0.01	1.2	<0.01
C07369	Prednisolone	↑		1.0	0.01		

P/L, pupal group vs. larval group; P/A, pupal group v.s. adult group; ↑, upregulation.

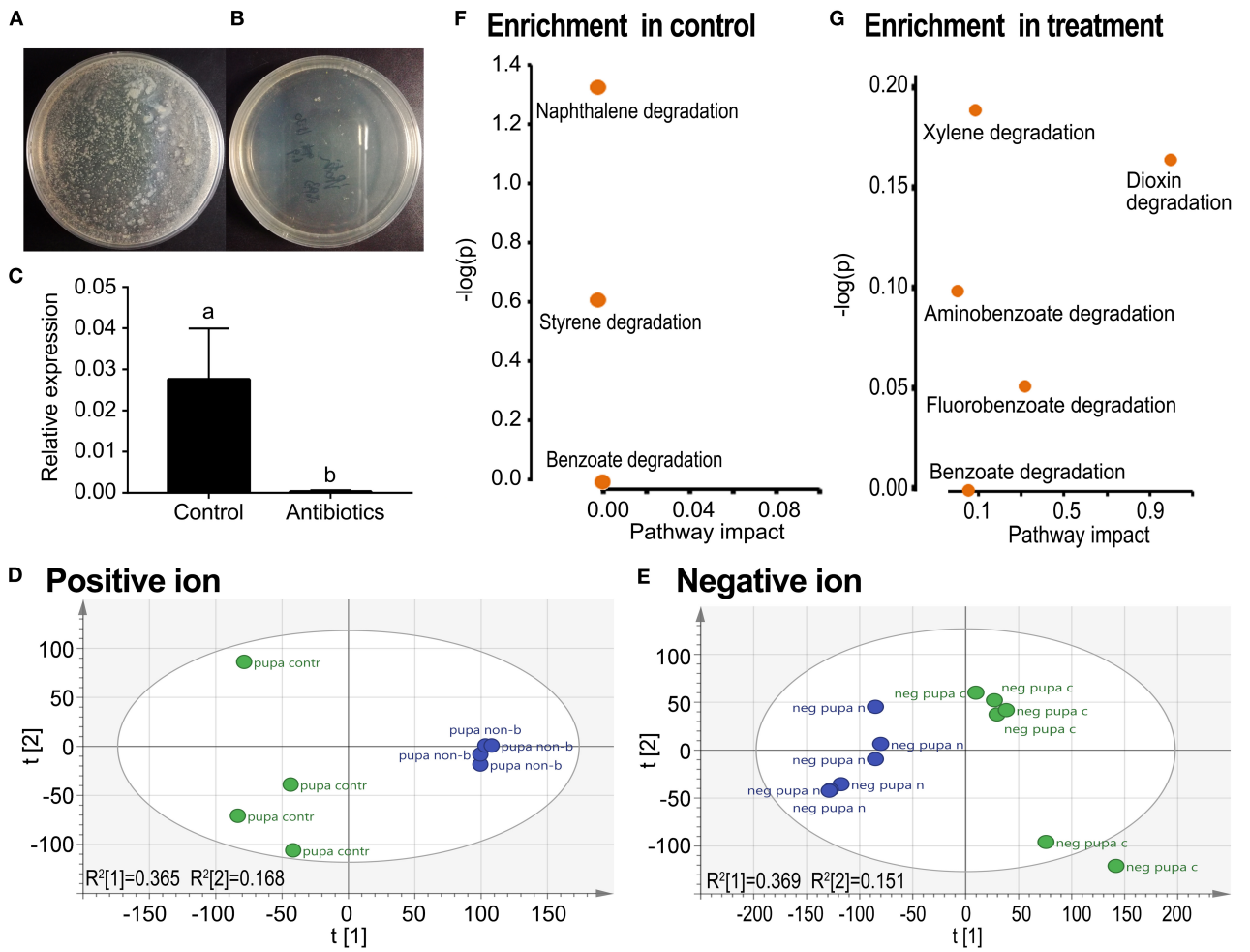

FIGURE 3 | Grouping comparison of metabolomics in control and antibiotic-fed pupae in *L. decemlineata*. The removal of bacteria was examined by plate culture **(A,B)** and qRT-PCR using a pair of universal primers of 16S rDNA from the Domain Bacteria **(C)**. Relative expression level of 16S rDNA was calculated by the $2^{-\Delta\Delta CT}$ method. Different letters indicate significant difference at p-value < 0.05 using analysis of variance with the Tukey–Kramer test. The UPLC-Q-TOF-MS resultant data were analyzed by PCA. Positive and negative ion mode PCA score maps **(D,E)** and pathway enrichment analyses **(F,G)** in control vs. antibiotic-fed pupal samples are shown. Green and blue colors in the **(D,E)** represented control and aposymbiontic pupal groups and each point represented a sample.

TABLE 3 | Differential xenobiotic and other secondary metabolite biomarkers with higher levels in controls than antibiotic-fed pupae in positive ion mode.

KEGG CID	Metabolites	C/T	VIP	*P*
C06758	4-Methylbenzaldehyde	↑	3.0	<0.01
C07209	3-Methylbenzaldehyde	↑	3.0	<0.01
C07214	2-Methylbenzaldehyde	↑	3.0	<0.01
C05775	N1-(alpha-D-ribosyl)-5,6-dimethylbenzimidazole	↑	1.5	<0.01
C06846	Benztropine	↑	1.4	<0.01
NA	2,3-Dimethylbenzofuran	↓	1.3	<0.01
NA	4-(1-Methylethenyl)benzaldehyde	↓	1.3	<0.01
C06578	4-Isopropylbenzoic acid	↓	1.5	<0.01
C00601	Phenylacetaldehyde	↑	3.0	<0.01
C05332	Phenylethylamine	↑	1.1	0.02
C02455	1-Phenylethylamine	↑	1.1	0.02
C12288	alpha-Amylcinnamaldehyde	↑	3.0	<0.01
C02083	Styrene oxide	↑	3.0	<0.01
C07083	Styrene	↓	1.4	0.03
C05627	4-Hydroxystyrene	↑	3.0	<0.01
C01455	Toluene	↓	1.5	0.01
C07113	Acetophenone	↑	3.0	<0.01
C02909	(2-Naphthyl)methanol	↑	2.0	<0.01
NA	2-(2-Methylpropoxy)naphthalene	↑	2.4	0.012
C12303	Phenethyl acetate	↓	1.5	<0.01
NA	2-Phenyl-2-butenal	↓	1.3	<0.01
NA	4-Phenyl-2-butenal	↓	1.3	<0.01
NA	4-(1-Methylethenyl)benzaldehyde	↓	1.3	<0.01
NA	2-Methyl-3-phenyl-2-propenal	↓	1.3	<0.01
NA	3-(4-Methylphenyl)-2-propenal	↓	1.3	<0.01
C08155	Nandrolone phenpropionate	↓	3.0	0.011
NA	2,3-Dimethylbenzofuran	↓	1.3	<0.01
C10453	Eugenol	↓	1.5	<0.01
C10469	Isoeugenol	↓	1.5	<0.01
C10469	trans-Isoeugenol	↓	1.5	<0.01
C15520	7α,25-Dihydroxycholesterol	↓	2.0	<0.01
C06341	7α,27-Dihydroxycholesterol	↓	2.0	<0.01
C15518	7α,24S-Dihydroxycholesterol	↓	2.0	<0.01
C05453	7α,12α-Dihydroxy-5β-cholestan-3-one	↓	2.0	<0.01
C05458	7α,12α-Dihydroxy-5α-cholestan-3-one	↓	2.0	<0.01
NA	(3α,17α,23S)-17,23-Epoxy-3,29-dihydroxy-27-norlanost-8-en-24-one	↓	2.7	<0.01
NA	γ-Chaconine	↑	1.2	<0.01

C/T, pupal control group v.s. pupae treated with antibiotics group; ↑, upregulation; ↓, downregulation.

4-hydroxymethylcatechol, and 4-methylsalicylate were higher in the pupae than those in the larvae and adults. It appears that the same naphthalene transformation way is present in the *L. decemlineata* pupae. Consistent with the metabolomic result, our microbiome analysis revealed that both *Pseudomonas* and *Stenotrophomonas* are among the 18 pupa-specific genera identified recently (Kang et al., 2021).

Both biogenic (natural) and anthropogenic steroids are frequently detected in soils and aquatic environments in China (Chiang et al., 2020). For example, oestrogens, androgens, progestogens, glucocorticoids, and mineralocorticoids are detected in the surface water of urban rivers in Beijing (Chang et al., 2009). Bacteria are responsible for mineralizing polycyclic aromatic hydrocarbons from the biosphere (Chiang et al., 2020). Among 18 pupa-specific bacterial genera (Kang et al., 2021), *Nocardia* (Coombe et al., 1966), *Rhodococcus* (Fernandez de las Heras et al., 2009; Li et al., 2018), and *Stenotrophomonas* (Juhasz et al., 2000; Tachibana et al., 2003; Guan et al., 2019; Xiong et al., 2019) have been documented to degrade steroids from other environments. Whether the three bacterial genera in *L. decemlineata* can break down steroids deserves further research.

Saponins are a class of secondary plant metabolites which includes triterpenoids, steroids, and steroidal alkaloids glycosylated with one or more sugar chains. They are produced by many plant species (Zhang et al., 2020). Saponins provoke molting defects in, and exert deleterious effects on insects (De

TABLE 4 | Differential xenobiotics with higher levels in controls than antibiotic-fed pupae in negative ion mode.

KEGG CID	Metabolites	P/L	VIP	*P*
C01408	Benzoin	↑	1.4	<0.01
NA	Benzosimuline	↑	1.9	<0.01
NA	Phenylmethyl benzeneacetate	↑	1.1	<0.01
NA	2-Phenylethyl benzoate	↑	1.1	<0.01
C13632	4,4′-Dihydroxy-α-methylstilbene	↑	1.1	<0.01
C09814	Benzonitrile	↓	1.4	<0.01
C07178	Trimethobenzamide	↓	2.8	<0.01
C02351	1,2-Benzoquinone	↓	1.7	<0.01
NA	N-[2-(4-Hydroxyphenyl)ethyl]benzamide	↓	1.1	<0.01
C07527	Benzocaine	↓	1.1	<0.01
C12537	Benzyl benzoate	↑	1.4	<0.01
C15513	Benzyl acetate	↓	1.0	<0.01
C02351	1,2-Benzoquinone	↓	1.7	<0.01
C00230	3,4-Dihydroxybenzoic acid	↓	1.7	<0.01
C00196	2,3-Dihydroxybenzoic acid	↓	1.7	<0.01
NA	2,6-Dihydroxybenzoic acid	↓	1.7	<0.01
NA	3,5-Dihydroxybenzoic acid	↓	1.7	<0.01
NA	2-Dodecylbenzenesulfonic acid	↓	9.6	<0.01
C06433	5′-Benzoylphosphoadenosine	↑	1.7	0.014
C04221	trans-1,2-Dihydrobenzene-1,2-diol	↓	2.4	<0.01
C10812	3,4-Methylenedioxybenzaldehyde	↓	1.1	<0.01
C03574	2-Formylaminobenzaldehyde	↓	1.4	<0.01
NA	N-Undecylbenzenesulfonic acid	↓	10.2	<0.01
NA	2-Dodecylbenzenesulfonic acid	↓	9.6	<0.01
NA	N1-(2,4-Dimethoxybenzyl)-n2-(2-(pyridin-2-yl) ethyl)oxalamide	↑	1.4	<0.01
NA	N1-(2-Methoxy-4-methylbenzyl)-n2-(2-(pyridin-2-yl) ethyl)oxalamide	↓	1.2	<0.01
NA	N1-(2-Methoxy-4-methylbenzyl)-n2-(2-(5-methylpyridin-2-yl)ethyl)oxalamide	↑	1.2	<0.01
NA	α-(Methoxyimino)-N-methyl-2-[[[1-[3-(trifluoromethyl) phenyl]ethoxy]imino]methyl]benzeneacetamide	↓	1.1	<0.01
C05775	N1-(α-D-ribosyl)-5,6-dimethylbenzimidazole	↑	1.1	<0.01
C06433	5′-Benzoylphosphoadenosine	↑	1.7	0.014
C02372	4-Aminophenol	↑	1.1	<0.01
C01987	2-Aminophenol	↑	1.1	<0.01
C08061	2′-Aminobiphenyl-2,3-diol	↓	2.6	<0.01
NA	3-Pentadecylphenol	↓	1.1	<0.01
NA	Ethyl 4-phenylbutanoate	↓	2.0	<0.01
C02137	Phenylglyoxylic acid	↓	1.1	<0.01
NA	4-Phenyl-2-butyl acetate	↓	2.0	<0.01
NA	2-Methyl-1-phenyl-2-propanyl acetate	↓	2.0	<0.01
NA	(Z)-3-Phenyl-2-propenal	↑	1.1	<0.01
C06746	N-(2-Phenylethyl)-acetamide	↓	1.5	<0.01
C07734	2-Hydroxy-6-oxo-6-(2-hydroxyphenoxy)-hexa-2,4-dienoate	↓	1.1	<0.01
D05095	Mycophenolate sodium	↑	1.7	<0.01
NA	Phenethylamine glucuronide	↑	1.3	<0.01
C07437	Phensuximide	↑	1.8	<0.01
C04468	(+)-cis-3,4-Dihydrophenanthrene-3,4-diol	↑	1.4	<0.01
NA	2-Phenylethyl β-D-glucopyranoside	↑	2.3	<0.01
C07440	Phenylbutazone	↑	1.9	<0.01
NA	7-(4-Hydroxyphenyl)-1-phenyl-4-hepten-3-one	↑	1.2	<0.01
C07911	Phenylpropanolamine	↑	1.1	<0.01

(Continued)

TABLE 4 | Continued

KEGG CID	Metabolites	P/L	VIP	*P*
NA	(Z)-3-Phenyl-2-propenal	↑	1.1	<0.01
NA	Phenylmethyl benzeneacetate	↑	1.1	<0.01
C03719	Phenylacetothiohydroximate	↑	5.3	<0.01
NA	2-Phenylethyl benzoate	↑	1.1	<0.01
NA	1-(5-Acetyl-2-hydroxyphenyl)-3-methyl-1-butanone	↑	1.4	<0.01
C18043	Cholesterol sulfate	↑	6.2	<0.01
C00477	Ecdysone	↑	1.4	<0.01
C02633	20-Hydroxyecdysone	↑	1.4	<0.01
C02513	3-Dehydroecdysone	↑	1.1	<0.01
NA	16-Oxoestrone	↑	2.1	<0.01
C00468	Estrone	↑	1.9	<0.01
C02537	17α-Estradiol	↑	4.4	<0.01
C05302	2-Methoxyestradiol	↑	4.4	<0.01
C05301	2-Hydroxyestradiol	↑	1.5	<0.01
C14209	4-Hydroxyestradiol	↑	1.5	<0.01
C05295	19-Oxotestosterone	↑	4.4	<0.01
NA	Zapotin	↑	1.7	<0.01
C05485	21-Hydroxypregnenolone	↓	3.8	<0.01
C18038	7α-Hydroxypregnenolone	↓	3.8	<0.01
C06390	16α-Hydroxypregnenolone	↓	3.8	<0.01
C05138	17α-Hydroxypregnenolone	↓	3.8	<0.01
C04518	(20S)-17,20-Dihydroxypregn-4-en-3-one	↓	3.8	<0.01
C18040	5α-Dihydrodeoxycorticosterone	↓	3.8	<0.01

C/T, pupal control group v.s. pupae treated with antibiotics group; ↑, upregulation; ↓, downregulation.

Geyter et al., 2007; Podolak et al., 2010; Cai et al., 2016; Dolma et al., 2017). Therefore, tea saponin has been widely used as an insecticide in China (Cai et al., 2016). We herein demonstrated that the contents of saponin H and assamsaponin D were higher in the pupae compared with those in the larvae and adults in *L. decemlineata* (**Figure 4**).

Although a considerable amount of saponins is indicated in the soil, *L. decemlineata* pupae could still develop into adults, indicating that other factors may help *L. decemlineata* resist saponins. Some bacteria, for instance, *Acinetobacter calcoaceticus* and *A. oleivorans*, are known to detoxify saponins (Zhang et al., 2020). Moreover, the mixed cultures of *Methanobrevibacter* spp. and *Methanosphaera stadtmanae* in the crop of the avian foregut fermenter in *Opisthocomus hoazin* are able to reduce the hemolytic activity of Quillaja saponins by 80% within a few hours (García-Amado et al., 2007). Consistent with these results, *Acinetobacter* is a pupa-specific genus (Kang et al., 2021), and it may be responsible for the metabolism of saponins in the *L. decemlineata* pupae.

Elimination of Aromatics in the Larvae and Adults

Potato plants contain many aromatics, where some exert noxious effects when accumulated to high concentrations within insect bodies (Gandia-Herrero and Garcia-Carmona, 2013; Kostyn et al., 2020). In this survey, we discovered that only 6 and 7 aromatics were accumulated in the larvae and adults, respectively, in contrast to 42 cumulated aromatics in the pupae (**Tables 1**, **2**). The less accumulation implies the more active elimination of aromatics in the *L. decemlineata* larvae and adults.

Consistently, the microbiota are widely distributed in the larval or/and adult guts (Jing et al., 2020). These gut microbiota are involved in the breakdown of noxious compounds in numerous insect species in Coleoptera (Ceja-Navarro et al., 2015; Berasategui et al., 2017; Zhang et al., 2020), Lepidoptera (Vilanova et al., 2016; Zeng et al., 2020), Diptera (Griffin and Reed, 2020), Hymenoptera (Wu et al., 2020), and Isoptera (Van Dexter and Boopathy, 2019).

In this survey, the bacterial OTU data (Kang et al., 2021) revealed that the catabolism of aromatics was less active in the larvae and adults compared with that in *L. decemlineata* pupae (**Figure 1**). Therefore, the bacterial biodegradation of aromatics only partially contributes to the removal of excessive aromatics. Intestinal excretion should be another route to eliminate superfluous aromatics (Rozman, 1985). In fact, insecticides can be excreted by insects, directly or indirectly (modified forms) (Quesada et al., 2020). In *L. decemlineata* larvae and adults, superfluous aromatics in food may be excreted through the guts directly, or transferred to more hydrophilic forms. Only those potato aromatics absorbed by *L. decemlineata* larvae and adults need to be biodegraded by bacteria. Conversely, the alimentary canal is not well-developed in *L. decemlineata* pupae and cannot actively remove excessive aromatics. The pupae mainly depend on bacteria to catabolize the noxious substances.

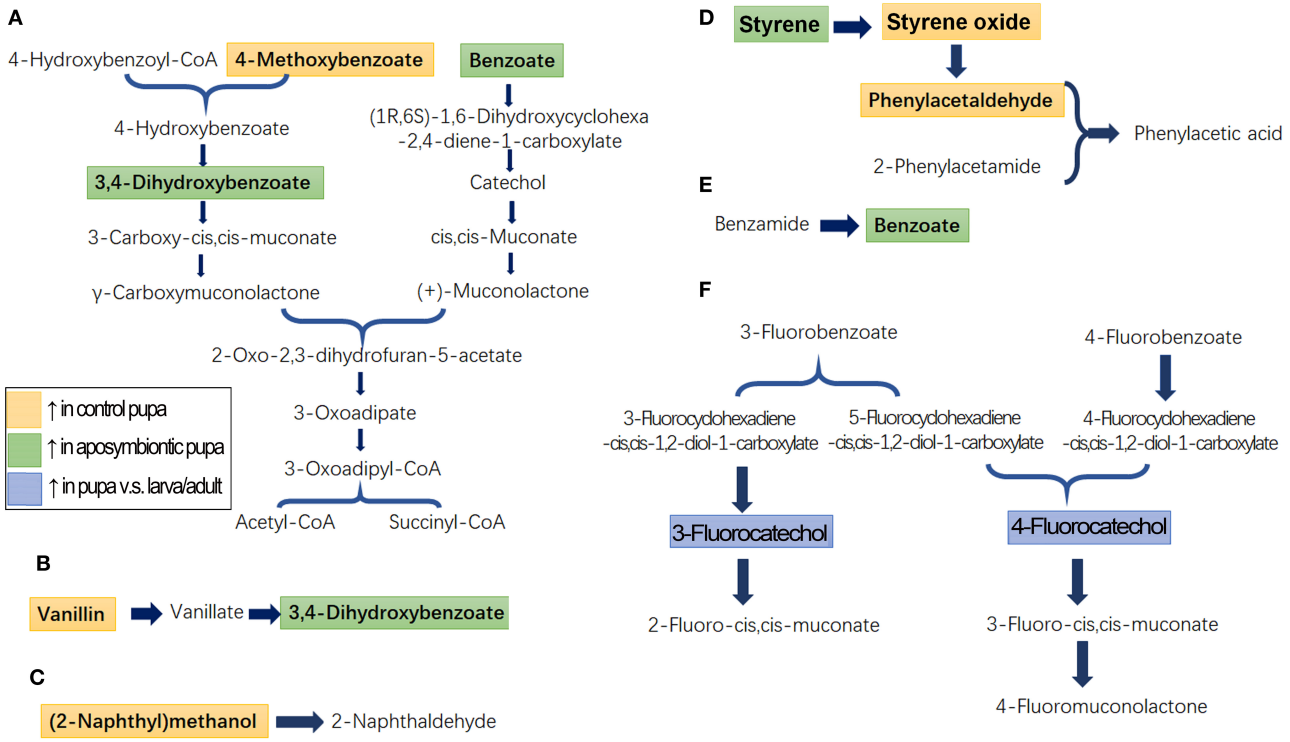

FIGURE 4 | Schematic diagram of the disturbed metabolic pathways in pupae. A total of seven active pathways were enriched in the pupal specimen by KEGG (http://www.kegg.jp) analysis. These ways were associated with the biodegradation of benzoate and 4-methoxybenzoate **(A)**, vanillin **(B)**, naphthalene **(C)**, styrene **(D)**, benzamide **(E)**, and fluorobenzoate **(F)**. The light orange and light green boxes indicate metabolites significantly higher and lower in the control pupal group than in the antibiotic-fed group, respectively. The light blue boxes mark metabolites significantly higher in the pupal group than in the larval and adult samples.

In summary, we uncovered the stage-dependent alterations in bacterial degradation of aromatics in *L. decemlineata*. The candidate bacterial genera contributing to aromatic catabolism were *Nocardia*, *Rhodococcus*, *Enterococcus*, *Acinetobacter*, *Pseudomonas*, and *Stenotrophomonas*, among others. This study provides new insights into the adaptation of *L. decemlineata* to different environmental niches and offers a better understanding of the relationship between ONS and a shift of bacterial flora. Moreover, since removal of the symbiotic bacteria inhibited the breakdown of superfluous aromatics (this study) and results in a decrease in the emergence rate and adult weight (Kang et al., 2021), disruption of bacterial communities may be a potential strategy to control *L. decemlineata*.

DATA AVAILABILITY STATEMENT

The datasets presented in this study can be found in online repositories. The names of the repository/repositories and accession number(s) can be found in the article/supplementary material.

AUTHOR CONTRIBUTIONS

W-NK, LJ, H-YM, and G-QL conceived the study, and participated in the design of the experiments and the interpretation of the results. W-NK, LJ, and H-YM performed the experiments. W-NK, LJ, and G-QL wrote the first draft of the manuscript. All authors contributed to the article and approved the submitted version.

FUNDING

This research was supported by the National Natural Science Foundation of China (32072416), and the China Agriculture Research System of MOF and MARA (CARS-09-P22).

REFERENCES

Berasategui, A., Salem, H., Paetz, C., Santoro, M., Gershenzon, J., Kaltenpoth, M., et al. (2017). Gut microbiota of the pine weevil degrades conifer diterpenes and increases insect fitness. *Mol. Ecol.* 26, 4099–4110. doi: 10.1111/mec.14186

Cai, H., Bai, Y., Wei, H., Lin, S., Chen, Y., Tian, H., et al. (2016). Effects of tea saponin on growth and development, nutritional indicators, and hormone titers in diamondback moths feeding on different host plant species. *Pesticide Biochem. Physiol.* 131, 53–59. doi: 10.1016/j.pestbp.2015.12.010

Ceja-Navarro, J. A., Vega, F. E., Karaoz, U., Hao, Z., Jenkins, S., Lim, H. C., et al. (2015). Gut microbiota mediate caffeine detoxification in the primary insect pest of coffee. *Nat. Commun.* 6:7618. doi: 10.1038/ncomms8618

Chang, H., Wan, Y., and Hu, J. (2009). Determination and source apportionment of five classes of steroid hormones in urban rivers. *Environ. Sci. Technol.* 43, 7691–7698. doi: 10.1021/es803653j

Chen, B., Teh, B. S., Sun, C., Hu, S., Lu, X., Boland, W., et al. (2016). Biodiversity and activity of the gut microbiota across the life history of the insect herbivore *Spodoptera littoralis*. *Sci. Rep.* 6:29505. doi: 10.1038/srep29505

Chen, J., Zhang, L., Jin, Q., Su, C., Zhao, L., Liu, X., et al. (2017). Bioremediation of phenol in soil through using a mobile plant-endophyte system. *Chemosphere* 182, 194–202. doi: 10.1016/j.chemosphere.2017.05.017

Chiang, Y.-R., Wei, S. T.-S., Wang, P.-H., Wu, P.-H., and Yu, C.-P. (2020). Microbial degradation of steroid sex hormones: implications for environmental and ecological studies. *Microb. Biotechnol.* 13, 926–949. doi: 10.1111/1751-7915.13504

Coates, J. D., Chakraborty, R., Lack, J. G., O'Connor, S. M., Cole, K. A., Bender, K. S., et al. (2001). Anaerobic benzene oxidation coupled to nitrate reduction in pure culture by two strains of *Dechloromonas*. *Nature* 411, 1039–1043. doi: 10.1038/35082545

Coombe, R. G., Tsong, Y. Y., Hamilton, P. B., and Sih, C. J. (1966). Mechanisms of steroid oxidation by microorganisms. X. Oxidative cleavage of estrone. *J. Biol. Chem.* 241, 1587–1595. doi: 10.1016/S0021-9258(18)96753-0

De Geyter, E., Lambert, E., Geelen, D., and Smagghe, G. (2007). "Novel advances with plant saponins as natural insecticides to control pest insects," in *Pest Technology Global Science Books*, 96–105.

Dolma, S. K., Sharma, E., Gulati, A., and Reddy, S. G. E. (2017). Insecticidal activities of tea saponin against diamondback moth, *Plutella xylostella* and aphid, *Aphis craccivora*. *Toxin Rev.* 37, 52–55. doi: 10.1080/15569543.2017.1318405

Fernandez de las Heras, L., Garcia Fernandez, E., Maria Navarro Llorens, J., Perera, J., and Drzyzga, O. (2009). Morphological, physiological, and molecular characterization of a newly isolated steroid-degrading actinomycete, identified as *Rhodococcus ruber* strain Chol-4. *Curr. Microbiol.* 59, 548–553. doi: 10.1007/s00284-009-9474-z

Fürstenberg-Hägg, J., Zagrobelny, M., and Bak, S. (2013). Plant defense against insect herbivores. *Int. J. Mol. Sci.* 14, 10242–10297. doi: 10.3390/ijms140510242

Gandia-Herrero, F., and Garcia-Carmona, F. (2013). Biosynthesis of betalains: yellow and violet plant pigments. *Trends Plant Sci.* 18, 334–343. doi: 10.1016/j.tplants.2013.01.003

García-Amado, M. A., Michelangeli, F., Gueneau, P., Perez, M. E., and Dominguez-Bello, M. G. (2007). Bacterial detoxification of saponins in the crop of the avian foregut fermenter *Opisthocomus hoazin*. *J. Anim. Feed Sci.* 16, 82–85. doi: 10.22358/jafs/74460/2007

Griffin, L. H., and Reed, L. K. (2020). Effect of gut microbiota on α-amanitin tolerance in *Drosophila tripunctata*. *Ecol. Evol.* 10, 9419–9427. doi: 10.1002/ece3.6630

Guan, J., Wang, H., Zhu, Y., and Xu, J. (2019). Whole-genome sequencing of *S. maltophilia* and degradation of fluoranthene. *Genomics Appl. Biol.* 38, 3037–3045. doi: 10.13417/j.gab.038.003037

Hammer, T. J., and Bowers, M. D. (2015). Gut microbes may facilitate insect herbivory of chemically defended plants. *Oecologia* 179, 1–14. doi: 10.1007/s00442-015-3327-1

Hanselman, T. A., Graetz, D. A., and Wilkie, A. C. (2003). Manure-borne estrogens as potential environmental contaminants: a review. *Environ. Sci. Technol.* 37, 5471–5478. doi: 10.1021/es034410+

Hartmans, S., Smits, J. P., van der Werf, M. J., Volkering, F., and de Bont, J. A. (1989). Metabolism of styrene oxide and 2-phenylethanol in the styrene-degrading *Xanthobacter* strain 124X. *Appl. Environ. Microbiol.* 55, 2850–2855. doi: 10.1128/aem.55.11.2850-2855.1989

Hartmans, S., van der Werf, M. J., and de Bont, J. A. (1990). Bacterial degradation of styrene involving a novel flavin adenine dinucleotide-dependent styrene monooxygenase. *Appl. Environ. Microbiol.* 56, 1347–1351. doi: 10.1128/aem.56.5.1347-1351.1990

Izmalkova, T. Y., Mavrodi, D. V., Sokolov, S. L., Kosheleva, I. A., Smalla, K., Thomas, C. M., et al. (2006). Molecular classification of IncP-9 naphthalene degradation plasmids. *Plasmid* 56, 1–10. doi: 10.1016/j.plasmid.2005.12.004

Jing, T. Z., Qi, F. H., and Wang, Z. Y. (2020). Most dominant roles of insect gut bacteria: digestion, detoxification, or essential nutrient provision? *Microbiome* 8:38. doi: 10.1186/s40168-020-00823-y

Juhasz, A. L., Stanley, G. A., and Britz, M. L. (2000). Microbial degradation and detoxification of high molecular weight polycyclic aromatic hydrocarbons by *Stenotrophomonas maltophilia* strain VUN 10,003. *Lett. Appl. Microbiol.* 30, 396–401. doi: 10.1046/j.1472-765x.2000.00733.x

Kanehisa, M., Goto, S., Sato, Y., Furumichi, M., and Tanabe, M. (2012). KEGG for integration and interpretation of largescale molecular data sets. *Nucleic Acids Res.* 40, 109–114. doi: 10.1093/nar/gkr988

Kang, W.-N., Jin, L., Fu, K.-Y., Guo, W.-C., and Li, G.-Q. (2021). A switch of microbial flora coupled with ontogenetic niche shift in *Leptinotarsa decemlineata*. *Arch. Insect Biochem. Physiol.* 106:e21782. doi: 10.1002/arch.21782

Kjaer, J., Olsen, P., Bach, K., Barlebo, H. C., Ingerslev, F., Hansen, M., et al. (2007). Leaching of estrogenic hormones from manure-treated structured soils. *Environ. Sci. Technol.* 41, 3911–3917. doi: 10.1021/es0627747

Kostyn, K., Boba, A., Kostyn, A., Kozak, B., Starzycki, M., Kulma, A., et al. (2020). Expression of the tyrosine hydroxylase gene from rat leads to oxidative stress in potato plants. *Antioxidants* 9:717. doi: 10.3390/antiox9080717

Kumar, K., and Goh, K. M. (2000). Crop residues and management practices: effects on soil quality, soil nitrogen dynamics, crop yield, and nitrogen recovery. *Adv. Agron.* 68, 197–319. doi: 10.1016/S0065-2113(08)60846-9

Lesperance, D. N., and Broderick, N. A. (2020). Microbiomes as modulators of *Drosophila melanogaster* homeostasis and disease. *Curr. Opin. Insect Sci.* 39, 84–90. doi: 10.1016/j.cois.2020.03.003

Li, Y., Wang, H. Q., Wu, X. X., and Xu, J. (2018). Study on the trans-membrane transport process of fluoranthene by *Rhodococcus* sp. BAP-1. *China Environ. Sci.* 38, 1441–1448. doi: 10.19674/j.cnki.issn1000-6923.2018.0174

Löfmark, S., Edlund, C., and Nord, C. E. (2010). Metronidazole is still the drug of choice for treatment of anaerobic infections. *Clin. Infect. Dis.* 50, S16–S23. doi: 10.1086/647939

Marconi, A. M., Beltrametti, F., Bestetti, G., Solinas, F., Ruzzi, M., Galli, E., et al. (1996). Cloning and characterisation of styrene catabolism genes from *Pseudomonas fuorescens* ST. *Appl. Environ. Microbiol.* 62, 121–127. doi: 10.1128/aem.62.1.121-127.1996

Mawad, A. M. M., Abdel-Mageed, W. S., and Hesham, A. E. (2020). Quantification of naphthalene dioxygenase (NahAC) and catechol dioxygenase (C23O) catabolic genes produced by phenanthrene-degrading *Pseudomonas fluorescens* AH-40. *Curr. Genomics* 21, 111–118. doi: 10.2174/1389202921666200224101742

Meng, Q.-W., Xu, Q.-Y., Zhu, T.-T., Jin, L., Fu, K.-Y., Guo, W.-C., et al. (2019). Hormonal signaling cascades required for phototaxis switch in wandering *Leptinotarsa decemlineata* larvae. *PLoS Genet.* 15:e1007423. doi: 10.1371/journal.pgen.1007423

Mushtaq, M. N., Sunohara, Y., and Matsumoto, H. (2013). Bioactive l-DOPA induced quinoprotein formation to inhibit root growth of cucumber seedlings. *J. Pesticide Sci.* 38, 68–73. doi: 10.1584/jpestics.D13-005

Nadkarni, M. A., Martin, F. E., Jacques, N. A., and Hunter, N. (2002). Determination of bacterial load by real-time PCR using a broad-range (universal) probe and primers set. *Microbiology* 148, 257–266. doi: 10.1099/00221287-148-1-257

O'Connor, K. E., Buckley, C. M., Hartmans, S., and Dobson, A. D. W. (1995). Possible regulatory role for non-aromatic carbon sources in styrene degradation by *Pseudomonas putida* CA-3. *Appl. Environ. Microbiol.* 61, 544–548. doi: 10.1128/aem.61.2.544-548.1995

O'Connor, K. E., and Dobson, A. D. W. (1996). Microbial degradation of alkenylbenzenes. *World J. Microbiol. Biotechnol.* 12, 207–212. doi: 10.1007/BF00360916

O'Leary, N. D., O'Connor, K. E., and Dobson, A. D. W. (2002). Biochemistry, genetics and physiology of microbial styrene degradation. *FEMS Microbiol. Rev.* 26, 403–417. doi: 10.1111/j.1574-6976.2002.tb00622.x

Panke, S., de Lorenzo, V., Kaiser, A., Witholt, B., and Wubbolts, M. G. (1999). Engineering of a stable whole-cell biocatalyst capable of (S)-styrene oxide formation for continuous two-liquid-phase applications. *Appl. Environ. Microbiol.* 65, 5619–5623. doi: 10.1128/AEM.65.12.5619-5623.1999

Patel, K., and Patel, M. (2020). Improving bioremediation process of petroleum wastewater using biosurfactants producing *Stenotrophomonas* sp. S1VKR-26 and assessment of phytotoxicity. *Bioresour. Technol.* 315:123861. doi: 10.1016/j.biortech.2020.123861

Podolak, I., Galanty, A., and Sobolewska, D. (2010). Saponins as cytotoxic agents: a review. *Phytochem. Rev.* 9, 425–474. doi: 10.1007/s11101-010-9183-z

Pozdnyakova-Filatova, I., Petrikov, K., Vetrova, A., Frolova, A., Streletskii, R., and Zakharova, M. (2020). The naphthalene catabolic genes of *Pseudomonas putida* BS3701: additional regulatory control. *Front. Microbiol.* 11:1217. doi: 10.3389/fmicb.2020.01217

Quesada, C. R., Scharf, M. E., and Sadof, C. S. (2020). Excretion of non-metabolized insecticides in honeydew of striped pine scale. *Chemosphere* 249:126167. doi: 10.1016/j.chemosphere.2020.126167

Rodgers, K. J., and Shiozawa, N. (2008). Misincorporation of amino acid analogues into proteins by biosynthesis. *Int. J. Biochem. Cell Biol.* 40, 1452–1466. doi: 10.1016/j.biocel.2008.01.009

Rozman, K. (1985). Intestinal excretion of toxic substances. *Arch. Toxicol. Suppl.* 8, 87–93. doi: 10.1007/978-3-642-69928-3_10

Shi, X.-Q., Guo, W.-C., Wan, P.-J., Zhou, L.-T., Ren, X.-L., Ahmat, T., et al. (2013). Validation of reference genes for expression analysis by quantitative real-time PCR in *Leptinotarsa decemlineata* (Say). *BMC Res. Notes* 6:93. doi: 10.1186/1756-0500-6-93

Silkie, S. S., and Nelson, K. L. (2009). Concentrations of host-specific and generic fecal markers measured by quantitative PCR in raw sewage and fresh animal feces. *Water Res.* 43, 4860–4871. doi: 10.1016/j.watres.2009.08.017

Steinmetz, Z., Kurtz, M. P., Zubrod, J. P., Meyer, A. H., Elsner, M., and Schaumann, G. E. (2019). Biodegradation and photooxidation of phenolic compounds in soil-A compound-specific stable isotope approach. *Chemosphere* 230, 210–218. doi: 10.1016/j.chemosphere.2019.05.030

Tachibana, S., Kuba, N., Kawai, F., Duine, J. A., and Yasuda, M. (2003). Involvement of a quinoprotein (PQQ-containing) alcohol dehydrogenase in the degradation of polypropylene glycols by the bacterium *Stenotrophomonas maltophilia*. *FEMS Microbiol. Lett.* 218, 345–349. doi: 10.1111/j.1574-6968.2003.tb11540.x

Utkin, I. B., Yakimov, M. M., Mateeva, L. N., Kozlyak, E. I., Rogozhin, I. S., Solomon, Z. G., et al. (1991). Degradation of styrene and ethylbenzene by *Pseudomonas* species Y2. *FEMS Microbiol. Lett.* 77, 237–242. doi: 10.1111/j.1574-6968.1991.tb04355.x

Van Dexter, S., and Boopathy, R. (2019). Biodegradation of phenol by *Acinetobacter tandoii* isolated from the gut of the termite. *Environ. Sci. Pollut. Res.* 26, 34067–33072. doi: 10.1007/s11356-018-3292-4

Velasco, A., Alonso, S., Garcia, J. L., Perera, J., and Diaz, E. (1998). Genetic and functional analysis of the styrene catabolic cluster of *Pseudomonas* sp. strain Y2. *J. Bacteriol.* 180, 1063–1071. doi: 10.1128/JB.180.5.1063-1071.1998

Vilanova, C., Baixeras, J., Latorre, A., and Porcar, M. (2016). The generalist inside the specialist: gut bacterial communities of two insect species feeding on toxic plants are dominated by *Enterococcus* sp. *Front. Microbiol.* 7:1005. doi: 10.3389/fmicb.2016.01005

Wu, Y., Zheng, Y., Chen, Y., Wang, S., Chen, Y., Hu, F., et al. (2020). Honey bee (*Apis mellifera*) gut microbiota promotes host endogenous detoxification capability via regulation of P450 gene expression in the digestive tract. *Microb. Biotechnol.* 13, 1201–1212. doi: 10.1111/1751-7915.13579

Xia, X., Lan, B., Tao, X., Lin, J., and You, M. (2020). Characterization of *Spodoptera litura* gut bacteria and their role in feeding and growth of the host. *Front. Microbiol.* 11:1492. doi: 10.3389/fmicb.2020.01492

Xiong, W., Yin, C., Peng, W., Deng, Z., Lin, S., and Liang, R. (2019). Characterization of an 17β-estradiol-degrading bacterium *Stenotrophomonas maltophilia* SJTL3 tolerant to adverse environmental factors. *Appl. Microbiol. Biotechnol.* 104, 1291–1305. doi: 10.1007/s00253-019-10281-8

Yen, K. M., and Gunsalus, I. C. (1982). Plasmid gene organization: naphthalene/salicylate oxidation. *Proc. Natl. Acad. Sci. U.S.A.* 79, 874–878. doi: 10.1073/pnas.79.3.874

Zeng, J. Y., Wu, D. D., Shi, Z. B., Yang, J., Zhang, G. C., and Zhang, J. (2020). Influence of dietary aconitine and nicotine on the gut microbiota of two lepidopteran herbivores. *Arch. Insect Biochem. Physiol.* 23:e21676. doi: 10.1002/arch.21676

Zhang, S., Shu, J., Xue, H., Zhang, W., Zhang, Y., Liu, Y., et al. (2020). The gut microbiota in *Camellia* weevils are influenced by plant secondary metabolites and contribute to saponin degradation. *mSystems* 5, e00692–e00619. doi: 10.1128/mSystems.00692-19

Conflict of Interest: The authors declare that the research was conducted in the absence of any commercial or financial relationships that could be construed as a potential conflict of interest.

Publisher's Note: All claims expressed in this article are solely those of the authors and do not necessarily represent those of their affiliated organizations, or those of the publisher, the editors and the reviewers. Any product that may be evaluated in this article, or claim that may be made by its manufacturer, is not guaranteed or endorsed by the publisher.

frontiers in Physiology

ORIGINAL RESEARCH
published: 13 December 2021
doi: 10.3389/fphys.2021.780255

Bacillus thuringiensis and Chlorantraniliprole Trigger the Expression of Detoxification-Related Genes in the Larval Midgut of *Plutella xylostella*

*Muhammad Zeeshan Shabbir[1,2], Xiangbing Yang[3], Raufa Batool[4], Fei Yin[1,2], Paul E. Kendra[3] and Zhen-Yu Li[1,2]**

[1] Institute of Plant Protection, Guangdong Academy of Agricultural Sciences, Guangzhou, China, [2] Guangdong Provincial Key Laboratory of High Technology for Plant Protection, Guangzhou, China, [3] USDA-ARS, Subtropical Horticulture Research Station, Miami, FL, United States, [4] State Key Laboratory for Biology of Plant Diseases and Insect Pests, Institute of Plant Protection, Chinese Academy of Agricultural Sciences, Beijing, China

OPEN ACCESS

Edited by:
Ran Wang,
Beijing Academy of Agriculture and Forestry Sciences, China

Reviewed by:
Youssef Dewer,
Agricultural Research Center, Egypt
Lin Jin,
Nanjing Agricultural University, China
Yajun Yang,
Zhejiang Academy of Agricultural Sciences, China

***Correspondence:**
Zhen-Yu Li
lizhenyu@gdaas.cn

Specialty section:
This article was submitted to Invertebrate Physiology, a section of the journal Frontiers in Physiology

Received: 20 September 2021
Accepted: 01 November 2021
Published: 13 December 2021

Citation:
Shabbir MZ, Yang X, Batool R, Yin F, Kendra PE and Li Z-Y (2021) Bacillus thuringiensis and Chlorantraniliprole Trigger the Expression of Detoxification-Related Genes in the Larval Midgut of Plutella xylostella. Front. Physiol. 12:780255. doi: 10.3389/fphys.2021.780255

Background: Diamondback moth (DBM), *Plutella xylostella* (L.), has developed resistance to many insecticides. The molecular mechanism of DBM resistance to Bt-G033A combined with chlorantraniliprole (CL) remains undefined.

Methods: In this study, field-resistant strains of *Plutella xylostella* to three pesticides, namely, *Bacillus thuringiensis* (Bt) toxin (Bt-G033A), CL, and a mixture of Bt + CL, were selected to evaluate the resistance level. Additionally, transcriptomic profiles of a susceptible (SS-DBM), field-resistant (FOH-DBM), Bt-resistant (Bt-DBM), CL-resistant (CL-DBM), and Bt + CL-resistant (BtC-DBM) strains were performed by comparative analysis to identify genes responsible for detoxification.

Results: The Bt-G033A was the most toxic chemical to all the DBM strains among the three insecticides. The comparative analysis identified 25,518 differentially expressed genes (DEGs) between pairs/combinations of strains. DEGs were enriched in pathways related to metabolic and catalytic activity and ABC transporter in resistant strains. In total, 17 metabolic resistance-related candidate genes were identified in resistance to Bt-G033A, CL, and Bt + CL by co-expression network analysis. Within candidate genes, the majority was upregulated in key genes including cytochrome P450, glutathione *S*-transferase (GST), carboxylesterase, and acetylcholinesterase in CL- and BtC-resistant strains. Furthermore, aminopeptidase N (APN), alkaline phosphatase (ALP), cadherin, trypsin, and ABC transporter genes were eminent as Bt-resistance-related genes. Expression patterns of key genes by the quantitative real-time PCR

(qRT-PCR) proved the credibility of transcriptome data and suggest their association in the detoxification process.

Conclusion: To date, this study is the most comprehensive research presenting functional transcriptome analysis of DBM using Bt-G033A and CL combined insecticidal activity.

Keywords: *Bacillus thuringiensis*, chlorantraniliprole, *Plutella xylostella*, resistance management, RNA sequencing, gene expression

INTRODUCTION

The diamondback moth (DBM), *Plutella xylostella* (L.) (*P. xylostella*) (Lepidoptera: Plutellidae), is a global pest of *Brassica* crops worldwide (Li et al., 2016; Jaleel et al., 2020). It can rapidly develop with extensive generation overlap and disperse quickly over substantial distances, which have made this pest particularly difficult to control. Currently, the control of *P. xylostella* is heavily dependent on pesticides causing several environmental problems including health issues and pollution and the development of resistance of the target insects (Pu et al., 2010; Yin et al., 2019). To the best of our knowledge, *P. xylostella* has developed resistance to over 95 insecticide compounds (Guo et al., 2013; Liu et al., 2015; Lima Neto et al., 2016). Although chlorantraniliprole (CL) is a novel diamide insecticide that is effective for control of *P. xylostella* (Guo et al., 2014), a field population of DBM has developed a 2,000-fold resistance to CL after 2 years of exposure in Southern China and Southeast Asia (Edralin et al., 2011; Wang and Wu, 2012). Also, the resistance level of DBM in field populations can vary among field sites, making resistance management more difficult (Wang et al., 2010). Therefore, effective management of this destructive pest is urgently needed.

Since repeated applications of conventional insecticides have resulted in a substantial increase in resistance in DBM populations, biological pesticides including Bt insecticides have been adopted as alternatives for managing Lepidoptera pests (Melatti et al., 2010; Shabbir et al., 2018; Prabu et al., 2020). However, DBM has rapidly developed significant resistance to various Bt toxins, although Bt insecticides showed negligible impact on non-target organisms (Jiang et al., 2015; Yin et al., 2016). Therefore, to cope with DBM resistance, rotation of insecticides with different modes of action has been utilized to lower the selection pressure (Zhao et al., 2010). To delay resistance evolution, combining various insecticides for target pests is necessary to ensure crop protection (Stemele, 2017; Yang et al., 2018; Zhao et al., 2018). Although different types of chemical combinations are commonly applied against lepidopteran pests (Cang et al., 2017; Zhao et al., 2018; Wang et al., 2019), studies on combinations of Bt products and insecticides have been little reported.

The evolution of resistance is a natural and unavoidable process. The mechanism of increased resistance to different insecticides is the enrichment of xenobiotic detoxification and target site mutation (James and Davey, 2009). The roles of major detoxification genes such as glutathione S-transferase (GST), carboxylesterases (CarE), and cytochrome P450 monooxygenases in metabolic resistance in lepidopteran pests have been widely reported (Li et al., 2007; Eziah et al., 2009; Pauchet et al., 2010). In addition, several Bt-binding proteins have been documented in *P. xylostella* (Gahan et al., 2010; Tiewsiri and Wang, 2011; Zhu et al., 2011). Previous studies have focused on mutations primarily correlated with insecticide resistance (Guo et al., 2014; Troczka et al., 2015). The role of mutation in diamide insecticide resistance has been confirmed by the CRISPR-Cas9-mediated genome editing in lepidopteran pests (Zuo et al., 2017). Similarly, genes (G4946E and I4790K) have also been associated with diamide resistance in DBM (Jouraku et al., 2020). Still, the occurrence of insecticide mutation is unclear, as information is insufficient about selecting ryanodine receptors (RyRs) allele in the field (Troczka et al., 2015). Thus, in-depth knowledge about the characterization of detoxification factors is essential for understanding the metabolic resistance mechanism to Cry toxins and insecticides in target pests.

Although the mechanism of resistance to insecticides in *P. xylostella* has been studied widely, complete information about the expression of genes linked to pesticides and Cry toxins is limited. To the best of our knowledge, no previous studies have addressed the molecular mechanism of resistance in *P. xylostella* by using a combination of Bt toxins and insecticides. A combination of Bt-G033A [*Bacillus thuringiensis* (Bt) subsp. *aizawai* G03, contains *cry1Ac*, *cry1Ac*, *cry1Ca*, and *cry2Ab* genes] and CL was used for the first time to determine the gene networks and molecular mechanism of resistance in *P. xylostella*. Recently, advancements in transcriptome analysis have provided several approaches for investigating the metabolic response of insects and comparing gene regulation in resistant and susceptible strains (Wang et al., 2010; Chen et al., 2011). In this study, we compared midgut tissues of susceptible (SS-DBM) and resistant strains [field-resistant (FOH-DBM), CL-resistant (CL-DBM), Bt-resistant (Bt-DBM), and Bt + CL-resistant (BtC-DBM)] of *P. xylostella* using transcriptome analysis to identify common genes that respond to different insecticides (CL, Bt-G033A, and mixture/combination of Bt and CL). Furthermore, the differentially expressed genes (DEGs) in DBM strains linked to metabolic resistance to Bt, CL, and Bt + CL (a mixture of Bt and CL) were identified and validated using qRT-PCR analysis. Current data will be useful for studying systemic differences between DBM strains and identifying genes that might confer resistance to Bt and CL.

MATERIALS AND METHODS

Diamondback Moth Strains

A colony of *P. xylostella* was originally collected from the vegetable fields of Guangdong province of China in 2002 and reared without exposure to any insecticides under constant laboratory conditions of 25 ± 2°C, 70–80% relative humidity (RH), and a photoperiod of 16:8 h [light:dark (L:D)]. A high-resistant strain of DBM was collected from the Shijing county of Guangdong province in 2017 and named as FOH-DBM. Detailed information with respect to insecticide resistance of FOH-DBM is given in **Supplementary Figure 1** and also discussed in our previous manuscript (Shabbir et al., 2021). Later, this population was established in the greenhouse and reared on cabbage without exposure to insecticide. The CL-DBM, Bt-DBM, and BtC-DBM strains were derived from FOH-DBM strain by two rounds of selection with CL, Bt (Bt-G033A), and mixture of Bt + CL, respectively (Shabbir et al., 2021). The rearing conditions in the greenhouse were maintained at 25 ± 2°C, 70–80% RH, and a photoperiod of 16:8 h (L:D). In September 2017, the greenhouse was divided into four compartments (1–4). Compartment 1 was used for maintaining DBM larvae with no treatment; compartment 2 was used to rear DBM on cabbage plants treated with Bt 4,000X, 1.5 g (Bt powder), and 6 L water; compartment 3 was used to rear DBM on cabbage plants sprayed with mixture treatment of Bt and CL 2,000–1,000X, 3 g (Bt powder), and 6 ml CL into 6 L water; and in compartment 4, DBM was reared on cabbage plants sprayed with CL 300X, 20 ml (5% CL) plus 6 L water. In March 2018, these four compartments were treated again as following: compartment 1, no treatment applied; compartment 2, sprayed cabbage plants with Bt 8,000X, 1.25 g (Bt powder), and 10 L water; compartment 3, sprayed plants with 16,000–3,200X, 0.625 g (Bt powder), 0.125 ml (5% CL), and 10 L water; and compartment 4, treated with CL 1,600X and 6.25 ml (5% CL) plus 10 L water (Shabbir et al., 2021).

Insecticides

The chemicals used in this experiment included CL (200 g L^{-1} SC) purchased from the DuPont Agricultural Chemicals Ltd. (United States) and Bt-G033A, which was provided by the Huazhong Agricultural University, China.

Leaf Bioassay

Leaf-dip bioassays were conducted to determine the resistance level of DBM from the CL, Bt-G033A, and Bt + CL treatment. Median lethal concentration (LC_{50}) values were determined in DBM strains to compare the resistance level. For bioassay studies, we adopted the cabbage leaf-dip method of Tabashnik et al. (1987). Insecticides were dissolved in 100 ml distilled water and solutions of different concentrations were prepared with 0.1% Triton X-100. The second instar larvae from each strain were exposed to seven to eight concentrations of each insecticide. The concentrations ranging from 0.5 to 35 ppm for Bt, 10.5 to 700 ppm for CL, and 5.7 to 368 ppm for Bt + CL [17.5 ppm of Bt + 350 ppm of CL dissolved in 100 ml double-distilled water (ddH_2O)] were used for bioassay. The concentrations (0, 0.03, 0.06, 0.013, 0.25, 0.50, 1, and 2 ppm) of Bt, CL, and Bt + CL were used for SS-DBM. Each dose was replicated three times for all the DBM strains. To conduct the leaf-dip bioassay, at each concentration, three cabbage leaf disks (d = 6 cm) were dipped in each insecticide solution for 15 s, and then air-dried for 2 h at room temperature. The control cabbage leaf disks were immersed in distilled water solution and then air-dried. The treated and control cabbage leaves were placed individually into petri dishes (2.5 cm H × 8.5 cm D). At each dose for each insecticide, 10 second instar larvae were placed on a treated leaf disk in plastic petri dish and kept at 25 ± 2°C and 65 ± 5% RH. Mortality was recorded after 48 h. The control mortality was also documented.

Ribonucleic Acid Extraction, Library Construction, and Sequencing

The SS-DBM, Bt-DBM, CL-DBM, BtC-DBM, and FOH-DBM strains were selected to detect the resistance-related genes to Bt-G033A, CL, and Bt + CL, respectively. To induce resistance, these resistant strains were further treated with the highest doses of each insecticide by leaf-dipping test as discussed above. At 2 days posttreatment, treated DBM was collected for midgut extraction. A total of 50–60 larvae were collected for RNA extraction from midgut of each sample using the RNAprep Pure Kit DP432 (Tiangen Biotech, Beijing, China). Three biological replicates for each sample were collected and used for Illumina sequencing and gene expression analysis. RNA samples from all the DBM strains were evaluated for their stability using the Qsep1 instrument. 3 μg of total RNA was used to construct RNA libraries with the MGIEasy mRNA Library Prep Kit (Xu et al., 2019).

Bioinformatics Analysis of RNA Sequencing

The adapter and low-quality reads were filtered through cutadapt (version 1.11). Clean reads were mapped to the contigs with paired-end reads by Hisat2 (version 2.1.0), allowing up to two mismatches (Su et al., 2019). These genes were subjected to alignment against public protein databases: Pfam (Pfam protein families) and UniProt (Swiss-Prot). It comprised RNA-seq by expectation-maximization (RSEM) (version 1.2.6) for transcript abundance estimation and normalization of expression values as fragments per kilobase of transcript per million mapped reads (FPKM) (Li and Dewey, 2011). DEGs were identified with DESeq2 with a filter threshold of adjusted q-value <0.05 and | log2 fold change| > 1 (Bakhtiarizadeh et al., 2019).

The clusterProfiler[1] in R package (Yu et al., 2012) was employed to perform the Gene Ontology (GO) and the Kyoto Encyclopedia of Genes and Genomes (KEGG)[2] enrichment analysis. The GO and the KEGG enrichment analysis were calculated using a hypergeometric distribution with a Q value cutoff of 0.05. Q value obtained by the Fisher's exact test was adjusted with false discovery rate (FDR) for multiple comparisons (Liu et al., 2019).

[1]http://bioconductor.org/packages/release/bioc/html/clusterProfiler.html
[2]http://www.genome.jp/kegg/

TABLE 1 | Median lethal concentration (LC_{50}) of Bt-G033A, chlorantraniliprole, and Bt + chlorantraniliprole against five strains of *Plutella xylostella*.

Insecticide	Strains	LC_{50} (95% FL) (mg/l)	df	χ^2	RR[a]
Chlorantraniliprole	SS-DBM[c]	0.189 (0.054–0.479)	5	1.505	–
	FOH-DBM[d]	7.485 (6.225–8.436)	5	0.744	39.6
	Bt-DBM[e]	93.691 (65.582–113.493)	5	1.642	495.7
	CL-DBM[f]	230.728 (151.731–383.323)	5	1.069	>1000
	BtC-DBM[g]	166.292 (109.621–342.673)	5	0.731	879.8
Bt-G033A	SS-DBM	0.053 (0.015–0.101)	5	1.230	–
	FOH-DBM	0.344 (0.003–0.361)	5	0.686	6.5
	Bt-DBM	2.294 (0.499–4.465)	5	0.627	43.3
	CL-DBM	0.871 (0.362–1.618)	5	4.577	16.4
	BtC-DBM	1.072 (0.351–1.979)	5	1.756	20.2
Bt + CL[b]	SS-DBM	0.141 (0.064–0.249)	5	2.043	–
	FOH-DBM	5.084 (3.696–7.506)	5	2.251	36.1
	Bt-DBM	30.289 (14.583–60.023)	5	3.395	214.8
	CL-DBM	24.398 (11.453–42.942)	5	1.403	173.1
	BtC-DBM	25.832 (18.919–35.853)	5	0.811	183.2

[a] *RR, resistance ratio = LC_{50} of a particular strain divided by LC_{50} of susceptible strain.*
[b] *Bt + CL is the insecticide mixture of Bt and chlorantraniliprole (1:1).*
[c] *SS-DBM is laboratory susceptible strain.*
[d] *FOH-DBM is the field high-resistant strain.*
[e] *Bt-DBM is the resistant strain treated with Bt-G033A.*
[f] *CL-DBM is the resistant strain treated with chlorantraniliprole insecticide.*
[g] *BtC-DBM is the resistant strain of DMB selected with a mixture of Bt and chlorantraniliprole.*

TABLE 2 | Summary of reads in resistant and susceptible strains of *Plutella xylostella* transcriptomes.

Samples	Raw reads	Clean reads	Total mapped %	Clean ratio	Q30 (%)	GC (%)
SS-DBM	160,430,796	160,256,478	62.41%	99.92%	93.29%	55.64%
FOH-DBM	150,250,928	149,997,438	54.94%	99.74%	93.68%	53.41%
Bt-DBM	138,498,530	138,101,022	64.71%	99.85%	92.87%	54.18%
CL-DBM	118,990,394	118,757,080	63.33%	99.80%	92.90%	51.73%
BtC-DBM	120,013,556	119,484,296	60.61%	99.70%	92.61%	49.42%

Co-expression Network Analysis of Genes

To explore the association of genes to insecticide resistance, co-expression network analyses were performed using a correlation calculator. Cytoscape software (3.7.2, Cytoscape, San Diego, CA, United States) was used to build the regulation network analysis for insecticide resistance-related genes. A threshold level of $\geq$2-fold, FDR $\geq$ 0.05 for upregulated and ≤ -2-fold, and FDR $\geq$ 0.05 for downregulated genes were taken to construct the co-expression network map.

Validation of Key Genes by Quantitative Real-Time PCR

Expression levels of key genes selected after co-expression network analysis were determined by the quantitative real-time PCR (qRT-PCR) in DBM strains. Total RNA was extracted from midgut of DBM larvae using the Easy-spin RNA Isolation Kit (Biomed, Beijing, China). Moloney murine leukemia virus (M-MLV) Reverse Transcriptase (Takara, Japan) was used for the first-strand complementary DNA (cDNA) synthesis. The primers were synthesized by the Invitrogen Trading (Shanghai) Corporation Ltd. The details of primers are shown in **Supplementary Table 1**. The qRT-PCR was performed according to our previous research protocol (Shabbir et al., 2020). Actin was used as a reference gene. The $2^{-\Delta\Delta CT}$ method was used to calculate the relative gene expression level in DBM strains.

Statistical Analysis

The LC_{50} with fiducial limits and the chi-square (x^2) values were determined by probit analysis using Probit Or LOgit (POLO-PC) LeOra software (Parma, MO, United States). The one-way ANOVA followed by the Tukey's honestly significant difference (HSD) for multiple comparisons was used to analyze the significant expression of key genes in the qRT-PCR analyses. All the statistical analyses were carried out using the SPSS software (SPSS Inc., Chicago, IL, United States).

RESULTS

Determination of Toxicity

The leaf bioassay indicated that the DBM populations showed variable degrees of resistance to insecticides tested (Bt-G033A, CL, and Bt + CL) (**Table 1**). The LC_{50} values for Bt-G033A, CL,

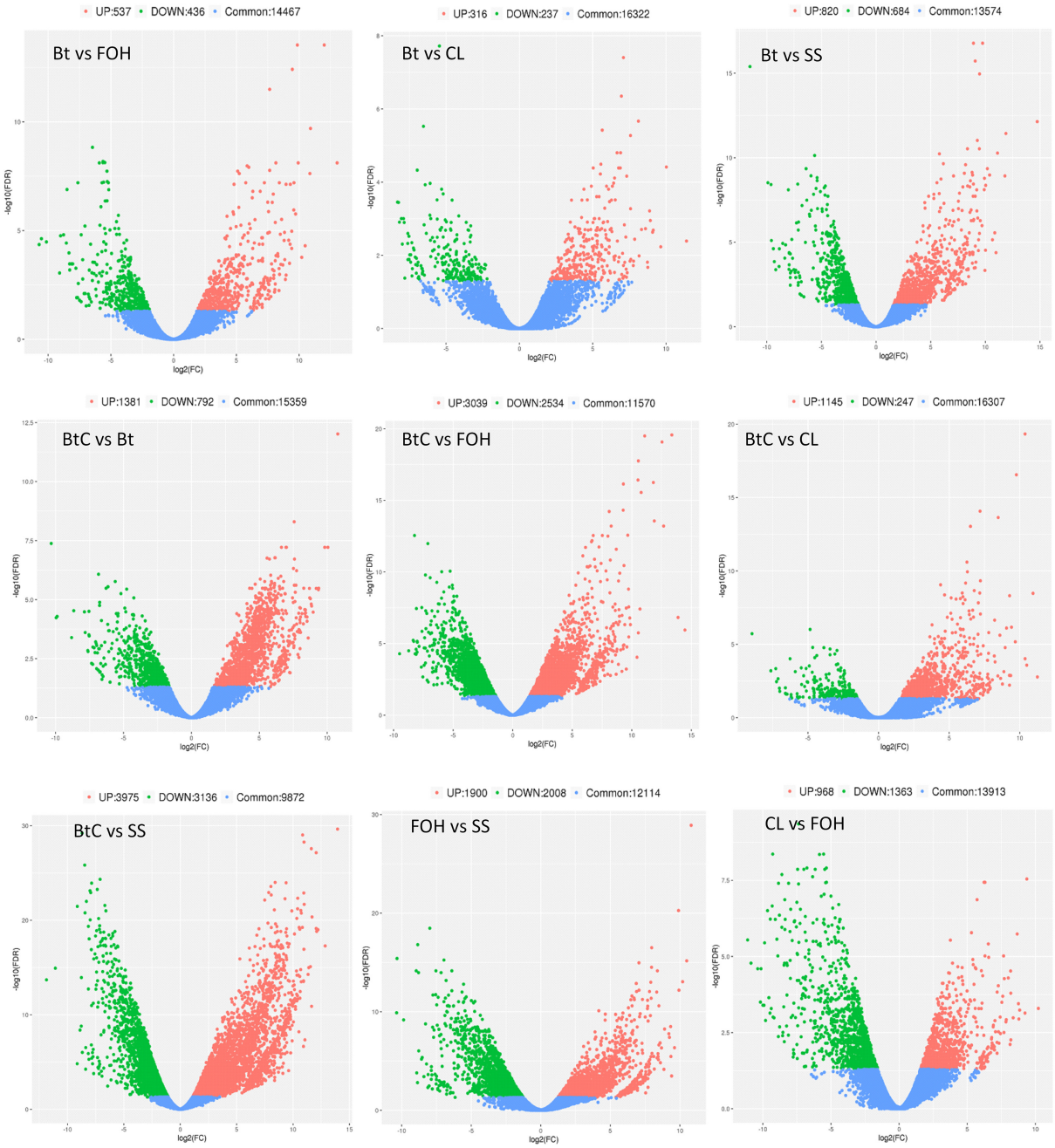

FIGURE 1 | Differentially expressed genes (DEGs) (>2-fold change, FDR < 0.05) between pairwise comparisons of resistant and susceptible strains of *Plutella xylostella*. The scatter in the figure represents each gene. Red indicates upregulated genes, green indicates downregulated genes, and blue are common genes.

and mixture insecticide (Bt + CL) were significantly higher in FOH-DBM and resistant strains (Bt-DBM, CL-DBM, and BtC-DBM) compared to SS-DBM strain. The resistance level of these DBM strains is different due to different generations of the strains from the results of our previous article (Shabbir et al., 2021). The results revealed that Bt-G033A was the most toxic to all the DBM strains among the tested insecticides. Concisely, the susceptibility level of DBM strains to tested chemicals from the most to least was Bt-G033A > Bt + CL > CL (**Table 1**).

Ribonucleic Acid Sequencing and Read Assembly

The cDNA samples of midgut tissue from resistant strains (FOH-DBM, Bt-DBM, CL-DBM, and BtC-DBM) and SS-DBM strain of *P. xylostella* were subjected to high-throughput Illumina sequencing to obtain an overview of gene expression profile. RNA sequencing from resistant and SS-DBM strains ranged from 118,757,080 to 160,256,478. The numbers of reads

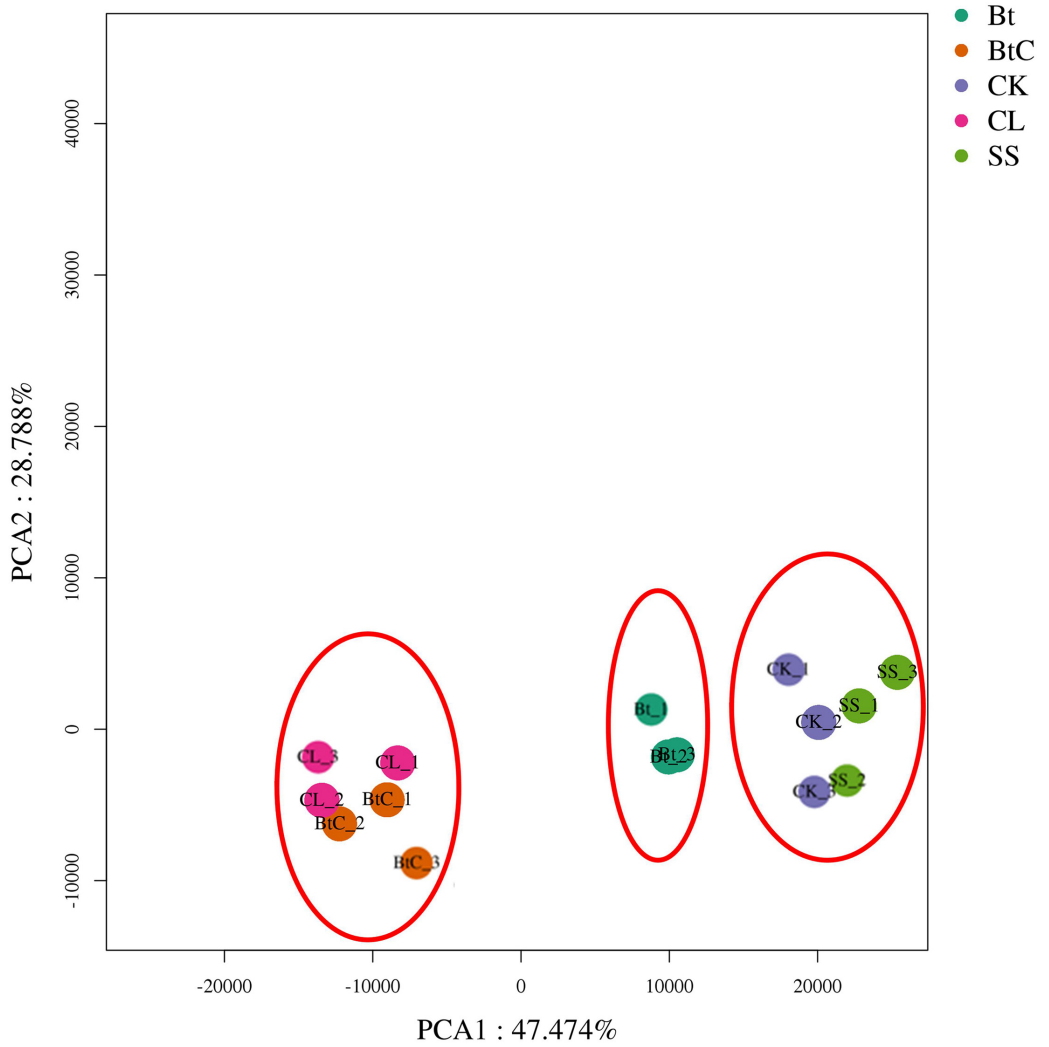

FIGURE 2 | Principal component analysis (PCA) analysis of samples in transcriptomic analysis showing expression level of DEGs in all the DBM groups.

ranged from 60.61 to 64.71% and were mapped to trinity spliced transcriptomes. The GC contents ranged from 49.42 to 55.64% (**Table 2**).

Identification of Differentially Expressed Genes

Pairwise comparisons were made to understand the expression patterns of genes between DBM strains. The DEGs (>2-fold change, FDR < 0.05) were identified in nine combinations of DBM strains. There were 973 DEGs (537 upregulated and 436 downregulated) in Bt-DBM vs. FOH-DBM groups; 553 (316 upregulated and 237 downregulated) in Bt-DBM vs. CL-DBM groups; 1,504 (820 upregulated and 684 downregulated) in Bt-DBM vs. SS-DBM groups; 2,173 (1,381 upregulated and 792 downregulated) in BtC-DBM vs. Bt-DBM groups; 5,573 (3,039 upregulated and 2,534 downregulated) in BtC-DBM vs. FOH-DBM groups; 1,392 (1,145 upregulated and 247 downregulated) in BtC-DBM vs. CL-DBM groups; 7,111 (3,975 upregulated and 3,136 downregulated) in BtC-DBM vs. SS-DBM groups; 3,908 (1,900 upregulated and 2,008 downregulated) in FOH-DBM vs. SS-DBM groups; and 2,331 (968 upregulated and 1,363 downregulated) in CL-DBM vs. FOH-DBM groups (**Figure 1**). These pair/group comparisons showed more upregulated DEG than downregulated genes, except for two pairs, BtC-DBM vs. SS-DBM groups and CL-DBM vs. FOH-DBM groups (**Figure 1**). Variability of data was checked by principal component analysis (PCA) analysis, which suggests that experimental data are reliable stable and can be used for further analysis (**Figure 2**).

Gene Ontology and the Kyoto Encyclopedia of Genes and Genomes Pathway Enrichment

The genes annotated in the GO classification were comprised of three major domains: biological process, cellular component, and molecular function. DEGs ($p \geq 0.05$, FDR > 2) analysis

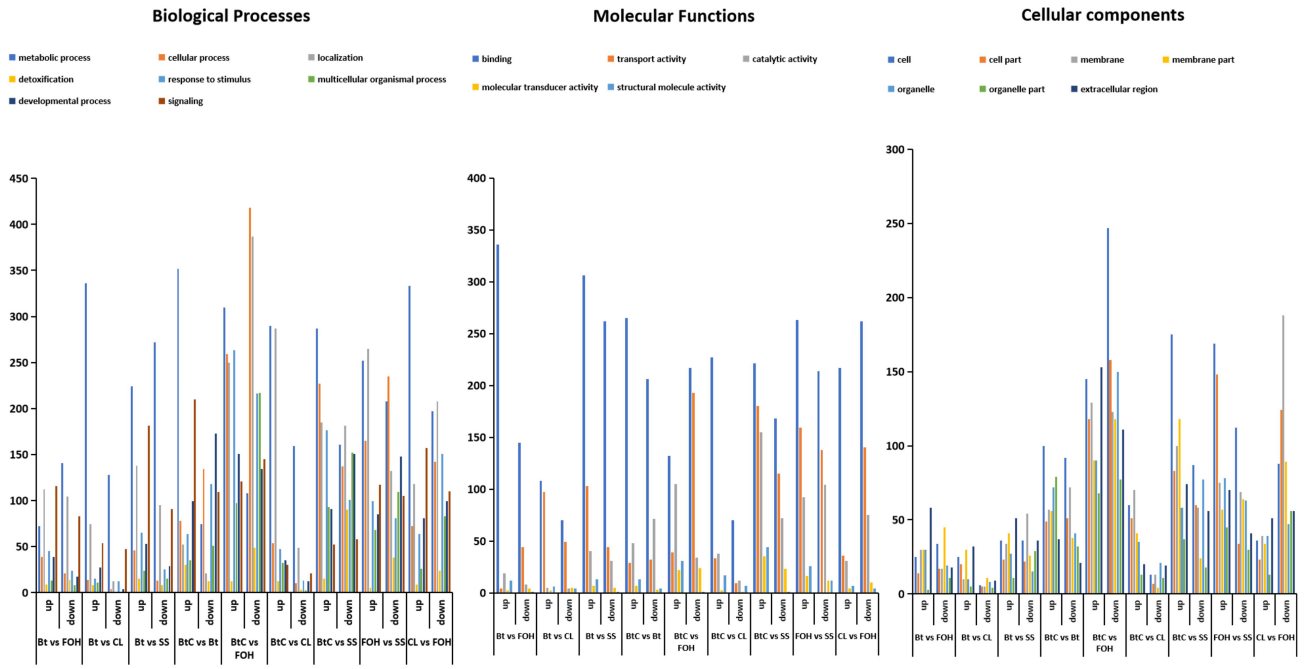

FIGURE 3 | The Gene Ontology (GO) classifications of DEGs between pairwise comparisons following the treatment of Bt-G033A, chlorantraniliprole (CL), and Bt + CL insecticides. DEGs are classified into three categories: molecular function, cellular components, and biological process. The *Y*-axis represents the number of downregulation and upregulation of genes in each GO term.

revealed that 172, 24, 264, 78, 584, 4, 768, 287, and 258 DEGs were downregulated, whereas 75, 17, 61, 242, 70, 211, 91, 43, and 69 DEGs were upregulated in the pairs/combinations of DBM strains (**Figure 3**), respectively. Most genes affected by Bt-G033A and CL and their combination treatments were assigned to binding, transport activity, and catalytic activity in molecular function; cell, cell part, and signaling in the cellular process; and metabolic process, cellular process, and localization in biological process (**Figure 3**). DEGs analysis showed no noticeable difference when compared among different pairs of strains, except for BtC-DBM vs. FOH-DBM groups. This pair showed a relatively higher proportion of downregulated genes in terms of cellular process and localization than other pairs of strains (**Figure 3**).

The KEGG analysis of DEGs identified from pairwise comparisons between susceptible and resistant strains provided information of pathways and gene functions associated with Bt and CL molecular mechanism (**Supplementary Table 2**). In the KEGG database, 20 highly enriched ($p \leq 0.05$) pathways comprised of "valine, leucine, and isoleucine degradation," "drug metabolism-cytochrome P450," and "glutathione metabolism" in all the pairwise comparisons (**Figure 4**).

Differentially Expressed Genes Following Insecticides Treatment

In the pairwise comparison between susceptible and treated larvae, we found detoxification genes such as cytochrome P450 monooxygenase, GST, acetylcholinesterase (AChE), CarE, glucuronosyltransferase, trypsin, nicotinamide adenine dinucleotide (NADH) dehydrogenase, and glutamate receptors potentially involved in insecticide resistance in pairs of DBM strains. Similarly, Bt resistance-related genes such as alkaline phosphatase, aminopeptidase N (APN), chitinase, cadherin, and ABC transporter were also identified (**Supplementary Table 3**).

The genes likely responsible for xenobiotic metabolism such as P450, CarE, AChE, and GST were more upregulated in CL-DBM vs. FOH-DBM groups with the rising of CL resistance level. Two upregulated putative insecticide target genes glutamate receptors were identified in the pair of CL-DBM vs. FOH-DBM comparison. The genes related to cuticle formation such as dehydrogenase and chitinase were mostly upregulated in pairs of DBM strains. Two downregulated RyR genes were identified in BtC-DBM vs. SS-DBM and CL-DBM vs. FOH-DBM pairs. Some immune-related genes such as serine protease were also found to be more upregulated in all the pairs of comparisons (**Table 3**).

Bt resistance-related genes, especially aminopeptidase N and ABC transporter, were downregulated. In the pair of Bt-DBM vs. FOH-DBM, trypsin genes were mostly upregulated, whereas more downregulated genes were identified in the pair of Bt-DBM vs. SS-DBM comparison. Similarly, we identified two alkaline phosphatase (ALP) genes that were upregulated in the pair of Bt-DBM vs. FOH-DBM and one upregulated in the pair of Bt-DBM vs. SS-DBM. However, two of these genes were upregulated and one was downregulated in the pair of BtC-DBM vs. FOH-DBM. Chitinase and cadherin genes

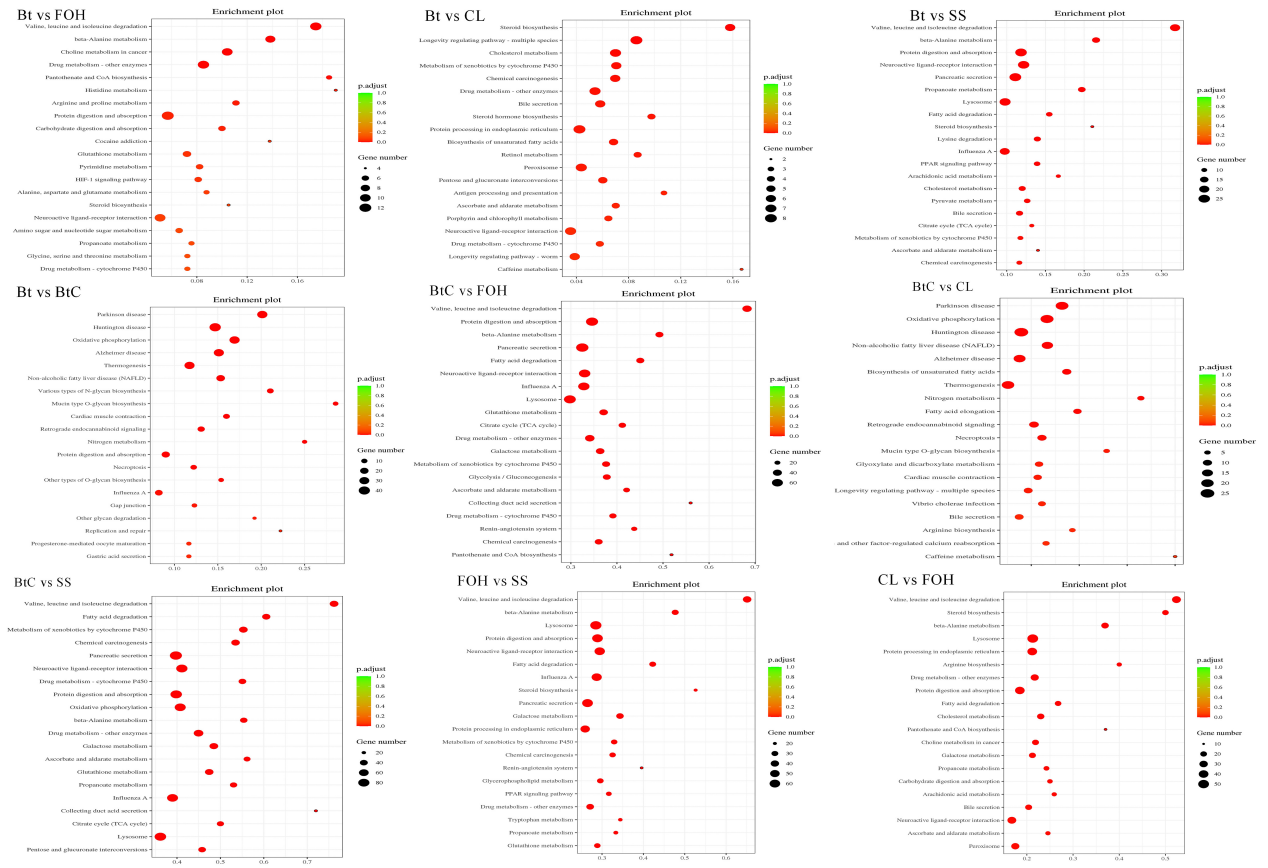

FIGURE 4 | The Kyoto Encyclopedia of Genes and Genomes (KEGG) pathway enrichment scatter plot among pairwise comparison of Diamondback moth (DBM) strains. The horizontal axis represents the rich path plotted and horizontal axis represents path factor corresponding to rich factor. The size of *p*-value is represented by the color of the point. The numbers of genes in each pathway are expressed by the size of the point.

were more upregulated in the pairwise comparisons of DBM strains (**Table 3**).

Co-expression Network Analysis of Genes Related to Resistance

To identify the key genes associated with resistance to Bt-G033A, CL, and Bt + CL, DEGs from all the pairs were subjected to co-expression network analysis. Based on the DEGs, a total of 30 highly enriched metabolic detoxification enzymes potentially involved in insecticide resistance were identified from all the pairs after the insecticide treatments. Furthermore, annotations of all these selected DEGs were obtained from the RNA-seq database to screen candidate genes that contributed to major resistance increase in each pairwise comparison (**Figure 5**).

The pairwise comparison of DBM strains revealed that most of the hub genes involved in metabolic detoxification were upregulated. We identified key genes such as CarE in pair of Bt-DBM vs. BtC-DBM, AChE in pair of BtC-DBM vs. CL-DBM, GST in pairs of BtC-DBM vs. SS-DBM and FOH-DBM vs. SS-DBM, whereas cytochrome P450 was identified in pairs of CL-DBM vs. FOH-DBM, BtC-DBM vs. CL-DBM, and BtC-DBM vs. SS-DBM. We identified trypsin upregulated in pairs of Bt-DBM vs. CL-DBM and BtC-DBM vs. CL-DBM, but downregulated in CL-DBM vs. FOH-DBM pair. Similarly, multidrug resistance genes, ABCC4, were downregulated key genes identified in the pairs of BtC-DBM vs. SS-DBM and FOH-DBM vs. SS-DBM, respectively (**Supplementary Table 4**).

Confirmation of Key Genes by Quantitative Real-Time PCR

Nine key genes, related to insecticide resistance and identified in pairs of DBM strains, were subjected to qRT-PCR analysis to validate the findings from RNA-seq data. The expression patterns of all the tested genes confirmed the trend with the data obtained from transcriptome analysis (**Figure 6**). Among the key genes, CarE, GST, cytochrome P450, AChE, and serpin were highly expressed in CL-induced DBM strain compared to other strains. Chitinase and trypsin showed higher expression levels in larvae treated with Bt-G033A. The expression level of genes encoding for ABCC4 and UDP-glycosyltransferase UGT5 in Bt-induced DBM was not significantly different compared to susceptible strain. In general, our results revealed that the expressions of detoxifying genes were higher in resistant strains than those insusceptible- and FOH-resistant strains (**Figure 6**).

TABLE 3 | Differentially expressed genes that potentially involved in detoxification metabolism.

Genes	Upregulated/Downregulated								
	Bt vs. FOH	Bt vs. CL	Bt vs. SS	Bt vs. BtC	BtC vs. FOH	BtC vs. CL	BtC vs. SS	FOH vs. SS	CL vs. FOH
Insecticide target genes									
Cytochrome P450	4/3	5/3	10/6	3/8	11/8	6/4	16/8	14/10	22/9
Glutathione S-transferase (GST)	0/2	2/1	0/4	1/1	1/11	3/2	1/16	1/4	7/2
Carboxylesterase	0/1	1/2	2/1	1/3	2/7	2/1	3/7	0/1	6/2
bbAcetylcholinesterase (AChE)	1/0	2/1	0/2	6/5	2/12	2/1	2/13	1/10	10/4
NADH dehydrogenase	2/3	1/1	1/1	10/2	3/7	8/1	12/12	5/6	1/4
UDP-glucuronosyltransferase	3/2	3/0	1/3	1/6	1/8	1/2	2/8	0/2	5/3
Sodium channel	2/5	1/0	0/0	7/5	1/1	5/1	3/1	4/4	2/7
Glutamate receptors	0/1	0/2	1/3	1/0	6/1	0/1	5/1	3/0	2/0
neurotransmitter gamma-aminobutyric acid (GABA) receptors	0/0	1/0	1/3	1/2	1/5	0/0	0/5	0/4	0/1‘
Ryanodine receptor	0/0	0/0	0/0	0/0	0/0	0/0	0/1	0/0	0/1
Trehalose transporter	0/9	1/2	7/5	3/1	2/6	9/2	12/10	5/15	1/8
Catalase	0/0	2/1	4/0	1/2	1/3	4/0	4/2	1/3	0/5
N-acetylgalactosaminyltransferase	0/0	4/2	0/0	6/1	5/2	6/1	9/2	3/2	0/2
ATPase synthase subunit	1/1	1/1	3/7	12/3	4/3	2/2	8/7	8/10	3/2
Serpin	2/0	3/2	2/0	1/0	4/1	1/1	6/1	9/0	4/0
Serine protease	7/3	5/0	4/1	1/0	5/0	6/0	4/2	2/0	6/8
Bt target genes									
Cadherin	2/1	1/0	3/1	2/1	2/2	2/1	2/3	0/2	0/0
Aminopeptidase N	0/6	1/3	2/6	1/10	3/8	1/2	3/7	3/10	0/8
Trypsin	16/8	10/6	6/11	14/11	17/5	9/8	9/7	6/10	3/14
Alkaline phosphatase	2/0	1/0	1/0	1/0	2/1	0/0	0/2	0/1	0/0
ABC transporter	0/2	1/1	0/5	1/3	1/14	4/1	5/12	1/10	1/11
Chitinase	5/3	1/1	7/2	1/1	6/1	2/0	5/2	3/2	4/2

Genes were identified in pairwise comparison of Plutella xylostella strains.
Differentially expressed genes are upregulated (FDR ≥ 0.05, logFC > 2-fold) and downregulated (FDR ≥ 0.05, FDR > −2-fold) between susceptible and resistant strains of Plutella xylostella.

DISCUSSION

The rapid evolution of resistance to pesticides and Cry toxins is a major challenge for managing lepidopteran pests including *P. xylostella* (Tabashnik et al., 2013). Assessment of insect resistance becomes necessary to guide appropriate implementation of chemical control and Bt products to understand the molecular mechanisms underlying development of resistance. In this study, we collected a DBM strain from one location and subjected it to two rounds of selection with Bt-G033A, CL, and a combination of the two insecticides. The resistant level of DBM strains to three tested insecticides from the most to the least ranked as Bt-G033A > Bt + CL > CL. Our results indicated that the combination of insecticides did not increase efficacy against DBM strains compared to Bt-G033A applied alone. These results are consistent with previous reports that a combination of two toxins may not delay resistance increase in lepidopteran pests as much as a single toxin in resistance management (Yang et al., 2018; Wang et al., 2019). However, the development of resistance under selection of a mixture of insecticides is dependent on multiple factors including the mode of inheritance of resistance to each insecticide (Tabashnik, 1989).

The molecular mechanism underlying the resistance to Bt-G033A, CL, or their mixture has not been fully understood yet. In this study, we investigated the molecular resistance mechanism for Bt-G033A, CL, and their combination in susceptible and resistance strains of DBM through transcriptomic analyses. We obtained a total of 25,518 DEGs from the pairs/comparisons of susceptible and resistant DBM strains. Comparative transcriptomic analysis showed more upregulation of DEGs in pairwise comparisons with the exception of two pairs (BtC-DBM vs. SS-DBM and CL-DBM vs. FOH-DBM) (**Figure 1**). Similarly, a previous study also reported more upregulated genes in Cry1Ac-resistant strain of DBM were identified (Lei et al., 2014).

The overall GO analysis identified a high proportion of genes related to cellular process, metabolic process, binding and localization, response to stimulus, transport activity, and catalytic activity. Mostly DEGs related to these categories had upregulated expression in pairwise comparisons (**Figure 3**). As these GO terms may be linked to detoxification xenobiotic process, the upregulation of these DEGs in treated larvae is responsible for resistance evolution. The KEGG analysis between pairwise comparisons of DBM strains showed that genes expression level was enriched in metabolic pathways. The genes involved in

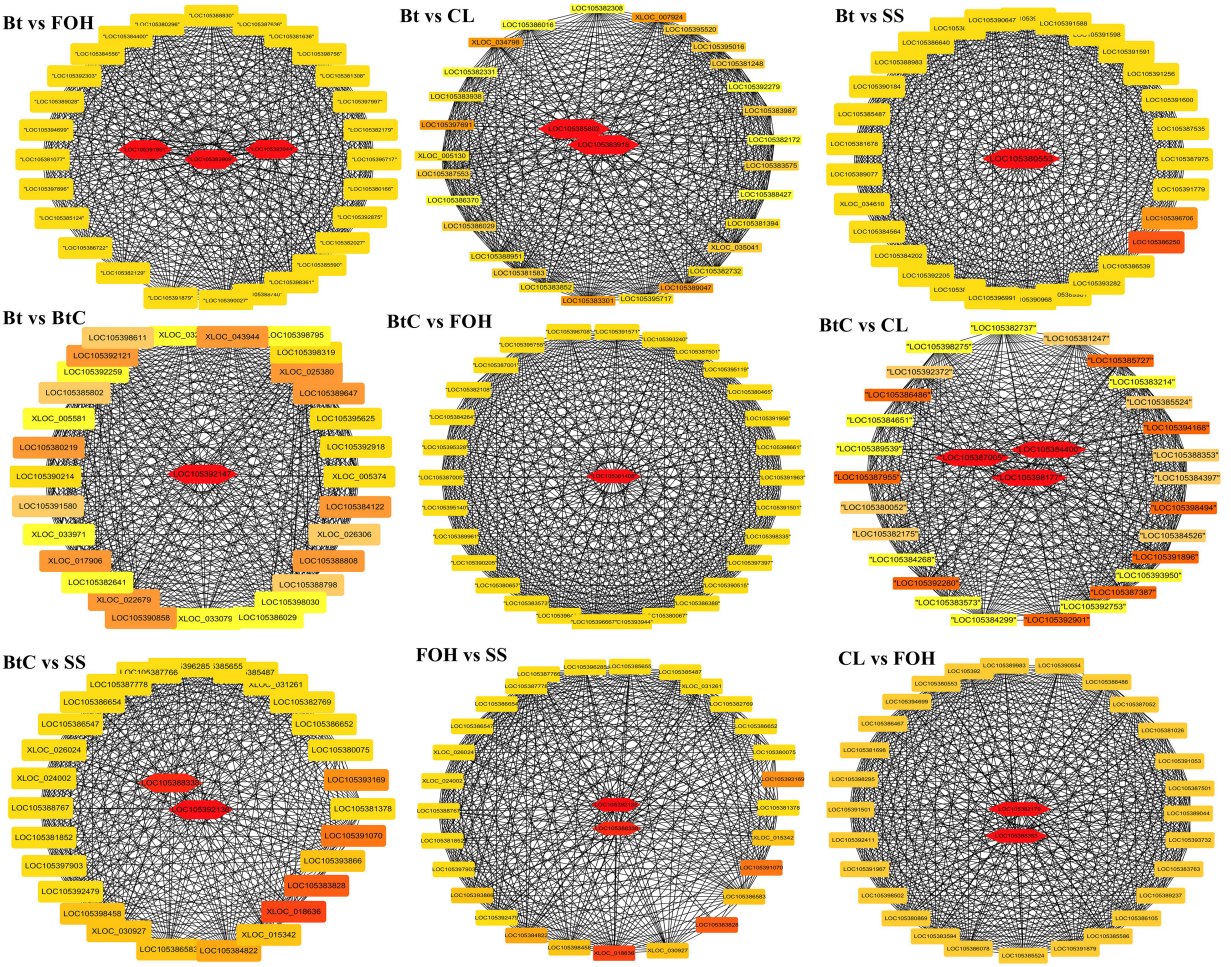

FIGURE 5 | Gene networks and key genes involved in metabolic resistance among pairwise comparison of DBM strains identified by weighted correlation network analysis (WGCNA). Key genes within (highlighted with red) each network are related to insecticide target and metabolism.

pathways such as glutathione metabolism and drug metabolism cytochrome P450 were upregulated (**Figure 4**). Other genes involved in signaling pathways and muscle control pathways were also identified as upregulated in pairs of BtC-DBM vs. Bt-DBM and BtC-DBM vs. CL-DBM. These results are consistent with a previous study, which revealed in CL-resistant *P. xylostella* strain, that upregulation of genes was involved in metabolic pathways such as drug metabolism and xenobiotic enzyme metabolism (Lin et al., 2013). Similarly, in the Cry1Ac-resistant *P. xylostella* strains, most DEGs involved in metabolic pathways and drug metabolism were upregulated (Lei et al., 2014). These results suggest that multiple genes involved in metabolic pathways, muscle contraction pathways, and drug metabolism pathways play dominant roles in resistance to Bt-G033A and CL.

In this study, detoxification genes were identified from insecticide-treated larvae. Detoxification of insecticides occurs in all the insects and involved several enzymes encoded for GST, P450, and Carboxylesterases (COE) families (Li et al., 2007). The genes related to insecticide resistance such as GST, cytochrome P450, and CarE were identified by the pairwise comparison of DBM strains (**Supplementary Table 3**). Cytochrome P450s are important detoxification enzymes, which are involved in xenobiotic metabolism and act on substrates to reduce the toxicity (Zimmer et al., 2014). In *P. xylostella*, cytochrome P450 was linked with resistance to abamectin and tebufenozide (Qian et al., 2008). In this study, most DEGs of cytochrome genes (31) were identified in the pair of CL-DBM vs. FOH-DBM strain (**Table 3**). Other more abundant genes of detoxification were identified in pair of CL-DBM vs. FOH-DBM, including GST (9), CarE (8), and AChE (14), and they were mostly upregulated. The identified genes encoding P450, GST, AChE, and CarE were less abundant in the CL treatment than those in the Bt-G033A or mixed insecticide treatments (**Table 3**). Previously, a study reported that cytochrome family genes (*Cyp301a1 and Cyp9e2*) were overtranscribed responding to insecticide treatment in a *P. xylostella* strain (Gao et al., 2018). Thus, increased expression of these detoxification genes might link directly to CL resistance in *P. xylostella* strains. Overexpression of the *CYP6BGI* gene was reported in a permethrin-resistant *P. xylostella* strain (Bautista et al., 2009). Likewise, overexpression of *P450s* genes

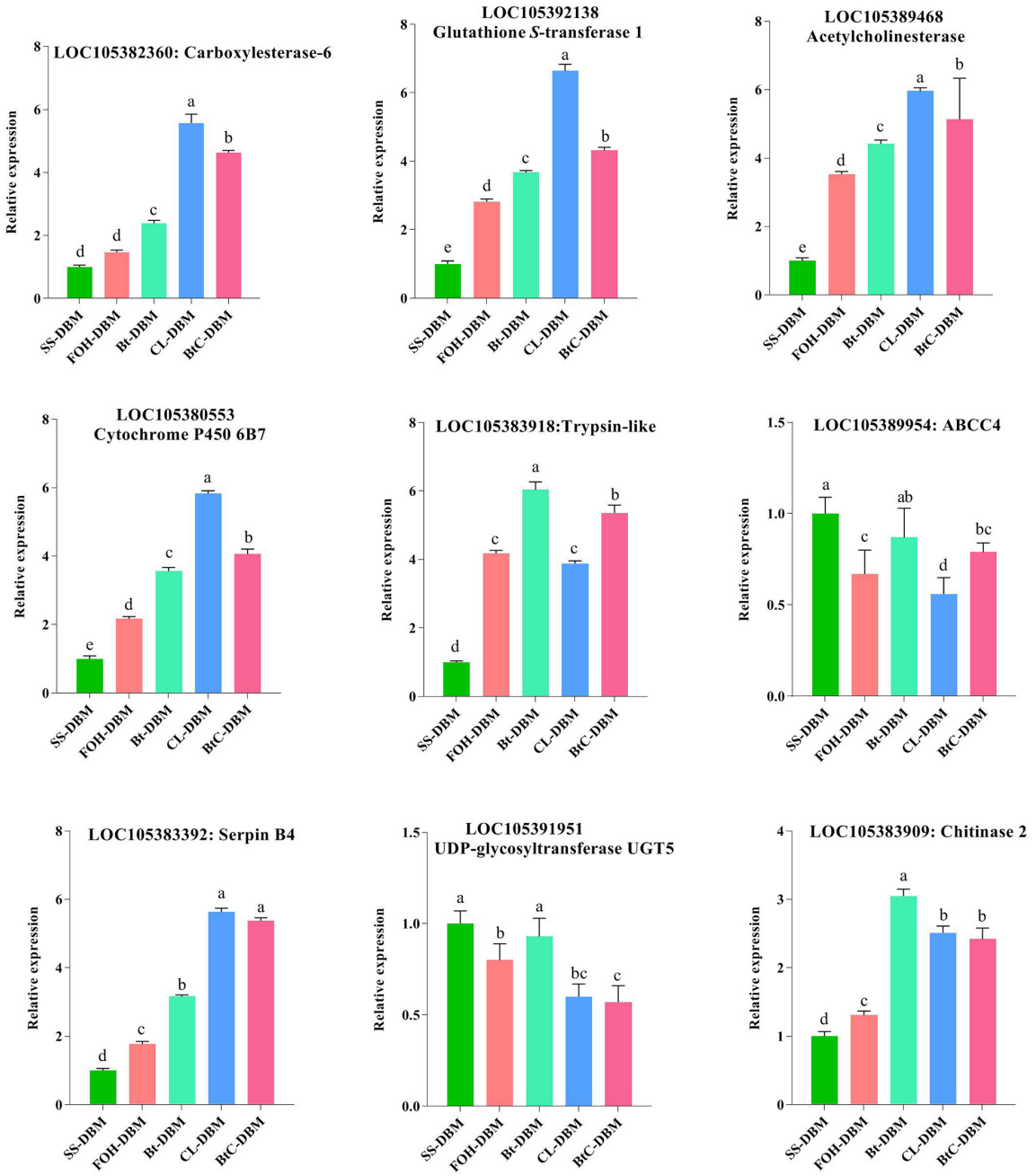

FIGURE 6 | The quantitative real-time PCR (qRT-PCR)-based validation of selected key genes from susceptible and resistant strains of *Plutella xylostella*. Same letter on top of the bars indicated no significant difference was found [general linear model (GLM), least significant difference (LSD), $p < 0.05$].

was associated with neonicotinoid resistance in *Bemisia tabaci* (Karunker et al., 2008) and led to deltamethrin resistance in *Tribolium castaneum* (Zhu et al., 2010). Furthermore, the detoxification enzyme GST was reported in *P. xylostella* to confer resistance to CL, organophosphates, and chlorfluazuron insecticides (Sonoda and Tsumuki, 2005; Lin et al., 2013). CarE and GST were also reported to be involved in fufenozide resistance (Tang et al., 2011). The expression of detoxification genes to all the pairs of different insecticide treatments in this study suggests that these genes are likely responsive to insecticide resistance and xenobiotic detoxification process.

Several genes such as serpin, serine protease, GABA receptors, and glutamate receptors that may contribute to insecticide resistance were also upregulated in most treated pairs of DBM strains, but not all. These results are consistent with a previous study on identification of insecticide target

genes including GABA receptor, AChE, nicotinic acetylcholine receptors (nAChRs), and RyR in the asian corn borer (ACB) transcriptome (Cui et al., 2017). AChEs are the principal targets of carbamates and organophosphate insecticides in insects, reflecting their role in neurotransmission. GABA receptors are a members of the cys-loop neurotransmitter receptors and the GABA-regulated chloride channel plays an important role in phenylpyrazole and organochlorine insecticides (Hosie et al., 1995). Some genes involved in cellular catabolism such as serine protease and trypsin were also identified in this study. The downregulated gene related to cuticular in CL-treated DBM indicated that this insecticide might play a role in thinning the cuticles in DBM. These thinned cuticles will help to accelerate the transportation of CL insecticide to the target site and improve its efficacy against the pest.

In this study, we identified two RyR genes with downregulation patterns: one was identified from the BtC-DBM vs. SS-DBM pair and the other from the CL-DBM vs. FOH-DBM comparison. A previous study reported that RyRs are major factors for *P. xylostella* resistance to CL (Troczka et al., 2012). As RyRs control the muscle contraction/excitation, it is speculated that the downregulation of RyRs is likely to reduce muscle excitability. Since the RyR was also identified in DBM treated with the mixture of Bt-G033A and CL, it remains to be determined whether the receptor is downregulated by the mixture. Also, NADH dehydrogenase genes were found more downregulated in the treatment of CL.

Bt resistance-related genes encoding for APN, ALP, cadherin, chitinase, trypsin, and ABC transporter were identified in this study (**Supplementary Table 2**). Most of *APN* genes were downregulated in Bt-resistant strains, whereas cadherin was upregulated in most pairs when compared with susceptible and FOH-DBM strains (**Table 3**). Downregulation of *APN* genes is involved in Bt resistance to different Cry toxins (Zhang et al., 2017; Shabbir et al., 2019). Different isoforms of APN, ALP, and cadherin are involved with different Cry toxin resistance (Flannagan et al., 2005; Pigott and Ellar, 2007). ABC transporter genes associated with drug resistance were also identified and most of them were downregulated in all the pairs of treated DBM compared to susceptible strains. ABC transporters identified in both the susceptible and resistant DBM strains included ABCC4, ABCC10, ABCB1, and ABCC1 in this study. Previous studies reported that ABC transporter (ABCB1) had been linked to multidrug resistance in mammalian systems (Shanker et al., 2010) and ABCC2 was linked with Cry1Ac resistance in lepidopteran insects (Gahan et al., 2010; Baxter et al., 2011). However, further studies are needed to determine the downregulation of these genes in DBM treated with Bt-G033A and the mixture insecticide.

We identified 17 gene networks, highly correlated with metabolic detoxification, muscle contraction pathways, and drug metabolism (**Supplementary Table 4** and **Figure 5**). We identified key genes including cytochrome P450, CarE, GSTs, and UDP-glycosyltransferase UGT5 related to insecticide metabolism from the network built from top DEGs. ABC transporter was previously found to be related to Bt resistance (Gahan et al., 2010). Trypsin is considered as the main proteinase involved in Bt toxin activation and detoxification (Liu et al., 2015). We selected nine detoxification-related key genes to analyze their gene expression in DBM strains. The results showed that CarE, GST, AChE, cytochrome P450, and serpin genes were expressed significantly higher in response to CL followed by the mixture insecticide (**Figure 6**). These results further validated the association of these genes with CL detoxification. Chitinase and trypsin were highly expressed in the Bt-G033A treatment. Furthermore, our findings suggested that multiple genes involved in drug metabolism, muscle control, and metabolic pathways that play dominant roles in CL and Bt-G033A detoxification. Further investigations are needed to explain the phenomenon of upregulated or downregulated genes in CL and Bt-treated DBM, so as to provide practical guidance for Bt-G033A and CL resistance management of DBM.

Bacillus thuringiensis subsp. *aizawai* and the binary combination of Bt-G033A with CL can delay resistance development in *P. xylostella* compared to CL alone. To date, this study is the most comprehensive study presenting functional transcriptome analysis of DBM using the combined insecticidal activity of Bt-G033A and CL. Comparative transcriptome analysis of three insecticides enabled the identification of commonly responding genes involved in drug metabolism and the xenobiotic detoxification process. The prominent genes identified in this study include cytochrome P450, GST, and CarE with more upregulation and downregulation of RyRs in the CL treatment. Bt and the mixture insecticide are involved in DBM metabolic and catalytic pathways with the downregulation and upregulation of cadherin, APN, ALP, and ABC transporter genes. Considering the physiological functions of key/hub genes identified through co-expression network analysis, their downregulation or upregulation appears to be involved in the direct or indirect detoxification process. The expression of these key genes further supported our findings. The common response of key DEGs to three tested insecticides via pairs/combinations of DBM strains suggests their roles of key candidates in catalytic, metabolic, and drug xenobiotic detoxification pathways. Consequently, precise identification of such key genes following exposure to Bt and CL insecticides could serve as a landmark for searching metabolic factors to provide information on improving resistance management of DBM.

DATA AVAILABILITY STATEMENT

The datasets presented in this study can be found in online repositories. The names of the repository and accession number(s) can be found below: BioProject (https://www.ncbi.nlm.nih.gov/bioproject), PRJNA785284.

AUTHOR CONTRIBUTIONS

MZS and Z-YL conceived and designed the research. MZS conducted the experiment and drafted the original manuscript. MZS, RB, and FY analyzed the data. Z-YL, XY, and PK reviewed and edited the manuscript. All authors read and approved the final manuscript.

FUNDING

This study was supported by the Guangdong Provincial Special Fund for Modern Agriculture Industry Technology Innovation Teams (Grant No. 2020KJ122), National Key Project of Research and Development Plan (2017YFD0201204 and 2018YFD0201200), Discipline Team Building Projects of Guangdong Academy of Agricultural Sciences in the 14th Five-Year Plan Period (202105TD), and President Foundation of Guangdong Academy of Agricultural Sciences (Grant No. BZ201911).

SUPPLEMENTARY MATERIAL

The Supplementary Material for this article can be found online at: https://www.frontiersin.org/articles/10.3389/fphys.2021.780255/full#supplementary-material

REFERENCES

Bakhtiarizadeh, M. R., Salehi, A., Alamouti, A. A., Abdollahi-Arpanahi, R., and Salami, S. A. (2019). Deep transcriptome analysis using RNA-Seq suggests novel insights into molecular aspects of fat-tail metabolism in sheep. *Sci. Rep*. 9, 1–14. doi: 10.1038/s41598-019-45665-3

Bautista, M. A. M., Miyata, T., Miura, K., and Tanaka, T. (2009). RNA interference-mediated knockdown of a cytochrome P450, CYP6BG1, from the diamondback moth, *Plutella xylostella*, reduces larval resistance to permethrin. *Insect Biochem. Mol. Biol* 39, 38–46. doi: 10.1016/j.ibmb.2008.09.005

Baxter, S. W., Badenes-Pérez, F. R., Morrison, A., Vogel, H., Crickmore, N., Kain, W., et al. (2011). Parallel evolution of *Bacillus thuringiensis* toxin resistance in *Lepidoptera*. *Genetics* 189, 675–679.

Cang, T., Dai, D., Yang, G., Yu, Y., Lv, L., Cai, L., et al. (2017). Combined toxicity of imidacloprid and three insecticides to the earthworm, *Eisenia fetida* (Annelida, Oligochaeta). *Sci. Pollut. Res. Int.* 24, 8722–8730. doi: 10.1007/s11356-017-8627-z

Chen, C., Ai, H., Ren, J., Li, W., Li, P., Qiao, R., et al. (2011). A global view of porcine transcriptome in three tissues from a full-sib pair with extreme phenotypes in growth and fat deposition by paired-end RNA sequencing. *BMC Genomics* 12:448. doi: 10.1186/1471-2164-12-448

Cui, L., Rui, C., Yang, D., Wang, Z., and Yuan, H. (2017). De novo transcriptome and expression profile analyses of the Asian corn borer (*Ostrinia furnacalis*) reveals relevant flubendiamide response genes. *BMC Genomics* 18:20. doi: 10.1186/s12864-016-3431-6

Edralin, O., Macatula, R., Vasquez, F., Anico, A., and Saavedra, N. (2011). "Update on DBM diamide resistance from the Philippines: causal factors and learnings," in *Proceedings Of The The Sixth International Workshop On Management Of The Diamondback Moth And Other Crucifer Insect Pests*, (Nakhon Pathom: Kasetsart University).

Eziah, V. Y., Rose, H. A., Wilkes, M., and Clift, A. D. J. (2009). Biochemical mechanisms of insecticide resistance in the diamondback moth (DBM), *Plutella xylostella* L.(Lepidopterata: Yponomeutidae), in the Sydney region, Australia. *Australian J. Entomol.* 48, 321–327. doi: 10.1111/j.1440-6055.2009.00723.x

Flannagan, R. D., Yu, C.-G., Mathis, J. P., Meyer, T. E., Shi, X., Siqueira, H. A., et al. (2005). Identification, cloning and expression of a Cry1Ab cadherin receptor from European corn borer, *Ostrinia nubilalis* (Hübner)(Lepidoptera: Crambidae). *Biochem. Mol. Biol.* 35, 33–40. doi: 10.1016/j.ibmb.2004.10.001

Gahan, L. J., Pauchet, Y., Vogel, H., and Heckel, D. G. J. (2010). An ABC transporter mutation is correlated with insect resistance to *Bacillus thuringiensis* Cry1Ac toxin. *PLoS Genet*. 6:e1001248. doi: 10.1371/journal.pgen.1001248

Gao, Y., Kim, K., Kwon, D. H., Jeong, I. H., Clark, J. M., and Lee, S. H. (2018). Transcriptome-based identification and characterization of genes commonly responding to five different insecticides in the diamondback moth, *Plutella xylostella*. *Pestic. Biochem. Physiol*. 144, 1–9. doi: 10.1016/j.pestbp.2017.11.007

Guo, L., Desneux, N., Sonoda, S., Liang, P., Han, P., and Gao, X.-W. J. (2013). Sublethal and transgenerational effects of chlorantraniliprole on biological traits of the diamondback moth, *Plutella xylostella* L. *Crop Prot.* 48, 29–34.

Guo, L., Wang, Y., Zhou, X., Li, Z., Liu, S., Pei, L., et al. (2014). Functional analysis of a point mutation in the ryanodine receptor of *Plutella xylostella* (L.) associated with resistance to chlorantraniliprole. *Pest Manag. Sci.* 70, 1083–1089. doi: 10.1002/ps.3651

Hosie, A. M., Baylis, H. A., Buckingham, S. D., and Sattelle, D. B. (1995). Actions of the insecticide fipronil, on dieldrin-sensitive and-resistant GABA receptors of *Drosophila melanogaster*. *Br. J. Pharmacol*. 115, 909–912. doi: 10.1111/j.1476-5381.1995.tb15896.x

Jaleel, W., Saeed, S., Naqqash, M. N., Sial, M. U., Ali, M., Zaka, S. M., et al. (2020). Effects of temperature on baseline susceptibility and stability of insecticide resistance against *Plutella xylostella* (Lepidoptera: Plutellidae) in the absence of selection pressure. *Saudi J. Biol. Sci.* 27, 1–5. doi: 10.1016/j.sjbs.2019.03.004

James, C. E., and Davey, M. W. (2009). Increased expression of ABC transport proteins is associated with ivermectin resistance in the model nematode *Caenorhabditis elegans*. *Int. J. Parasitol*. 39, 213–220. doi: 10.1016/j.ijpara.2008.06.009

Jiang, T., Wu, S., Yang, T., Zhu, C., and Gao, C. (2015). Monitoring field populations of *Plutella xylostella* (Lepidoptera: Plutellidae) for resistance to eight insecticides in China. *Florida Entomol.* 98, 65–73. doi: 10.1653/024.098.0112

Jouraku, A., Kuwazaki, S., Miyamoto, K., Uchiyama, M., Kurokawa, T., Mori, E., et al. (2020). Ryanodine receptor mutations (G4946E and I4790K) differentially responsible for diamide insecticide resistance in diamondback moth, *Plutella xylostella* L. *Insect Biochem. Mol. Biol.* 118:103308. doi: 10.1016/j.ibmb.2019.103308

Karunker, I., Benting, J., Lueke, B., Ponge, T., Nauen, R., Roditakis, E., et al. (2008). Over-expression of cytochrome P450 CYP6CM1 is associated with high resistance to imidacloprid in the B and Q biotypes of *Bemisia tabaci* (Hemiptera: Aleyrodidae). *Insect Biochem. Mol. Biol.* 38, 634–644. doi: 10.1016/j.ibmb.2008.03.008

Lei, Y., Zhu, X., Xie, W., Wu, Q., Wang, S., Guo, Z., et al. (2014). Midgut transcriptome response to a Cry toxin in the diamondback moth, *Plutella xylostella* (Lepidoptera: Plutellidae). *Gene* 533, 180–187. doi: 10.1016/j.gene.2013.09.091

Li, B., and Dewey, C. N. J. (2011). RSEM: accurate transcript quantification from RNA-Seq data with or without a reference genome. *BMC Bioinformatics* 12:323. doi: 10.1186/1471-2105-12-323

Li, X., Schuler, M. A., and Berenbaum, M. R. (2007). Molecular mechanisms of metabolic resistance to synthetic and natural xenobiotics. *J. Econ. Entomol.* 52, 231–253.

Li, Z., Feng, X., Liu, S. S., You, M., and Furlong, M. J. (2016). Biology, ecology, and management of the diamondback moth in China. *Annu. Rev. Entomol.* 61, 277–296. doi: 10.1146/annurev-ento-010715-023622

Lima Neto, J. E., Amaral, M. H. P., Siqueira, H. A. A., Barros, R., and Silva, P. A. F. (2016). Resistance monitoring of *Plutella xylostella* (L.) (Lepidoptera: Plutellidae) to risk-reduced insecticides and cross resistance to spinetoram. *Phytoparasitica* 44, 631–640. doi: 10.1007/s12600-016-0553-y

Lin, Q., Jin, F., Hu, Z., Chen, H., Yin, F., Li, Z., et al. (2013). Transcriptome analysis of chlorantraniliprole resistance development in the diamondback moth *Plutella xylostella*. *PLoS One* 8:e72314. doi: 10.1371/journal.pone.0072314

Liu, N., Cheng, F., Zhong, Y., and Guo, X. J. (2019). Comparative transcriptome and coexpression network analysis of carpel quantitative variation in *Paeonia rockii*. *BMC Genomics* 20:683. doi: 10.1186/s12864-019-6036-z

Liu, X., Ning, Y., Wang, H., and Wang, K. J. (2015). Cross−resistance, mode of inheritance, synergism, and fitness effects of cyantraniliprole resistance in *Plutella xylostella*. *Entomol. Exp. Appl.* 157, 271–278.

Melatti, V., Praça, L., Martins, E., Sujii, E., Berry, C., and De Pontes, R. J. (2010). Selection of *Bacillus thuringiensis* strains toxic against cotton aphid, *Aphis gossypii* glover (Hemiptera: Aphididae). *BioAssay* 5:2.

Pauchet, Y., Wilkinson, P., Vogel, H., Nelson, D., Reynolds, S., Heckel, D. G., et al. (2010). Pyrosequencing the *Manduca sexta* larval midgut transcriptome: messages for digestion, detoxification and defence. *Insect Mol. Biol.* 19, 61–75. doi: 10.1111/j.1365-2583.2009.00936.x

Pigott, C. R., and Ellar, D. J. (2007). Role of receptors in *Bacillus thuringiensis* crystal toxin activity. *Microbiol. Mol. Biol. Rev*. 71, 255–281.

Prabu, S., Jing, D., Shabbir, M. Z., Yuan, W., Wang, Z., and He, K. (2020). Contribution of phenoloxidase activation mechanism to Bt insecticidal protein resistance in Asian corn borer. *Int. J. Biol. Macromol*. 153, 88–99. doi: 10.1016/j.ijbiomac.2020.03.003

Pu, X., Yang, Y., Wu, S., and Wu, Y. (2010). Characterisation of abamectin resistance in a field-evolved multiresistant population of *Plutella xylostella*. *Pest Manag. Sci.* 66, 371–378. doi: 10.1002/ps.1885

Qian, L., Cao, G., Song, J., Yin, Q., and Han, Z. (2008). Biochemical mechanisms conferring cross-resistance between tebufenozide and abamectin in *Plutella xylostella*.*Pestic. Biochem. Physiol*. 91, 175–179. doi: 10.1016/j.pestbp.2008.03.011

Shabbir, M. Z., He, L., Shu, C., Yin, F., Zhang, J., and Li, Z.-Y. (2021). Assessing the single and combined toxicity of chlorantraniliprole and *Bacillus thuringiensis* (GO33A) against four selected strains of *Plutella xylostella* (Lepidoptera: Plutellidae), and a gene expression analysis. *Toxins* 13:227. doi: 10.3390/toxins13030227

Shabbir, M. Z., Quan, Y., Wang, Z., Bravo, A., Soberón, M., and He, K. (2018). Characterization of the Cry1Ah resistance in Asian corn borer and its cross-resistance to other *Bacillus thuringiensis* toxins. *Sci. Rep*. 8, 1–9. doi: 10.1038/s41598-017-18586-2

Shabbir, M. Z., Zhang, T., Prabu, S., Wang, Y., Wang, Z., Bravo, A., et al. (2020). Identification of Cry1Ah-binding proteins through pull down and gene expression analysis in Cry1Ah-resistant and susceptible strains of *Ostrinia furnacalis*. *Pestic. Biochem. Physiol*. 163, 200–208. doi: 10.1016/j.pestbp.2019.11.014

Shabbir, M. Z., Zhang, T., Wang, Z., and He, K. (2019). Transcriptome and proteome alternation with resistance to *Bacillus thuringiensis* Cry1Ah toxin in *Ostrinia furnacalis*. *Front. Physiol.* 10:27. doi: 10.3389/fphys.2019.00027

Shanker, M., Willcutts, D., Roth, J. A., and Ramesh, R. (2010). Drug resistance in lung cancer. *Lung Cancer (Auckl)* 1:23. doi: 10.2147/lctt.s6861

Sonoda, S., and Tsumuki, H. (2005). Studies on glutathione S-transferase gene involved in chlorfluazuron resistance of the diamondback moth, *Plutella xylostella* L.(Lepidoptera: Yponomeutidae). *Pestic. Biochem. Physiol*. 82, 94–101.

Stemele, M. (2017). Comparative effects of a selective insecticide, *Bacillus thuringiensis* var. kurstaki and the broad-spectrum insecticide cypermethrin on diamondback moth and its parasitoid *Cotesia vestalis* (Hymenoptera; Braconidae). *Crop Prot*. 101, 35–42.

Su, W.-L., Liu, N., Mei, L., Luo, J., Zhu, Y.-J., and Liang, Z. J. B. (2019). Global transcriptomic profile analysis of genes involved in lignin biosynthesis and accumulation induced by boron deficiency in poplar roots. *Biomolecules* 9:156. doi: 10.3390/biom9040156

Tabashnik, B. E. (1989). Managing resistance with multiple pesticide tactics: theory, evidence, and recommendations. *J. Econ. Entomol.* 82, 1263–1269. doi: 10.1093/jee/82.5.1263

Tabashnik, B. E., Brévault, T., and Carrière, Y. (2013). Insect resistance to Bt crops: lessons from the first billion acres. *Nat. Biotechnol*. 31, 510–521. doi: 10.1038/nbt.2597

Tabashnik, B. E., Cushing, N. L., and Finson, N. (1987). Leaf residue vs topical bioassay for assessing resistance in the diamondback moth (Lepidoptera: Plutellidae). *FAO Plant Prot. Bull.* 35, 11–14.

Tang, B., Sun, J., Zhou, X., Gao, X., and Liang, P. (2011). The stability and biochemical basis of fufenozide resistance in a laboratory-selected strain of *Plutella xylostella*. *Pestic. Biochem. Physiol*. 101, 80–85. doi: 10.1016/j.pestbp.2011.08.003

Tiewsiri, K., and Wang, P. J. (2011). Differential alteration of two aminopeptidases N associated with resistance to *Bacillus thuringiensis* toxin Cry1Ac in cabbage looper. *Proc. Natl. Acad. Sci. U.S.A.* 108, 14037–14042. doi: 10.1073/pnas.1102555108

Troczka, B. J., Williams, A. J., Williamson, M. S., Field, L. M., Lüemmen, P., and Davies, T. E. (2015). Stable expression and functional characterisation of the diamondback moth ryanodine receptor G4946E variant conferring resistance to diamide insecticides. *Insect Biochem. Mol. Biol.* 5, 1–11. doi: 10.1038/srep14680

Troczka, B., Zimmer, C. T., Elias, J., Schorn, C., Bass, C., Davies, T. E., et al. (2012). Resistance to diamide insecticides in diamondback moth, *Plutella xylostella* (Lepidoptera: Plutellidae) is associated with a mutation in the membrane-spanning domain of the ryanodine receptor. *Insect Biochem. Mol. Biol.* 42, 873–880. doi: 10.1016/j.ibmb.2012.09.001

Wang, X., and Wu, Y. (2012). High levels of resistance to chlorantraniliprole evolved in field populations of *Plutella xylostella*. *J. Econ. Entomol.* 105, 1019–1023. doi: 10.1603/ec12059

Wang, X., Li, X., Shen, A., and Wu, Y. (2010). Baseline susceptibility of the diamondback moth (Lepidoptera: Plutellidae) to chlorantraniliprole in China. *J. Econ. Entomol.* 103, 843–848. doi: 10.1603/EC09367

Wang, Y., Quan, Y., Yang, J., Shu, C., Wang, Z., Zhang, J., et al. (2019). Evolution of Asian corn borer resistance to Bt toxins used singly or in pairs. *Toxins* 11:461. doi: 10.3390/toxins11080461

Xu, L., Li, S., Shabala, S., Jian, T., and Zhang, W. (2019). Plants grown in Parafilm-wrapped Petri dishes are stressed and possess altered gene expression profile. *Plant Sci.* 10, 637. doi: 10.3389/fpls.2019.00637

Yang, J., Quan, Y., Sivaprasath, P., Shabbir, M. Z., Wang, Z., Ferré, J., et al. (2018). Insecticidal activity and synergistic combinations of ten different Bt toxins against *Mythimna separata* (Walker). *Toxins* 10:454. doi: 10.3390/toxins10110454

Yin, C., Wang, R., Luo, C., Zhao, K., Wu, Q., Wang, Z., et al. (2019). Monitoring, cross-resistance, inheritance, and Synergism of *Plutella xylostella* (Lepidoptera: Plutellidae) resistance to pyridalyl in China. *J. Econ. Entomol.* 112, 329–334. doi: 10.1093/jee/toy334

Yin, S., Zhang, C., Zhang, Y., and Li, X. (2016). Resistance status of diamondback moth *Plutella xylostella* (L.) to nine insecticides in Shaanxi. *J. Northwest A F Uni. Nat. Sci. Edi* 44, 102–110.

Yu, G., Wang, L.-G., Han, Y., and He, Q.-Y. (2012). clusterProfiler: an R package for comparing biological themes among gene clusters. *OMICS* 16, 284–287. doi: 10.1089/omi.2011.0118

Zhang, T., Coates, B. S., Wang, Y., Wang, Y., Bai, S., Wang, Z., et al. (2017). Down-regulation of aminopeptidase N and ABC transporter subfamily G transcripts in Cry1Ab and Cry1Ac resistant Asian corn borer, *Ostrinia furnacalis* (Lepidoptera: Crambidae). *Int. J. Biol. Sci.* 13:835. doi: 10.7150/ijbs.18868

Zhao, F., Li, Y., Huang, L., Gu, Y., Zhang, H., Zeng, D., et al. (2018). Individual and combined toxicity of atrazine, butachlor, halosulfuron-methyl and mesotrione on the microalga *Selenastrum capricornutum*. *Ecotoxicol. Environ. Saf.* 148, 969–975. doi: 10.1016/j.ecoenv.2017.11.069

Zhao, J. Z., Collins, H. L., and Shelton, A. M. (2010). Testing insecticide resistance management strategies: mosaic versus rotations. *Pest Manag. Sci.* 66, 1101–1105. doi: 10.1002/ps.1985

Zhu, F., Parthasarathy, R., Bai, H., Woithe, K., Kaussmann, M., Nauen, R., et al. (2010). A brain-specific cytochrome P450 responsible for the majority of deltamethrin resistance in the QTC279 strain of *Tribolium*

castaneum. *Proc. Natl. Acad. Sci. U.S.A.* 107, 8557–8562. doi: 10.1073/pnas.1000059107

Zhu, Y. C., Guo, Z., Chen, M.-S., Zhu, K. Y., Liu, X. F., and Scheffler, B. (2011). Major putative pesticide receptors, detoxification enzymes, and transcriptional profile of the midgut of the tobacco budworm, *Heliothis virescens* (Lepidoptera: Noctuidae). *J. Invertebr. Pathol.* 106, 296–307. doi: 10.1016/j.jip.2010.10.007

Zimmer, C., Maiwald, F., Schorn, C., Bass, C., Ott, M. C., and Nauen, R. (2014). A de novo transcriptome of European pollen beetle populations and its analysis, with special reference to insecticide action and resistance. *Insect Mol. Biol.* 23, 511–526. doi: 10.1111/imb.12099

Zuo, Y., Wang, H., Xu, Y., Huang, J., Wu, S., Wu, Y., et al. (2017). CRISPR/Cas9 mediated G4946E substitution in the ryanodine receptor of *Spodoptera exigua* confers high levels of resistance to diamide insecticides. *Insect Mol. Biol.* 89, 79–85. doi: 10.1016/j.ibmb.2017.09.005

Conflict of Interest: The authors declare that the research was conducted in the absence of any commercial or financial relationships that could be construed as a potential conflict of interest.

frontiers in Physiology

ORIGINAL RESEARCH
published: 11 January 2022
doi: 10.3389/fphys.2021.818210

Selection and Validation of Reference Genes for RT-qPCR Normalization in *Bradysia odoriphaga* (Diptera: Sciaridae) Under Insecticides Stress

*Haiyan Fu[1,2,3], Tubiao Huang[1,2], Cheng Yin[1,2], Zhenhua Xu[1,2], Chao Li[1,2], Chunguang Liu[1,2], Tong Wu[1,2], Fuqiang Song[1,2], Fujuan Feng[3] and Fengshan Yang[1,2]**

[1] Engineering Research Center of Agricultural Microbiology Technology, Ministry of Education, Heilongjiang University, Harbin, China, [2] Heilongjiang Provincial Key Laboratory of Ecological Restoration and Resource Utilization for Cold Region, School of Life Sciences, Heilongjiang University, Harbin, China, [3] College of Life Science, Northeast Forestry University, Harbin, China

OPEN ACCESS

Edited by:
Ran Wang,
Institute of Plant Protection and Environmental Protection, Beijing Academy of Agricultural and Forestry Sciences, China

Reviewed by:
Xingliang Wang,
Nanjing Agricultural University, China
Huipeng Pan,
South China Agricultural University, China
Haipeng Zhao,
Shandong Agricultural University, China

***Correspondence:**
Fengshan Yang
2004064@hlju.edu.cn

Specialty section:
This article was submitted to Invertebrate Physiology, a section of the journal Frontiers in Physiology

Received: 19 November 2021
Accepted: 08 December 2021
Published: 11 January 2022

Citation:
Fu H, Huang T, Yin C, Xu Z, Li C, Liu C, Wu T, Song F, Feng F and Yang F (2022) Selection and Validation of Reference Genes for RT-qPCR Normalization in Bradysia odoriphaga (Diptera: Sciaridae) Under Insecticides Stress. Front. Physiol. 12:818210. doi: 10.3389/fphys.2021.818210

Bradysia odoriphaga (Diptera: Sciaridae) is the most serious root maggot pest which causes substantial damage to the Chinese chive. Organophosphate (OP) and neonicotinoid insecticides are widely used chemical pesticides and play important roles in controlling *B. odoriphaga*. However, a strong selection pressure following repeated pesticide applications has led to the development of resistant populations of this insect. To understand the insecticide resistance mechanism in *B. odoriphaga*, gene expression analysis might be required. Appropriate reference gene selection is a critical prerequisite for gene expression studies, as the expression stability of reference genes can be affected by experimental conditions, resulting in biased or erroneous results. The present study shows the expression profile of nine commonly used reference genes [*elongation factor 1α (EF-1α)*, *actin2 (ACT)*, *elongation factor 2α (EF-2α)*, *glucose-6-phosphate dehydrogenase (G6PDH)*, *glyceraldehyde-3-phosphate dehydrogenase (GAPDH)*, *ribosomal protein L10 (RPL10)*, *ribosomal protein S3 (RPS3)*, *ubiquitin-conjugating enzyme (UBC)*, and *α-tubulin (TUB)*] was systematically analyzed under insecticide stress. Moreover, we also evaluated their expression stability in other experimental conditions, including developmental stages, sexes, and tissues. Five programs (NormFinder, geNorm, BestKeeper, RefFinder, and Δ*Ct*) were used to validate the suitability of candidate reference genes. The results revealed that the most appropriate sets of reference genes were *RPL10* and *ACT* across phoxim; *ACT* and *TUB* across chlorpyrifos and chlorfluazuron; *EF1α* and *TUB* across imidacloprid; *EF1α* and *EF2α* across developmental stages; *RPL10* and *TUB* across larvae; *EF1α* and *ACT* across tissues, and *ACT* and *G6PDH* across sex. These results will facilitate the standardization of RT-qPCR and contribute to further research on *B. odoriphaga* gene function under insecticides stress.

Keywords: *Bradysia odoriphaga*, RT-qPCR, reference gene, insecticides stress, normalization

INTRODUCTION

Bradysia odoriphaga Yang et Zhang (Diptera: Sciaridae) is a serious soil pest in China that feeds on 7 plant families and more than 30 plant species, including Chinese chive (Liliaceae), onion (Liliaceae), Chinese cabbage (Cruciferae), lettuce (Asteraceae), and so on (Li W. X. et al., 2015; Yang Y. T. et al., 2015). The main host plant of *B. odoriphaga* is Chinese chive (*Allium tuberosum* Rottle ex Spreng). Chinese chive is a perennial vegetable with a high economic value and is grown over a vast geographic area from Asia through the Middle East, to Europe and North America, and is widely cultivated in China. *B. odoriphaga* larvae usually gather in the roots, bulbs, and even in immature stems of Chinese chives, making the pest hard to control and allowing it to cause significant production losses of Chinese chives (Zhang et al., 2013; Chen et al., 2018). Yield loss of Chinese chive caused by *B. odoriphaga* has been reported to vary from 40 to 60% (Li et al., 2007). So far, the control efforts against *B. odoriphaga* still largely rely on the application of chemical insecticides, such as organophosphate (OP) and neonicotinoid insecticides (Chen et al., 2017). Phoxim, chlorpyrifos, imidacloprid, and chlorfluazuron are very popular insecticides that are used extensively for the purpose of *B. odoriphaga* control. Unfortunately, *B. odoriphaga* has developed increased resistance to insecticides because of heavy reliance on chemical insecticides (Chen et al., 2017). To investigate insecticide resistance mechanisms and promote integrated pest management (IPM) strategies, researchers have studied several pests over the past few decades and achieved important progress in several areas, including genomics (Xiao et al., 2021), transcriptomics (Cheng et al., 2020; Nazar et al., 2020; Nor Muhammad et al., 2020; Wang et al., 2020; Fu et al., 2021; Zou et al., 2021), proteomics (Prajapati et al., 2020; Chen et al., 2021), insecticide resistance (Wang et al., 2020; Gong et al., 2021; Ullah et al., 2021), RNA interference (Koo et al., 2020; Silver et al., 2021), and gene functions (Yu et al., 2020; Li L. L. et al., 2021; Luo et al., 2021). However, further studies on the mechanism of insecticide resistance are required to clarify the genes directly involved in resistance and regulatory mechanisms associated with those genes.

At present, real-time quantitative PCR is considered a reliable method to determine minor deviations in mRNA expression levels of a target gene due to its speed, accuracy, sensibility, throughput, cost, and reproducibility. The results of RT-qPCR must be normalized using reference genes because the threshold cycle (*Ct*) values are influenced by RNA quality and quantity, primer characteristics, PCR conditions, and variable transcriptional efficiencies. Since the validity and accuracy of RT-qPCR are highly dependent on the reference genes, it is imperative to identify the ideal candidate reference genes. An ideal reference gene should be constitutively and equally expressed in different cell types and tissues, regardless of internal and external factors or physiological cycles (Castanera et al., 2015). Many housekeeping genes that are necessary for regular cell functions have been universally used to normalize gene expression (Adeyinka et al., 2019; Chen et al., 2020). The top 10 most frequently used reference genes are *Actin*, *RPL*, *Tubulin*, *GAPDH*, *RPS*, *18S*, *EF1α*, *TATA*, *HSP*, and *SDHA* (Lü et al., 2018). Several methods and programs have been developed to evaluate the stability of reference genes, including the ΔCt method (Silver et al., 2006), BestKeeper (Pfaffl et al., 2004), NormFinder (Andersen et al., 2004), geNorm (Vandesompele et al., 2002), and a web-based tool RefFinder (Xie et al., 2012). However, accumulating data of reference genes studies showed that an ideal reference gene that can keep stability in various experimental conditions does not exist (Yuan et al., 2014). Therefore, the reference genes should be selected cautiously, and their stability be validated before they are used under specific experimental conditions.

Consideration of the significance and diverse specificity of reference genes, many reference gene sets have been validated in various insect species, such as *Spodoptera frugiperda* (Zhou et al., 2021), *Rhopalosiphum padi* (Li M. et al., 2021), *Aquatica leii* (Fu and Meyer-Rochow, 2021), *Tuta absoluta* (Yan et al., 2021), *Dichelops melacanthus* (Pinheiro et al., 2020), *Thermobia domestica* (Bai et al., 2020), *Apolygus lucorum* (Luo et al., 2020), *Lymantria dispar* (Yin et al., 2020), *Drosophila melanogaster* (Kim et al., 2020), *Phenacoccus solenopsis* (Zheng et al., 2019), *Chilo partellus* (Adeyinka et al., 2019), *Harmonia axyridis* (Yang et al., 2018), *Liriomyza trifolii* (Chang et al., 2017), *Myzus persicae* (Kang et al., 2017), and *B. odoriphaga* (Shi et al., 2016) under various experimental conditions. However, a universal reference gene has not yet been identified. Therefore, the lack of a single universal reference for *B. odoriphaga* is not surprising. In this case, it's important to choose reliable reference genes for gene expression analysis under various experimental conditions. Though appropriate references genes have been identified in *B. odoriphaga* under different biotic and abiotic conditions (Shi et al., 2016; Tang et al., 2019), a piece of comprehensive information is lacking for *B. odoriphaga* stressed by different groups of insecticides. Therefore, in this study, nine commonly used reference genes *elongation factor 1α (EF-1α)*, *actin2 (ACT)*, *elongation factor 2α (EF-2α)*, *glucose-6-phosphate dehydrogenase (G6PDH)*, *glyceraldehyde-3-phosphate dehydrogenase (GAPDH)*, *ribosomal protein L10 (RPL10)*, *ribosomal protein S3 (RPS3)*, *ubiquitin-conjugating enzyme (UBC)*, and *α-tubulin (TUB)* were analyzed to assess their suitability for normalizing RT-qPCR data for *B. odoriphaga* under the stress of insecticides (phoxim, chlorpyrifos, imidacloprid, and chlorfluazuron). Additionally, the effects of developmental stages, tissues, and sexes were also evaluated. The objective of the present work was to identify different sets of suitable reference genes for further studies of toxicology-related target genes in *B. odoriphaga*.

MATERIALS AND METHODS

Insects

B. odoriphaga was originally collected from The Institute of Plant Protection, Academy of Agricultural Sciences, Tianjin, China (39°10′36″N, 117°05′86″E) in 2018. The individuals were reared on scallions in an incubator at 20 ± 1°C, and 65 ± 5% relative humidity with a 12-h light:12-h dark photoperiod in culture

dishes (Φ = 90 mm) filled with 2.5% agar solution at the liquid level of 0.5 mm and covered with filter paper.

Chemicals

Formulated insecticides, 50% phoxim EC, 40% chlorpyrifos EC, 20% imidacloprid SE, and 5% chlorfluazuron SE were manufactured by Xuzhou Shennong Chemical Co., Ltd., JiangSu, China, and kept in a refrigerator.

Analyzed Factors

The effects of the following factors on candidate reference genes mRNA were measured: insecticides (phoxim, chlorpyrifos, imidacloprid, and chlorfluazuron), developmental stages, tissues, and sexes. The samples processed by each factor were flash-frozen in liquid nitrogen and then stored at −80°C until analyzed by RT-qPCR. Each factor was assessed in four independent experiments.

Determination of LC_{50} Value of Insecticides

Groups of 15, third instar larvae were sprayed in a culture dish with 600 μL phoxim, chlorpyrifos, imidacloprid or chlorfluazuron, half on the body, half around, and fed scallion stained with pesticide (Li Z. N. et al., 2015). The control group was sprayed with distilled water. The number of dead individuals was checked after 24 h at 20°C and RH: 60–70%. LC_{50} was calculated for all the samples by survival analysis using SPSS 19.0 software for Windows (SPSS Inc., Chicago, IL, United States).

Insecticides Stress

The treatment groups of third instar larvae were sprayed with the LC_{50} value of phoxim, chlorpyrifos, imidacloprid, or chlorfluazuron. The control group was sprayed with distilled water. After 24, 48, and 72 h, 23 larvae in total were collected, flash-frozen, and stored.

Developmental Stages

B. odoriphaga samples were collected in a dish at each of the six developmental stages: first instar larvae, second instar larvae, third instar larvae, fourth instar larvae, pupa, and adult. Each dish contained 100 samples.

Tissues

The head, thorax, and abdomen from the fourth instar larvae were dissected by a dissection needle and a tweezer under a stereomicroscope. For each tissue, four replicates of 100 samples were collected.

Sexes

Hundred male and 100 female wingless *B. odoriphaga* adults were collected, flash-frozen in liquid nitrogen, and stored at −80°C until analyzed by RT-qPCR.

Primer Design

A set of nine candidate reference genes included *EF1α*, *EF2α*, *ACT*, *GAPDH*, *G6PDH*, *RPL10*, *RPS3*, *TUB*, and *UBC*. All of these genes are commonly used as reference genes in RT-qPCR analysis of other insects (Lü et al., 2018). The sequences of genes were obtained from *B. odoriphaga* transcriptome data (Chen et al., 2019). Primers were designed by NCBI Primer-BLAST[1]. The secondary structure of DNA template was predicted by the mfold web server[2]. Parameters were set as PCR products size 80–200 bp and size of primer 18–25 bp. Primers were synthetized by JINKAIRUI company, Wuhan, China. The details regarding the RT-qPCR primers are provided in **Table 1**.

Total RNA Extraction and cDNA Synthesis

Total RNA was extracted using the TRNzol Universal Reagent as described by the manufacturer (TaKaRa Bio, Dalian, China). The quantity and quality of RNA samples were assessed with a spectrophotometer 2000 (Thermo Scientific, Wilmington, DE, United States). RNA samples with OD ratio (A_{260}/A_{280}) ranging between 1.9 and 2.12 were selected for reverse transcription. Following the manufacturer's instructions, the cDNA was synthesized using the Prime script TMRT reagent kit (TaKaRa Bio, Dalian, China). The synthesized cDNA was stored at −20°C.

RT-qPCR

The PCR reaction system was structured by SYBR Premix Ex Taq II kit (TaKaRa, Dalian, China). Each reaction was operated in a 20-μL solution including 2 μL mixture, 10 μL SYBR Premix Ex Taq II, 0.8 μL forward primer, 0.8 μL reverse primer, and 6.4 μL distilled water. The mixture was cDNA synthesized in different reverse transcription conditions. The amplification conditions for the RT-qPCR were set as following: 95°C for 30 s; followed by 40 cycles of 95°C for 5 s, 60°C for 34 s. The corresponding RT-qPCR efficiencies (*E*) were counted employing the equation: $E = (10^{[-1/\text{slope}]} - 1) \times 100$, with cDNA gradient dilution (1, 1/5, 1/25, 1/125, 1/625, and 1/3125) set as abscissa and *Ct* value as ordinate (Pfaffl, 2001). All samples were set three biological replicates and three technical replicates. The *Ct* values were obtained by analyzing the result from RT-qPCR using the SDS software of ABI 7500 (version 1.4).

Data Analysis

Data from RT-qPCR were analyzed by software SDS Shell.exe for ABI7500. The values were given as cycle threshold (*Ct*) numbers. All the *Ct* values were the average means of three biological replicates. The Δ*Ct* method and three analysis applets NormFinder version 0.953[3], GeNorm version 3.5[4], and BestKeeper[5] were used to validate the stability of candidate reference genes. The comprehensive rank and a suitable number of reference genes were calculated by RefFinder[6] and GeNorm, respectively.

[1]http://www.ncbi.nlm.nih.gov/tools/primer-blast/index.cgi?LINK_LOC=BlastHome

[2]http://mfold.rna.albany.edu/?q=mfold/DNA-Folding-Form

[3]http://www.mdl.dk/publications NormFinder.htm

[4]http://GeNorm.cmgg.be

[5]http://www.wzw.tum.de/gene-quantification/bestkeeper.html

[6]https://www.heartcure.com.au/for-researchers

TABLE 1 | Primer sequences and amplicon characteristics of the nine reference genes in *B. odoriphaga* samples.

Gene symbol	Gene name	(Putative)function	Primer sequences (5′ → 3′)	Amplicon length (bp)	*E* (%) *	R^{2**}
EF1α	*Elongation factor 1α*	Structural constituent of ribosome	F: TTTTGGCCTTCACCCTTGGT R: AACGGTTCTCGCTGAATGGT	87	108.2	0.996
ACT	*Actin2*	Structural constituent of ribosome	F: AGAGCAAACGTGGTATCCTTACTT R: CTGGATGTTCTTCGGGTGCG	132	103.7	0.997
EF2α	*Elongation factor 2α*	Involved in cell motility, structure, and integrity	F: CTGCTGCAATCACAGCCAAG R: GGAAAGCTTGACCGCCAGTA	237	102.3	0.996
G6PDH	*Glucose-6-phosphate dehydrogenase*		F: ATCACTCATTCGGCGCTCTT R: CGGTACAAGTACCACAGCGT	150	98.8	0.998
GAPDH	*Glyceraldehyde-3-phosphate dehydrogenase*	Glycolytic enzyme	F: GGTCGTTTGGTACTTCGTGC R: GACCACCAAGAAGCCACCTT	162	98.7	0.998
RPL10	*Ribosomal protein L10*	Structural constituent of ribosome	F: AAGCGTTTCTCCGGAACTGT R: TATGCGGGTAACCAAGAGCG	115	106.4	0.997
RPS3	*Ribosomal protein S3*	Structural constituent of ribosome	F: TCTACGCAGAAAAGGTGGCA R: ACGAACGGCTAATCCACCAG	92	101.4	0.998
UBC	*Ubiquitin-conjugating enzyme*		F: CTTCTTCAGGAGCCCGTACC R: CTCGAATGGGGAGTCTGACG	102	101.2	0.998
TUB	*α-Tubulin*	Cytoskeleton structural protein	F: CACGTGCCGTTTTGGTTGAT R: TTACCGGCACCAGATTGACC	115	100.2	0.999

**Real-time qPCR efficiency (calculated by the standard curve method).*
***Regression coefficient calculated from the regression line of the standard curve.*

RESULTS

Verification of PCR Amplicons and PCR Amplification Efficiencies

The specific amplification of all primer pairs of candidate reference genes was confirmed with regular PCR and RT-qPCR. The PCR amplifications were identified by sequencing clones of the open reading frame (ORF). The results were consistent with the results of transcriptome sequencing. A single amplification peak for each candidate reference gene was observed in the melting curve (**Figure 1**). The size of amplicons ranged from 87 to 237 bp. The amplification efficiencies (*E*) for these genes varied from 98.7% for *GAPDH* to 108.2% for *EF1*α, and the correlation coefficients (R^2) varied from 0.999 to 0.996 (**Table 1**).

Expression Profiles of Candidate Reference Genes

The raw *Ct* values of the nine candidate reference genes for RT-qPCR were collected and are shown in **Figure 2**. The *Ct* values varied from 15.02 (*EF-1*α) to 37.26 (*GAPDH*), and the average *Ct* values ranged from 17.30 (*EF-1*α) to 22.10 (*UBC*), which indicates that noticeable differences exist in the expression profiles. Low *Ct* values correspond to high expression levels. Therefore, *EF-1*α exhibited the highest expression abundance, and *UBC* expressed the lowest level. Moreover, *Ct* values have also shown the differential expression variability, and *EF-1*α and *TUB* had a relatively narrow *Ct* range than other genes, indicating that these two genes might be expressed more stably.

Stability of Candidate Reference Genes

Imidacloprid

Based on Δ*Ct* and the BestKeeper analyses, *TUB* and *EF1*α were the most stable genes (**Table 2**). However, the NormFinder analysis indicated *RPL10* and *ACT* as the most stable genes (**Table 2**). All four analyses revealed *G6PDH* and *GAPDH* as the least stable genes (**Table 2**). The rank order for gene stability in the imidacloprid determined using RefFinder was as follows (most to least stable): *EF1*α, *TUB*, *UBC*, *EF2*α, *RPL10*, *ACT*, *RPS3*, *G6PDH*, and *GAPDH* (**Figure 3A**). The geNorm data indicated that the pairwise variation value for V2/3 was less than the proposed 0.15 cut-off (**Figure 4**). The RefFinder analysis suggested that *EF1*α and *TUB* are required to normalize target gene expression levels under imidacloprid stress (**Table 3**).

Chlorpyrifos

Both Δ*Ct* and NormFinder identified *ACT* and *RPL10* as the most stable genes across chlorpyrifos samples (**Table 2**). In contrast, BestKeeper and geNorm detected *TUB* and *EF1*α as the most stable genes (**Table 2**). All analyses indicated that *EF2*α and *GAPDH* were the least stable genes. The RefFinder results for chlorpyrifos indicated the rank order for gene stability was as follows (most to least stable): *ACT*, *TUB*, *EF1*α, *RPL10*, *RPS3*, *G6PDH*, *EF2*α, *UBC*, and *GAPDH* (**Figure 3B**). The geNorm data indicated that all pairwise values were less than the proposed 0.15 cut-off (**Figure 4**). Based on the RefFinder analysis, *ACT* and *TUB* are required to normalize target gene expression levels across chlorpyrifos (**Table 3**).

Chlorfluazuron

The Δ*Ct* analyses identified *RPS3*, *RPL10*, and *UBC* as the most stable genes across chlorfluazuron samples (**Table 2**). Similar results were obtained by geNorm (**Table 2**). However, BestKeeper identified *TUB* as the most stable gene (**Table 2**). The least stable gene was identified as *TUB* according to Δ*Ct*, NormFinder, and geNorm. The RefFinder data indicated that the rank order for gene stability among chlorfluazuron samples was as follows (most

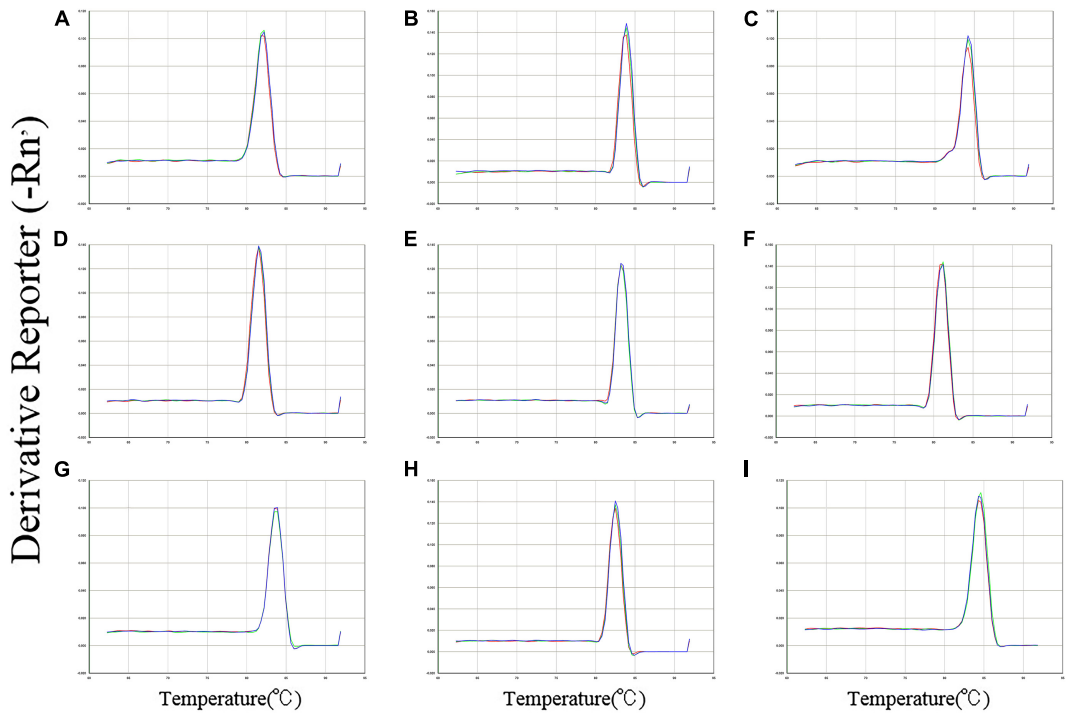

FIGURE 1 | Specificity of primer pairs for RT-qPCR amplification in *B. odoriphaga*. Melting curves with single peaks were produced for all amplicons. **(A)** *EF1α*; **(B)** *EF2α*; **(C)** *ACT*; **(D)** *GAPDH*; **(E)** *G6PDH*; **(F)** *RPL10*; **(G)** *RPS3*; **(H)** *TUB*; and **(I)** *UBC*.

to least stable): *ACT*, *TUB*, *EF1α*, *RPL10*, *RPS3*, *G6PDH*, *EF2α*, *UBC*, and *GAPDH* (**Figure 3C**). The geNorm analysis revealed that all pairwise variation values were less than the proposed 0.15 cut-off (**Figure 4**). The RefFinder analysis suggested that *ACT* and *TUB* are required to normalize target gene expression levels in chlorfluazuron-treated *B. odoriphaga* (**Table 3**).

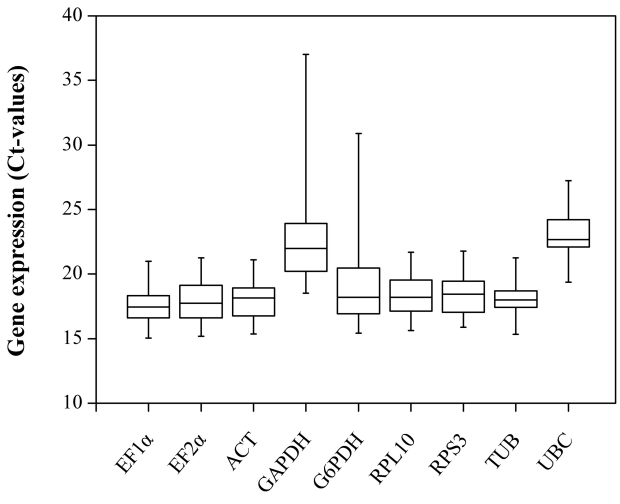

FIGURE 2 | Candidate reference genes expression profiles in *B. odoriphaga*. The expression data are presented as mean *Ct* values for duplicate samples. Whiskers represent the maximum and minimum values. The lower and upper borders of boxes represent the 25th and 75th percentiles, respectively. The line across the box indicates the median *Ct* value.

Phoxim

All analyses except the BestKeeper indicated that *RPL10*, *ACT*, and *RPS3* were the most stable genes, while *GAPDH* and *TUB* were the least stable genes (**Table 2**). In contrast, BestKeeper identified *TUB* as the most stable gene (**Table 2**). The rank order for gene stability determined using RefFinder was as follows (most to least stable): *RPL10*, *ACT*, *RPS3*, *EF1α*, *UBC*, *EF2α*, *TUB*, *G6PDH*, and *GAPDH* (**Figure 3D**). The geNorm data indicated that the pairwise variation value for V2/3 was less than the proposed 0.15 cut-off (**Figure 4**). The RefFinder analysis showed that target gene expression levels under phoxim stress conditions should be normalized against the expression of *RPL10* and *ACT* (**Table 3**).

Integrative Analysis of Reference Genes Under Insecticides' Stress

Regarding the insecticides' stress effects, the Δ*Ct*, geNorm, and NormFinder analyses indicated that the most stable genes were *RPL10*, *ACT*, and *RPS3*, whereas BestKeeper identified *TUB*, *EF1α*, and *EF2α* as the most stable genes (**Table 2**). All four analyses identified *GAPDH* and *G6PDH* as the least stable genes (**Table 2**). The RefFinder data indicated the rank order for gene stability was as follows (most to least stable): *ACT*, *RPL10*, *EF1α*, *RPS3*, *TUB*, *EF2α*, *UBC*, *G6PDH*, and *GAPDH* (**Figure 3E**). The geNorm analysis revealed that the pairwise variation value of V4/5 was less than the proposed 0.15 cut-off

TABLE 2 | Expression stability of the nine candidate reference genes in *B. odoriphaga* under various experimental conditions.

Condition	Rank	*ΔCt*		BestKeeper		NormFinder		geNorm	
		Gene Name	SV	Gene Name	SD	Gene Name	SV	Gene Name	SV
Imidacloprid	1	TUB	1.60	EF1α	0.32	RPL10	0.36	EF1α	0.25
	2	EF1α	1.70	TUB	0.38	ACT	0.40	EF2α	0.25
	3	UBC	1.72	UBC	0.41	TUB	1.05	UBC	0.38
	4	RPL10	1.73	EF2α	0.50	RPS3	1.07	TUB	0.40
	5	EF2α	1.74	RPS3	1.16	UBC	1.22	RPS3	0.61
	6	ACT	1.76	ACT	1.25	EF1α	1.30	ACT	0.82
	7	RPS3	1.80	RPL10	1.25	EF2α	1.40	RPL10	0.97
	8	G6PDH	3.42	G6PDH	2.82	G6PDH	3.18	G6PDH	1.64
	9	GAPDH	4.00	GAPDH	3.21	GAPDH	4.00	GAPDH	2.18
Chlorpyrifos	1	ACT	0.37	TUB	1.30	ACT	0.12	EF1α	0.15
	2	RPL10	0.39	EF1α	1.31	RPL10	0.18	TUB	0.16
	3	EF1α	0.40	EF2α	1.32	G6PDH	0.20	RPS3	0.20
	4	RPS3	0.41	RPS3	1.38	UBC	0.25	ACT	0.26
	5	TUB	0.41	RPL10	1.46	EF1α	0.26	RPL10	0.28
	6	G6PDH	0.44	ACT	1.53	RPS3	0.28	G6PDH	0.31
	7	UBC	0.48	G6PDH	1.60	TUB	0.30	UBC	0.34
	8	EF2α	0.58	UBC	1.68	EF2α	0.47	EF2α	0.37
	9	GAPDH	0.89	GAPDH	2.15	GAPDH	0.88	GAPDH	0.48
Chlorfluazuron	1	RPS3	061	TUB	0.27	ACT	0.18	RPS3	0.28
	2	RPL10	0.62	EF2α	0.50	EF1α	0.24	UBC	0.28
	3	UBC	0.65	EF1α	0.62	RPS3	0.24	RPL10	0.30
	4	ACT	0.68	ACT	1.01	UBC	0.25	ACT	0.39
	5	EF1α	0.69	UBC	1.03	RPL10	0.28	EF1α	0.41
	6	G6PDH	0.73	RPS3	1.08	G6PDH	0.49	G6PDH	0.47
	7	EF2α	0.77	RPL10	1.14	EF2α	0.60	EF2α	0.55
	8	GAPDH	1.15	G6PDH	1.23	GAPDH	1.07	GAPDH	0.63
	9	TUB	1.28	GAPDH	1.58	TUB	1.20	TUB	0.81
Phoxim	1	RPL10	1.33	TUB	0.60	RPL10	0.13	ACT	0.22
	2	ACT	1.35	EF2α	1.15	ACT	0.13	RPL10	0.23
	3	RPS3	1.44	EF1α	1.19	RPS3	0.15	RPS3	0.29
	4	UBC	1.50	RPS3	2.23	UBC	0.20	EF1α	0.32
	5	EF1α	1.52	RPL10	1.32	EF1α	0.35	UBC	0.38
	6	G6PDH	1.52	ACT	1.35	G6PDH	0.68	G6PDH	0.51
	7	EF2α	1.58	UBC	1.55	EF2α	0.78	EF2α	0.65
	8	GAPDH	2.20	G6PDH	1.88	GAPDH	1.52	GAPDH	0.84
	9	TUB	2.48	GAPDH	2.40	TUB	1.78	TUB	1.12
Insecticides	1	RPL10	1.12	TUB	0.68	ACT	0.20	ACT	0.55
	2	ACT	1.15	EF1α	1.08	RPL10	0.21	RPL10	0.55
	3	RPS3	1.18	EF2α	1.17	RPS3	0.52	RPS3	0.62
	4	EF1α	1.20	ACT	1.32	EF1α	0.69	EF1α	0.67
	5	EF2α	1.31	RPS3	1.32	UBC	0.90	UBC	0.71
	6	UBC	1.31	RPL10	1.50	EF2α	0.90	EF2α	0.74
	7	TUB	1.70	UBC	1.57	TUB	1.39	TUB	0.91
	8	G6PDH	1.90	G6PDH	1.84	G6PDH	1.58	G6PDH	1.21
	9	GAPDH	2.42	GAPDH	2.40	GAPDH	2.29	GAPDH	1.49
Developmental stages	1	EF1α	0.69	RPS3	0.38	EF1α	0.21	EF1α	0.35
	2	EF2α	0.70	RPL10	0.41	EF2α	0.24	ACT	0.36
	3	G6PDH	0.73	G6PDH	0.59	G6PDH	0.31	EF2α	0.38
	4	ACT	0.74	EF2α	0.61	ACT	0.44	G6PDH	0.51
	5	RPL10	0.79	EF1α	0.62	RPL10	0.55	RPL10	0.54
	6	RPS3	0.81	ACT	0.75	RPS3	0.56	RPS3	0.55

(Continued)

TABLE 2 | (Continued)

Condition	Rank	ΔCt		BestKeeper		NormFinder		geNorm	
		Gene Name	SV	Gene Name	SD	Gene Name	SV	Gene Name	SV
	7	UBC	0.99	TUB	0.93	UBC	0.79	UBC	0.69
	8	TUB	1.04	GAPDH	1.04	TUB	0.91	TUB	0.77
	9	GAPDH	1.19	UBC	1.10	GAPDH	1.12	GAPDH	0.90
Larvae	1	EF1α	0.62	RPL10	0.46	EF2α	0.26	RPL10	0.24
	2	EF2α	0.63	RPS3	0.49	EF1α	0.40	TUB	0.25
	3	TUB	0.64	TUB	0.53	UBC	0.45	G6PDH	046
	4	UBC	0.65	G6PDH	0.64	TUB	0.48	RPS3	0.48
	5	RPL10	0.70	EF1α	0.81	G6PDH	0.50	EF1α	0.52
	6	G6PDH	0.71	EF2α	0.83	ACT	0.54	UBC	0.58
	7	ACT	0.73	UBC	0.88	RPL10	0.55	EF2α	0.60
	8	RPS3	0.75	ACT	0.94	RPS3	0.55	ACT	0.63
	9	GAPDH	1.42	GAPDH	1.35	GAPDH	1.23	GAPDH	0.78
Tissues	1	EF1α	0.41	EF1α	0.33	EF1α	0.12	EF1α	0.15
	2	RPL10	0.41	ACT	0.39	RPL10	0.13	ACT	0.16
	3	RPS3	0.42	G6PDH	0.39	RPS3	0.15	G6PDH	0.21
	4	G6PDH	0.43	RPS3	0.48	ACT	0.20	RPL10	0.23
	5	ACT	0.45	RPL10	0.50	G6PDH	0.21	RPS3	0.27
	6	EF2α	0.50	EF2α	0.60	EF2α	0.32	EF2α	0.32
	7	UBC	0.61	UBC	0.64	UBC	0.48	TUB	0.41
	8	TUB	0.66	TUB	0.73	TUB	0.57	UBC	0.49
	9	GAPDH	0.87	GAPDH	0.81	GAPDH	0.79	GAPDH	0.55
Sex	1	ACT	0.45	G6PDH	0.13	G6PDH	0.14	ACT	0.15
	2	GAPDH	0.46	UBC	0.16	ACT	0.18	GAPDH	0.16
	3	G6PDH	0.48	ACT	0.17	UBC	0.23	EF1α	0.19
	4	UBC	0.50	GAPDH	0.21	GAPDH	0.25	UBC	0.20
	5	EF1α	0.51	RPS3	0.29	EF1α	0.38	G6PDH	0.25
	6	RPL10	0.57	EF1α	0.32	RPL10	0.47	RPL10	0.29
	7	RPS3	0.64	RPL10	0.38	RPS3	0.48	RPS3	0.36
	8	EF2α	0.85	EF2α	0.71	EF2α	0.75	EF2α	0.49
	9	TUB	0.92	TUB	0.82	TUB	0.87	TUB	0.62
All samples	1	RPL10	1.06	TUB	0.84	RPL10	0.32	RPL10	0.52
	2	ACT	1.07	EF1α	0.95	ACT	0.43	RPS3	0.53
	3	RPS3	1.11	EF2α	1.17	RPS3	0.51	ACT	0.64
	4	EF1α	1.13	ACT	1.21	EF1α	0.64	EF1α	0.65
	5	EF2α	1.22	RPS3	1.34	EF2α	0.71	EF2α	0.68
	6	UBC	1.23	UBC	1.40	UBC	0.87	UBC	0.70
	7	G6PDH	1.56	RPL10	1.42	G6PDH	1.23	TUB	0.92
	8	TUB	1.62	G6PDH	1.68	TUB	1.44	G6PDH	1.15
	9	GAPDH	2.05	GAPDH	2.15	GAPDH	1.98	GAPDH	1.34

(**Figure 4**). The RefFinder analysis suggested that *EF1α*, *TUB*, and *UBC* are required to normalize target gene expression levels in *B. odoriphaga* under insecticides stress (**Table 3**).

Developmental Stages

Regarding the analyzed developmental stages, the Δ*Ct* method, NormFinder, and geNorm, but not BestKeeper, indicated that *EF-1α* was the most stable gene and *GAPDH* and *TUB* were the least stable genes (**Table 2**). The BestKeeper analysis identified *RPS3* and *RPL10* as the most stable genes. In contrast, *UBC* was the least stable gene. The RefFinder analysis indicated the rank order for reference gene stability as follows (most to least stable): *EF1α*, *EF2α*, *ACT*, *G6PDH*, *RPS3*, *RPL10*, *UBC*, *TUB*, and *GAPDH* (**Figure 3F**). The geNorm analysis revealed that all pairwise variation values were less than the proposed 0.15 cut-off, except for V8/9 (**Figure 4**). A value less than 0.15 indicates that adding another reference gene will not change the normalization. The RefFinder analysis revealed that *EF1α* and *EF2α* are required for normalizing target gene expression levels in different *B. odoriphaga* developmental stages (**Table 3**).

Larvae

Both Δ*Ct* and NormFinder identified *EF1α* and *EF2α* as the most stable genes and *RPL10* as a moderately stable gene in

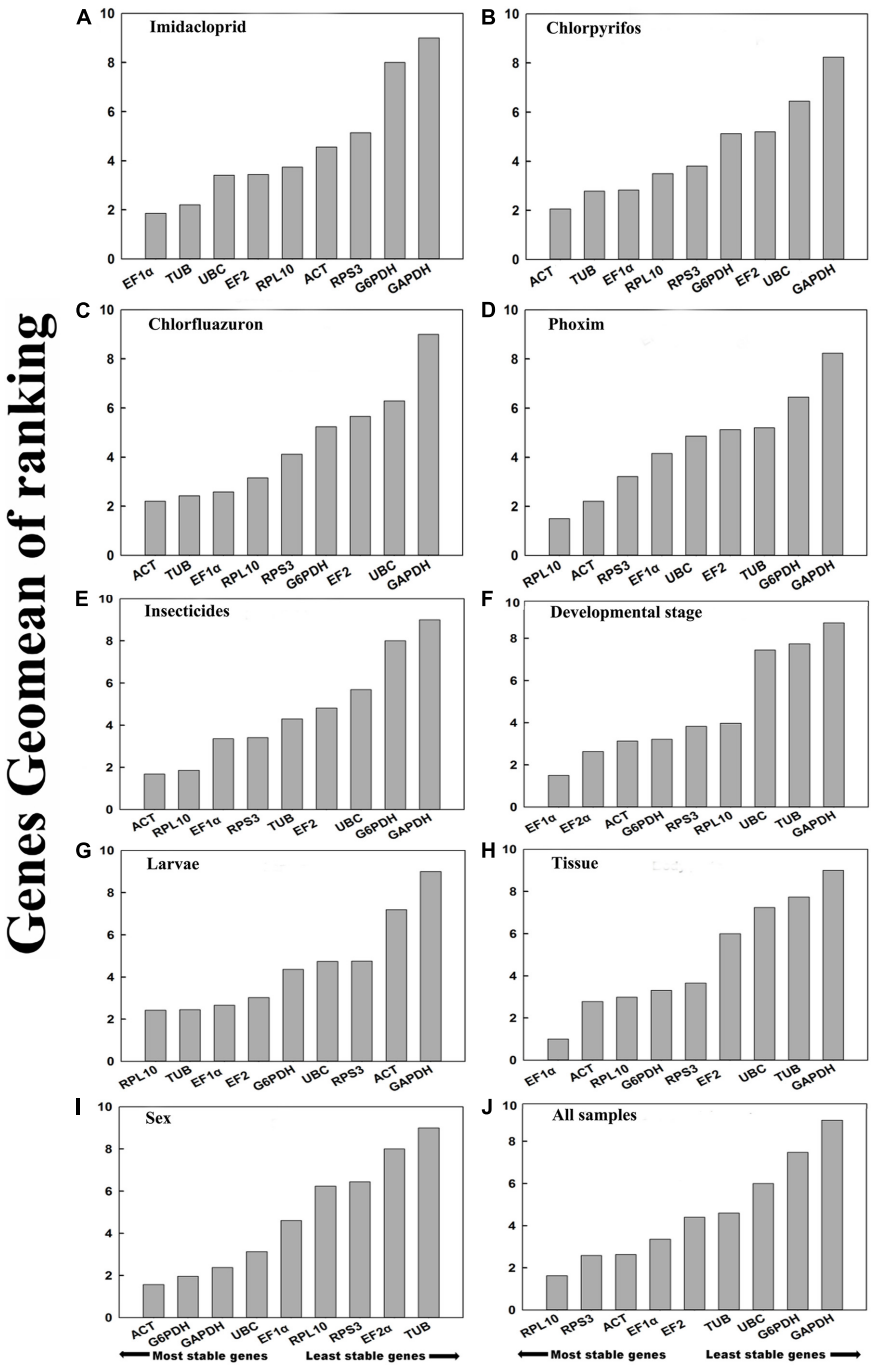

FIGURE 3 | Stability of candidate reference genes in *B. odoriphaga* under various experimental conditions. In a RefFinder analysis, increasing Geomean values correspond to decreasing gene expression stability. The Geomean values for the following *B. odoriphaga* samples are presented: **(A)** imidacloprid: samples treated with imidacloprid; **(B)** chlorpyrifos: samples treated with chlorpyrifos; **(C)** chlorfluazuron: samples treated with chlorfluazuron; **(D)** phoxim:samples treated with phoxim; **(E)** insecticide treatment: adult samples treated with different insecticides; **(F)** developmental stage: samples for all developmental stages; **(G)** larvae: samples for larvae; **(H)** tissue: samples for different tissues; **(I)** adult samples for different sex; and **(J)** all samples: all samples for all treatments. The candidate reference genes are as follows: *EF-1α*, *elongation factor 1α*; *ACT*, *actin2*; *EF-2α*, *elongation factor 2α*; *G6PDH*, *glucose-6-phosphate dehydrogenase*; *GAPDH*, *glyceraldehyde-3-phosphate dehydrogenase*; *RPL10*, *ribosomal protein L10*; *RPS3*, *ribosomal protein S3*; *UBC*, *ubiquitin-conjugating enzyme*; *TUB*, *α-tubulin*.

larval samples (**Table 2**). However, the BestKeeper and geNorm analysis identified *RPL10* as the most stable gene. According to the four algorithms, *GAPDH* was considered the least stable gene (**Table 2**). The rank order for gene stability based on the RefFinder results was as follows (most to least stable): *RPL10*, *TUB*, *EF1α*, *EF2α*, *G6PDH*, *UBC*, *RPS3*, *ACT*, and

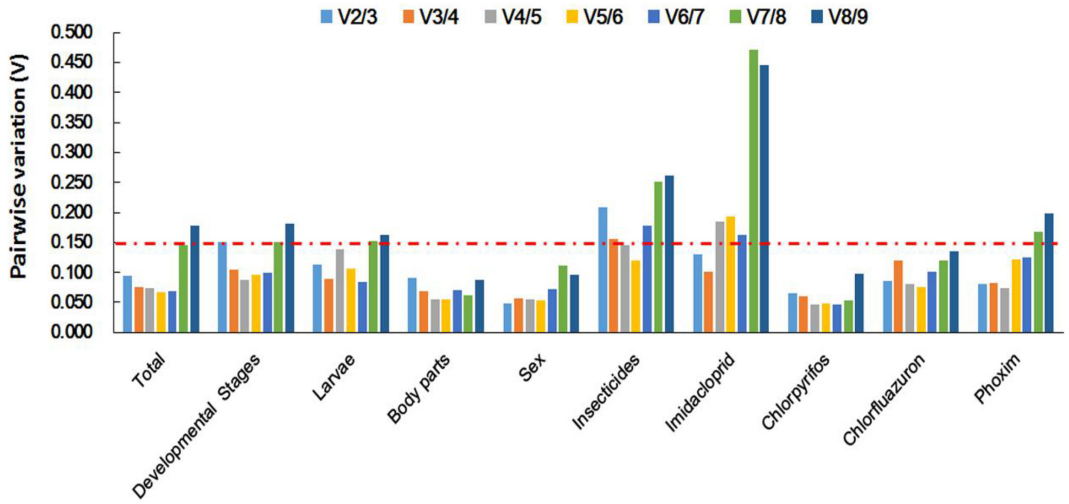

FIGURE 4 | Optimal number of reference genes for accurate normalization as determined by geNorm. The V*n*/*n* + 1 value indicates the pairwise variation (*Y*-axis) between two sequential normalization factors and was used to determine the optimal number of reference genes for an accurate data normalization. *A*-value < 0.15 indicates that an additional reference gene will not significantly improve the normalization.

GAPDH (**Figure 3G**). The geNorm analysis indicated that the pairwise value of V2/3 was less than the proposed 0.15 cut-off (**Figure 4**). The RefFinder analysis suggested that *RPL10* and *TUB* are required to normalize target gene expression levels in *B. odoriphaga* larval samples (**Table 3**).

Tissues

According to the four algorithms, the most stable gene was *EF1α*, and the least stable genes were *GAPDH*, *UBC*, and *TUB* across the tissues (**Table 2**). According to RefFinder, the reference gene stability rank order across tissues was as follows (most to least stable): *EF1α*, *ACT*, *RPL10*, *G6PDH*, *RPS3*, *EF2α*, *UBC*, *TUB*, and *GAPDH* (**Figure 3H**). The geNorm analysis results showed that all pair-wise variation values were less than the proposed 0.15 cut-off. The RefFinder analysis indicated *EF1α* and *ACT* are required for normalizing target gene expression levels in different *B. odoriphaga* tissues (**Table 3**).

Sex

Both Δ*Ct* and geNorm identified *ACT* and *GAPDH* as the most stable genes across sex samples (**Table 2**). The BestKeeper and NormFinder analysis also identified *G6PDH* as the most stable gene, while *UBC* and *ACT* were the second and third stable genes, respectively (**Table 2**). According to the four algorithms, *EF2α* and *TUB* were identified as the least stable genes (**Table 2**). The rank order for gene stability among the examined sex samples based on the RefFinder results was as follows (most to least stable): *ACT*, *G6PDH*, *GAPDH*, *UBC*, *EF1α*, *RPL10*, *RPS3*, *EF2α*, and *TUB* (**Figure 3I**). The geNorm analysis indicated that the pairwise value of V2/3 was less than the proposed 0.15 cut-off (**Figure 4**). The RefFinder analysis suggested that *ACT* and *G6PDH* are required to normalize target gene expression levels in *B. odoriphaga* sex samples (**Table 3**).

Overall Ranking of *Bradysia odoriphaga* Reference Genes

Based on the RefFinder analysis, the overall rank order for the stability of *B. odoriphaga* genes was as follows (most to least stable): *RPL10*, *RPS3*, *ACT*, *EF1α*, *EF2α*, *TUB*, *UBC*, *G6PDH*, and *GAPDH* (**Figure 3J**). The geNorm analysis indicated that all pairwise variation values were less than the proposed 0.15 cut-off, except for V8/9 (**Figure 4**). The RefFinder data suggested that *RPL10* and *RPS3* are suitable internal reference genes for normalizing target gene expression levels in *B. odoriphaga* (**Table 3**).

TABLE 3 | Most stable reference genes in *B. odoriphaga* under different experimental conditions.

Experimental conditions	Reference genes (most stable)	Experimental conditions	Reference genes (most stable)
Imidacloprid	*EF1α, TUB*	Developmental stage	*EF1α, EF2α*
Chlorpyrifos	*ACT, TUB*	Larvae	*RPL10, TUB*
Chlorfluazuron	*ACT, TUB*	Tissue	*EF1α, ACT*
Phoxim	*RPL10, ACT*	Sex	*ACT, G6PDH*
Insecticides	*ACT, RPL10, EF1α*	All samples	*RPL10, RPS3*

DISCUSSION

It is unquestionably true that gene expression quantification has never been easier than it is now, thanks to RT-qPCR technology. However, extreme care must be taken to avoid erroneous results (Liang et al., 2014). One of the most common strategies for correcting experimental errors introduced during the steps of RT-qPCR analysis is the normalization of RT-qPCR data with reference genes (Pinheiro et al., 2020). Inappropriate reference gene selection can obscure or magnify real biological changes

caused by changes in reference gene expression (Zhu et al., 2014). Therefore, a reference gene with low expression variation must be chosen to ensure accurate normalization and avoid inaccurate quantification of gene expression (Huggett et al., 2005).

Earlier studies on reference genes evaluation and validation in insects under insecticide stress reported that the expression of reference genes varies under different insecticide stress even if they belong to the same group of insecticides (Liang et al., 2014). These findings further demonstrate that there is no single universal reference available under different conditions. Therefore, identifying suitable reference genes is critical for obtaining a reliable estimate for gene expression levels under different conditions.

The present study evaluated the expression stability of nine candidate reference genes in *B. odoriphaga* under four insecticides commonly applied for controlling this pest. Moreover, the stability of these selected candidate genes was also assessed in developmental stages, sexes, and different tissues of *B. odoriphaga*.

The assessment of RNA integrity and amplification efficiency must be conducted prior to RT-qPCR based analysis of genes expression. In the present work, RNA integrity results showed that the OD ratio (A260/A280) of all RNA samples varied between 1.8 and 2.0, and the amplification efficiency of the nine candidates ranged from 90 to 110% ($R^2 > 0.996$) (**Table 1**). Thus, RNA quality and amplification were of sufficient quality to be used in RT-qPCR. Our RNA quality and amplification results agree with other reference gene validation studies conducted on the other insects (Shakeel et al., 2015; Pinheiro et al., 2020).

Our results of reference genes expression stability offered by five algorithms (geNorm, NormFinder, BestKeeper, Delta Ct, and RefFinder) indicated that the ranking order was different, such as *TUB* and *EF1*α were ranked as the most stable reference genes by ΔCt. In contrast, NormFinder ranked *RPL10* and *ACT* as the most stable reference genes under imidacloprid stress. Similarly, geNorm indicated *RPS3* and *UBC* as the most stable reference genes, whereas BestKeeper ranked *TUB* and *EF2*α as the most stable reference genes under chlorfluazuron stress. These discrepancies in the ranking order by different algorithms within the same tested insecticide might be because of the various analytical methods used (Shakeel et al., 2018). On the other hand, the difference in ranking of the reference genes under the stress of different insecticides in this study demonstrates the importance of evaluating their use under different sets of insecticides. Our findings provide more comprehensive information regarding reference genes selection under insecticide stress compared to the previous studies on *B. odoriphaga* (Shi et al., 2016; Tang et al., 2019).

The *ACT* gene, which is most frequently used as a reference gene, encodes a major structural protein that maintains organisms' life activity and exhibits conservative structure during evolution. In the present study, our results demonstrated that *ACT* expression was highly stable under insecticide stress (chlorpyrifos, chlorfluazuron) and other experimental conditions, including tissues and both sexes, and developmental stages. Coincidentally, the results are consistent with the earlier reports. For example, *ACT* was identified as one of the most stable reference genes for normalizing target gene expression in *Spodoptera litura* treated with insecticides (Lu et al., 2013). Additionally, *ACT* expression was revealed to be most stable in *Locusta migratoria* under different insecticides stress (Yang et al., 2014). *ACT* also showed high stability in other insects under different experimental sets, such as in *Plutella xylostella* and *Chilo suppressalis* under different development stages (Teng et al., 2012), *D. melanogaster* after heat-stress (Ponton et al., 2011), *Schistocerca gregaria* in fifth instar nymphs (Van Hiel et al., 2009), and *Orchesella cincta* overall treatments (de Boer et al., 2009). Quite the contrary, *ACT* was a less stable reference gene for gene expression analyses in *Bombyx mori*, *Spodoptera exigua* (Teng et al., 2012), *Coleomegilla maculata* (Yang C. et al., 2015), *Coccinella septempunctata* (Yang et al., 2016), and *Hippodamia convergens* (Pan et al., 2015). In this study, *ACT* was not an ideal reference gene for the larval stage in *B. odoriphaga*. Thus, there is no single universal reference gene suitable for all insects and under all conditions, even the most commonly used housekeeping gene responds differently to various experimental conditions.

The *TUB* gene is assigned to the Eukaryotic structural gene family, and encodes cytoskeletal structure proteins that involve in the regulation of cell division, shape, motility, and intracellular activity. In previous studies, *TUB* exhibited a stable expression, for example, *Nilaparvata lugens* for geographic population (Yuan et al., 2014), *Sogatella furcifera* at different developmental stages and under different temperature stress (An et al., 2016), *Thitarodes armoricanus* for the fungal infections (Liu et al., 2016), and *Bemisia tabaci* MED across all sample sets (Dai et al., 2017). In this study, the stability of *TUB* was variable under different treatments in *B. odoriphaga*. It exhibited a stable expression under chlorpyrifos, imidacloprid, and chlorfluazuron stress, whereas its expression was unstable across different developmental stages and tissues. Similar results have also been noted in *C. maculata* (Yang C. et al., 2015). The above results clearly suggest that determining candidates and evaluating their suitability is required for each experimental condition.

In the present study, the *EF1*α gene expression levels was stable across different developmental stages, tissues, and under the treatment of imidacloprid. Indeed, *EF1*α has been commonly picked as reference genes across different developmental stages and temperature in many other insect species, such as *Sesamia inferens* (Sun et al., 2015), *L. migratoria* (Yang et al., 2014), *Frankliniella occidentalis* (Zheng et al., 2014), and *H. convergens* (Pan et al., 2015). However, *EF1*α was considered unstable in developmental stages and tissues, again, in *B. odoriphaga* (Shi et al., 2016). This discrepancy between our study and previous study might be caused by different candidate reference genes, diet, population, temperature, and photoperiods.

Notably, the *GAPDH* gene, which encodes a key enzyme involved in the energy metabolism and ranked as the fourth most widely used reference gene, showed poor stability among almost all experimental conditions in this study. There are also some reports suggesting that the *GAPDH* was not suitable to be used as reference gene under the specific condition in some species, for example, *Bactrocera dorsalis* in difference tissues (Shen et al., 2010), *Musca domestica* (Zheng et al., 2014), and *Lucilia cuprina*

(Bagnall and Kotze, 2010) in difference developmental stages. On the other hand, *GADPH* was used as the most stable reference gene, such as *S. litura* in developmental stage and under temperature stress (Lu et al., 2013), *P. xylostella* in mechanical injury (Fu et al., 2013), *Euscelidius variegatus*, and *Macrosteles quadripunctulatus* by phytoplasma infection (Galetto et al., 2013). The results showed that the expression of candidate reference genes was not stable in all the tested conditions. Thus it is necessary to select different genes to normalize expression under different experimental conditions.

CONCLUSION

In summary, there was no single universal reference gene that could be used in all situations. It is indispensable to validate the expression of candidate genes before using them as the internal controls in qPCR. A suite of reference genes was specifically recommended for each experimental condition in this study. The suitable reference genes in different experimental conditions were *EF1α* and *EF2α* in development stages; *EF1α* and *ACT* in tissues; *ACT* and *G6PDH* in sex; *RPL10* and *ACT* in phoxim treatment; *ACT* and *TUB* in chlorpyrifos treatment; *EF1α* and *TUB* in imidacloprid treatment; and *ACT* and *TUB* in chlorfluazuron treatment. The results of our experiment can be used for the further studies in *B. odoriphaga*.

DATA AVAILABILITY STATEMENT

The original contributions presented in the study are included in the article/supplementary material, further inquiries can be directed to the corresponding author.

ETHICS STATEMENT

The animal study was reviewed and approved by the Animal Ethics Committee of Heilongjiang University. Written informed consent was obtained from the owners for the participation of their animals in this study.

AUTHOR CONTRIBUTIONS

FY and HF conceived and designed the research. TH, ZX, ChaoL, and CY conducted the experiments. ChunL and TW analyzed the data. HF wrote the manuscript. FS, FF, and FY revised the manuscript. All authors have read and approved the manuscript.

FUNDING

This study was supported by the Heilongjiang University Postdoctoral Research Fund (194359), National Natural Science Foundation of China (31672060), and Nature Scientific Foundation of Heilongjiang Province (ZD2017004). This work was supported by the Key Laboratory of Molecular Biology, College of Heilongjiang Province, and Heilongjiang Vegetable Collaborative Innovation and Extension System of Modern Agricultural Industry Technology.

ACKNOWLEDGMENTS

We thank Researchersview, Shakeel M. for editing the English text of the draft of this manuscript.

REFERENCES

Adeyinka, O. S., Tabassum, B., Nasir, I. A., Yousaf, I., Sajid, I. A., Shehzad, K., et al. (2019). Identification and validation of potential reference gene for effective dsRNA knockdown analysis in *Chilo partellus*. *Sci Rep.* 9:13629. doi: 10.1038/s41598-019-49810-w

An, X. K., Hou, M. L., and Liu, Y. D. (2016). Reference Gene Selection and Evaluation for Gene Expression Studies Using qRT-PCR in the White-Backed Plant hopper, *Sogatella furcifera* (Hemiptera: delphacidae). *J. Econ. Entomol.* 109, 879–886. doi: 10.1093/jee/tov333

Andersen, C. L., Jensen, J. L., and Orntoft, T. F. (2004). Normalization of real-time quantitative reverse transcription-PCR data: a model-based variance estimation approach to identify genes suited for normalization, applied to bladder and colon cancer data sets. *Cancer Res.* 64, 5245–5250. doi: 10.1158/0008-5472.CAN-04-0496

Bagnall, N. H., and Kotze, A. C. (2010). Evaluation of reference genes for real-time PCR quantification of gene expression in the Australian sheep blowfly, *Lucilia cuprina*. *Med. Vet. Entomol.* 24, 176–181. doi: 10.1111/j.1365-2915.2010.00866.x

Bai, Y., Lv, Y. N., Zeng, M., Jia, P. Y., Lu, H. N., Zhu, Y. B., et al. (2020). Selection of Reference Genes for Normalization of Gene Expression in *Thermobia domestica* (Insecta: zygentoma: lepismatidae). *Genes* 12:21. doi: 10.3390/genes12010021

Castanera, R., López-Varas, L., Pisabarro, A. G., and Ramírez, L. (2015). Validation of reference genes for transcriptional analyses in *pleurotus ostreatus* by using reverse transcription-quantitative PCR. *Appl. Environ. Microbiol.* 81, 4120–4129. doi: 10.1128/AEM.00402-15

Chang, Y., Chen, J., Lu, M., Gao, Y., Tian, Z., Gong, W., et al. (2017). Selection and validation of reference genes for quantitative real-time PCR analysis under different experimental conditions in the leafminer *Liriomyza trifolii* (Diptera: agromyzidae). *PLoS One* 12:e0181862. doi: 10.1371/journal.pone.0181862

Chen, C., Li, S., Zhu, H., Fan, B., Wang, Y., and Hao, D. (2020). Identification and evaluation of reference genes for gene expression analysis in the weevil pest *Pagiophloeus tsushimanus* using RT-qPCR. *J. Asia Pacif. Entomol.* 23, 336–344. doi: 10.1016/j.aspen.2020.01.010

Chen, C., Shi, X., Desneux, N., Han, P., and Gao, X. (2017). Detection of insecticide resistance in *Bradysia odoriphaga* Yang et Zhang (Diptera: sciaridae) in China. *Ecotoxicology* 26, 868–875. doi: 10.1007/s10646-017-1817-0

Chen, C., Wang, C., Liu, Y., Shi, X., and Gao, X. (2018). Transcriptome analysis and identification of P450 genes relevant to imidacloprid detoxification in *Bradysia odoriphaga*. *Sci Rep.* 8:2564. doi: 10.1038/s41598-018-20981-2

Chen, H., Lin, L., Xie, M., Zhong, Y., Zhang, G., and Su, W. (2019). Survey of the *Bradysia odoriphaga* Transcriptome Using PacBio Single-Molecule Long-Read Sequencing. *Genes* 10:481. doi: 10.3390/genes10060481

Chen, J., Guo, Y., Huang, S., Zhan, H., Zhang, M., Wang, J., et al. (2021). Integration of transcriptome and proteome reveals molecular mechanisms underlying stress responses of the cutworm, *Spodoptera litura*, exposed to different levels of lead (Pb). *Chemosphere* 283:131205. doi: 10.1016/j.chemosphere.2021.131205

Cheng, J., Su, Q., Xia, J., Yang, Z., Shi, C., Wang, S., et al. (2020). Comparative transcriptome analysis of differentially expressed genes in *Bradysia odoriphaga* Yang et Zhang (Diptera: sciaridae) at different acute stress temperatures. *Genomics* 112, 3739–3750. doi: 10.1016/j.ygeno.2020.04.019

Dai, T. M., Lü, Z. C., Liu, W. X., and Wan, F. H. (2017). Selection and validation of reference genes for qRT-PCR analysis during biological invasions: the thermal adaptability of *Bemisia tabaci* MED. *PLoS One* 12:e0173821. doi: 10.1371/journal.pone.0173821

de Boer, M. E., de Boer, T. E., Mariën, J., Timmermans, M. J., Nota, B., van Straalen, N. M., et al. (2009). Reference genes for QRT-PCR tested under various stress conditions in *Folsomia candida* and *Orchesella cincta* (Insecta, Collembola). *BMC Mol. Biol.* 10:54. doi: 10.1186/1471-2199-10-54

Fu, S., Duan, Y., Wang, S., Ren, Y., and Bu, W. (2021). Comparative transcriptomic analysis of *Riptortus pedestris* (Hemiptera: alydidae) to characterize wing formation across all developmental stages. *Insects* 12:226. doi: 10.3390/insects12030226

Fu, W., Xie, W., Zhang, Z., Wang, S., Wu, Q., Liu, Y., et al. (2013). Exploring valid reference genes for quantitative real-time PCR analysis in *Plutella xylostella* (Lepidoptera: plutellidae). *Int. J. Biol. Sci.* 9, 792–802. doi: 10.7150/ijbs.5862

Fu, X., and Meyer-Rochow, V. B. (2021). Selection and validation of suitable reference genes for RT-qPCR analysis in the rare aquatic firefly *Aquatica leii* (Coleoptera: lampyridae). *Insects* 12:359. doi: 10.3390/insects12040359

Galetto, L., Bosco, D., and Marzachì, C. (2013). Selection of reference genes from two leafhopper species challenged by phytoplasma infection, for gene expression studies by RT-qPCR. *BMC Res. Notes* 6:409. doi: 10.1186/1756-0500-6-409

Gong, P., Li, X., Gao, H., Wang, C., Li, M., Zhang, Y., et al. (2021). Field evolved resistance to pyrethroids, neonicotinoids, organophosphates and macrolides in *Rhopalosiphum padi* (Linnaeus) and *Sitobion avenae* (Fabricius) from China. *Chemosphere* 269:128747. doi: 10.1016/j.chemosphere.2020.128747

Huggett, J., Dheda, K., Bustin, S., and Zumla, A. (2005). Real-time RT-PCR normalisation; strategies and considerations. *Genes Immun.* 6, 279–284. doi: 10.1038/sj.gene.6364190

Kang, Z., Liu, F., Tian, H., Zhang, M., Guo, S., and Liu, T. (2017). Evaluation of the reference genes for expression analysis using quantitative real-time polymerase chain reaction in the green peach aphid. *Myzus persicae. Insect Sci.* 24, 222–234. doi: 10.1111/1744-7917.12310

Kim, Y., Kim, Y., and Kim, Y. H. (2020). Evaluation of reference genes for gene expression studies using quantitative real-time PCR in *Drosophila melanogaster* after chemical exposures. *J. Asia Pacif. Entomol.* 23, 385–394.

Koo, J., Chereddy, S. C. R. R., and Palli, S. R. (2020). RNA interference-mediated control of cigarette beetle, *Lasioderma serricorne*. *Arch Insect Biochem Physiol.* 104:e21680. doi: 10.1002/arch.21680

Li, H. J., He, X. K., Zeng, A. J., Liu, Y. J., and Jiang, S. R. (2007). *Bradysia odoriphaga* copulatory behavior and evidence of a female sex pheromone. *J. Agric. Urban Entomol.* 24, 27–34. doi: 10.3954/1523-5475-24.1.27

Li, L. L., Xu, J. W., Yao, W. C., Yang, H. H., Dewer, Y., Zhang, F., et al. (2021). Chemosensory genes in the head of *Spodoptera litura* larvae. *Bull. Entomol. Res.* 111, 454–463. doi: 10.1017/S0007485321000109

Li, M., Li, X., Wang, C., Li, Q., Zhu, S., Zhang, Y., et al. (2021). Selection and validation of reference genes for qRT-PCR analysis of *Rhopalosiphum padi* (Hemiptera: aphididae). *Front. Physiol.* 12:663338. doi: 10.3389/fphys.2021.663338

Li, W. X., Yang, Y. T., Xie, W., Wu, Q. J., Xu, B. Y., Wang, S. L., et al. (2015). Effects of temperature on the age-stage, two-sex life table of *Bradysia odoriphaga* (Diptera: sciaridae). *J. Econ. Entomol.* 108, 126–134. doi: 10.1093/jee/tou011

Li, Z. N., Gu, X. S., Xu, W. H., Xu, J. Y., and Chen, J. R. (2015). Study on toxic effect of 8 kinds of insecticides to *Bradysia odoriphaga*. *Shandong Agric. Sci.* 47, 107–108.

Liang, P., Guo, Y., Zhou, X., and Gao, X. (2014). Expression profiling in *Bemisia tabaci* under insecticide treatment: indicating the necessity for custom reference gene selection. *PLoS One* 9:e87514. doi: 10.1371/journal.pone.0087514

Liu, G., Qiu, X., Cao, L., Zhang, Y., Zhan, Z., and Han, R. (2016). Evaluation of reference genes for reverse transcription quantitative PCR Studies of Physiological Responses in the Ghost Moth, *Thitarodes armoricanus* (Lepidoptera, Hepialidae). *PLoS One* 11:e0159060. doi: 10.1371/journal.pone.0159060

Lü, J., Yang, C., Zhang, Y., and Pan, H. (2018). Selection of reference genes for the normalization of RT-qPCR data in gene expression studies in insects: a systematic review. *Front. Physiol.* 9:1560. doi: 10.3389/fphys.2018.01560

Lu, Y., Yuan, M., Gao, X., Kang, T., Zhan, S., Wan, H., et al. (2013). Identification and validation of reference genes for gene expression analysis using quantitative PCR in *Spodoptera litura* (Lepidoptera: noctuidae). *PLoS One* 8:e68059. doi: 10.1371/journal.pone.0068059

Luo, J., Wang, A., Cheng, Y., Rong, H., Guo, L., Peng, Y., et al. (2020). Selection and validation of suitable reference genes for RT-qPCR analysis in *Apolygus lucorum* (Hemiptera: miridae). *J. Econ. Entomol.* 113, 451–460. doi: 10.1093/jee/toz301

Luo, J., Zhang, Z., Li, D., Liu, J., Li, K., Sun, X., et al. (2021). Identification and functional analysis of SlitOBP11 from *Spodoptera litura*. *Front. Physiol.* 12:619816. doi: 10.3389/fphys.2021.619816

Nazar, M. Z., Freed, S., Hussain, S., Sumra, M. W., Shah, M. S., and Naeem, A. (2020). Characteristics of biochemical resistance mechanism of novel insecticides in *Phenacoccus solenopsis* Tinsley (Hemiptera: pseudococcidae). *Crop Protect.* 138:105320. doi: 10.1016/j.cropro.2020.105320

Nor Muhammad, N. A., Ramlee, I. A., Mohd Nor, D., Satyavenathan, M. V., Rahmat, N. L., Awang, A., et al. (2020). Data on RNA-seq analysis of the cocoa pod borer pest *Conopomorpha cramerella* (Snellen) (Lepidoptera: gracillariidae). *Data Brief.* 34:106638. doi: 10.1016/j.dib.2020.106638

Pan, H., Yang, X., Siegfried, B. D., and Zhou, X. (2015). A Comprehensive Selection of Reference Genes for RT-qPCR Analysis in a Predatory Lady Beetle, *Hippodamia convergens* (Coleoptera: coccinellidae). *PLoS One* 10:e0125868. doi: 10.1371/journal.pone.0125868

Pfaffl, M. W. (2001). A new mathematical model for relative quantification in real-time RT-PCR. *Nucleic Acids Res.* 29:e45. doi: 10.1093/nar/29.9.e45

Pfaffl, M. W., Tichopad, A., Prgomet, C., and Neuvians, T. P. (2004). Determination of stable housekeeping genes, differentially regulated target genes and sample integrity: bestkeeper – excel-based tool using pair-wise correlations. *Biotechnol. Lett.* 26, 509–515. doi: 10.1023/b:bile.0000019559.84305.47

Pinheiro, D. H., Moreira, R. O., Leite, N. A., Redoan, A. C., Xavier, A. D. S., Barros, B. A., et al. (2020). Suitable reference genes for RT-qPCR analysis in *Dichelops melacanthus* (Hemiptera: pentatomidae). *Mol. Biol. Rep.* 47, 4989–5000. doi: 10.1007/s11033-020-05550-z

Ponton, F., Chapuis, M. P., Pernice, M., Sword, G. A., and Simpson, S. J. (2011). Evaluation of potential reference genes for reverse transcription-qPCR studies of physiological responses in *Drosophila melanogaster*. *J. Insect Physiol.* 57, 840–850. doi: 10.1016/j.jinsphys.2011.03.014

Prajapati, V. K., Varma, M., and Vadassery, J. (2020). In silico identifification of effector proteins from generalist herbivore *Spodoptera litura*. *BMC Genom.* 21:819. doi: 10.1186/s12864-020-07196-4

Shakeel, M., Rodriguez, A., Tahir, U. B., and Jin, F. (2018). Gene expression studies of reference genes for quantitative real-time PCR: an overview in insects. *Biotechnol. Lett.* 40, 227–236. doi: 10.1007/s10529-017-2465-4

Shakeel, M., Zhu, X., Kang, T., Wan, H., and Li, J. (2015). Selection and evaluation of reference genes for quantitative gene expression studies in cotton bollworm, *Helicoverpa armigera* (Lepidoptera: Noctuidae). *J. Asia Pacif. Entomol.* 18, 123–130. doi: 10.1016/j.aspen.2015.01.001

Shen, G. M., Jiang, H. B., Wang, X. N., and Wang, J. J. (2010). Evaluation of endogenous references for gene expression profiling in different tissues of the oriental fruit fly *Bactrocera dorsalis* (Diptera: tephritidae). *BMC Mol. Biol.* 11:76. doi: 10.1186/1471-2199-11-76

Shi, C., Yang, F., Zhu, X., Du, E., Yang, Y., Wang, S., et al. (2016). Evaluation of housekeeping genes for Quantitative Real-Time PCR analysis of *Bradysia odoriphaga* (Diptera: sciaridae). *Int. J. Mol. Sci.* 17:1034. doi: 10.3390/ijms17071034

Silver, K., Cooper, A. M., and Zhu, K. Y. (2021). Strategies for enhancing the efficiency of RNA interference in insects. *Pest. Manag. Sci.* 77, 2645–2658. doi: 10.1002/ps.6277

Silver, N., Best, S., Jiang, J., and Thein, S. L. (2006). Selection of housekeeping genes for gene expression studies in human reticulocytes using real-time PCR. *BMC Mol. Biol.* 7:33. doi: 10.1186/1471-2199-7-33

Sun, M., Lu, M. X., Tang, X. T., and Du, Y. Z. (2015). Exploring valid reference genes for quantitative real-time PCR analysis in *Sesamia inferens* (Lepidoptera: noctuidae). *PLoS One* 10:e0115979. doi: 10.1371/journal.pone.0115979

Tang, B., Dai, W., and Zhang, C. (2019). Selection of reference genes for quantitative real-time polymerase chain reaction normalization in *Bradysia odoriphaga* (Diptera: sciaridae). *Entomol. Sci.* 22, 422–436. doi: 10.1111/ens.12383

Teng, X., Zhang, Z., He, G., Yang, L., and Li, F. (2012). Validation of reference genes for quantitative expression analysis by real-time rt-PCR in four lepidopteran insects. *J. Insect Sci.* 12:60. doi: 10.1673/031.012.6001

Ullah, I., Wazir, S., Abbas, N., Naeem, M., Abdullah, K., Mahmood, Z., et al. (2021). Monitoring of field-evolved resistance to flonicamid, neonicotinoid, and conventional insecticides in the *Oxycarenus hyalinipennis costa*. *Environ. Monit. Assess.* 193:382. doi: 10.1007/s10661-021-09158-z

Vandesompele, J., Preter, K. D., Pattyn, F., Poppe, B., Roy, N. V., Paepe, A. D., et al. (2002). Accurate normalization of real-time quantitative RT-PCR data by geometric averaging of multiple internal control genes. *Genome Biol.* 3:research0034.1. doi: 10.1186/gb-2002-3-7-research0034

Van Hiel, M. B., Van Wielendaele, P., Temmerman, L., Van Soest, S., Vuerinckx, K., Huybrechts, R., et al. (2009). Identification and validation of housekeeping genes in brains of the desert locust *Schistocerca gregaria* under different developmental conditions. *BMC Mol. Biol.* 10:56. doi: 10.1186/1471-2199-10-56

Wang, R., Che, W., Wang, J., and Luo, C. (2020). Monitoring insecticide resistance and diagnostics of resistance mechanisms in *Bemisia tabaci* Mediterranean (Q biotype) in China. *Pestic. Biochem. Physiol.* 163, 117–122.

Xiao, H. Y., Li, G. C., Wang, Z. Q., Guo, Y. R., and Liu, N. Y. (2021). Combined transcriptomic, proteomic and genomic analysis identifies reproductive-related proteins and potential modulators of female behaviors in *Spodoptera litura*. *Genomics* 113, 1876–1894. doi: 10.1016/j.ygeno.2021.04.006

Xie, F., Xiao, P., Chen, D., Xu, L., and Zhang, B. (2012). miRDeepFinder: a miRNA analysis tool for deep sequencing of plant small RNAs. *Plant Mol. Biol.* 80, 75–84. doi: 10.1007/s11103-012-9885-2

Yan, X., Zhang, Y., Xu, K., Wang, Y., and Yang, W. (2021). Selection and validation of reference genes for gene expression analysis in *Tuta absoluta* Meyrick (Lepidoptera: gelechiidae). *Insects* 12:589. doi: 10.3390/insects12070589

Yang, C., Pan, H., Noland, J. E., Zhang, D., Zhang, Z., Liu, Y., et al. (2015). Selection of reference genes for RT-qPCR analysis in a predatory biological control agent, *Coleomegilla maculata* (Coleoptera: coccinellidae). *Sci Rep.* 5:18201. doi: 10.1038/srep18201

Yang, C., Preisser, E. L., Zhang, H., Liu, Y., Dai, L., Pan, H., et al. (2016). Selection of Reference Genes for RT-qPCR Analysis in *Coccinella septempunctata* to Assess Un-intended Effects of RNAi Transgenic Plants. *Front Plant Sci.* 7:1672. doi: 10.3389/fpls.2016.01672

Yang, Q., Li, Z., Cao, J., Zhang, S., Zhang, H., Wu, X., et al. (2014). Selection and assessment of reference genes for quantitative PCR normalization in migratory locust *Locusta migratoria* (Orthoptera: acrididae). *PLoS One* 9:e98164. doi: 10.1371/journal.pone.0098164

Yang, X., Pan, H., Yuan, L., and Zhou, X. (2018). Reference gene selection for RT-qPCR analysis in Harmonia axyridis, a global invasive lady beetle. *Sci. Rep.* 8:2689. doi: 10.1038/s41598-018-20612-w

Yang, Y. T., Li, W. X., Xie, W., Wu, Q. J., Xu, B. Y., Wang, S. L., et al. (2015). Development of *Bradysia odoriphaga* (Diptera: sciaridae) as affected by humidity: an age–stage, two-sex, life-table study. *Appl. Entomol. Zool.* 50, 3–10. doi: 10.1007/s13355-014-0295-6

Yin, J., Sun, L., Zhang, Q., and Cao, C. (2020). Screening and evaluation of the stability of expression of reference genes in *Lymantria dispar* (Lepidoptera: erebidae) using qRT-PCR. *Gene* 749:144712. doi: 10.1016/j.gene.2020.144712

Yu, H. Z., Li, N. Y., Xie, Y. X., Zhang, Q., Wang, Y., and Lu, Z. J. (2020). Identification and functional analysis of two chitin synthase genes in the common cutworm, *Spodoptera litura*. *Insects* 11:253. doi: 10.3390/insects11040253

Yuan, M., Lu, Y., Zhu, X., Wan, H., Shakeel, M., Zhan, S., et al. (2014). Selection and evaluation of potential reference genes for gene expression analysis in the brown planthopper, *Nilaparvata lugens* (Hemiptera: delphacidae) using reverse-transcription quantitative PCR. *PLoS One* 9:e86503. doi: 10.1371/journal.pone.0086503

Zhang, H., Mallik, A., and Zeng, R. S. (2013). Control of Panama disease of banana by rotating and intercropping with Chinese chive (*Allium tuberosum* Rottler): role of plant volatiles. *J. Chem. Ecol.* 39, 243–252. doi: 10.1007/s10886-013-0243-x

Zheng, L., Zhang, Z., Zhang, J., Li, X., Huang, J., Lin, W., et al. (2019). Selection of reference genes for RT-qPCR analysis of *Phenacoccus solenopsis* (Hemiptera: pseudococcidae) sex-dimorphic development. *J. Integr. Agric.* 18, 854–864. doi: 10.1016/s2095-3119(18)61973-2

Zheng, Y. T., Li, H. B., Lu, M. X., and Du, Y. Z. (2014). Evaluation and validation of reference genes for qRT-PCR normalization in *Frankliniella occidentalis* (Thysanoptera: thripidae). *PLoS One* 9:e111369. doi: 10.1371/journal.pone.0111369

Zhou, L., Meng, J. Y., Ruan, H. Y., Yang, C. L., and Zhang, C. Y. (2021). Expression stability of candidate RT-qPCR housekeeping genes in *Spodoptera frugiperda* (Lepidoptera: noctuidae). *Arch. Insect. Biochem. Physiol.* 108:e21831. doi: 10.1002/arch.21831

Zhu, X., Yuan, M., Shakeel, M., Zhang, Y., Wang, S., Wang, X., et al. (2014). Selection and evaluation of reference genes for expression analysis using qRT-PCR in the beet armyworm *Spodoptera exigua* (Hübner) (Lepidoptera: Noctuidae). *PLoS One* 9:e84730. doi: 10.1371/journal.pone.0084730

Zou, X. P., Lin, Y. G., Cen, Y. J., Ma, K., Qiu, B. B., Feng, Q. L., et al. (2021). Analyses of microRNAs and transcriptomes in the midgut of *Spodoptera litura* feeding on *Brassica juncea*. *Insect Sci.* 28, 533–547. doi: 10.1111/1744-7917.12779

Conflict of Interest: The authors declare that the research was conducted in the absence of any commercial or financial relationships that could be construed as a potential conflict of interest.

Publisher's Note: All claims expressed in this article are solely those of the authors and do not necessarily represent those of their affiliated organizations, or those of the publisher, the editors and the reviewers. Any product that may be evaluated in this article, or claim that may be made by its manufacturer, is not guaranteed or endorsed by the publisher.

frontiers in Physiology

ORIGINAL RESEARCH
published: 04 February 2022
doi: 10.3389/fphys.2021.816675

Transcriptome Responses to Defined Insecticide Selection Pressures in the German Cockroach (*Blattella germanica* L.)

Michael E. Scharf[1]†, Zachery M. Wolfe[1], Kapil R. Raje[1], Mahsa Fardisi[1], Jyothi Thimmapuram[2], Ketaki Bhide[2] and Ameya D. Gondhalekar[1]*

[1] Department of Entomology, Purdue University, West Lafayette, IN, United States, [2] Bioinformatics Core, Purdue University, West Lafayette, IN, United States

OPEN ACCESS

Edited by:
Ran Wang,
Institute of Plant Protection and Environmental Protection, Beijing Academy of Agricultural and Forestry Sciences, China

Reviewed by:
Fan Zhang,
Shandong Normal University, China
Ana Elena Pérez-Cobas,
Ramón y Cajal Institute for Health Research, Spain

***Correspondence:**
Michael E. Scharf
mescharf@ufl.edu

†Present address:
Michael E. Scharf,
Department of Entomology and Nematology, University of Florida, Gainesville, FL, United States

Specialty section:
This article was submitted to Invertebrate Physiology, a section of the journal Frontiers in Physiology

Received: 17 November 2021
Accepted: 29 December 2021
Published: 04 February 2022

Citation:
Scharf ME, Wolfe ZM, Raje KR, Fardisi M, Thimmapuram J, Bhide K and Gondhalekar AD (2022) Transcriptome Responses to Defined Insecticide Selection Pressures in the German Cockroach (Blattella germanica L.). Front. Physiol. 12:816675. doi: 10.3389/fphys.2021.816675

Cockroaches are important global urban pests from aesthetic and health perspectives. Insecticides represent the most cost-effective way to control cockroaches and limit their impacts on human health. However, cockroaches readily develop insecticide resistance, which can quickly limit efficacy of even the newest and most effective insecticide products. The goal of this research was to understand whole-body physiological responses in German cockroaches, at the metatranscriptome level, to defined insecticide selection pressures. We used the insecticide indoxacarb as the selecting insecticide, which is an important bait active ingredient for cockroach control. Six generations of selection with indoxacarb bait produced a strain with substantial (>20×) resistance relative to inbred control lines originating from the same parental stock. Metatranscriptome sequencing revealed 1,123 significantly differentially expressed (DE) genes in ≥two of three statistical models (81 upregulated and 1,042 downregulated; FDR $P < 0.001$; log2FC of ±1). Upregulated DE genes represented many detoxification enzyme families including cytochrome-P450 oxidative enzymes, hydrolases and glutathione-*S*-transferases. Interestingly, the majority of downregulated DE genes were from microbial and viral origins, indicating that selection for resistance is also associated with elimination of commensal, pathogenic and/or parasitic microbes. These microbial impacts could result from: (i) direct effects of indoxacarb, (ii) indirect effects of antimicrobial preservatives included in the selecting bait matrix, or (iii) selection for general stress response mechanisms that confer both xenobiotic resistance and immunity. These results provide novel physiological insights into insecticide resistance evolution and mechanisms, as well as novel insights into parallel fitness benefits associated with selection for insecticide resistance.

Keywords: cockroach genome, gregarine, baculovirus, resistance, P450, FE4 esterase

INTRODUCTION

The German cockroach, *Blattella germanica* L. is an international urban pest that affects millions of residences on a global scale (Vargo, 2021). *B. germanica* impacts human health through the production of asthma and rhinitis-causing allergens, transmission of food-borne pathogens and psychological stress (Kopanic et al., 1994; Elgderi et al., 2006; Sohn and Kim, 2012). Up to 85% of

inner city homes in the United States test positive for cockroach allergens and 60–93% of inner-city children with asthma are sensitized to cockroaches (Gore and Schal, 2007; Do et al., 2016; Pomés et al., 2017). Cockroaches also host pro- and eukaryotic microbes that contribute to house-dust microbiomes that intensify asthma (Roth and Willis, 1960; Pai et al., 2003; Carrasco et al., 2014; Crawford et al., 2015; Thorne et al., 2015; Wada-Katsumata et al., 2015; Lai, 2017; Turturice et al., 2017).

Insecticides are essential for efficiently overcoming health impacts of cockroaches (Schal and Hamilton, 1990; Pomés et al., 2017). However, insecticide resistance has been a formidable recurring barrier to effective cockroach control for decades (Scharf and Gondhalekar, 2021). As of 2016, the German cockroach was reported as having developed resistance worldwide to 42 distinct insecticide active ingredients in at least 219 documented cases (Zhu et al., 2016). Because cockroaches live in relatively closed populations (Crissman et al., 2010; Vargo et al., 2014; Vargo, 2021), resistance can build quickly, even with moderate insecticide selection pressure (Scharf et al., 1997a,b; Gondhalekar et al., 2013; Fardisi et al., 2019). Cockroach baits are widely used in management programs and have been an effective tool for controlling cockroaches and reducing pesticide loads in urban housing (e.g., Miller and Smith, 2020); however, resistance can readily develop even to bait insecticides (Gondhalekar et al., 2011, 2013, 2016; Gondhalekar and Scharf, 2012, 2013; Ko et al., 2016; Fardisi et al., 2019).

The goal of this research was to use a quantitative metatranscriptomics approach to better understand whole-body physiological responses in *B. germanica* to defined insecticide selection pressures. The insecticide indoxacarb was used as the selecting insecticide, which is an important bait active ingredient for cockroach control (Appel, 2003; Buczkowski et al., 2008; Gondhalekar et al., 2011). Through previous studies we documented early stages of resistance evolution to indoxacarb among field populations (Gondhalekar et al., 2011, 2013) and verified hydrolysis and cytochrome P450-based oxidation as important steps in indoxacarb bioactivation and detoxification (Gondhalekar et al., 2016). Our specific objectives here were to: (1) identify whole-body mRNA expression profiles and candidate genes associated with indoxacarb resistance, and (2) investigate a subset of candidate resistance-associated genes in an independent and highly resistant field strain. Our findings reveal novel physiological insights into insecticide resistance evolution in this important global health pest; mainly that resistance evolves rapidly as a complex phenotype with multiple underlying mechanisms that include both xenobiotic detoxification and microbial clearance.

MATERIALS AND METHODS

Cockroach Strains and Rearing

The Arbor Park (AP) strain was used for indoxacarb selection experiments within 12 months of its collection and is the source of the "Parental-F0," "Selected-F6," and "Control-F6" lines (**Figure 1A**). The AP strain was collected from an apartment in Gainesville, FL, United States after control failures with multiple insecticide products. The highly resistant field-collected "Oviedo-R" strain and the standard susceptible Johnson Wax (JWax-S) strain were included in *post hoc* validation experiments. The Oviedo-R strain was collected from a restaurant near Orlando, FL, United States, where indoxacarb-containing cockroach baits were used regularly for at least 3–4 years and was tested within 6 months of its collection. The JWax-S strain has been in culture for over 70 years and has never been exposed to synthetic organic insecticides. All of the above cockroach strains were reared in mixed life stages in 1,000 cm × 400 cm × 300 cm (L × W × H) plastic boxes with aerated lids, greased walls, cardboard harborage, and an *ad libitum* water source and rodent diet (#8604, Harlan Teklad, Madison, WI, United States). Rearing conditions consisted of a 12:12 (L:D) photocycle, 25–27°C and ∼50% RH.

Chemicals

Technical grade indoxacarb (99.1% AI), blank bait matrix and formulated gel bait product containing indoxacarb (Advion®) were provided by DuPont Inc. (Wilmington, DE, United States). All solvents and buffer components were purchased from Fisher Scientific (Pittsburgh, PA, United States) or Sigma (St. Louis, MO, United States). Other chemicals used in enzyme assays and other procedures are detailed in a previous report (Gondhalekar, 2011). These chemicals include the P450 substrate *p*-Nitroanisole, the esterase substrates *p*-nitrophenyl acetate and naphthyl acetate, the GST substrate chloro-dinitro benzene, protein extraction buffers, and native PAGE reagents and stains.

Selection Procedures

For selection experiments, >1,200 large nymphs (4th to 5th instar) were separated from the AP lab cultures and divided into six sub populations of ca. 200 nymphs. These life stages were used because they are among the most tolerant cockroach life stages (Koehler et al., 1993). A feeding delivery method was used for selections because it exactly represents field exposure to indoxacarb baits (Gondhalekar et al., 2011, 2013; Gondhalekar and Scharf, 2012). In brief, pellets of blank gel bait matrix (ca. 5–10 mg wet weight) were prepared manually and treated with a dose of indoxacarb in acetone that provided ca. 60 to 80% mortality (**Supplementary Table 1**). Large nymphs that were pre-starved for 24-h were held individually with a single indoxacarb treated pellet in 1 oz. (30 mL) cups with vented lids. After 3 days, nymphs that had completely eaten bait pellets were transferred in groups of 100 into 17.8 cm × 17.8 cm × 6 cm disposable plastic Glad®boxes under conditions detailed above, where they remained for 7–10 days. Almost all nymphs exhibited intoxication symptoms at 3 days; however, ca. 25–35% completely recovered over the next 7–10 days. These surviving individuals were reared to adulthood and used as founders for the next generation (Scharf et al., 1997b). Selections continued in this manner for six generations (Parental or F0 to F5 generation). The above process happened with three replicate "selected" and "control" lines; control lines received lab diet only. Details of indoxacarb doses used and percent survival for each round of selection are given in **Supplementary Table 1**.

A **Selection Regime**

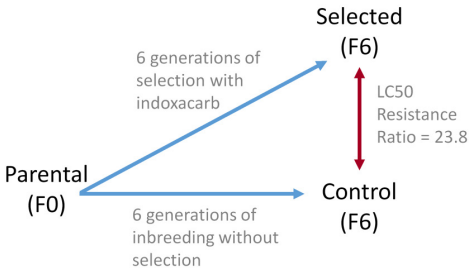

B **Indoxacarb toxicity with selection**

Strain	n	Chi-square (df)	Slope (± SE)	LC50 (95 % FL)	Resistance ratio
Selected (F6)	240	3.21 (5)	6.81 (1.62)	473.13 (414.51 – 528.15)	23.82* (14.95 – 37.96)
Control (F6)	240	3.81 (5)	1.47 (0.20)	18.87 (13.16 – 25.93)	0.96
Parental (F0)	240	2.03 (5)	1.50 (0.19)	19.74 (14.22 – 26.67)	-.--

n: total number of adult males used in vial bioassays.
Chi-square: goodness of fit to probit model and (df) degrees of freedom.
Slope: Slope of probit-mortality line with std. error (SE).
LC50: Lethal concentration estimates with 95% confidence intervals. Values are expressed in µg indoxacarb per vial.
Resistance ratio: LC50 selected or control ÷ LC50 Parental. Ratios were considered significant if the 95% CIs did not include the number 1 (P<0.05).

C **Esterase activity in F6 generations**

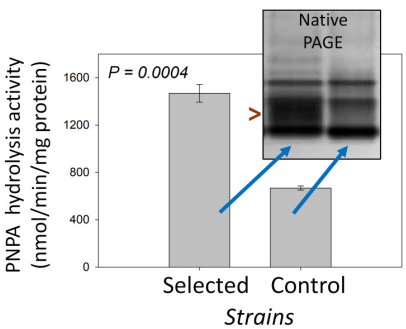

D **P450 O-demethylation activity in F6 generations**

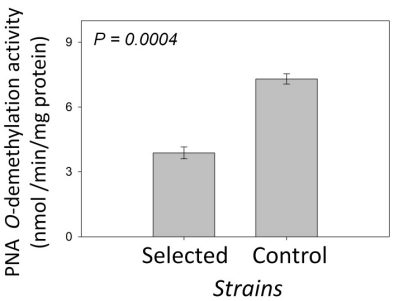

FIGURE 1 | Overview of the indoxacarb selection process and key associated findings. **(A)** Diagram of the selection regime over six generations resulting in a F6-selected strain having 23.3-fold indoxacarb resistance. **(B)** Concentration-response vial bioassay results on selected F6, control F6 and Parental F0 lines showing LC50 determination outcomes and resistance ratios. **(C)** Cytosolic esterase activity in the F6 selected and F6 control lines using the model substrate *p*-Nitrophenylacetate (PNPA) and also by native PAGE visualization (inset). **(D)** Microsomal cytochrome P450 *O*-demethylation activity in the F6 selected and F6 control lines using the model substrate *p*-Nitroanisole (PNA).

Bioassays

Bioassays performed included vial and feeding bioassays, each in two formats.

Vial Bioassays

Vial bioassays were done in concentration-response and diagnostic-concentration formats. Concentration-response bioassays were done with adult males from the Parental (F0), Control F6 and Selected F6 generations following established protocols (Gondhalekar et al., 2011; Fardisi et al., 2019). Four to five concentrations providing 10–90% mortality were used for calculating lethal concentration (LC) estimates and associated parameters using probit analysis (see below). Diagnostic concentration bioassays were done by testing adult males of the JWax-S and Oviedo-R strains at previously-established concentrations of 30 and 60 µg indoxacarb per vial (Gondhalekar et al., 2011, 2013). Three replicates of ten insects were conducted per concentration and isolate (n = 90). Control vials received acetone only.

Feeding Bioassays

Feeding bioassays were done in dose-response and no-choice formats. Dose-response bioassays were conducted with Parental (F0), Control F6 and Selected F6 generation adult males using a published protocol (Gondhalekar et al., 2011). At least four doses producing 10–90% mortality were tested against each sub-population. Each replicate had ten insects and bioassays were repeated three times for each dose and sub-population. The dose-response data were analyzed by probit analysis (details below) and used for calculating lethal doses (LD) and associated parameters. Realized heritability (h^2) estimation was done on oral dose-response data to determine the proportion of phenotypic variance in resistance caused by additive genetic variation (Falconer, 1989; Tabashnik, 1992).

No-choice assays used formulated indoxacarb gel bait product (0.6% indoxacarb) with adult males of JWax-S strain and the field-selected highly resistant Mid-Florida strain using published protocols (Gondhalekar et al., 2011). The same protocols were followed for control treatments that were conducted using blank gel bait without indoxacarb. These tests were done on lab-reared individuals within 6 months of collecting the Oviedo-R strain. In these tests no alternative/competing food other than gel bait was present in the bioassay arenas. No-choice bait feeding assays were preferred for testing the Oviedo-R strain because within 6 months after field collection the population numbers were relatively low and the bait feeding bioassay required less insects as

compared to the traditional dose or concentration-response tests. Disposable plastic GladWare boxes (17.8 cm × 17.8 cm × 6 cm; Clorox Co., Oakland, CA, United States) served as bioassay arenas and were provisioned with a water source, harborage and 0.5 g of formulated indoxacarb gel bait product in a plastic dish (Gondhalekar et al., 2011). Additional bait or blank matrix was provided if the insects consumed a majority of the initially provided bait. Mortality was recorded at 1, 3, 7, 14, and 21 days. Five replicates with 10 adult males per replicate (n = 50) were performed for each strain.

Enzyme Activity Assays

Enzyme assay methods were detailed previously (Gondhalekar, 2011). Esterase (hydrolysis) and P450 (*O*-demethylation) activity assays were done on F6-selected and control lines using the model substrates *p*-nitrophenyl acetate and *p*-nitroanisole, respectively. Esterase native PAGE was done using the model substrate beta-naphthyl acetate. Esterase and P450 investigations were done on soluble and microsomal protein preparations, respectively, made from the same insect homogenates. Protein content was normalized using a commercial Bradford assay (Bio-Rad) with bovine serum albumin as a standard. All enzyme and protein assays were performed in triplicates representing three F6-selected and three control lines.

Transcriptome Sequencing

Total RNA was isolated from three independent biological replicate samples of 10 whole adult male cockroaches from each of F6-selected and control lines. A two-step process was used that included the Promega SV Total RNA Isolation Kit (Madison, WI, United States) followed by the Bioline TRIsure kit (Taunton, MA, United States). Manufacturer protocols were followed for both kits with the exception that DNase treatment was excluded as the final step for the second kit. The use of two kits ensured the RNA samples were free of excess protein. Total RNA yields ranged from 5.8–18.6 μg with A260/280 and 260/230 ratios in the range of 1.8–2.1. Sample quality was further assessed using an Agilent Bioanalyzer (Agilent Technologies, Santa Clara, CA, United States) which verified above yields and provided acceptable RIN scores of 7.20–7.76. RNA samples were enhanced for messenger RNA (mRNA) using the Agilent TruSeq RNA prep kit before bar-coded sequencing libraries were made. Sequencing was done on the Illumina HiSeq 2000 platform by the Purdue University Genomics Core (West Lafayette, IN, United States). Sequencing reads were filtered using Phred quality scores and other parameters, and *de novo* transcriptome assembly performed from all six pooled replicate samples (3 selected and 3 control) using Trinity (Grabherr et al., 2011). Paired reads for individual replicate samples were then mapped to the *de novo* transcriptome using Bowtie2 (Langmead and Salzberg, 2012), which provided read counts used for differential expression analyses as detailed below. The *de novo* transcriptome assembly was used because a reference German cockroach genome was not yet available at the time sequencing was completed; however, new blast searches with significant contigs were performed in 2021 which confirmed origins in either the *B. germanica* genome or from other microbial sources.

GO and KAAS Annotation Analyses

The assembled contiguous sequences, i.e., "contigs" were analyzed by BLAST, Blast2GO and KAAS to assign identities and functional annotations. The contigs, as well as single-read "singletons," were annotated using "Blast2GO" for cellular location (CL), biological process (BP), and molecular function (MF) (Conesa et al., 2005). BLAST searches were performed against the Genbank "nr" database available as of May 2012 at www.ncbi.nlm.nih.gov and re-verified in June 2021 (file provided). KAAS analysis was done to gain insights into possible pathways and gene networks involved in resistance (Moriya et al., 2007). KAAS is a rapid method that establishes orthologies to genes operating within conserved pathways using best hit information and Smith–Waterman scores.

Differential Expression Analysis Methods

Basic exploration of the data such as accessing data range, library sizes etc. was performed to ensure data quality. Three models were used for analysis of read-count data obtained for each contig and singleton: edgeR (v 2.9), DESeq (v 1.8.3), and voom-limma (v 1.2.0). An edgeR object was created by combining the counts matrix, library sizes, and experimental design (3 replicates each for selected and control lines, i.e., "samples") using the edgeR package. Normalization factors were calculated for the counts matrix, followed by estimation of common dispersion of counts. An Exact test for differences between the negative binomial distribution of counts for the selected and control replicates resulted in finding differential expression, which was then adjusted for multiple-hypothesis testing to generate a result file. A DESeq object analogous to the aforementioned edgeR object was created and used to generate normalization factors followed by dispersion estimates using DESeq package. The DESeq method tests for differences between the base means of the experimental conditions and differential expression (DE) results were reported in another result file (DE_analysis_DESeq.csv). A third method called 'voom' from the limma package was also used for DE analysis. The 'voom' function carries out log2 transformation of counts followed by mean-variance estimation and assigns weight to each transformed value. Linear model coefficients were then calculated using limma's design matrix and log2 transformed values. The linear model was fitted using an empirical Bayes method and differences between counts between selected and control replicates were calculated, which was then adjusted for multiple-hypothesis testing, and reported as result file. Venn diagrams were generated displaying the DE contigs with false discovery rate (FDR) $P < 0.05$ that were found to be common among all three analysis methods using the online tool Venny[1].

Quantitative Real-Time PCR

Expression levels of 48 significantly up- and down-regulated genes identified from Illumina sequencing (**Table 1**) were investigated for validative purposes by qRT-PCR in the F6-selected and control lines (three biological replicates each). PCR primers for target and reference genes were designed

[1]http://bioinfogp.cnb.csic.es/tools/venny/index.html

using Primer 3[2] (Untergasser et al., 2012) and are given in **Supplementary Table 2**. The efficiencies of qPCR primers used in this experiment were empirically determined and they were within the recommended range of 90–110%. Validative qRT-PCR was done on aliquots of the same RNA preparations used for Illumina sequencing above using an iCycler iQ real-time PCR detection system (Bio-Rad, Hercules, CA, United States) with Sybr Green product tagging (2x SensiMix Sybr and Fluorescein Kit; Quantace, Norwood, MA, United States). Each 20 μL qRT-PCR reaction in a 96-well format consisted of 10 μL SensiMix (Bioline, Taunton, MA, United States), 7 μL nanopure water, 1 μL each of forward and reverse primer (0.5 μM final concentration) and 1 μL cDNA. A published qRT-PCR temperature program was followed (Scharf et al., 2008). Three technical replicates were performed for each gene and cDNA preparation. The resulting critical threshold (*C*q) data were analyzed by the $2^{-\Delta CT \Delta CT}$ method (Livak and Schmittgen, 2001).

Expression of a subset of 21 genes (indicated by asterisks* in **Table 1** and **Supplementary Table 2**) that showed significant differential expression in transcriptome analyses was also quantified in the lab-susceptible JWax-S and resistant Oviedo-R strains. These genes included 13 host cockroach genes (8 P450s, 2 carboxylesterases, 1 chitinase, 1 transposable element, and 1 hypothetical protein) and 8 genes from eukaryotic/viral microbiota (4 virus, 2 gregarine, 1 coccidia, and 1 unknown). Total RNA was extracted from 1 to 2 weeks old adult males in three replicate groups of 10 for the above two strains. RNA extractions were done using the two- step process described under "Transcriptome Sequencing." cDNA synthesis was done from 500 ng total RNA using the iScript^{TM} cDNA synthesis kit (Bio-Rad, Hercules, CA, United States). All qPCR procedures and expression analysis methods were similar to those mentioned above.

Statistical Analyses

Probit analysis was used for LD and LC determinations using SAS software Version 9.2. Mortality data were corrected for control mortality (<10%) using Abbott's transformation prior to conducting Probit analysis. Resistance ratios (RRs) were calculated by dividing LC or LD estimates for the selected lines by corresponding values for susceptible lines. Significance of RRs was determined according to the procedure outlined by Robertson and Preisler (1992). Mean-separation analyses of insecticide toxicity (vial diagnostic and no choice bait feeding bioassays) were done by ANOVA and paired t-tests ($P < 0.05$) after arcsine transformation of raw mortality data. For enzyme activity assays, specific activity values for the F6-selected and susceptible sub-populations were compared by non-parametric Mann–Whitney *U* tests ($P < 0.05$). Methods used for differential gene expression analysis of read-count data from transcriptome sequencing are explained in a separate section above. Regression analyses were done using JMP Pro 15 software (SAS Institute, Cary, NC, United States) to compare (i) qRT-PCR results to Illumina read counts for the F6-selected and control lines ($n = 48$ genes), and (ii) the F6-selected and control lines to each other and the Oviedo-R and JWax-S strains ($n = 21$ genes).

[2]https://bioinfo.ut.ee/primer3-0.4.0/

RESULTS

Selection and Resistance Evolution

Six generations of selection of the parental AP strain with indoxacarb bait (**Figure 1A**) resulted in a selected strain having significant levels of resistance in both surface contact (23.8×; **Figure 1B**) and feeding bioassays (4.5×; **Supplementary Table 2**). The control strain left to inbreed without selection over the same timeframe acquired no resistance. The selection process led to heritable genetic changes with a realized heritability estimate (h2) of 0.28 (**Supplementary Table 3**). Biochemical assays on the F6-selected and control lines revealed >2× elevated esterase activity ($P = 0.0004$; **Figure 1C**) and ∼0.5× decreased P450 *O*-demethylation activity ($P = 0.0004$; **Figure 1D**).

Metatranscriptome Sequencing and Assembly

From six total libraries representing three replicates each of the selected and control lines, 133 million paired-end sequence reads were obtained that contained >1.3 billion total nucleotide bases having an average read length of 98 base pairs (bp). The resulting overlapping sequences were assembled into 207,672 contiguous sequences, hereafter referred to as "contigs." Sequence reads are deposited in the NCBI GEO archive under accession number GSE188950.

Validation of *de novo* Transcriptome and Differentially Expressed Contigs

Contig length ranged from 201 to 30,113 bp with an average length of 1,777 bp and a N50 size of 4,805 bp; i.e., half of the assembled metatranscriptome is covered by contigs ≥ 4,805 bp. Next, a subset of 48 assembled contigs was chosen for validation analysis by qRT-PCR using the same RNA preparations as were used for Illumina sequencing (**Table 1**). A regression plot of log2 transformed Illumina transcriptome read count (X) vs. log2 transformed qRT-PCR Cq values (Y) revealed a highly significant correlation ($P < 0.0001$, $r^2 = 0.51$) (**Supplementary Figure 1**). The latter result independently verifies the accuracy of the metatranscriptome results.

DE analysis by three different models yielded differing numbers of passing contigs (**Figure 2**). Different FDR *p*-values were considered ($P < 0.05, 0.01, 0.001$) but the greatest emphasis is placed on the $P < 0.001$ level. The most stringent analysis model was edgeR with 473 passing contigs (**Figure 2A**), followed by voom-limma with 1,089 (**Figure 2B**) and DESeq with 2,209 (**Figure 2C**). Another interesting feature of the datasets for all three models was the higher ratio of downregulated:upregulated contigs in the selected strain; i.e., 424:49 for edgeR, 960:129 for voom-limma, and 2,083:126 for DESeq. Overall, there were 236 significant DE contigs shared among all three analysis models at the FDR $P < 0.01$ level and log2FC of ±1 (**Figure 2D**). Only

TABLE 1 | An overview of 53 transcript contigs that were significantly differentially expressed with selection for indoxacarb resistance.

Contig no.	Best blastX match (Genbank, 2021)[1]	Best *Blattella germanica* genome match	Fold change	FDR adj. *P*-Value	Contig length
1*	Hypothetical protein C0J52_04259 (*Blattella germanica*) short match of 92%	Hypothetical protein C0J52_04259 (*B. germanica*) short 92% match	83.94	0.00009	792
2*	PiggyBac transposable element-derived protein 3 (*Cryptotermessecundus* LOC111875436)	No match	67.05	0.00001	501
3*	Cytochrome P450 6k1 (*Blattella germanica*)	97% match to hypothetical protein C0J52_26426 (*B. germanica*)	48.15	0.00012	694
4*	Putative Cytochrome P450 6a14 (*Blattella germanica*)	100% match to PSN34612.1 from *B. germanica* genome	39.40	0.00003	1142
5*	Cytochrome P450 6j1 (*Cryptotermes secundus*)	66% match to hypothetical protein C0J52_26426 (*B. germanica*)	34.22	0.00003	1095
6*	Cytochrome P450 6j1 (*Cryptotermes secundus*)	70% match to hypothetical protein C0J52_26426 (*B. germanica*)	33.82	0.00019	2042
7*	Cytochrome P450 6j1 (*Cryptotermes secundus*)	79% match to hypothetical protein C0J52_26426 (*B. germanica*)	33.54	0.00002	476
8*	Cytochrome P450 6j1 (*Cryptotermes secundus*)	100% match to hypothetical protein C0J52_26426 (*B. germanica*)	31.25	0.00054	531
9*	Cytochrome P450 6j1-like (*Cryptotermes secundus*)	81% match to hypothetical protein C0J52_26426 (*B. germanica*)	30.45	0.00037	1105
10*	Cytochrome P450 6k1-like (*Zootermopsis nevadensis*)	100% match to hypothetical protein C0J52_20551 (*B. germanica*)	17.44	0.00018	546
11	Putative Cytochrome P450 6a14 (*Blattella germanica*)	86% match to hypothetical protein C0J52_20551 ((*B. germanica*)	7.85	0.00018	2940
12	Cytochrome P450 6j1 (*Cryptotermes secundus*)	66% match to hypothetical protein C0J52_26426 (*B. germanica*)	6.83	0.00001	2807
13	Cytochrome p450 15F1 (*Reticulitermes flavipes*)	99% match to Methyl farnesoate epoxidase, partial (*B. germanica*)	6.81	0.00003	2003
14	Cytochrome P450 4C1; AltName: Full = CYPIVC1 (*Blaberus discoidalis*)	53% match to Cytochrome P450 4C1 (*B. germanica*)	6.33	0.00026	1974
15	Cytochrome P450 6j1 (*Cryptotermes secundus*)	85% match to hypothetical protein C0J52_26834 (*B. germanica*)	5.31	0.00000	2390
16	Cytochrome P450 4C1 (*Cryptotermes secundus*)	54% match to Cytochrome P450 4c21 (*B. germanica*)	5.13	0.00030	1687
17	1,5-anhydro-D-fructose reductase (*Cryptotermes secundus*) 75% match	63% match to 1,5-anhydro-D-fructose reductase (*B. germanica*)	4.91	0.00014	997
18	Per a allergen (*Periplaneta americana*)	63% match to Glutathione *S*-transferase (*B. germanica*)	4.11	0.00003	991
19	Cytochrome P450 6j1 (*Cryptotermes secundus*)	82% match to hypothetical protein C0J52_12805 (*B. germanica*)	3.83	0.00000	2083
20	Cytochrome P450 6j1 (*Cryptotermes secundus*)	48% match to Cytochrome P450 6j1 (*B. germanica*)	3.36	0.00003	1830
21	Peritrophic membrane protein 4, partial (*Holotrichia oblita*)	80% match to hypothetical protein C0J52_18875 (*B. germanica*)	2.64	0.00003	294
22	Venom carboxylesterase-6-like (*Zootermopsis nevadensis*)	99% match to hypothetical protein C0J52_16277 (*B. germanica*)	2.60	0.00082	3127
23	Cytochrome P450 6j1 (*Cryptotermes secundus*)	99% match to hypothetical protein C0J52_26834 (*B. germanica*)	2.30	0.00000	2568
24	Esterase FE4 (*Zootermopsis nevadensis*)	62% match to hypothetical protein C0J52_03840 (*B. germanica*)	1.77	0.00033	2177
25	Aldehyde dehydrogenase, partial (*Blattella germanica*) 100% match	Aldehyde dehydrogenase, partial (*B. germanica*) 100% match	1.70	0.00000	5007
26*	Chitinase-3-like protein 1 isoform X2 (Zootermopsis nevadensis)	73% match to hypothetical protein C0J52_01400 (*B. germanica*)	1.60	0.00060	2432
27	Chitin deacetylase 2 (*Nilaparvata lugens*)	100% match to hypothetical protein C0J52_26402 (*B. germanica*)	0.603	0.00038	2454
28	Bacterial aldo/keto reductase (Ruminococcus sp.)	No match	0.601	0.00058	2418
29	Cytochrome P450 4C1 (*Blattella germanica*) 100% match	Cytochrome P450 4C1 (*B. germanica*) 100% match	0.482	0.00082	2742
30*	Esterase FE4 (*Blattella germanica*) 99% match	Esterase FE4 (*B. germanica*) 99% match	0.405	0.00029	2208

(Continued)

TABLE 1 | (Continued)

Contig no.	Best blastX match (Genbank, 2021)[1]	Best *Blattella germanica* genome match	Fold change	FDR adj. *P*-Value	Contig length
31	Cytochrome P450 9e2 (*Zootermopsis nevadensis*)	78% similar to hypothetical protein C0J52_03714 (*B. germanica*)	0.381	0.00028	2335
32	Protist ERD2 (endoplasmic reticulum retention receptor) (*Symbiodinium necroappetens*)	No match	0.163	0.00044	4453
33*	Venom carboxylesterase-6 (*Blattella germanica*) 55% identity	Venom carboxylesterase-6 (*B. germanica*) 55% identity	0.153	0.00036	2132
34	Fungal membrane transporter (*Diplocarpon rosae*)	No match	0.142	0.00090	5851
35	GREGARINE piwi domain protein (*Gregarina niphandrodes*)	No match	0.136	0.00070	3424
36	Bacterial chitinase (*Legionella nagasakiensis*)	No match	0.123	0.00028	2674
37	PROTIST lysophospholipase II (*Nannochloropsis gaditana* CCMP526)	No match	0.113	0.00058	3625
38	GREGARINE chitinase (*Gregarina niphandrodes*)	No match	0.109	0.00026	1840
39	GREGARINE glutathione *S*-transferase (*Gregarina niphandrodes*)	No match	0.108	0.00022	2616
40	GREGARINE chitinase/lysozyme protein (*Gregarina niphandrodes*)	No match	0.107	0.00029	857
41	GREGARINE indolepyruvate decarboxylase (*Gregarina niphandrodes*)	No match	0.104	0.00022	2027
42	GREGARINE aldehyde dehydrogenase (*Gregarina niphandrodes*)	No match	0.101	0.00035	1772
43	Insect glutathione *S*-transferase 1-like (*Aricia agestis*)	No match	0.096	0.00051	4634
44	COCCIDIA ABC1 family protein (*Toxoplasma gondii* VEG)	No match	0.092	0.00028	4696
45	GREGARINE ATP-binding ABC transporter, partial (*Gregarina niphandrodes*)	No match	0.082	0.00078	2531
46*	GREGARINE superoxide dismutase (*Gregarina niphandrodes*)	No match	0.078	0.00044	830
47*	COCCIDIA phospholipase/carboxylesterase (*Toxoplasma gondii* GT1)	No match	0.072	0.00061	1338
48*	GREGARINE glutathione *S*-transferase (*Gregarina niphandrodes*)	No match	0.069	0.00026	2156
49*	BACTERIAL NAD-dependent formate dehydrogenase (*Granulicella* sp. S156)	No match	0.034	0.00086	1358
50*	Virus polyprotein 1 (Praha dicistro-like virus 2) 97% match	No match	0.013	0.00000	1897
51*	No match	No match	0.007	0.00001	1218
52*	Virus polyprotein 2 (Praha dicistro-like virus 2) 96% identity	No match	0.005	0.00000	2499
53*	Virus RNA-dependent RNA polymerase RdRp (Hubei permutotetra-like virus 8)	No match	0.001	0.00002	5487

The order shown is ranked from most highly upregulated (top) to most downregulated (bottom). All 53 contigs were tested in qRT-PCR validations against Illumina read count data, and a subset of 21 contigs indicated by asterisks was used for post hoc regression comparisons between different strains (see **Figure 6**). Values shown are based on voom-limma analysis. See **Supplementary Table 2** for primer sequences. [1]nr database at ncbi.nlm.nih.gov/genbank/.*

contigs passing in two or more models at the FDR < 0.001 log2FC ± 1 level were considered for further analysis as detailed below.

GO Annotation and KAAS Pathway Analyses

BLAST2GO analyses for gene annotation revealed that 36.6% of contigs were annotated (76,053). For $P < 0.001$ passing contigs there were 779 GO terms for cellular location (CL; 99 upregulated, 680 downregulated), 1,514 for molecular function (MF; 209 up, 1,305 down) and 1,493 for biological process (BP; 265 up, 1,288 down) (**Supplementary Figure 2A**). CL terms potentially related to insecticide resistance include membrane, ribosome, mitochondria, microsome, endoplasmic reticulum and dendrite (**Supplementary Figures 2B–D**). Potentially relevant MF terms include electron carrier, hydrolase, monooxygenase, oxidoreductase, transferase and catalytic activity; and ATP, calcium, iron, heme, nucleotide and sugar binding. Lastly, relevant BP terms potentially linked to resistance include metabolic, transport, phosphorylation, glutathione conjugation and response to drug.

KAAS analysis was used to gain further insights into responsive pathways and gene networks (**Supplementary Figure 3**). Upregulated pathways potentially linked to resistance

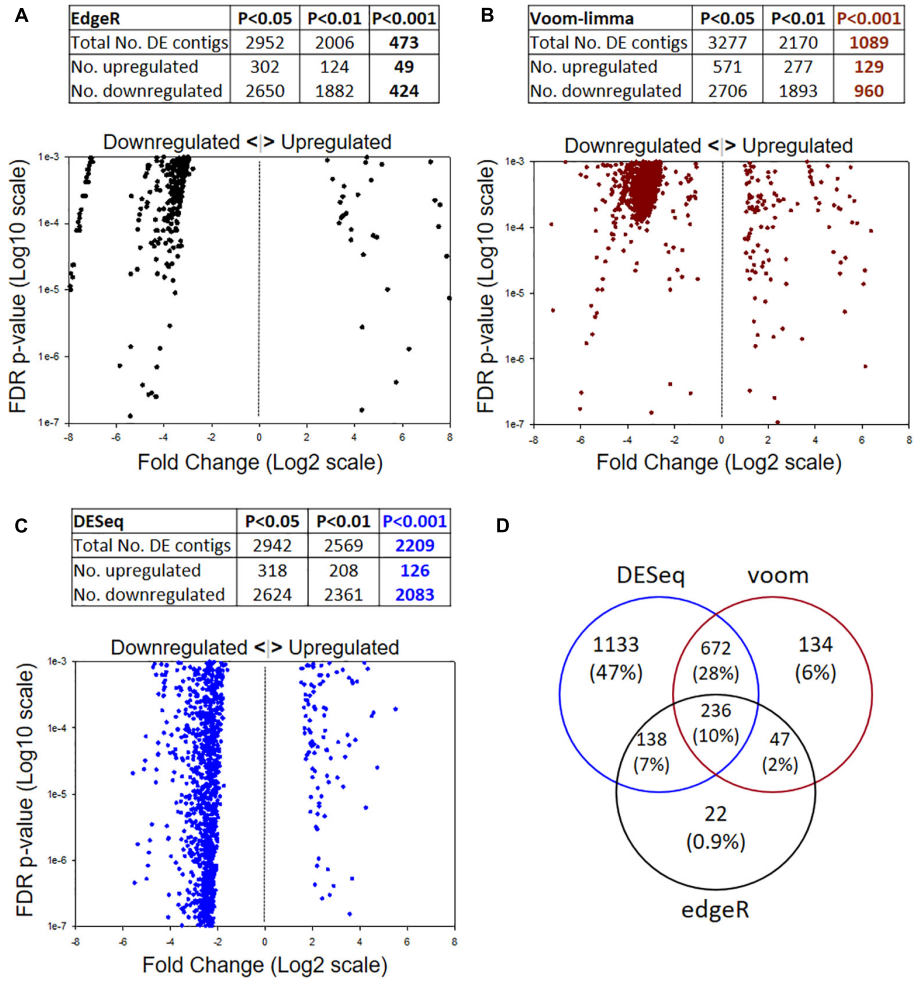

FIGURE 2 | Illumina metatranscriptome analysis by three different models: **(A)** edgeR, **(B)** voom-limma and **(C)** DESeq. The top of each panel shows summary statistics for differentially expressed contigs and different false discovery rate (FDR) *p*-values. The bottom of each panel shows scatter plots of Log2 Fold Change (*x*) by *p*-value (*y*) for the FDR $P < 0.001$ datasets. **(D)** Venn diagram showing the numbers of passing contigs at the $P < 0.001$ level shared among different analysis models. The edgeR model was the most stringent at the $P < 0.001$ level.

included drug metabolism by Cytochrome P450, fatty acid biosynthesis and pentose/glucuronate interconversion. Key downregulated pathways were related to microbial metabolism, viral infection, ribosome function/biogenesis, phagosomes, RNA degradation and epithelial cell signaling.

Candidate Genes and Taxonomic Matches of Differentially Expressed Transcripts

The blastx identities of many upregulated transcripts had logical links to resistance and detoxification. Upregulated cockroach genes included many gene families commonly associated with insecticide resistance including P450 oxidases and hydrolases (**Figure 3**) and glutathione-*S*-transferases (GSTs). **Table 1** overviews the 21 contigs (shown by asterisks*) used for *post hoc* validations and gives a general overview of upregulated transcripts that mainly match the *B. germanica* genome, along with downregulated transcripts that originate mainly from microbial sources. The identities of sequences from either cockroach or microbial origins were re-verified by Genbank blastX searches performed in September 2021 (**Table 1**).

Taxonomic compositions of significant DE contigs ($P < 0.001$), based on blastx database queries, indicate the majority of upregulated contigs are from the cockroach genome; whereas, the majority of downregulated contigs come from viruses and eukaryotic microbes (**Figure 4**). Top upregulated taxonomic matches at the domain level were overwhelmingly eukaryotic whereas downregulated contigs had >10-fold more numbers of matches to bacteria, viruses and archaea than insects. At the genera level the top taxonomic matches for upregulated contigs were nearly all insects (*Blattella*, *Cryptotermes*, *Zootermopsis*, *Coptotermes*, *Timema,* and *Periplaneta*). Downregulated transcripts at the genus level were dominated by eukaryotic microbes that are apparently commensal, pathogenic and/or parasitic

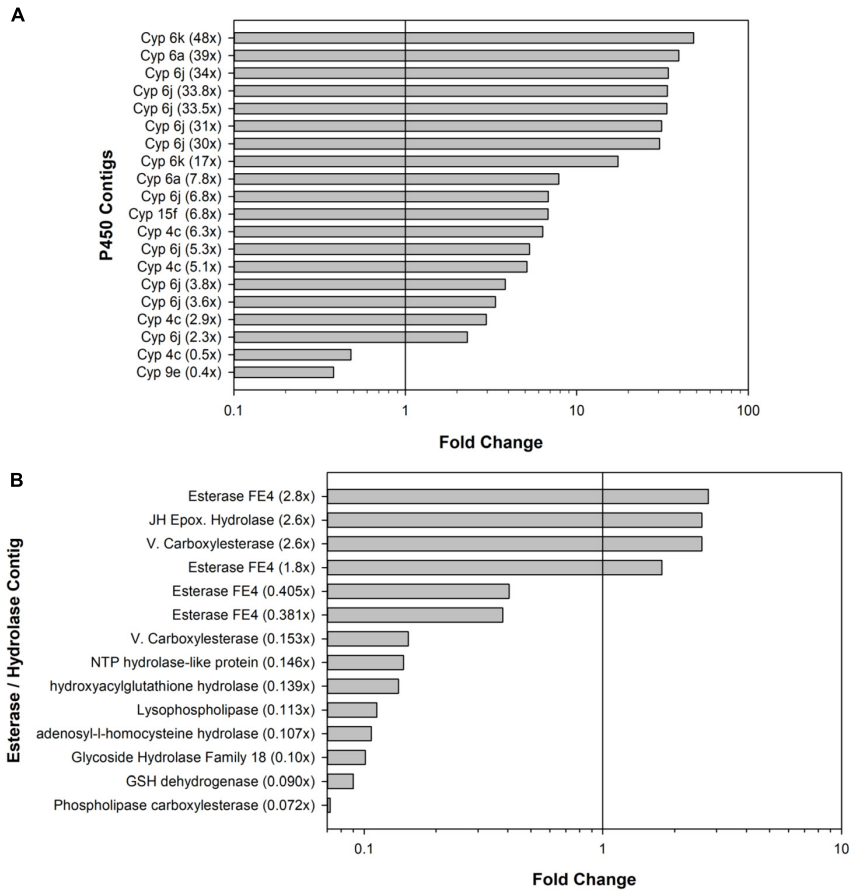

FIGURE 3 | Bar graphs showing the numbers of significant differentially expressed contigs. **(A)** Cytochrome P450 (Cyp) contigs and **(B)** esterase and hydrolase contigs. Bars to the right of vertical black lines indicate upregulated contigs; bars to the left indicate downregulated contigs.

(*Gregarina*, *Cryptosporidium*, *Toxoplasma*, *Vitrella*, *Plasmodium*, *Neospora*, etc.).

Post hoc Validations in an Independent Resistant Strain

An independent resistant strain, Oviedo-R, was collected from the field after indoxacarb bait control failures and assayed alongside the standard susceptible JWax-S strain. The Oviedo-R strain was highly resistant with 0% mortality in vial bioassays on diagnostic concentrations of indoxacarb (**Figure 5A**). These diagnostic concentrations were approximately two and fourfold higher than the indoxacarb LC50 for the Control (F6) strain shown in **Figure 1B**. The JWax-S strain was highly susceptible with 100% mortality in the same assays. When tested in no-choice feeding bioassays with commercially-formulated indoxacarb bait, the Oviedo-R strain displayed exceptionally high resistance (ANOVA df = 1,48, $F = 130.50$, $P < 0.001$) (**Figure 5B**). The Oviedo-R strain entirely consumed 0.5 g indoxacarb bait per assay replicate by Days 7 and 14, at which time the bait was replenished. These results show high levels of physiological resistance to indoxacarb in the Oviedo-R strain with no involvement of a behavioral "aversion" component.

Finally, to test for common patterns of gene expression across strains, qRT-PCR analyses were performed on a subset of 21 significant up- and down-regulated contigs identified from the transcriptome analysis presented above (**Table 1** and **Supplementary Table 2**). The four strains included in this analysis were Oviedo-R, JWax-S, indoxacarb Selected-F6 and Control-F6. From a series of regression analyses, there was significantly correlated transcript abundance between the Selected-F6 and Oviedo-R strains (**Figure 6A**), but no correlation when comparing Oviedo-R vs. Control-F6 (**Figure 6B**), Control-F6 vs. Selected-F6 (**Figure 6C**), and JWax-S vs. Selected F6 (**Figure 6D**). These results suggest common processes associated with indoxacarb resistance evolution in lab and field-selected cockroach populations.

DISCUSSION

Overview

This study reveals new insights into cockroach insecticide resistance evolution from multiple physiological perspectives. Through a combination of approaches including selection for

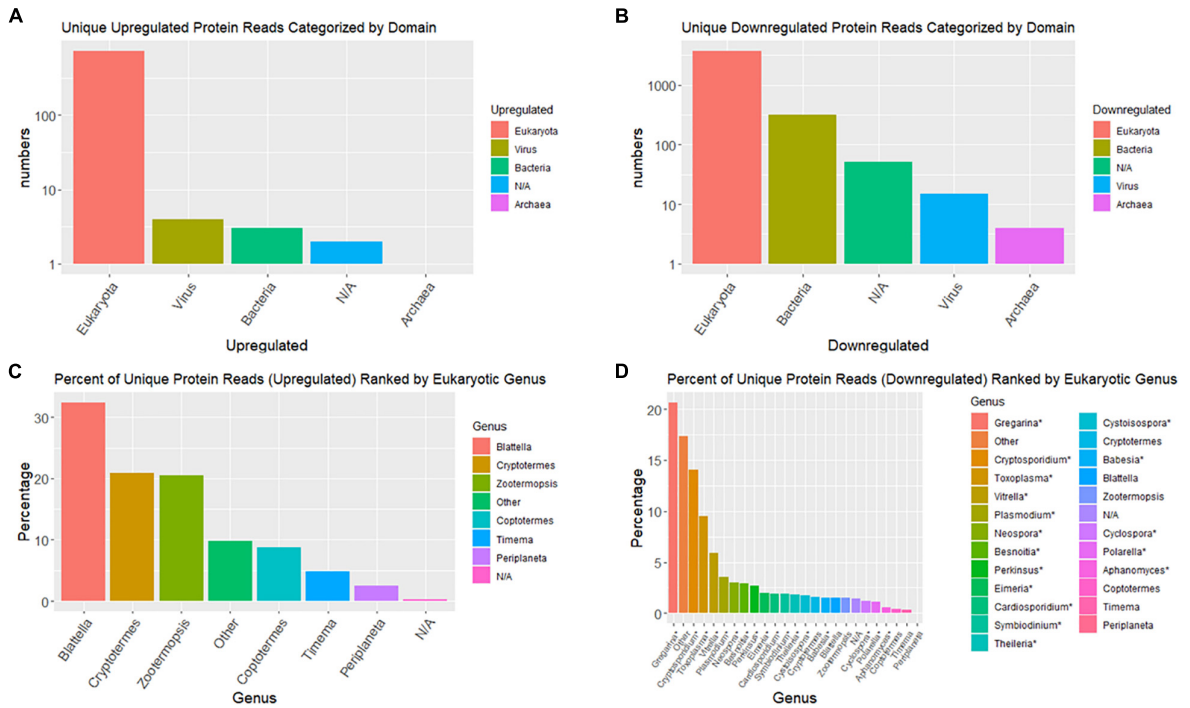

FIGURE 4 | Bar graphs summarizing top taxonomic matches of top BlastX hits for differentially expressed contigs. **(A,B)** Are domain-level taxonomic matches and **(C,D)** are genus-level. **(A,C)** Are upregulated contigs and **(B,D)** are downregulated.

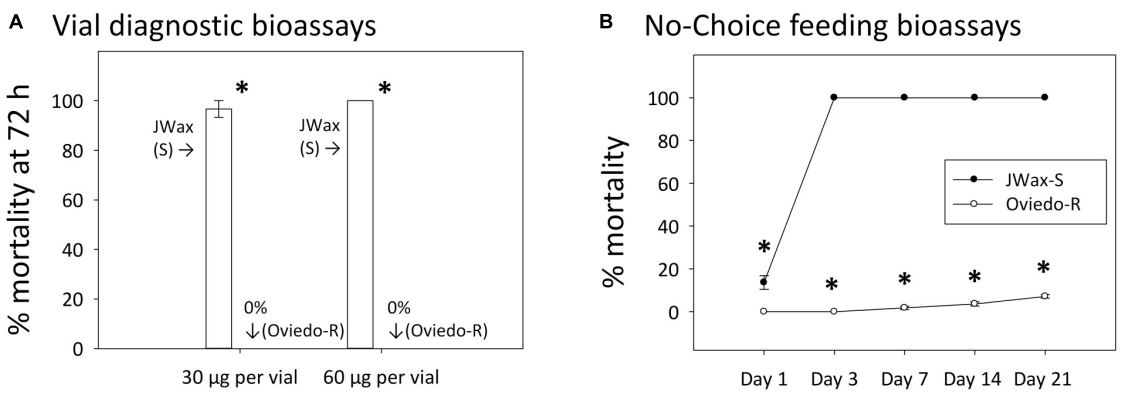

FIGURE 5 | Indoxacarb bioassay results for the highly resistant Oviedo-R strain and the standard susceptible JWax-S strain. **(A)** Vial diagnostic concentration bioassays at two concentrations showing high-level mortality and the JWax-S strain and 0% mortality in the Oviedo-R strain. **(B)** No-choice feeding bioassays using commercial formulated indoxacarb bait showing rapid high-level mortality in the JWax-S strain and virtually no mortality in the Oviedo-R strain. *Asterisks indicate significant differences between strains at $P < 0.0001$.

resistance via feeding on insecticidal bait, coupled with different bioassay formats and metatranscriptome sequencing, we were able to observe that (1) the host cockroach mainly upregulates a range of detoxification resistance mechanisms, and (2) at the same time decreases its internal virus, parasite and/or pathogen levels. Further investigation of candidate gene expression in the highly resistant Oviedo-R strain suggests common phenomena that underlie resistance evolution. Taken together, these findings support the idea that high-level resistance evolution results from a dual process whereby the host tolerates the selecting insecticide through a number of potential mechanisms, and in parallel, host fitness is further increased as the body is cleared of parasites and pathogens. At present it remains unclear if the microbial impacts result from (i) direct effects of indoxacarb, (ii) indirect effects of antimicrobial preservatives included in the selecting bait matrix, or (iii) selection for general stress response mechanisms that confer both xenobiotic resistance and microbial immunity. With respect to the first two possibilities, it is unclear if these processes are associated generally with all insecticides, or specifically with ingested indoxacarb.

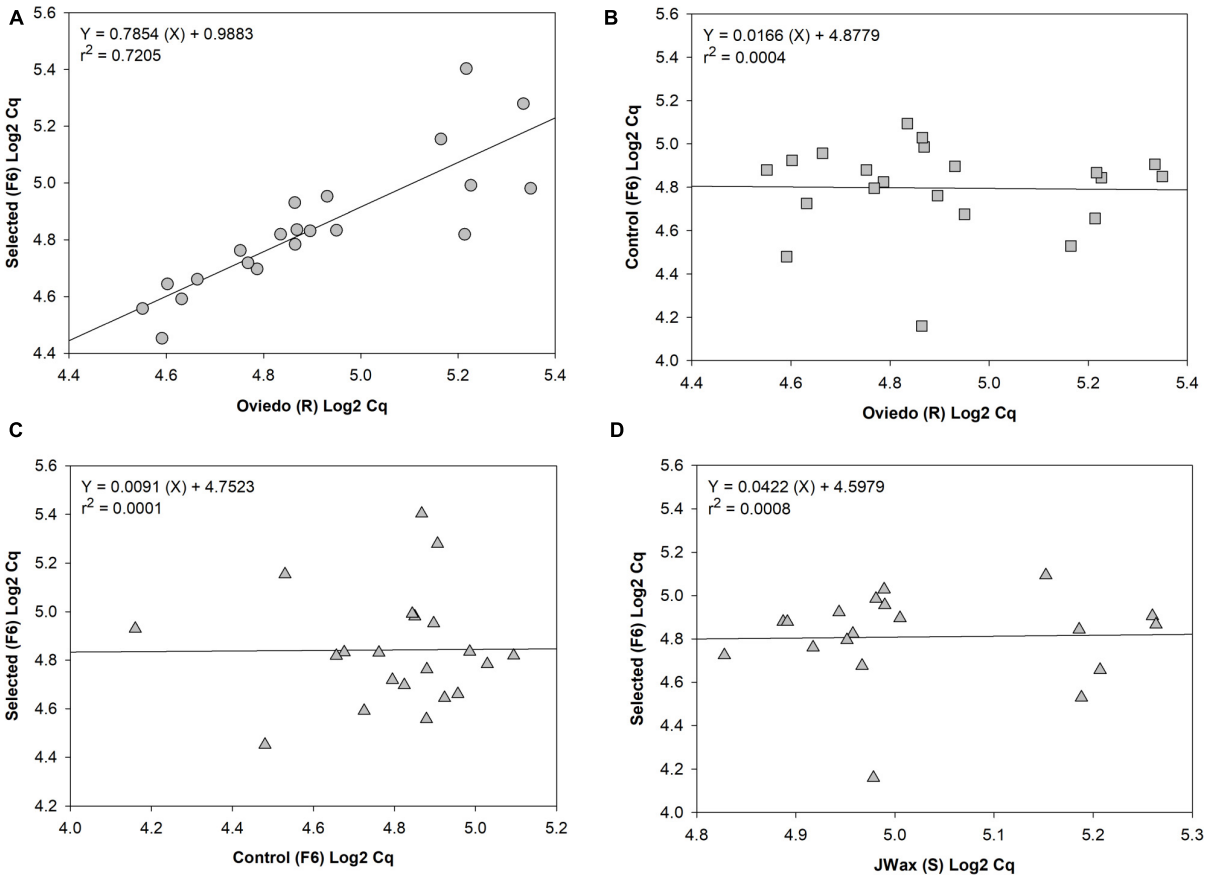

FIGURE 6 | Regression analyses of qRT-PCR relative expression data for 21 significant differentially expressed contigs. Results show **(A)** well-correlated gene expression between the selected-F6 and highly resistant Oviedo-R strains, but no correlation when comparing **(B)** Oviedo vs. Control-F6, **(C)** Control-F6 vs. Selected-F6, or **(D)** JWax-S vs. Selected F6. All *Cq* data were Log2 transformed before performing regressions.

Transcriptome sequencing revealed dozens of candidate upregulated genes from the host cockroach potentially involved in resistance, including detoxification enzymes (discussed below), transport mechanisms, host gut penetration barriers, and others. An unanticipated result was the downregulation thereby indicating disappearance of commensal, pathogenic and/or parasitic microbe transcript contigs after insecticide selection (also discussed below). Findings in both categories are corroborated by the GO and KAAS analyses, which provide additional independent confirmation for the sequence composition results relating to detoxification and parasite/pathogen disappearance. The qPCR correlation analyses between resistant and susceptible strains lends further strength to the above findings. Specifically, the regression analyses showed similar trends between independently-selected resistant strains for upregulation and downregulation of host detox mechanisms, and disappearance of a wide range of microbes. However, there appears to be wider variation with respect to disappearance of microbial contigs (right side of **Figure 6A**). This finding is logical given that different environments have different microbiomes associated with them that can, in turn, shape internal microbiomes of higher organisms living within them (Renelies-Hamilton et al., 2021; Tinker and Ottesen, 2021).

Detoxification and Metabolism Mechanisms

In terms of detoxification and metabolism, indoxacarb is a unique pro-insecticide that requires hydrolytic activation to its decarbomethoxyllated "DCJW" metabolite to become an active insecticide (Wing et al., 2000; Alves et al., 2008). A prior study investigating indoxacarb metabolism pathways in resistant and susceptible *B. germanica* strains revealed that hydrolysis and P450-oxidation were important to activation and resistance-associated detoxification, respectively (Gondhalekar et al., 2016). The current study reveals candidate genes involved in both oxidative and hydrolytic metabolism of indoxacarb; specifically, 20 differentially expressed (DE) P450 contigs and 14 DE esterase/hydrolase contigs. In theory, resistance could result from both upregulation of P450 oxidative enzymes and downregulation of hydrolases, both of which were detected in the present study.

With respect to detoxification genes and the *B. germanica* genome, a targeted analysis revealed 158 P450 genes total, which

represents some gene expansions in relation to the available genomes of close insect relatives (Harrison et al., 2018a,b). The most expanded P450 families were Cyp4 (n = 59), followed by a subset of Cyp6 (n = 8). The present study identified resistance-associated changes of expression of 12.6% of the *B. germanica* "cypome," with the majority (14) being Cyp6 members and fewer being Cyp4s (4). It is also noteworthy that a transposable element potentially associated with Cyp4 expansion (Harrison et al., 2018b) had higher resistance-associated expression in both the indoxacarb-selected line and the field-selected Oviedo-R strain. Expansions previously identified for other detoxification genes in the *B. germanica* genome included 62 E4 esterases and a subgroup of 23 GST genes (Harrison et al., 2018b). The present study identified 14 DE esterases (4 up- and 10 down-regulated) and 11 GSTs (6 up- and 5 down-regulated). Significant changes in both P450 and esterase activity were noted with selection (**Figure 1**) but not GST activity (Gondhalekar, 2011).

Numerous DE P450 contigs identified here were close homologs to Cyp6J1 and 6K1 of *B. germanica* (Wen and Scott, 2001), but none were identical matches. Some of these Cyp6 homologs had 20–50× upregulation with indoxacarb selection. Based on these results it is likely that there is Cyp6 involvement in the detoxification pathway for indoxacarb (Gondhalekar et al., 2016) and more Cyp6 diversity in the *B. germanica* genome than initially suggested (Wen and Scott, 2001; Harrison et al., 2018b). A previous study found Cyp4G19 over expression in association with fipronil and imidacloprid resistance in *B. germanica*, but not indoxacarb resistance, which agrees with results of the present study finding no change of expression for Cyp4G P450s. Cyp4G19 was also linked to pyrethroid resistance, cuticular hydrocarbon production and cuticular penetration-based resistance (Pridgeon et al., 2003; Guo et al., 2010; Pei et al., 2019; Chen et al., 2020; Hu et al., 2021), which are seemingly unrelated to the ingestion and gut uptake that occurred during the six generations of indoxacarb selection that were done in the present study.

The current study also identified DE homologs of Cyp9e2 and Cyp4C21 with possible roles in indoxacarb biotransformation. Both Cyp9e2 and Cyp4C21 were previously identified from *B. germanica* along with apparent homologous pseudogenes that may confound gene identification (Wen et al., 2001). Another upregulated P450 in the present study was Cyp15F1, which catalyzes the last step in juvenile hormone biosynthesis (Maestro et al., 2010; Tarver et al., 2012; Zhou et al., 2014). The Cyp15F1 homolog identified in the present study had a strong match to its corresponding genomic sequence reported in the *B. germanica* genome (Harrison et al., 2018a,b). It is not clear if Cyp15F1 participates in indoxacarb detoxification or another physiological process related to gut tissue remodeling after indoxacarb exposure, or in response to clearance of gut microbes (e.g., Sen et al., 2015). A previous study identified the P450 protein "P450MA" from a multi-resistant *B. germanica* strain (Scharf et al., 1998). P450MA was overexpressed after organophosphate insecticide selection and also was found to be over-expressed in organophosphate resistant *B. germanica* strains from different global origins (Scharf et al., 1997b, 1999). While the molecular identity of P450MA remains unknown, it may be among the P450s identified in the present study, of which Cyp6 members were the most abundant.

Lastly, the identification of decreased P450 *O*-demethylation activity in the F6-selected strain does not appear to be an erroneous or trivial result. This is because there is good agreement between reduced *O*-demethylation activity in our F6-selected indoxacarb-resistant strain and transcriptome results showing downregulation of several P450 contigs in the same genetic lineage. This latter finding also suggests that increased *O*-demethylation activity may not be a useful biomarker for indoxacarb resistance.

With regard to hydrolytic activity, it is considered more important for indoxacarb activation in *B. germanica* than detoxification (Gondhalekar et al., 2016). Esterases and associated hydrolases are overall not as well studied as the P450s discussed above, but several DE hydrolase and esterase homologs were identified through the current study. Several of these DE esterase contigs had significant matches to FE4 esterases from other insects with well-established roles in insecticide metabolism (Field and Foster, 2002; Srigiriraju et al., 2009). Esterase activity toward model substrates was also elevated in the F6-selected strain, which is consistent with the several upregulated esterase/hydrolase contigs that were identified through transcriptome sequencing. It is also possible that, despite being important for indoxacarb activation, increased hydrolytic activation could still enable greater detoxification by P450 and other detox enzymes and subsequent clearance from the body (Gondhalekar et al., 2016) by Glutathione-*S*-transferases, some of which were also upregulated.

Microbial Disappearance

Invertebrates were the first hosts of apicomplexan parasites like *Plasmodium* and *Toxoplasma* which later switched to vertebrate hosts during their evolution (Kopecná et al., 2006). Biotic associations of cockroaches with microbes have been known for over 100 years and include bacteria, archaea, viruses, protists, fungi, gregarines, and nematodes (Roth and Willis, 1960; Kakumanu et al., 2018). In the present study, transcript contigs from representatives of all of these groups were greatly reduced with indoxacarb selection. Omics approaches similar to those used here have previously identified gregarines and other eukaryotic microbes in insects and thus it should not be surprising that similar eukaryotic microbe transcripts were identified in the present study through the use of poly-A RNA tagging (McCarthy et al., 2011; Scharf, 2015; Scharf et al., 2017). Many of the microbial genera that were reduced by the selection process are potential pathogens to humans and companion animals (e.g., *Cryptosporidium*, *Toxoplasma*, *Vitrella*, *Plasmodium*, *Neospora*, etc.) and thus our findings on their disappearance may be highlighting a previously unknown/unacknowledged benefit of cockroach baits.

Gregarine protist contigs were the dominant downregulated contigs in the F6-indoxacarb selected line. One common parasitic gregarine, *Gregarine blattarum*, can infect multiple cockroach species including *B. germanica*, as well as other invertebrates (Yahaya et al., 2017). Gregarine infection has been shown to cause pathological effects in *B. germanica* as well as increase

susceptibility to the fungal pathogen *Metarhizium anisopliae* and the growth regulator insecticide triflumuron (Lopes and Alves, 2005), which compels us to ask the question: *is insecticide susceptibility caused in part by microbial pathogens or parasite stress*? Cockroaches in culture are particularly susceptible to gregarine infections and such infections can be reduced by antimicrobial drugs (Clopton and Smith, 2002; Smith and Clopton, 2003). However, it does not appear that many of the sampled microbial groups are exclusively associated with laboratory rearing (Kakumanu et al., 2018). Gregarines are further known to accelerate larval development in cat fleas, *Ctenocephalides felis* (Alarcón et al., 2017) and have recently been identified in cucumber beetles, *Acalymma vittatum*, with no apparent impacts on fitness (Coco et al., 2020). To our knowledge no prior reports are available describing the effects of insecticides on gregarines, but a prior report does document impacts on related termite gut protists by the nicotinoid insecticide imidacloprid (Sen et al., 2015). While it is not clear if the disappearance of these internal microbes enhances host fitness to enable a rapid buildup of xenobiotic resistance, or *vice-versa* (i.e., if resistance happens first), our findings provide important new insights into the potential stepwise basis of resistance evolution and the complex physiological interactions involved.

CONCLUSION

This study provides new insights into cockroach insecticide resistance evolution from multiple physiological perspectives ranging from xenobiotic metabolism and excretion to pathogen and parasite resistance. The identities of dozens of candidate bioactivation and detoxification enzymes were revealed, namely cytochrome P450s and esterases/hydrolases, which agrees strongly with outcomes of preceding indoxacarb metabolomics work in *B. germanica* (Gondhalekar et al., 2016). Many of the genes studied here also had strong matches to the *B. germanica* genome (Harrison et al., 2018a,b) and thus our findings provide important annotations that have been lacking in many cases. Because we used a selection-based approach with temporally parallel non-selected controls that originated from the same genetic stock, and compared strains from both common and distinct genetic origins in a stepwise fashion, the insights provided have limited caveats. Thus, the correlated expression for a subset of candidate genes between independently-selected resistant strains suggests there are common, predictable patterns to resistance evolution across populations.

An unanticipated outcome was that numerous microbial transcripts were reduced with insecticide selection. In terms of the causative agents behind microbial disappearance, three possibilities exist: (i) direct antimicrobial effects by indoxacarb, (ii) indirect effects of antimicrobial preservatives in the bait matrix, or (iii) co-selection for dual detoxification and immune pathways. While the potentially direct effects of the selecting insecticide or bait matrix preservatives on eukaryotic microbes are logical, the causative factors underlying virus and bacterial declines are less clear and should be further investigated. Findings also revealed a potential added benefit of cockroach baits for curing cockroaches of potentially deleterious pathogens and associated allergens that can affect both humans and companion animals. *A priori* goals of this study did not include identification of effects on cockroach parasites and pathogens, and thus our experimental design was not optimized for gaining insights into host-microbial interactions. Future work thus needs to examine for similarities in genes, microbes and processes revealed here, with the ultimate goal of reducing impacts of insecticide resistance and concurrently creating healthier indoor urban environments.

DATA AVAILABILITY STATEMENT

The datasets presented in this study can be found in provided **Supplementary Material**, as well as in online repositories. The names of the repository/repositories and accession number(s) can be found below: NCBI GEO, accession no: GSE188950.

AUTHOR CONTRIBUTIONS

MS designed the research, performed data analysis, and drafted the initial manuscript. ZW performed taxonomic analyses. KR and MF conducted qPCR analyses. JT and KB performed bioinformatics analyses and statistics. AG designed and conducted the research, performed data analyses, and edited the manuscript. All authors contributed to the article and approved the submitted version.

FUNDING

The funding sources for enabling this research: O. W. Rollins/Orkin Endowment in the Department of Entomology at Purdue University, DuPont Inc., HUD grant No. INHHU0026-14 to MS and AG and USDA-NIFA-Hatch support to MS (project No. 1010572).

ACKNOWLEDGMENTS

We thank the Purdue University Genomics Core for transcriptome sequencing.

SUPPLEMENTARY MATERIAL

The Supplementary Material for this article can be found online at: https://www.frontiersin.org/articles/10.3389/fphys.2021.816675/full#supplementary-material

Supplementary Table 1 | Supplementary Tables & Figures.

Supplementary Table 2 | Upregulated contig summary statistics.

Supplementary Table 3 | Downregulated contig summary statistics.

Supplementary Data Sheet 1 | FASTA sequences of upregulated contigs.

Supplementary Data Sheet 2 | FASTA sequences of downregulated contigs.

REFERENCES

Alarcón, M. E., Jara-F, A., Briones, R. C., Dubey, A. K., and Slamovits, C. H. (2017). Gregarine infection accelerates larval development of the cat flea *Ctenocephalides felis* (Bouché). *Parasitology* 144, 419–425. doi: 10.1017/S0031182016002122

Alves, A. P., Allgeier, W. J., and Siegfried, B. D. (2008). Effects of the synergist S,S,S-tributyl phosphorotrithioate on indoxacarb toxicity and metabolism in the European corn borer, *Ostrinia nubilalis* (Hübner). *Pestic. Biochem. Physiol.* 90, 26–30. doi: 10.1016/j.pestbp.2007.07.005

Appel, A. G. (2003). Laboratory and field performance of an indoxacarb bait against German cockroaches. *J. Econ. Entomol.* 96, 863–870. doi: 10.1093/jee/96.3.863

Buczkowski, G., Scherer, C. W., and Bennett, G. W. (2008). Horizontal transfer of bait in the German cockroach: indoxacarb causes secondary and tertiary mortality. *J. Econ. Entomol.* 101, 894–901.

Carrasco, P., Pérez-Cobas, A. E., van de Pol, C., Baixeras, J., Moya, A., and Latorre, A. (2014). Succession of the gut microbiota in the cockroach *Blattella germanica*. *Int. Microbiol.* 17, 99–109. doi: 10.2436/20.1501.01.212

Chen, N., Pei, X. J., Li, S., Fan, Y. L., and Liu, T. X. (2020). Involvement of integument-rich CYP4G19 in hydrocarbon biosynthesis and cuticular penetration resistance in *Blattella germanica* (L.). *Pest Manag. Sci.* 76, 215–226. doi: 10.1002/ps.5499

Clopton, R. E., and Smith, A. (2002). Efficacy of oral sulfadimethoxine against two gregarine parasites, *Protomagalhaensia granulosae* and *Gregarina cubensis* (Apicomplexa: Eugregarinida), infecting the Death's Head cockroach, *Blaberus discoidalis*. *J. Parasitol.* 88, 786–789.

Coco, A. M., Lewis, M. T., Fleischer, S. J., and Tooker, J. F. (2020). Parasitoids, nematodes, and protists in populations of striped cucumber beetle (Coleoptera: Chrysomelidae). *Environ. Entomol.* 49, 1316–1326. doi: 10.1093/ee/nvaa116

Conesa, A., Götz, S., García-Gómez, J. M., Terol, J., Talón, M., and Robles, M. (2005). Blast2GO: a universal tool for annotation, visualization and analysis in functional genomics research. *Bioinformatics* 21, 3674–3676. doi: 10.1093/bioinformatics/bti610

Crawford, J. A., Rosenbaum, P. F., Anagnost, S. E., Hunt, A., and Abraham, J. L. (2015). Indicators of airborne fungal concentrations in urban homes: understanding the conditions that affect indoor fungal exposures. *Sci. Total Environ.* 517, 113–124. doi: 10.1016/j.scitotenv.2015.02.060

Crissman, J. R., Booth, W., Santangelo, R. G., Mukha, D. V., Vargo, E. L., and Schal, C. (2010). Population genetic structure of the German cockroach in apartment buildings. *J. Med. Entomol.* 47, 553–564. doi: 10.1603/me09036

Do, D. C., Zhao, Y., and Gao, P. (2016). Cockroach allergen exposure and risk of asthma. *Allergy* 71, 463–474. doi: 10.1111/all.12827

Elgderi, R. M., Ghenghesh, K. S., and Berbash, N. (2006). Carriage by the German cockroach (*Blattella germanica*) of multiple-antibiotic-resistant bacteria that are potentially pathogenic to humans, in hospitals and households in Tripoli, Libya. *Ann. Trop. Med. Parasitol.* 100:55. doi: 10.1179/136485906X78463

Falconer, D. S. (1989). *An Introduction To Quantitative Genetics*. London: Wiley.

Fardisi, M., Gondhalekar, A. D., Ashbrook, A. R., and Scharf, M. E. (2019). Rapid evolutionary responses to insecticide resistance management interventions by the German cockroach. *Sci. Rep.* 9:8292. doi: 10.1038/s41598-019-44296-y

Field, L. M., and Foster, S. P. (2002). Amplified esterase genes and their relationship with other insecticide resistance mechanisms in English field populations of the aphid, *Myzus persicae* (Sulzer). *Pest Manag. Sci.* 58, 889–894. doi: 10.1002/ps.552

Gondhalekar, A. D. (2011). *Indoxacarb Toxicology And Susceptibility Monitoring In The German Cockroach*. Ph.D. Dissertation. Gainesville, FL: University of Florida.

Gondhalekar, A. D., and Scharf, M. E. (2012). Mechanisms underlying fipronil resistance in a multi-resistant field strain of the German cockroach. *J. Med. Entomol.* 49, 122–131. doi: 10.1603/me11106

Gondhalekar, A. D., and Scharf, M. E. (2013). Preventing resistance to bait products. *Pest Control Technol.* 41, 42–47.

Gondhalekar, A. D., Nakayasu, E. S., Silva, I., Cooper, B., and Scharf, M. E. (2016). Indoxacarb biotransformation in the German cockroach. *Pestic. Biochem. Physiol.* 134, 14–23. doi: 10.1016/j.pestbp.2016.05.003

Gondhalekar, A. D., Scherer, C. W., Saran, R. K., and Scharf, M. E. (2013). Implementation of an indoxacarb susceptibility monitoring program using field-collected German cockroach isolates from the United States. *J. Econ. Entomol.* 106, 945–953. doi: 10.1603/ec12384

Gondhalekar, A. D., Song, C., and Scharf, M. E. (2011). Development of strategies for monitoring indoxacarb and gel bait susceptibility in the German cockroach. *Pest Manag. Sci.* 67, 262–270. doi: 10.1002/ps.2057

Gore, J. C., and Schal, C. (2007). Cockroach allergen biology and mitigation in the indoor environment. *Annu. Rev. Entomol.* 52, 439–463. doi: 10.1146/annurev.ento.52.110405.091313

Grabherr, M. G., Haas, B. J., Yassour, M., Levin, J. Z., Thompson, D. A., Amit, I., et al. (2011). Full-length transcriptome assembly from RNA-seq data without a reference genome. *Nat. Biotechnol.* 29, 644–652. doi: 10.1038/nbt.1883

Guo, G. Z., Geng, Y. J., Huang, D. N., Xue, C. F., and Zhang, R. L. (2010). Level of CYP4G19 Expression is associated with pyrethroid resistance in *Blattella germanica*. *J. Parasitol. Res.* 2010, 517534. doi: 10.1155/2010/517534

Harrison, M. C., Arning, N., Kremer, L. P. M., Ylla, G., Belles, X., and Bornberg-Bauer, E. (2018b). Expansions of key protein families in the German cockroach highlight the molecular basis of its remarkable success as a global indoor pest. *J. Exp. Zool. B Mol. Dev. Evol.* 330, 254–264.

Harrison, M. C., Jongepier, E., Robertson, H. M., Arning, N., Bitard-Feildel, T., Chao, H., et al. (2018a). Hemimetabolous genomes reveal molecular basis of termite eusociality. *Nat. Ecol. Evol.* 2, 557–566.

Hu, I. H., Tzeng, H. Y., Chen, M. E., Lee, C. Y., and Neoh, K. B. (2021). Association of CYP4G19 expression with gel bait performance in pyrethroid-resistant german cockroaches from taiwan. *J. Econ. Entomol.* 114, 1764–1770. doi: 10.1093/jee/toab104

Kakumanu, M. L., Maritz, J. M., Carlton, J. M., and Schal, C. (2018). Overlapping community compositions of gut and fecal microbiomes in lab-reared and field-collected german cockroaches. *Appl. Environ. Microbiol.* 84:e01037–18. doi: 10.1128/AEM.01037-18

Ko, A. E., Bieman, D. N., Schal, C., and Silverman, J. (2016). Insecticide resistance and diminished secondary kill performance of bait formulations against German cockroaches. *Pest Manag. Sci.* 729, 1778–1784. doi: 10.1002/ps.4211

Koehler, P. G., Strong, C. A., Patterson, R. S., and Valles, S. M. (1993). Differential susceptibility of German cockroach (Dictyoptera: Blattellidae) sexes and nymphal age classes to insecticides. *J. Econ. Entomol.* 86, 785–792.

Kopanic, R. J., Sheldon, B. W., and Wright, C. G. (1994). Cockroaches as vectors of *Salmonella* : laboratory and field trials. *J. Food Protect.* 57:125. doi: 10.4315/0362-028X-57.2.125

Kopecná, J., Jirkù, M., Oborník, M., Tokarev, Y. S., Lukes, J., and Modrı, D. (2006). Phylogenetic analysis of coccidian parasites from invertebrates: search for missing links. *Protist* 157, 173–183. doi: 10.1016/j.protis.2006.02.005

Lai, K. M. (2017). Are cockroaches an important source of indoor endotoxins? *Int. J. Environ. Res. Public Health* 14:E91. doi: 10.3390/ijerph14010091

Langmead, B., and Salzberg, S. (2012). Fast gapped-read alignment with Bowtie 2. *Nat. Methods* 9, 357–359. doi: 10.1038/nmeth.1923

Livak, K. J., and Schmittgen, T. D. (2001). Analysis of relative gene expression data using real-time quantitative PCR and 2-ΔΔCT method. *Methods* 25, 402–408. doi: 10.1006/meth.2001.1262

Lopes, R. B., and Alves, S. B. (2005). Effect of *Gregarina* sp. parasitism on the susceptibility of *Blattella germanica* to some control agents. *J. Invertebr. Pathol.* 88, 261–264. doi: 10.1016/j.jip.2005.01.010

Maestro, J. L., Pascual, N., Treiblmayr, K., Lozano, J., and Belles, X. (2010). Juvenile hormone and allatostatins in the German cockroach embryo. *Insect Biochem. Mol. Biol.* 40, 660–665. doi: 10.1016/j.ibmb.2010.06.006

McCarthy, C. B., Diambra, L. A., and Rivera Pomar, R. V. (2011). Metagenomic analysis of taxa associated with *Lutzomyia longipalpis*, vector of visceral leishmaniasis, using an unbiased high-throughput approach. *PLoS Negl. Trop. Dis.* 5:e1304. doi: 10.1371/journal.pntd.0001304

Miller, D. M., and Smith, E. P. (2020). Quantifying the efficacy of an assessment-based pest management (APM) program for german cockroach control in low-income public housing units. *J. Econ. Entomol.* 113, 375–384. doi: 10.1093/jee/toz302

Moriya, Y., Itoh, M., Okuda, S., Yoshizawa, A. C., and Kanehisa, M. (2007). KAAS: an automatic genome annotation and pathway reconstruction server. *Nucleic Acids Res.* 35, W182–W185. doi: 10.1093/nar/gkm321

Pai, H. H., Ko, Y. C., and Chen, E. R. (2003). Cockroaches (*Periplaneta americana* and *Blattella germanica*) as potential mechanical disseminators of *Entamoeba histolytica*. *Acta Trop.* 87, 355–359. doi: 10.1016/s0001-706x(03)00140-2

Pei, X. J., Chen, N., Bai, Y., Qiao, J. W., Li, S., Fan, Y. L., et al. (2019). BgFas1: A fatty acid synthase gene required for both hydrocarbon and cuticular fatty acid biosynthesis in the German cockroach, *Blattella germanica* (L.). *Insect Biochem. Mol. Biol.* 112:103203. doi: 10.1016/j.ibmb.2019.103203

Pomés, A., Mueller, G. A., Randall, T. A., Chapman, M. D., and Arruda, L. K. (2017). New insights into cockroach allergens. *Curr. Allergy Asthma Rep.* 17:25. doi: 10.1007/s11882-017-0694-1

Pridgeon, J. W., Zhang, L., and Liu, N. (2003). Overexpression of CYP4G19 associated with a pyrethroid-resistant strain of the German cockroach, *Blattella germanica* (L.). *Gene* 314, 157–163. doi: 10.1016/s0378-1119(03)00725-x

Renelies-Hamilton, J., Germer, K., Sillam-Dussès, D., Bodawatta, K. H., and Poulsen, M. (2021). Disentangling the relative roles of vertical transmission, subsequent colonizations, and diet on cockroach microbiome assembly. *mSphere* 6:e01023–20. doi: 10.1128/mSphere.01023-20

Robertson, J. L., and Preisler, H. K. (1992). *Pesticide Bioassays with Arthropods*. Boca Raton, FL: CRC Press.

Roth, L. M., and Willis, E. R. (1960). *The Biotic Associations Of Cockroaches – Publication No. 4422 of the Smithsonian Institution*. Baltimore, MD: Baltimore Press, 470.

Schal, C., and Hamilton, R. (1990). Integrated suppression of synanthropic cockroaches. *Annu. Rev. Entomol.* 35:521. doi: 10.1146/annurev.en.35.010190.002513

Scharf, M. E. (2015). Omic research in termites: an overview and a roadmap. *Front. Genet.* 6:76. doi: 10.3389/fgene.2015.00076

Scharf, M. E., and Gondhalekar, A. D. (2021). "Chapter 11: insecticide resistance: perspectives on evolution, monitoring, mechanisms and management," in *Biology and Management of the German Cockroach*, eds C. Wang, C.-Y. Lee, and M. K. Rust (Wallingford: CABI International), 321–356.

Scharf, M. E., Cai, Y., Sun, Y., Sen, R., Raychoudhury, R., and Boucias, D. G. (2017). A meta-analysis testing eusocial co-option theories in termite gut physiology and symbiosis. *Commun. Integr. Biol.* 10:e1295187.

Scharf, M. E., Kaakeh, W., and Bennett, G. W. (1997a). Changes in an insecticide resistant field-population of German cockroach following exposure to an insecticide mixture. *J. Econ. Entomol.* 90, 38–48.

Scharf, M. E., Neal, J. J., and Bennett, G. W. (1997b). Changes of insecticide resistance levels and detoxication enzymes following insecticide selection in the German cockroach. *Pestic. Biochem. Physiol.* 59, 67–79.

Scharf, M. E., Neal, J. J., Marcus, C. B., and Bennett, G. W. (1998). Cytochrome P450 purification and immunological detection in an insecticide resistant strain of German cockroach (*Blattella germanica*, L.). *Insect Biochem. Mol Biol.* 28, 1–9. doi: 10.1016/s0965-1748(97)00060-x

Scharf, M. E., Lee, C. Y., Neal, J. J., and Bennett, G. W. (1999). Cytochrome P450 MA expression in insecticide-resistant German cockroaches. *J. Econ. Entomol.* 92, 788–793. doi: 10.1093/jee/92.4.788

Scharf, M. E., Zhou, X., and Schwinghammer, M. A. (2008). "Application of RNA interference in functional-genomics studies of a social insect," in *Methods in Molecular Biology: siRNA, shRNA and miRNA Protocols*, Vol. 442, ed. S. Barik (Totowa, NJ: Humana Press), 205–229. doi: 10.1007/978-1-59745-191-8_15

Sen, R., Raychoudhury, R., Cai, Y., Sun, Y., Lietze, V. U., Peterson, B. F., et al. (2015). Molecular signatures of nicotinoid-pathogen synergy in the termite gut. *PLoS One* 10:e0123391. doi: 10.1371/journal.pone.0123391

Smith, A. J., and Clopton, R. E. (2003). Efficacy of oral metronidazole and potassium sorbate against two gregarine parasites, *Protomagalhaensia granulosae* and *Gregarina cubensis* (Apicomplexa: Eugregarinidae), Infecting the death's head cockroach, *Blaberus discoidalis*. *Comp. Parasitol.* 70, 196–199.

Sohn, M. H., and Kim, K. E. (2012). The cockroach and allergic diseases. *Allergy Asthma Immunol. Res.* 4:264. doi: 10.4168/aair.2012.4.5.264

Srigiriraju, L., Semtner, P. J., Anderson, T. D., and Bloomquist, J. R. (2009). Esterase-based resistance in the tobacco-adapted form of the green peach aphid, *Myzus persicae* (Sulzer) (Hemiptera: Aphididae) in the eastern United States. *Arch. Insect Biochem. Physiol.* 72, 105–123. doi: 10.1002/arch.20326

Tabashnik, B. E. (1992). Resistance risk assessment: realized heritability of resistance to *Bacillus thuringenesis* in diamondback moth (Lepidoptera: Plutellidae), tobacco budworm (Lepidoptera: Noctuidae) and colorado potato beetle (Coleoptera: Chrysonmelidae). *J Econ Entomol* 85, 1551–1559.

Tarver, M. R., Coy, M. R., and Scharf, M. E. (2012). Cyp15F1: a novel cytochrome P450 gene linked to juvenile hormone-dependent caste differention in the termite *Reticulitermes flavipes*. *Arch. Insect Biochem. Physiol.* 80, 92–108. doi: 10.1002/arch.21030

Thorne, P. S., Mendy, A., Metwali, N., Salo, P., Co, C., Jaramillo, R., et al. (2015). Endotoxin exposure: predictors and prevalence of associated asthma outcomes in the United States. *Am. J. Resp. Crit. Care Med.* 192, 1287–1297. doi: 10.1164/rccm.201502-0251OC

Tinker, K. A., and Ottesen, E. A. (2021). Differences in gut microbiome composition between sympatric wild and allopatric laboratory populations of omnivorous cockroaches. *Front. Microbiol.* 12:703785. doi: 10.3389/fmicb.2021.703785

Turturice, B. A., Ranjan, R., Nguyen, B., Hughes, L. M., Andropolis, K. E., Gold, D. R., et al. (2017). Perinatal bacterial exposure contributes to IL-13 aeroallergen response. *Am. J. Respir. Cell Mol. Biol.* 57, 419–427. doi: 10.1165/rcmb.2017-0027OC

Untergasser, A., Cutcutache, I., Koressaar, T., Ye, J., Faircloth, B. C., Remm, M., et al. (2012). Primer3 - new capabilities and interfaces. *Nucleic Acids Res.* 40:e115. doi: 10.1093/nar/gks596

Vargo, E. L. (2021). "Chapter 7: dispersal and population genetics," in *Biology and Management of the German Cockroach*, eds C. Wang, C.-Y. Lee, and M. K. Rust (Wallingford: CABI International), 143–152.

Vargo, E. L., Crissman, J. R., Booth, W., Santangelo, R. G., Mukha, D. V., Schal, C., et al. (2014). Hierarchical genetic analysis of German cockroach populations from within buildings to across continents. *PLoS One* 9:e102321. doi: 10.1371/journal.pone.0102321

Wada-Katsumata, A., Zurek, L., Nalyanya, G., Roelofs, W. L., Zhang, A., Schal, C., et al. (2015). Gut bacteria mediate aggregation in the German cockroach. *Proc. Natl. Acad. Sci. U.S.A.* 112, 15678–15683. doi: 10.1073/pnas.1504031112

Wen, Z., and Scott, J. G. (2001). Cloning of two novel P450 cDNAs from German cockroaches, *Blattella germanica* (L.): CYP6K1 and CYP6J1. *Insect Mol. Biol.* 10, 131–137. doi: 10.1046/j.1365-2583.2001.00247.x

Wen, Z., Horak, C. E., and Scott, J. G. (2001). CYP9E2, CYP4C21 and related pseudogenes from German cockroaches, *Blattella germanica*: implications for molecular evolution, expression studies and nomenclature of P450s. *Gene* 272, 257–266. doi: 10.1016/s0378-1119(01)00529-7

Wing, K. D., Sacher, M., Kagaya, Y., Tsurubuchi, Y., Mulderig, L., Connair, M., et al. (2000). Bioactivation and mode of action of the oxadiazine indoxacarb in insects. *Crop Protect.* 19, 537–545. doi: 10.1016/S0261-2194(00)00070-3

Yahaya, Z. S., Izzaudin, N. A., and Razak, A. F. (2017). Parasitic *Gregarine blattarum* found infecting american cockroaches, *Periplaneta americana*, in a population in pulau pinang, Malaysia. *Trop. Life Sci. Res.* 28, 145–149. doi: 10.21315/tlsr2017.28.1.10

Zhou, X., Qian, K., Tong, Y., Zhu, J. J., Qiu, X., and Zeng, X. (2014). De novo transcriptome of the Hemimetabolous German cockroach (*Blattella germanica*). *PLoS One* 9:e106932. doi: 10.1371/journal.pone.0106932

Zhu, F., Lavine, L., O'Neal, S., Lavine, M., Foss, C., and Walsh, D. (2016). Insecticide resistance and management strategies in urban ecosystems. *Insects* 7:2. doi: 10.3390/insects7010002

Conflict of Interest: This study received gift funding from DuPont Inc. The funder was not involved in the study design, collection, analysis, interpretation of data, the writing of this article or the decision to submit it for publication.

The authors declare that the research was conducted in the absence of any commercial or financial relationships that could be construed as a potential conflict of interest.

frontiers in Physiology

ORIGINAL RESEARCH
published: 17 February 2022
doi: 10.3389/fphys.2022.842314

Assessment of Sex-Specific Toxicity and Physiological Responses to Thymol in a Common Bean Pest *Acanthoscelides obtectus* Say

Jelica Lazarević[1]†, Stojan Jevremović[2], Igor Kostić[3]†, Ana Vuleta[1], Sanja Manitašević Jovanović[1], Miroslav Kostić[4] and Darka Šešlija Jovanović[1]†*

[1] Institute for Biological Research "Siniša Stanković" - National Institute of Republic of Serbia, University of Belgrade, Belgrade, Serbia, [2] Bayer d.o.o., Belgrade, Serbia, [3] Institute for Multidisciplinary Research, University of Belgrade, Belgrade, Serbia, [4] Institute for Medicinal Plants Research "Dr. Josif Pančić", Belgrade, Serbia

OPEN ACCESS

Edited by:
Ran Wang,
Institute of Plant Protection and Environmental Protection, Beijing Academy of Agricultural and Forestry Sciences, China

Reviewed by:
Jinda Wang,
Fujian Agriculture and Forestry University, China
Shaukat Ali,
South China Agricultural University, China

***Correspondence:**
Jelica Lazarević
jellaz@ibiss.bg.ac.rs

†These authors share senior authorship

Specialty section:
This article was submitted to Invertebrate Physiology, a section of the journal Frontiers in Physiology

Received: 23 December 2021
Accepted: 25 January 2022
Published: 17 February 2022

Citation:
Lazarević J, Jevremović S, Kostić I, Vuleta A, Manitašević Jovanović S, Kostić M and Šešlija Jovanović D (2022) Assessment of Sex-Specific Toxicity and Physiological Responses to Thymol in a Common Bean Pest Acanthoscelides obtectus Say. Front. Physiol. 13:842314. doi: 10.3389/fphys.2022.842314

Acanthoscelides obtectus Say (Coleoptera: Chrysomelidae: Bruchinae), is one of the most important pests of the common bean *Phaseolus vulgaris* L. Without appropriate management it may cause significant seed loss in storages. In search for means of environmentally safe and effective protection of beans we assessed biological activity of thymol, an oxygenated monoterpene present in essential oils of many aromatic plants. We studied contact toxicity of thymol on bean seeds and its effects on adult longevity and emergence in F1 generation. Furthermore, we determined acetylcholinesterase (AChE), superoxide dismutase (SOD), catalase (CAT), mixed-function oxidase (MFO), carboxylesterases (CarE) and glutathione S-transferase (GST) activities in response to 24 h exposure of beetles to sublethal and lethal thymol concentrations. Our results showed that thymol decreased adult survival, longevity and percentage of adult emergence. Higher median lethal concentration (LC_{50}) was recorded in females indicating their higher tolerance comparing to males. Overall, activities of SOD, CAT and CarE increased at sublethal and MFO increased at both sublethal and lethal thymol concentrations. On the other hand, GST and AChE activities decreased along with the increase in thymol concentrations from sublethal (1/5 of LC_{50}, 1/2 of LC_{50}) to lethal (LC_{50}). Enzyme responses to the presence of thymol on bean seed were sex-specific. In the control group females had lower CarE and higher SOD, CAT and GST activity than males. In treatment groups, females had much higher CAT activity and much lower CarE activity than males. Our results contribute to deeper understanding of physiological mechanisms underlying thymol toxicity and tolerance which should be taken into account in future formulation of a thymol-based insecticide.

Keywords: *Acanthoscelides obtectus*, seed protection, thymol, insecticidal activity, antioxidative defense, detoxification, sexual dimorphism

INTRODUCTION

The bean weevil *Acanthoscelides obtectus* Say (Coleoptera: Chrysomelidae: Bruchine) is an economically important pest of leguminous crops. Beside the primary host common bean *Phaseolus vulgaris* L. it can also feed on other crops belonging to 11 different genera (Johnson, 1981; Labeyrie, 1990). In a study of Szentesi (2021) 18 legume species are shown to be acceptable, and nine of them support complete development to adults even if seed coat was intact. *A. obtectus* originates from South America but widened its areal of distribution to Europe, North America, Australia and Africa due to human-mediated migrations and tolerance to broad range of environmental conditions (Alvarez et al., 2005). Bean infestation starts in fields by female oviposition into pods and then spreads in storages causing rapid destruction of bean seeds in subsequent generations (Schmale et al., 2002). Larvae feed inside the seeds leading to changes in their mass and nutritional quality (Keszthelyi et al., 2018). Quantitative post-harvest losses in storages due to insect infestation may reach value of 30% in developing countries (Nayak and Daglish, 2018).

Chemical fumigants and contact insecticides are still the main method for storage seed protection (Obeng-Ofori, 2010). However, environmental pollution and threats to human health due to insecticide residues as well as the risk of pest resistance evolution (Guedes et al., 2017; Dar et al., 2020) forced searching for alternative management tools (reviewed in Mohapatra et al., 2015; Daglish et al., 2018; Rajendran, 2020). For example, recent studies on *A. obtectus* have evaluated efficacy of hermetic storage (Freitas et al., 2016), inert dusts (Floros et al., 2018; Lazarević et al., 2018; Prasantha et al., 2019), predators and parasitoids (Iturralde-García et al., 2020), insecticidal products of entomopatogenic bacteria and fungi (Rodríguez-González et al., 2018, 2020), as well as plant-derived products (Kısa et al., 2018; Jevremović et al., 2019; Hategekimana and Erler, 2020; Lazarević et al., 2020).

Among plant-derived products, essential oils (EOs) and their compounds terpenoids and phenylpropanoids exhibit various biological activities against stored product insects including toxicity and sublethal effects on behavior and physiology (reviewed in Nerio et al., 2010; Zibaee, 2011; Kim S. I. et al., 2012; Ebadollahi and Sendi, 2015; Chaudhari et al., 2021). The complex nature of essential oils and artificial blends of their compounds may slow down evolution of pest resistance, whereas low persistence of the volatiles minimizes harmful impact on the environment (Pavela, 2016; Isman, 2020). Additionally, these natural products may contribute to sustainable plant protection through synergy with chemical insecticides (Norris et al., 2018; Reynoso et al., 2018; Ruttanaphan et al., 2019).

Physiological mechanisms of EOs and EOs compounds activity against insects involve neurotoxic interference on cholinergic, GABA-ergic and octopamine pathways (Jankowska et al., 2018), and metabolic reorganization mostly at the level of xenobiotic detoxification, mitochondrial function and antioxidative defense (Liao et al., 2016; Huang et al., 2018; Gao et al., 2020). The activity of acetylcholinesterase (AChE), the enzyme which degrades neurotransmitter acethylcholine, can be inhibited by many terpenoids (López and Pascual-Villalobos, 2010, 2015; Herrera et al., 2015; Al-Nagar et al., 2020; Liu et al., 2021). EOs and EOs compounds may also decrease the activity of enzymes in the mitochondrial electron transport chain, which further provoke increase in free radicals and oxidative damage to macromolecules (Pinho et al., 2014; da Cunha et al., 2015; Kiran et al., 2017; Liao et al., 2018). To defend from oxidative stress, insects induce various enzymatic and non-enzymatic antioxidants (da Cunha et al., 2015; Kiran and Prakash, 2015a,b; Agliassa and Maffei, 2018; Chen et al., 2021). For example, dietary α-pinene, trans-anethole and thymol elevate activities of superoxide dismutase (SOD), catalase (CAT) and glutathione S-transferase (GST) in *Ephestia kuehniella* Zeller larvae (Shahriari et al., 2018). SOD catalyzes the conversion of superoxide anion radical (O_2^-) into oxygen (O_2) and hydrogen peroxide (H_2O_2) after which CAT decomposes H_2O_2 to water and O_2. GST metabolizes lipid peroxides and as a major phase II detoxification enzyme catalyzes conjugation of electrophilic xenobiotics with low-molecular antioxidant glutathione. Formed conjugates are less toxic and more water soluble which facilitates their excretion. Mixed-function oxidase (MFO) and carboxylesterase (CarE), phase I detoxification enzymes involved in decomposition of exogenous toxins, can be also induced in the presence of terpenoids (Yotavong et al., 2015; Vasantha-Srinivasan et al., 2018; Gao et al., 2020; Piri et al., 2020; Subaharan et al., 2021). However, inhibition of detoxification enzymes by EOs and EOs compounds has also been reported in insects (Liao et al., 2017; Tak et al., 2017; de Souza et al., 2019; Hu et al., 2019; Shang et al., 2019; Chen et al., 2021; Gaire et al., 2021).

The present study evaluates insecticidal potential of thymol, a natural monoterpenoid phenol, against *A. obtectus*. Thymol (2-isopropyl-5-methylphenol) is the major ingredient of essential oils extracted from aromatic plants belonging to families of Lamiaceae, Apiaceae, Verbenaceae, Asteraceae, Ranunculaceae, Scrophulariaceae and Saururaceae (Escobar et al., 2020). Many of these plants are used as seasonings in human nutrition and as medicinal herbs with anti-inflammatory, analgesic, antimicrobial, antioxidant and other properties (Peter and Shylaja, 2012; Mancini et al., 2015). FEMA expert panel included thymol and thymol containing essential oils in a list of "generally recognized as safe" (GRAS) natural flavors (Cohen et al., 2021). These compounds also show low toxicity to non-target organisms (Charpentier et al., 2014; Yotavong et al., 2015; Pavela et al., 2020) and various adverse effects on fitness of pest insects (Abdelgaleil et al., 2021b).

In *A. obtectus* thymol applied as fumigant induced high mortality and decreased adult longevity, fecundity, penetration of larvae into bean seeds and adult emergence (Regnault-Roger and Hamraoui, 1995). Our study was aimed to determine residual contact toxicity of thymol by monitoring adult survival and progeny production and to explore the physiological basis of thymol toxicity by measuring activities of AChE, SOD, CAT, MFO, CarE, and GST. Additionally, since females and males of this species differently responded to various chemical stressors (Papachristos and Stamopoulos, 2002; Papachristos et al., 2004; Lazarević et al., 2013, 2018, 2020; Šešlija Jovanović et al., 2014) we assessed if changes in survival and enzyme activities were sex-specific.

MATERIALS AND METHODS

Insects and Rearing Conditions

Acanthoscelides obtectus used in this study originated from the laboratory population maintained on the common bean (*Phaseolus vulgaris* c.v. "gradištanac") seeds for more than 250 generations. During the experiment, beetles were kept in heating incubators at 27 ± 1°C, 12 h:12 h light:dark photoperiod and 55 ± 10% relative humidity. Bean seeds were chemically untreated and frozen prior to usage to avoid any possible infestation with external pests.

Residual Contact Toxicity of Thymol on Bean Seeds

Thymol purchased from Sigma-Aldrich (cat. no. W306606) was dissolved in acetone. Bean seeds (10 g) were put in 90 mL glass jars and treated with 300 μL of either thymol solutions or solvent (control). Five thymol concentrations were applied for females (60, 90, 105, 120, and 150 mg/kg of beans) and males (30, 45, 60, 75, and 90 mg/kg of beans). Treated seeds were mixed manually for 5 min and left in open jars for 20 min to evaporate the solvent. Then, 10 adult females or males (one day old) were introduced into the jar, covered with a piece of cloth fixed with rubber. Eight replicates per sex per thymol concentration and control (acetone) were analyzed. The number of dead insects was estimated daily until all insects died. Percentage of dead insects after 24 h of treatment was used to determine lethal thymol concentrations. Beetle longevity and age-specific mortality were also observed.

Thymol Effects on F1 Progeny Production

Bean seeds (20 g) were put in 200 mL glass jars and treated with 600 μL of either thymol solution or solvent (control). Applied thymol concentrations were 30, 45, 60, 75, 90, 105, and 120 mg/kg of beans. After 5 min of treated seed mixing and 20 min of solvent evaporation, five pairs of one day old bean weevils, i.e., five females and five males, were introduced into each jar, covered with a piece of cloth fixed with rubber and kept in heating incubators until the emergence of the progeny. Emerged adults were counted daily until the end of emergence. Total number of emerged insects as well as the number of emerged females and males were used to determine the inhibition rate (IR%) of emergence according to the formula:

$$IR\% = \frac{Nc - Nt}{Nc} \times 100$$

where N_c and N_t were total numbers of emerged adults in control and treatment jars, respectively.

Enzyme Assays

Activities of enzymes (AChE, SOD, CAT, MFO, CarE, GST) were determined in female and male beetles exposed to sublethal (1/5 of LC_{50}, 1/2 of LC_{50}) and lethal concentrations (LC_{50}) of thymol for 24 h. The enzyme extracts were prepared by pulverization of batches of 20 frozen beetles under liquid nitrogen in a mortar with the pestle. After the addition of cold 50 mM K-phosphate buffer pH 7.4 containing 1 mM EDTA and 1 mM PMSF (1:10 tissue to buffer ratio), homogenates were sonicated (2 × 15 s) and centrifuged at 4°C, 16,000 × *g* for 30 min. The supernatants were collected and used for the determination of enzymes activities and total protein content. All enzyme assays were performed at 30°C. The total protein content was quantified according to Bradford (1976) with bovine serum albumin (BSA) as the standard and enzyme activities were expressed in units (U) per mg of proteins.

The activity of AChE was determined according to the method of Ellman et al. (1961). During the reaction, thiol groups released from substrate acetyl-thiocholine iodide (ACTH) bind to 5,5′-dithio-bis(2-nitrobenzoic acid) (DTNB) and form yellow 5-thio-2-nitrobenzene (TNB). The reaction was carried out in 50 mM phosphate buffer pH 7.9 and the change in absorbance was monitored at 406 nm (ε = 13,330 M^{-1} cm^{-1}). One enzyme unit (U) was defined as the amount of enzyme that forms 1 nmol TNB per min.

The activity of SOD was assayed by the method of Misra and Fridovich (1972), which is based on the capacity of SOD to inhibit autoxidation of adrenaline to adrenochrome at pH 10.2 (50 mM sodium carbonate buffer). The change in absorbance was monitored at 480 nm. One unit of SOD activity was defined as the amount of enzyme causing 50 % inhibition of the adrenaline autoxidation.

CAT activity was determined by the method of Claiborne (1984). The rate of hydrogen peroxide (H_2O_2) decomposition in 50 mM phosphate buffer pH 7.0 was determined according to the change in absorbance at 240 nm (ε = 43.6 M^{-1} cm^{-1}). One unit of CAT activity was defined as the amount of enzyme that catalyzed the decomposition of 1 μmol of H_2O_2 per min.

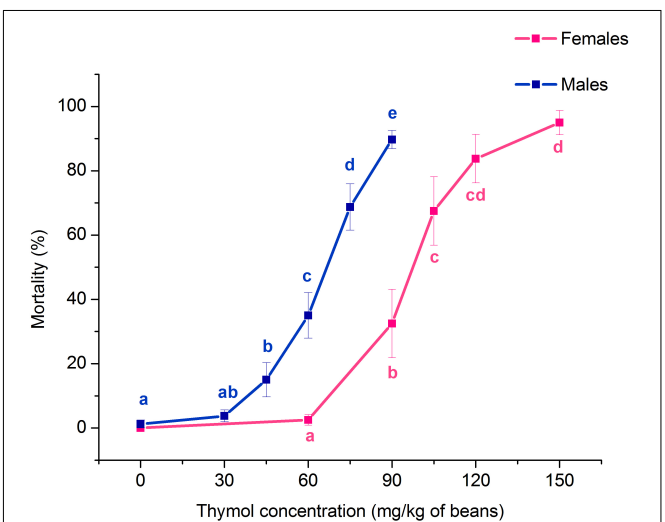

FIGURE 1 | Impact of different concentrations of thymol on *Acanthoscelides obtectus* mortality after 24 h of exposure to thymol treated bean seeds (means ± SE for 8 replicates). Significant differences among experimental groups within each sex are marked with different letters (a – e) (Duncan's *post-hoc* test, $p < 0.05$).

TABLE 1 | Residual contact toxicity of thymol against adult females and males of *Acanthoscelides obtectus*.

	Slope (CI)	LC_{30} (CI)	LC_{50} (CI)	LC_{99} (CI)	χ^2	*p*
Females	8.73 ± 0.79 (7.17, 10.28)	85.8 (80.7, 89.7)	98.4 (94.2, 102.3)	181.8 (165.6, 207.0)	3.84	0.279
Males	8.68 ± 0.80 (7.11, 10.25)	55.2 (51.3, 58.5)	66.0 (62.7, 69.0)	108.9 (100.8, 120.9)	1.02	0.795

LC – lethal thymol concentrations expressed in mg/kg of beans leading to 30, 50 and 99% beetle mortality (LC_{30}, LC_{50}, and LC_{99}, respectively); CI – 95% confidence interval; χ^2 and P – Pearson's goodness-of-fit test (df = 3).

The activity of MFO was quantified indirectly by the heme peroxidation method (Brogdon et al., 1997). TMBZ (3, 3′, 5, 5′-tetra-methylbenzidine) dissolved in methanol and sodium acetate buffer pH 5.0 was used as a hydrogen donor substrate. The reaction started with adding a drop of hydrogen peroxide. After 5 minutes of incubation absorbance was read at 630 nm. Cytochrome c was used as an internal standard and the enzyme unit was expressed as pmol of cytochrome c equivalents per min.

CarE activity was determined by the method of Wu et al. (1998) by using p-nitrophenyl acetate (p-NA) as a substrate. The enzyme hydrolyzes acetate ester and forms p-nitrophenol (p-NP) which absorbs at 405 nm (ε = 12,800 M^{-1} cm^{-1}). The enzyme unit was defined as the amount of enzyme which generates 1 nmol of p-NP per min.

The activity of GST was determined by the method of Habig et al. (1974). The method is based on the reaction of CDNB with the SH group of GSH which was performed in 100 mM potassium phosphate buffer pH 6.5. The change in absorbance was measured at 340 nm (ε = 9,600 M^{-1} cm^{-1}) and the enzyme unit was defined as the amount of enzyme that generate 1 nmol of CDNB-GSH conjugate per min.

Statistical Methods

Lethal thymol concentrations after 24 h of exposure were estimated by probit analysis (Finney, 1971) and their values were compared between females and males according to overlapping confidence intervals. Based on mortality data during the beetles life time Kaplan-Meier survival probability was calculated, survival analysis was performed and survival distribution was compared among thymol concentrations by log-rank test. Parameters *a* (initial mortality) and *b* (exponential increase in mortality over time) of the Gompertz model (instantaneous mortality at age $x = a \times e^{bx}$) were determined by using WinModest software and compared between control and thymol treated beetles by using the log-likelihood-ratio test (Pletcher, 1999). Also, Gompertz parameters were compared between females and males of the control group and group treated with 60 mg of thymol/kg of beans.

Kolmogorov-Smirnov test of normality and Bartlett's test for homogeneity of variances were applied on data transformed in order to achieve assumptions for parametric ANOVA. Arcus sinus square root transformation was used for the percentage of 24 h adult mortality and the percentage of adult emergence inhibition. Data on the number of emerged adults and adult longevity were square root transformed. Assumption of normality of distribution was violated for square root transformed female and male longevities. Accordingly, to assess the impact of thymol concentration on adult longevity we used non-parametric Kruskal-Wallis ANOVA and Dunn's *post-hoc* test, whereas 24 h mortality and adult emergence were analyzed by parametric 1-way ANOVA and Duncan's *post-hoc* test. To reveal the significance of the differences in the number of emerged females and males we performed 1-way repeated measures ANOVA with sex as within-subject factor and thymol concentration as between-subject factor.

Enzyme activities were analyzed by 2-way ANOVA with thymol concentration and sex as fixed factors. Carboxylesterase activity was log-transformed whereas untransformed data on other enzyme activities satisfied parametric ANOVA assumptions. A posteriori comparisons (least square means contrasts) were applied to assess the significance of enzyme activity differences between sexes within each thymol concentration. Also, 1-way ANOVAs followed by Duncan's *post-hoc* test were carried out to reveal the significance of thymol concentration effects on enzyme activities separately in females and males. All analyses were carried out with the software Statistica 7.0 (StatSoft, Inc., Tulsa, OK, United States).

RESULTS

Acute Thymol Toxicity Against *Acanthoscelides obtectus*

Thymol concentration significantly affected the percentage of *A. obtectus* mortality both in females ($F_{4,35} = 24.81$, $p < 0.001$) and males ($F_{5,42} = 43.17$, $p < 0.001$). Mortality of females and males was significantly increased at concentrations equal or higher than 90 and 45 mg/kg of beans, respectively (**Figure 1**). Concentration-mortality response fitted the probit distribution (Pearson's test in **Table 1**). Higher resistance of females than males to thymol was confirmed by higher low lethal (LC_{30}) and lethal concentrations (LC_{50}, LC_{99}) with non-overlapping confidence intervals.

Acanthoscelides obtectus Longevity and Time-Mortality Responses to Thymol

Exposure to thymol negatively affected *A. obtectus* adult longevity. Both females and males lived shorter comparing to control beetles (Kruskal-Wallis ANOVA, females: $H_{4,399} = 227.68$, $p < 0.001$; males: $H_{5,479} = 125.48$, $p < 0.001$). Significant longevity decrease can be observed

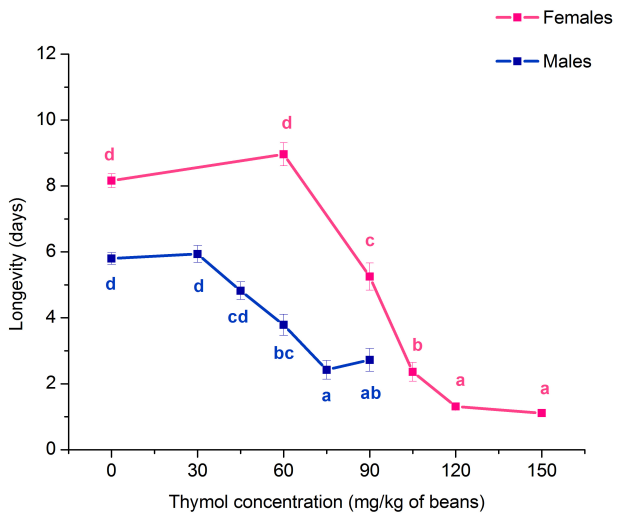

FIGURE 2 | Changes in longevity of *Acanthoscelides obtectus* females and males (means ± SE for 8 replicates) in response to chronic exposure to thymol treated bean seeds. Significant differences among experimental groups within each sex are marked with different letters (a - d) (Dunn's *post-hoc* test, $p < 0.05$).

at concentrations ≥ 90 mg/kg of beans in females and 60 mg/kg of beans in males (**Figure 2**).

As revealed by Kaplan-Meier analysis thymol applied on bean seeds also affected survival distribution over time in females ($\chi^2 = 368.12$, df = 5, $p < 0.001$) and males ($\chi^2 = 58.35$, df = 5, $p < 0.001$). Beetles from the treatment groups started to die earlier than control beetles (**Figure 3**) and had higher initial mortality at thymol concentrations ≥ 90 mg/kg of beans in females and 30 mg/kg of beans in males (Gompertz parameter *a* in **Table 2**). This higher initial mortality was related to slower mortality increase with advanced age and higher maximum longevity (**Figure 3**, Gompertz parameter *b* in **Table 2**). In the control group males lived shorter due to accelerated aging rate, whereas in beetles exposed to 60 mg of thymol / kg of beans shorter life of males was a consequence of much higher initial mortality (higher parameter *a*) which could not be compensated by retarded aging (lower parameter *b*) (**Table 2**).

Thymol Impact on *Acanthoscelides obtectus* Adult Emergence

Results presented in **Table 3** show that the number of emerged adults decreased significantly at concentrations ≥ 60 mg/kg of beans (female emergence: $F_{5,42} = 21.12$, $p < 0.001$; male emergence: $F_{5,42} = 21.14$, $p < 0.001$; total emergence: $F_{5,42} = 22.19$, $p < 0.001$). Similarly, the percentage of emergence inhibition was significantly affected by thymol concentration (females: $F_{4,35} = 19.51$, $p < 0.001$; males: $F_{4,35} = 16.81$, $p < 0.001$; females+males: $F_{4,35} = 18.80$, $p < 0.001$). The concentration that provoked 50% emergence inhibition was estimated to be 57.3 mg/kg of beans (CI = 0.179; 0.201). Significant influence of thymol concentration on adult emergence and emergence inhibition was also confirmed by repeated measures ANOVA ($F_{5,42} = 22.32$, $p < 0.001$ and $F_{4,35} = 19.05$, $p < 0.001$, respectively). On average, more males than females emerged in F1 generation (within-subject sex: $F_{1,42} = 8.20$, $p = 0.007$) but emergence inhibition was not sex specific ($F_{1,35} = 0.04$, $p = 0.846$). Additionally, slope of thymol concentration – F1 progeny number and thymol concentration – emergence inhibition response did not differ between females and males (concentration × sex interaction: $F_{5,42} = 0.19$, $p = 0.964$ and $F_{4,35} = 0.50$, $p = 0.734$, respectively).

Enzyme Activities in *Acanthoscelides obtectus* Exposed to Sublethal and Lethal Thymol Concentrations

The neurotoxic effect of thymol on *A. obtectus* adults was revealed by inhibition of AChE activity both at sublethal and lethal concentrations (**Figure 4**; significant "concentration" term in **Table 4**). The slope of AChE inhibition differed between females and males (significant "sex × concentration" term in **Table 4**). Influence of thymol concentration was highly significant in females ($F_{3,16} = 18.77$, $p < 0.001$), and males ($F_{3,16} = 3.40$, $p = 0.044$). At median lethal concentration LC_{50} AchE was inhibited about 38% in females and 15% in males (**Figure 4**).

On average, activities of antioxidative enzymes SOD and CAT were elevated in the presence of thymol (**Figure 5**; significant "concentration" term in **Table 4**). Shape of thymol concentration – activity response depended on sex (significant "sex × concentration" terms in **Table 4**) although both females (SOD: $F_{3,16} = 4.6$, $p = 0.017$; CAT: $F_{3,16} = 8.35$, $p = 0.001$) and males (SOD: $F_{3,16} = 10.97$, $p < 0.001$; CAT: $F_{3,16} = 19.47$, $p < 0.001$) were significantly affected by thymol concentration. Activity of catalase was about 2.5 times higher in females than males across all examined concentrations. In contrast, differences in SOD activity were recorded only in control (higher activity in females) and LC_{50} group (higher activity in males) (**Figures 5A,B**).

Activity of mixed-function oxidases was elevated in treated beetles (**Figure 6A**; significant "concentration" term in **Table 4**). Both females ($F_{3,16} = 21.93$, $p < 0.001$) and males ($F_{3,16} = 22.88$, $p < 0.001$) were significantly affected by thymol concentration but female MFO was less sensitive (**Figure 6A**; significant "sex × concentration" term in **Table 4**). Males exposed to thymol had higher MFO activity than females (**Figure 6A**; significant "sex" term in **Table 4**).

Carboxylesterase activity was induced at sublethal thymol concentrations (**Figure 6B**; significant "concentration" term in **Table 4**). Significant thymol influence was detected both in females ($F_{3,16} = 5.38$, $p = 0.009$) and males ($F_{3,16} = 17.49$, $p < 0.001$) but induction was more expressed in males than females (**Figure 6B**; significant "sex × concentration" term in **Table 4**). At all examined concentrations CarE activity was higher in males than females (**Figure 6B**; significant "sex" term in **Table 4**).

Inhibition of glutathione S-transferase activity by thymol is another possible mechanism of its toxicity (**Figure 6C**; significant "concentration" term in **Table 4**). Both females ($F_{3,16} = 136.13$, $p < 0.001$) and males ($F_{3,16} = 30.73$, $p < 0.001$) were significantly

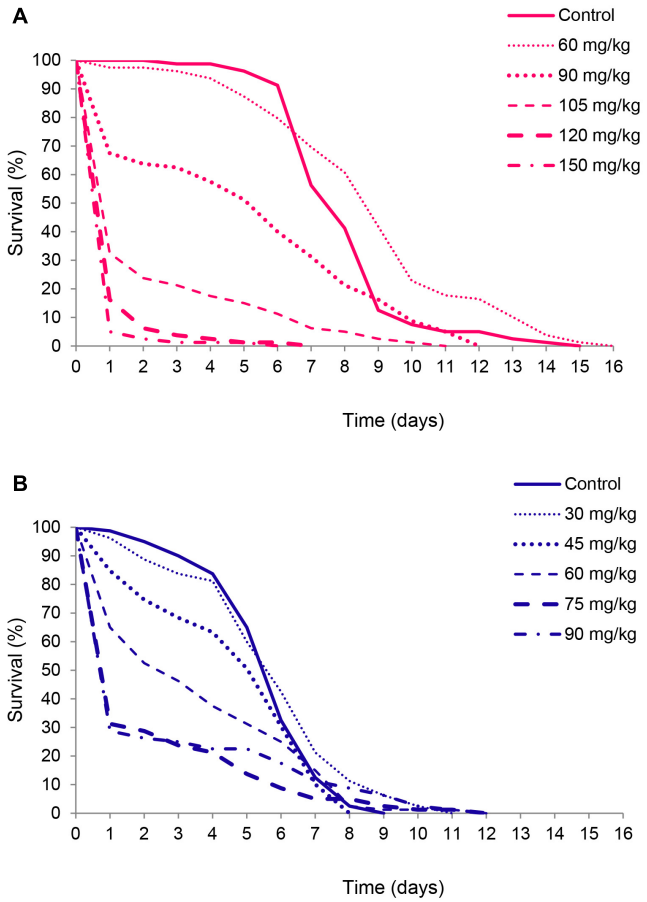

FIGURE 3 | Survival curves for female **(A)** and male *Acanthoscelides obtectus* **(B)** exposed to different thymol concentrations.

affected by thymol concentration but inhibition was steeper in females than males (**Figure 6C**; significant "sex × concentration" term in **Table 4**). Control and 1/5 of LC_{50} females had about 40% higher GST activity than males, whereas no difference could be recorded at LC_{50} (**Figure 6C**).

DISCUSSION

Adverse Effects of Thymol on Adult Fitness Traits

Similar to the results on residual contact toxicity of thyme EO against the bean weevil (Lazarević et al., 2020) we found that its major compound thymol also significantly affected 24 h mortality and longevity of females and males, and progeny production in F1 generation. The ratio of median lethal concentrations obtained for thymol and thyme EO (98.4 vs. 255.0 mg/kg of beans in females and 66.0 vs. 172.2 mg/kg of beans in males) corresponds to thymol concentration of 43.52% in thyme EO (Jevremović et al., 2019) and suggests that thymol was the major determinant of bean weevil mortality induced by thyme EO. It appeared that other EO compounds either had negligible impact on the acute toxicity of EO or some compounds contribution counteracted the antagonistic effects of others. In difference to our results studies on fumigant toxicity of thyme EO containing 47.5% thymol (Regnault-Roger et al., 1993) and pure thymol (Regnault-Roger and Hamraoui, 1995) point to the significant contribution of other compounds. Using different bean weevil populations and different modes of botanical application may account for disagreement between results of the studies. Besides, although both EOs were extracted from thyme belonging to thymol chemotype their composition was different. For example, thyme EO from the study of Regnault-Roger and colaborators contained caryophyllene, bicyclic sesquiterpene, which had both fumigant and residual toxic effects on stored product insects (Lee et al., 2008; Sun et al., 2020).

On the other hand, ratio of median effective concentration (EC_{50}) for adult emergence inhibition rate on thymol (57.3 mg/kg of beans) and thyme EO (65.7 mg/kg of beans, Lazarević et al., 2020) suggests an important role of other compounds in reducing adult emergence. Since pure thymol seems to affect F1 progeny number mainly through the adverse effect on male survival (similarity of EC_{50} value for adult emergence inhibition to LC_{50} for males on thymol) it is possible that other compounds in thyme EO additionally reduced emergence through adverse effects on mating, fecundity, larval penetration into seeds and/or preadult

survival. Even sublethal concentrations of monoterpenes could have a significant impact on fitness traits and behavior of the bean weevil (Regnault-Roger and Hamraoui, 1995; Jevremović et al., 2019; Hategekimana and Erler, 2020) and other pests (Hummelbrunner and Isman, 2001; Wang et al., 2009; Tak and Isman, 2017; de Melo et al., 2018; Abdelgaleil et al., 2021a; Barbosa et al., 2021; de Andrade Brito et al., 2021; Ruiz et al., 2021). Because thymol also affects bean weevil fitness traits (Regnault-Roger and Hamraoui, 1995) and deters oviposition (Jevremović et al., 2019) we suppose that various synergistic and antagonistic interactions of thymol with other monoterpenes might take part in determining the number of emerged adults. In other pest species such interactions can affect repellence, feeding deterrence, female attraction to males, egg viability, adult emergence and locomotion (Singh et al., 2009; Tak and Isman, 2017; Youssefi et al., 2019; Ataide et al., 2020; López et al., 2021).

Insecticidal, repellent, antifeedant, oviposition deterrent and growth reducing effects of thymol have been confirmed in stored products (Kim et al., 2010; Szczepanik et al., 2012; Brari and Thakur, 2015; Oliveira et al., 2017, 2018; Shahriari et al., 2017; Wahba et al., 2018; da Camara et al., 2022), agricultural (Hummelbrunner and Isman, 2001; Wilson and Isman, 2006; Pavela, 2011a; Koul et al., 2013; Lima et al., 2020; Valcárcel et al., 2021) and medically important pest insects (Pavela, 2011b; Zahran and Abdelgaleil, 2011; Govindarajan et al., 2013; Youssefi et al., 2019). Influence of thymol on stored products insects depends on insect species, mode of application and sex. For example, in residual contact assays, *Tribolium castaneum* was more sensitive than *Sitophilus oryzae* (Kanda et al., 2017), whereas in fumigant assays efficacy of thymol was equal in these species (Brari and Thakur, 2015). Relative ranking of terpene efficacy also depended on the mode of application. Comparisons of thymol and linalool revealed similar toxicity and oviposition inhibition effect of thymol against the bean weevil in fumigant assay (Regnault-Roger and Hamraoui, 1995), whereas in residual contact assays thymol was more effective in reducing survival and oviposition (Jevremović et al., 2019). About ten times higher vapor pressure of linalool than thymol (0.157 and 0.016 mmHg, respectively) may account for such a relationship. This result is consistent with the findings of other authors that thymol bioactivity is superior in contact assays (Waliwitiya et al., 2005; Hieu et al., 2014; Wahba et al., 2018).

Thymol Toxicity Is Sex-Specific

Bean weevil females are more tolerant to monoterpenes and essential oils (Regnault-Roger and Hamraoui, 1995; Papachristos and Stamopoulos, 2002; Papachristos et al., 2004; Lazarević et al., 2020), which is confirmed in our study with residual contact toxicity of thymol where we recorded higher median lethal concentration and lower initial mortality in females than males. In other insect species, females are usually more tolerant to plant-derived compounds (Yeom et al., 2012; Theou et al., 2013; Jang et al., 2017; Park et al., 2017; Pavela et al., 2021). Sex differences depend on applied compounds and the method of application. Jang et al. (2017) detected higher tolerance of female *Drosophila suzuki* to topically applied citronellal, citronellol and isopulegol, but not after fumigant application. Only essential oils rich in α-pinene were more toxic to *Musca domestica* males (Pavela et al., 2021). In the bean weevil, females were about 3.5 times more resistant to α-terpineol and only 1.2 times more resistant to α-pinene (Papachristos et al., 2004). Likewise, bean weevil females were about 5 times more resistant to *Mentha microphylla* EO and 1.5 times more resistant to *Lavandula hybrida* EO (Papachristos and Stamopoulos, 2002) and thymol (present results). Possible explanations of sexual dimorphism in toxicity of plant-derived compounds against bean weevil are differences in body size and cuticle composition (Tucić et al., 1996; Gołębiowski et al., 2008) as well as differences in physiology (Šešlija et al., 1999; Lazarević et al., 2012, 2020; Arnqvist et al., 2017; Zhang et al., 2020) that may affect compound bioavailability and bean weevils' innate ability to cope with chemical stressors.

Our results showing a lower exponential increase in mortality with age in thymol treatment groups and higher maximum longevity at sublethal thymol concentrations imply that individuals that survived after 24 h of exposure possibly had and/or induced some kind of defense responses. To explore mechanisms of thymol toxicity and tolerance, we determined the activity of six enzymes and found that thymol gradually inhibited activities of AChE and GST, elevated activities of SOD, CAT and CarE at sublethal concentrations and MFO at both sublethal and lethal concentrations. Generally, insects resistant to chemical insecticides and plant-derived compounds have higher activities of AChE, SOD and detoxification enzymes (Attia et al., 2017; Roy and Prasad, 2018; Akami et al., 2019; Senthil-Nathan, 2020). In agreement with this, we found that in the absence of thymol females, the more tolerant sex, contained a higher level of low-molecular thiols (Lazarević et al., 2020) and had higher activities of SOD, CAT and GST (present results).

TABLE 2 | Gompertz mortality parameters (*a* – initial mortality; *b* – exponential increase in mortality with age) and 95% confidence intervals (CI) in *Acanthoscelides obtectus* females and males exposed to different thymol concentrations.

	Gompertz mortality parameters			
Concentration (mg/kg of beans)	***a*** **(× 10^{-2})**	**(CI)**	***b***	**(CI)**
Females				
0	1.09	(0.61, 1.95)	0.40	(0.34, 0.47)
60	1.35	(0.74, 2.46)	0.30*	(0.25, 0.37)
90	9.48*	(6.08, 14.77)	0.15*	(0.10, 0.25)
105	61.63*	(46.24, 82.14)	0.19*	(0.09, 0.41)
Males				
0	0.72	(0.33, 1.57)	0.70^{C}	(0.58, 0.84)
30	2.49*	(1.41, 4.40)	0.41*	(0.33, 0.51)
45	3.60*	(1.96, 6.61)	0.45*	(0.34, 0.58)
60	16.47*,^{C}	(11.01, 24.66)	0.14*,^{B}	(0.08, 0.26)

Significant differences from the control group are marked with asterisks (log-likelihood ratio test, df = 1, $p < 0.05$). Significant differences between females and males of control and 60 mg of thymol / kg of beans treatment group are marked with B ($p < 0.01$) and C ($p < 0.001$).

TABLE 3 | Adult emergence in F1 generation and emergence inhibition (means ± SE for 8 replicates) in *Acanthoscelides obtectus* depending on thymol concentration (Conc) in parental generation.

Thymol	Number of emerged adults			Emergence inhibition (%)		
Conc (mg/kg of beans)	Females	Males	Total	Females	Males	Total
0	43.5 ± 6.6^{c}	47.5 ± 5.2^{c}	91.0 ± 11.3^{c}			
30	48.4 ± 3.4^{c}	55.1 ± 6.3^{c}	103.5 ± 9.3^{c}	−11.2 ± 7.8^{a}	−16.1 ± 13.3^{a}	−13.7 ± 10.2^{a}
45	33.9 ± 4.6^{c}	35.5 ± 4.0^{c}	69.4 ± 8.3^{c}	22.1 ± 10.5^{b}	25.3 ± 8.4^{b}	23.8 ± 9.1^{b}
60	18.6 ± 5.9^{b}	19.5 ± 5.8^{b}	38.1 ± 11.6^{b}	57.2 ± 13.6^{c}	58.9 ± 12.1^{bc}	58.1 ± 12.7^{b}
75	5.8 ± 2.9^{a}	8.9 ± 4.1^{a}	14.6 ± 6.7^{a}	86.8 ± 6.7^{d}	81.3 ± 8.7^{cd}	83.9 ± 7.4^{c}
90	3.4 ± 1.9^{a}	3.9 ± 1.8^{a}	7.3 ± 3.7^{a}	92.2 ± 4.4^{d}	91.8 ± 3.9^{d}	92.0 ± 4.0^{c}

Values marked with different letters (a, b, c, d) within columns indicate significant differences among treatments (Duncan's post-hoc test, $p < 0.05$).

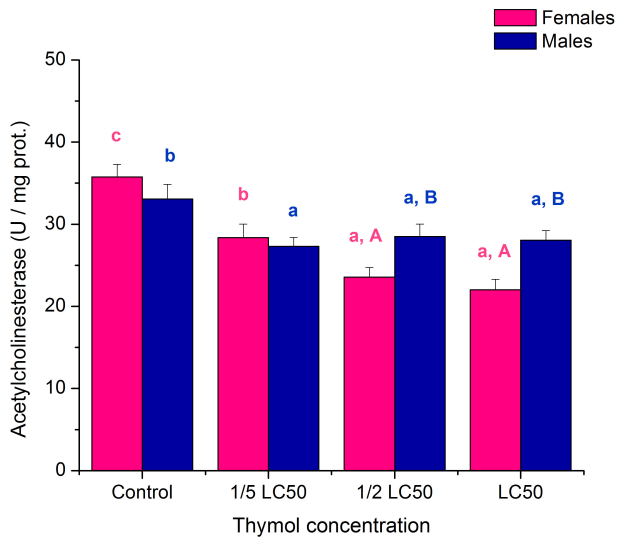

FIGURE 4 | Activity of acetylcholinesterase (mean ± SE for 5 replicates) in females and males of *Acanthoscelides obtectus* exposed to different thymol concentrations. Different lowercase letters (a, b, c) mark significant differences among concentrations within each sex (Duncan's *post-hoc* test, $p < 0.05$), whereas different uppercase letters (A, B) show significant differences between females and males within each thymol concentration (LSM contrasts, $p < 0.05$).

Role of Antioxidative Enzymes in Tolerance to Thymol

After exposure to sublethal thymol concentrations, SOD increased both in females and males whereas at lethal concentration it was increased only in males. SOD responds first to oxidative stress induced by xenobiotics and protects cells from dangerous free radicals. Without efficient scavenging of its product of reaction H_2O_2 by catalase and other peroxidases, it may damage macromolecules, accelerate aging and reduce insect survival and longevity. For instance, bean weevil females exposed to thyme essential oil had lower a level of damaged lipids (Lazarević et al., 2020). In consistence with our results, SOD and CAT were elevated by thymol in *Ephestia kuehniella* larvae (Shahriari et al., 2018), by carvacrol, p-cymene and γ-terpinene in *S. littoralis* larvae (Agliassa and Maffei, 2018), by carvacrol in *Lymantria dispar* larvae (Chen et al., 2021), by ethanolic extract of *Acalypha wilkesiana* leaves in *Callosobruchus maculatus* adults (Oni et al., 2019) and by *Boswellia carterii* EO in adults of two *Callosobruchus* species (Kiran et al., 2017). SOD and CAT responses to botanicals may vary depending on insect species, duration of exposure, botanical type and concentration. Several studies have shown that more resistant species had higher SOD and CAT activity, higher induction of activity and/or higher CAT to SOD ratio (Kiran et al., 2017; Petrović et al., 2019). Also, in some species, botanicals can reduce SOD and/or CAT activity at high concentrations (Oni et al., 2019; Rajkumar et al., 2019).

Here we recorded higher CAT activity and CAT to SOD activity ratio in females across all examined thymol concentrations that could account for sex-specific differences in tolerance to thymol. Similar result was obtained in *A. obtectus* populations selected for early and late reproduction (Šešlija et al., 1999) indicating that a higher CAT and CAT to SOD ratio is characteristic of this species. Tasaki et al. (2017) suggested that females of eusocial Isoptera and Hymenoptera have high CAT activity whereas in solitary insects CAT activity is lower in females than males. However, there are also examples of higher CAT activity in females of solitary species under control (Sharma et al., 1995) and stressful conditions (Rovenko et al., 2015; Manna et al., 2020; Wang et al., 2020). Several studies have shown that CAT accumulates in insect ovaries providing protection to developing oocytes from oxidative damage (e.g., de Jong et al., 2007; Diaz-Albiter et al., 2011). We speculate that such mechanism might contribute to higher CAT activity in *A. obtectus* females which emerge with about 30 mature chorionated eggs in the lateral oviduct (Leroi, 1981). In the absence of mating antioxidants accumulated in eggs would be fully available for defense against xenobiotics.

Thymol Inhibits Activities of AChE and GST

Our observation about inhibition of neurotransmitter enzyme AChE and detoxification enzyme GST by thymol in bean weevil females and males agrees with findings of other studies on physiological mechanisms of monoterpenes and essential oils toxicity (Mojarab-Mahboubkar et al., 2015; Liao et al., 2016, 2017; Agliassa and Maffei, 2018; Yang et al., 2018; Chen et al., 2021; Fouad and Abotaleb, 2021). Inhibition of AChE leads

TABLE 4 | F and *p* values from 2-way ANOVA testing significance of main and interaction effects of sex and thymol concentration on activities of acetylcholinesterase (AChE), superoxide dismutase (SOD), catalase (CAT), mixed-function oxidase (MFO), carboxylesterase (CarE), and glutathione S-transferase (GST) in *Acanthoscelides obtectus*.

Source of	AChE		SOD		CAT		MFO		CarE		GST	
variation	F	*p*	F	*p*	F	*p*	F	*p*	F	*p*	F	*p*
Sex (df: 1, 32)	3.2	0.082	0.0	0.935	2366.0	**<0.001**	31.4	**<0.001**	682.7	**<0.001**	22.5	**<0.001**
Concentration (df: 3, 32)	17.6	**<0.001**	9.7	**<0.001**	19.8	**<0.001**	41.6	**<0.001**	21.3	**<0.001**	150.1	**<0.001**
Sex × Concentration (df: 3, 32)	4.6	**0.009**	8.6	**<0.001**	1.2	0.329	3.4	**0.029**	7.0	**<0.001**	43.6	**<0.001**

Significant effects are marked in bold.

to accumulation of acetylcholine at nerve synapses, and thus permanent conduction of nerve impulses, ataxia, convulsions and death (Rattan, 2010). AChE activity was more reduced in females than males so that males had higher activity at thymol concentration 1/2 of LC_{50} and LC_{50}. In difference to our results, AChE of female adults of *Blatella germanica* and *Drosophila suzuki* were less sensitive to in vitro inhibition with thymol (Yeom et al., 2012; Park et al., 2016). The discrepancy between toxicity and AChE inhibition by botanical insecticides suggests differences in other neurological or enzymatic target sites. A weak correlation has been found between AChE activity and insecticide resistance in *D. melanogaster* (Charpentier and Fournier, 2001). Therefore, the relationship between AChE activity and resistance to chemical stress may depend on insect species and population or applied compound. For example, although more resistant to fumigation with lemongrass essential oil AChE activity in treated females of *Callosobrucus maculatus* was lower than in males (de Souza et al., 2019). To fully understand AChE-thymol resistance relationship further researches are needed to reveal how thymol affects the level of cholinergic and non-cholinergic AChE isoforms. Non-cholinergic AChE is important for insect fecundity and defense against xenobiotics, and, compared to cholinergic isoform, exhibits lower catalytic efficiency and higher resistance to inhibiton by insecticides (Kim Y. H. et al., 2012; Kim et al., 2014; Lu et al., 2012; Hwang et al., 2014; Lee et al., 2015; Kim and Lee, 2018). Therefore, a higher level of protective non-cholinergic isoform might provide higher thymol resistance to females despite the lower activity. Several studies have shown sex-dependant relative expression of genes encoding the two isoforms (Zhao et al., 2013; Salim et al., 2017).

Inhibition of GST by thymol is an important feature from the pest management point of view because it could interfere with the detoxification in insects and lead to enhanced activity of conventional insecticides (Ismail, 2021). In *Trichoplusia ni* larvae, topical application of thymol inhibited GST activity by 41% (Tak et al., 2017), whereas topical application of thymol on larvae of *Plutella xylostella* (Kumrungsee et al., 2014), and oral administration in *Ephestia kuehniella* (Shahriari et al., 2018) and *Tuta absoluta* (Piri et al., 2020) increased GST activity. At LC_{50} of thymol we obtained that there was no difference in GST activity between females and males. However, because initial activity in control females was higher, a higher percentage of inhibition was recorded in females than males (58 vs. 35%). Sexual dimorphism in detoxification enzyme activity has also been revealed in other studies where pest insects were exposed to plant-derived compounds. In *C. maculatus* GST, p-NPA esterase and α-esterase were not affected by lemongrass oil, whereas β-esterase was inhibited only in females (de Souza et al., 2019).

Thymol Increases Activities of Phase I Detoxification Enzymes

Two enzymes involved in the phase I detoxification, CarE and MFO, increased the activity in response to thymol suggesting that they could have an important role in thymol metabolism in the bean weevil females and males. Further investigations are needed to elucidate how bean weevils detoxify thymol. In mammals, the majority of thymol is rapidly excreted unchanged or as a conjugate but oxidation of methyl and isopropyl groups also occurred (Austgulen et al., 1987). In difference to our results, thymol did not change the activity of CarE and MFO in *Trichoplusia ni* (Tak et al., 2017) which larvae excreted thymol bound to glucose without the change in its monoterpenoid structure (Passreiter et al., 2004). Highly diverse results have been obtained in other insect species where thymol had insignificant effect on esterase and MFO activities (Yotavong et al., 2015) or provoked their induction (Boncristiani et al., 2012; Kumrungsee et al., 2014; Piri et al., 2020) or inhibition (Waliwitiya et al., 2012; Shahriari et al., 2017; Gaire et al., 2021).

Comparison between thymol treated females and males revealed that males had higher CarE and MFO activity and provoked activity increase at lower thymol concentrations than females. It is not clear how detoxification enzyme activity variation contributes to the higher tolerance of females to insecticides. For example, females of *Helopeltis theivora* that are more tolerant to organophosphates had similar MFO activity to males and higher activity of α-esterase and GST (Roy and Prasad, 2018). Females of tortricid species *Lobesia botrana* and *Grapholita molesta* that are more tolerant to neonicotinoid insecticide thiacloprid and less tolerant to organophosphate insecticide chloropyrifos, exhibited sex-specific differences in detoxification enzymes (Navarro-Roldán et al., 2017, 2020). Namely, females of *L. botrana* had higher activities of MFO and GST and lower sensitivity of esterase to specific inhibitor DEF, whereas *G. molesta* females exhibited faster inhibition of MFO with specific

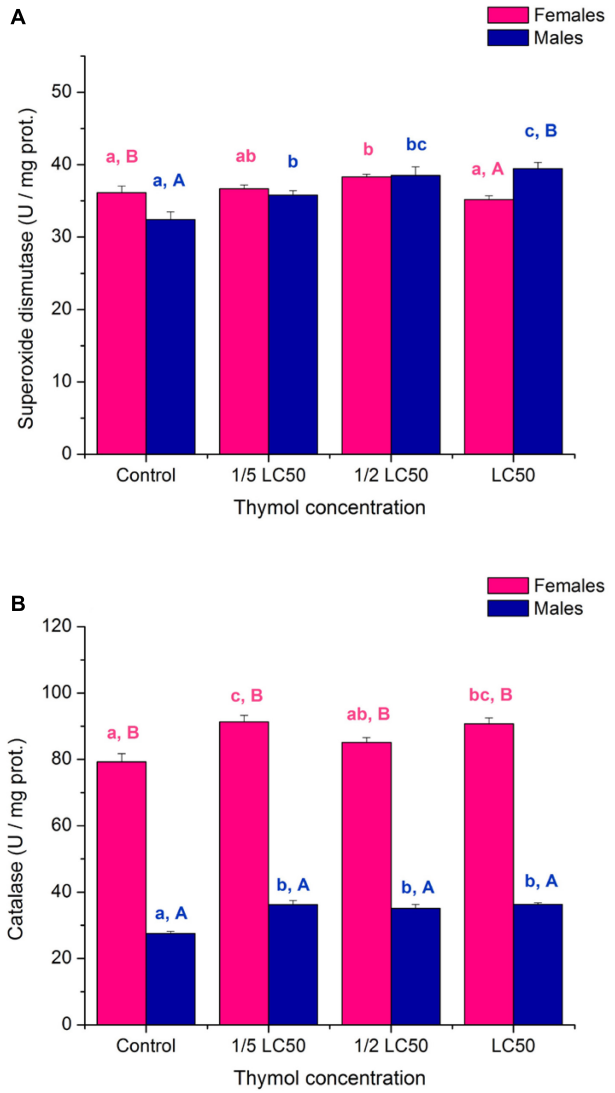

FIGURE 5 | Activity of superoxide dismutase **(A)** and catalase **(B)** in females and males of *Acanthoscelides obtectus* exposed to different thymol concentrations (mean ± SE for 5 replicates). Different lowercase letters (a, b, c) mark significant differences among concentrations within each sex (Duncan's *post-hoc* test, $p < 0.05$), whereas different uppercase letters (A, B) show significant differences between females and males within each thymol concentration (LSM contrasts, $p < 0.01$).

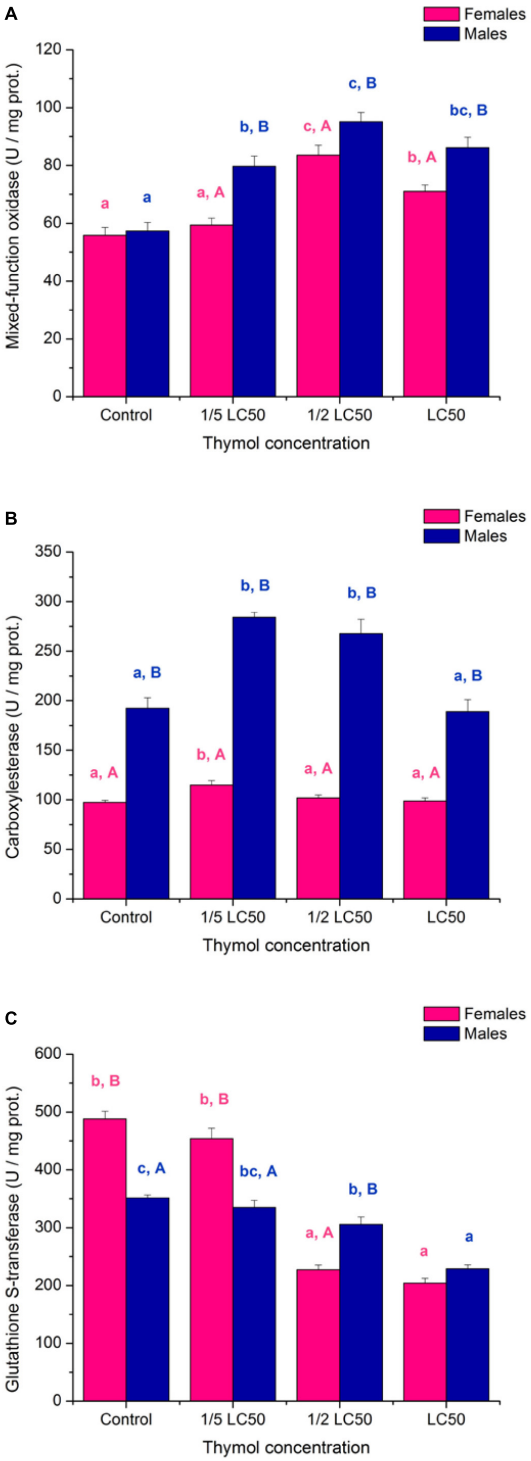

FIGURE 6 | Activity of mixed-function oxidases **(A)**, carboxylesterase **(B)** and glutathione S-transferase **(C)** in females and males of *Acanthoscelides obtectus* exposed to different thymol concentrations (means ± SE for 5 replicates). Different lowercase letters (a, b, c) mark significant differences among concentrations within each sex (Duncan's *post-hoc* test, $p < 0.05$), whereas different uppercase letters (A, B) show significant differences between females and males within each thymol concentration (LSM contrasts, $p < 0.05$).

inhibitor PBO. In *C. macullatus* treated with lemongrass oil females had higher p-NPA esterase activity (de Souza et al., 2019). Evidently, our results on lower activity of detoxification enzymes in more tolerant sex disagree with other studies on chemical and botanical insecticides. This may suggest an involvement of other mechanisms of tolerance such as better behavioral avoidance of a toxic compound or cuticle structure which slows-down thymol penetration (Panini et al., 2016). Besides, esterases and MFO are multifunctional enzymes encoded by a large number of genes organized into families (Feyereisen, 2012; Montella et al., 2012). Change in

detoxification gene expression in response to xenobiotics is sex-biased and can be related to sex-specific differences in xenobiotic metabolism or other sex-specific physiological functions such as the production of pheromones and hormones by MFO and odorant degradation by esterases (Le Goff et al., 2006; Robert et al., 2013; Liu et al., 2019). High CarE activity that we recorded in male weevils might be related to its role in reproduction. It is known that carboxylesterases are overexpressed in the male reproductive tract of insects where they provide protection against xenobiotics and take part in sperm differentiation, maturation and function (Mikhailov and Torrado, 1999, 2000). In agreement with our results much higher esterase activity in males than females have been detected in whole body homogenates of *Lygus hesperus* (Zhu and Brindley, 1990) and abdomens of *Grapholita molesta* (de Lame et al., 2001) and *Cydia pomonella* (Fuentes-Contreras et al., 2007).

Conclusion

In conclusion, we showed insecticidal activity of thymol against the bean weevil. Since thymol has been approved by the Environmental protection agency for use on food crops (EPA Code 080402, 2021) and has many human health promoting effects (de Alvarenga et al., 2021) it can be safely used as a contact insecticide on bean seeds. Results on bean weevil physiological responses have implications for designing of future thymol-based insecticides. Inhibition of AChE is responsible for fast mortality response. However, thymol-induced inhibition was weak and thus involvement of other neurotoxicity and/or metabolic targets cannot be excluded. Due to inhibition of GST thymol can be used to synergize effects of chemical insecticides for which GST activity is crucial and thus reduce applied doses of these dangerous compounds. Since thymol induce the activity of MFO and CarE future formulations of thymol-based insecticides should involve inhibitors of these enzymes. Sex-specific differences in tolerance to thymol and sex-specific physiological responses to thymol exposure (especially high CAT and CAT to SOD activity ratio in females, and high CarE activity in males) should be also taken into account in bean weevil management. Further studies are needed to fully elucidate mechanisms of thymol toxicity and tolerance.

DATA AVAILABILITY STATEMENT

The raw data supporting the conclusions of this article will be made available by the authors, without undue reservation.

AUTHOR CONTRIBUTIONS

JL, IK, and DŠJ designed the experiment. JL, DŠJ, and SJ conducted the experiment. AV and SMJ determined enzyme activities. DŠJ and MK performed statistical analysis. JL, DŠJ, and IK prepared the manuscript. All authors have read and agreed to the published version of the manuscript.

FUNDING

This research was funded by the Ministry of Education, Science and Technological Development of the Republic of Serbia, grant no. 451-03-9/2021-14/200007.

REFERENCES

Abdelgaleil, S. A. M., Gad, H. A., Ramadan, G. R., El-Bakry, A. M., and El-Sabrout, A. M. (2021b). Monoterpenes: chemistry, insecticidal activity against stored product insects and modes of action—a review. *Int. J. Pest Manag.* 2, 1–23. doi: 10.1080/09670874.2021.1982067

Abdelgaleil, S. A. M., Al-Nagar, N. M., Abou-Taleb, H. K., and Shawir, M. S. (2021a). Effect of monoterpenes, phenylpropenes and sesquiterpenes on development, fecundity and fertility of *Spodoptera littoralis* (Boisduval). *Int. J. Trop. Insect Sci.* 2, 1–9. doi: 10.1007/s42690-021-00539-y

Agliassa, C., and Maffei, M. E. (2018). Origanum vulgare terpenoids induce oxidative stress and reduce the feeding activity of *Spodoptera littoralis*. *Int. J. Mol. Sci.* 19:2805. doi: 10.3390/ijms19092805

Akami, M., Njintang, N. Y., Gbaye, O., Niu, C. Y., and Nukenine, E. N. (2019). Comparative expression of two detoxification genes by *Callosobruchus maculatus* in response to dichlorvos and *Lippia adoensis* essential oil treatments. *J. Pest Sci.* 92, 665–676. doi: 10.1007/s10340-018-01075-4

Al-Nagar, N. M., Abou-Taleb, H. K., Shawir, M. S., and Abdelgaleil, S. A. (2020). Comparative toxicity, growth inhibitory and biochemical effects of terpenes and phenylpropenes on *Spodoptera littoralis* (Boisd.). *J. Asia-Pac. Entomol.* 23, 67–75. doi: 10.1016/j.aspen.2019.09.005

Alvarez, N., McKey, D., Hossaert-Mckey, M., Born, C., Mercier, L., and Benrey, B. (2005). Ancient and recent evolutionary history of the bruchid beetle, *Acanthoscelides obtectus* Say, a cosmopolitan pest of beans. *Mol. Ecol.* 14, 1015–1024. doi: 10.1111/j.1365-294X.2005.02470.x

Arnqvist, G., Stojković, B., Rönn, J. L., and Immonen, E. (2017). The pace-of-life: A sex-specific link between metabolic rate and life history in bean beetles. *Funct. Ecol.* 31, 2299–2309. doi: 10.1111/1365-2435.12927

Ataide, J. O., Holtz, F. G., Destefani, F., Deolindo, A. H., Zago, H. B., Menini, L., et al. (2020). Exposure to major components of essential oils and their mixtures cause mortality, sublethal effect and behavioral disturbance of *Sitophilus zeamais* (Motschulsky) (Coleoptera: Curculionidae). *J. Pharmacogn. Phytochem.* 9, 1329–1335. doi: 10.22271/phyto.2020.v9.i2v.11038

Attia, M. A., Wahba, T. F., Mackled, M. I., and Shawir, M. S. (2017). Resistance status and associated resistance mechanisms to certain insecticides in rice weevil *Sitophilus oryzae* (Coleoptera: Curculionidae). *Alexandria J. Agricult. Sci.* 62, 331–340. doi: 10.21608/alexja.2017.67624

Austgulen, L. T., Solheim, E., and Scheline, R. R. (1987). Metabolism in rats of p-cymene derivatives: carvacrol and thymol. *Pharmacol. Toxicol.* 61, 98–102. doi: 10.1111/j.1600-0773.1987.tb01783.x

Barbosa, D. R. S., de Oliveira, J. V., da Silva, P. H. S., Santana, M. F., Breda, M. O., de França, S. M., et al. (2021). Lethal and sublethal effects of chemical constituents from essential oils on *Callosobruchus maculatus* (F.) (Coleoptera: Chrysomelidae: Bruchinae) in cowpea stored grains. *J. Plant Dis. Prot.* 128, 1575–1586. doi: 10.1007/s41348-021-00543-x

Boncristiani, H., Underwood, R., Schwarz, R., Evans, J. D., and Pettis, J. (2012). Direct effect of acaricides on pathogen loads and gene expression levels in honey bees *Apis mellifera*. *J. Insect Physiol.* 58, 613–620. doi: 10.1016/j.jinsphys.2011.12.011

Bradford, M. M. (1976). A rapid and sensitive method for the quantitation of microgram quantities of protein utilizing the principle of protein-dye binding. *Anal. Biochem.* 72, 248–254. doi: 10.1016/j.jinsphys.2011.12.011

Brari, J., and Thakur, D. R. (2015). Fumigant toxicity and cytotoxicity evaluation of monoterpenes against four stored products pests. *Int. J. Dev. Res.* 5, 5661–5667.

Brogdon, W. G., McAllister, J. C., and Vulule, J. (1997). Heme peroxidase activity measured in single mosquitoes identifies individuals expressing an elevated oxidase for insecticide resistance. *J. Am. Mosq. Control Assoc.* 13, 233–237.

Charpentier, A., and Fournier, D. (2001). Levels of total acetylcholinesterase in *Drosophila melanogaster* in relation to insecticide resistance. *Pestic. Biochem. Physiol.* 70, 100–107. doi: 10.1006/pest.2001.2549

Charpentier, G., Vidau, C., Ferdy, J. B., Tabart, J., and Vetillard, A. (2014). Lethal and sub-lethal effects of thymol on honeybee (*Apis mellifera*) larvae reared in vitro. *Pest Manag. Sci.* 70, 140–147. doi: 10.1002/ps.3539

Chaudhari, A. K., Singh, V. K., Kedia, A., Das, S., and Dubey, N. K. (2021). Essential oils and their bioactive compounds as eco-friendly novel green pesticides for management of storage insect pests: prospects and retrospects. *Environ. Sci. Pollut. Res.* 28, 18918–18940. doi: 10.1007/s11356-021-12841-w

Chen, Y. Z., Zhang, B. W., Yang, J., Zou, C. S., Li, T., Zhang, G. C., et al. (2021). Detoxification, antioxidant, and digestive enzyme activities and gene expression analysis of *Lymantria dispar* larvae under carvacrol. *J. Asia-Pac. Entomol.* 24, 208–216. doi: 10.1016/j.aspen.2020.12.014

Claiborne, A. (1984). "Catalase activity," in *Handbook of Methods for Oxygen Radical Research*, ed. R. A. Greenwald (Boca Raton, FL: CRC Press), 283–284. doi: 10.1201/9781351072922

Cohen, S. M., Eisenbrand, G., Fukushima, S., Gooderham, N. J., Guengerich, F. P., Hecht, S. S., et al. (2021). FEMA GRAS assessment of natural flavor complexes: origanum oil, thyme oil and related phenol derivative-containing flavoring ingredients. *Food Chem. Toxicol.* 155:112378. doi: 10.1016/j.fct.2021.112378

da Camara, C. A., Doboszewski, B., de Melo, J. P., Nazarenko, A. Y., dos Santosa, R. B., and Moraesa, M. M. (2022). Novel insecticides from alkylated and acylated derivatives of thymol and eugenol for the control of *Plutella xylostella* (Lepidoptera: Plutellidae). *J. Braz. Chem. Soc.* 33, 196–204. doi: 10.21577/0103-5053.20210137

da Cunha, F. A. B., Wallau, G. L., Pinho, A. I., Nunes, M. E. M., Leite, N. F., Tintino, S. R., et al. (2015). *Eugenia uniflora* leaves essential oil induces toxicity in *Drosophila melanogaster*: involvement of oxidative stress mechanisms. *Toxicol. Res.* 4, 634–644. doi: 10.1039/c4tx00162a

Daglish, G. J., Nayak, M. K., Arthur, F. H., and Athanassiou, C. G. (2018). "Insect pest management in stored grain," in *Recent Advances in Stored Product Protection*, eds C. G. Athanassiou and F. H. Arthur (Berlin: Springer), 45–63. doi: 10.1007/978-3-662-56125-6_3

Dar, M. A., Kaushik, G., and Chiu, J. F. V. (2020). "Pollution status and biodegradation of organophosphate pesticides in the environment," in *Abatement of Environmental Pollutants*, eds P. Singh, A. Kumar, and A. Borthakur (Amsterdam: Elsevier), 25–66. doi: 10.1016/B978-0-12-818095-2.00002-3

de Alvarenga, J. F. R., Genaro, B., Costa, B. L., Purgatto, E., Manach, C., and Fiamoncini, J. (2021). Monoterpenes: current knowledge on food source, metabolism, and health effects. *Crit. Rev. Food Sci. Nutr.* 2, 1–38. doi: 10.1080/10408398.2021.1963945

de Andrade Brito, F., Bacci, L., da Silva Santana, A., da Silva, J. E., de Castro Nizio, D. A., de Lima Nogueira, P. C., et al. (2021). Toxicity and behavioral alterations caused by essential oils of *Croton tetradenius* and their major compounds on *Acromyrmex balzani*. *Crop. Prot.* 137:105259. doi: 10.1016/j.cropro.2020.105259

de Jong, R. J., Miller, L. M., Molina-Cruz, A., Gupta, L., Kumar, S., and Barillas-Mury, C. (2007). Reactive oxygen species detoxification by catalase is a major determinant of fecundity in the mosquito *Anopheles gambiae*. *Proc. Natl. Acad. Sci. U.S.A.* 104, 2121–2126. doi: 10.1073/pnas.0608407104

de Lame, F. M., Hong, J. J., Shearer, P. W., and Brattsten, L. B. (2001). Sex-related differences in the tolerance of Oriental fruit moth (*Grapholita molesta*) to organophosphate insecticides. *Pest. Manage. Sci.* 57, 827–832. doi: 10.1002/ps.368

de Melo, C. R., Picanco, M. C., Santos, A. A., Santos, I. B., Pimentel, M. F., Santos, A. C., et al. (2018). Toxicity of essential oils of *Lippia gracilis* chemotypes and their major compounds on *Diaphania hyalinata* and non-target species. *Crop Prot.* 104, 47–51. doi: 10.1016/j.cropro.2017.10.013

de Souza, A. M., Campos, I. M., de Brito, D. D. M. C., Cardoso, C. M., Pontes, E. G., and de Souza, M. A. A. (2019). Efficacy of lemongrass essential oil and citral in controlling *Callosobruchus maculatus* (Coleoptera: Chrysomelidae), a post-harvest cowpea insect pest. *Crop Prot.* 119, 191–196. doi: 10.1016/j.cropro.2019.02.007

Diaz-Albiter, H., Mitford, R., Genta, F. A., Sant'Anna, M. R., and Dillon, R. J. (2011). Reactive oxygen species scavenging by catalase is important for female *Lutzomyia longipalpis* fecundity and mortality. *PLoS One* 6:e17486. doi: 10.1371/journal.pone.0017486

Ebadollahi, A., and Sendi, J. J. (2015). A review on recent research results on bio-effects of plant essential oils against major Coleopteran insect pests. *Toxin Rev.* 34, 76–91. doi: 10.3109/15569543.2015.1023956

Ellman, G. L., Courtney, K. D., Andres, V. Jr., and Featherstone, R. M. (1961). A new and rapid colorimetric determination of acetylcholinesterase activity. *Biochem. Pharmacol.* 7, 88–95. doi: 10.1016/0006-2952(61)90145-9

EPA Code 080402 (2021). Available online at: https://www3.epa.gov/pesticides/chem_search/reg_actions/registration/decision_PC-080402_23-Mar-06.pdf (accessed December 22, 2021).

Escobar, C. A. M., Pérez, M. C., Romanelli, G. P., and Blustein, G. (2020). Thymol bioactivity: a review focusing on practical applications. *Arab. J. Chem.* 13, 9243–9269. doi: 10.1016/j.arabjc.2020.11.009

Feyereisen, R. (2012). "Insect CYP genes and P450 enzymes ," in *Insect Molecular Biology and Biochemistry*, ed. L. I. Gilbert (Cambridge, MA: Academic Press), 236–316. doi: 10.1016/B978-0-12-384747-8.10008-X

Finney, D. J. (1971). *Probit Analysis*, 3th Edn. Cambridge: Cambridge University Press. doi: 10.1002/jps.2600600940

Floros, G. D., Kokkari, A. I., Kouloussis, N. A., Kantiranis, N. A., Damos, P., Filippidis, A. A., et al. (2018). Evaluation of the natural zeolite lethal effects on adults of the bean weevil under different temperatures and relative humidity regimes. *J. Econ. Entomol.* 111, 482–490. doi: 10.1093/jee/tox305

Fouad, E. A., and Abotaleb, A. O. (2021). Sublethal effects of two insecticides, deltamethrin, thiamethoxam and the botanical insecticide (*Foeniculum vulgare* Mill.) on *Callosobruchus maculates* (Fabr.) (Coleoptera: Bruchidae). *Egypt. Acad. J. Biol. Sci. A Entomol.* 14, 255–269. doi: 10.21608/EAJBSA.2021.161753

Freitas, R. S., Faroni, L. R. A., and Sousa, A. H. (2016). Hermetic storage for control of common bean weevil, *Acanthoscelides obtectus* (Say). *J. Stored Prod. Res.* 66, 1–5. doi: 10.1016/j.jspr.2015.12.004

Fuentes-Contreras, E., Reyes, M., Barros, W., and Sauphanor, B. (2007). Evaluation of azinphos-methyl resistance and activity of detoxifying enzymes in codling moth (Lepidoptera: Tortricidae) from central Chile. *J. Econ. Entomol.* 100, 551–556. doi: 10.1093/jee/100.2.551

Gaire, S., Zheng, W., Scharf, M. E., and Gondhalekar, A. D. (2021). Plant essential oil constituents enhance deltamethrin toxicity in a resistant population of bed bugs (*Cimexlectularius* L.) by inhibiting cytochrome P450 enzymes. *Pestic. Biochem. Phys.* 175:104829. doi: 10.1016/j.pestbp.2021.104829

Gao, S., Zhang, K., Wei, L., Wei, G., Xiong, W., Lu, Y., et al. (2020). Insecticidal activity of *Artemisia vulgaris* essential oil and transcriptome analysis of *Tribolium castaneum* in response to oil exposure. *Front. Genet.* 11:589. doi: 10.3389/fgene.2020.00589

Gołębiowski, M., Malinski, E., Nawrot, J., and Stepnowski, P. (2008). Identification andcharacterization of surface lipid components of the dried-bean beetle *Acanthoscelides obtectus* (Say) (Coleoptera: Bruchidae). *J. Stored Prod. Res.* 44, 386–388. doi: 10.1016/j.jspr.2008.02.010

Govindarajan, M., Sivakumar, R., Rajeswary, M., and Veerakumar, K. (2013). Mosquito larvicidal activity of thymol from essential oil of *Coleus aromaticus* Benth. against *Culex tritaeniorhynchus*, *Aedes albopictus*, and *Anopheles subpictus* (Diptera: Culicidae). *Parasitol. Res.* 112, 3713–3721. doi: 10.1007/s00436-013-3557-2

Guedes, R. N. C., Walse, S. S., and Throne, J. E. (2017). Sublethal exposure, insecticide resistance, and community stress. *Curr. Opin. Insect Sci.* 21, 47–53. doi: 10.1016/j.cois.2017.04.010

Habig, W. H., Pabst, M. J., and Jakoby, W. B. (1974). Glutathione S-transferases. The first enzymatic step in mercapturic acid formation. *J. Biol. Chem.* 249, 7130–7139. doi: 10.1016/S0021-9258(19)42083-8

Hategekimana, A., and Erler, F. (2020). Fecundity and fertility inhibition effects of some plant essential oils and their major components against *Acanthoscelides obtectus* Say (Coleoptera: Bruchidae). *J. Plant Dis. Prot.* 127, 615–623. doi: 10.1007/s41348-020-00311-3

Herrera, J. M., Zunino, M. P., Dambolena, J. S., Pizzolitto, R. P., Gañan, N. A., Lucini, E. I., et al. (2015). Terpene ketones as natural insecticides against *Sitophilus zeamais*. *Ind. Crops Prod.* 70, 435–442. doi: 10.1016/j.indcrop.2015.03.074

Hieu, T. T., Kim, S. I., and Ahn, Y. J. (2014). Toxicity of *Zanthoxylum piperitum* and *Zanthoxylum armatum* oil constituents and related compounds to *Stomoxys calcitrans* (Diptera: Muscidae). *J. Med. Entomol.* 49, 1084–1091. doi: 10.1603/ME12047

Hu, J., Wang, W., Dai, J., and Zhu, L. (2019). Chemical composition and biological activity against *Tribolium castaneum* (Coleoptera: Tenebrionidae) of *Artemisia brachyloba* essential oil. *Ind. Crops Prod.* 128, 29–37. doi: 10.1016/j.indcrop.2018.10.076

Huang, Y., Liao, M., Yang, Q., Xiao, J., Hu, Z., Zhou, L., et al. (2018). Transcriptome profiling reveals differential gene expression of detoxification enzymes in *Sitophilus zeamais* responding to terpinen-4-ol fumigation. *Pestic. Biochem. Physiol.* 149, 44–53. doi: 10.1016/j.pestbp.2018.05.008

Hummelbrunner, L. A., and Isman, M. B. (2001). Acute, sublethal, antifeedant, and synergistic effects of monoterpenoid essential oil compounds on the tobacco cutworm, *Spodoptera litura* (Lep., Noctuidae). *J. Agric. Food Chem.* 49, 715–720. doi: 10.1021/jf000749t

Hwang, C. E., Kim, Y. H., Kwon, D. H., Seong, K. M., Choi, J. Y., Je, Y. H., et al. (2014). Biochemical and toxicological properties of two acetylcholinesterases from the common bed bug, *Cimex lectularius*. *Pestic. Biochem. Physiol.* 110, 20–26. doi: 10.1016/j.pestbp.2014.02.002

Ismail, S. (2021). Synergistic efficacy of plant essential oils with cypermethrin and chlorpyrifos against *Spodoptera littoralis*, field populations in Egypt. *Int. J. Adv. Biol. Biomed. Res.* 9, 128–137. doi: 10.22034/ijabbr.2021.239417

Isman, M. B. (2020). Bioinsecticides based on plant essential oils: a short overview. *Z. Naturforsch.* C 75, 179–182. doi: 10.1515/znc-2020-0038

Iturralde-García, R. D., Castañé, C., Wong-Corral, F. J., and Riudavets, J. (2020). Biological control of *Acanthoscelides obtectus* and *Zabrotes subfasciatus* in stored dried beans. *Bio. Control* 65, 693–701. doi: 10.1007/s10526-020-10048-5

Jang, M., Kim, J., Yoon, K. A., Lee, S. H., and Park, C. G. (2017). Biological activity of Myrtaceae plant essential oils and their major components against *Drosophila suzukii* (Diptera: Drosophilidae). *Pest Manag. Sci.* 73, 404–409. doi: 10.1002/ps.4430

Jankowska, M., Rogalska, J., Wyszkowska, J., and Stankiewicz, M. (2018). Molecular targets for components of essential oils in the insect nervous system – a review. *Molecules* 23:34. doi: 10.3390/molecules23010034

Jevremović, S., Lazarević, J., Kostić, M., Krnjajić, S., Ugrenović, V., Radonjić, A., et al. (2019). Contact application of Lamiaceae botanicals reduces bean weevil infestation in stored beans. *Arch. Biol. Sci.* 71, 665–676. doi: 10.2298/ABS190617049J

Johnson, C. D. (1981). "Relations of *Acanthoscelides* with their plant hosts," in *The Ecology of Bruchids Attacking Legumes (Pulses)*, ed. V. Labeyrie (Dordrecht: Springer), 73–81. doi: 10.1007/978-94-017-3286-4_7

Kanda, D., Kaur, S., and Koul, O. (2017). A comparative study of monoterpenoids and phenylpropanoids from essential oils against stored grain insects: acute toxins or feeding deterrents. *J. Pest Sci.* 90, 531–545. doi: 10.1007/s10340-016-0800-5

Keszthelyi, S., Bosnyakne, E. H., Horváth, D., Csóka, Á, Kovacs, G., and Tamas, D. (2018). Nutrient content restructuring and CT-measured density, volume attritions on damaged beans caused by *Acanthoscelides obtectus* Say (Coleoptera: Chrysomelidae). *J. Plant Prot. Res.* 58, 91–95. doi: 10.24425/119123

Kim, S. I., Ahn, Y. J., and Kwon, H. W. (2012). "Toxicity of aromatic plants and their constituents against coleopteran stored products insect pests," in *New Perspectives in Plant Protection*, ed. A. R. Bandani (London: InTech), 93–120. doi: 10.5772/36288_5

Kim, S. I., Yoon, J. S., Jung, J. W., Hong, K. B., Ahn, Y. J., and Kwon, H. W. (2010). Toxicity and repellency of origanum essential oil and its components against *Tribolium castaneum* (Coleoptera: Tenebrionidae) adults. *J. Asia-Pac. Entomol.* 13, 369–373. doi: 10.1016/j.aspen.2010.06.011

Kim, Y. H., and Lee, S. H. (2018). Invertebrate acetylcholinesterases: insights into their evolution and non-classical functions. *J. Asia-Pac. Entomol.* 21, 186–195. doi: 10.1016/j.aspen.2017.11.017

Kim, Y. H., Cha, D. J., Jung, J. W., Kwon, H. W., and Lee, S. H. (2012). Molecular and kinetic properties of two acetylcholinesterases from the western honey bee, *Apis mellifera*. *PLoS One* 7:e48838. doi: 10.1371/journal.pone.0048838

Kim, Y. H., Kwon, D. H., Ahn, H. M., Koh, Y. H., and Lee, S. H. (2014). Induction of soluble AChE expression via alternative splicing by chemical stress in *Drosophila melanogaster*. *Insect Biochem. Mol. Biol.* 48, 75–82. doi: 10.1016/j.ibmb.2014.03.001

Kiran, S., and Prakash, B. (2015a). Assessment of toxicity, antifeedant activity, and biochemical responses in stored-grain insects exposed to lethal and sublethal doses of *Gaultheria procumbens* L. essential oil. *J. Agric. Food Chem.* 63, 10518–10524. doi: 10.1021/acs.jafc.5b03797

Kiran, S., and Prakash, B. (2015b). Toxicity and biochemical efficacy of chemically characterized *Rosmarinus officinalis* essential oil against *Sitophilus oryzae* and *Oryzaephilus surinamensis*. *Ind. Crops Prod.* 74, 817–823. doi: 10.1016/j.indcrop.2015.05.073

Kiran, S., Kujur, A., Patel, L., Ramalakshmi, K., and Prakash, B. (2017). Assessment of toxicity and biochemical mechanisms underlying the insecticidal activity of chemically characterized *Boswellia carterii* essential oil against insect pest of legume seeds. *Pestic. Biochem. Phys.* 139, 17–23. doi: 10.1016/j.pestbp.2017.04.004

Kısa, A., Akyüz, M., Çoğun, H. Y., Kordali, Ş, Bozhüyük, A. U., Tezel, B., et al. (2018). Effects of *Olea europaea* L. leaf metabolites on the tilapia (*Oreochromis niloticus*) and three stored pests, *Sitophilus granarius*, *Tribolium confusum* and *Acanthoscelides obtectus*. *Rec. Nat. Prod.* 12, 201–215. doi: 10.25135/rnp.23.17.07.126

Koul, O., Singh, R., Kaur, B., and Kanda, D. (2013). Comparative study on the behavioral response and acute toxicity of some essential oil compounds and their binary mixtures to larvae of *Helicoverpa armigera*, *Spodoptera litura* and *Chilo partellus*. *Ind. Crops Prod.* 49, 428–436. doi: 10.1007/s10340-018-01075-4

Kumrungsee, N., Pluempanupat, W., Koul, O., and Bullangpoti, V. (2014). Toxicity of essential oil compounds against diamondback moth, *Plutella xylostella*, and their impact on detoxification enzyme activities. *J. Pest Sci.* 87, 721–729. doi: 10.1007/s10340-014-0602-6

Labeyrie, V. (1990). "The bean beetle (*Acanthoscelides obtectus*) and its host, the French bean (*Phaseolus vulgaris*): a two-way colonization story," in *Biological Invasions in Europe and the Mediterranean Basin*, eds F. di Castri, A. J. Hansen, and M. Debussche (Dordrecht: Springer), 229–243. doi: 10.1007/s10340-014-0602-6

Lazarević, J., Đorđević, M., Stojković, B., and Tucić, N. (2013). Resistance to prooxidant agent paraquat in the short-and long-lived lines of the seed beetle (*Acanthoscelides obtectus*). *Biogerontology* 14, 141–152. doi: 10.1007/s10522-013-9417-8

Lazarević, J., Jevremović, S., Kostić, I., Kostić, M., Vuleta, A., Manitašević Jovanović, S., et al. (2020). Toxic, oviposition deterrent and oxidative stress effects of *Thymus vulgaris* essential oil against *Acanthoscelides obtectus*. *Insects* 11:563. doi: 10.3390/insects11090563

Lazarević, J., Radojković, A., Kostić, I., Krnjajić, S., Mitrović, J., Kostić, M. B., et al. (2018). Insecticidal impact of alumina powders against *Acanthoscelides obtectus* (Say). *J. Stored Prod. Res.* 77, 45–54. doi: 10.1016/j.jspr.2018.02.006

Lazarević, J., Tucić, N., Šešlija Jovanović, D., Veèeøa, J., and Kodrík, D. (2012). The effects of selection for early and late reproduction on metabolite pools in *Acanthoscelides obtectus* Say. *Insect Sci.* 19, 303–314. doi: 10.1111/j.1744-7917.2011.01457.x

Le Goff, G., Hilliou, F., Siegfried, B. D., Boundy, S., Wajnberg, E., Sofer, L., et al. (2006). Xenobiotic response in *Drosophila melanogaster*: sex dependence of P450 and GST gene induction. *Insect Biochem. Mol. Biol.* 36, 674–682. doi: 10.1016/j.ibmb.2006.05.009

Lee, E. J., Kim, J. R., Choi, D. R., and Ahn, Y. J. (2008). Toxicity of cassia and cinnamon oil compounds and cinnamaldehyde-related compounds to *Sitophilus oryzae* (Coleoptera: Curculionidae). *J. Econ. Entomol.* 101, 1960–1966. doi: 10.1603/0022-0493-101.6.1960

Lee, S. H., Kim, Y. H., Kwon, D. H., Cha, D. J., and Kim, J. H. (2015). Mutation and duplication of arthropod acetylcholinesterase: implications for pesticide resistance and tolerance. *Pestic. Biochem. Physiol.* 120, 118–124. doi: 10.1016/j.pestbp.2014.11.004

Leroi, B. (1981). "Feeding, longevity and reproduction of adults of *Acanthoscelides obtectus* Say in laboratory conditions," in *The Ecology of Bruchids Attacking Legumes (Pulses)*, (Dordrecht: Springer), 101–111. doi: 10.1007/978-94-017-3286-4_10

Liao, M., Xiao, J. J., Zhou, L. J., Liu, Y., Wu, X. W., Hua, R. M., et al. (2016). Insecticidal activity of *Melaleuca alternifolia* essential oil and RNA-Seq analysis of *Sitophilus zeamais* transcriptome in response to oil fumigation. *PLoS One* 11:e0167748. doi: 10.1371/journal.pone.0167748

Liao, M., Xiao, J. J., Zhou, L. J., Yao, X., Tang, F., Hua, R. M., et al. (2017). Chemical composition, insecticidal and biochemical effects of *Melaleuca alternifolia* essential oil on the *Helicoverpa armigera*. *J. Appl. Entomol.* 141, 721–728. doi: 10.1111/jen.12397

Liao, M., Yang, Q. Q., Xiao, J. J., Huang, Y., Zhou, L. J., Hua, R. M., et al. (2018). Toxicity of *Melaleuca alternifolia* essential oil to the mitochondrion and NAD+/NADH dehydrogenase in *Tribolium confusum*. *Peer J.* 6:e5693. doi: 10.7717/peerj.5693

Lima, A. P., Santana, E. D., Santos, A. C., Silva, J. E., Ribeiro, G. T., Pinheiro, A. M., et al. (2020). Insecticide activity of botanical compounds against *Spodoptera frugiperda* and selectivity to the predatory bug *Podisus nigrispinus*. *Crop Prot.* 136:105230. doi: 10.1016/j.cropro.2020.105230

Liu, H., Lei, X., Du, L., Yin, J., Shi, H., Zhang, T., et al. (2019). Antennae-specific carboxylesterase genes from Indian meal moth: identification, tissue distribution and the response to semiochemicals. *J. Stored Prod. Res.* 84:101528. doi: 10.1016/j.jspr.2019.101528

Liu, J., Hua, J., Qu, B., Guo, X., Wang, Y., Shao, M., et al. (2021). Insecticidal terpenes from the essential oils of *Artemisia nakaii* and their inhibitory effects on acetylcholinesterase. *Front. Plant Sci.* 12:720816. doi: 10.3389/fpls.2021.720816

López, M. D., and Pascual-Villalobos, M. J. (2010). Mode of inhibition of acetylcholinesterase by monoterpenoids and implications for pest control. *Ind. Crops Prod.* 31, 284–288. doi: 10.1016/j.indcrop.2009.11.005

López, M. D., and Pascual-Villalobos, M. J. (2015). Are monoterpenoids and phenylpropanoids efficient inhibitors of acetylcholinesterase from stored product insect strains? *Flavour Frag. J.* 30, 108–112. doi: 10.1002/ffj.3220

López, S., Domínguez, A., Guerrero, Á, and Quero, C. (2021). Inhibitory effect of thymol on pheromone-mediated attraction in two pest moth species. *Sci. Rep.* 11, 1–10. doi: 10.1038/s41598-020-79550-1

Lu, Y., Park, Y., Gao, X., Zhang, X., Yao, J., Pang, Y. P., et al. (2012). Cholinergic and non-cholinergic functions of two acetylcholinesterase genes revealed by gene-silencing in *Tribolium castaneum*. *Sci. Rep.* 2, 1–7. doi: 10.1038/srep00288

Mancini, E., Senatore, F., Del Monte, D., De Martino, L., Grulova, D., Scognamiglio, M., et al. (2015). Studies on chemical composition, antimicrobial and antioxidant activities of five *Thymus vulgaris* L. essential oils. *Molecules* 20, 12016–12028. doi: 10.3390/molecules200712016

Manna, B., Maiti, S., and Das, A. (2020). Bioindicator potential of *Spathosternum prasiniferum prasiniferum* (Orthoptera; Acridoidea) in pesticide (azadirachtin)-induced radical toxicity in gonadal/nymphal tissues; correlation with eco-sustainability. *J. Asia Pac. Entomol.* 23, 350–357. doi: 10.1016/j.aspen.2020.02.007

Mikhailov, A. T., and Torrado, M. (1999). Carboxylesterase overexpression in the male reproductive tract: a universal safeguarding mechanism? *Reprod. Fertil. Dev.* 11, 133–146. doi: 10.1071/RD99011

Mikhailov, A. T., and Torrado, M. (2000). Carboxylesterases moonlight in the male reproductive tract: a functional shift pivotal for male fertility. *Front. Biosci.* 5:e53–e62. doi: 10.2741/mikhail

Misra, H. P., and Fridovich, I. (1972). The role of superoxide anion in the autoxidation of epinephrine and simple assay for superoxide dismutase. *J. Biol. Chem.* 247, 3170–3175. doi: 10.1016/S0021-9258(19)45228-9

Mohapatra, D., Kar, A., and Giri, S. K. (2015). Insect pest management in stored pulses: an overview. *Food Bioproc. Tech.* 8, 239–265. doi: 10.1007/s11947-014-1399-2

Mojarab-Mahboubkar, M., Sendi, J. J., and Aliakbar, A. (2015). Effect of *Artemisia annua* L. essential oil on toxicity, enzyme activities, and energy reserves of cotton bollworm *Helicoverpa armigera* (Hübner) (Lepidoptera: Noctuidae). *J. Plant Prot. Res.* 55:49. doi: 10.1515/jppr-2015-0049

Montella, I. R., Schama, R., and Valle, D. (2012). The classification of esterases: an important gene family involved in insecticide resistance-A review. *Mem. Inst. Oswaldo Cruz.* 107, 437–449. doi: 10.1590/s0074-02762012000400001

Navarro-Roldán, M. A., Avilla, J., Bosch, D., Valls, J., and Gemeno, C. (2017). Comparative effect of three neurotoxic insecticides with different modes of action on adult males and females of three tortricid moth pests. *J. Econom. Entomol.* 110, 1740–1749. doi: 10.1093/jee/tox113

Navarro-Roldán, M. A., Bosch, D., Gemeno, C., and Siegwart, M. (2020). Enzymatic detoxification strategies for neurotoxic insecticides in adults of three tortricid pests. *Bull. Entomol. Res.* 110, 144–154. doi: 10.1017/S0007485319000415

Nayak, M. K., and Daglish, G. J. (2018). "Importance of stored product insects," in *Recent Advances in Stored Product Protection*, eds G. Athanassiou and F. H. Arthur (Berlin: Springer), 1–17. doi: 10.1007/978-3-662-56125-6_1

Nerio, L. S., Oliver-Verbal, J., and Stashenko, E. (2010). Repellent activity of essential oils: a review. *Bioresour. Technol.* 101, 372–378. doi: 10.1016/j.biortech.2009.07.048

Norris, E. J., Bartholomay, L., and Coats, J. (2018). "Present and future outlook: the potential of green chemistry in vector control," in *Advances in the Biorational Control of Medical and Veterinary Pests*, eds E. J. Norris, J. R. Coats, A. D. Gross, and J. M. Clark (Washington, DC: ACS), 43–62. doi: 10.1021/bk-2018-1289.ch004

Obeng-Ofori, D. (2010). "Residual insecticides, inert dusts and botanicals for the protection of durable stored products against pest infestation in developing countries," in *Proceedings of the Sixth International Working Conference on Stored-product Protection*, eds M. O. Carvalho, P. G. Fields, C. S. Adler, F. H. Arthur, C. G. Athanassiou, J. F. Campbell, et al. (Estoril: Julius-Kühn-Archiv), 774–788. doi: 10.5073/jka.2010.425.141

Oliveira, A. P., Santana, A. S., Santana, E. D., Lima, A. P. S., Faro, R. R., Nunes, R. S., et al. (2017). Nanoformulation prototype of the essential oil of *Lippia sidoides* and thymol to population management of *Sitophilus zeamais* (Coleoptera: Curculionidae). *Ind. Crops Prod.* 107, 198–205. doi: 10.1016/j.indcrop.2017.05.046

Oliveira, A. P., Santos, A. A., Santana, A. S., Lima, A. P. S., Melo, C. R., Santana, E. D., et al. (2018). Essential oil of *Lippia sidoides* and its major compound thymol: toxicity and walking response of populations of *Sitophilus zeamais* (Coleoptera: Curculionidae). *Crop Prot.* 112, 33–38. doi: 10.1016/j.cropro.2018.05.011

Oni, M. O., Ogungbite, O. C., Oguntuase, S. O., Bamidele, O. S., and Ofuya, T. I. (2019). Inhibitory effects of oil extract of green Acalypha (*Acalypha wilkesiana*) on antioxidant and neurotransmitter enzymes in *Callosobruchus maculatus*. *J. Basic Appl. Zool.* 80, 1–13. doi: 10.1186/s41936-019-0116-0

Panini, M., Manicardi, G. C., Moores, G. D., and Mazzoni, E. (2016). An overview of the main pathways of metabolic resistance in insects. *Invertebr. Surviv. J.* 13, 326–335. doi: 10.25431/1824-307X/isj.v13i1.326-335

Papachristos, D. P., and Stamopoulos, D. C. (2002). Repellent, toxic and reproduction inhibitory effects of essential oil vapours on *Acanthoscelides obtectus* (Say) (Coleoptera: Bruchidae). *J. Stored Prod. Res.* 38, 117–128. doi: 10.1016/S0022-474X(01)00007-8

Papachristos, D. P., Karamanoli, K. I, Stamopoulos, D. C., and Menkissoglu-Spiroudi, U. (2004). The relationship between the chemical composition of three essential oils and their insecticidal activity against *Acanthoscelides obtectus* (Say). *Pest Manag. Sci.* 60, 514–520. doi: 10.1002/ps.798

Park, C. G., Jang, M., Yoon, K. A., and Kim, J. (2016). Insecticidal and acetylcholinesterase inhibitory activities of Lamiaceae plant essential oils and their major components against *Drosophila suzukii* (Diptera: Drosophilidae). *Ind. Crops Prod.* 89, 507–513. doi: 10.1016/j.indcrop.2016.06.008

Park, J. H., Jeon, Y. J., Lee, C. H., Chung, N., and Lee, H. S. (2017). Insecticidal toxicities of carvacrol and thymol derived from *Thymus vulgaris* Lin. against *Pochazia shantungensis* Chou & Lu., newly recorded pest. *Sci. Rep.* 7, 1–7. doi: 10.1038/srep40902

Passreiter, C. M., Wilson, J., Andersen, R., and Isman, M. B. (2004). Metabolism of thymol and trans-anethole in larvae of *Spodoptera litura* and *Trichoplusia ni* (Lepidoptera: Noctuidae). *J. Agri. Food Chem.* 52, 2549–2551. doi: 10.1021/jf035386m

Pavela, R. (2011a). Antifeedant and larvicidal effects of some phenolic components of essential oils lasp lines of introduction against *Spodoptera littoralis* (Boisd.). *J. Essent. Oil Bear. Plants* 14, 266–273. doi: 10.1080/0972060X.2011.10643932

Pavela, R. (2011b). Insecticidal properties of phenols on *Culex quinquefasciatus* Say and *Musca domestica* L. *Parasitol. Res.* 109, 1547–1553. doi: 10.1007/s00436-011-2395-3

Pavela, R. (2016). History, presence and perspective of using plant extracts as commercial botanical insecticides and farm products for protection against insects–a review. *Plant Prot. Sci.* 52, 229–241. doi: 10.17221/31/2016-PPS

Pavela, R., Maggi, F., Mazzara, E., Torresi, J., Cianfaglione, K., Benelli, G., et al. (2021). Prolonged sublethal effects of essential oils from non-wood parts of nine conifers on key insect pests and vectors. *Ind. Crops Prod.* 168:113590. doi: 10.1016/j.indcrop.2021.113590

Pavela, R., Morshedloo, M. R., Mumivand, H., Khorsand, G. J., Karami, A., Maggi, F., et al. (2020). Phenolic monoterpene-rich essential oils from Apiaceae and Lamiaceae species: insecticidal activity and safety evaluation on non-target earthworms. *Entomol. Gen*. 40, 421–435. doi: 10.1127/entomologia/2020/1131

Peter, K. V., and Shylaja, M. R. (2012). "Introduction to herbs and spices: definitions, trade and applications," in *Handbook of Herbs and Spices*, ed. K. V. Peter (Cambridge: Woodhead Publishing), 1–24. doi: 10.1533/9780857095671.1

Petrović, M., Popović, A., Kojić, D., Šućur, J., Bursić, V., Aćimović, M., et al. (2019). Assessment of toxicity and biochemical response of *Tenebrio molitor* and *Tribolium confusum* exposed to *Carum carvi* essential oil. *Entomol. Gen*. 38, 333–348. doi: 10.1127/entomologia/2019/0697

Pinho, A. I., Wallau, G. L., Nunes, M. E. M., Leite, N. F., Tintino, S. R., da Cruz, L. C., et al. (2014). Fumigant activity of the *Psidium guajava var. pomifera* (Myrtaceae) essential oil in *Drosophila melanogaster* by means of oxidative stress. *Oxid. Med. Cell. Longev*. 4:696785. doi: 10.1155/2014/696785

Piri, A., Sahebzadeh, N., Zibaee, A., Sendi, J. J., Shamakhi, L., and Shahriari, M. (2020). Toxicity and physiological effects of ajwain (*Carum copticum*, Apiaceae) essential oil and its major constituents against *Tuta absoluta* (Meyrick) (Lepidoptera: Gelechiidae). *Chemosphere* 256:127103. doi: 10.1016/j.chemosphere.2020.127103

Pletcher, S. D. (1999). Model fitting and hypothesis testing for age-specific mortality data. *J. Evol. Biol*. 12, 430–439. doi: 10.1046/j.1420-9101.1999.00058.x

Prasantha, B. R., Reichmuth, C. H., and Adler, C. (2019). Lethality and kinetic of diatomaceous earth uptake by the bean weevil (*Acanthoscelides obtectus* [Say] Coleoptera: Bruchinae): Influence of short-term exposure period. *J. Stored Prod. Res*. 84:101509. doi: 10.1016/j.jspr.2019.101509

Rajendran, S. (2020). Insect pest management in stored products. *Outlooks Pest Manag*. 31, 24–35. doi: 10.1564/v31_feb_05

Rajkumar, V., Gunasekaran, C., Christy, I. K., Dharmaraj, J., Chinnaraj, P., and Paul, C. A. (2019). Toxicity, antifeedant and biochemical efficacy of *Mentha piperita* L. essential oil and their major constituents against stored grain pest. *Pestic. Biochem. Physiol.* 156, 138–144. doi: 10.1016/j.pestbp.2019.02.016

Rattan, R. S. (2010). Mechanism of action of insecticidal secondary metabolites of plant origin. *Crop Prot*. 29, 913–920. doi: 10.1016/j.cropro.2010.05.008

Regnault-Roger, C., and Hamraoui, A. (1995). Fumigant toxic activity and reproductive inhibition induced by monoterpenes on *Acanthoscelides obtectus* (Say) (Coleoptera), a bruchid of kidney bean (*Phaseolus vulgaris* L.). *J. Stored Prod. Res*. 31, 291–299. doi: 10.1016/0022-474X(95)00025-3

Regnault-Roger, C., Hamraoui, A., Holeman, M., Theron, E., and Pinel, R. (1993). Insecticidal effect of essential oils from mediterranean plants upon *Acanthoscelides obtectus* Say (Coleoptera, Bruchidae), a pest of kidney bean (*Phaseolus vulgaris* L.). *J. Chem. Ecol*. 19, 1233–1244. doi: 10.1007/BF00987383

Reynoso, M. M. N., Lucia, A., Zerba, E. N., and Alzogaray, R. A. (2018). Eugenol-hyperactivated nymphs of *Triatoma infestans* become intoxicated faster than non-hyperactivated nymphs when exposed to a permethrin-treated surface. *Parasite. Vector*. 11, 1–9. doi: 10.1186/s13071-018-3146-4

Robert, J. A., Pitt, C., Bonnett, T. R., Yuen, M. M., Keeling, C. I., Bohlmann, J., et al. (2013). Disentangling detoxification: gene expression analysis of feeding mountain pine beetle illuminates molecular-level host chemical defense detoxification mechanisms. *PLoS One* 8:e77777. doi: 10.1371/journal.pone.0077777

Rodríguez-González, Á, Casquero, P. A., Suárez-Villanueva, V., Carro-Huerga, G., Álvarez-García, S., Mayo-Prieto, S., et al. (2018). Effect of trichodiene production by *Trichoderma harzianum* on *Acanthoscelides obtectus*. *J. Stored Prod. Res*. 77, 231–239. doi: 10.1016/j.jspr.2018.05.001

Rodríguez-González, Á, Porteous-Álvarez, A. J., Del Val, M., Casquero, P. A., and Escriche, B. (2020). Toxicity of five Cry proteins against the insect pest *Acanthoscelides obtectus* (Coleoptera: Chrisomelidae: Bruchinae). *J. Invertebr. Pathol*. 169:107295. doi: 10.1016/j.jip.2019.107295

Rovenko, B. M., Kubrak, O. I., Gospodaryov, D. V., Perkhulyn, N. V., Yurkevych, I. S., Sanz, A., et al. (2015). High sucrose consumption promotes obesity whereas its low consumption induces oxidative stress in *Drosophila melanogaster*. *J. Insect Physiol.* 79, 42–54. doi: 10.1016/j.jinsphys.2015.05.007

Roy, S., and Prasad, A. K. (2018). Sex-based variation in insecticide susceptibility and tolerance related biochemical parameters in tea mosquito bug *Helopeltis theivora*. *Phytoparasitica* 46, 405–410. doi: 10.1007/s12600-018-0670-x

Ruiz, M. J., Juárez, M. L., Jofré Barud, F., Goane, L., Valladares, G. A., Bachmann, G. E., et al. (2021). Lemon and *Schinus polygama* essential oils enhance male mating success of *Anastrepha fraterculus*. *Entomol. Exp. Appl*. 169, 172–182. doi: 10.1111/eea.13005

Ruttanaphan, T., Pluempanupat, W., Aungsirisawat, C., Boonyarit, P., Goff, G. L., and Bullangpoti, V. (2019). Effect of plant essential oils and their major constituents on cypermethrin tolerance associated detoxification enzyme activities in *Spodoptera litura* (Lepidoptera: Noctuidae). *J. Econom. Entomol*. 112, 2167–2176. doi: 10.1093/jee/toz126

Salim, A. M., Shakeel, M., Ji, J., Kang, T., Zhang, Y., Ali, E., et al. (2017). Cloning, expression, and functional analysis of two acetylcholinesterase genes in *Spodoptera litura* (Lepidoptera: Noctuidae). *Comp. Biochem. Physiol. B: Biochem. Mol. Biol.* 206, 16–25. doi: 10.1016/j.cbpb.2017.01.007

Schmale, I., Wäckers, F. L., Cardona, C., and Dorn, S. (2002). Field infestation of *Phaseolus vulgaris* by *Acanthoscelides obtectus* (Coleoptera: Bruchidae), parasitoid abundance, and consequences for storage pest control. *Environ. Entomol*. 31, 859–863. doi: 10.1603/0046-225X-31.5.859

Senthil-Nathan, S. (2020). A review of resistance mechanisms of synthetic insecticides and botanicals, phytochemicals, and essential oils as alternative larvicidal agents against mosquitoes. *Front. Physiol*. 10:1591. doi: 10.3389/fphys.2019.01591

Šešlija Jovanović, D., Đorđević, M., Savković, U., and Lazarević, J. (2014). The effect of mitochondrial complex I inhibitor on longevity of short-lived and long-lived seed beetles and its mitonuclear hybrids. *Biogerontology* 15, 487–501. doi: 10.1007/s10522-014-9520-5

Šešlija, D., Blagojević, D., Spasić, M., and Tucić, N. (1999). Activity of superoxide dismutase and catalase in the bean weevil (*Acanthoscelides obtectus*) selected for postponed senescence. *Exp. Gerontol*. 34, 185–195. doi: 10.1016/S0531-5565(98)00078-3

Shahriari, M., Sahbzadeh, N., Zibaee, A., Khani, A., and Senthil-Nathan, S. (2017). Metabolic response of *Ephestia kuehniella* Zeller (Lepidoptera: Pyralidae) to essential oil of Ajwain and thymol. *Toxin Rev*. 36, 204–209. doi: 10.1080/15569543.2017.1294605

Shahriari, M., Zibaee, A., Sahebzadeh, N., and Shamakhi, L. (2018). Effects of α-pinene, trans-anethole, and thymol as the essential oil constituents on antioxidant system and acetylcholine esterase of *Ephestia kuehniella* Zeller (Lepidoptera: Pyralidae). *Pestic. Biochem. Physiol*. 150, 40–47. doi: 10.1016/j.pestbp.2018.06.015

Shang, X. F., Dai, L. X., Liu, Y. Q., Zhao, Z. M., Li, J. C., Yang, G. Z., et al. (2019). Acaricidal activity and enzyme inhibitory activity of active compounds of essential oils against *Psoroptes cuniculi*. *Vet. Parasitol*. 267, 54–59. doi: 10.1016/j.vetpar.2019.01.013

Sharma, S. P., Sharma, M., and Kakkar, R. (1995). Methionine-lnduced Alterations in the Life Span, Antioxidant Enzymes, and Peroxide Levels in *Aging Zaprionus paravittiger* (Diptera). *Gerontology* 41, 86–93. doi: 10.1159/000213668

Singh, R., Koul, O., Rup, P. J., and Jindal, J. (2009). Toxicity of some essential oil constituents and their binary mixtures against *Chilo partellus* (Lepidoptera: Pyralidae). *Int. J. Trop. Insect Sci*. 29, 93–101. doi: 10.1017/S1742758409990087

Subaharan, K., Senthoorraja, R., Manjunath, S., Thimmegowda, G. G., Pragadheesh, V. S., Bakthavatsalam, N., et al. (2021). Toxicity, behavioural and biochemical effect of *Piper betle* L. essential oil and its constituents against housefly, *Musca domestica* L. *Pestic. Biochem. Physiol*. 174:104804. doi: 10.1016/j.pestbp.2021.104804

Sun, J., Feng, Y., Wang, Y., Li, J., Zou, K., Liu, H., et al. (2020). Investigation of pesticidal effects of *Peucedanum terebinthinaceum* essential oil on three stored-product insects. *Rec. Nat. Prod*. 14, 177–189. doi: 10.25135/rnp.149.19.05.1287

Szczepanik, M., Zawitowska, B., and Szumny, A. (2012). Insecticidal activities of *Thymus vulgaris* essential oil and its components (thymol and carvacrol) against larvae of lesser mealworm, *Alphitobius diaperinus* Panzer (Coleoptera: Tenebrionidae). *Allelopathy* J. 30, 129–142.

Szentesi, Á (2021). How the seed coat affects the mother's oviposition preference and larval performance in the bean beetle (*Acanthoscelides obtectus*, Coleoptera: Chrysomelidae, Bruchinae) in leguminous species. *BMC Ecol. Evol.* 21:1–14. doi: 10.1186/s12862-021-01892-9

Tak, J. H., and Isman, M. B. (2017). Acaricidal and repellent activity of plant essential oil-derived terpenes and the effect of binary mixtures against *Tetranychus urticae* Koch (Acari: Tetranychidae). *Ind. Crops Prod*. 108, 786–792. doi: 10.1016/j.indcrop.2017.08.003

Tak, J. H., Jovel, E., and Isman, M. B. (2017). Effects of rosemary, thyme and lemongrass oils and their major constituents on detoxifying enzyme activity and insecticidal activity in *Trichoplusia ni*. *Pestic. Biochem. Physiol*. 140, 9–16. doi: 10.1016/j.pestbp.2017.01.012

Tasaki, E., Kobayashi, K., Matsuura, K., and Iuchi, Y. (2017). An efficient antioxidant system in a long-lived termite queen. *PLoS One* 12:e0167412. doi: 10.1371/journal.pone.0167412

Theou, G., Papachristos, D. P., and Stamopoulos, D. C. (2013). Fumigant toxicity of six essential oils to the immature stages and adults of *Tribolium confusum*. *Hell. Plant Prot. J*. 6, 29–39.

Tucić, N., Gliksman, I., Šešlija, D., Milanović, D., Mikuljanac, S., and Stojković, O. (1996). Laboratory evolution of longevity in the bean weevil (*Acanthoscelides obtectus*). *J. Evol. Biol*. 9, 485–503. doi: 10.1046/j.1420-9101.1996.9040485.x

Valcárcel, F., Olmeda, A. S., González, M. G., Andrés, M. F., Navarro-Rocha, J., and González-Coloma, A. (2021). Acaricidal and insect antifeedant effects of essential oils from selected aromatic plants and their main components. *Front. Agron*. 3:662802. doi: 10.3389/fagro.2021.662802

Vasantha-Srinivasan, P., Chellappandian, M., Senthil-Nathan, S., Ponsankar, A., Thanigaivel, A., Karthi, S., et al. (2018). A novel herbal product based on *Piper betle* and *Sphaeranthus indicus* essential oils: Toxicity, repellent activity and impact on detoxifying enzymes GST and CYP450 of *Aedes aegypti* Liston (Diptera: Culicidae). *J. Asia Pac. Entomol*. 21, 1466–1472. doi: 10.1016/j.aspen.2018.10.008

Wahba, T. F., Mackled, M. I., Selim, S., and El-Zemity, S. R. (2018). Toxicity and reproduction inhibitory effects of some monoterpenes against the cowpea weevil *Callosobruchus maculatus* F. (Coleoptera: Chrysomelidae: Bruchinae). *Middle East J. Appl. Sci*. 8, 1061–1070.

Waliwitiya, R., Isman, M. B., Vernon, R. S., and Riseman, A. (2005). Insecticidal activity of selected monoterpenoids and rosemary oil to *Agriotes obscurus* (Coleoptera: Elateridae). *J. Econom. Entomol*. 98, 1560–1565. doi: 10.1093/jee/98.5.1560

Waliwitiya, R., Nicholson, R. A., Kennedy, C. J., and Lowenberger, C. A. (2012). The synergistic effects of insecticidal essential oils and piperonyl butoxide on biotransformational enzyme activities in *Aedes aegypti* (Diptera: Culicidae). *J. Med. Entomol*. 49, 614–623. doi: 10.1603/ME10272

Wang, J. L., Li, Y., and Lei, C. L. (2009). Evaluation of monoterpenes for the control of *Tribolium castaneum* (Herbst) and *Sitophilus zeamais* Motschulsky. *Nat. Prod. Res*. 23, 1080–1088. doi: 10.1080/14786410802267759

Wang, W., Gao, C., Ren, L., and Luo, Y. (2020). The effect of longwave ultraviolet light radiation on *Dendrolimus tabulaeformis* antioxidant and detoxifying enzymes. *Insects* 11:1. doi: 10.3390/insects11010001

Wilson, J. A., and Isman, M. B. (2006). Influence of essential oils on toxicity and pharmacokinetics of the plant toxin thymol in the larvae of *Trichoplusia ni*. *Can. Entomol*. 138, 578–589. doi: 10.4039/n06-801

Wu, D., Scharf, M. E., Neal, J. J., Suiter, D. R., and Bennett, G. W. (1998). Mechanisms of fenvalerate resistance in the German cockroach, *Blattella germanica* (L.). *Pestic. Biochem. Physiol*. 61, 53–62. doi: 10.1006/pest.1998.2343

Yang, H., Piao, X., Zhang, L., Song, S., and Xu, Y. (2018). Ginsenosides from the stems and leaves of *Panax ginseng* show antifeedant activity against *Plutella xylostella* (Linnaeus). *Ind. Crops Prod*. 124, 412–417. doi: 10.1016/j.indcrop.2018.07.054

Yeom, H. J., Kang, J. S., Kim, G. H., and Park, I. K. (2012). Insecticidal and acetylcholine esterase inhibition activity of Apiaceae plant essential oils and their constituents against adults of German cockroach (*Blattella germanica*). *J. Agric. Food Chem*. 60, 7194–7203. doi: 10.1021/jf302009w

Yotavong, P., Boonsoong, B., Pluempanupat, W., Koul, O., and Bullangpoti, V. (2015). Effects of the botanical insecticide thymol on biology of a braconid, *Cotesia plutellae* (Kurdjumov), parasitizing the diamondback moth, *Plutella xylostella* L. *Int. J. Pest Manag*. 61, 171–178. doi: 10.1080/09670874.2015.1030001

Youssefi, M. R., Tabari, M. A., Esfandiari, A., Kazemi, S., Moghadamnia, A. A., Sut, S., et al. (2019). Efficacy of two monoterpenoids, carvacrol and thymol, and their combinations against eggs and larvae of the West Nile vector *Culex pipiens*. *Molecules* 24:1867. doi: 10.3390/molecules24101867

Zahran, H. E. D. M., and Abdelgaleil, S. A. (2011). Insecticidal and developmental inhibitory properties of monoterpenes on *Culex pipiens* L. (Diptera: Culicidae). *J. Asia Pac. Entomol*. 14, 46–51. doi: 10.1016/j.aspen.2010.11.013

Zhang, S., Wang, X., Gu, F., Gong, C., Chen, L., Zhang, Y., et al. (2020). Sublethal effects of triflumezopyrim on biological traits and detoxification enzyme activities in the small brown planthopper *Laodelphax striatellus* (Hemiptera: Delphacidae). *Front. Physiol*. 11:261. doi: 10.3389/fphys.2020.00261

Zhao, P., Wang, Y., and Jiang, H. (2013). Biochemical properties, expression profiles, and tissue localization of orthologous acetylcholinesterase-2 in the mosquito, *Anopheles gambiae*. *Insect Biochem. Mol. Biol.* 43, 260–271. doi: 10.1016/j.ibmb.2012.12.005

Zhu, K. Y., and Brindley, W. A. (1990). Properties of esterases from *Lygus hesperus* Knight (Hemiptera: Miridae) and the roles of the esterases in insecticide resistance. *J. Econ. Entomol*. 83, 725–732. doi: 10.1093/jee/83.3.725

Zibaee, A. (2011). "Botanical insecticides and their effects on insect biochemistry and immunity," in *Pesticides in the Modern World-Pests Control and Pesticides Exposure and Toxicity Assessment*, ed. M. Stoytcheva (London: InTech), 55–68.

Conflict of Interest: The authors declare that the research was conducted in the absence of any commercial or financial relationships that could be construed as a potential conflict of interest.

Publisher's Note: All claims expressed in this article are solely those of the authors and do not necessarily represent those of their affiliated organizations, or those of the publisher, the editors and the reviewers. Any product that may be evaluated in this article, or claim that may be made by its manufacturer, is not guaranteed or endorsed by the publisher.

frontiers in Physiology

ORIGINAL RESEARCH
published: 24 February 2022
doi: 10.3389/fphys.2022.829675

Silencing of *Adc* and *Ebony* Causes Abnormal Darkening of Cuticle in *Henosepilachna vigintioctopunctata*

Long-Ji Ze, Lin Jin and Guo-Qing Li*

Education Ministry Key Laboratory of Integrated Management of Crop Diseases and Pests/State & Local Joint Engineering Research Center of Green Pesticide Invention and Application, Department of Entomology, College of Plant Protection, Nanjing Agricultural University, Nanjing, China

N-β-alanyldopamine (NBAD) is a precursor of N-acylquinone sclerotin utilized for cross-linking between cuticular proteins for cuticle during insect molting. The importance of NBAD in cuticle tanning has not been well compared among different developing stages of insects. *Henosepilachna vigintioctopunctata*, a typical polyphagous pest feeding on a large number of Solanaceae and Cucurbitaceae plants in Asian countries, displays diverse cuticle pigmentation patterns among developing stages and body regions. Here, we found that the expression of three genes (*Hvadc*, *Hvebony*, and *Hvtan*) involved in NBAD biosynthesis peaked in the 4-day-old pupae or 0-day-old adults of *H. vigintioctopunctata*. At the first, second, third, and fourth larval instar and pupal stage, their transcript levels were high just before and/or right after the molting. Moreover, they were more abundantly transcribed at the larval heads than in the bodies. RNA interference (RNAi) of either *Hvadc* or *Hvebony* at the third instar larvae selectively deepened the color of the larval head capsules, antennae, mouthpart, scoli, strumae, and legs; and depletion of the two genes blackened the pupal head capsules, antennae, mouthpart, and legs. However, the knockdown of either *Hvadc* or *Hvebony* darkened the whole bodies of the adults. Conversely, RNAi of *Hvtan* at the third instar stage had little influence on the pigmentation in the larvae, pupae, and adults. These findings demonstrated that Adc and Ebony are important in cuticle pigmentation of *H. vigintioctopunctata* and suggested that larger quantities of NBAD were present in adults and play more important roles in pigmentation than larvae/pupae.

Keywords: N-β-alanyldopamine, biosynthesis, adult cuticle, pigmentation, *Henosepilachna vigintioctopunctata*

OPEN ACCESS

Edited by:
Ran Wang,
Institute of Plant Protection and Environmental Protection, Beijing Academy of Agricultural and Forestry Sciences, China

Reviewed by:
Yuichiro Suzuki,
Wellesley College, United States
Qi Su,
Yangtze University, China
Honglin Feng,
Boyce Thompson Institute, United States

****Correspondence:***
Lin Jin
jinlin@njau.edu.cn

Specialty section:
This article was submitted to Invertebrate Physiology, a section of the journal Frontiers in Physiology

Received: *06 December 2021*
Accepted: *10 January 2022*
Published: *24 February 2022*

Citation:
Ze L-J, Jin L and Li G-Q (2022) Silencing of Adc and Ebony Causes Abnormal Darkening of Cuticle in Henosepilachna vigintioctopunctata. Front. Physiol. 13:829675. doi: 10.3389/fphys.2022.829675

INTRODUCTION

In insects, the cuticle provides protection against physical injury and water loss, rigidness for muscle attachment and mechanical support, and flexibility in intersegmental and joint areas for mobility. During growth and metamorphosis, insects need to regularly shed off old exoskeletons and synthesize new cuticles to fit the continuously increasing body sizes and the stage-specific body shapes. The newly formed cuticle, mainly composed of cuticular proteins, chitin, and sclerotized reagents, needs to be tanned, a process involved in melanization and sclerotization (Sugumaran and Barek, 2016). Moreover, melanization and sclerotization of insect cuticles also

determine pigmentation and play an important role in ecological adaption, such as in escaping predation, mimicry, sexual selection, signaling, and thermoregulation (Wright, 1987; True, 2003; Wittkopp and Beldade, 2009; van't Hof et al., 2011).

From a biochemical perspective, melanization and sclerotization of insect cuticles result from a combination of dark black and brown melanin and light yellow and colorless sclerotins (Wright, 1987; True, 2003; Wittkopp et al., 2003; Wittkopp and Beldade, 2009; Zhan et al., 2010). These melanizing and sclerotized reagents are produced from tyrosine. The tyrosine hydroxylase (TH) converts tyrosine to dopa. Subsequently, the dopa decarboxylase (DDC) converts dopa into dopamine. Dopa and dopamine are further converted to corresponding melanins (Andersen, 2010). The production of sclerotins from dopamine has been clarified in *Drosophila melanogaster* (Phillips et al., 2005). There are four reaction steps: (1) N-acylation of dopamine with acetyl-CoA to N-acetyldopamine (NADA). (2) Decarboxylation of aspartic acid to β-alanine by aspartate 1-decarboxylase (ADC, Black). (3) N-acylation of dopamine with β-alanine to produce N-β-alanyldopamine (NBAD) by NBAD synthase (Ebony). This reaction is reversible, with the reverse reaction catalyzed by an NBAD hydrolase (Tan). (4) Oxidation of NADA and NBAD to NADA-quinone and NBAD-quinone, which are polymerized to form the corresponding N-acylquinoid sclerotins (Phillips et al., 2005; Simon et al., 2009; Noh et al., 2016; Mun et al., 2020).

The importance of normal pigmentation of two enzymes, ADC and Ebony, has been confirmed (Mun et al., 2020). For ADC, levels of β-alanine are reduced in the heads of *adc* mutants compared to wild type in *D. melanogaster* (Hodgetts and Choi, 1974; Phillips et al., 2005; Borycz et al., 2012; Ziegler et al., 2013), in black body color mutant *Tribolium castaneum* (Kramer et al., 1984) and the black pupal (*bp*) mutant of *Bombyx mori* (Dai et al., 2015). Deficiency of β-alanine causes a lack of NBAD and leads to black body color (Kramer et al., 1984; Dai et al., 2015). Treatment with β-alanine can restore these mutants to wild-type phenotype (Jacobs, 1974; Kramer et al., 1984; Roseland et al., 1987; Wappner et al., 1996a,b; Phillips et al., 2005).

As for Ebony, the mutation in or knockdown of *ebony* increases black pigments in Dipteran insects *D. melanogaster* and *Ceratitis capitata* (Bridges and Morgan, 1923), Lepidopteran insects *B. mori* (Futahashi et al., 2008) and *Spodoptera litura* (Bi et al., 2019), Coleopteran insects *Tenebrio molitor* (Mun et al., 2020) and *T. castaneum* (Tomoyasu et al., 2009), and Hemipteran insect *Oncopeltus fasciatus* (Liu et al., 2016). Similarly, Tan has been recognized as an additional factor that promotes melanization in *Heliconius* (Ferguson et al., 2011). In *D. melanogaster*, loss of Tan causes a global reduction of melanin patterns (True et al., 2005; Jeong et al., 2008). However, the importance of NBAD in cuticle tanning has not been well compared among different developing stages of insects.

Henosepilachna vigintioctopunctata (Fabricius) (Coleoptera: Coccinellidae) is a typical polyphagous pest that feeds on a large number of Solanaceae and Cucurbitaceae plants in Asian countries (Zhang et al., 2018). The color markings in the beetle are distinctive and variable in different developing stages (Casari and Teixeira, 2015). This offers a very suitable model to test the pigmentation patterns. Here, using RNA interference (RNAi) technology, the three genes *adc*, *ebony,* or *tan* reported being involved in NBAD biosynthesis were knockdown at the third larval instar stage of *H. vigintioctopunctata*. The cuticle pigmentation patterns were detected and compared during larval–larval, larval–pupal, and pupal–adult molting. The results demonstrate that Adc and Ebony are important in cuticle pigmentation of *H. vigintioctopunctata* and suggest that larger quantities of NBAD were present in adults and play more important roles in pigmentation than larvae/pupae.

MATERIALS AND METHODS

Insect

Henosepilachna vigintioctopunctata adults were collected from *Solanum melongena* L. in Nanjing city, Jiangsu Province, China, in the summer of 2018. The beetles were routinely maintained in an insectary at 28 ± 1°C under a 14:10 h light-dark photoperiod and 50–60% relative humidity using potato (*Solanum tuberosum*) foliage at the vegetative growth or young tuber stages to assure sufficient nutrition. Under this feeding protocol, the larvae progressed through four distinct instars, with approximate periods of the first, second, third, and fourth instar stages of 3, 2, 2, and 3 days, respectively. Upon reaching full size, the fourth larval instars stopped feeding, fixed their abdomen ends to the substrate surface, and entered the prepupal stage. The prepupae spent approximately 2 days to pupate. The pupae lasted about 4 days and the adults emerged.

Molecular Cloning

TRIzol reagent (Invitrogen, New York, NY, United States) was used to extract the total RNA following the protocols of the manufacturer. The NanoDrop 2000 spectrophotometer (Thermo Fisher Scientific, New York, NY, United States) was applied to perform the RNA quantification. RNA purity was determined by assessing optical density (OD) absorbance ratios at OD260/280 and OD260/230. The integrity of RNA was analyzed *via* 1% agarose gel electrophoresis with ethidium bromide staining. Reverse transcription was performed using a PrimeScript™ RT reagent Kit with a gDNA Eraser (TaKaRa Biotechnology Corporation Ltd., Dalian, China). Briefly, the reaction was incubated at 37°C for 15 min and then 85°C for 5 s. The synthesized cDNAs were preserved at −20°C for further use.

The putative *adc*, *ebony,* and *tan* genes were obtained from *H. vigintioctopunctata* transcriptome data (Zhang et al., 2018). The correctness of the sequences was substantiated by PCR using primers in **Supplementary Table 1**. The sequenced cDNAs were submitted to GenBank (accession numbers: *adc*, MW380963; *ebony*, MW380964; and *tan*, MW380968).

The protein sequences of ADC, Ebony, and Tan from other species were acquired from the NCBI.[1] Phylogenetic analysis was conducted using MEGA-X software[2] and the neighbor-joining method with 1,000 bootstrap replications.

[1]https://www.ncbi.nlm.nih.gov/

[2]https://sourceforge.net/projects/mega5/

Synthesis of dsRNA Molecules

The cDNA fragments derived from *adc*, *ebony*, *tan*, and enhanced green fluorescent protein (*egfp*) were, respectively, amplified by PCR using specific primers (**Supplementary Table 1**) conjugated with the T7 RNA polymerase promoter. These targeted regions were further BLAST (BLASTN) searched against *H. vigintioctopunctata* transcriptome data (Zhang et al., 2018) to identify any possible off-target sequences that had an identical match of 20 bp or more. The dsRNA was synthesized using the MEGAscript T7 High Yield Transcription Kit (Ambion, Austin, TX, United States) according to the instructions of the manufacturer. Subsequently, the synthesized dsRNA (at a concentration of 5–8 μg/μl) was determined by agarose gel electrophoresis and the NanoDrop 1,000 spectrophotometer (Thermo Fisher Scientific, Waltham, MA, United States) (data not shown) and kept at −80°C until used in the subsequent experiment.

Larval RNA Interference

RNA interference of larvae was performed according to a previously described method (Xu et al., 2020; Ze et al., 2021). Briefly, an aliquot (0.1 μl) of the solution including 300 ng dsRNA was injected into the newly ecdysed third instar larvae. Blank and negative control larvae were injected with the same volume of PBS and ds*egfp* solutions, respectively. A group of 15 injected larvae was set as a replicate. Each dsRNA injection was repeated 8 times. Three replicates (each replicate contained at least six individuals) were sampled at 48 and 72 h after injection for qRT-PCR to test RNAi efficacy. Another two replicates were used to observe the phenotype.

Three biological independent experiments were carried out using the newly ecdysed third instar larvae and were planned to determine the RNAi effects of *Hvadc*, *Hvebony*, and *Hvtan* on the performances and cuticle tanning of the resultant larvae, pupae, and adults. Three treatments were set as follows: phosphate-buffered saline (PBS), 300 ng ds*egfp* and 300 ng ds*adc*; PBS, 300 ng ds*egfp* and 300 ng ds*ebony*; or PBS, 300 ng ds*egfp* and 300 ng ds*tan*.

Real-Time Quantitative PCR

For temporal expression analysis, cDNA templates were derived from 3-day-old eggs, the first, second, third, and fourth larval instar, the prepupae, pupae, and adults at an interval of 1 day (D0 indicates newly molted larvae, pupae, or newly emerged adults). For comparison of the expression levels in different portions, the heads and the remaining portions (bodies) were separately collected from 2-day-old third instar larvae, and 1-, 2-, and 3-day-old fourth instar larvae. Each sample contained 10 individuals and repeated three times. For analysis of the effects of treatments, total RNA was extracted from treated larvae. Each sample contained at least six individuals and repeated three times. The RNA was extracted using SV Total RNA Isolation System Kit (Promega, Madison, WI, United States). cDNA was prepared according to the instructions by using HiScript III RT SuperMix for qPCR (+gDNA wiper) kit (Vazyme, Nanjing, China). The qPCR performed on Applied Biosystems 7500 System (Life Technologies, Carlsbad, CA, United States) with ChamQ Universal SYBR qPCR Master Mix (Vazyme, Nanjing, China) according to the instructions of the manufacturer. Each 20 μl reaction solution containing 10 μl of 2 × ChamQ Universal SYBR qPCR Master Mix, 0.4 μl of each primer (10 μM), 1 μl of cDNA template, and 8.2 μl of nuclease-free water. The cycling parameters were: 1 cycle of 95°C for 3 min; 40 cycles of 95°C and 60°C for 10 s and 30 s, respectively. Quantitative mRNA measurements were performed by qRT-PCR in technical triplicate, using two internal control genes (*ribosomal protein S18*, *HvRPS18*; *ribosomal protein L13*, *HvRPL13*; and the primers listed in **Supplementary Table 1**) according to the published results (Lü et al., 2018). An RT negative control (without reverse transcriptase) and a non-template negative control were included for each primer set to confirm the absence of genome DNA and to check for primer-dimer or contamination in the reactions, respectively.

According to a previously described method (Bustin et al., 2009), the generation of specific PCR products was confirmed by gel electrophoresis. The primer pair for each gene was tested with a 10-fold logarithmic dilution of a cDNA mixture to generate a linear standard curve [crossing point (CP) plotted vs. log of template concentration], which was used to calculate the primer pair efficiency. All primer pairs amplified a single PCR product with the expected sizes, showed a slope less than −3.0, and exhibited efficiency values ranging from 2.5 to 2.6. Data were analyzed by the $2^{-\Delta\Delta CT}$ method, using the geometric mean of the four internal control genes for normalization.

Image Processing and Color Intensity Measurement

Digital photographs of all the phenotypes were taken with Nikon SMZ 25 stereo microscopy (Nikon, Japan). Images of hindwings, dissected from 7-day-old adults whose third instar larvae were treated with dsRNA, were transferred to RGB stack images, and color intensity in equivalent regions was determined as mean grayscale values (average luminance) *via* ImageJ software. Under this measurement, the lower color intensity indicates the darker cuticle pigmentation (Noh et al., 2016). All the treated groups and the corresponding control groups were photographed under the same conditions.

Data Analysis

Statistical significance of differences in the mRNA expression or other biological experiments among PBS, ds*egfp,* and dsRNA treatment groups was determined by one-way ANOVA and Turkey's test in SPSS Statistics 20.0 software (at $P < 0.05$). In the color intensity measurement of hindwings, the statistical significance of differences in mean gray values between the dsRNA-treated groups was assessed by Student's *t*-test.

RESULTS

Temporal Expression Pattern of *Adc*, *Ebony,* and *Tan* Transcript

By mining of *H. vigintioctopunctata* transcriptome data and constructing the phylogenetic trees, *Hvadc*, *Hvebony,* and *Hvtan* were identified (**Supplementary Figures 1–3**).

To detect the expression patterns of *Hvadc*, *Hvebony,* and *Hvtan* during different developmental stages, qRT-PCR was performed. The results revealed that *Hvadc*, *Hvebony,* and *Hvtan* were detectable from the embryo (egg) to adults. They peaked in the 4-day-old pupae or 0-day-old adults. Moreover, at the first, second, third, and fourth larval instar and pupal stages, the transcription levels of *Hvadc*, *Hvebony,* and *Hvtan* were high just before and/or right after the molt, and were low at the intermediate stages (**Figures 1A–C**).

The expression levels of *Hvadc*, *Hvebony,* and *Hvtan* in larval heads were compared to those in the bodies of 2-day-old third instar larvae, and 1-, 2-, and 3-day-old fourth instar larvae. Both *Hvadc* and *Hvebony* were abundantly transcribed in the larval heads of 2-day-old third instar larvae and 1-day-old four instar larvae (**Figures 1D,E**). Similarly, the levels of *Hvtan* in the head samples of 1- to 3-day-old fourth instar larvae were higher than those in the bodies (**Figure 1F**).

RNA Interference of *Adc* Blackens the Larvae

Three days after the introduction of ds*adc* into the newly ecdysed third instar larvae, the accumulated mRNA level of the target transcript was heavily suppressed (**Figure 2A**).

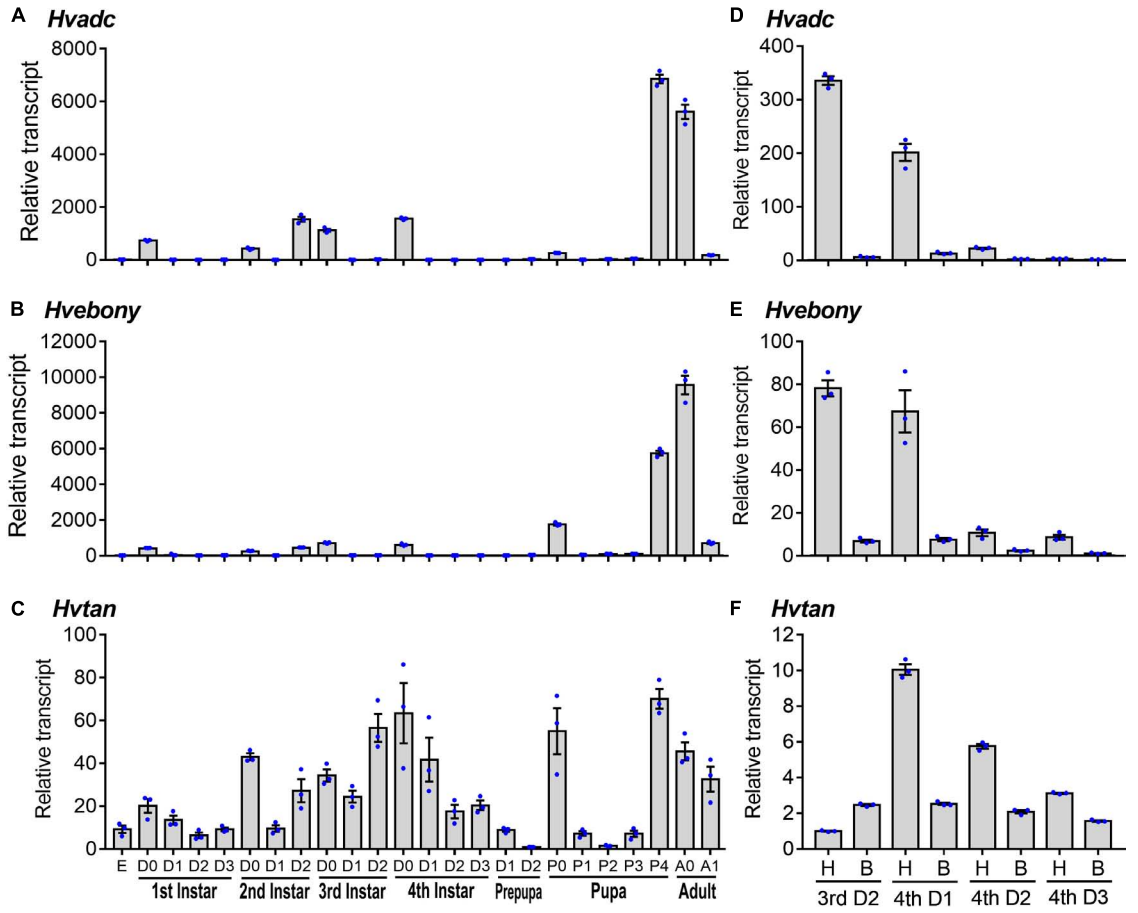

FIGURE 1 | Transcription patterns of *adc*, *ebony,* and *tan* genes in *Henosepilachna vigintioctopunctata*. For temporal expression analysis **(A–C)**, RNA templates were derived from day 3 eggs, the larvae from the first through the fourth instar, prepupae, pupae, and adults (D0 indicated newly ecdysed larvae or pupae, or newly emerged adults). Each repeat included 20–30 individuals and there were three independent pools. For analysis of the expression levels in different regions **(D–F)**, the heads and the remaining bodies were separately collected from the 2-day-old third instar larvae, and 1-, 2- and 3-day-old fourth instar larvae. A replicate included 10 individuals and each sample repeated 3 times. All the samples were measured in technical triplicate using qRT-PCR. The values were calculated using the $2^{-\Delta\Delta CT}$ method. The lowest transcript level of each of the three mRNAs at a specific developing time is set as 1. The relative transcripts are the ratios of copy numbers in different developing stages relative to larvae at the specific developing time. The genes for *ribosomal protein S18* (*HvRPS18*) and *ribosomal protein L13* (*HvRPS13*) were used as internal controls. The columns represent averages with vertical lines indicating ± SE. E, egg; H, head; B, remaining body without head.

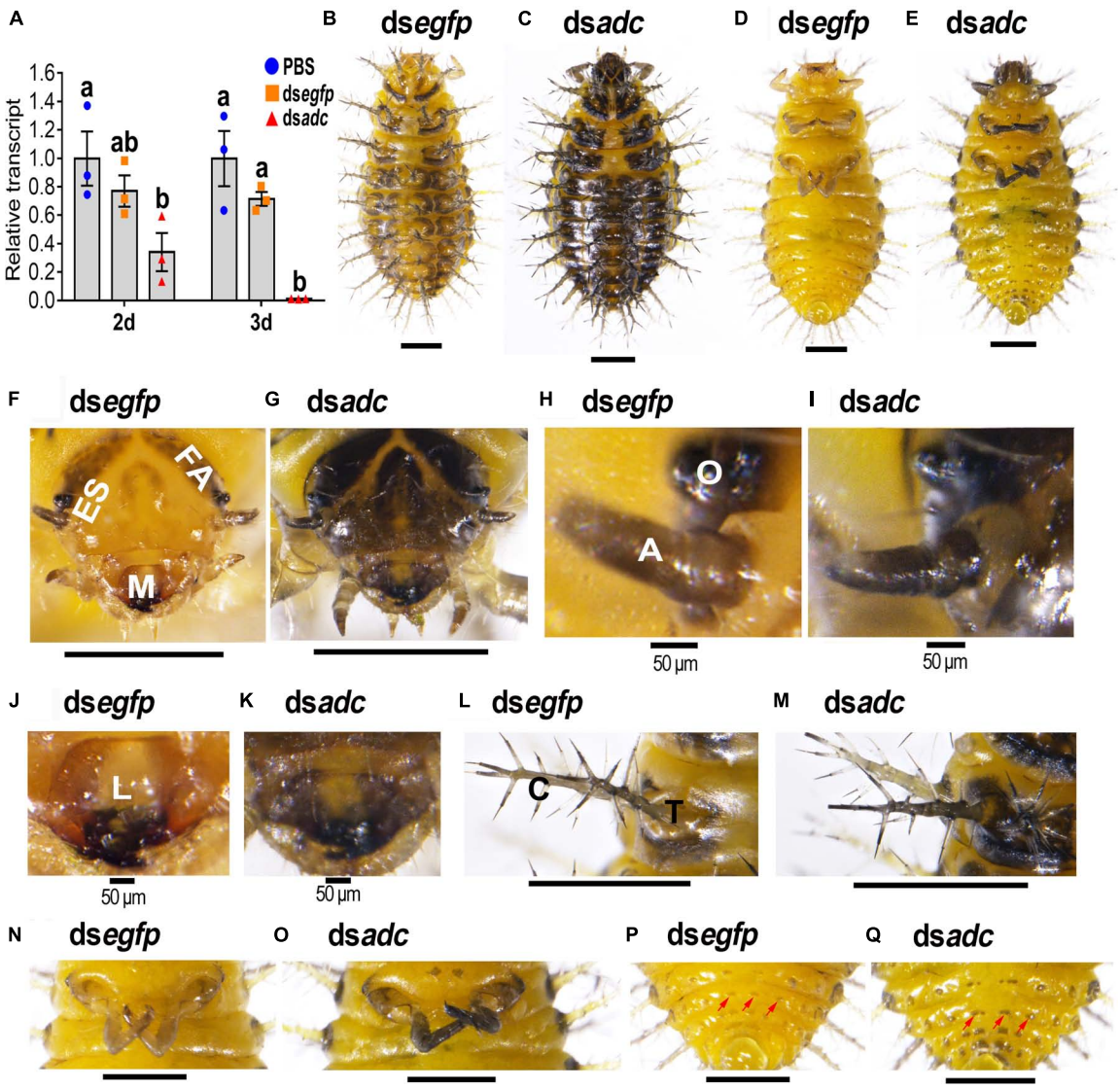

FIGURE 2 | RNA interference of *Hvadc* darkens larvae of *H. vigintioctopunctata*. The newly ecdysed third instar larvae were injected with an aliquot (0.1 μl) of PBS, or solution including 300 ng ds*egfp* or 300 ng ds*adc*. The larvae were then transferred to potato foliage. Two days and three days after injection, the expression level of *Hvadc* was measured **(A)**. Relative transcripts are the ratios of relative copy numbers in treated individuals to that in PBS-injected ones, which is set as 1. Different letters indicate significant differences at *P*-value < 0.05 using ANOVA with the Tukey–Kramer test. The dorsal and ventral views of ds*egfp*- **(B,D)** and ds*adc*- **(C,E)** treated larvae are shown. The heads **(F,G)**, ocelli and antennae **(H,I)**, mouthpart **(J,K)**, scoli and strumae **(L,M)**, hind legs **(N,O)**, and the end of abdomens **(P,Q)** were further amplified. ES, epicranial suture; FA, frontal arms; M, mouthpart; O, ocelli; A, antennae; C, scolus; T, struma. Red arrows point to mastoids on the abdomen.

All the controls (PBS- and ds*egfp*-introduced) and ds*adc*-treated larvae normally molted to the fourth instar larvae. However, the color was darkened in the heads of the *Hvadc* RNAi larvae, compared with those of the PBS- and ds*egfp*-treated ones (**Figures 2B,D** vs. **C,E**), especially the mouthparts (**Figures 2F** vs. **G**) and the patches around larval ocelli and the antennae (**Figures 2H** vs. **I**). In addition, a wide cream band called epicranial suture (ES) was narrowed, and the V-shaped frontal arms and the U-shaped patch on the head top were widened in the *Hvadc* RNAi larvae (**Figures 2F** vs. **G**).

In the mouthparts of the control fourth instar larvae (PBS- and ds*egfp*-injected), the median part of the labrum is cream, while the lateral and anterior parts are brownish narrow bands. Other appendages of the mouthparts, namely, mandibles, maxilla, and labium were black in color (**Figures 2F,J**). By contrast, in the *Hvadc* RNAi larvae, the color of all the pigmented regions was deepened and blackened (**Figures 2F,J** vs. **G,K**). Moreover, the scoli, strumae, and legs were all darker-colored in the *Hvadc* silenced larvae (**Figures 2L,N** vs. **M,O**). In addition, small mastoids queuing up on the abdomen were darker pigmented

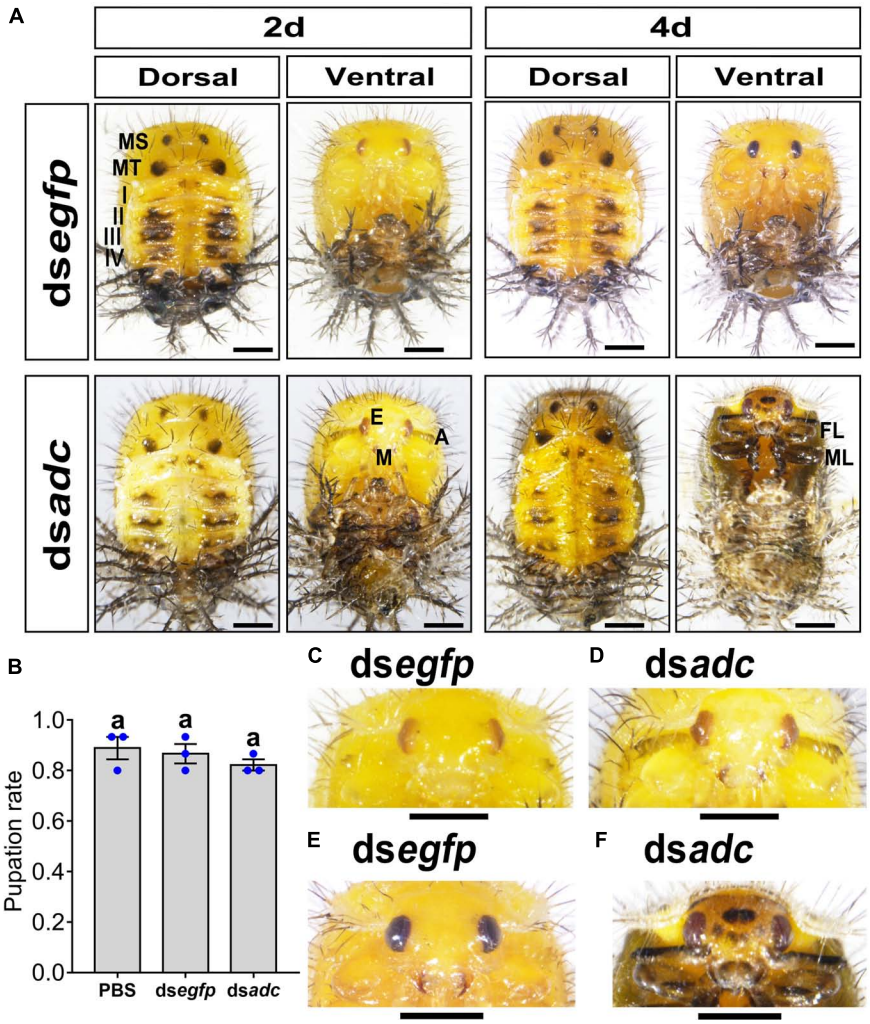

FIGURE 3 | Knockdown of *Hvadc* darkens pupa color in *H. vigintioctopunctata*. The newly molted third instar larvae were injected with an aliquot (0.1 μl) of PBS, or solution including 300 ng ds*egfp* or 300 ng ds*adc*. The larvae were then transferred to potato foliage. The pupation rate was recorded during a 3-week trial period **(B)**. The averages (±SE) following different letters indicate significant differences at *P*-value < 0.05 using ANOVA with the Tukey–Kramer test. The dorsal and ventral views of 2-day-old and 4-day-old pupae whose third instar larvae had been subjected to ds*egfp* and ds*adc* injection are shown **(A)**. The heads of 2-day-old pupae **(C,D)** and 4-day-old pupae **(E,F)** were further amplified. MS, meso thorax; MT, meta thorax; I–IV, tergites I–IV; E, compound eye; A, antenna; M, mouthpart; FL, foreleg; ML, midleg. Scale bars: 1 mm.

in ds*adc*-injected larvae, compared with that of ds*egfp*-injected larvae (**Figures 2D,P** vs. **E,Q**).

Silencing *Adc* Affects Coloration of Pupae

Knockdown of *Hvadc* did not affect the pupal morphology (**Figure 3A**) and the pupation rate (**Figure 3B**), but the coloration.

The integument of the 2-day-old pupae developed from the third instar larvae treated with ds*egfp* or ds*adc* were generally pale yellow, especially on the ventral one (**Figure 3A**, left panel). Then, the overall color shifted to dull yellow in the 4-day-old pupae (**Figure 3A**, right panel). From the dorsal views, the paired black markings in the meso and meta thoraxes, and the dark patches in tergite I–IV were similar between the control (ds*egfp*-treated) and the *Hvadc* RNAi pupae (**Figure 3A**).

However, the antennae and mouthparts of the 2-day-old *Hvadc*-silenced pupae were blackened (**Figure 3D**), while those parts in 2-day-old pupae treated with ds*egfp* exhibited no obvious pigmentation (**Figure 3C**). Four days after pupation, the mouthparts of control displayed rufous color, and the color of antennae and legs did not obviously change (**Figure 3E**). By contrast, the cuticle color between two compound eyes of the *Hvadc*-silenced pupae was obviously darker, and obvious central black patches and several small dark spots were present (**Figures 3E** vs. **F**). The antennae, mouthparts, and legs became darker (**Figure 3F**).

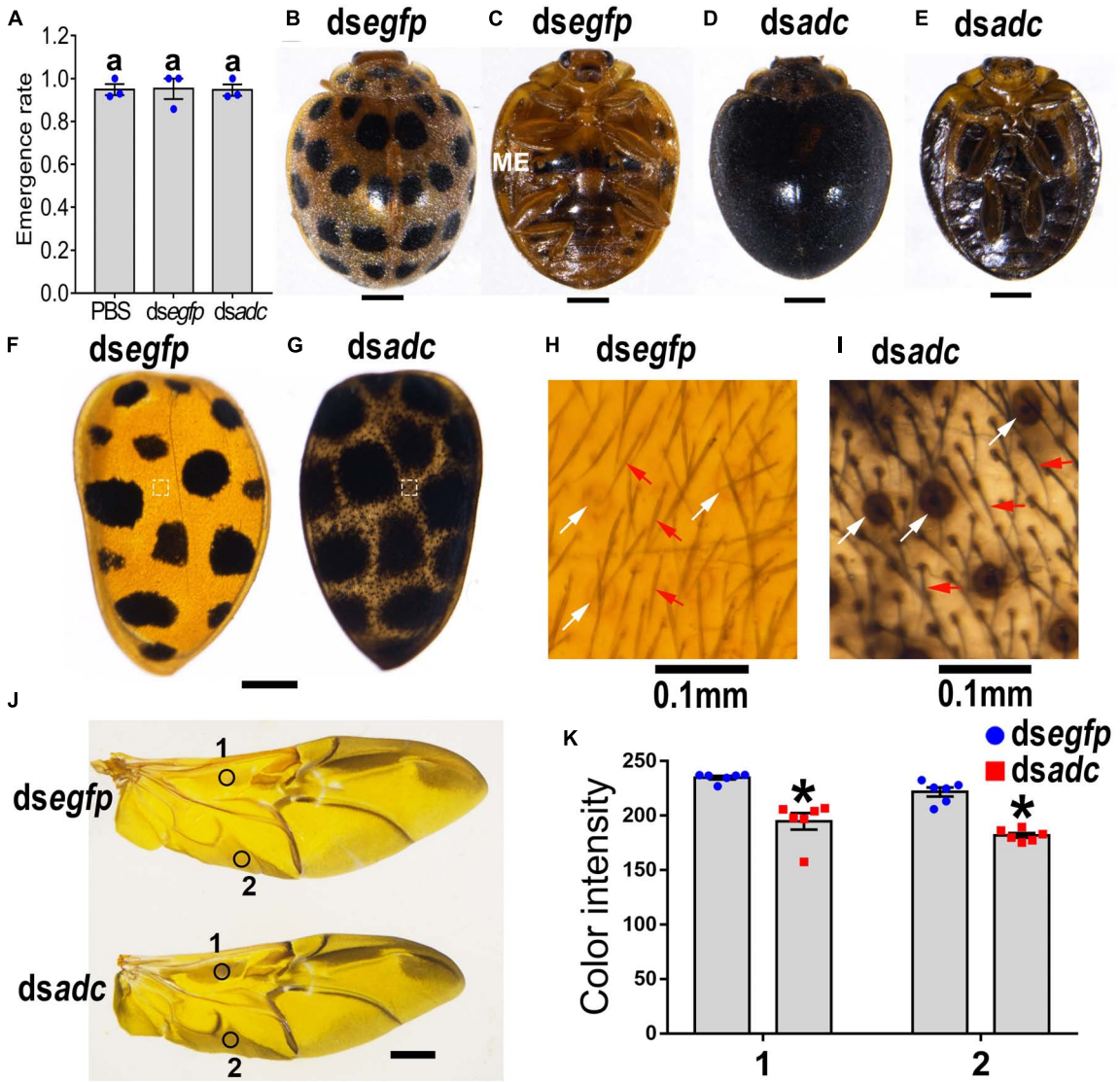

FIGURE 4 | Silencing *Hvadc* affects pigmentation in adults of *H. vigintioctopunctata*. The newly molted third instar larvae were injected with an aliquot (0.1 μl) of PBS, or solution including 300 ng ds*egfp* or 300 ng ds*adc*. The larvae were then transferred to potato foliage. The emergence rates and the rates of normal adults were recorded during a 3-week trial period **(A)**. The average values (±SE) followed by different letters indicate significant differences at *P*-value < 0.05 using ANOVA with the Tukey–Kramer test. The dorsal **(B,D)** and ventral **(C,E)** views of 7-day-old adults whose third instar larvae had been subjected to ds*egfp* or ds*adc* treatment are shown. The elytra **(F,G)** and the elytral surfaces were further amplified **(H,I)**. The hindwings **(J)** and the color intensity **(K)** in equivalent regions of them (circles 1 and 2 in **J**) were determined as mean gray values (average luminance) by ImageJ software. Data are shown as the mean values ± SE ($n = 6$). The asterisk indicates a significant difference in color intensity between control and test beetles ($P < 0.01$, *t*-test). White and red arrows point to the circle pits and setae, respectively. ME, metathorax.

Knockdown of *Adc* Affects the Color of Adult Cuticle and Wings

The emergence rate of the pupae in the ds*adc*-treated group was 95% on average, showing no significant difference with the one in the PBS- or ds*egfp*-treated group (**Figure 4A**). For *Hvadc* RNAi adults, 28 black markings were distributed symmetrically on two hard elytra 1 day after emergence. Then, the black pigments were gradually deposited and finally covered the whole body from the dorsal view 7 days after emergence, while the pigmentation of the control (ds*egfp*-treated) adult remained the same (**Figures 4B** vs. **D**). Similarly, a pair of black markings on the sternum of the metathorax was seen in the control and 1-day-old *Hvadc* RNAi adults; while the whole body from the ventral view was blackened in the 7-day-old *Hvadc* RNAi adults (**Figures 4C** vs. **E**). Knockdown of *Hvadc* caused the overall darkening pigmentation in elytra, which seems to be due to the enlargement of the black spots (**Figures 4F** vs. **G**). Moreover, the view of the amplified elytra from *Hvadc* RNAi adults showed that the setae and circle pits were all dark-colored, in contrast to the reddish-brown color in the control beetles (**Figures 4H** vs. **I**).

Further dissection of the head, pronotum, scutellum, hindlegs, and hindwing revealed that these regions all shifted to the darker pigmentation (**Figure 4J** and **Supplementary Figure 4**). The color intensity of the corresponding regions of hindwings showed a significant difference between ds*adc* and ds*egfp* treated groups (**Figure 4K**).

RNA Interference of *Ebony* on the Third Instar Larvae

Since both the Adc and Ebony play central roles in the synthesis of the NBAD (Massey et al., 2019), we have knocked down the expression of *Hvebony* by injection of ds*ebony* to the newly ecdysed third instar larvae (**Figure 5A**).

The pupation rate and the emergence rate of the *Hvebony* RNAi larvae were similar to those of the control larvae which were injected PBS or ds*egfp* (**Figures 5B,C**). The mandibles were darker-colored in the ds*ebony*-introduced newly molted fourth instar larvae, compared with those in the control larvae treated with PBS or ds*egfp* (**Figures 5D,E**, 15 min). Eight hours postmolting, the scoli and strumae from the larval thorax to the eighth segment of the abdomen, along with head and leg, became brownish in the PBS- and ds*egfp*-introduced larvae (**Figures 5D,E**, above panel). By contrast, the color of the body parts, namely, head, scoli, strumae, and legs became dark brown in the ds*ebony*-treated larvae (**Figures 5D,E**, lower panels).

Similarly, at the wandering stage, the cuticles of the larvae head capsules, scoli, strumae, legs, and spots on the abdomen were more blackened in *Hvebony* RNAi larvae than those in the control larvae (**Figures 5F,H,J** vs. **G,I,K**).

In the ds*ebony*-introduced pupae, the black dorsal markings in the meso and meta thoraxes and the dark patches in tergite I–IV showed no significant difference with PBS or ds*egfp*-treated pupae (**Figure 6A**). However, the mandibles were darker in the 3-day/4-day-old *Hvebony*-silenced pupae, than those in control groups (**Figure 6A**). Similar to the phenotype of the *Hvadc* depleted pupae, several small dark spots appeared in the cuticle between two compound eyes of the ds*ebony*-introduced 4-day-old pupae (**Figures 6B** vs. **C**). Furthermore, the cuticle of the head, legs, elytra, and pronotum in ds*ebony*-introduced 4-day-old pupae became significantly darker than that of pupae injected with PBS or ds*egfp* (**Figures 6B,D,F** vs. **C,E,G**). The enlarged dorsal view displayed that many short black setae and dots appeared on the cuticle of the ds*ebony*-injected 4-day-old pupae to make the cuticle blacker in color than the control (**Figures 6F** vs. **G**).

Thirty minutes after emergence, the elytra of the control adults treated with PBS or ds*egfp* still exhibited light yellow in color. Subsequently, the elytra turned copper yellow, and 28 spots appeared, gradually darkened (**Figure 7A**, ds*egfp*-dorsal view). By contrast, knockdown of *Hvebony* led to an overall gray pigmentation and enlarged 28 dark spots in elytra within 30 min after emergence. The elytra of the *Hvebony* RNAi adults also gradually darkened (**Figure 7A**, ds*ebony*-dorsal view), but they looked completely black in color 7 days after emergence (**Figures 7B** vs. **C**). Further dissection of the head, pronotum, scutellum, and hindlegs of the *Hvebony* RNAi adults showed that these regions all turned to darker pigmentation than control adults (**Supplementary Figure 4**). Similar to the *Hvadc*-silenced adults, the 28 black spots on the elytra of the *Hvebony*-silenced adults became larger than those on the control elytra (**Figures 7D** vs. **E**), and the color of the setae and pits on the surface of the elytra was darker than that of the control elytra (**Figures 7F** vs. **G**). In addition, the pigment regions of the hindwing from the *Hvebony* RNAi adults were darker than controls (**Figures 7H,I**).

From the ventral view, six pairs of dark patches appeared along the lateral portions on the abdomen segments of the *Hvebony* RNAi adults, and the last two pairs extended and merged together. The pale-yellow color outside the dark patches was gradually darkened, until merging the dark patches 2 days after emergence (**Figure 7A**, ds*ebony*-ventral view). The legs and the abdomen of the *Hvebony*-depleted adults were blacker in color than the control beetles (**Figure 7A**, ds*ebony*-ventral view).

RNA Interference of *Tan* on the Third Instar Larvae

Two days and three days after injection of ds*tan* to the third instar larvae, the expression of the target *Hvtan* transcript was significantly reduced, compared with the control larvae injected PBS or ds*egfp* (**Supplementary Figure 5A**).

Depletion of *Hvtan* exerted little influence on pupation and emergence rates (**Supplementary Figure 7**). The results of color intensity measurement (data not shown) indicated that knockdown of *Hvtan* had a very limited influence on the cuticle pigmentation at the larval, pupal, and adult stages, compared with the controls subjected to PBS or ds*egfp* injection (**Supplementary Figures 5B,C**, **6A–M**). In addition, there was no significant difference in the color intensity of the hindwings between ds*egfp*- and ds*tan*-treated ladybirds (**Supplementary Figure 6N**).

DISCUSSION

The conjugation and cross-linking of cuticle proteins during cuticle tanning lead to an insoluble, hard, and darkened red-brown exoskeleton in Coleoptera (Roseland et al., 1987). NBAD, a sclerotic reagent, and a pigment precursor play critical roles in cuticle pigmentation and hardening (Kramer et al., 1984). In this article, three genes (*Hvadc*, *Hvebony,* and *Hvtan*) reported to be involved in NBAD biosynthesis were identified and their role in the pigmentation of cuticle on the larvae, pupae, and adults of *H. vigintioctopunctata* was explored by RNAi in the newly ecdysed third instar larvae. Three pieces of experimental evidence suggested that NBAD plays more important roles in the pigmentation in adults than that in the larvae and pupae of *H. vigintioctopunctata*.

First, we found that *Hvadc*, *Hvebony,* and *Hvtan* were detected from the embryo (egg) to adults. Moreover, the transcription levels of *Hvadc*, *Hvebony,* and *Hvtan* were high just before and/or right after the molt at the first, second, third, and fourth larval instar and pupal stages (**Figure 1**). In *S. litura*, *Slebony* was expressed at all developing stages, namely, egg, the first through sixth larval instar larvae, prepupa, pupa, and adult (Bi et al., 2019). Similarly, *ebony* is abundantly expressed at the larval, pupal, and adult stages in *P*apilio *xuthus* and

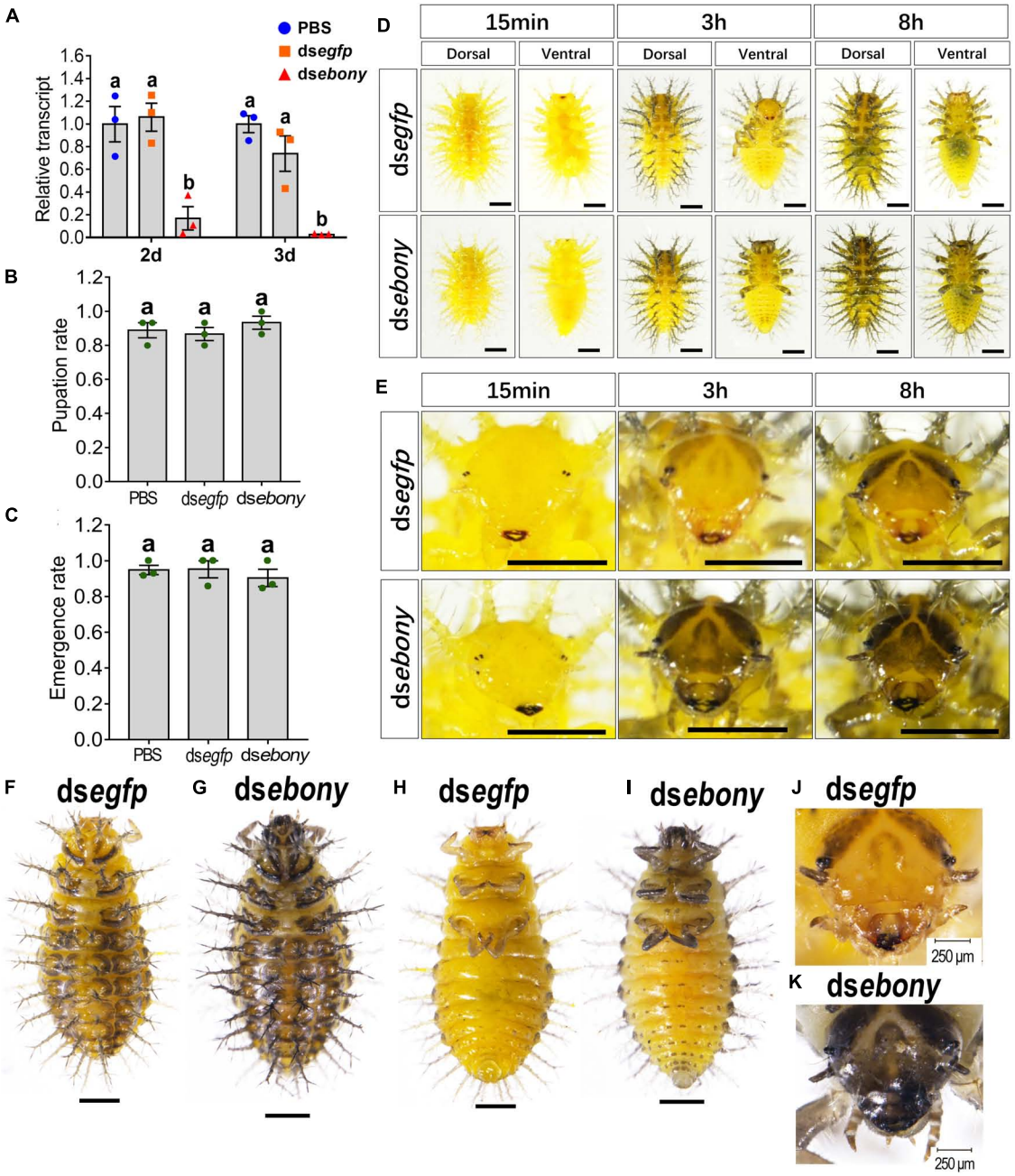

FIGURE 5 | Depletion of *Hvebony* influences pigmentation in larvae of *H. vigintioctopunctata*. The newly molted third instar larvae were injected with an aliquot (0.1 μl) of PBS, or solution including 300 ng ds*egfp* or 300 ng ds*ebony*. The larvae were then transferred to potato foliage. Two days and three days after injection, the expression level of *Hvebony* was measured **(A)**. Relative transcripts are the ratios of relative copy numbers in treated individuals to that of PBS-treated ones, which is set as 1. The pupation and emergence rates were recorded during a 3-week trial period **(B,C)**. Different letters indicate significant difference at *P*-value < 0.05 using ANOVA with the Tukey–Kramer test. The dorsal and ventral views of ds*egfp*- and ds*ebony*-treated larvae **(D)** and amplified larval heads **(E)** at different times after molting to the fourth instar, and the dorsal and ventral views of larvae in the wandering stage **(F–I)** are shown. The heads of the wandering stage larvae were further amplified **(J,K)**. The unlabeled scale bars: 1 mm.

Papilio machaon (Li et al., 2015). In *T. molitor*, the abundant transcripts were confirmed at late stages of development from pharate pupae through 10-day-old adults (Mun et al., 2020). The expression profiles of *Hvadc*, *Hvebony,* and *Hvtan* suggest that the three functional enzymes catalyze the formation of melanin and sclerotins after each molting during the developing stages.

Second, the expression of the *Hvadc*, *Hvebony,* and *Hvtan* peaked in the 4-day-old pupae or 0-day-old *H. vigintioctopunctata* adults (**Figure 1**). The highest expression levels at the late pupal and early adult phrases suggest that abundant NBAD were produced in the preadults and adults. In agreement with these results, the highest level of *Tmadc* is seen

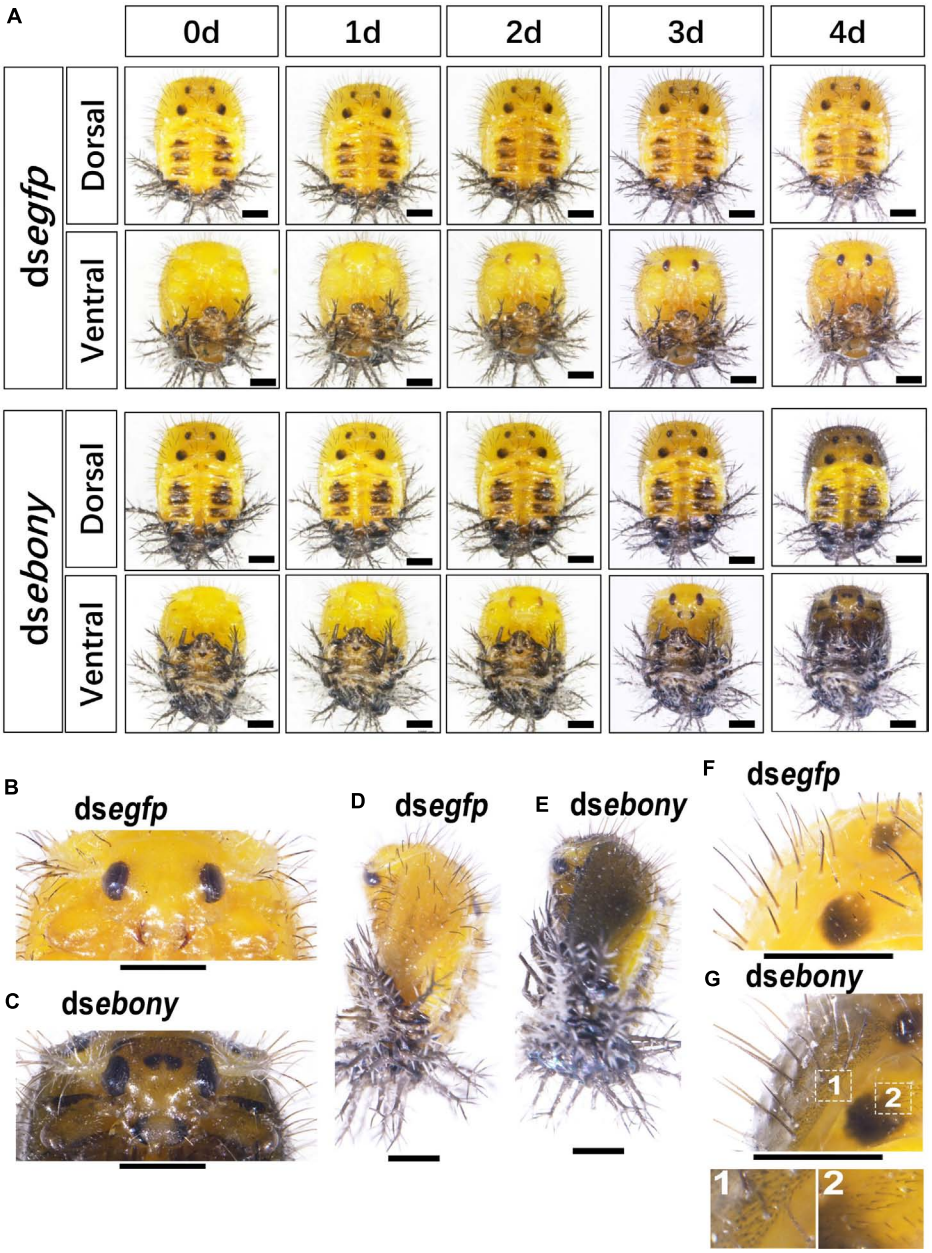

FIGURE 6 | RNA interference of *Hvebony* affects the pigmentation in pupae of *H. vigintioctopunctata*. The dorsal and ventral views of 0-day, 1-day, 2-day, 3-day, and 4-day old pupae from the third instar larvae injected with ds*egfp* and ds*ebony* **(A)** are shown. The heads **(B,C)** and the dorsal view **(F,G)** of the 4-day-old pupae were further amplified. The lateral views of 4-day-old pupae **(D,E)** are shown. The unlabeled scale bars: 1 mm.

right after adult emergence (adult day 0) in *T. molitor* (Mun et al., 2020). Similarly, high levels of *Slebony* were found just before and right after adult emergence in *S. litura* (Bi et al., 2019). Moreover, *Dmadc* was expressed at high levels at the end of the pupae period (96 h after pupation) in *D. melanogaster* (Sobala and Adler, 2016).

Lastly, the results revealed that RNAi of either *Hvadc* or *Hvebony* selectively deepened the color of the larval head capsules, scoli, strumae, and legs (**Figures 2**, **5**), and depletion of *Hvadc* or *Hvebony* blackened the pupal head capsules, antennae, mouthpart, and legs (**Figures 3**, **6**), while knockdown of either *Hvadc* or *Hvebony* darkened whole bodies of the adults (**Figures 4**, **7**) of *H. vigintioctopunctata*. The greater accumulation of black pigments in the *Hvadc* or *Hvebony* depleted adults likely resulted from the conversion of larger quantities of dopamine to brown dopamine-melanin than in the larvae. Therefore, we infer that larger quantities of NBAD were present in adults than larvae/pupae.

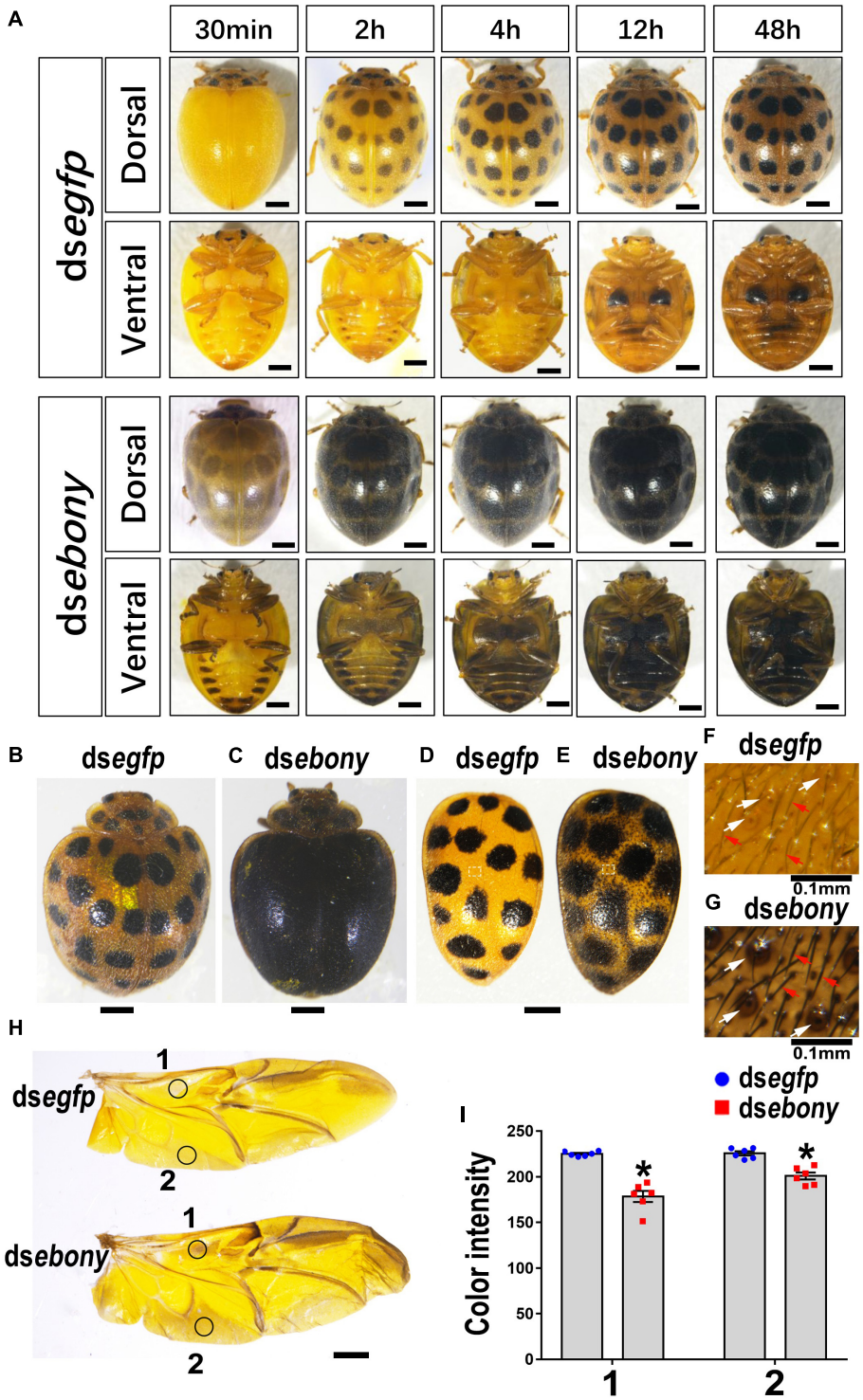

FIGURE 7 | Depletion of *Hvebony* deepens color of adults in *H. vigintioctopunctata*. The dorsal and ventral views of adults from different times after emergence **(A)**. The 7-day-old adults **(B,C)** and elytra dissected from 7-day-old adults **(D,E)** are shown. The surfaces of elytra were further amplified **(F,G)**. The hindwings **(H)** and the color intensity **(I)** in equivalent regions of them (circles 1 and 2 in **H**) were determined as mean gray values (average luminance) by ImageJ software. Data are shown as the mean values ± SE ($n = 6$). The asterisk indicates a significant difference in color intensity between control and test beetles ($P < 0.01$, *t*-test). The unlabeled scale bars: 1 mm. White and red arrows point to the pits and setae, respectively.

In contrast, microinjection of ds*adc* into penultimate-instar larvae does not cause obvious phenotype in the *T. castaneum* old larvae but leads to a darkened body pigmentation in pupae and adults when compared with controls (Arakane et al., 2009). In the *Bmadc* mutant strain of *B. mori*, β-alanine and NBAD were deficient but dopamine is accumulated. As a result, deep coloration was induced in pupae (Dai et al., 2015). It appears that NBAD is as important in pupae as that in adults in both *T. castaneum* (Arakane et al., 2009) and *B. mori* (Dai et al., 2015).

As for *ebony*, CRISPR/Cas9-mediated *ebony* knockout did not change the pigmentation in larvae but led to darker coloration in the pupae and adults in *S. litura* (Bi et al., 2019). In *D. melanogaster*, homozygous mutations of *ebony* bring about dark body pigmentation in adult flies, but not larvae and pupae (Massey et al., 2019). Moreover, the core enhancers in the *ebony* gene determine thoracic pigmentation intensity in different *D. melanogaster* strains across geographical gradients (Telonis-Scott et al., 2011; Telonis-Scott and Hoffmann, 2018). These results suggest that reduced synthesis of NBAD leads to abnormal accumulations of high levels of dopamine, which likely undergoes dopamine-melanin synthesis to cause a dark coloration of cuticle in adults of insects from different orders. Interestingly, although the elytra of adults treated with ds*adc* and ds*ebony* appear to be almost completely black in color, we found that the main regions of elytra got dark pigmented were pits and setae (**Figures 4**, **7**). Similarly, as early as the end of the pupae, the epidermal setae were already black in coloration in the *Hvebony* depleted pupae (**Figure 6**). It suggested that NBAD may be mainly accumulated in pits and setae of *H. vigintioctopunctata* cuticle.

It is known that NBAD is a major sclerotizing precursor that is secreted during the cuticle tanning process. It is further oxidized and used to cross-link cuticular proteins to form a rigid coleopteran exoskeleton at the adult stage (Noh et al., 2016). Moreover, some pigmentation gene transcripts, such as *ebony* and *tan*, are pleiotropic genes that affect more than one trait. In *D. melanogaster*, loss-of-function mutations in *ebony* and *tan* also affect cuticular hydrocarbon composition (Massey et al., 2019). A bias for long-chain hydrocarbon increases the melting temperatures and enables the flies to live longer in dry climates (Gibbs, 1998). *H. vigintioctopunctata* is a diurnal herbivorous ladybird. The adults are frequently exposed to a dry environment to forage for food, oviposition sites, and copulation mates. Hard exoskeleton in the adults confers greater tolerance to desiccation and ultraviolet during the foraging stage (Matute and Harris, 2013; Bastide et al., 2014).

In addition, we noticed that the change of cuticle pigmentation was very limited in the beetles treated with ds*tan* (**Supplementary Figures 5**, **6**). The enzyme encoded by *tan* is required for the production of dopamine in *D. melanogaster* (True et al., 2005). In *B. mori*, *tan* is suggested to be the responsible gene for larval color mutant *rouge*, and Tan plays a significant role in emphasizing the black markings of the larvae (Futahashi et al., 2010). Previous studies have shown that Tan catalyzes the production of dopamine from NBAD during pigment development (True et al., 2005). This role of Tan seems to be not obvious in *H. vigintioctopunctata*. Combined with the results of RNAi of *Hvadc* and *Hvebony*, we speculated that *Hvtan* plays a weak role in the process of converting NBAD to dopamine in *H. vigintioctopunctata*.

CONCLUSION

In conclusion, the study has determined the important role of Adc and Ebony in cuticle pigmentation in the 28-spotted ladybird. Larger quantities of NBAD were suggested to be present in adults and play more important roles in pigmentation than larvae/pupae. Abundant NBAD in the adults may be an adaptation strategy in the tanning process to form inconspicuous pigmentation in *H. vigintioctopunctata* beetles.

DATA AVAILABILITY STATEMENT

The datasets presented in this study can be found in online repositories. The names of the repository/repositories and accession number(s) can be found in the article/**Supplementary Material**.

AUTHOR CONTRIBUTIONS

L-JZ, LJ, and G-QL conceived the study, participated in the design of the experiments and the interpretation of the results, and wrote the first draft of the manuscript. L-JZ and LJ performed the experiments. LJ and G-QL revised the manuscript. All authors contributed to the article and approved the submitted version of the manuscript.

FUNDING

This study was supported by the National Natural Science Foundation of China (32072416) and the China Agriculture Research System of MOF and MARA (CARS-09-P22).

SUPPLEMENTARY MATERIAL

The Supplementary Material for this article can be found online at: https://www.frontiersin.org/articles/10.3389/fphys.2022.829675/full#supplementary-material

REFERENCES

Andersen, S. O. (2010). Insect cuticular sclerotization: a review. *Insect Biochem. Mol. Biol.* 40, 166–178. doi: 10.1016/j.ibmb.2009.10.007

Arakane, Y., Lomakin, J., Beeman, R. W., Muthukrishnan, S., Gehrke, S. H., Kanost, M. R., et al. (2009). Molecular and functional analyses of amino acid decarboxylases involved in cuticle tanning in *Tribolium castaneum*. *J. Biol. Chem.* 284, 16584–16594. doi: 10.1074/jbc.M901629200

Bastide, H., Yassin, A., Johanning, E. J., and Pool, J. E. (2014). Pigmentation in *Drosophila melanogaster* reaches its maximum in Ethiopia and correlates most strongly with ultra-violet radiation in sub-Saharan Africa. *BMC Evol. Biol.* 14:179. doi: 10.1186/s12862-014-0179-y

Bi, H. L., Xu, J., He, L., Zhang, Y., Li, K., and Huang, Y. P. (2019). CRISPR/Cas9-mediated ebony knockout results in puparium melanism in *Spodoptera litura*. *Insect Sci.* 26, 1011–1019. doi: 10.1111/1744-7917.12663

Borycz, J., Borycz, J. A., Edwards, T. N., Boulianne, G. L., and Meinertzhagen, I. A. (2012). The metabolism of histamine in the *Drosophila* optic lobe involves an ommatidial pathway: β-alanine recycles through the retina. *J. Exp. Biol.* 215, 1399–1411. doi: 10.1242/jeb.060699

Bridges, C. B., and Morgan, T. H. (1923). *The Third-Chromosome Group of Mutant Characters of Drosophila melanogaster*. Washington, DC: Carnegie Institution of Washington.

Bustin, S. A., Benes, V., Garson, J. A., Hellemans, J., Huggett, J., Kubista, M., et al. (2009). The MIQE guidelines: minimum information for publication of quantitative real-time PCR experiments. *Clin. Chem.* 55, 611–622. doi: 10.1373/clinchem.2008.112797

Casari, S. A., and Teixeira, E. P. (2015). Immatures of epilachna chevrolat (Coleoptera, Coccinellidae, Epilachninae). *Rev. Bras. Entomol.* 59, 113–120. doi: 10.1016/j.rbe.2015.03.006

Dai, F. Y., Qiao, L., Cao, C., Liu, X. F., Tong, X. L., He, S. Z., et al. (2015). Aspartate decarboxylase is required for a normal pupa pigmentation pattern in the silkworm, *Bombyx mori*. *Sci. Rep.* 5:10885. doi: 10.1038/srep10885

Ferguson, L. C., Maroja, L., and Jiggins, C. D. (2011). Convergent, modular expression of ebony and tan in the mimetic wing patterns of *Heliconius butterflies*. *Dev. Genes Evol.* 221, 297–308. doi: 10.1007/s00427-011-0380-6

Futahashi, R., Banno, Y., and Fujiwara, H. (2010). Caterpillar color patterns are determined by a two-phase melanin gene prepatterning process: new evidence from tan and laccase2. *Evol. Dev.* 12, 157–167. doi: 10.1111/j.1525-142X.2010.00401.x

Futahashi, R., Sato, J., Meng, Y., Okamoto, S., Daimon, T., Yamamoto, K., et al. (2008). yellow and ebony are the responsible genes for the larval color mutants of the silkworm *Bombyx Mori*. *Genetics* 180, 1995–2005. doi: 10.1534/genetics.108.096388

Gibbs, A. G. (1998). Water-proofing properties of cuticular lipids. *Am. Zool.* 38, 471–482. doi: 10.1093/icb/38.3.471

Hodgetts, R., and Choi, A. (1974). β Alanine and cuticle maturation in *Drosophila*. *Nature* 252, 710–711. doi: 10.1038/252710a0

Jacobs, M. E. (1974). Beta-alanine and adaptation in *Drosophila*. *J. Insect Physiol.* 20, 859–866. doi: 10.1016/0022-1910(74)90175-9

Jeong, S., Rebeiz, M., Andolfatto, P., Werner, T., True, J., and Carroll, S. B. (2008). The evolution of gene regulation underlies a morphological difference between two *Drosophila* sister species. *Cell* 132, 783–793. doi: 10.1016/j.cell.2008.01.014

Kramer, K. J., Morgan, T. D., Hopkins, T. L., Roseland, C. R., Aso, Y., Beeman, R. W., et al. (1984). Catecholamines and β-alanine in the red flour beetle, *Tribolium castaneum*: roles in cuticle sclerotization and melanization. *Insect Biochem.* 14, 293–298. doi: 10.1016/0020-1790(84)90063-5

Li, X. Y., Fan, D. D., Zhang, W., Liu, G. C., Zhang, L., Zhao, L., et al. (2015). Outbred genome sequencing and CRISPR/Cas9 gene editing in butterflies. *Nat. Commun.* 6:8212. doi: 10.1038/Ncomms9212

Liu, J., Lemonds, T. R., Marden, J. H., and Popadic, A. (2016). A pathway analysis of melanin patterning in a *Hemimetabolous* insect. *Genetics* 203:403. doi: 10.1534/genetics.115.186684

Lü, J., Chen, S. M., Guo, M. J., Ye, C. Y., Qiu, B. L., Wu, J. H., et al. (2018). Selection and validation of reference genes for RT-qPCR analysis of the ladybird beetle *Henosepilachna vigintioctomaculata*. *Front. Physiol.* 9:1614. doi: 10.3389/Fphys.2018.01614

Massey, J. H., Akiyama, N., Bien, T., Dreisewerd, K., Wittkopp, P. J., Yew, J. Y., et al. (2019). Pleiotropic effects of ebony and tan on pigmentation and cuticular hydrocarbon composition in *Drosophila melanogaster*. *Front. Physiol.* 10:518. doi: 10.3389/Fphys.2019.00518

Matute, D. R., and Harris, A. (2013). The influence of abdominal pigmentation on desiccation and ultraviolet resistance in two species of *Drosophila*. *Evolution* 67, 2451–2460. doi: 10.1111/evo.12122

Mun, S., Noh, M. Y., Kramer, K. J., Muthukrishnan, S., and Arakane, Y. (2020). Gene functions in adult cuticle pigmentation of the yellow mealworm, *Tenebrio molitor*. *Insect Biochem. Mol. Biol.* 117:103291. doi: 10.1016/J.Ibmb.2019.103291

Noh, M. Y., Koo, B., Kramer, K. J., Muthukrishnan, S., and Arakane, Y. (2016). Arylalkylamine N-acetyltransferase 1 gene (TcAANAT1) is required for cuticle morphology and pigmentation of the adult red flour beetle, *Tribolium castaneum*. *Insect Biochem. Mol. Biol.* 79, 119–129. doi: 10.1016/j.ibmb.2016.10.013

Phillips, A. M., Smart, R., Strauss, R., Brembs, B., and Kelly, L. E. (2005). The *Drosophila* black enigma: the molecular characterization of the black1 mutant and behavioural allele. *Gene* 351, 131–142. doi: 10.1016/j.gene.2005.03.013

Roseland, C. R., Kramer, K. J., and Hopkins, T. L. (1987). Cuticular strength and pigmentation of rust-red and black strains of *Tribolium castaneum*: correlation with catecholamine and β-alanine content. *Insect Biochem.* 17, 21–28. doi: 10.1016/0020-1790(87)90139-9

Simon, J. D., Peles, D., Wakamatsu, K., and Ito, S. (2009). Current challenges in understanding melanogenesis: bridging chemistry, biological control, morphology, and function. *Pigm. Cell Melanoma R.* 22, 563–579. doi: 10.1111/j.1755-148X.2009.00610.x

Sobala, L. F., and Adler, P. N. (2016). The gene expression program for the formation of wing cuticle in *Drosophila*. *PLoS Genet.* 12:e1006100. doi: 10.1371/journal.pgen.1006100

Sugumaran, M., and Barek, H. (2016). Critical analysis of the melanogenic pathway in insects and higher animals. *Int. J. Mol. Sci.* 17:1753. doi: 10.3390/Ijms17101753

Telonis-Scott, M., and Hoffmann, A. A. (2018). Enhancing ebony? common associations with a cis-regulatory haplotype for *Drosophila melanogaster* thoracic pigmentation in a Japanese population and Australian populations. *Front. Physiol.* 9:822. doi: 10.3389/Fphys.2018.00822

Telonis-Scott, M., Hoffmann, A. A., and Sgro, C. M. (2011). The molecular genetics of clinal variation: a case study of ebony and thoracic trident pigmentation in *Drosophila melanogaster* from eastern Australia. *Mol. Ecol.* 20, 2100–2110. doi: 10.1111/j.1365-294X.2011.05089.x

Tomoyasu, Y., Arakane, Y., Kramer, K. J., and Denell, R. E. (2009). Repeated co-options of exoskeleton formation during wing-to-elytron evolution in beetles. *Curr. Biol.* 19, 2057–2065. doi: 10.1016/j.cub.2009.11.014

True, J. R. (2003). Insect melanism: the molecules matter. *Trends Ecol. Evol.* 18, 640–647. doi: 10.1016/j.tree.2003.09.006

True, J. R., Yeh, S. D., Hovemann, B. T., Kemme, T., Meinertzhagen, I. A., Edwards, T. N., et al. (2005). *Drosophila* tan encodes a novel hydrolase required in pigmentation and vision. *PLoS Genet.* 1:e63. doi: 10.1371/journal.pgen.0010063

van't Hof, A. E., Edmonds, N., Dalikova, M., Marec, F., and Saccheri, I. J. (2011). Industrial melanism in British peppered moths has a singular and recent mutational origin. *Science* 332, 958–960. doi: 10.1126/science.1203043

Wappner, P., Hopkins, T. L., Kramer, K. J., Cladera, J. L., Manso, F., and QuesadaAllue, L. A. (1996a). Role of catecholamines and β-alanine in puparial color of wild-type and melanic mutants of the Mediterranean fruit fly (*Ceratitis capitata*). *J. Insect Physiol.* 42, 455–461. doi: 10.1016/0022-1910(95)00131-X

Wappner, P., Kramer, K. J., Manso, F., Hopkins, T. L., and QuesadaAllue, L. A. (1996b). N-β-alanyldopamine metabolism for puparial tanning in wild-type and mutant Niger strains of the Mediterranean fruit fly, *Ceratitis capitata*. *Insect Biochem. Mol. Biol.* 26, 585–592. doi: 10.1016/S0965-1748(96)00012-4

Wittkopp, P. J., and Beldade, P. (2009). Development and evolution of insect pigmentation: genetic mechanisms and the potential consequences of pleiotropy. *Semin. Cell Dev. Biol.* 20, 65–71. doi: 10.1016/j.semcdb.2008.10.002

Wittkopp, P. J., Carroll, S. B., and Kopp, A. (2003). Evolution in black and white: genetic control of pigment patterns in *Drosophila*. *Trends Genet.* 19, 495–504. doi: 10.1016/S0168-9525(03)00194-X

Wright, T. R. F. (1987). The genetics of biogenic amine metabolism, sclerotization, and melanization in *Drosophila melanogaster*. *Adv. Genet.* 24, 127–222. doi: 10.1016/s0065-2660(08)60008-5

Xu, P., Ze, L. J., Kang, W. N., Wu, J. J., Jin, L., Anjum, A. A., et al. (2020). Functional divergence of white genes in *Henosepilachna vigintioctopunctata* revealed by RNA interference. *Insect Mol. Biol.* 29, 466–476. doi: 10.1111/imb.12656

Ze, L. J., Xu, P., Kang, W. N., Wu, J. J., Jin, L., Anjum, A. A., et al. (2021). Disruption of kynurenine pathway reveals physiological importance of tryptophan catabolism in *Henosepilachna vigintioctopunctata*. *Amino Acids* 53, 1091–1104. doi: 10.1007/s00726-021-03009-4

Zhan, S., Guo, Q., Li, M., Li, M., Li, J., Miao, X., et al. (2010). Disruption of an N-acetyltransferase gene in the silkworm reveals a novel role in pigmentation. *Development* 137, 4083–4090. doi: 10.1242/dev.053678

Zhang, Q. L., Wang, F., Guo, J., Deng, X. Y., Chen, J. Y., and Lin, L. B. (2018). Characterization of ladybird *Henosepilachna vigintioctopunctata* transcriptomes across various life stages. *Sci. Data* 5:180093. doi: 10.1038/Sdata.2018.93

Ziegler, A. B., Brusselbach, F., and Hovemann, B. T. (2013). Activity and coexpression of *Drosophila* black with ebony in fly optic lobes reveals putative cooperative tasks in vision that evade electroretinographic detection. *J. Comp. Neurol.* 521, 1207–1224. doi: 10.1002/cne.23247

Conflict of Interest: The authors declare that the research was conducted in the absence of any commercial or financial relationships that could be construed as a potential conflict of interest.

Publisher's Note: All claims expressed in this article are solely those of the authors and do not necessarily represent those of their affiliated organizations, or those of the publisher, the editors and the reviewers. Any product that may be evaluated in this article, or claim that may be made by its manufacturer, is not guaranteed or endorsed by the publisher.

frontiers in Physiology

ORIGINAL RESEARCH
published: 08 March 2022
doi: 10.3389/fphys.2022.829766

Binding Affinity Characterization of Four Antennae-Enriched Odorant-Binding Proteins From *Harmonia axyridis* (Coleoptera: Coccinellidae)

Cheng Qu[1†], Zhao-kai Yang[2†], Su Wang[1], Hai-peng Zhao[3], Feng-qi Li[1], Xin-ling Yang[2] and Chen Luo[1*]*

[1]*Institute of Plant Protection, Beijing Academy of Agriculture and Forestry Sciences, Beijing, China,* [2]*Department of Applied Chemistry, Innovation Center of Pesticide Research, China Agricultural University, Beijing, China,* [3]*College of Plant Protection, Shandong Agricultural University, Taian, China*

OPEN ACCESS

Edited by:
Qingjun Wu,
Insititute of Vegetables and Flowers (CAAS), China

Reviewed by:
Na Yu,
Nanjing Agricultural University, China
Tiantao Zhang,
State Key Laboratory for Biology of Plant Diseases and Insect Pests, Institute of Plant Protection (CAAS), China

***Correspondence:**
Chen Luo
luochen1010@126.com
Xin-ling Yang
yangxl@cau.edu.cn

†These authors have contributed equally to this work

Specialty section:
This article was submitted to Invertebrate Physiology, a section of the journal Frontiers in Physiology

Received: *06 December 2021*
Accepted: *24 January 2022*
Published: *08 March 2022*

Citation:
Qu C, Yang Z-k, Wang S, Zhao H-p, Li F-q, Yang X-l and Luo C (2022) Binding Affinity Characterization of Four Antennae-Enriched Odorant-Binding Proteins From Harmonia axyridis (Coleoptera: Coccinellidae). Front. Physiol. 13:829766. doi: 10.3389/fphys.2022.829766

Harmonia axyridis is an important natural enemy that consumes many agricultural and forestry pests. It relies on a sensitive olfactory system to find prey and mates. Odorant-binding proteins (OBPs) as the first-step of recognizing volatiles, transport odors through sensillum lymph to odorant receptors (ORs). However, little is known about the molecular mechanisms of *H. axyridis* olfaction. In this study, four *H. axyridis* antenna specific OBP genes, *HaxyOBP3*, *5*, *12*, and *15*, were bacterially expressed and the binding features of the four recombinant proteins to 40 substances were investigated using fluorescence competitive binding assays. Three-dimensional structure modeling and molecular docking analysis predicted the binding sites between HaxyOBPs and candidate volatiles. Developmental expression analyses showed that the four HaxyOBP genes displayed a variety of expression patterns at different development stages. The expression levels of *HaxyOBP3* and *HaxyOBP15* were higher in the adult stage than in the other developmental stages, and *HaxyOBP15* was significantly transcriptionally enriched in adult stage. Ligand-binding analysis demonstrated that HaxyOBP3 and HaxyOBP12 only combined with two compounds, β-ionone and p-anisaldehyde. HaxyOBP5 protein displayed binding affinities with methyl salicylate, β-ionone, and p-anisaldehyde (K_i = 18.15, 11.71, and 13.45 μM). HaxyOBP15 protein had a broad binding profile with (E)-β-farnesene, β-ionone, α-ionone, geranyl acetate, nonyl aldehyde, dihydro-β-ionone, and linalyl acetate (K_i = 4.33–31.01 μM), and hydrophobic interactions played a key role in the binding of HaxyOBP15 to these substances according to molecular docking. Taken together, HaxyOBP15 exhibited a broader ligand-binding spectrum and a higher expression in adult stage than HaxyOBP3, 5, and 12, indicating HaxyOBP15 may play a greater role in binding volatiles than other three HaxyOBPs. The results will increase our understanding of the molecular mechanism of *H. axyridis* olfaction and may also result in new management strategies (attractants/repellents) that increase the biological control efficacy of *H. axyridis*.

Keywords: *Harmonia axyridis*, odorant-binding proteins, fluorescence competitive binding assays, molecular docking, volatile compounds

INTRODUCTION

Insects rely on sensitive olfactory systems to perceive chemical signals from the environment, which are important in locating mates, detecting food sources, and finding suitable oviposition sites (Sato et al., 2008; Brito et al., 2016). The interaction between odorant-binding proteins (OBPs) and odorants is the first-step to recognize chemicals, transporting external odors through sensillum lymph to odorant receptors (ORs; Laughlin et al., 2008; Glaser et al., 2015; Elfekih et al., 2016; Pelosi et al., 2018). In *Antheraea polyphemus*, the first OBP was identified showing the function of sex pheromone binding (Vogt and Riddiford, 1981). Since then, many OBPs have been identified in species from different insect orders, including Lepidoptera (Zhu et al., 2013; Yang et al., 2017; Zhang et al., 2017b), Diptera (Zhao et al., 2018; Chen et al., 2019), Hemiptera (Wang et al., 2017; Sun et al., 2020), Neuroptera (Li et al., 2015), and Coleoptera (Bin et al., 2017; Liu et al., 2018).

It is helpful for identifying the function to study the OBPs expression patterns (Gong et al., 2014; Tang et al., 2019). OBPs have a variety of functions depending on their distribution (Sun et al., 2012; Xue et al., 2016; Li et al., 2019b). Antennae-specific OBPs play important roles in detecting sex pheromones and plant volatiles (Sun et al., 2014; Liu et al., 2020).

The Asian multicolored ladybird beetle, *H. axyridis* (Coleoptera: Coccinellidae), as an important natural enemy, can prey on many pests, including aphids, whiteflies, and thrips. Since the early 21 century, this species has been successfully used to control pests of crops (Koch, 2003; Pervez and Omkar, 2006; Wang et al., 2015). *Harmonia axyridis* is an effective biological control agent, but it can also be a pest in some situations (Soares et al., 2007; Koch and Costamagna, 2016; Ovchinnikov et al., 2019). It may compete with native predators for common food resources, and bring pollution to wine production (Pickering et al., 2004; Katsanis et al., 2013; Grez et al., 2016).

Predators used aphid alarm pheromones and pest-induced volatiles to locate pest (Al Abassi et al., 2000; Hatt et al., 2019), which is an important communication way of pest-crop-natural enemy interactions in agricultural fields. It is necessary for enhancing natural enemies' biological control efficacy to understand their olfactory systems. Therefore, the interaction of *H. axyridis* with plant volatiles and aphid pheromones may be important for enhancing the effectiveness of *H. axyridis* as a biological control agent.

We previously identified 19 putative OBPs and characterized their tissue expression patterns by quantitative real-time PCR (qRT-PCR) based on antennae and whole-body transcriptomes of *H. axyridis* (Qu et al., 2021). *HaxyOBP3* (NCBI accession number MT150141), *HaxyOBP5* (NCBI accession number MT150143), *HaxyOBP12* (NCBI accession number MT150150), and *HaxyOBP15* (NCBI accession number MT150153), specifically expressed in adult antennae, may play a more important role in the olfactory perception of *H. axyridis*. In the present study, these four antennae-specific OBPs were selected for detailed study. The development stage expression profiles of these genes were generated, and their binding characteristics to ligands were also conducted. In addition, protein structures were modeled in three dimensions, and their potential binding sites were studied by molecular docking. The results increase our comprehending of the molecular basis of olfaction of *H. axyridis* and may help to enhance their biological control effectiveness.

MATERIALS AND METHODS

Insect Samples

Harmonia axyridis was obtained from Beijing Kuoye Tianyuan Biological Technology Co., Ltd., rearing in a growth chamber of the Beijing Academy of Agriculture and Forestry Sciences with the temperature of 23 ± 1°C, 16:8 h (L:D) photoperiod and 70% relative humidity. The adults and larvae were fed with aphid *Aphis craccivora* Koch (Qu et al., 2018). To determine the transcript levels of *HaxyOBP3*, *5*, *12*, and *15* under various developmental stages (eggs, first, second, third, and fourth instar, pupae, and male and female adults), samples were collected and stored at −80°C. Three biological replicates were conducted.

Specific Expression of OBP Genes

The TRIzol reagent (Invitrogen, Carlsbad, CA, United States) was used to extract total RNA samples based on the manufacturer's instructions. The first-strand cDNA was synthesized using the PrimeScript™ RT reagent Kit (TAKARA, Japan) following the provided protocol. The development stage expression pattern of HaxyOBPs was assessed by qRT-PCR. qRT-PCR was performed on ABI PRISM 7500 (Applied Biosystems, United States). The reaction consisted of 10 μl SYBR Premix *Ex Taq*TM II (TaKaRa, Japan), 1 μl of each primer (10 μmol L^{-1}), 2 μl cDNA, 0.4 μl Rox Reference Dye II (Takara, Japan), and 5.6 μl nuclease free water. The reaction conditions were 95°C for 30 s, followed by 40 cycles of 95°C for 5 s and 60°C for 34 s. Primers of HaxyOBPs were based on Qu et al. (2021). EF1A and RPS13 genes were used as housekeeping genes (Qu et al., 2018). All samples were tested in three biological replicates. The $2^{-\triangle\triangle CT}$ method was used for relative quantification (Schmittgen and Livak, 2008). The differences in the transcript levels of HaxyOBPs in different developmental stages were compared by One-way ANOVA (SPSS 19.0, Chicago, IL, United States), followed by Tukey's test. Heat map illustrating the $\log_2$ transformation of HaxyOBPs mRNA expression levels in different developmental stages.

Expression and Purification of Recombinant OBPs

The DNA sequences that encode the HaxyOBP3, 5, 12, and 15 proteins were chemically synthesized and cloned into pET30a (+) by GenScript (Nanjing, China; Wang et al., 2020b). The positive plasmid was then transformed into BL21 (DE3) cells for the expression of recombinant proteins, and proteins induced with 0.5 mmol/L isopropyl *β*-D-1-thiogalactopyranoside (IPTG) for 4 h at 37°C (HaxyOBP3) or 16 h at 15°C (HaxyOBP5, 12, and 15). HaxyOBP5 was expressed in the supernatant. HaxyOBP3, 12, and 15 were mainly found in inclusion bodies. Inclusion bodies were denatured by 8 M urea. Recombinant proteins of

HaxyOBP3, 12, and 15 were dissolved and refolded based on the reported methods (Zhang et al., 2012).

Protein purification was performed with His-Tag Purification Resin column (Genscript Biology Company, Nanjing, Jiangsu, China) and purified by gradient imidazole buffer (20, 50, 100, 250, and 500 mmol·L^{-1}). The purity and size of proteins were detected by SDS-PAGE, and concentrations of proteins were measured with bicinchoninic acid (BCA) Protein Assay Kit (ThermoFisher Scientific-Life Technologies, Carlsbad, CA, United States).

Competitive Fluorescence Binding Assay

A Cary Eclipse Fluorescence Spectrophotometer (Agilent Technologies, United States) was used to determine the results of the binding assay. *N*-phenyl-1-naphthylamine (1-NPN) for HaxyOBP15 and 4,4′-Dianilino-1,1′-binaphthyl-5,5′-disulfonic acid dipotassium salt (bis-ANS) for HaxyOBP3, 5, and 12 were chosen as the fluorescent probe. The excitation wavelength was 337 nm of 1-NPN and 295 nm of bis-ANS, and the emission spectrum was recorded between 350 and 500 nm for 1-NPN and between 300 and 550 nm for bis-ANS. The recombinant proteins prepared in Tris–HCl (50 mM, pH 7.4) was titrated with aliquots of 1 mM 1-NPN or bis-ANS to final concentrations ranging from 2 to 16 μM to measure the binding affinity. To further measure the binding affinity of ligands to HaxyOBPs, proteins and fluorescent probe at 2 μM were titrated with aliquots of 1 mM odorants. The binding constant ($K_{1\text{-NPN/bis-ANS}}$) of 1-NPN or bis-ANS to HaxyOBPs was calculated by GraphPad Prism 5 software (GraphPad Software Inc.) with the equation $K_i = [IC_{50}]/(1 + [1\text{-NPN}]/K_{1\text{-NPN}})$ or $[IC_{50}]/(1 + [\text{bis-ANS}]/K_{\text{bis-ANS}})$, where [1-NPN]/[bis-ANS] is the free concentration of 1-NPN/bis-ANS, and $K_{1\text{-NPN}}/K_{\text{bis-ANS}}$ is the dissociation constant of the protein/1-NPN (bis-ANS).

Three-Dimensional Modeling and Molecular Docking

Three-dimensional structure of HaxyOBP12 and HaxyOBP15, more than 30% homology with the OBP templates in the Protein Database,[1] was modeled by Program MODELLER (Martí-Renom et al., 2000; Fiser et al., 2010), while HaxyOBP3 and HaxyOBP5 that had less than 30% homology were also generated using a deep residual neural network trRosetta (https://yanglab.nankai.edu.cn/trRosetta; Yang et al., 2020). Three methods, including Verify_3D, Procheck, and ERRAT were used to assess the final 3D model of HaxyOBPs protein (Laskowski et al., 1996; Webb and Sali, 2016). AutoDock Vina (version 1.1.2) was selected to analyze the binding mode between HaxyOBPs protein and compounds with the default parameters (Morris et al., 2009). The top ranked binding mode was evaluated according to the Vina docking score, and visually analyzed by PyMOL (version 1.9.0; http://www.pymol.org/).

RESULTS

Developmental Stage Expression of HaxyOBPs

qRT-PCR was used to determine the expression levels of *HaxyOBP3*, *5*, *12*, and *15* in different developmental stages (**Figure 1**). *HaxyOBP3* and *HaxyOBP15* were both highly expressed in adults, and *HaxyOBP15* had a significantly higher expression

[1]http://www.rcsb.org

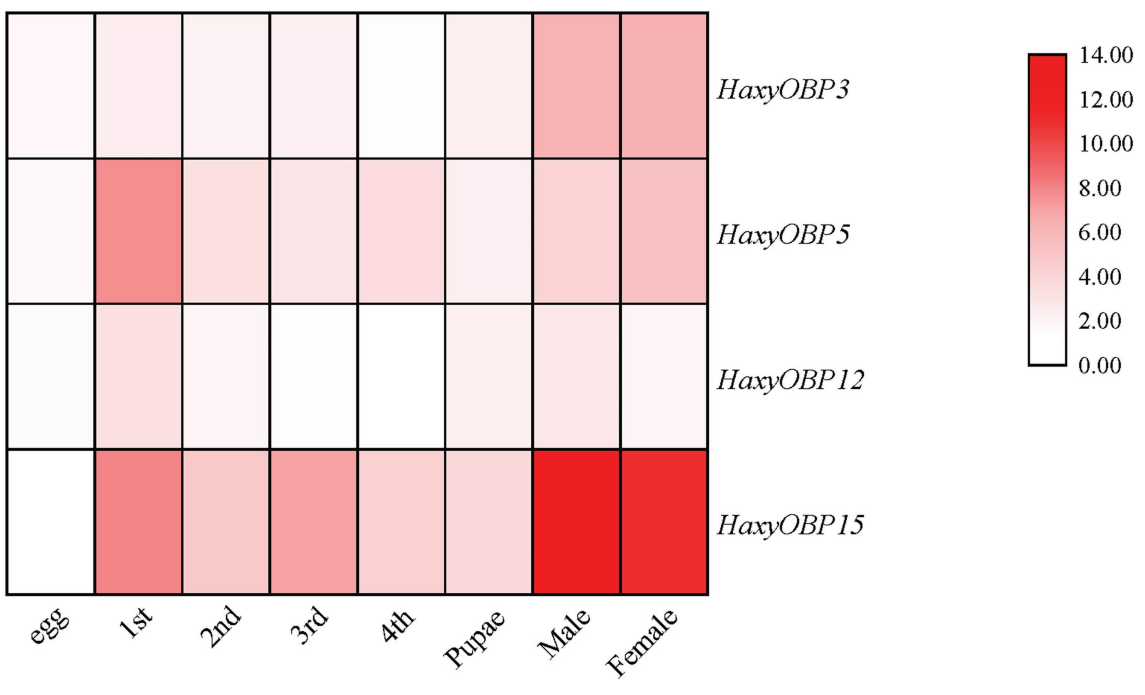

FIGURE 1 | Relative expression levels of *HaxyOBP3*, *5*, *12*, and *15* genes in different developmental stages.

level in this stage. Transcripts of *HaxyOBP5* were especially abundant in the first instar. In addition, *HaxyOBP12* showed similar relative transcript levels in all developmental stages.

Expression and Purification of HaxyOBPs

The recombinant proteins of HaxyOBP3, 5, 12, and 15 were successfully expressed in the *E. coli* system induced by IPTG. HaxyOBP5 was mainly detected in the supernatant, while HaxyOBP3, 12, and 15 were present in inclusion bodies (**Supplementary Figure S1**). Therefore, 8 mol/L urea was used to extract the protein of HaxyOBP3, 12, and 15 before the purification. Renaturation, dialysis, and ultrafiltration were then used to obtain the purified target proteins of HaxyOBP3, 12, and 15. The OBPs were purified by nickel affinity chromatography. SDS-PAGE analysis revealed the final purified proteins as a single band, a molecular weight of about 15 kDa, consistent with the predicted molecular mass (**Figure 2**).

Binding Characteristics of HaxyOBPs

To determine the binding spectra of four HaxyOBPs recombinant proteins, fluorescence competitive binding assay was conducted. The binding characteristics of HaxyOBP3, 5, and 12 with fluorescent probe bis-ANS were detected by molecular fluorescence spectrometry, and the dissociation constants (K_i value) of HaxyOBP3, HaxyOBP5, and HaxyOBP12 were 3.07 ± 057, 2.23 ± 0.36, and 1.84 ± 0.10 μM, respectively. Using the same method, we detected the binding characteristics of HaxyOBP15 with 1-NPN, and the dissociation constant was 5.07 ± 0.31 μM (**Figure 3**).

Using 1-NPN or bis-ANS as a probe, 40 chemicals were used in competitive binding assay. HaxyOBP15 showed a broad binding profile with (E)-β-Farnesene, β-ionone, α-ionone, geranyl acetate, dihydro-β-ionone, nonyl aldehyde, and linalyl acetate, with the K_i values between 4.33 and 40.02 μM. HaxyOBP5 could bind methyl salicylate, β-ionone, and p-anisaldehyde, with the K_i values of 11.71, 13.45, and 18.15 μM, respectively. HaxyOBP3 and HaxyOBP12 showed narrow binding spectra and were able to only bind β-ionone and p-anisaldehyde, with the K_i values of 18.78 and 24.43 μM for HaxyOBP3 and 15.22 and 16.15 μM for HaxyOBP12, respectively (**Figure 4**; **Table 1**).

Homology Modeling and Molecular Docking

Sequence alignments showed that HaxyOBP12 and HaxyOBP15 share 44 and 31% amino acid identities with 6JPM and 4Z45, respectively. Sequence alignments showed that HaxyOBP3 and HaxyOBP5 share 29.27 and 28.93% amino acid identities, respectively, with the templates 1C3Y and 6QQ4, less than 30.00% (**Table 2**). The low identity may decrease the accuracy of the predicted model. So, we used the other method, trRosetta, to predict the model of HaxyOBP3 and HaxyOBP5. The trRosetta can predict the protein more accurately for the low identity sequence. The models predicted by Homology modeling were named Mod-HaxyOBP12 and Mod-HaxyOBP15. The models predicted by trRosetta were named trR-HaxyOBP3 and trR-HaxyOBP5.

For all of the predicted protein models, VERIFY3D, ERRAT, and Procheck were used to analyze the accuracy and reliability. The VERIFY3D (**Supplementary Figure S2**), ERRAT (**Supplementary Figure S3**), and Procheck (**Supplementary Figure S4**) showed that the models of Mod-HaxyOBP12, Mod-HaxyOBP15, trR-HaxyOBP3, and trR-HaxyOBP5 were reasonable.

The protein structures of HaxyOBP3, 5, 12, and 15 were composed of six typical α-helices, forming a hydrophobic binding cavity, which are the important features of insect OBPs (**Figure 5**).

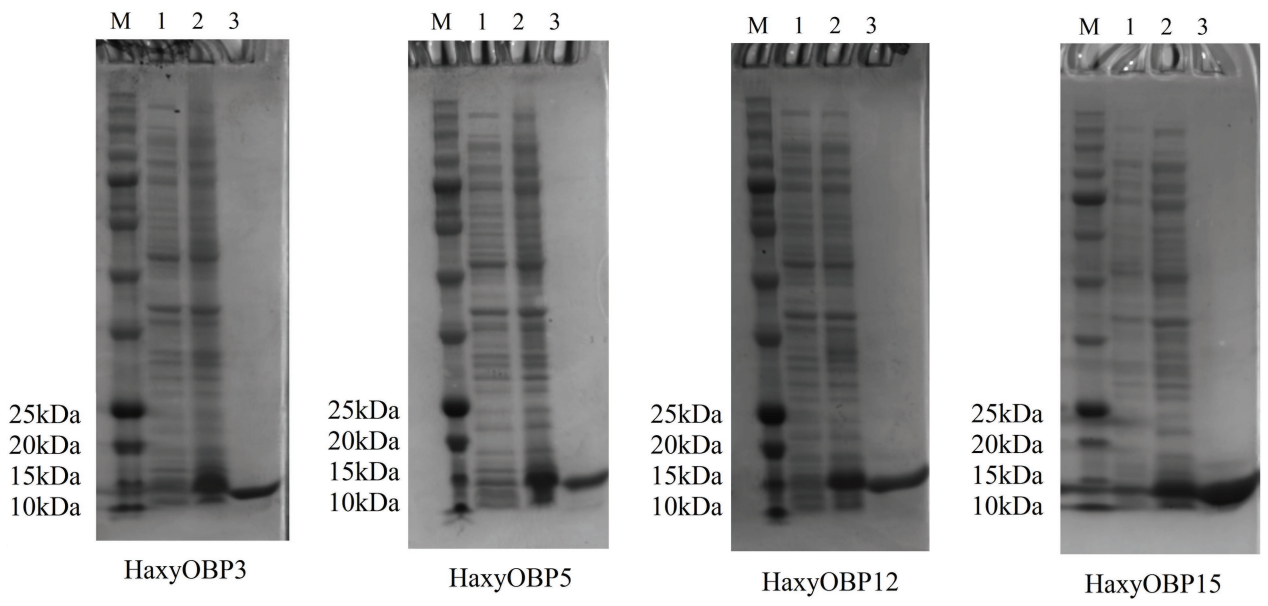

FIGURE 2 | Expression and purification of HaxyOBP3, HaxyOBP5, HaxyOBP12, and HaxyOBP15. M: Marker; 1: Uninduced recombinant protein; 2: IPTG-induced recombinant protein; and 3: Purified proteins.

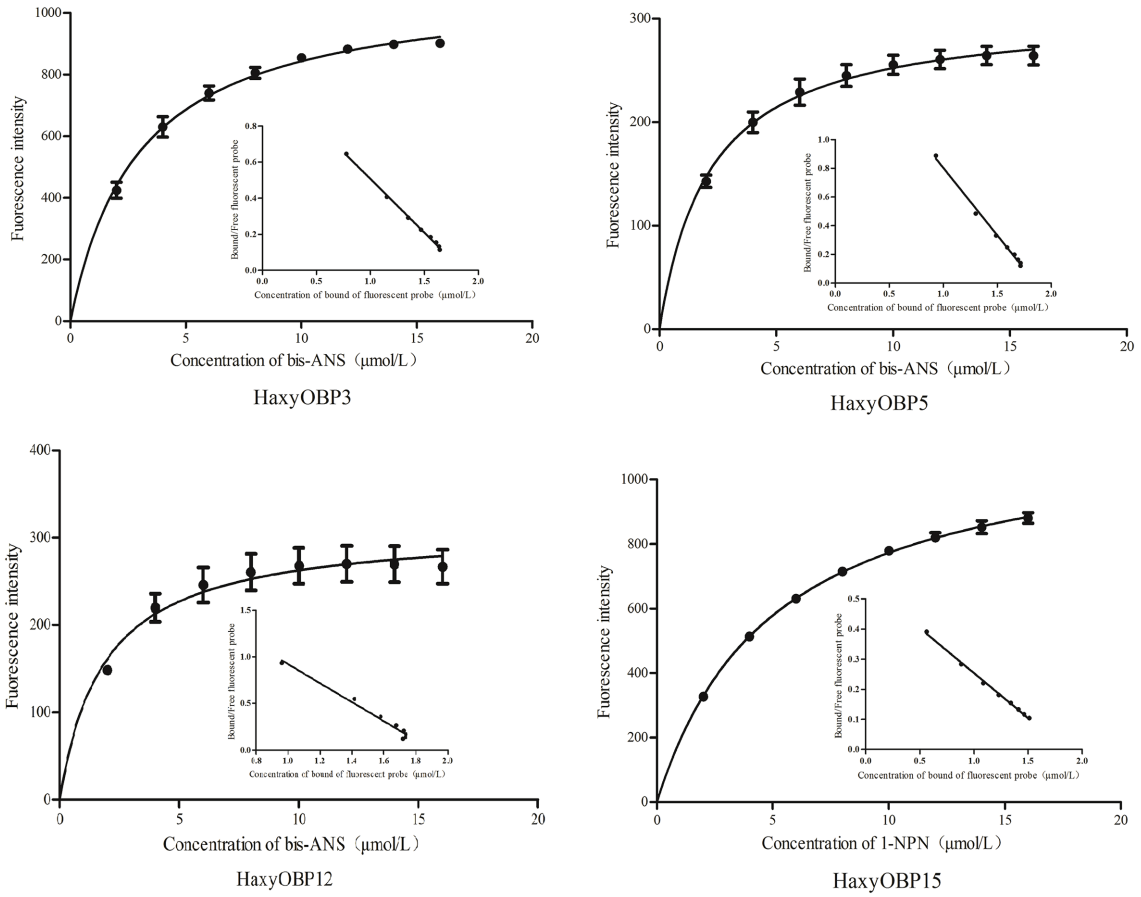

FIGURE 3 | Binding curves and scatchard plots (insert) of probe to HaxyOBPs.

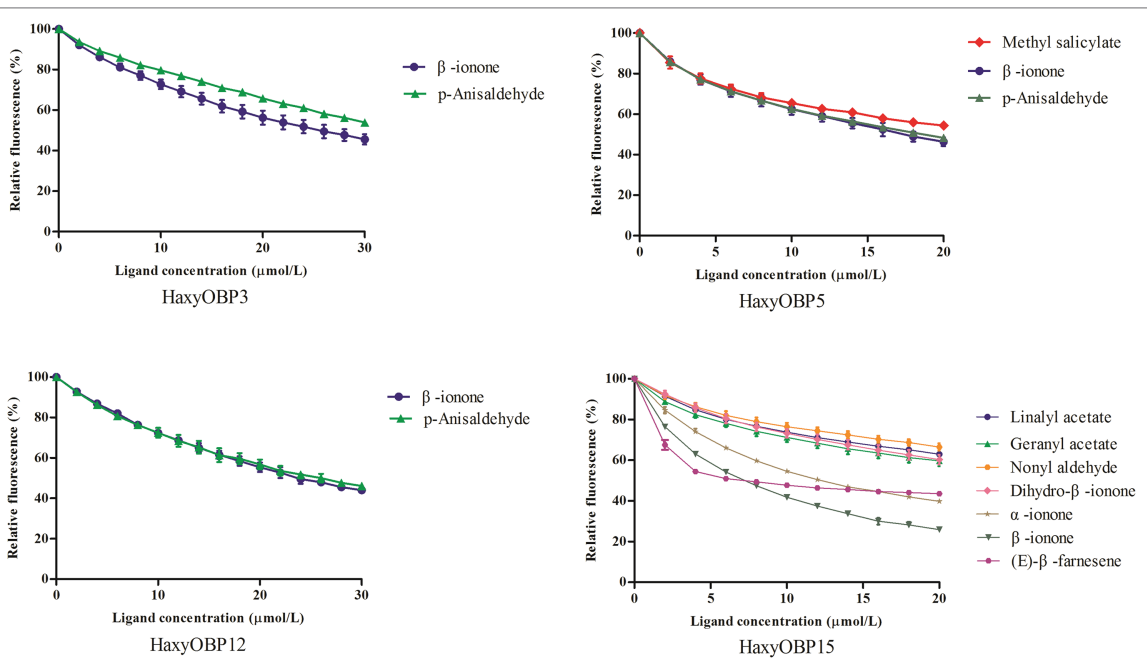

FIGURE 4 | Competitive binding curves of compounds to HaxyOBP3, HaxyOBP5, HaxyOBP12, and HaxyOBP15.

TABLE 1 | Binding affinities of HaxyOBPs with the compounds.

Name	HaxyOBP3		HaxyOBP5		HaxyOBP12		HaxyOBP15	
	IC_{50} (μM)	K_i (μM)	IC_{50} (μM)	K_i (μM)	IC_{50} (μM)	K_i (μM)	IC_{50} (μM)	K_i (μM)
p-Anisaldehyde	34.10 ± 1.06	24.43 ± 0.37	19.93 ± 0.70	13.45 ± 0.67	25.45 ± 1.99	16.15 ± 1.21	--	--
4-Allyl-1,2-dimethoxybenzene	--	--	--	--	--	--	--	--
Nonyl aldehyde	--	--	--	--	--	--	38.49 ± 2.03	29.60 ± 1.86
α-Caryophyllene	--	--	--	--	--	--	--	--
N,N-Diethyl-m-toluamide	--	--	--	--	--	--	--	--
Cis-3-hexenyl butyate	--	--	--	--	--	--	--	--
3-Methyl-1-butanol	--	--	--	--	--	--	--	--
1-Octene	--	--	--	--	--	--	--	--
β-Caryophyllene	--	--	--	--	--	--	--	--
(–)-trans-Caryophyllene	--	--	--	--	--	--	--	--
(+)-α-Pinene	--	--	--	--	--	--	--	--
1-Octen-3-ol	--	--	--	--	--	--	--	--
Cis-3-hexen-1-ol	--	--	--	--	--	--	--	--
Phenylacetaldehyde	--	--	--	--	--	--	--	--
2-Phenylethanol	--	--	--	--	--	--	--	--
Terpinolene	--	--	--	--	--	--	--	--
Acetoin	--	--	--	--	--	--	--	--
α-Terpinene	--	--	--	--	--	--	--	--
β-Cyclocitral	--	--	--	--	--	--	--	--
β-Citronellol	--	--	--	--	--	--	--	--
(+)-2-Carene	--	--	--	--	--	--	--	--
Methyl jasmonate	--	--	--	--	--	--	--	--
α-Pinene	--	--	--	--	--	--	--	--
Geraniol	--	--	--	--	--	--	--	--
β-Ionone	25.87 ± 2.85	18.78 ± 2.14	17.77 ± 1.52	11.71 ± 0.86	24.03 ± 1.56	15.22 ± 1.06	6.99 ± 0.21	5.34 ± 0.18
P-Cymene	--	--	--	--	--	--	--	--
Tetradecane	--	--	--	--	--	--	--	--
Methyl laurate	--	--	--	--	--	--	--	--
Carvacrol	--	--	--	--	--	--	--	--
Linalool	--	--	--	--	--	--	--	--
Dihydro-β-ionone	--	--	--	--	--	--	30.89 ± 3.01	24.01 ± 2.65
α-Ionone	--	--	--	--	--	--	12.03 ± 0.56	9.21 ± 0.44
(E)-β-Farnesene	--	--	--	--	--	--	5.81 ± 0.46	4.33 ± 0.40
Methyl salicylate	--	--	26.44 ± 1.96	18.15 ± 1.33	--	--	--	--
(s)-(–)-Limonone	--	--	--	--	--	--	--	--
α-Humulene	--	--	--	--	--	--	--	--
Geranyl acetate	--	--	--	--	--	--	30.26 ± 3.58	23.38 ± 3.04
Linalyl acetate	--	--	--	--	--	--	40.02 ± 2.91	31.01 ± 2.49
Ethyl octanoate	--	--	--	--	--	--	--	--
β-Elemene	--	--	--	--	--	--	--	--

TABLE 2 | Homologous templates of odorant-binding proteins (OBPs) in *Harmonia axyridis*.

Name	BLAST X match result				
	Species	PDB number of template protein	*E*-value	Identify	Score
HaxyOBP3	*Tenebrio molitor*	1C3Y	$2e^{-04}$	29.27%	38.9
HaxyOBP5	*Drosophila melanogaster*	6QQ4	$1e^{-09}$	28.93%	53.5
HaxyOBP12	*Chrysopa pallens*	6JPM	$2e^{-27}$	44.00%	98.6
HaxyOBP15	*Nasonovia ribisnigri*	4Z45	$3e^{-09}$	31.03%	52.0

According to the affinities between recombinant proteins and chemicals, we selected different numbers of ligands to study the docking conformation and binding energy with four HaxyOBPs proteins, including two ligands (β-ionone and p-anisaldehyde) for HaxyOBP3 and HaxyOBP12, three ligands (methyl salicylate, β-ionone, and p-anisaldehyde) for HaxyOBP5, and seven ligands [(E)-β-Farnesene, β-ionone, α-ionone, geranyl acetate, dihydro-β-ionone, nonyl aldehyde, and linalyl acetateone] for HaxyOBP15. The binding energy values were all negative and ranged from −5.13 to −7.31 kcal mol^{-1} (**Table 3**).

For HaxyOBP3, p-anisaldehyde bound the protein with Y46 and I115 and formed a "π-π" interaction with Y46. β-ionone bound the protein with F52, L68, V103, I113, and I115. The ligand formed hydrogen bond interactions with Y106. I115 is a common key residue for two ligands (**Figure 6**).

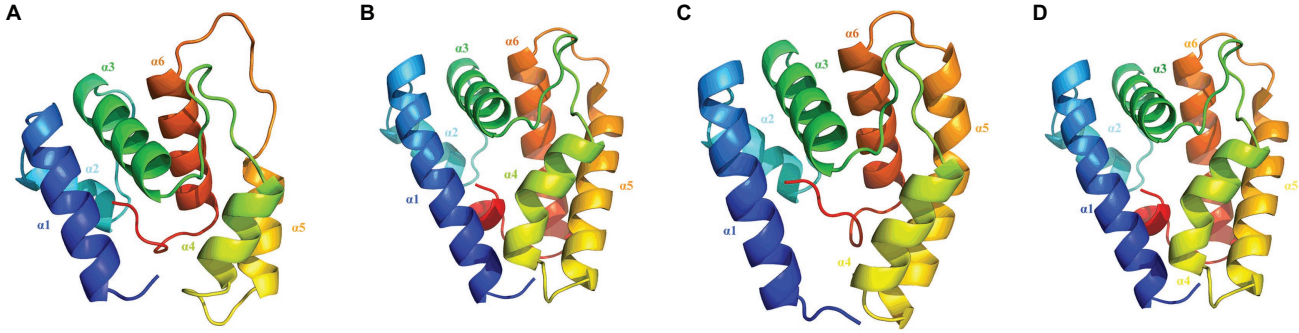

FIGURE 5 | Three-dimensional structure mode of odorant binding proteins in *Harmonia axyridis* (**A**: HaxyOBP3; **B**: HaxyOBP5; **C**: HaxyOBP12; and **D**: HaxyOBP15).

TABLE 3 | Molecular docking analysis of ligands and its binding energy toward HaxyOBPs.

Ligand	HaxyOBP3 (kcal mol^{-1})	HaxyOBP5 (kcal mol^{-1})	HaxyOBP12 (kcal mol^{-1})	HaxyOBP15 (kcal mol^{-1})
β-Ionone	−6.11	−5.95	−5.60	−6.13
p-Anisaldehyde	−5.89	−5.84	−5.86	--
Methyl salicylate	--	−5.13	--	--
Dihydro-β-ionone	--	--	--	−6.19
α-Ionone	--	--	--	−5.83
(E)-β-Farnesene	--	--	--	−7.31
Geranyl acetate	--	--	--	−6.94
Linalyl acetate	--	--	--	−6.09
Nonyl aldehyde	--	--	--	−6.32

For HaxyOBP5, seven residues, including H73, I78, V85, A90, Y112, C115, and L131, were critical for binding affinity to β-ionone based on hydrophobic interactions. P-anisaldehyde formed a "π-π" interaction with Y112 of HaxyOBP5 and formed hydrophobic interactions with V85, A90, and L131. Methyl salicylate formed hydrogen bond interactions with L131 of HaxyOBP5 and hydrophobic interactions with V85, V87, A90, and Y112 (**Figure 7**).

Hydrophobic interactions were the important linkages between HaxyOBP12 and β-ionone and p-anisaldehyde. Three residues, including I91, A103, and A138, were critical for binding affinity to p-anisaldehyde. Four residues, including I91, L131, Y139, and L141, were critical for binding affinity to β-ionone (**Figure 8**).

For HaxyOBP15, hydrophobic interactions were the important linkages between HaxyOBP15 and β-ionone, dihydro-β-ionone, and α-ionone. Three residues, including H53, L58, and I130, appeared to be involved in the binding affinity to the three substances. (E)-β-Farnesene and HaxyOBP15 also have hydrophobic interactions, mediated by F9, L34, M48, I49, F52, H53, and L58. A hydrogen bonding interaction existed between HaxyOBP15 and geranyl acetate and linalyl acetate, with the key residue H53, and there were some hydrophobic residues involved in the interactions (**Figure 9**).

DISCUSSION

Odorant-binding proteins are the front-line environmental odorant sensors, playing an essential role in insect behavior (Pelosi et al., 2006). Temporal and spatial expression patterns of OBPs in insects are interrelated with their specific physiological functions (Song et al., 2014; Sun et al., 2016; Zhang et al., 2017b). The transcripts of *HaxyOBP3*, *5*, *12*, and *15* were mainly restricted to adult antennae in our previous study (Qu et al., 2021), implying a role of these proteins in olfactory chemoreception. Clarifying the expression characteristics of insects' OBPs at different developmental stages can also help to understand their functions in olfactory recognition (Ju et al., 2014). In this study, qRT-PCR indicated that *HaxyOBP3*, *5*, *12*, and *15* had different transcript levels during the different developmental stages of *H. axyridis*. *HaxyOBP5* and *HaxyOBP12* were abundant in the larval stage, indicating their connection to larval biological characteristics of *H. axyridis*. However, *HaxyOBP3* and *HaxyOBP15* were both highly expressed in adult stage, and the expression level of *HaxyOBP15* was significantly higher in this stage, indicating they might be involved in adult-specific behaviors.

The results of the fluorescence binding assay also showed that HaxyOBP15 had a broader ligand-binding affinity, and it could bind seven substances including (E)-β-Farnesene, β-ionone, α-ionone, geranyl acetate, dihydro-β-ionone, nonyl aldehyde, and linalyl acetate, comparing with HaxyOBP3, 5, 12. These results were consistent with the fact that *HaxyOBP15* gene showed significantly higher expression level in adult stage, indicating that *HaxyOBP15* played a key role in olfactory communication of adult *H. axyridis*. *Harmonia axyridis* is an important natural enemy in many crops (Koch, 2003; Pervez and Omkar, 2006). Plant volatiles and sex pheromone are essential signal chemicals in pest-crop-natural enemy interactions

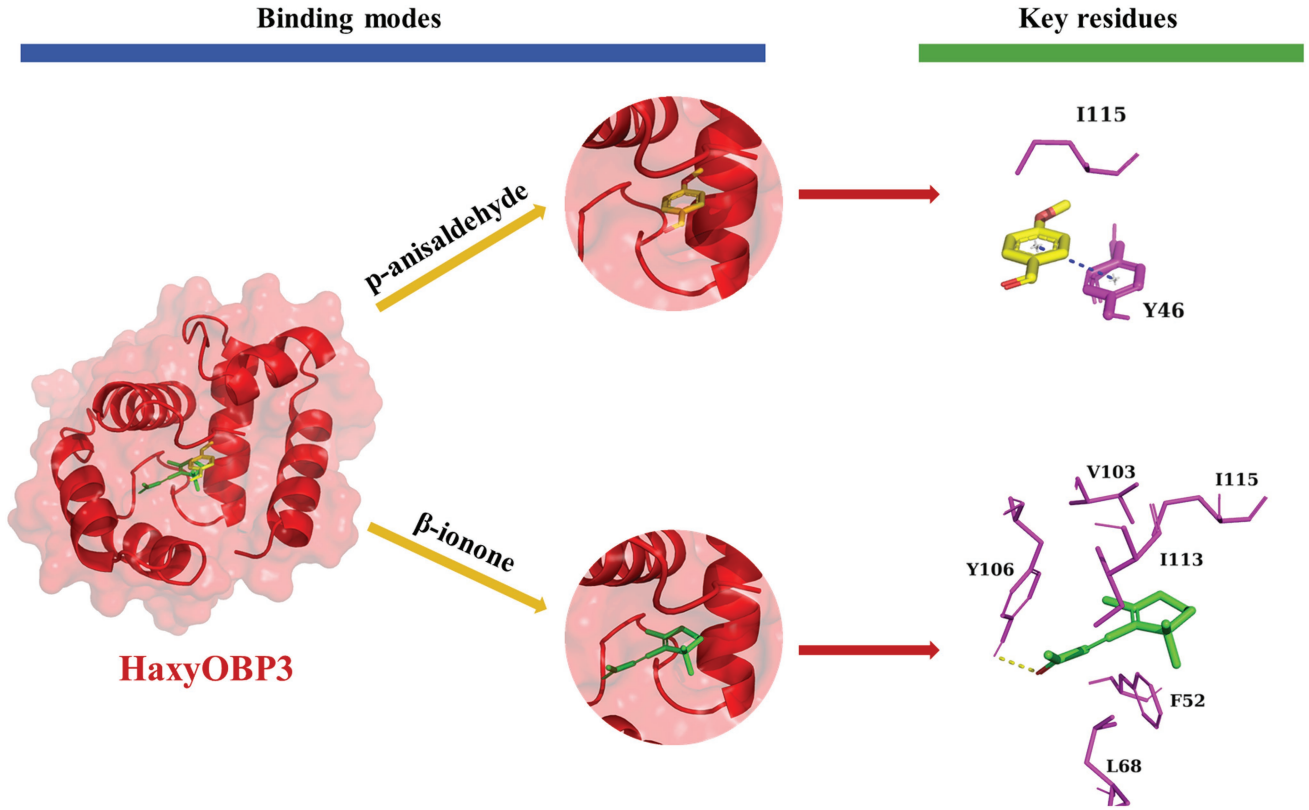

FIGURE 6 | Binding pattern of HaxyOBP3 with p-anisaldehyde and β-ionone.

(Li et al., 2018). Compared with larvae, adults of *H. axyridis* have a wider range of activities due to their ability to fly, and they need to recognize more odorants, so as to detect food sources or find suitable oviposition sites.

Homology modeling and molecular docking were used to further study the specific binding characteristics of OBPs. Classic OBPs usually has six α-helical domains, and fold together to form a compact pocket for combing odors (Pelosi et al., 2014). The present study showed that the predicted 3D structures of the four HaxyOBPs were consistent with those of classic OBPs, having six α-helical domains. Ligands are usually bound in a hydrophobic cavity of insect OBPs (Wogulis et al., 2006; Northey et al., 2016). In this study, molecular docking results showed that HaxyOBP15 broadly bound with more substances, suggesting that HaxyOBP15 may have adapted to binding to substances with different shapes and sizes. Some residues of HaxyOBP15 may specifically interact with functional groups of substances. For instance, HaxyOBP15 possess a key amino acid residue, H53, which appears to be involved in the recognition of a broad range of substances.

Among the 40 candidate compounds, nine compounds, including β-ionone, α-ionone, dihydro-β-ionone, geranyl acetate, nonanal, linalyl acetate, EBF, p-anisaldehyde, and methyl salicylate, bound to four HaxyOBPs according to fluorescence binding assay and molecular docking. β-ionone as a fragrance compound, existing in the flowers and fruits of many plants (Beekwilder et al., 2014; Fu et al., 2019; Guarino et al., 2021) and having a strong repellent effect on flea beetles, spider mites, and whiteflies (Caceres et al., 2016), could bind with the four HaxyOBPs proteins. Moreover, HaxyOBP15 could also bind with α-ionone and dihydro-β-ionone, the analogs of β-ionone. For HaxyOBP15, hydrophobic interactions played a key role in the binding of HaxyOBP15 to three substances based on molecular docking. Three substances have similar chemical structures, and also commonly exist in plant volatiles, playing an important role in interactions between plants and insects (Li et al., 2019a). For example, Dihydro-β-ionone is attractive to the crucifer flea beetle (Caceres et al., 2016). The bouquet of *Philodendron adamantinum* is mainly composed of dihydro-β-ionone, which can attract the beetle *Erioscelis emarginata* and promote the pollination process (Pereira et al., 2014). The α-ionone was widely used as a male attractant for *Bractocera latifrons* (Nishida et al., 2009).

HaxyOBP15 could also bind geranyl acetate, nonanal, and linalyl acetate, and H53 was the key residue between HaxyOBP15 and these three substances by molecular docking. Geranyl acetate is similar to (E)-ß-farnesene (EBF) in structure, but the polarity and hydrophilicity of two compounds are different. Geranyl acetate is an ester, and EBF is a hydrocarbon. Previous studies reported that geranyl acetate is a strong activator of OR5 of aphids and also has binding affinity to OBP3 and OBP7, demonstrating features shared by several other behaviorally active repellents (Zhang et al., 2017a). Linalyl acetate is a monoterpene ester, which can be isolated from essential oils of *Chrysactinia mexicana*, *Lavandula angustifolia*, and *Thymus leptophyllus* (Jan et al., 2016).

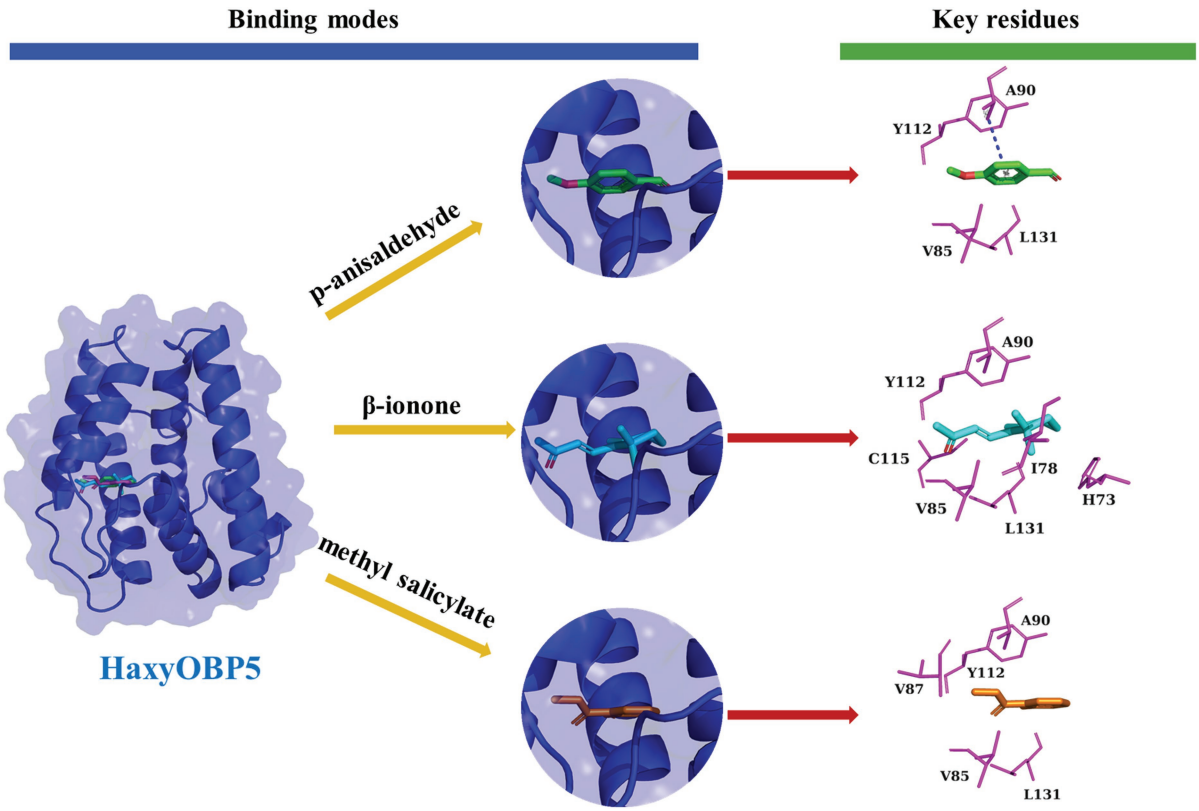

FIGURE 7 | Binding pattern of HaxyOBP5 with p-anisaldehyde, β-ionone, and methyl salicylate.

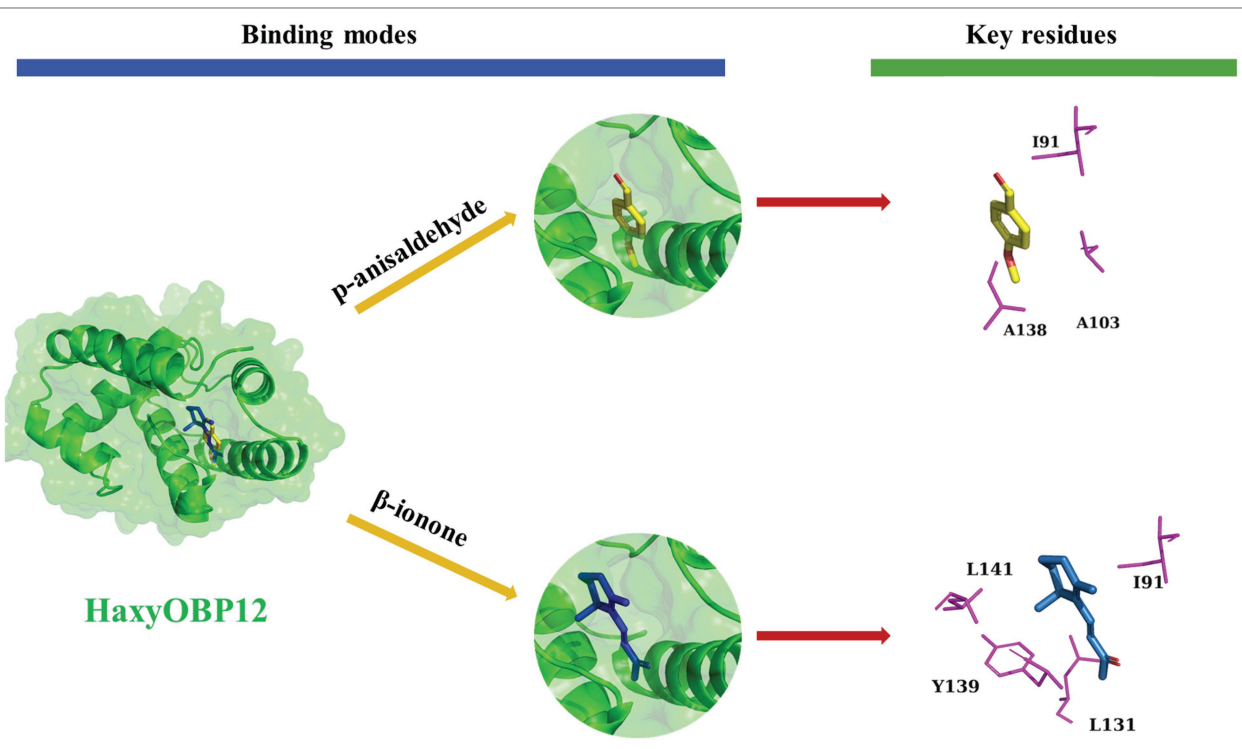

FIGURE 8 | Binding pattern of HaxyOBP12 with p-anisaldehyde and β-ionone.

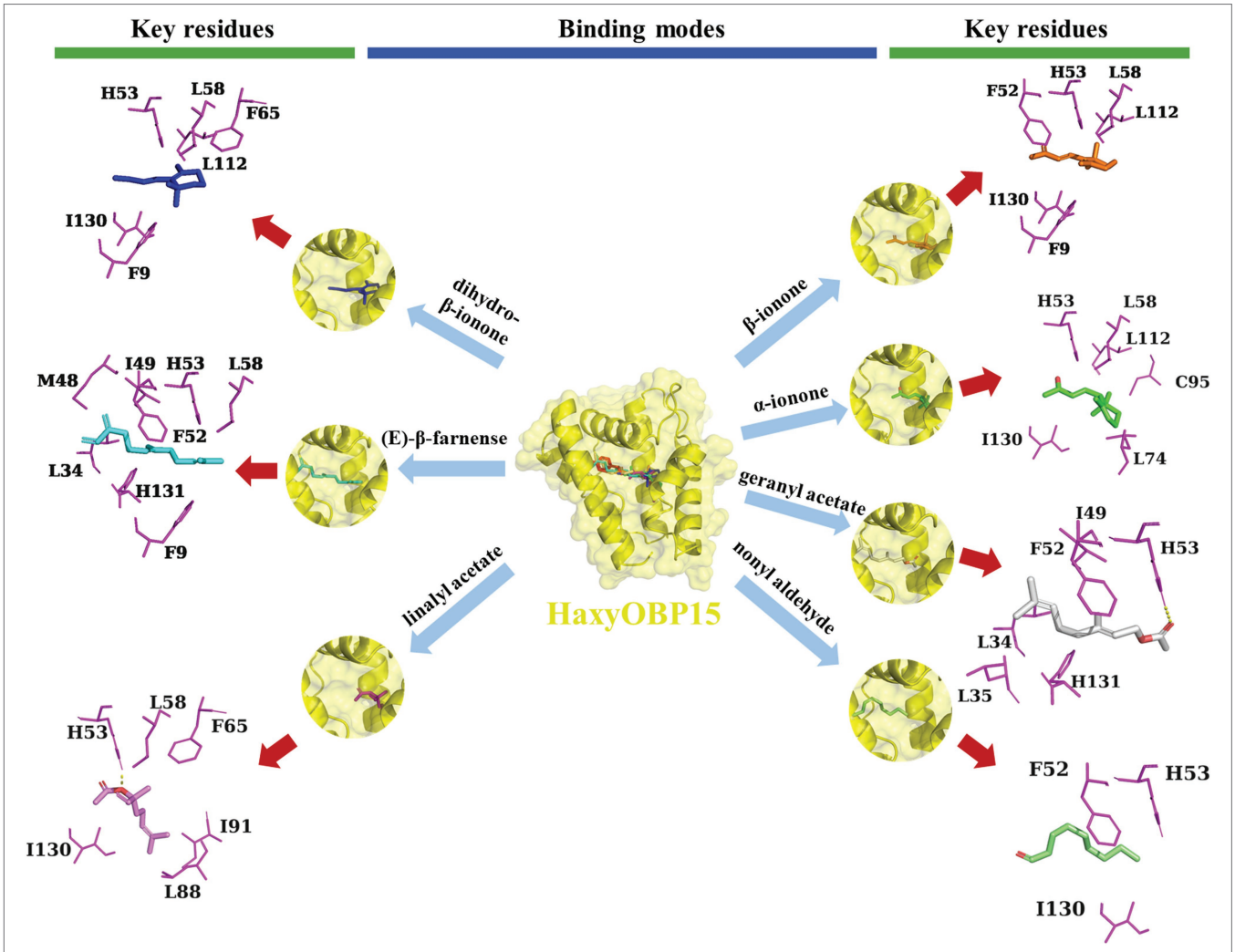

FIGURE 9 | Binding pattern of HaxyOBP15 with β-ionone, dihydro-β-ionone, α-ionone, EBF, geranyl acetate, linalyl acetate, and nonyl aldehyde.

In addition, the common volatile compound nonanal can attract female *Grapholitha molesta* in Y-tube experiment and is a critical volatile of tobacco for attracting female *Helicoverpa assulta* (Lu and Qiao, 2020; Wang et al., 2020a).

More importantly, fluorescence binding assay showed that HaxyOBP15 exhibited the strongest binding affinity with EBF. Molecular docking results also revealed that HaxyOBP15 and EBF displayed the strongest binding activity, having hydrophobic interactions mediated by F9, L34, M48, I49, F52, H53, and L58, with the lowest binding energy values. EBF, as main active component of aphid alarm pheromone (Bowers et al., 1977), can cause aphids to kick, stop feeding, and disperse from feeding site (Pickett et al., 1992), and mediates the winged morphs's production (Kunert et al., 2005). Many aphid predators, such as hoverflies (Harmel et al., 2007), ground beetles (Kielty et al., 1996), and lady beetles (Nakamuta, 1991; Verheggen et al., 2007; Liu et al., 2014), utilize the aphid alarm pheromone EBF as a foraging cue. OBP3, 7, and 9 are associated with EBF perception in aphids (Qiao et al., 2009; Sun et al., 2011; Northey et al., 2016; Fan et al., 2017; Qin et al., 2020; Wang et al., 2021). The OBP1 of *Chrysoperla sinica* was able to bind EBF (Li et al., 2018), and the OBP10 of *Chrysopa pallens* mediated the perception of EBF (Li et al., 2017).

Although HaxyOBP3, 5, and 12 had a relatively narrow binding spectrum, comparing with HaxyOBP15, but they all bound to p-anisaldehyde. P-anisaldehyde is a naturally occurring fragrant phenolic compound that exists in anise, cumin, fennel, garlic, and other plant species (Boulogne et al., 2012). P-anisaldehyde is also a chemical communication substance of many insects (El-Sayed et al., 2008; Mainali and Lim, 2011; Thoming et al., 2020). For example, p-anisaldehyde can attract *Frankliniella occidentalis* and *Thrips tabaci* (Hollister et al., 1995; Koschier et al., 2000), and is an effective attractant for adults of *Anthrenus verbasci* (Imai et al., 2002). However, p-anisaldehyde has a repellent effect on some species, including *Amblyomma americanum* (Showler and Harlien, 2018) and *Musca domestica* (Showler and Harlien, 2019). In addition, HaxyOBP5 could bind with methyl salicylate (MeSA), a herbivore-induced plant

volatile that is attractive to many predators such as ladybeetles (James, 2003a; Zhu and Park, 2005; Salamanca et al., 2017), lacewings (James, 2003b), hoverflies (Mallinger et al., 2011), mites (de Boer and Dicke, 2005), bugs (James, 2005), and aphid parasitoids (Gordon et al., 2013; Martini et al., 2014). In addition, MeSA has repellent effect on several aphid species (Ninkovic et al., 2003; Wang et al., 2019).

In summary, the expression levels of the four HaxyOBPs genes showed different in development stages, and HaxyOBP15 was significantly higher expressed in the adult of *H. axyridis* based on the results of qRT-PCR. Ligand binding assays and molecular docking demonstrated HaxyOBP15 exhibited high specificity for more substances, comparing with HaxyOBP3, 5, and 12, suggesting HaxyOBP15 may play the most prominent role in the olfactory chemoreception of *H. axyridis*. These results can provide insight into the mechanism of olfactory communication of *H. axyridis* and enhance the biological control effectiveness of *H. axyridis*.

DATA AVAILABILITY STATEMENT

The original contributions presented in the study are included in the article/**Supplementary Material**, further inquiries can be directed to the corresponding authors.

AUTHOR CONTRIBUTIONS

CQ and CL conceived and designed the experiments. CQ performed the experiments. CQ and F-qL analyzed the data. Z-kY and CQ provided the homology modeling and molecular docking and wrote the initial manuscript. CQ and H-pZ prepared the figures. CL, X-lY, and SW edited and reviewed the manuscript. All authors accepted the final version of the manuscript.

FUNDING

This work was supported by the China Agriculture Research System of MOF and MARA (CARS-24-C-03); the National Key Research and Development Program of China (2017YFD0200400); and the Shandong Province Modern Agricultural Technology System Peanut Innovation Team, China (SDAIT-04-08).

SUPPLEMENTARY MATERIAL

The Supplementary Material for this article can be found online at: https://www.frontiersin.org/articles/10.3389/fphys.2022.829766/full#supplementary-material

REFERENCES

Al Abassi, S., Birkett, M. A., Pettersson, J., Pickett, J. A., Wadhams, L. J., and Woodcock, C. M. (2000). Response of the seven-spot ladybird to an aphid alarm pheromone and an alarm pheromone inhibitor is mediated by paired olfactory cells. *J. Chem. Ecol.* 26, 1765–1771. doi: 10.1023/a:1005555300476

Beekwilder, J., van Rossum, H. M., Koopman, F., Sonntag, F., Buchhaupt, M., Schrader, J., et al. (2014). Polycistronic expression of a beta-carotene biosynthetic pathway in *Saccharomyces cerevisiae* coupled to beta-ionone production. *J. Biotechnol.* 192, 383–392. doi: 10.1016/j.jbiotec.2013.12.016

Bin, S. Y., Qu, M. Q., Li, K. M., Peng, Z. Q., Wu, Z. Z., and Lin, J. T. (2017). Antennal and abdominal transcriptomes reveal chemosensory gene families in the coconut hispine beetle, *Brontispa longissima*. *Sci. Rep.* 7:2809. doi: 10.1038/s41598-017-03263-1

Boulogne, I., Petit, P., Ozier-Lafontaine, H., Desfontaines, L., and Loranger-Merciris, G. (2012). Insecticidal and antifungal chemicals produced by plants: a review. *Environ. Chem. Lett.* 10, 325–347. doi: 10.1007/s10311-012-0359-1

Bowers, W. S., Nishino, C., Montgomery, M. E., and Nault, L. R. (1977). Structure-activity relationships of analogs of the aphid alarm pheromone, (E)-β-farnesene. *J. Insect Physiol.* 23, 697–701. doi: 10.1016/0022-1910(77)90086-5

Brito, N. F., Moreira, M. F., and Melo, A. C. A. (2016). A look inside odorant-binding proteins in insect chemoreception. *J. Insect Physiol.* 95, 51–65. doi: 10.1016/j.jinsphys.2016.09.008

Caceres, L. A., Lakshminarayan, S., Yeung, K. K. C., McGarvey, B. D., Hannoufa, A., Sumarah, M. W., et al. (2016). Repellent and attractive effects of alpha-, beta-, and Dihydro-beta- ionone to generalist and specialist herbivores. *J. Chem. Ecol.* 42, 107–117. doi: 10.1007/s10886-016-0669-z

Chen, J., Wang, F. L., Gui, L. Y., and Zhang, G. H. (2019). Identification and tissue distribution of odorant binding protein genes in the citrus fruit fly, *Bactrocera minax* (Enderlein) (Diptera: Tephritidae). *J. Asia Pac. Entomol.* 22, 256–262. doi: 10.1016/j.aspen.2019.01.011

de Boer, J. G., and Dicke, M. (2005). Information use by the predatory mite *Phytoseiulus persimilis* (Acari: Phytoseiidae), a specialised natural enemy of herbivorous spider mites. *Appl. Entomol. Zool.* 40, 1–12. doi: 10.1303/aez.2005.1

Elfekih, S., Chen, C. Y., Hsu, J. C., Belcaid, M., and Haymer, D. (2016). Identification and preliminary characterization of chemosensory perception-associated proteins in the melon fly *Bactrocera cucurbitae* using RNA-seq. *Sci. Rep.* 6:19112. doi: 10.1038/srep19112

El-Sayed, A. M., Byers, J. A., Manning, L. M., Juergens, A., Mitchell, V. J., and Suckling, D. M. (2008). Floral scent of Canada thistle and its potential as a generic insect attractant. *J. Econ. Entomol.* 101, 720–727. doi: 10.1603/0022-0493(2008)101[720:fsocta]2.0.co;2

Fan, J., Xue, W. X., Duan, H. X., Jiang, X., Zhang, Y., Yu, W. J., et al. (2017). Identification of an intraspecific alarm pheromone and two conserved odorant-binding proteins associated with (E)-beta-farnesene perception in aphid *Rhopalosiphum padi*. *J. Insect Physiol.* 101, 151–160. doi: 10.1016/j.jinsphys.2017.07.014

Fiser, A., Do, R. K. G., and Ali, A. (2010). Modeling of loops in protein structures. *Protein Sci.* 9, 1753–1773. doi: 10.1110/ps.9.9.1753

Fu, J. X., Hou, D., Wang, Y. G., Zhang, C., Bao, Z. Y., Zhao, H. B., et al. (2019). Identification of floral aromatic volatile compounds in 29 cultivars from four groups of *Osmanthus fragrans* by gas chromatography-mass spectrometry. *Hortic. Environ. Biotechnol.* 60, 611–623. doi: 10.1007/s13580-019-00153-5

Glaser, N., Gallot, A., Legeai, F., Harry, M., Kaiser, L., Le Ru, B., et al. (2015). Differential expression of the chemosensory transcriptome in two populations of the stemborer *Sesamia nonagrioides*. *Insect. Biochem. Molec.* 65, 28–34. doi: 10.1016/j.ibmb.2015.07.008

Gong, Z. J., Miao, J., Duan, Y., Jiang, Y. L., Li, T., and Wu, Y. Q. (2014). Identification and expression profile analysis of putative odorant-binding proteins in *Sitodiplosis mosellana* (Gehin) (Diptera: Cecidomyiidae). *Biochem. Biophys. Res. Commun.* 444, 164–170. doi: 10.1016/j.bbrc.2014.01.036

Gordon, G. U. S. O., Wratten, S. D., Jonsson, M., Simpson, M., and Hale, R. (2013). Attract and reward: combining a herbivore-induced plant volatile with floral resource supplementation—multi-trophic level effects. *Biol. Control* 64, 106–115. doi: 10.1016/j.biocontrol.2012.10.003

Grez, A. A., Zaviezo, T., Roy, H. E., Brown, P. M. J., and Bizama, G. (2016). Rapid spread of *Harmonia axyridis* in Chile and its effects on local coccinellid biodiversity. *Divers. Distrib.* 22, 982–994. doi: 10.1111/ddi.12455

Guarino, S., Basile, S., Arif, M. A., Manachini, B., and Peri, E. (2021). Odorants of *Capsicum* spp. dried fruits as candidate attractants for *Lasioderma serricorne* F (Coleoptera: Anobiidae). *Insects* 12:9. doi: 10.3390/insects12010061

Harmel, N., Almohamad, R., Fauconnier, M.-L., Du Jardin, P., Verheggen, F., Marlier, M., et al. (2007). Role of terpenes from aphid-infested potato on searching and oviposition behavior of *Episyrphus balteatus*. *Insect Sci.* 14, 57–63. doi: 10.1111/j.1744-7917.2007.00126.x

Hatt, S., Xu, Q. X., Francis, F., and Osawa, N. (2019). Aromatic plants of East Asia to enhance natural enemies towards biological control of insect pests. A review. *Entomol. Gen.* 38, 275–315. doi: 10.1127/entomologia/2019/0625

Hollister, B., Ca Meron, E. A., and Teulon, D. (1995). Effect of p-Anisaldehyde and a yellow color on behavior and capture of Western flower Thrips. *Thrips Biol. Manag.* 276, 571–574. doi: 10.1007/978-1-4899-1409-5_85

Imai, T., Maekawa, M., and Tsuchiya, S. (2002). Attractiveness of p-anisaldehyde to the varied carpet beetle, *Anthrenus verbasci* (L.) (Coleoptera: Dermestidae). *Appl. Entomol. Zool.* 37, 505–508. doi: 10.1303/aez.2002.505

James, D. G. (2003a). Field evaluation of herbivore-induced plant volatiles as attractants for beneficial insects: methyl salicylate and the green lacewing, *Chrysopa nigricornis*. *J. Chem. Ecol.* 29, 1601–1609. doi: 10.1023/a:1024270713493

James, D. G. (2003b). Synthetic herbivore-induced plant volatiles as field attractants for beneficial insects. *Environ. Entomol.* 32, 977–982. doi: 10.1603/0046-225x-32.5.977

James, D. G. (2005). Further field evaluation of synthetic herbivore-induced plant volatiles as attractants for beneficial insects. *J. Chem. Ecol.* 31, 481–495. doi: 10.1007/s10886-005-2020-y

Jan, S., Kamili, A. N., Parray, J. A., and Bedi, Y. S. (2016). Differential response of terpenes and anthraquinones derivatives in Rumex dentatus and Lavandula officinalis to harsh winters across north-western Himalaya. *Nat. Prod. Res.* 30, 608–612. doi: 10.1080/14786419.2015.1030404

Ju, Q., Li, X., Jiang, X. J., Qu, M. J., Guo, X. Q., Han, Z. J., et al. (2014). Transcriptome and tissue-specific expression analysis of OBP and CSP genes in the dark black chafer. *Arch. Insect. Biochem.* 87, 177–200. doi: 10.1002/arch.21188

Katsanis, A., Babendreier, D., Nentwig, W., and Kenis, M. (2013). Intraguild predation between the invasive ladybird *Harmonia axyridis* and non-target European coccinellid species. *BioControl* 58, 73–83. doi: 10.1007/s10526-012-9470-2

Kielty, J. P., Allen-Williams, L. J., Underwood, N., and Eastwood, E. A. (1996). Behavioral responses of three species of ground beetle (Coleoptera: Carabidae) to olfactory cues associated with prey and habitat. *J. Insect Behav.* 9, 237–250. doi: 10.1007/BF02213868

Koch, R. L. (2003). The multicolored Asian lady beetle, *Harmonia axyridis*: a review of its biology, uses in biological control, and non-target impacts. *J. Insect Sci.* 3:32. doi: 10.1093/jis/3.1.32

Koch, R. L., and Costamagna, A. C. (2016). Reaping benefits from an invasive species: role of *Harmonia axyridis* in natural biological control of Aphis glycines in North America. *BioControl* 62, 331–340. doi: 10.1007/s10526-016-9749-9

Koschier, E. H., Kogel, W., and Visser, J. H. (2000). Assessing the attractiveness of volatile plant compounds to Western flower thrips *Frankliniella occidentalis*. *J. Chem. Ecol.* 26, 2643–2655. doi: 10.1023/A:1026470122171

Kunert, G., Otto, S., Rose, U. S. R., Gershenzon, J., and Weisser, W. W. (2005). Alarm pheromone mediates production of winged dispersal morphs in aphids. *Ecol. Lett.* 8, 596–603. doi: 10.1111/j.1461-0248.2005.00754.x

Laskowski, R. A., Rullmann, J., Macarthur, M. W., Kaptein, R., and Thornton, J. M. (1996). AQUA and PROCHECK-NMR: programs for checking the quality of protein structures solved by NMR. *J. Biomol. NMR* 8, 477–486. doi: 10.1007/BF00228148

Laughlin, J. D., Ha, T. S., Jones, D. N. M., and Smith, D. P. (2008). Activation of pheromone-sensitive neurons is mediated by conformational activation of pheromone-binding protein. *Cell* 133, 1255–1265. doi: 10.1016/j.cell.2008.04.046

Li, F., Li, D., Dewer, Y., Qu, C., Yang, Z., Tian, J. H., et al. (2019a). Discrimination of Oviposition deterrent volatile β-ionone by odorant-binding proteins 1 and 4 in the whitefly *Bemisia tabaci*. *Biomol. Ther.* 9:563. doi: 10.3390/biom9100563

Li, Z. B., Wei, Y., Sun, L., An, X. K., Dhiloo, K. H., Wang, Q., et al. (2019b). Mouthparts enriched odorant binding protein AfasOBP11 plays a role in the gustatory perception of *Adelphocoris fasciaticollis*. *J. Insect Physiol.* 117:103915. doi: 10.1016/j.jinsphys.2019.103915

Li, Z. Q., Zhang, S., Cai, X. M., Luo, J. Y., Dong, S. L., Cui, J. J., et al. (2017). Three odorant binding proteins may regulate the behavioural response of Chrysopa pallens to plant volatiles and the aphid alarm pheromone (E)-beta-farnesene. *Insect Mol. Biol.* 26, 255–265. doi: 10.1111/imb.12295

Li, Z. Q., Zhang, S., Cai, X. M., Luo, J. Y., Dong, S. L., Cui, J. J., et al. (2018). Distinct binding affinities of odorant-binding proteins from the natural predator *Chrysoperla sinica* suggest different strategies-to-hunt-prey. *J. Insect Physiol.* 111, 25–31. doi: 10.1016/j.jinsphys.2018.10.004

Li, Z. Q., Zhang, S., Luo, J. Y., Wang, S. B., Wang, C. Y., Lv, L. M., et al. (2015). Identification and expression pattern of candidate olfactory genes in *Chrysoperla sinica* by antennal transcriptome analysis. *Comp. Biochem. Physiol. Part D Genom. Proteom.* 15, 28–38. doi: 10.1016/j.cbd.2015.05.002

Liu, Y., Chi, B., Bo, Y., Zhu, Y., and Yong, L. (2014). Effects of E-β-farnesene release on the spatial distribution patterns of cabbage aphids and lady beetles. *Acta Phytophy. Sin.* 41, 754–760.

Liu, N. Y., Li, Z. B., Zhao, N., Song, Q. S., Zhu, J. Y., and Yang, B. (2018). Identification and characterization of chemosensory gene families in the bark beetle, *Tomicus yunnanensis*. *Comp. Biochem. Physiol. Part D Genom. Proteom.* 25, 73–85. doi: 10.1016/j.cbd.2017.11.003

Liu, Z., Liang, X. F., Xu, L., Keesey, I. W., Lei, Z. R., Smagghe, G., et al. (2020). An antennae-specific odorant-binding protein is involved in *Bactrocera dorsalis* olfaction. *Front. Ecol. Evol.* 8:63. doi: 10.3389/fevo.2020.00063

Lu, P. F., and Qiao, H. L. (2020). Peach volatile emission and attractiveness of different host plant volatiles blends to *Cydia molesta* in adjacent peach and pear orchards. *Sci. Rep.* 10:13658. doi: 10.1038/s41598-020-70685-9

Mainali, B. P., and Lim, U. T. (2011). Behavioral response of Western flower thrips to visual and olfactory cues. *J. Insect Behav.* 24, 436–446. doi: 10.1007/s10905-011-9267-7

Mallinger, R. E., Hogg, D. B., and Gratton, C. (2011). Methyl salicylate attracts natural enemies and reduces populations of soybean aphids (Hemiptera: Aphididae) in soybean Agroecosystems. *J. Econ. Entomol.* 104, 115–124. doi: 10.1603/ec10253

Martini, X., Pelz-Stelinski, K. S., and Stelinski, L. L. (2014). Plant pathogen-induced volatiles attract parasitoids to increase parasitism of an insect vector. *Front. Ecol. Evol.* 2:8. doi: 10.3389/fevo.2014.00008

Martí-Renom, M. A., Stuart, A. C., Fiser, A., Sánchez, R., and Sali, A. (2000). Comparative protein structure modeling of genes and genomes. *Annu. Rev. Biophys.* 29, 291–325. doi: 10.1146/annurev.biophys.29.1.291

Morris, G. M., Huey, R., Lindstrom, W., Sanner, M. F., Belew, R. K., Goodsell, D. S., et al. (2009). AutoDock4 and AutoDockTools4: automated docking with selective receptor flexibility. *J. Comput. Chem.* 30, 2785–2791. doi: 10.1002/jcc.21256

Nakamuta, K. (1991). Aphid alarm pheromone component, (E)-β-farnesene, and local search by a predatory lady beetle, *Coccinella septempunctata* bruckii MULSANT(Coleoptera:Coccinellidae). *Appl. Entomol. Zool.* 26, 1–7. doi: 10.1303/aez.26.1

Ninkovic, V., Ahmed, E., Glinwood, R., and Pettersson, J. (2003). Effects of two types of semiochemical on population development of the bird cherry oat aphid *Rhopalosiphum padi* in a barley crop. *Agric. Forset. Entomol.* 5, 27–34. doi: 10.1046/j.1461-9563.2003.00159.x

Nishida, R., Enomoto, H., Shelly, T. E., and Ishida, T. (2009). Sequestration of 3-oxygenated alpha-ionone derivatives in the male rectal gland of the solanaceous fruit fly, *Bactrocera latifrons*. *Entomol. Exp. Appl.* 131, 85–92. doi: 10.1111/j.1570-7458.2009.00835.x

Northey, T., Venthur, H., De Biasio, F., Chauviac, F.-X., Cole, A., Lisboa Ribeiro Junior, K. A., et al. (2016). Crystal structures and binding dynamics of odorant-binding protein 3 from two aphid species *Megoura viciae* and *Nasonovia ribisnigri*. *Sci. Rep.* 6:24739. doi: 10.1038/srep24739

Ovchinnikov, A. N., Belyakova, N. A., Ovchinnikova, A. A., and Reznik, S. Y. (2019). Factors determining larval cannibalistic behavior in invasive and native populations of the multicolored Asian ladybird, *Harmonia axyridis*. *Entomol. Gen.* 38, 243–254. doi: 10.1127/entomologia/2019/0702

Pelosi, P., Iovinella, I., Felicioli, A., and Dani, F. R. (2014). Soluble proteins of chemical communication: an overview across arthropods. *Front. Physiol.* 5:320. doi: 10.3389/fphys.2014.00320

Pelosi, P., Iovinella, I., Zhu, J., Wang, G., and Dani, F. R. (2018). Beyond chemoreception: diverse tasks of soluble olfactory proteins in insects. *Biol. Rev.* 93, 184–200. doi: 10.1111/brv.12339

Pelosi, P., Zhou, J. J., Ban, L. P., and Calvello, M. (2006). Soluble proteins in insect chemical communication. *Cell. Mol. Life Sci.* 63, 1658–1676. doi: 10.1007/s00018-005-5607-0

Pereira, J., Schlindwein, C., Antonini, Y., Dalia Maia, A. C., Doetterl, S., Martins, C., et al. (2014). *Philodendron adamantinum* (Araceae) lures its single cyclocephaline scarab pollinator with specific dominant floral scent volatiles. *Biol. J. Linn. Soc.* 111, 679–691. doi: 10.1111/bij.12232

Pervez, A., and Omkar, (2006). Ecology and biological control application of multicoloured Asian ladybird, *Harmonia axyridis*: a review. *Biocontrol Sci. Tech.* 16, 111–128. doi: 10.1080/09583150500335350

Pickering, G., Lin, J., Riesen, R., Reynolds, A., Brindle, I., and Soleas, G. (2004). Influence of *Harmonia axyridis* on the sensory properties of white and red wine. *Am. J. Enol. Vitic.* 55, 153–159.

Pickett, J. A., Wadhams, L. J., and Woodcock, C. M. (1992). The chemical ecology of aphids. *Annu. Rev. Entomol.* 37, 67–90. doi: 10.1146/ annurev.en.37.010192.000435

Qiao, H. L., Tuccori, E., He, X. L., Gazzano, A., Field, L., Zhou, J. J., et al. (2009). Discrimination of alarm pheromone (E)-beta-farnesene by aphid odorant-binding proteins. *Insect. Biochem. Molec.* 39, 414–419. doi: 10.1016/j.ibmb.2009.03.004

Qin, Y. G., Yang, Z. K., Song, D. L., Wang, Q., Gu, S. H., Li, W. H., et al. (2020). Bioactivities of synthetic salicylate-substituted carboxyl (E)-β-Farnesene derivatives as ecofriendly agrochemicals and their binding mechanism with potential targets in aphid olfactory system. *Pest Manag. Sci.* 76, 2465–2472. doi: 10.1002/ps.5787

Qu, C., Wang, R., Che, W. N., Li, F. Q., Zhao, H. P., Wei, Y. Y., et al. (2021). Identification and tissue distribution of odorant binding protein genes in *Harmonia axyridis* (Coleoptera: Coccinellidae). *J. Integr. Agric.* 20, 2204–2213. doi: 10.1016/s2095-3119(20)63297-x

Qu, C., Wang, R., Che, W. N., Zhu, X. Q., Li, F. Q., and Luo, C. (2018). Selection and evaluation of reference genes for expression analysis using quantitative real-time PCR in the Asian ladybird *Harmonia axyridis* (Coleoptera: Coccinellidae). *PLoS One* 13:e0192521. doi: 10.1371/journal.pone.0192521

Salamanca, J., Souza, B., Lundgren, J. G., and Rodriguez-Saona, C. (2017). From laboratory to field: electro-antennographic and behavioral responsiveness of two insect predators to methyl salicylate. *Chemoecology* 27, 51–63. doi: 10.1007/s00049-017-0230-8

Sato, K., Pellegrino, M., Nakagawa, T., Nakagawa, T., Vosshall, L. B., and Touhara, K. (2008). Insect olfactory receptors are heteromeric liagnd-gated ion chanels. *Nature* 452, 1002–1006. doi: 10.1038/nature06850

Schmittgen, T. D., and Livak, K. J. (2008). Analyzing real-time PCR data by the comparative C-T method. *Nat. Protoc.* 3, 1101–1108. doi: 10.1038/nprot.2008.73

Showler, A. T., and Harlien, J. L. (2018). Botanical compound p-Anisaldehyde repels larval lone star tick (Acari: Ixodidae), and halts reproduction by gravid adults. *J. Med. Entomol.* 55, 200–209. doi: 10.1093/jme/tjx158

Showler, A. T., and Harlien, J. L. (2019). Lethal and repellent effects of the botanical p-Anisaldehyde on *Musca domestica* (Diptera: Muscidae). *J. Econ. Entomol.* 112, 485–493. doi: 10.1093/jee/toy351

Soares, A. O., Borges, I., Borges, P. A. V., Labrie, G., and Lucas, É. (2007). *Harmonia axyridis*: what will stop the invader? *BioControl* 53, 127–145. doi: 10.1007/s10526-007-9141-x

Song, Y. Q., Dong, J. F., Qiao, H. L., and Wu, J. X. (2014). Molecular characterization, expression patterns and binding properties of two pheromone-binding proteins from the oriental fruit moth, *Grapholita molesta* (Busck). *J. Integr. Agric.* 13, 2709–2720. doi: 10.1016/s2095-3119(13)60686-3

Sun, Y. L., Huang, L. Q., Pelosi, P., and Wang, C. Z. (2012). Expression in antennae and reproductive organs suggests a dual role of an odorant-binding protein in two sibling Helicoverpa species. *PLoS One* 7:e30040. doi: 10.1371/journal.pone.0030040

Sun, D. D., Huang, Y., Qin, Z. J., Zhan, H. X., Zhang, J. P., Liu, Y., et al. (2020). Identification of candidate olfactory genes in the antennal transcriptome of the stink bug *Halyomorpha halys*. *Front. Physiol.* 11:876. doi: 10.3389/fphys.2020.00876

Sun, Y. F., Qiao, H. L., Ling, Y., Yang, S. X., Rui, C. H., Pelosi, P., et al. (2011). New analogues of (E)-beta-Farnesene with insecticidal activity and binding affinity to aphid odorant-binding proteins. *J. Agric. Food Chem.* 59, 2456–2461. doi: 10.1021/jf104712c

Sun, L., Wei, Y., Zhang, D. D., Ma, X. Y., Xiao, Y., Zhang, Y. N., et al. (2016). The mouthparts enriched odorant binding protein 11 of the alfalfa plant bug *Adelphocoris lineolatus* displays a preferential binding behavior to host plant secondary metabolites. *Front. Physiol.* 7:201. doi: 10.3389/fphys.2016.00201

Sun, L., Xiao, H. J., Gu, S. H., Zhou, J. J., Guo, Y. Y., Liu, Z. W., et al. (2014). The antenna-specific odorant-binding protein AlinOBP13 of the alfalfa plant bug *Adelphocoris lineolatusis* expressed specifically in basiconic sensilla and has high binding affinity to terpenoids. *Insect Mol. Biol.* 23, 417–434. doi: 10.1111/imb.12089

Tang, Q. F., Shen, C., Zhang, Y., Yang, Z. P., Han, R. R., and Wang, J. (2019). Antennal transcriptome analysis of the maize weevil *Sitophilus zeamais*: identification and tissue expression profiling of candidate odorant-binding protein genes. *Arch. Insect. Biochem.* 101:e21542. doi: 10.1002/arch.21542

Thoming, G., Koczor, S., Szentkiralyi, F., Norli, H. R., Tasin, M., and Knudsen, G. K. (2020). Attraction of *Chrysotropia ciliata*(Neuroptera, Chrysopidae) males to P-Anisaldehyde, a compound with presumed pheromone function. *J. Chem. Ecol.* 46, 597–609. doi: 10.1007/s10886-020-01191-5

Verheggen, F. J., Fagel, Q., Heuskin, S., Lognay, G., Francis, F., and Haubruge, E. (2007). Electrophysiological and behavioral responses of the multicolored Asian lady beetle, *Harmonia axyridis* Pallas, to Sesquiterpene Semiochemicals. *J. Chem. Ecol.* 33, 2148–2155. doi: 10.1007/s10886-007-9370-6

Vogt, R. G., and Riddiford, L. M. (1981). Pheromone binding and inactivation by moth antennae. *Nature* 293, 161–163. doi: 10.1038/293161a0

Wang, C., Li, G. N., Miao, C. J., Zhao, M., Wang, B., and Guo, X. R. (2020a). Nonanal modulates oviposition preference in female *Helicoverpa assulta* (Lepidoptera: Noctuidae) via the activation of peripheral neurons. *Pest Manag. Sci.* 76, 3159–3167. doi: 10.1002/ps.5870

Wang, R., Li, F. Q., Zhang, W., Zhang, X. M., Qu, C., Tetreau, G., et al. (2017). Identification and expression profile analysis of odorant binding protein and chemosensory protein genes in *Bemisia tabaci* MED by head transcriptome. *PLoS One* 12:e0171739. doi: 10.1371/journal.pone.0171739

Wang, K., Liu, J. H., Zhan, Y. D., and Liu, Y. (2019). A new slow-release formulation of methyl salicylate optimizes the alternative control of *Sitobion avenae* (Fabricius; Hemiptera: Aphididae) in wheat fields. *Pest Manag. Sci.* 75, 676–682. doi: 10.1002/ps.5164

Wang, Q., Liu, J. T., Zhang, Y. J., Chen, J. L., Li, X. C., Liang, P., et al. (2021). Coordinative mediation of the response to alarm pheromones by three odorant binding proteins in the green peach aphid *Myzus persicae*. *Insect Biochem. Mol. Biol.* 130:103528. doi: 10.1016/j.ibmb.2021.103528

Wang, S. N., Shan, S., Yu, G. Y., Wang, H., Dhiloo, K. H., Khashaveh, A., et al. (2020b). Identification of odorant-binding proteins and functional analysis of antenna-specific AplaOBP1 in the emerald ash borer, *Agrilus planipennis*. *J. Pest. Sci.* 93, 853–865. doi: 10.1007/s10340-019-01188-4

Wang, S., Tan, X. L., Michaud, J. P., Shi, Z. K., and Zhang, F. (2015). Sexual selection drives the evolution of limb regeneration in *Harmonia axyridis* (Coleoptera: Coccinellidae). *Bull. Entomol. Res.* 105, 245–252. doi: 10.1017/s0007485315000036

Webb, B., and Sali, A. (2016). Comparative protein structure modeling using MODELLER. *Curr. Protoc. Bioinformatics* 47, 1–32. doi: 10.1002/0471250953.bi0506s47

Wogulis, M., Morgan, T., Ishida, Y., Leal, W. S., and Wilson, D. K. (2006). The crystal structure of an odorant binding protein from *Anopheles gambiae*: evidence for a common ligand release mechanism. *Biochem. Biophys. Res. Commun.* 339, 157–164. doi: 10.1016/j.bbrc.2005.10.191

Xue, W. X., Fan, J., Zhang, Y., Xu, Q. X., Han, Z. L., Sun, J. R., et al. (2016). Identification and expression analysis of candidate odorant-binding protein and chemosensory protein genes by antennal transcriptome of *Sitobion avenae*. *PLoS One* 11:e0161839. doi: 10.1371/journal.pone.0161839

Yang, J., Anishchenko, I., Park, H., Peng, Z., Ovchinnikov, S., and Baker, D. (2020). Improved protein structure prediction using predicted interresidue orientations. *Proc. Natl. Acad. Sci. U.S.A.* 117, 1496–1503. doi: 10.1073/pnas.1914677117

Yang, S. Y., Cao, D. P., Wang, G. R., and Liu, Y. (2017). Identification of genes involved in chemoreception in *Plutella xyllostella* by antennal transcriptome analysis. *Sci. Rep.* 7:11941. doi: 10.1038/s41598-017-11646-7

Zhang, T. T., Mei, X. D., Feng, J. N., Berg, B. G., Zhang, Y. J., and Guo, Y. Y. (2012). Characterization of three pheromone-binding proteins (PBPs) of *Helicoverpa armigera* (Hubner) and their binding properties. *J. Insect Physiol.* 58, 941–948. doi: 10.1016/j.jinsphys.2012.04.010

Zhang, R. B., Wang, B., Grossi, G., Falabella, P., Liu, Y., Yan, S. C., et al. (2017a). Molecular basis of alarm pheromone detection in aphids. *Curr. Biol.* 27, 55–61. doi: 10.1016/j.cub.2016.10.013

Zhang, Y. N., Zhu, X. Y., Ma, J. F., Dong, Z. P., Xu, J. W., Kang, K., et al. (2017b). Molecular identification and expression patterns of odorant binding protein and chemosensory protein genes in *Athetis lepigone* (Lepidoptera: Noctuidae). *Peer J* 5:e3157. doi: 10.7717/peerj.3157

Zhao, Y. H., Ding, J. F., Zhang, Z. Q., Liu, F., Zhou, C. G., and Mu, W. (2018). Sex- and tissue-specific expression profiles of odorant binding protein and chemosensory protein genes in *Bradysia odoriphaga* (Diptera: Sciaridae). *Front. Physiol.* 9:107. doi: 10.3389/fphys.2018.00107

Zhu, J. W., and Park, K. C. (2005). Methyl salicylate, a soybean aphid-induced plant volatile attractive to the predator *Coccinella septempunctata*. *J. Chem. Ecol.* 31, 1733–1746. doi: 10.1007/s10886-005-5923-8

Zhu, J. Y., Zhang, L. F., Ze, S. Z., Wang, D. W., and Yang, B. (2013). Identification and tissue distribution of odorant binding protein genes in the beet armyworm, *Spodoptera exigua*. *J. Insect Physiol.* 59, 722–728. doi: 10.1016/j.jinsphys.2013.02.011

Conflict of Interest: The authors declare that the research was conducted in the absence of any commercial or financial relationships that could be construed as a potential conflict of interest.

Publisher's Note: All claims expressed in this article are solely those of the authors and do not necessarily represent those of their affiliated organizations, or those of the publisher, the editors and the reviewers. Any product that may be evaluated in this article, or claim that may be made by its manufacturer, is not guaranteed or endorsed by the publisher.

frontiers | Frontiers in Physiology

ORIGINAL RESEARCH
published: 05 May 2022
doi: 10.3389/fphys.2022.850022

Multiple dsRNases Involved in Exogenous dsRNA Degradation of Fall Armyworm *Spodoptera frugiperda*

Yang Yao[1], Dong-Jiang Lin[1], Xiang-Yun Cai[2], Ran Wang[3], You-Ming Hou[2], Chao-Hua Hu[1], San-Ji Gao[1] and Jin-Da Wang[1]**

[1]National Engineering Research Center of Sugarcane, Fujian Agricultural and Forestry University, Fuzhou, China, [2]State Key Laboratory of Ecological Pest Control for Fujian and Taiwan Crops, Ministry of Education, College of Plant Protection, Fujian Agricultural and Forestry University, Fuzhou, China, [3]Institute of Plant Protection, Beijing Academy of Agriculture and Forestry, Beijing, China

RNAi is regarded as a promising technology for pest control. However, not all insects are sensitive to RNAi. Studies have confirmed that insect dsRNases are one of key factors affecting RNAi efficiency. In the current study, we identified four genes coding for dsRNases from the *Spodoptera frugiperda* genome. Spatial and temporal expression analysis showed that those dsRNases were highly expressed in the midgut and old larvae. Then a delivery method was applied for inducing efficient RNAi based on dsRNA encapsulated by liposome. Furthermore, we assessed degradation efficiency by incubation with dsRNA with gut juice or hemocoel to characterize potential roles of different SfdsRNases after suppression of *SfdsRNase*. The result showed that interferenced with any *sfdsRNase* reduced the degradation of exogenous dsRNA in midgut, interfered with *sfdsRNase1* and *sfdsRNase3* slowed down the degradation of exogenous dsRNA in hemolymph. Our data suggest the evolutionary expansion and multiple high activity dsRNase genes would take part in the RNAi obstinate in *S. frugiperda*, besides we also provide an efficient RNAi method for better use of RNAi in *S. frugiperda*.

Keywords: RNA inference, dsRNase, efficiency, liposome, *Spodoptera frugiperda*

OPEN ACCESS

Edited by:
Patrizia Falabella, University of Basilicata, Italy

Reviewed by:
Huipeng Pan, South China Agricultural University, China
Kang He, Zhejiang University, China
Kangxu Wang, Michigan State University, United States

****Correspondence:***
Ran Wang
rwang1105@126.com
Jin-Da Wang
jdwang@fafu.edu.cn

Specialty section:
This article was submitted to Invertebrate Physiology, a section of the journal Frontiers in Physiology

Received: *07 January 2022*
Accepted: *11 April 2022*
Published: *05 May 2022*

Citation:
Yao Y, Lin D-J, Cai X-Y, Wang R, Hou Y-M, Hu C-H, Gao S-J and Wang J-D (2022) Multiple dsRNases Involved in Exogenous dsRNA Degradation of Fall Armyworm Spodoptera frugiperda. Front. Physiol. 13:850022. doi: 10.3389/fphys.2022.850022

INTRODUCTION

RNA interference (RNAi) is a conserved regulatory process to induce sequence-specific gene silencing effect and modulated gene expression in a controlled manner. Therefore, the idea of silencing specific fatal genes in insects has been suggested as a potential strategy for pest management, such as expression of dsRNA in transgenic plants or by spraying absorbable dsRNA pesticide (Baum et al., 2007; Kunte et al., 2020; Zhu and Palli, 2020). Interestingly, the successful systemic RNAi has been established as an important tool for the development of potential insecticidal dsRNAs that can target essential genes in many other tissues of the insect pests (Huvenne and Smagghe, 2010). More recently, the use of the sprayable double-strand RNA-based biopesticide technology was proven to be effective strategy for controlling Colorado potato beetle *Leptinotarsa decemlineata* by GreenLight Biosciences (Rodrigues et al., 2021). Not all insects, viz., Lepidopteran and Hemipteran orders, however, show sensitivity to RNAi (Terenius et al., 2011) compared to the Coleopteran order (Wang et al., 2013; Guo et al., 2021). Furthermore, to induce systemic RNAi in these highly susceptible insects, a particularly intriguing aspect of RNAi is that the dsRNA is not only capable of entering gut cells but can spread to other tissues as well (Joga et al., 2016). Several factors

have been attributed to induce the variability of insect RNAi responses, such as the malfunction or deficiency of core RNAi machinery components, difficulty of cellular dsRNA uptake and systemic distribution, and fast digestion of dsRNA by double-stranded ribonucleases (dsRNases). The existence of dsRNases is deemed as one of the major obstacles influencing successful RNAi by affecting dsRNA integrity in body fluids (Shukla et al., 2016; Wang et al., 2016).

The dsRNases were first isolated from silkworm *Bombyx mori* (Arimatsu et al., 2007; Yuji et al., 2007). Subsequently, large amounts of dsRNases were identified from various insects (Prentice et al., 2019; Peng et al., 2020). However, the function of them was remained to be characterized. Generally, the dsRNases were participating in dsRNA degrading and reduced RNAi efficiency (Yuji et al., 2007; Song et al., 2019). For instance, five dsRNases were identified from the *S. litura,* and functional analysis revealed they may contribute to the lower and variable RNAi efficiency (Peng et al., 2020). While the report from cotton bollworm (*Helicoverpa armigera*) demonstrated an entirely different result: RNAi efficiency was not significantly upregulated when knocking out *HaREase* by CRISPR/Cas9 system (Guan et al., 2019). Therefore, a study of molecular and functional characteristics of dsRNases would make contributions for better applications of RNAi in both scientific research and pest management area.

The fall armyworm *Spodoptera frugiperda* is a devastating agricultural pest in many countries, the outbreak of this pest often leads to significant loss of many commercial crops such as corn, rice, and sugarcane. Repeated use of chemical pesticides causes a considerable decrease in pesticide resistance (Chi et al., 2021; Hafeez et al., 2021; Paredes-Sanchez et al., 2021). Therefore, the demand for new controlling strategies is eagerly excepted. The use of RNAi would provide a new way for *S. frugiperda* management. However, limited successful RNAi cases were reported (Christiaens et al., 2020; Kunte et al., 2020; Zhu and Palli, 2020). Injection of dsSfV-ATPase resulted in enlarged midgut and difficulty of nutrient absorption, significant lethal effect was only observed by continuous dsRNA feeding (Parsons et al., 2018). However, it is still unknown the details of dsRNases in *S. frugiperda* and whether those dsRNases contributed to lower RNAi efficiency. With the help of up-to-date genome sequencing technology, it is possible to identify functional genes from genome-scale. Hence, in the current study, we identified genes coding for dsRNases from the published *S. frugiperda* genome database (http://v2.insect-genome.com/Organism/715); then a delivery method was applied for inducing efficient RNAi *in vivo* based on previous studies in Sf9 cell lines (Gurusamy et al., 2020b); in addition, an assay was performed by suppressed those identified *SfdsRNases via* our efficient delivery method and assessed digestion efficiency by incubation with dsRNA with gut juice or hemocoel to characterize potential roles of different *SfdsRNases* on RNAi efficacy in *S. frugiperda*.

MATERIALS AND METHODS

Insect Rearing

The insects were originally collected from the countryside of Fuzhou, Fujian Province, China, and reared in a laboratory climate chamber at 26°C, relative humidity of 66%, and light for 14 h/10 h. Newly hatched larvae were fed with an artificial diet until pupation, the diet containing soybean powder, wheat bran, yeast powder, casein, ascorbic acid, choline chloride, sorbic acid, inositol, streptomycin, penicillin sodium, propylparaben and agar (Li et al., 2019). Then the adult was supplied with 10% honey solution for oviposition on fresh corn leaves.

Identification of *dsRNase* Gene Family of *S. frugiperda*

The genomic data of *S. frugiperda* was downloaded from the InsectBase2.0 (http://v2.insect-genome.com/) website. The conserved domain of Endonuclease_NS (PF01223) was downloaded from the protein family database (Pfam, http://pfam.xfam.org/) to search for the *dsRNase* gene family. The *dsRNase* genes were retrieved from the *S. frugiperda* genome database by using HMMER software under Linux system (Potter et al., 2018) with default parameters and significant e-value of 0.01. To ensure the complete identification of the *SfdsRNase* gene family, redundant and duplicated sequences were manually removed by confirmation using the BLASTX algorithm against a non-redundant protein database (https://blast.ncbi.nlm.nih.gov/Blast.cgi).

Bioinformatic Analysis of dsRNase From *S. frugiperda*

The online website Gene Structure Display Server version 2.0 (GSDS, http://gsds.cbi.pku.edu.cn/) was used to conduct gene structure analysis. The amino acid motifs present in the predicted SfdsRNase protein sequences were analyzed using the MEME program (http://meme-suite.org/tools/meme). The motif distribution type was set as 0 or 1 occurrence per sequence with the default setting. TBtools (Toolbox for biologists) (Chen et al., 2020) was then used for visual analysis.

The position data for the *SfdsRNase* gene family on the chromosomes was obtained from the genome annotation file, and the chromosomal locations of the *SfdsRNase* genes were visualized.

SfdsRNase protein sequences were retrieved from the NCBI database, and sequences from insects were used to conduct phylogenetic analysis (**Supplementary Table S1**). A maximum likelihood method was conducted in MEGA 7.0.14 (Kumar et al., 2016). Branch confidence was estimated *via* bootstrap analysis with 1,000 replicates using the default parameters, and the tree was visualized with Evolview (https://www.evolgenius.info//evolview/#login).

RNA Extraction and RT-qPCR Analysis

To study the spatial and temporal expression, RNA from different tissue parts (head, hemolymph, midgut, epidermis dissected from ten fifth instar larvae) and four to five larvae from different instars was extracted using the Trizol reagent following the MagZol™ Reagent instructions (Magen, Shanghai, China) with three biological replicates. The extracted RNA was tested for concentration with a multifunctional microplate reader and 1% agarose gel electrophoresis was used to verify the integrity and quality of the RNA. After obtaining the total RNA of *S. frugiperda*, HiScript® II Q RT SuperMix for qPCR (+gDNA wiper) reagent Kit (Perfect Real-time) (Vazyme, Nanjing, China) was used to synthesize cDNA. Total RNA and cDNA are stored at −80°C and −20°C, respectively for subsequent analysis.

Primer 5.0 software was used to design gene specific primers for cloning the detected *SfdsRNase* and *SfV-ATPase* sequences (**Supplementary Table S2**). Premix Taq™ (TaKaRa Taq™ Version 2.0) was used for amplification, and then amplified and purified products were connected to pMD 19-T Vector (TaKaRa, Dalian, China) for sequence verification.

Based on the cloning sequence of *SfdsRNase*, Primer 5.0 was used to design quantitative primers for nuclease genes (**Supplementary Table S2**). The real-time quantitative PCR was performed with ChamQ Universal SYBR qPCR Master Mix reagents (Vazyme) in an Applied Biosystems Q3 system. System configuration and program settings were performed according to the reagent instructions. β-actin was used as an internal reference gene (Rodrígues et al., 2010). Each experimental unit contains four biological replicates and three technical replicates. The $2^{-\Delta\Delta CT}$ was used to calculate the relative expression level.

DsRNA and Nano-dsRNA Synthesis

Using the plasmids containing the *SfdsRNase* and *SfV-ATPase* genes as templates, the fragments were amplified using T7 polymerase-specific primers (**Supplementary Table S2**), detected by 1.5% agarose gel electrophoresis followed by purification and recovery of the fragment. To eliminate the influence of the gene background level, the exogenous gene EGFP was used as a template to synthesize dsEGFP as a negative control. Using the above-amplified product as a template, the T7 RiboMAX™ Express RNAi System (Promega, Madison, United States) was used to synthesize dsRNA separately and the dsRNA needed in the experiment was synthesized *in vitro* according to manufacturer instructions. Take out 1 μl of synthetic dsRNA, dilute it with water ten times, draw apart and use a microplate reader to measure the concentration, then take the remaining diluted solution for gel electrophoresis to test the quality of dsRNA, and finally put it in a −80°C ultra-low temperature refrigerator for later storage.

Use 0.1 M sodium acetate solution to dissolve 75% acetylated chitosan and prepare a 0.02% (w/v) chitosan (Sigma-Aldrich, Shanghai, China) solution. Add 32 μg of dsRNA to 200 μl of chitosan-sodium sulfate solution, the ratio of chitosan solution to sodium sulfate is 1:1. Incubate at 55°C for 1 min, vortex, and mix at high speed for 30 s to form a chitosan dsRNA solution.

The microwave method was used to synthesize CQD nanoparticles (Das et al., 2015). Mix 9 ml polyethylene glycol (PEG200) (TCI, Shanghai, China) with 3 ml nuclease-free water. Mix 0.4 ml of polyethyleneimine (PEI) (TCI, Shanghai, China) with 1.6 ml of nuclease-free water, and then mix with the prepared polyethylene glycol solution. Then, put it in a microwave oven and heat for 3 min, then mix the configured CQD and the sodium sulfate solution containing dsRNA at a ratio of 20:1, and finally put it in 4°C and incubate overnight.

For LIP-dsRNA complexes, dsRNA was mixed with an appropriate amount of liposome transfection reagent Lipofectamine 2000 (Thermo Fisher Science, Waltham, United States) and incubated according to the instructions.

Administration of dsRNA by Oral Uptake and Injection

To test the RNAi efficiency of nanomaterial treated dsRNA on *S. frugiperda* larvae, we first evaluated the lethal effect of nanomaterial. Fresh 30 ml of dsEGFP with nanomaterial was added to artificial diet every day and fed with first instar for 1 week. The mortality is calculated every day. Then nanomaterial-treated dsRNA targets for *SfV-ATPase* were applied to determine RNAi efficiency by feeding method as described above. The mortality and weight were documented after 7 days of treatment. The dsEGFP diluted with ddH_2O was used as a control. Fifty larvae were treated as a biological replicate, and the experiment was repeated three times.

Furthermore, to test the potential mechanism of nanomaterial treated dsRNA on enhancing RNAi efficiency, we used the injection method to achieve a more efficient RNAi effect. Briefly, dsEGFP were incubated LIP-dsRNA (600 ng/μl) according to the instructions of LIP 2000. Use a microsyringe to inject 4 μl LIP-dsRNA into the abdominal cavity of the fourth instar larvae. The larvae were injected with an equal volume of water-dsEGFP as control. Twenty to thirty fourth instar larvae were injected in each treatment. The experiment was repeated three times, and the treated larvae were kept fed and observed with an artificial diet. The midgut juice and hemolymph were further collected for the detection content of dsEGFP.

Midgut Juice and Hemolymph Extraction

Midgut juice extraction refers to the extraction method (Ayra-Pardo et al., 2007). First, prepare 30–40 fourth-instar larvae and place them on ice to make them lose their activity. Then, use a dissecting needle to fix the worm body on the plate, use a scalpel to cut the abdomen, cut the midgut tissue, and place it in a PE tube containing 100 ul PBS. Put the midgut tissue at 4°C, 16000 × g, 20 min, take the supernatant into a new tube, repeat the above steps, and finally the supernatant and midgut juice, store it at −80°C.

The extraction of hemolymph refers to the method reported (Yang and Han, 2014). First, prepare 30–40 fourth instar larvae and place them on ice to make them lose their mobility. Then, use a dissecting needle to fix the worm body on the plate, use scissors to cut a small mouth in the abdomen of the worm body, and then use a 10 μl pipette tip to aspirate the hemolymph and transfer it to a nuclease-free 1.5 ml PE tube. Place the hemolymph melanin, put an appropriate amount of phenylthiourea in the PE tube in advance. The extracted hemolymph was 4°C, 16000 × g, 5 min, the supernatant was discarded, and the hemolymph extract was stored at −80°C.

DsRNA Content Detection

To accurately monitor the dsRNA content in both *in vivo* and *in vitro* conditions. EGFP was used to eliminate the influence of gene background level, and a dsRNA with a fragment length of 414 bp was designed. After the dsRNA feeding or incubation experiment, RNeasy Micro Kit was used to extract dsRNA in each sample, and cDNA was synthesized according to HiScript® II Q RT SuperMix for qPCR (+gDNA wiper) reagent Kit (Perfect Real time) (Vazyme) instructions.

Used modified qPCR method described by (Wang et al., 2020) to detect the absolute content of dsRNA in the sample. The dsRNA (10^5,10^4,10^3,10^2,10^1,10^0,10^{-1} pg/μl) was serially diluted and reverse transcribed into cDNA, and the CT values corresponding to different concentrations of dsRNA were detected by SYBR Green qPCR (Vazyme), and a linear regression model was established. Taking the calculated CT value as the X-axis and the Y-axis as the dsEGFP content in the sample, a linear regression model equation was constructed (**Supplementary Figure.S1**). After RNA extraction and RT-qPCR analysis of the sample, the corresponding CT value is substituted into the linear regression model to obtain the content of dsRNA in the sample.

Ex Vivo Degradation of dsRNA in Hemolymph and Midgut Fluid

To evaluate the roles of sfdsRNases on dsRNA stability, 4 μl dsRNA (1,500 ng/μl) target to four *sfdsRNase* (sfdsRNase1–4), respectively with LIP treated were injected into fourth instar larvae as described before. Twenty-four hours later, the gene expression level of *sfdsRNase1–4* was detected. The hemolymph and midgut fluid were then dissected and stored from treated larvae, also as described before. *Ex vivo* assays were conducted to evaluate the capability of those fluids in dsRNA degrading: first, the dsEGFP was incubated with 200 μl hemolymph or midgut fluid extract at room temperature for 10 min and 60 min. After each time point, the reaction was stored at −20°C to stop the enzymatic reaction. Then the dsEGFP content in the samples was calculated after RNA extraction, cDNA synthesis, and qPCR detection as described above. The relative content of dsEGFP to assess the ability of midgut juice and hemolymph to degrade dsRNA. In order to more accurately record the changes of dsRNA content during in *ex vivo*, the relative content was used for calculation in the experiment. Calculate the relative content with the following formula:

$$\text{Relative content of dsEGFP} = \frac{\text{Treatment group dsEGFP content}}{\text{Control group dsEGFP content}}$$

Statistical Analysis

IBM SPSS statistics was used to test the significance. To compare the treatment means 0.05 probability level was used. All statistical analysis is done on Prism 9.0 software (GraphPad, La Jolla, CA, United States).

RESULTS

Bioinformatics Screening of *S. frugiperda* Nuclease Gene

Four *dsRNases* were obtained from *S. frugiperda* genome after deleting redundant sequences and pseudogene sequences, named as *sfdsRNase1*, *sfdsRNase2*, *sfdsRNase3,* and *sfdsRNase4* according to those in *S. litura*. The predicted full length of CDS ranges from 957 to 1,341, encoding 318 (SfdsRNase1)-446 (SfdsRNase4) amino acids. The predicted protein weight ranges from 36.01 to 50.18 kDa, and the isoelectric point ranges from 5.25 to 9.45. Except for SfdsRNase2, the remaining three amino acid sequences are predicted to contain a signal peptide. The four sfdsRNases amino acid sequences all contain the Endonuclease_NS Structure domain (**Table 1**; **Supplementary Figure S2**).

The chromosome location information shows that the four dsRNase genes are located on three chromosomes (**Figure 1**). In addition, a total of 41 dsRNase gene protein sequences of different species (**Supplementary Table S1**) were obtained from NCBI. The results of the phylogenetic analysis showed that the dsRNase genes of insects are mainly distributed in the five categories of Lepidoptera, Diptera, Orthoptera, Coleoptera, and Hemiptera orders (**Figure 2**). Among them, the four dsRNase genes from *S. frugiperda* are clustered to those reported in *S. litura*, indicating that the dsRNase genes of the two species are closely related.

Spatial and Temporal Expression of Four *sfdsRNases*

The results showed that sfdsRNase1–4 were all highly expressed in the midgut (**Figures 3A–D**), among them, the high expression of *dsRNase3* is extraordinary, and the expression level is nearly 7,000 times higher than that of the other two tissues (**Figure 3C**). In addition, we also compared the expression level of four *sfdsRNases* from midgut and hemolymph. The *sfdsRNase3* was most abundant in the midgut, the expression level of *sfdsRNase3* is still 400 times that of *sfdsRNase1* and more than seven times that of *sfdsRNase1*. Since the mRNA levels of the four *sfdsRNases* in hemolymph reached the detection limit, we compared them horizontally and found that *sfdsRNase2* was the highest expression level among the four *S. frugiperda* dsRNases (**Figure 3F**). These results indicate that the expression levels of different dsRNase in the same tissue are also quite different.

TABLE 1 | Basic information and physical and chemical properties of four predicted *S. frugiperda* dsRNase.

Gene name	Gene ID	GenBank accession	Protein length	Mw (kDa)	Theoretical pI	Signal peptide	Endonuclease_NS (position)
SfdsRNase1	Sfru170710.1	OL960003	318	36.01	9.45	Yes	144–318
SfdsRNase2	Sfru175350.1	OL960002	395	44.80	5.66	No	135–378
SfdsRNase3	Sfru068710.1	OL960004	445	49.27	6.17	Yes	187–428
SfdsRNase4	Sfru003330.1	OM001111	446	50.18	5.25	Yes	185–429

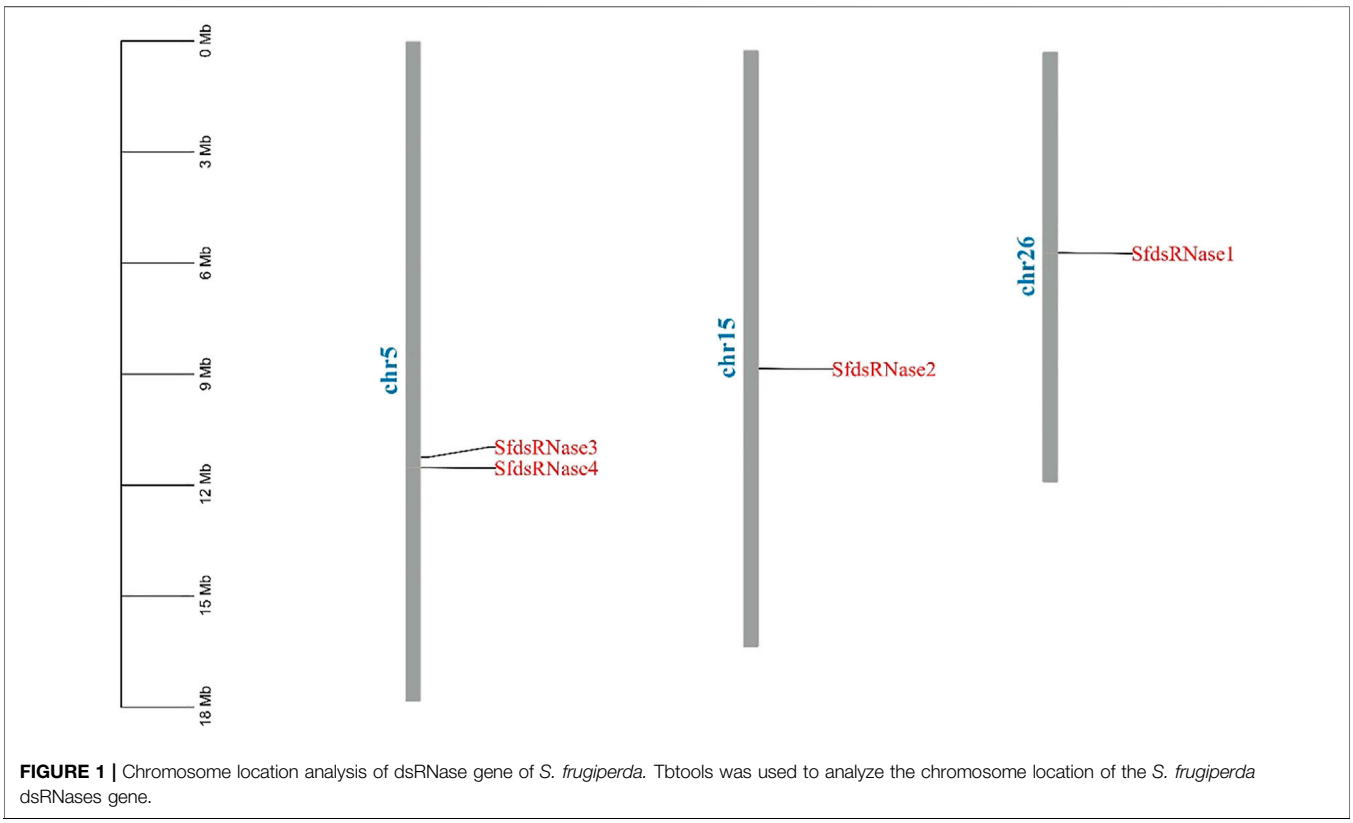

FIGURE 1 | Chromosome location analysis of dsRNase gene of *S. frugiperda*. Tbtools was used to analyze the chromosome location of the *S. frugiperda* dsRNases gene.

The temporal expression levels were analyzed from the six instar stages compared to in egg. It was found that *sfdsRNase1–4* could be detected at all instars, *sfdsRNase1* and *sfdsRNase3* had the highest expression in the third instar stage (**Figure 4A**), *sfdsRNase2* and *sfdsRNase4* had higher expression in the fifth and sixth instar (**Figures 4B,D**). In addition, the mRNA expression levels of adjacent ages are also very different. The expression level of *sfdsRNase2* at the sixth age is ten times as much as that at the fifth age (**Figure 4B**). And the mRNA expression level of fourth instar larvae of *sfdsRNA3* was significantly lower than that of other instar larvae, only one-tenth of that in first instar larvae (**Figure 4C**).

Lip-Encapsulated dsRNA Improves the Efficiency of RNAi

First, to verify whether the nanomaterial itself is toxic to *S. frugiperda* larvae, three nanomaterials were capsulated with dsEGFP and added into an artificial diet continuously for 5 days, and the same amount of dsRNA was incubated with water instead of nanomaterials as a control. We found the mortality of larvae fed with CQD-dsEGFP was significantly higher than that caused by LIP and CHS, and the mortality caused by LIP and CHS was close to the normal mortality of larvae (**Supplementary Figure S3**).

Due to the lethal effect of CQD, the remained LIP and CHS nanomaterials were used for further experiments. Then we synthesized dsRNA from the reported lethal target gene *SfV-ATPase*, and capsulated it with LIP and CHS. The results showed that the LIP-dsV-ATPase complex can significantly increase the mortality of *S. frugiperda* larvae, and the mortality of the larvae fed with the CHS-dsV-ATPase complex feed has no difference compared with the control. Analyzing the growth of larva, it is found that LIP-dsV-ATPase also significantly reduced the growth of larvae, indicating that interference with *SfV-ATPase* may affect the normal feeding of larvae, while the growth of larvae fed with CHS-dsEGFP showed no difference with control (**Table 2**). The target gene *SfV-ATPase* of *S. frugiperda* larvae was detected by

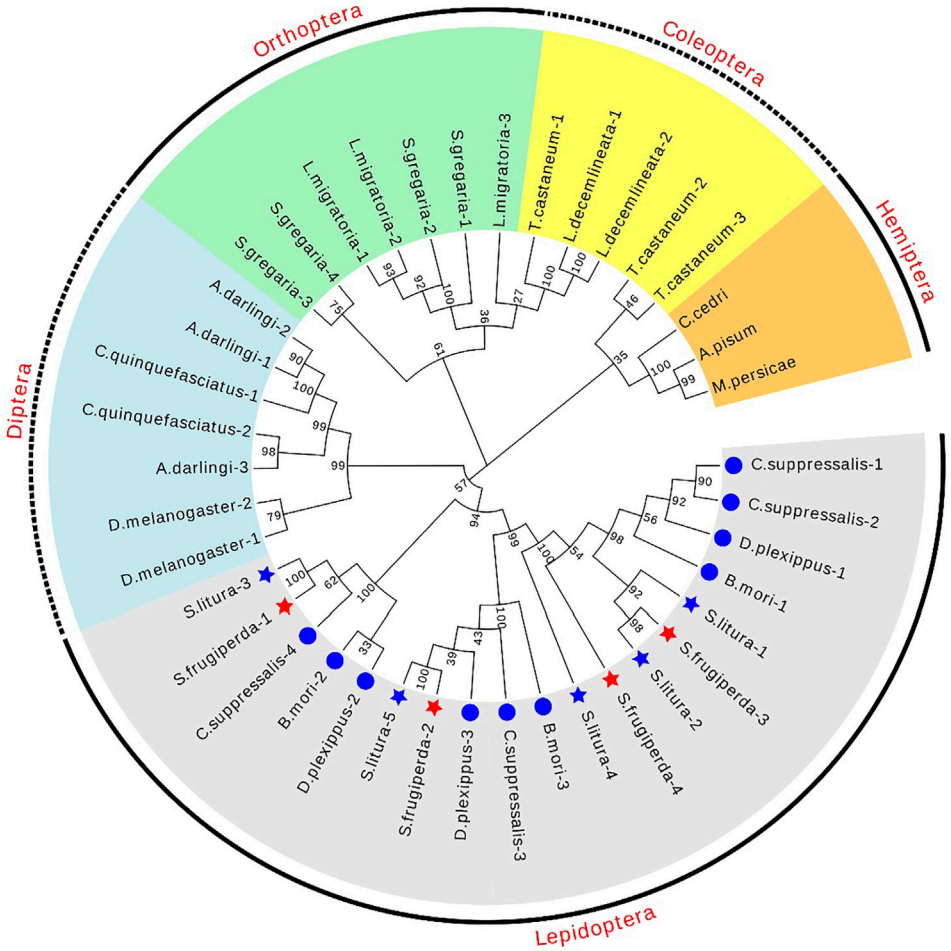

FIGURE 2 | Phylogenetic tree of different species dsRNase in insects. The maximum likelihood method was used to construct phylogenetic trees of different species of dsRNase in insects. *S. frugiperda* is represented by a red star, and *S. litura* is represented by a blue star. Its four sldsRNases GenBank numbers of *S. frugiperda* dsRNase (OL960003, OL960002, OL960004, and OM001111) and *S. litura* dsRNaseare respectively (QJD55609.1), (QJD55610.1), (QJD55611.1), (QJD55612.1).

qPCR for 24 h after feeding LIP-dsRNA complex feed, and it was found that the target gene mRNA level of LIP-dsV-ATPase larvae was significantly reduced (**Supplementary Figure S4**). These results further prove that liposome-encapsulated dsRNA can improve the efficiency of RNAi.

To further explore the potential mechanism of enhancing RNAi effect by lipid, the intestinal fluid and hemolymph of the fourth instar larvae were extracted and incubated with LIP-dsRNA *in vitro*. The data shows that in midgut juice, after incubation for 10 and 60 min, the relative content of dsEGFP without liposome encapsulation is significantly lower than that of liposome-encapsulated dsEGFP. After 60 min, the relative content of liposome-encapsulated dsRNA was nearly 12-fold higher than the control due to further degradation of dsEGFP (**Figure 5A**). In the hemolymph, after 10 min of incubation, the relative content of dsEGFP not encapsulated with liposomes was significantly lower than that of dsEGFP encapsulated with liposomes, but there was no significant difference compared with the control after 60 min (**Figure 5B**). These results indicate that LIP-dsRNA can improve the stability of dsRNA in the midgut fluid of *S. frugiperda*, thereby increasing the efficiency of RNAi.

S. frugiperda Nuclease Gene is Involved in the Degradation of dsRNA in the Midgut and Hemolymph

To verify the function of the *sfdsRNase1–4* genes of *S. frugiperda*, we synthesized dsRNA targeted to those four *sfdsRNases* and used the efficient RNAi delivery method described above. To achieve a more obvious RNAi effect, dsRNAs with lip-encapsulated were injected into fourth instar larvae and significant depression phenomena were observed after 24 h. The results showed that the expression of the four *sfdsRNase* genes was significantly downregulated respectively, compared to the control (**Figure 6**).

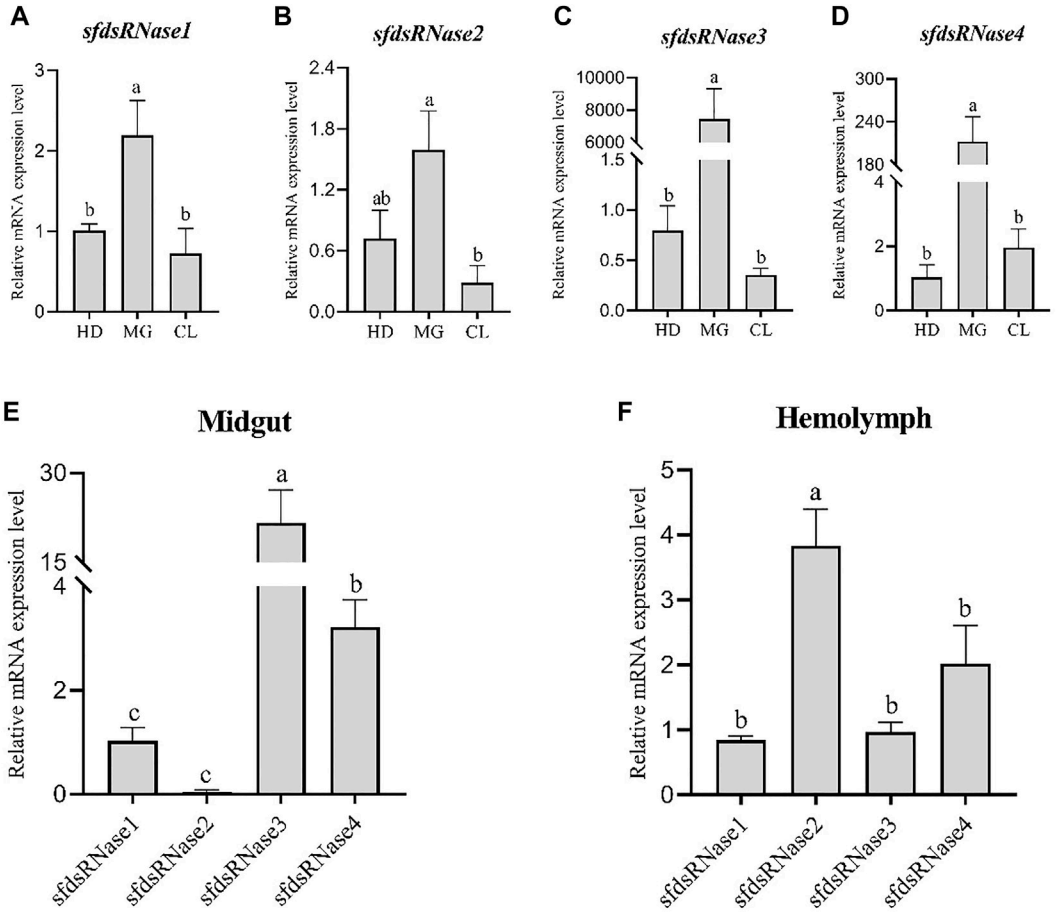

FIGURE 3 | Expression analysis of *S. frugiperda* dsRNase in different tissues. Collect three different tissues of sixth instar larvae, head (HD), midgut (MG), and epidermis (CL) for RT-qPCR, and calculate the expression levels of sfdsRNases in different tissues **(A–D)**. Using *sfdsRNase1* as a control, analyze the relative expression differences of the four sfdsRNases in the midgut and hemolymph **(E,F)**. Five larvae are a biological replicate, and this experiment was performed three times in total. The data shown are mean ± SE, $n = 15$, different letters indicate a significant difference among tissues [$p < 0.05$, one-way ANOVA followed by Duncan's multiple range test for **(A,B)**].

Next, the midgut juice and hemolymph were dissected from those successful silencing insects and incubated with dsEGFP for 10 and 60 min at room temperature, respectively. The results showed that in the midgut juice, there was no significant difference between all treatment groups and the control at 10 min (**Figure 7A**). After 60 min, while the relative content of dsEGFP was significantly higher than that in the control group especially after silencing with *sfdsRNase2* and *sfdsRNases3* , and the relative content of silencing *sfdsRNase2* was 2.5 times that of the water control, indicating all the *sfdsRNases* participated in exogenous dsRNA degradation (**Figure 7B**). A similar situation was detected in hemolymph, there was no significant difference between the treatment group and the control after 10 min incubation (**Figure 7C**). However, we found the ratio of dsEGFP from *sfdsRNase1* and *sfdsRNase3* treatment groups was much higher than that in other groups after 60 min incubation. Among them, the relative content of the treatment group after silencing *sfdsRNase1* was nearly twice that of the control (**Figure 7D**). The results suggest that *sfdsRNase1* and *sfdsRNase3* may be involved in the degradation of dsRNA in the hemolymph.

DISCUSSION

The development of RNAi encloses great potential to be strategies for pest control management (Baum et al., 2007; Song et al., 2019; Kunte et al., 2020; Zhu and Palli, 2020). However, the insensitive RNAi in different insects hindered the application of RNAi in practical fields. As one of the most important insects, the lepidopteran insect caused severe damages to crop. Unfortunately, those insects showed low efficiency to RNAi compared to coleopteran insects, including fall armyworm *S. frugiperda* (Christiaens et al., 2020). As noted, fast dsRNA degradation is one of the key factors affecting RNAi efficiency

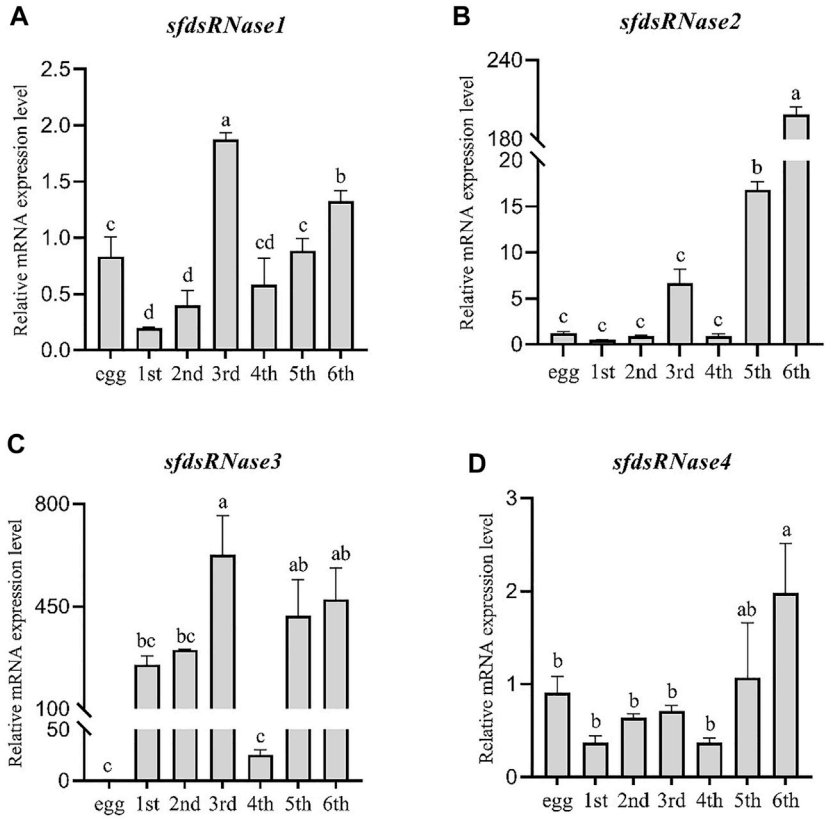

FIGURE 4 | Expression analysis of *S. frugiperda dsRNases* at different ages. Using egg, first instar larvae (first), second instar larvae (second), third instar larvae (third), fourth instar larvae (fourth), fifth instar larvae (fifth), and sixth instar larvae (sixth) as templates for qPCR and using the eggs as a control to calculate the dsRNases in different instars. The relative expression level of mRNA **(A–D)**. Five larvae are a biological replicate, and this experiment was performed three times in total. The data shown are mean ± SE, $n = 21$, different letters indicate a significant difference among ages [$p < 0.05$, one-way ANOVA followed by Duncan's multiple range test for **(A,B,C)**].

TABLE 2 | Effects of liposome-encapsulated dsRNA on the growth of *S. frugiperda* larvae.

NPs-dsRNA	Mortality rate (%)	Weight increase (mg)
W + dsV-ATPase	16.67 ± 5.773503b	22.55 ± 6.50a
LIP + dsV-ATPase	41.67 ± 10.40833a	13.80 ± 5.63b
CHS + dsV-ATPase	18.34 ± 7.637626b	17.51 ± 4.54ab

Note: V-ATPase*, an important gene for the growth and development of* S. frugiperda *(Parsons et al., 2018). dsV-ATPase is combined with two nanomaterials, liposome-encapsulated dsRNA (LIP-dsV-ATPase) and chitosan-encapsulated dsRNA (CHS + dsV-ATPase), using water instead of nanomaterials as a control (W+ dsV-ATPase). Apply the same amount of NPs-dsRNA to the artificial feed every day and feed the first instar larvae continuously for 1 week. Count the final mortality and weight gain. Five larvae were a biological replicate, and this experiment was performed three times in total. The data shown are mean ± SE,* n = *15 for the mortality and weight increase calculation, different letters indicate a significant difference among treatments* (p < *0.05, one-way ANOVA followed by Duncan's multiple range test).*

(Song et al., 2017; Spit et al., 2017). The dsRNases were well documented to play crucial roles in degrading dsRNA, study of *dsRNase* gene family would improve the understanding of RNAi mechanism and make contributions to better usage of RNAi.

To identify potential roles of dsRNases in reduced RNAi efficiency, a genome-scale search was carried in the presented study, and four homolog *dsRNase* genes were identified from *S. frugiperda* genome, named as *SfdsRNase1–4* based on their homology to *S. litura* (Peng et al., 2020). The endounuclease_NS domain was predicted from each protein (**Table 1**; **Supplementary Figure S2**), indicating they belong to DNA/RNA non-specific endonuclease family. In addition, those genes were clustered with other lepidopteran insect *dsRNases* from phylogenetic tree analysis, which also supported they are indeed *dsRNase* homolog (**Figure 2**). However, the number of dsRNases from each lepidopteran and hemipteran (insensitive to RNAi) varies from three to six, while most Coleopteran insects shared one to four homologs (**Figure 2**; **Supplementary Table S1**). Lepidopteran insects have evolved multiple copies of *dsRNase* homologs than other insects, therefore those expansions of *dsRNase* genes would be part of an explanation of low RNAi efficiency in lepidopteran and hemipteran insects. A detailed functional analysis of a specific gene is needed to be revealed. Furthermore, those functional hypotheses were supported by the expression profile (**Figures 3**, **4**). General, most dsRNases were highly expressed in midgut and elder larvae, indicating an increased

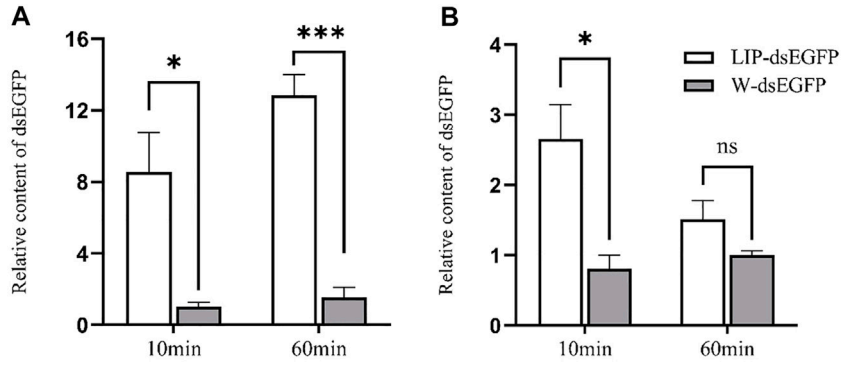

FIGURE 5 | *In vitro* degradation of Lip-dsRNA in midgut juice and hemolymph. The relative content of dsRNA was negatively correlated with the ability to degrade dsRNA. Degradation of liposome-encapsulated dsRNA in midgut juice **(A)**. Degradation of liposome-encapsulated dsRNA in hemolymph **(B)**. Liposome-encapsulated dsRNA (LIP-dsEGFP), dsRNA not encapsulated with liposomes, replaced liposomes with the same amount of water as a control (W-dsEGFP). The two forms of dsRNA were incubated with midgut juice and hemolymph for 10 and 60 min at room temperature, respectively. The dsRNA content after incubation was detected by qPCR, and the relative content ratio was calculated. The data shown are mean ± SE, $n = 12$ for the dsRNA relative content ratio calculation (One-way ANOVA, the least significant difference (LSD) test, ns = No significant difference, $^{*}p < 0.05$, $^{***}p < 0.001$).

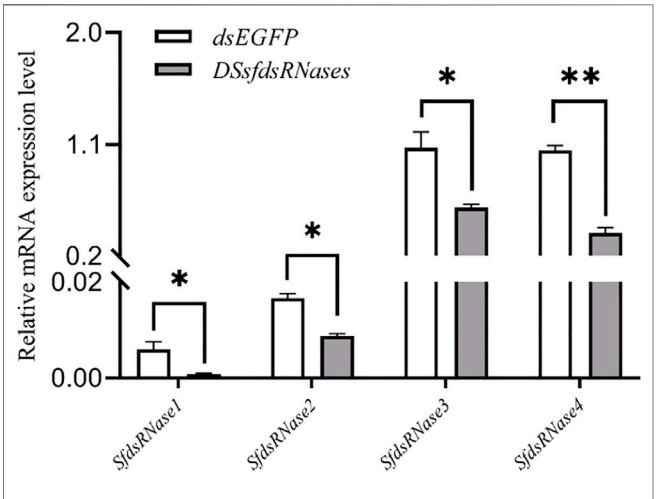

FIGURE 6 | Lip-dsRNA down-regulates the expression of *sfdsRNase*. DssfdsRNase represents the injection of 4 dsRNA of sfdsRNases into the fourth instar larvae, and the control injection of the same amount of dsEGFP. After 24 h, the expression level of sfdsRNase is measured by RT-qPCR. The data shown are mean ± SE, $n = 12$ for the Relative mRNA expression measurement of *sfdsRNases* (One-way ANOVA, the least significant difference (LSD) test, $^{*}p < 0.05$, $^{**}p < 0.01$) .

activity, and similar results were found in *S. exigua* and *S. litura*. They found a positive correlation between lower *dsRNase* activity and lower expression levels in young larvae (Vatanparast and Kim, 2017; Peng et al., 2020).

It is well known that naked dsRNA is vulnerable to degrade in fluid, whereas encapsulating dsRNA would protect it from degradation. To increase the RNAi effect and achieve the RNAi phenotype, three nanomaterials were used *in vivo*, as previously reported (Wang et al., 2020). To date, most related works were conducted in sf9 cells, and satisfying results were obtained in *S. frugiperda* (Gurusamy et al., 2020a; Gurusamy et al., 2020b). In the presence of our data, we found liposome significantly increased RNAi effect with successful target gene from previous work (Lin et al., 2017; Gurusamy et al., 2020b). Similar results were observed from the sf9 cell line and tephritid fruit flies, strong RNAi phenotypes were achieved by complexing dsRNA with liposomes (Tayler et al., 2019; Gurusamy et al., 2020b). In lepidopteran insects, the rapid degradation of dsRNA in the midgut and hemolymph is an important factor that limits the efficiency of RNAi. Therefore, to verify whether LIP-dsRNA can enhance the stability of dsRNA in the midgut and hemolymph, thereby improving the efficiency of RNAi. We detected dsRNA content from different time points after incubation with insect midgut and hemolymph and found those dsRNAs were more persistent than the naked ones (**Figure 5**). Together with the results from *in vivo* and *ex vivo* cell experiments, we speculated the liposome was mainly involved in protecting dsRNA from degradation by endonucleases and improved delivery of intact dsRNA into cells. Studies had also confirmed that oral administration of liposome-encapsulated dsRNA (*α-tubulin*) to German cockroaches *Blattella germanica* can reduce the degradation of dsRNA in the midgut and increase mortality (Lin et al., 2017). Furthermore, we used this method to conduct RNAi experiment targeted with different *SfdsRNase*, a desirable effect was observed (**Figure 7**). Therefore, the presence of our work provided successful examples for further RNAi experiments in *S. frugiperda*. While the CQD showed the lethal effect on *S. frugiperda* larvae, this result is quite different from works in striped stem borer (*Chilo suppressalis*) (Wang et al., 2020). However, we used the same dosage of CQD as reported in Wang's work, and we did not decrease the concentration of CQD and tested the lethal effect. Therefore, we deem this situation as the variation of sensitiveness to CQD among different insects.

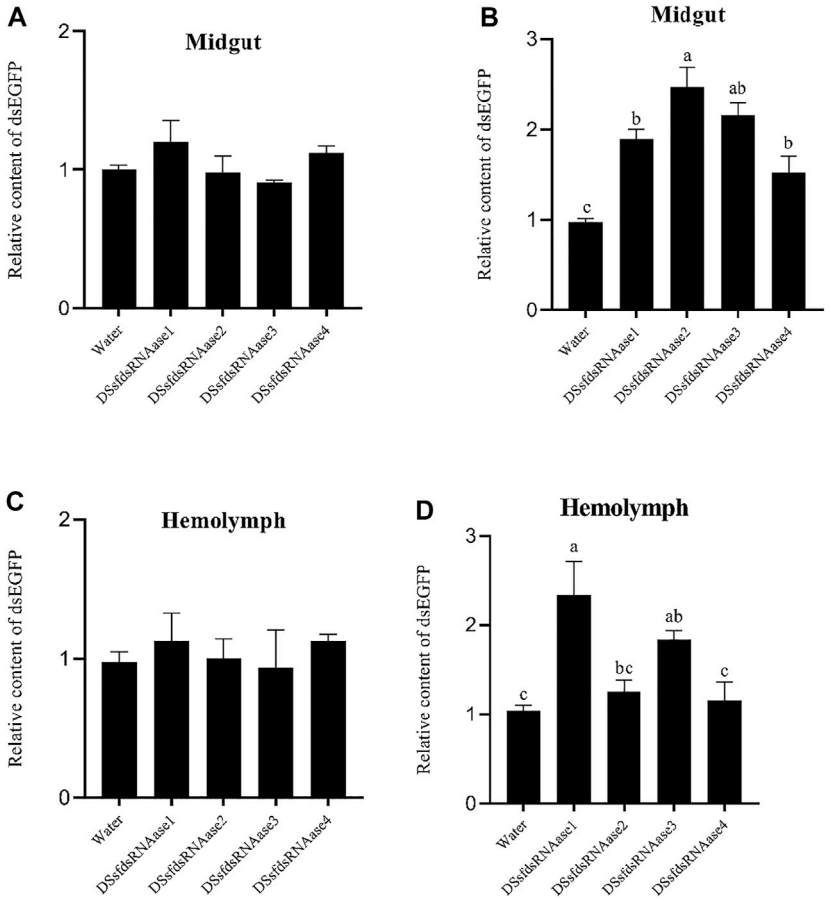

FIGURE 7 | *In vitro* incubation of dsRNA and midgut juice and hemolymph. Relative content of dsEGFP in the control group = 1. The relative content of dsRNA was negatively correlated with the ability to degrade dsRNA. *In vitro* incubation of dsRNA and midgut fluid, dsRNases are the midgut extract of *S. frugiperda* larvae after successfully interfering with 4 *sfdsRNase* genes. At the same time, to avoid the influence of dsEGFP injection on the detection of dsEGFP content after incubation, the larval midgut fluid injected with water was used as a control. The midgut extract was incubated with dsEGFP for 10 and 60 min at room temperature, and the midgut juice was replaced by water as a control. The dsRNA content after incubation was detected by qPCR, and the relative content ratio was calculated [**(A)** represented relative content of dsEGFP after 10 min in midgut, **(B)** represented relative content of dsEGFP after 60 min in midgut, **(C)** represented relative content of dsEGFP after 10 min in hemolymph, **(D)** represented relative content of dsEGFP after 60 min in hemolymph**]**. The data shown are mean ± SE, $n = 12$ for the dsRNA relative content ratio calculation, different letters indicate a significant difference among treatments [$p < 0.05$, one-way ANOVA followed by Duncan's multiple range test for **(A,B)**].

The role of dsRNase has been demonstrated by several insects and is mainly involved in the degradation of dsRNA in the midgut and hemolymph (Wang et al., 2016; Song et al., 2017; Prentice et al., 2019; Song et al., 2019). Therefore, the variation of insect RNAi efficiency may be the consequence of fast degrading exogenous dsRNA by endogenous dsRNases. The RNAi effect could be induced by considerable dose of dsRNA and most RNAi response is dependent on the concentration of dsRNA (Scott et al., 2013; Wang et al., 2015; Killiny and Kishk, 2017; Peng et al., 2020). In addition, most successful insect RNAi cases were reported from injection method than ingestion due to rapid dsRNA degradation before entering gut epithelial cells (Luo et al., 2013; Sapountzis et al., 2014; Joga et al., 2016; Wang et al., 2016). Therefore, impairing endogenous nucleases and protecting dsRNA from dsRNases degradation would be a feasible solution to improve insect RNAi efficiency. Consequently, a clear understanding of specific nuclease which is involved in dsRNA degradation is urgently needed. The *ex vivo* assays (incubation dsRNA with midgut juice or hemolymph) demonstrated depression of any of sfdsRNases increased the dsRNA persistence in midgut fluid (**Figures 7A,B**). In addition, silencing of two dsRNases (*sfdsRNase1* and *sfdsRNase3*) also reduced the ability of dsRNA degrading in hemolymph (**Figures 7C,D**). In *S. litura*, CRISPR-Cas9 mediated knockout of *SldsRNase1* and *SldsRNase2* increased dsRNA stability both in the gut and hemolymph (Peng et al., 2021). In the research of sweetpotato weevil *Cylas puncticollis*, they also found dsRNA degradation in the samples injected with dsCp-dsRNase-3 was significantly reduced (Prentice et al., 2019). Powell et al. (2017) demonstrated a clear relationship

between nuclease activity and RNAi effect *in vivo*. Silencing of digestive secretions expressed nuclease enhancing orally delivered RNAi effect in the small hive beetle *Aethina tumida*, which is insensitive to oral RNAi. Hence we believe our experiment provided a feasible scheme for the functional identification of dsRNase in insects. In the presence of our data, we found *sfdsRNase3* participated in both midgut and hemolymph dsRNA degradation. Therefore, we believe *sfdsRNase3* plays an important role in RNAi degradation of *S. frugiperda* larvae, and further work needs to be done to illustrate the process and mechanism of potential roles of *sfdsRNase3* affecting dsRNA stability *in vivo* and make practical use of the RNAi effect after the depression of *sfdsRNase3*. Successful application of RNAi by oral-delivery dsRNA is challengeable but overcoming these challenges will be greatly paid back in the field of pest control.

In summary, the characterized *dsRNases* genes from *S. frugiperda* were consistent with other reports from other insects, those dsRNases would contribute to dsRNA instability and lead to RNAi recalcitrance as other lepidopteran insects. Furthermore, analysis of dsRNases gene characters and their function from other insects would be helpful to make a solid conclusion whether the existence of multiple dsRNases is a general phenomenon and contribute to low RNAi efficiency in all lepidopteran insects. In addition, we found transfection reagents liposomes greatly protect dsRNA from nuclease degradation in *S. frugiperda*. Therefore, co-delivery of nuclease- and specific-dsRNA by Lip-encapsulated dsRNA is a good strategy for enhancing dsRNA stability in *S. frugiperda*, and hopefully improving RNAi efficiency. Hence RNAi-mediated pest control approach can be utilized in more practical applications. However, most dsRNase shared high similarities, and it is worth knowing whether the off-target effect was existence after suppression of any dsRNases. In addition, whether inhibition of cellular nucleases would affect the core RNAi mechanism is another critical issue that need to be clarified.

DATA AVAILABILITY STATEMENT

The original contributions presented in the study are included in the article/**Supplementary Material**, further inquiries can be directed to the corresponding authors.

AUTHOR CONTRIBUTIONS

J-DW, RW, and Y-MH designed the experiment. YY, D-JL, and X-YC conducted the experiment. C-HH and S-JG performed statistical analysis. J-DW and YY prepared the manuscript. All authors have read and agreed to the published version of the manuscript.

FUNDING

This work was supported by the National Key R & D Program of China (2018YFD201100), Talent Programs of Fujian Agriculture and Forestry University (xjq202119), the Sugar Crop Research System, CARS (CARS-17) and Special Technology Innovation Funding of Fujian Agriculture and Forestry University (KFA17523A).

SUPPLEMENTARY MATERIAL

The Supplementary Material for this article can be found online at: https://www.frontiersin.org/articles/10.3389/fphys.2022.850022/full#supplementary-material

REFERENCES

Arimatsu, Y., Furuno, T., Sugimura, Y., Togoh, M., Ishihara, R., Tokizan, M., et al. (2007). Purification and Properties of Double-Stranded RNA-Degrading Nuclease,dsRNase, from the Digestive Juice of the Silkworm, *Bombyx mori*. *J. Insect Biotechnol. Sericology* 76, 57–62. doi:10.11416/jibs.76.1_57

Arimatsu, Y., Kotani, E., Sugimura, Y., and Furusawa, T. (2007). Molecular Characterization of a cDNA Encoding Extracellular dsRNase and its Expression in the Silkworm, *Bombyx mori*. *Insect Biochem. Mol. Biol.* 37, 176–183. doi:10.1016/j.ibmb.2006.11.004

Ayra-Pardo, C., Davis, P., and Ellar, D. J. (2007). The Mutation R423S in the Bacillus Thuringiensis Hybrid Toxin CryAAC Slightly Increases Toxicity for Mamestra Brassicae L. *J. Invertebr. Pathol.* 95, 41–47. doi:10.1016/j.jip.2006.12.001

Baum, J. A., Bogaert, T., Clinton, W., Heck, G. R., Feldmann, P., Ilagan, O., et al. (2007). Control of Coleopteran Insect Pests through RNA Interference. *Nat. Biotechnol.* 25, 1322–1326. doi:10.1038/nbt1359

Chen, C., Chen, H., Zhang, Y., Thomas, H. R., Frank, M. H., He, Y., et al. (2020). TBtools: An Integrative Toolkit Developed for Interactive Analyses of Big Biological Data. *Mol. Plant* 13, 1194–1202. doi:10.1016/j.molp.2020.06.009

Chi, B.-j., Zhang, D.-m., and Dong, H.-z. (2021). Control of Cotton Pests and Diseases by Intercropping: A Review. *J. Integr. Agric.* 20, 3089–3100. doi:10.1016/S2095-3119(20)63318-4

Christiaens, O., Whyard, S., Vélez, A. M., and Smagghe, G. (2020). Double-Stranded RNA Technology to Control Insect Pests: Current Status and Challenges. *Front. Plant Sci.* 11, 451–460. doi:10.3389/fpls.2020.00451

Das, S., Debnath, N., Cui, Y., Unrine, J., and Palli, S. R. (2015). Chitosan, Carbon Quantum Dot, and Silica Nanoparticle Mediated dsRNA Delivery for Gene Silencing in *Aedes aegypti*: A Comparative Analysis. *ACS Appl. Mater. Inter.* 7, 19530–19535. doi:10.1021/acsami.5b05232

Guan, R., Chen, Q., Li, H., Hu, S., Miao, X., Wang, G., et al. (2019). Knockout of the HaREase Gene Improves the Stability of dsRNA and Increases the Sensitivity of Helicoverpa Armigera to Bacillus Thuringiensis Toxin. *Front. Physiol.* 10, 1368. doi:10.3389/fphys.2019.01368

Guo, M., Nanda, S., Chen, S., Lü, J., Yang, C., Liu, Z., et al. (2021). Oral RNAi Toxicity Assay Suggests Clathrin Heavy Chain as a Promising Molecular Target for Controlling the 28 -spotted Potato Ladybird, Henosepilachna Vigintioctopunctata. *Pest Manag. Sci.* 10, doi:10.1002/ps.6594

Gurusamy, D., Mogilicherla, K., and Palli, S. R. (2020a). Chitosan Nanoparticles Help Double-stranded RNA Escape from Endosomes and Improve RNA Interference in the Fall Armyworm, Spodoptera Frugiperda. *Arch. Insect Biochem. Physiol.* 104, e21677. doi:10.1002/arch.21677

Gurusamy, D., Mogilicherla, K., Shukla, J. N., and Palli, S. R. (2020b). Lipids Help Double-stranded RNA in Endosomal Escape and Improve RNA Interference in the Fall Armyworm, Spodoptera Frugiperda. *Arch. Insect Biochem. Physiol.* 104, e21678. doi:10.1002/arch.21678

Hafeez, M., Ullah, F., Khan, M. M., Li, X., Zhang, Z., Shah, S., et al. (2021). Metabolic-based Insecticide Resistance Mechanism and Ecofriendly Approaches for Controlling of Beet Armyworm Spodoptera Exigua: a Review. *Environ. Sci. Pollut. Res.* 29, 1746–1762. doi:10.1007/s11356-021-16974-w

Huvenne, H., and Smagghe, G. (2010). Mechanisms of dsRNA Uptake in Insects and Potential of RNAi for Pest Control: A Review. *J. Insect Physiol.* 56, 227–235. doi:10.1016/j.jinsphys.2009.10.004

Joga, M. R., Zotti, M. J., Smagghe, G., and Christiaens, O. (2016). RNAi Efficiency, Systemic Properties, and Novel Delivery Methods for Pest Insect Control: What We Know So Far. *Front. Physiol.* 7, 553. doi:10.3389/fphys.2016.00553

Killiny, N., and Kishk, A. (2017). Delivery of dsRNA through Topical Feeding for RNA Interference in the Citrus Sap Piercing-sucking Hemipteran, Diaphorina Citri. *Arch. Insect Biochem. Physiol.* 95 (2). doi:10.1002/arch.21394

Kumar, S., Stecher, G., and Tamura, K. (2016). MEGA7: Molecular Evolutionary Genetics Analysis Version 7.0 for Bigger Datasets. *Mol. Biol. Evol.* 33, 1870–1874. doi:10.1093/molbev/msw054

Kunte, N., Mcgraw, E., Bell, S., Held, D., and Avila, L. A. (2020). Prospects, Challenges and Current Status of RNAi through Insect Feeding. *Pest Manag. Sci.* 76, 26–41. doi:10.1002/ps.5588

Li, Z. Y., Dai, Q. X., Kuang, Z. L., Liang, M. R., Wang, T. J., Lu, Y. Y., et al. (2019). Effects of Three Artificial Diets on Development and Reproduction of the Fall Armyworm Spodoptera Frugiperda. *J. Enviro Entomol.* 41 (06), 1147–1154. doi:10.3969/j.issn.1674-0858

Lin, Y.-H., Huang, J.-H., Liu, Y., Belles, X., and Lee, H.-J. (2017). Oral Delivery of dsRNA Lipoplexes to German Cockroach Protects dsRNA from Degradation and Induces RNAi Response. *Pest Manag. Sci.* 73, 960–966. doi:10.1002/ps.4407

Luo, Y., Wang, X., Wang, X., Yu, D., Chen, B., and Kang, L. (2013). Differential Responses of Migratory Locusts to Systemic RNA Interference via Double-Stranded RNA Injection and Feeding. *Insect Mol. Biol.* 22, 574–583. doi:10.1111/imb.12046

Paredes-Sánchez, F. A., Rivera, G., Bocanegra-García, V., Martínez-Padrón, H. Y., Berrones-Morales, M., Niño-García, N., et al. (2021). Advances in Control Strategies against Spodoptera Frugiperda. A Review. *Molecules* 26, 5587. doi:10.3390/molecules26185587

Parsons, K. H., Mondal, M. H., Mccormick, C. L., and Flynt, A. S. (2018). Guanidinium-Functionalized Interpolyelectrolyte Complexes Enabling RNAi in Resistant Insect Pests. *Biomacromolecules* 19, 1111–1117. doi:10.1021/acs.biomac.7b01717

Peng, Y., Wang, K., Zhu, G., Han, Q., Chen, J., Elzaki, M. E. A., et al. (2020). Identification and Characterization of Multiple dsRNases from a Lepidopteran Insect, the Tobacco Cutworm, Spodoptera Litura (Lepidoptera: Noctuidae). *Pestic. Biochem. Physiol.* 162, 86–95. doi:10.1016/j.pestbp.2019.09.011

Peng, Y., Zhu, G.-H., Wang, K., Chen, J., Liu, X., Wu, M., et al. (2021). Knockout of SldsRNase1 and SldsRNase2 Revealed Their Function in dsRNA Degradation and Contribution to RNAi Efficiency in the Tobacco Cutworm, Spodoptera Litura. *J. Pest Sci.* 94, 1449–1460. doi:10.1007/s10340-021-01335-w

Potter, S. C., Luciani, A., Eddy, S. R., Park, Y., Lopez, R., and Finn, R. D. (2018). HMMER Web Server: 2018 Update. *Nucleic Acids Res.* 46 (W1), W200–W204. doi:10.1093/nar/gky448

Powell, M. E., Bradish, H. M., Gatehouse, J. A., and Fitches, E. C. (2017). Systemic RNAi in the Small Hive beetleAethina tumidaMurray (Coleoptera: Nitidulidae), a Serious Pest of the European Honey beeApis Mellifera. *Pest Manag. Sci.* 73, 53–63. doi:10.1002/ps.4365

Prentice, K., Smagghe, G., Gheysen, G., and Christiaens, O. (2019). Nuclease Activity Decreases the RNAi Response in the Sweetpotato Weevil Cylas Puncticollis. *Insect Biochem. Mol. Biol.* 110, 80–89. doi:10.1016/j.ibmb.2019.04.001

Rodrigues, T. B., Mishra, S. K., Sridharan, K., Barnes, E. R., Alyokhin, A., Tuttle, R., et al. (2021). First Sprayable Double-Stranded RNA-Based Biopesticide Product Targets Proteasome Subunit Beta Type-5 in Colorado Potato Beetle (*Leptinotarsa decemlineata*). *Front. Plant Sci.* 12, 728652. doi:10.3389/fpls.2021.728652

Sapountzis, P., Duport, G., Balmand, S., Gaget, K., Jaubert-Possamai, S., Febvay, G., et al. (2014). New Insight into the RNA Interference Response against Cathepsin-L Gene in the Pea Aphid, *Acyrthosiphon pisum*: Molting or Gut Phenotypes Specifically Induced by Injection or Feeding Treatments. *Insect Biochem. Mol. Biol.* 51, 20–32. doi:10.1016/j.ibmb.2014.05.005

Scott, J. G., Michel, K., Bartholomay, L. C., Siegfried, B. D., Hunter, W. B., Smagghe, G., et al. (2013). Towards the Elements of Successful Insect RNAi. *J. Insect Physiol.* 59, 1212–1221. doi:10.1016/j.jinsphys.2013.08.014

Shukla, J. N., Kalsi, M., Sethi, A., Narva, K. E., Fishilevich, E., Singh, S., et al. (2016). Reduced Stability and Intracellular Transport of dsRNA Contribute to Poor RNAi Response in Lepidopteran Insects. *RNA Biol.* 13, 656–669. doi:10.1080/15476286.2016.1191728

Song, H., Fan, Y., Zhang, J., Cooper, A. M., Silver, K., Li, D., et al. (2019). Contributions of dsRNases to Differential RNAi Efficiencies between the Injection and Oral Delivery of dsRNA in *Locusta migratoria*. *Pest Manag. Sci.* 75, 1707–1717. doi:10.1002/ps.5291

Song, H., Zhang, J., Li, D., Cooper, A. M. W., Silver, K., Li, T., et al. (2017). A Double-Stranded RNA Degrading Enzyme Reduces the Efficiency of Oral RNA Interference in Migratory Locust. *Insect Biochem. Mol. Biol.* 86, 68–80. doi:10.1016/j.ibmb.2017.05.008

Spit, J., Philips, A., Wynant, N., Santos, D., Plaetinck, G., and Vanden Broeck, J. (2017). Knockdown of Nuclease Activity in the Gut Enhances RNAi Efficiency in the Colorado Potato Beetle, *Leptinotarsa decemlineata* , but Not in the Desert Locust, *Schistocerca gregaria*. *Insect Biochem. Mol. Biol.* 81, 103–116. doi:10.1016/j.ibmb.2017.01.004

Tayler, A., Heschuk, D., Giesbrecht, D., Park, J. Y., and Whyard, S. (2019). Efficiency of RNA Interference Is Improved by Knockdown of dsRNA Nucleases in Tephritid Fruit Flies. *Open Biol.* 9 (12), 190198. doi:10.1098/rsob.190198

Terenius, O., Papanicolaou, A., Garbutt, J. S., Eleftherianos, I., Huvenne, H., Kanginakudru, S., et al. (2011). RNA Interference in Lepidoptera: An Overview of Successful and Unsuccessful Studies and Implications for Experimental Design. *J. Insect Physiol.* 57, 231–245. doi:10.1016/j.jinsphys.2010.11.006

Vatanparast, M., and Kim, Y. (2017). Optimization of Recombinant Bacteria Expressing dsRNA to Enhance Insecticidal Activity against a Lepidopteran Insect, Spodoptera Exigua. *Plos One* 12 (8), e0183054. doi:10.1371/journal.pone.0183054

Wang, J., Gu, L., Ireland, S., Garczynski, S. F., and Knipple, D. C. (2015). Phenotypic Screen for RNAi Effects in the Codling Moth Cydia Pomonella. *Gene* 572, 184–190. doi:10.1016/j.gene.2015.07.006

Wang, J., Wu, M., Wang, B., and Han, Z. (2013). Comparison of the RNA Interference Effects Triggered by dsRNA and siRNA inTriboliumcastaneum. *Pest Manag. Sci.* 69, 781–786. doi:10.1002/ps.3432

Wang, K., Peng, Y., Chen, J., Peng, Y., Wang, X., Shen, Z., et al. (2020). Comparison of Efficacy of RNAi Mediated by Various Nanoparticles in the rice Striped Stem Borer (Chilo Suppressalis). *Pestic. Biochem. Physiol.* 165, 104467. doi:10.1016/j.pestbp.2019.10.005

Wang, K., Peng, Y., Pu, J., Fu, W., Wang, J., and Han, Z. (2016). Variation in RNAi Efficacy Among Insect Species Is Attributable to dsRNA Degradation *In Vivo*. *Insect Biochem. Mol. Biol.* 77, 1–9. doi:10.1016/j.ibmb.2016.07.007

Yang, J., and Han, Z.-j. (2014). Efficiency of Different Methods for dsRNA Delivery in Cotton Bollworm (Helicoverpa Armigera). *J. Integr. Agric.* 13, 115–123. doi:10.1016/S2095-3119(13)60511-0

Zhu, K. Y., and Palli, S. R. (2020). Mechanisms, Applications, and Challenges of Insect RNA Interference. *Annu. Rev. Entomol.* 65, 293–311. doi:10.1146/annurev-ento-011019-025224

Conflict of Interest: The authors declare that the research was conducted in the absence of any commercial or financial relationships that could be construed as a potential conflict of interest.

Publisher's Note: All claims expressed in this article are solely those of the authors and do not necessarily represent those of their affiliated organizations, or those of the publisher, the editors and the reviewers. Any product that may be evaluated in this article, or claim that may be made by its manufacturer, is not guaranteed or endorsed by the publisher.

frontiers | Frontiers in Physiology

ORIGINAL RESEARCH
published: 09 May 2022
doi: 10.3389/fphys.2022.884447

Down-Regulation of P450 Genes Enhances Susceptibility to Indoxacarb and Alters Physiology and Development of Fall Armyworm, *Spodoptera frugipreda* (Lepidoptera: Noctuidae)

Muhammad Hafeez[1,2], *Xiaowei Li*[1], *Farman Ullah*[3], *Zhijun Zhang*[1], *Jinming Zhang*[1], *Jun Huang*[1], *G. Mandela Fernández-Grandon*[4], *Muhammad Musa Khan*[5], *Junaid Ali Siddiqui*[6], *Limin Chen*[1,7], *Xiao Yun Ren*[1], *Shuxing Zhou*[1], *Yonggen Lou*[2]* and *Yaobin Lu*[1]*

[1]State Key Laboratory for Managing Biotic and Chemical Threats to the Quality and Safety of Agro-products, Institute of Plant Protection and Microbiology, Zhejiang Academy of Agricultural Sciences, Hangzhou, China, [2]State Key Laboratory of Rice Biology and Ministry of Agriculture Key Lab of Molecular Biology of Crop Pathogens and Insects, Institute of Insect Sciences, Zhejiang University, Hangzhou, China, [3]Department of Plant Biosecurity, College of Plant Protection, China Agricultural University, Beijing, China, [4]Natural Resources Institute, University of Greenwich, Greenwich, United Kingdom, [5]Key Laboratory of Bio-Pesticide Innovation and Application, South China Agricultural University, Guangzhou, China, [6]Red Imported Fire Ant Research Centre, South China Agricultural University, Guangzhou, China, [7]Integrated Plant Protection Center, Lishui Academy of Agricultural and Forestry Sciences, Lishui, China

OPEN ACCESS

Edited by:
Qingjun Wu,
Insititute of Vegetables and Flowers (CAAS), China

Reviewed by:
Hu Wan,
Huazhong Agricultural University, China
Shaoli Wang,
Insititute of Vegetables and Flowers (CAAS), China

***Correspondence:**
Yonggen Lou
yglou@zju.edu.cn
Yaobin Lu
luybcn@163.com

Specialty section:
This article was submitted to Invertebrate Physiology, a section of the journal Frontiers in Physiology

Received: 26 February 2022
Accepted: 11 April 2022
Published: 09 May 2022

Citation:
Hafeez M, Li X, Ullah F, Zhang Z, Zhang J, Huang J, Fernández-Grandon GM, Khan MM, Siddiqui JA, Chen L, Ren XY, Zhou S, Lou Y and Lu Y (2022) Down-Regulation of P450 Genes Enhances Susceptibility to Indoxacarb and Alters Physiology and Development of Fall Armyworm, Spodoptera frugipreda (Lepidoptera: Noctuidae). Front. Physiol. 13:884447. doi: 10.3389/fphys.2022.884447

The fall armyworm (FAW), *Spodoptera frugiperda* (J.E. Smith), is a pest of many important crops globally. Effective control is challenging, with the pest exhibiting resistance to different synthetic pesticides across various groups. However, the mechanisms employed by resistant insects for overexpression of relevant detoxification genes remain unclear. The activity of detoxification enzymes was investigated in this study. Additionally, using RNA interference (RNAi), a functional analysis was completed of two P450s genes in an indoxacarb resistant population of fall armyworms. Elevated resistance levels (resistance ratio = 31.37-fold) in indoxacarb-selected populations of FAW were observed after 14 generations. The qRT-PCR showed higher expression of two cytochrome P450 genes, *CYP321A7* and *CYP6AE43*, in this selected population compared to the control population. RNAi was applied to knock down the P450 ds*CYP321A7* and ds*CYP6AE43* genes in the FAW larvae. Droplet feeding of the dsRNAs (*CYP321A7* and *CYP6AE43*) via an artificial diet significantly increased mortality rates in the indoxacarb treated population. A shorter larval developmental time of FAW was detected in all dsRNAs-fed larvae. Correspondingly, larval mass was reduced by dsRNAs in indoxacarb resistant populations of fall armyworm. Larval feeding assays demonstrate that dsRNAs targeting, specifically of *CYP321A7* and *CYP6AE43* enzymes, could be a beneficial technique in the management of indoxacarb resistant populations. Further study on the potential use of dsRNA and its application should be

conducted in efforts to counter the development of resistance in FAW against various insecticides in the field.

Keywords: Fall armyworm, Detoxification enzymes, P450 genes, indoxacarb resistance, RNAi

INTRODUCTION

The fall armyworm (FAW), *Spodoptera frugiperda* (J.E. Smith), is an invasive polyphagous insect pest, causing serious damage to major crops such as corn, rice, sorghum, and peanut (Goergen et al., 2016; Montezano et al., 2018). This pest, which originated in the Americas, has spread rapidly around the world, causing significant crop losses in each new location where it has been discovered (Goergen et al., 2016). FAW has spread in West and Central Africa in recent years, and it has recently been discovered in Indonesia and Southwest China (Southwest Yunnan province) (Goergen et al., 2016; Ginting et al., 2020; Li et al., 2020). FAW has the potential to cause 8.3 to 20.6 million tons of corn losses across Africa each year, according to the International Centre for Agricultural and Biological Sciences (Day et al., 2017).

Traditionally, various synthetic insecticides have been used to control insect pests in major crops (Desneux et al., 2007; Burtet et al., 2017; Hafeez et al., 2019b; Gul et al., 2021). Currently, the application of synthetic insecticides remains the primary approach to control FAW in China. However, the long-term use in large quantities of chemical insecticides could easily lead to resistance strains developing as well as create serious problems for human health, destruction of non-target organisms, hormesis and further environmental pollution (Desneux et al., 2006; Davis 1993; Aktar et al., 2009; Nawaz et al., 2018; Hafeez et al., 2019c; Ullah et al., 2019; Iftikhar et al., 2020). These issues are exacerbated once pests have developed resistance to large groups of insecticides, which directly reduces their efficacy (Mallet 1989; Zhang et al., 2020; Ullah et al., 2021). In the field, insecticides such as indoxacarb, chlorantraniliprole, emamectin benzoate, and *Bacillus thuringiensis* are mainly used to control lepidopteran pests (Cordova et al., 2006; Xiao et al., 2016; Wang et al., 2019; Hafez et al., 2020; Zhang et al., 2021). The genetic malleability and the exhaustive selection pressure of insecticide applications has led insect pests such as *Plutella xylostella*, *Mythimna separate, Choristoneura rosaceana* and *S. frugiperda* to develop effective resistance to chlorantraniliprole, emamectin benzoate, indoxacarb and *Bacillus thuringiensis* (Wang et al., 2013, 2019; Monnerat et al., 2015; Liu et al., 2016; Hafez et al., 2020). Indoxacarb is an oxadiazine insecticide discovered in 1992 by the E.I. DuPont Co. and commercialized to the open market in 2000 (McCann et al., 2001; Thompson and Dutton, 2003). Indoxacarb is highly active when ingested, but there have been few reports of contact activity when applied topically (Alves et al., 2008; Nehare et al., 2010). This is the premise for indoxacarb's exceptional activity against several lepidopteran species, regardless of the fact that some field populations of major insect pests, including FAW, have evolved a high level of resistance to indoxacarb (Wing et al., 2000; Ahmad et al., 2008; Hafeez et al., 2020; Zhang et al., 2021). To develop effective FAW management practices, we must first understand the mechanisms underlying their resistance to these insecticides.

Insect resistance to synthetic insecticides is an ongoing challenge to sustainable pest management while also providing a suitable model system to study adaptive evolution. One of the molecular alterations frequently implicated in resistant insect populations is the increased production of metabolic enzymes that detoxify or sequester insecticides before they reach the target site (Feyereisen, 2012; Yang et al., 2020). High metabolic activity of detoxifying enzymes such as cytochrome P450 monooxygenase, esterases (Ests), and glutathione *S*-transferase (GSTs) has been identified as among the key mechanisms that underlie insecticide resistance (Li et al., 2007; Li and Liu, 2017). A key enzyme system in this regard is insect cytochrome P450s, which play a central role in the metabolism of a wide range of natural and synthetic xenobiotics, including insecticides, and have been classified into four major clades: CYP2, CYP3, CYP4, and the mitochondrial CYP (Scott, 1999a; Feyereisen, 2012). Among them, the clade *CYP3* is further subdivided into different CYP families and subfamilies. The subfamilies *CYP321* and *CYP6* of clade *CYP3* are known to play a significant role in the metabolism of xenobiotics and, accordingly, insecticide resistance (Feyereisen, 2006a; Li et al., 2007). Induction of P450 genes is commonly seen in insects and may be initiated by a variety of compounds found in their environment. For example, research has shown that increased metabolic enzyme activity caused by increased mRNA expression levels of detoxification genes facilitates insecticide resistance in insects (Vontas et al., 2000; Arain et al., 2018; Hafeez et al., 2019c). In Lepidoptera, numerous key P450 genes such as *CYP6AB14* and *CYP9A98* in *Spodoptera exigua*, *CYP9A14*, *CYP337B1*, *CYP9A12*, *CYP6AE11* and *CYP6B7* in *Helicoverpa armigera*, and *CYP321A8*, *CYP321A9*, and *CYP321B1* in *Spodoptera frugiperda* were frequently identified as being associated with various insecticide resistance mechanisms (Hafeez et al., 2019d; Wee et al., 2008; Zhao et al., 2014; Bai-Zhong et al., 2020; Tang et al., 2020). As a result, it is critical to investigate the induction effect of this insecticide on FAW to assess its potential for use in pest control.

RNAi, which uses gene silencing based on the conserved biological defense response at the cellular level triggered by double-stranded RNA (dsRNA), is a promising technology in agriculture. This method could pave the way for the next generation of insect-resistant GM crops (Mello and Conte, 2004; Zhang et al., 2017; Chen et al., 2019; Bennett et al., 2020). The roles of multiple P450 genes of various insects in insecticide resistance and phytochemical detoxification have been functionally confirmed by the induction experiments. These demonstrate the increased larval sensitivity to toxins after RNAi-mediated silencing of specific P450 genes (Sun et al., 2019; Lu et al., 2020; Wang et al., 2022). When dsRNA is

ingested via an artificial diet or through droplet feeding, it can knock down genes through the RNAi pathway, resulting in a reduction in the target pest's growth and mortality (Ehrlich and Raven 1964; Ahmad et al., 2008; Lim et al., 2016; Zhang et al., 2017; Hafeez et al., 2019e; Ullah et al., 2020a).

The primary goal of this study was to identify the expression and function of P450 genes in an FAW population that has developed significant levels of resistance to indoxacarb in the laboratory. Two up regulated P450 genes (*CYP321A7* and *CYP6AE43*) related to resistance were selected to study the expression and function in an indoxacarb resistant population of FAW. These findings provide a better understanding of the molecular functions of P450 genes and insecticide resistance mechanisms, findings that may facilitate future pest management strategies for FAW.

MATERIALS AND METHODS

Insect Collection and Rearing

In August 2019, 200 fall armyworm larvae of various instars were collected from two different cornfields in Ping Hu, Zhejiang province, to establish a laboratory population. Larvae were raised on a semi-solid artificial diet based on pinto bean powder, as previously described (Zhao et al., 2020). They were kept at 25 ± 2°C on a 14:10 h light: dark photoperiod in a climate control chamber. Following pupation, newly hatched adults were segregated into mating pairs and fed a 10% sugar solution as an additional food source. Two generations were reared before conducting selection bioassays. The population was divided into two subpopulations: those exposed to no insecticide treatment denoted as Indox-UNSEL and those exposed to indoxacarb denoted as Indox-SEL. After 14 generations of selection with indoxacarb, the Indox-SEL population were identified as a resistant strain.

Chemicals

Indoxacarb 15% (commercial formulation) was purchased from Mesa Tech International Inc (China). 7-ethoxycoumarin and 7-hydroxycoumarin were bought from Sigma-Aldrich (St. Louis, MO, United States). The synergist, piperonyl butoxide (PBO) was obtained from Shanghai Aladdin Bio-chem Technology Co., Ltd (China). Bovine serum albumin was purchased from Beyotime Biotechnology (Jiangsu, China).

Toxicity Bioassays

The toxicity bioassay at generation one (G1) on two-day-old second-instar larvae was conducted using the previously described diet incorporation method (Hafeez et al., 2019a). In brief, six concentrations of insecticide were diluted from the stock (via serial dilutions) with distilled water including a control (without insecticide). In each concentration, there were four replicates and the semisynthetic diet was thoroughly mixed using a well-established method (Gupta et al., 2005). The required concentrations were mixed gently before the agar solidified (40–45°C), then placed into new sterile transparent plastic cups to prevent cross-contamination (3 cm diameter, 3.5 cm height). The artificial diet without insecticide was established as a control treatment. Ten two-day-old second-instar larvae were placed in each transparent plastic cup containing an insecticide-supplemented diet. Four replicates were completed for each, providing a total of 40 larvae per concentration. Similarly, the control treatment was performed with larvae exposed to the artificial diet without insecticide. Control mortality was less than 10%. The bioassays were kept in a climate control chamber at 25 ± 2°C (14:10 h) light: dark photoperiod with 60 ± 5% RH. Mortality was evaluated 72 h after exposure to indoxacarb. Larvae that did not move after being touched with a fine paintbrush were deemed dead.

Resistance Selection of FAW to Indoxacarb

The selection with indoxacarb from generations 1–14 of *S. frugiperda* was done by a diet incorporation method as previously described to create the Indox-SEL population. From generation 1 to generation 14, two-day-old second-instar larvae were exposed to various concentrations (4–110 μg g^{-1}) throughout their rearing. The field-collected population of FAW developed high levels of resistance to indoxacarb after 14 generations of continuous selection. The LC_{50} value was calculated 72 h after treatment to indoxacarb and the surviving larvae of every selection were raised on an artificial diet to obtain the next generation. Two-day-old second-instar larvae selected per generation ranged from 200 to 300 individuals. The laboratory reared population without exposure to any insecticide, Indox-UNSEL, was used as a reference strain for resistance monitoring.

Synergism Bioassay

To evaluate the metabolic resistance to indoxacarb, the larvae were exposed to known pesticide synergists, piperonyl butoxide (PBO), triphenyl phosphate (TPP) and diethyl maleate (DEM) then subjected to the test insecticide. Synergistic mechanisms associated with PBO, TPP and DEM were evaluated using a previously described method (Zhao et al., 2020). Solutions of PBO, TPP and DEM at the concentration of 50 mg/L, 50 mg/L and 100 mg/L were prepared in 1% (v/v) acetone. For both Indox-SEL and Indox-UNSEL groups, acetone solutions (1 μL) of PBO TPP and DEM were applied to the pronotum of individual third instar larvae using a hand applicator. Larvae were left for 2 h before indoxacarb treatment. There was no mortality in FAW after exposure to any of these synergists. The FAW larvae were then moved into the transparent plastic cup containing an indoxacarb-treated diet of different concentrations for 72 h. There were two control groups: one exposed and then fed an artificial diet containing 1% (v/v) acetone, and the other exposed and then fed an artificial diet only. All population were maintained in a controlled environment matching their rearing conditions.

Measurement of Enzyme Activity

Sample Preparation

The detoxification enzyme activity of P450 and esterase in the midgut homogenates of the Indox-SEL and Indox-UNSEL

populations was measured. For the Indox-SEL population, late third-instar larvae of a similar size were selected and transferred into transparent plastic cups containing diets supplemented with an LC_{20} dose of indoxacarb. The Indox-UNSEL population was fed on control diet without insecticide for 48, 72, and 96 h. The midguts from treated (Indox-SEL population) and untreated (Indox-UNSEL population) groups were dissected and gently shaken to release their contents before being washed in a cold aqueous solution. The crude homogenates of FAW midguts from treated and untreated groups were prepared according to Liu et al. (2006). It was done in biological triplicate for every treatment that was given.

P450 Enzyme Activity Measurement

Evaluation P450 enzyme activity followed the methodology from Chen et al. (2018), with slight modification. A total of 100 μL of 2 mM p-nitroanisole solution was put into each well of a clear 96-well plate containing 90 μL of crude enzyme, and the microplate was incubated for 3 min at 27°C before adding 10 μL of 9.6 mM NADPH to initiate the reaction. The absorbance was measured using a microplate reader. The activity was recorded as nmol p-nitroanisole/min/mg protein.

Protein concentration was determined using the Bradford method (Bradford, 1976).

Measurement of the Activity of Esterase

The activity of the esterase (EST) enzyme was determined using established methodologies (van Asperen, 1962; Wu et al., 2011). A total of 200 μL of substrate solution (0.1 ml 100 mM a-NA, 10 mg 10 mg Fast Blue RR salt, and 5 ml 0.2 M pH 6.0 phosphate buffer) and 10 μL enzyme solution were gently mixed and added to each well. Enzyme activity was measured using an xMark Microplate Spectrophotometer (BIO-RAD) and recorded every 15 s. The activity of the enzyme was denoted as nmol a-naphthol/min/mg protein.

Extraction of RNA and Preparation of cDNA

Trizol reagent (Takara, Japan) was used to extract total RNAs from different tissues of larvae and adults (male and female) of Indox-UNSEL and Indox-SEL populations after 72 h following the manufacturer's protocol. First-strand complementary DNA (cDNA) was synthesized by using TransScript® One-Step gDNA Removal and cDNA Synthesis SuperMix in 20 μL reactions containing 1 μg of total RNA (500 ng), 1 μL Anchord Oligo (dT)18 Prime (0.5 μg/uL), 10 μL 2xTS Reaction mixture, TransScript® RT/RI EnzymeMix and gDNA Remover at 42°C for 30 min and preserved until use.

Expression Analysis of P450 Genes in Indox-UNSEL and Indox-SEL Populations

qRT-PCR was performed using a CFX Connect TM Real-Time System (Bio-Rad, United States) to check the expression patterns of selected P450 genes. The RT-qPCR reaction mixtures contained 10 μL SsoFast EvoGreen® qPCR SuperMix, 0.5 μL forward and reverse primers (10 μM each), 1 μL of cDNA template, and nuclease free water to a total volume of 20 μL. The thermo cycling protocol used was 94°C for 3 min, followed by 40 cycles of 94°C for 15 s, 57–60°C for 30 s and 70°C for 30 s. The gene sequences were downloaded from NCBI and primers were designed using Primer Premier 5 software (Premier Biosoft, United States) (**Supplementary Table S1**). The mean expression of the two reference genes, GAPDH (KC262638.1) and ribosomal protein S30 (AF400225.1) were used for data normalization according to (Bustin et al., 2009) (**Supplementary Table S1**). The $2^{-\Delta\Delta Ct}$ method described by Livak & Schmittgen (2001) was used to estimate mRNA expression levels. Three biological and three technical replicates were used in the qRT-PCR analysis.

Bioinformatic and Phylogenetic Analysis of Selected P450 Genes

The protein sequences of all selected P450 genes from *CYP3*, *CYP2*, *CYP4* and Mito-clade were aligned using DNAMAN software. MEGA 7 software was used to construct a neighbour-joining tree with the Minimum-Evolution method (1000 bootstrap replications). The protein sequence was queried against the pdb database to find a template in NCBI blast. Then against both queries, 5cd1 was found to be highly homozygous with more than 30 percent sequence similarity. The modelling was performed using modeller 9.1.

dsRNA Preparation and Feeding Bioassays

For dsRNA synthesis, The ORF and the conserved domains of *CYP321A7* and *CYP6AE43* sequences were found using NCBI. Primer Premier 5 software (Premier Biosoft, United States) was used to design primers with respective fragment sizes of 506 bp and 679 bp and were amplified by PCR. In addition, pGEM T-easy plasmid carrying the *dsRED* gene with fragment sizes of 421 bp was used as the template for PCR of the products to synthesize dsRNA (Jan et al., 2017). The primers for the targets (*CYP321A7* and *CYP6AE43*) and *dsRED* as a control gene amplification were designed using the T7 polymerase promoter sequence at the 5 ends of each strand (**Table 1**). To prepare dsRNA, we used the purified PCR-generated templates from *T7-CYP331A7*, *T7-CYP6AE43*, and T7-RED using the T7 RiboMAX Express RNAi System (Promega, Madison, WI, United States). MEGA clearTM Kit (Ambion) was used for the purification of dsRNA. The dsRNA was resuspended in diethyl pyrocarbonate (DEPC)-treated water to a final concentration of (500 ng/μL) and stored at 80°C for further use. In line with previous work, droplet-feeding was used for dsRNA feeding bioassays (Wang et al., 2018a; Hafeez et al., 2019c). The DEPC-treated water was used to prepare the dsRNA solution (500 ng/μL). The larvae were given 0.5 μL of dsRNA solution in droplets. A preliminary trial was performed to establish the effect of dsRNAs on mortality and development of FAW larvae. The artificial diet (1 g) was poured into each well of the sterilized 24-orifice tissue culture

TABLE 1 | Primers used in this study for RNAi.

Primers Used for RNAi	Sense Primers	Anti-sense Primers	–
dsCYP6AE43	5′-ggatcctaatacgactcactatagg GATATGCTGAACGCCGACCT-3′	5′-ggatcctaatacgactcactatagg CTATCACCGGGTACATCCGC-3	679
dsCYP321A7	5′-ggatcctaatacgactcactatagg GCTACTGGAAAAAGCGTGGC-3′	5′-ggatcctaatacgactcactataggTGAGTTCGTTCCAATGCCGA-3′	506
dsRED	5′-ggatcctaatacgactcactatagg GCAAGCTATGCATCCAACGCGTTG GG-3′	5′-ggatcctaatacgactcactatagg CAAGCTATGCATCCAACGCGTTGG GAG-3′	421
S30	CACCCTCGGTGTTAGACGTT	CCACCGGGAAAGTGATACTGT	119
GAPDH	CGGTGTCTTCACAACCACAG	TTGACACCAACGACGAACAT	111

plate before solidification. A single drop of dsRNA solution 0.5 μL (500 ng/μL) was placed at the center of each well of diet using a 2 μL pipette (www.eppendorf.com) for 24 h followed by the exposure to an artificial diet supplemented with 6.84 μg g^{-1} of indoxacarb after 48, 72 and 96 h. The same method was applied for the dsRED as a control group. The artificial diet + DEPC without exposure to indoxacarb was also used as a control. Each treatment consisted of sixty starved larvae, three replicates of 20 larvae each. The mortality data were recorded at 48, 72 and 96 h. To evaluate the efficacy of RNAi-mediated knockdown of two selected P450 genes, the midguts were dissected from larvae that fed on dsRNAs (*dsCYP332A7* and *dsCYP6AE43*, *dsRED*, and DEPC-water) for 24 h followed by the exposure to an artificial diet supplemented with 6.84 μg g^{-1} of indoxacarb after 48, 72 and 96 h for RNA extraction and RT-qPCR analysis.

The Single and Combined Effects of ds*CYP332A1* and ds*CYP6AE43* on Mortality and Development

To examine the combined effect of the two target genes, 250 ng of each dsRNA was used (ds*CYP332A7* + ds*CYP6AE43*). The droplet-feeding method described above was used to administer dsRNA in all treatments.

The larval mortality, developmental time, and weight were observed after feeding larvae on dsRNAs for 24 h. A total of 60 FAW larvae from each treatment (three replicates each of 20 larvae) were individually transferred into a 24-orifice tissue culture plate containing artificial diet supplemented with indoxacarb LC_{50} as described above. All tests were done in triplicate. All treatment groups recorded mortality at 48, 72, and 96 h, and larval weight at 72 h after feeding on dsRNA of each target gene. The surviving larvae were used to estimate the larval developmental period, larval weight, midgut physiology and pupal duration. Three triplicates were used for each treatment in all experiments. Midguts of larvae were dissected after 72 h of treatment with dsRNAs and control. The physiology of the midgut from each treated and control larva was observed under the microscope (Olympus, SZX2-ILLK, Tokyo, Japan) using a digital camera fed into a computer.

Statistical Analysis

The lethal concentrations from the mortality bioassay data were estimated using Polo-PC software (Robertson and Preisler, 1992; Hafeez et al., 2019a). Data related to all experiments and the relative mRNA expression levels of P450 genes, were analyzed using SPSS 20.0 Software Package (SPSS Inc., Chicago, IL, United States).

RESULTS

Toxicity of Indoxacarb to Indox-UNSEL and Indox-SEL Populations of FAW

The indoxacarb resistance in FAW was obtained by continuous selection of the population for 14 generations under laboratory conditions (**Table 2**). The unselected population (Indox-UNSEL) was found to have a lower LC_{50} (0.67 μg g^{-1}) to indoxacarb than the selected population (Indox-SEL) which, after 14 generations of exposure and selection, had an LC_{50} (21.02 μg g^{-1}) (**Table 2**). This high level of resistance is 31.37-fold compared to the unselected control group.

Synergistic Assessment

An assay was conducted on the effect of indoxacarb synergists PBO, TPP and DEM on the Indox-UNSEL and Indox-SEL population (**Table 3**). The highest synergistic ratio for the Indox-SEL population was found for PBO (2.39), followed by

TABLE 2 | Resistance to indoxacarb in field-collected populations of *S. frugiperda* after 14 generations of selection.

Insecticide	*N*	(μg-G-1) (95% CI)		Slope ±S.E.	X^2	*df*	Sr
		LC_{50}	LC_{20}				
Indox-UNSEL	630	0.67 (0.57 ± 0.79)	0.343 (0.24 ± 0.39)	2.03 ± 0.19	0.43	4	1
Indox-SEL (G-14)	630	21.02 (17.96 ± 24.38)	6.84 (5.04 ± 8.67)	1.88 ± 0.16	1.53	4	31.37

The 95% CI of RR were calculated according to Robertson and Preisler (1992) and considered significant if these did not include the value of 1. N: *Number of individuals exposed was 630 insects and constant across all bioassays; degrees of freedom (df) was 4. CI = Confidence interval. RR = Resistance ratio a RR = LC_{50} value of insecticides of Indox-SEL-G14 divided by LC_{50} value of insecticides of Indox-UNSEL.*

TABLE 3 | Synergism by PBO, TPP and DEM in indoxacarb-treated larvae of *S. frugiperda*.

Insecticide	*N*	LC50 (μg-G-1) (95% CI)	Slope ±S.E.	SR[a]
Indoxacarb + UNSEL	630	0.67 (0.57 ± 0.79)	2.03 ± 0.19	–
Indoxacarb + PBO	315	0.549 (0.47 ± 0.67)	1.90 ± 0.16	–
Indoxacarb + TPP	315	0.58 (0.49 ± 0.68)	1.94 ± 0.17	–
Indoxacarb + DEM	315	0.785 (0.65 ± 0.92)	2.02 ± 0.20	–
Indoxacarb + SEL	630	21.02 (17.96 ± 24.38)	1.88 ± 0.16	–
Indoxacarb + PBO	315	8.81 (7.53 ± 10.16)	1.85 ± 0.15	2.39
Indoxacarb + TPP	315	16.11 (13.57 ± 18.90)	1.75 ± 0.16	1.31
Indoxacarb + DEM	315	20.13 (16.20 ± 23.70)	1.72 ± 0.16	1.04

[a]*SR[a] (synergism ratio) = LC_{50} of a population treated with indoxacarb alone divided by LC_{50} of the same population treated with indoxacarb plus a synergist.*

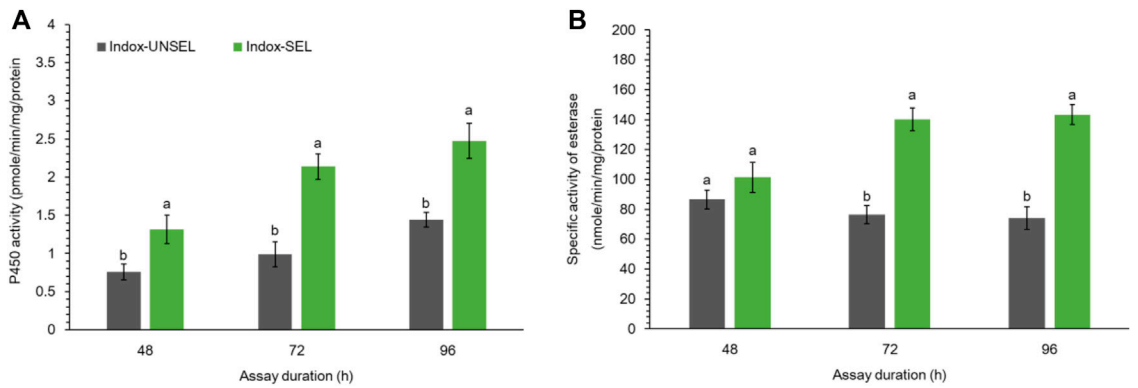

FIGURE 1 | Activity of P450 enzyme **(A)** and specific activity of esterase **(B)** in midguts of the fourth-instar larvae of Indox-UNSEL and Indox-SEL population of FAW after 48, 72 and 96 h exposure to LC_{20} (6.84 μg g^{-1}) concentration of indoxacarb. The data were expressed as the means ± SE. The bars with lowercase letters indicate significant differences within the same treatment time at the $p < 0.05$ level, based on Student's *t* test.

TPP (at 1.31) and DEM (at 1.04). Results suggest that the cytochrome P450 may be involved in the detoxification mechanism of indoxacarb causing resistance in FAW (**Table 3**).

Detoxification Enzymes Activity of P450 and Esterase

Detoxification enzyme activity of P450 using 7-ethoxycoumarin (7-EC) as the substrate was assayed from the midgut of Indox-UNSEL and Indox-SEL populations (**Figure 1A**). The enzyme activity of cytochrome P450 with 7-EC substrate was significantly increased with time after an exposure to an LC_{20} (6.84 μg g^{-1}) dosage of indoxacarb, whereas the highest P450 activity was noted after 96 h, in the midgut of the Indox-SEL larvae (**Figure 1A**). Similarly, higher activity of esterase was observed at 96 h for the Indox-SEL population after exposure to indoxacarb compared to the Indox-UNSEL population (**Figure 1B**).

Expression pattern of P450s genes in the midgut of *S. frugiperda* and phylogenetic analysis

Expression patterns of selected P450s genes from FAW larvae midguts of both Indox-SEL and Indox-UNSEL populations were analyzed by qRT-PCR (**Figure 2**). The 14 selected genes from clade-3 were; *CYP321A9*, *CYP6AN4*, *CYP6AE43*, *CYP337B5*, *CYP9A59*, *CYP321A7*, *CYP6AB12*, *CYP321B1*, *CYP321A10*, *CYP6B50*, *CYP321A8*, *CYP340L1*, *CYP321A9* and *CYP6AN4*. The eight selected genes from clade-4 were; *CYP4L4*, *CYP4C3*, *CYP4G74*, *CYP4G108*, *CYP4CG16*, *CYP321B1*, *CYP366A1*, and *CYP341A11*. The six selected genes from clade-2 were; *CYP306A1*, *CYP307A1*, *CYP18A1*, *CYP305A1*, *CYP301B1* and *CYP15C1*. In addition, 5 genes from the mitochondrial clade were selected; *CYP302A1*, *CYP49A1*, *CYP314A1*, *CYP315A1* and *CYP12B1*. It was shown that some cytochrome P450 genes from the four clades displayed significantly different expression patterns in the Indox-SEL population compared to the Indox-UNSEL population. Significantly higher mRNA transcript levels of two P450 genes, *CYP321A7* and *CYP6AE43*, from clade-3 were detected (11.22 and 9.07) in the midgut of Indox-SEL compared to the UNSEL population (**Figure 2**). Similarly, the highest expression level of *CYP6AE43* and *CYP321A7* was observed in the midguts of the larvae compared to the other tissues (**Figure 3A**). Meanwhile, significantly higher relative expression level of *CYP321A7* genes was detected in wings of adults as compared to other tissues (**Figure 3B**).

MEGA 7 was used to perform phylogenetic analysis with the Minimum-Evolution method based on the amino acid

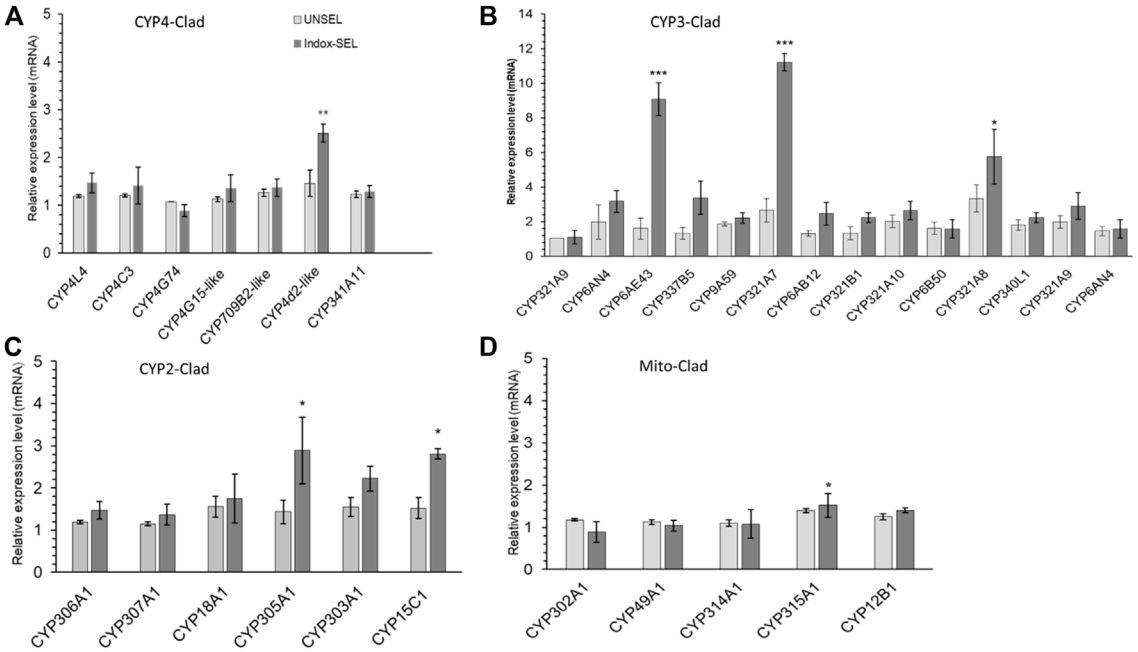

FIGURE 2 | Midgut expression profiles of CYP4-clade **(A)**, CYP3-clade **(B)**, CYP2-clade **(C)** and Mito-clade **(D)** from *S. frugiperda* larvae. Bars represent relative expression (mean ± SE). All biological groups contained three replicates for each treatment, and there were three technical replicates. The transcription levels of all P450s genes determined by quantitative real-time PCR, normalized to two reference genes. The data were expressed as the means ± SE. The bars with astriks indicate significant differences within the same treatment at the $p < 0.05$ level, based on Student's *t* test.

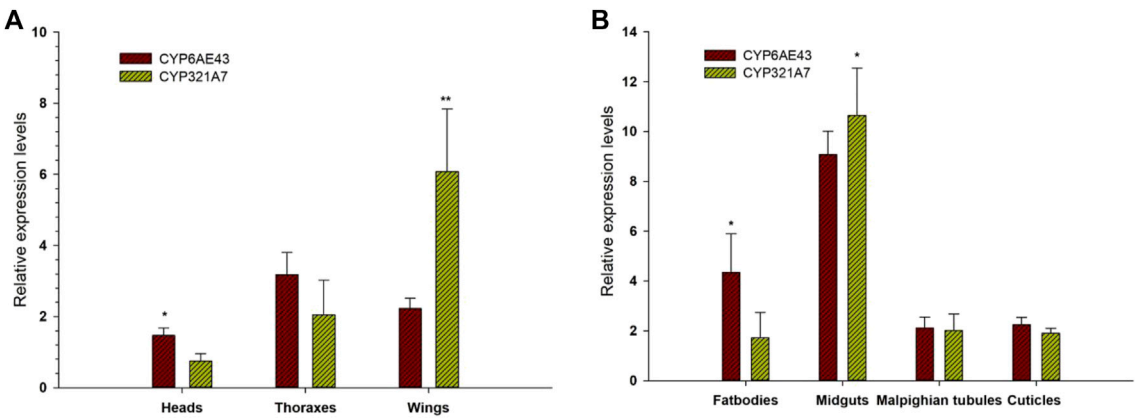

FIGURE 3 | Tissue specific expression pattern of CYP6AE43 and CYP321A7 in midguts, bodies, malpighian tubules and cuticles of FAW larvae **(A)** and the heads, thoraxes and wings of adults **(B)**. Data shown are means ± SE derived from three biological replicates. Bars represent relative expression (mean ± SE). All biological groups contained three replicates for each treatment, and there were three technical replicates. The relative expression was calculated using the $2^{-\Delta\Delta CT}$ method based on the value of the egg expression, which was ascribed an arbitrary value of 1. The astriks on the bar represent significant differences ($p < 0.05$) using one-way ANOVA, followed by Tukey's HSD multiple comparison tests.

sequences of all selected P450 genes belonging to CYP3, CYP2, CYP4 and the Mito-clade. The results showed that the mitochondrial clan and CYP4 appeared to share the maximum sequence similarity (**Supplementary Figure S2**). Amino acid alignments with different P450s of the *CYP6AE* and *CYP321A* subfamilies also indicated that the *CYP6AE43* and *CYP321A7* protein contains shared conserved motifs found in other P450s, including the helix C motif WKVQR (WxxxR), the helix I motif GFETS (Gx [ED]T [TS]), the helix K motif EALR (ExLR), the PERF motif PEQFRPER (PxxFxP [ED]RE) and the heme-binding motif PFGEGPRLCIG (PFxxGxRxCx [GA]) (**Figure 4** and **Supplementary Figure S1**).

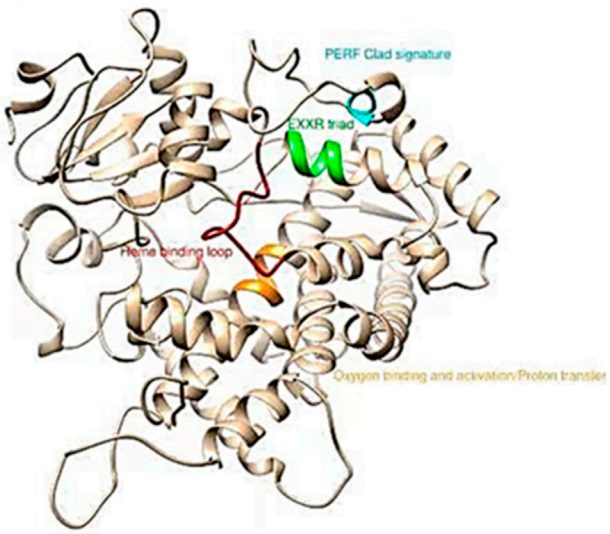

FIGURE 4 | Conserved motifs in *S. frugiperda CYP6AE43* and *CYP321A7*. The protein sequences were queried against the pdb database to find template in ncbi blast.

The Integrity of Resulting dsRNAs

The integrity of all three resulting dsRNAs were analyzed by 1% agarose gel electrophoresis which showed the expected size of two P450 genes and control dsRED fragments as 679, 506 and 421 bp respectively (**Supplementary Figure S3A** and **Supplementary Figure S3B**).

RNAi-mediated downregulation of ds*CYP321A7* and ds*CYP6AE43* genes in *S. frugiperda* via qRT-PCR

Two target P450 genes were selected to evaluate their function in indoxacarb resistant FAW. To find the RNAi efficiency, qRT-PCR was conducted to check the relative change in mRNA expression of targeted genes in FAW larval fed on dsRNAs, *dsCYP321A7* and *dsCYP6AE43* along with the dsRED control for 48, 72 and 96 h (**Figure 4A–C**). Dramatically lower mRNA transcript levels of *dsCYP321A7* and *dsCYP6AE43* genes were observed in Indox-SEL after 48, 72 and 96 h compared with the *dsRED* control (**Figure 4A–C**). We evaluated the effect of two dsRNAs targeting *CYP321A7* and *CYP6AE43* on the mortality of the indoxacarb resistant FAW larvae at different time points after feeding on dsRNA-supplemented diet followed by exposure to a lethal concentration (21.02 μg g^{-1}) of indoxacarb (**Figure 5D–F**). After 48 h, a significantly higher mortality rate was observed in the *dsCYP321A7* and the *dsCYP6AE43*-fed larvae compared to the *dsRED* control (**Figure 5D**). The highest mortality was observed for the *dsCYP321A7* treatment. Feeding on a *dsCYP321A7+dsCYP6AE43*-supplemented diet significantly increased the mortality rate compared to all other treatments (**Figure 5D**). Similarly, a significantly higher mortality rate was observed in *dsCYP321A7* and *dsCYP6AE43*-fed larvae after 72 h compared to the *dsRED* control (**Figure 5E**). At 72 h, as previously, the highest mortality was observed in the combined treatment (**Figure 5E**). Furthermore, this trend was observed in the mortality rate recorded after 96 h (**Figure 5F**). The overall mortality rate was significantly increased in *dsCYP321A7*-fed larvae and, to a lesser extent, in *dsCYP6AE43*-fed larvae compared to the *dsRED* control (**Figure 5F**). However, the greatest mortality was observed when a combined treatment of *dsCYP321A7+dsCYP6AE43* supplemented diet was used (**Figure 5F**).

The single and combined effect of dsRNA on the larval development, pupal development, and midgut physiology of FAW

The larval developmental period of FAW in different treatment groups was assessed. Larvae were fed with dsRNA-supplemented diets targeting *dsCYP321A7* and *dsCYP6AE43*, or a combination of both, followed by exposure of LC_{20} (6.84 μg g^{-1}) of indoxacarb after 3 days (**Figure 6**). It was found that these single target dsRNA-supplemented diets of *dsCYP321A7*, *dsCYP6AE43* and combined target dsRNA-supplemented diets of *dsCYP321A7+dsCYP6AE43* significantly reduced the larval duration in the Indox-SEL population compared to the *dsRED* and DEPC-water as control treatments (**Figure 6A**). While no significant decrease in larval duration between *dsCYP321A7* and *dsCYP6AE43* treatments was found (**Figure 6A**). Weight gain of the FAW larvae was found to be greatest in the control diet followed by the *dsRED* control group (**Figure 6B**). A significant reduction of the larvae weight gain was observed when the Indox-SEL population was fed on dsRNA-supplemented diet targeting *dsCYP321A7*, *dsCYP6AE43,* or a combination of both for 24 h followed by the exposure to LC_{20} (6.84 μg g^{-1}) of indoxacarb after 3 days (**Figure 6B**). Furthermore, it was found that these single effects of *dsCYP321A7* and *dsCYP6AE43* did not affect the pupal duration, meanwhile pupal duration significantly increased when a combined *dsCYP321A7+dsCYP6AE43* treatment was applied in the Indox-SEL population compared to the *dsRED* and DEPC-water control treatments (**Figure 6C**).

The changes in the larval and midguts physiology of the FAW after feeding on ds*CYP321A7* + *dsCYP6AE43*, *dsCYP321A7*, *dsCYP6AE43* for 24 h followed by the exposure to an artificial diet supplemented with LC_{20} (6.84 μg g^{-1}) of indoxacarb for 72 h was assessed (**Figure 7A–E**). After exposure to dsRNAs for 24 h followed by LC_{20} (6.84 μg g^{-1}) of indoxacarb insecticide, toxic symptoms including reduced appetite, shorter body length of larvae, the development and growth of most FAW were delayed. Furthermore, damaged midguts can be observed in single and combined dsRNAs-treated groups compared to the *dsRED* and DEPC-water control treatments (**Figure 7F–J**).

DISCUSSION

Synthetic insecticides are still the mainstay of insect pest management. Synthetic insecticides, including indoxacarb,

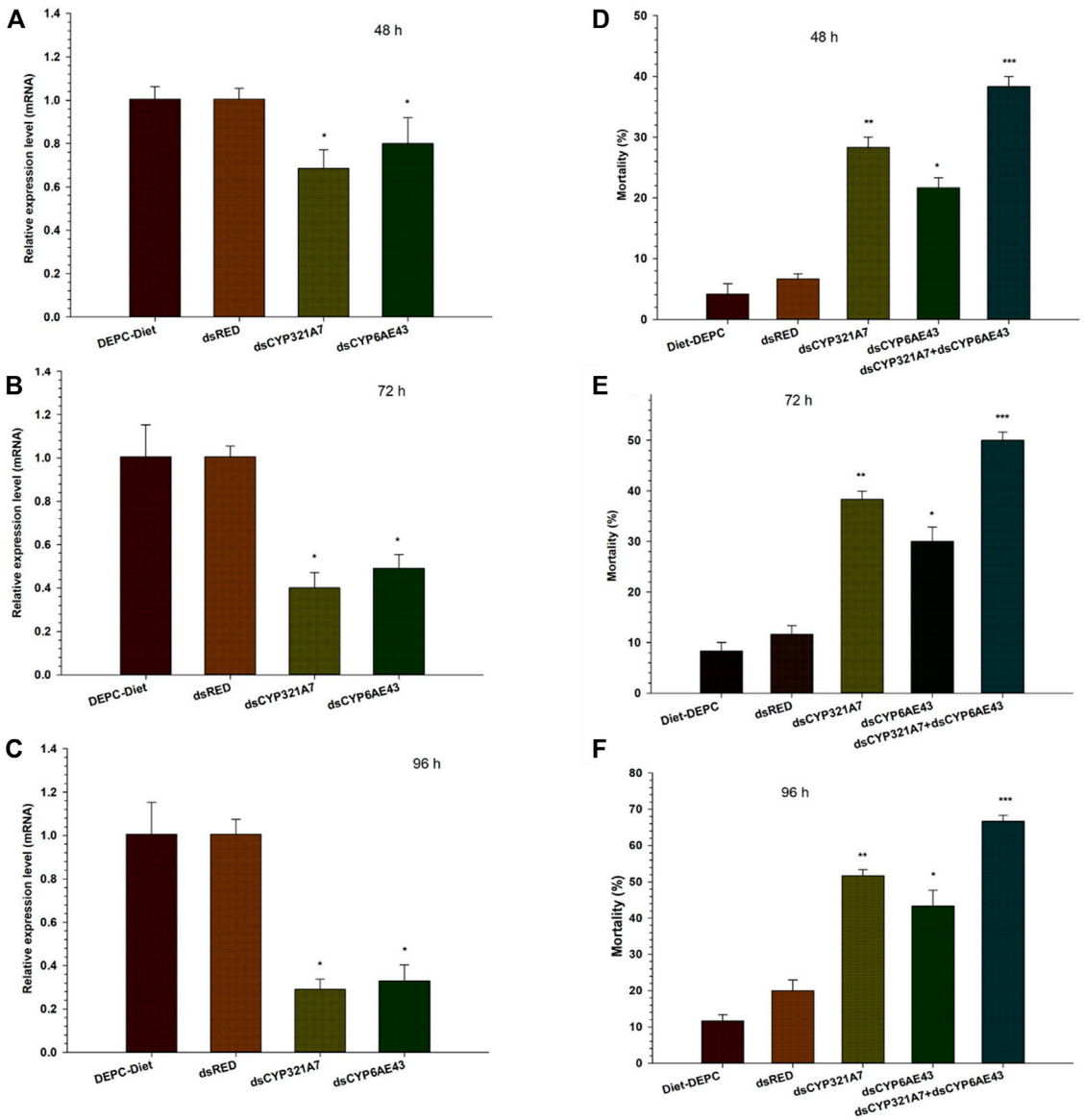

FIGURE 5 | The relative mRNA transcript levels in the midguts of *S. frugiperda* larvae (Indox-SEL population) after feeding on dsCYP321A7, dsCYP6AE43 and dsRED for 48 h **(A)**, 72 h **(B)** and 96 h **(C)**. Similarly, the single dsCYP321A7, dsCYP6AE43 and combined dsCYP321A7+dsCYP6AE43) or dsRED effect of dsRNAs on the sensibility to indoxacarb in third-instar larvae of *S. frugiperda* after exposure with LC_{20}: 6.84 μg g^{-1} concentration of indoxacarb. After feeding with dsRNAs and dsRED for 24 h followed by the exposed third instar larvae were transferred individually into 12-oriface tissue culture plate containing artificial diets supplemented with LC_{20}: 6.84 μg g^{-1} of indoxacarb for 48 h **(D)**, 72 and 96 h **(F)**. DEPC-Diet as a control (Indox-UNSEL population) without exposure to indoxacarb. The mortality data were recorded at 48, 72 and 96 h. Data shown are means ± SE derived from three biological replicates. The astriks on the bar represent significant differences ($p < 0.05$) using one-way ANOVA, followed by Tukey's HSD multiple comparison tests.

have been extensively used against a variety of agricultural insect pests (Zhao et al., 2020), however, due to the development of insecticide resistance, these synthetic insecticides often fail to provide effective control (Gutirrez-Moreno et al., 2019; Boaventura et al., 2020; Zhang et al., 2020). The fall armyworm (FAW) has developed resistance to a range of different groups of synthetic insecticides including pyrethroids. An example is the now commonly observed resistance of FAW to lambda-cyhalothrin (Zhao et al., 2020).

To understand more about the important phenomena of indoxacarb resistance, we looked at the effect of silencing two important encoding P450 genes in FAW: *CYP321A7* and *CYP6AE43*. Our results indicated that PBO and TPP enhanced the toxicity of indoxacarb for the indoxacarb-resistant laboratory selected population (Indox-SEL). This indicates that cytochrome P450 monooxygenases may play a significant role in the resistance mechanism, because PBO as a synergist, can also block the non-specific esterase activity (Moores et al., 2009). It has been previously

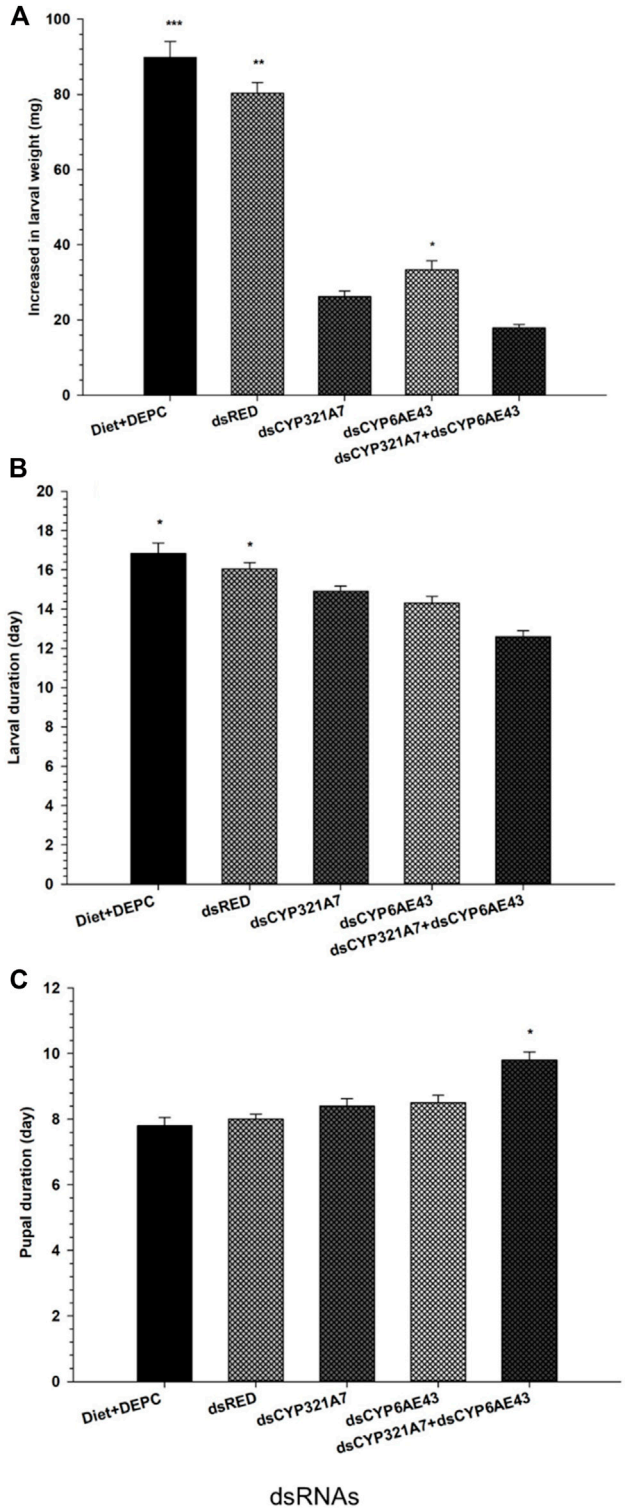

FIGURE 6 | Single and combined effect of dsCYP321A7, dsCYP6AE43 and dsCYP321A7+dsCYP6AE43) or dsRED on larval duration **(A)**, increased in larval weight **(B)** pupal duration **(C)** of Indox-SEL population after feeding on dsRNAs, or the dsRED for 24 h followed by the exposed larvae were transferred individually into 12-oriface tissue culture plate containing artificial diets supplemented with LC_{20}: 6.84 μg g^{-1} of indoxacarb for 72 h. DEPC-Diet (*Continued*)

FIGURE 6 | as a control (Indox-UNSEL population) without exposure to indoxacarb. Data shown are means ± SE derived from three biological replicates. The astriks on the bar represent significant differences ($p < 0.05$) using one-way ANOVA, followed by Tukey's HSD multiple comparison tests.

been identified that synthetic insecticides are converted into non-toxic compounds due to increased metabolic activity of detoxifying enzymes and reduced target sensitivity of pesticides, which is one of the key detoxification mechanisms in insect pests (Scott, 1999b; Feyereisen, 2006b; Li et al., 2007). We found that the enzyme activity of P450s monooxygenase in the Indox-SEL population was significantly enhanced after 24 h and up to 96 h following the exposure to indoxacarb. This pattern is similar to previous studies which have shown the greater detoxification activity of P450 enzymes in resistant populations of other insect pests (Chen et al., 2018; Wang et al., 2018c, 2018b). In addition to the involvement of P450s in resistance, the effects of esterase and GST contributing to indoxacarb resistance of FAW larvae should be further examined in future work.

The elevated activity of P450 enzymes due to the up-regulation of P450 genes is ostensibly a major mechanism for insecticide resistance (Elzaki et al., 2017; Ullah et al., 2020b). In the current study, we evaluated clades-3, 4, 2 and the mitochondrial clade P450 genes and found that two genes *CYP321A7* and *CYP6AE43* from clade CYP3 were associated with indoxacarb-resistant populations of FAW. Two P450 genes out of ten showed significantly higher expression levels in the midgut of FAW larvae after 14 generations of selection with indoxacarb. These findings were consistent with previous findings that some of the *CYP321* subfamily genes, as well as the CYP6 and CYP9 subfamily genes, may be involved in mechanisms of detoxication or regulation of insecticides. These findings elucidated P450 functions on insect biology and physiology, and that the midgut and fat body tissue of insects are considered important as detoxification organs (Giraudo et al., 2015; Hou et al., 2021). It has been previously reported that the development of insecticide resistance by enhancing metabolic detoxification enzymes in various insects is closely related to the elevated expression of P450 genes and subsequent increases in P450 protein levels (Riveron et al., 2013; Xu et al., 2018). In this study, we tested whether the resistant populations of *S. frugiperda* differ in expression of P450 genes of CYP4, CYP6 and CYP9 subfamilies, which are expected to be associated with insecticide resistance (Bai-Zhong et al., 2020; Wang et al., 2022; Zhao et al., 2022). Among the differentially expressed *S. frugiperda* P450 genes identified in this study, CYP321A7 and CYP6AE43 genes were particularly overexpressed in larvae of indoxacarb-resistant populations (11.6 and 9.4 fold higher in resistant compared to control populations). These results are in line with previous findings showing that the insecticide-induced P450 genes (*CYP6BG1, CYP321A8, CYP321B1, CYP9A32, CYP333B3, CYP9A26, CYP321A9, CYP337B5*, and *CYP6AE44*) that play a role in insect metabolic resistance (Bautista et al., 2009; Giraudo et al., 2015; Bai-Zhong et al., 2020). Similarly, transcriptome analysis has revealed higher mRNA expression level of five P450 genes in indoxacarb-fed larvae of *Spodoptera exigua* (Hu et al., 2019). The induced mRNA expression of some P450 genes, *CYP9A9, CYP321A1* and *CYP321B1* has been reported in the midgut of FAW and *Spodoptera litura* after exposure to different insecticides (Nascimento et al., 2015; Wang

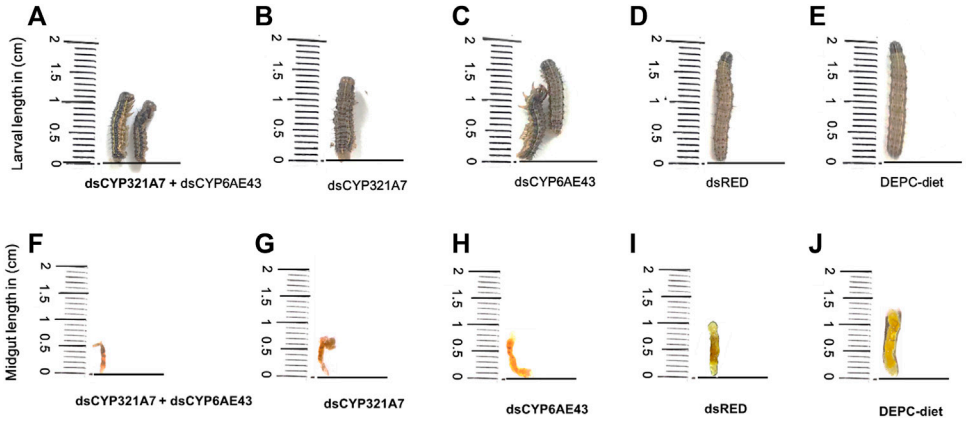

FIGURE 7 | The effect of dsCYP321A7+dsCYP6AE43, dsCYP321A7, dsCYP6AE43, dsRED on the *S. frugiperda* larvae physiology and growth (Indox-SEL population) after feeding on dsRNAs, or the dsRED as a control for 24 h followed by exposure to diet supplemented with LC_{20}: 6.84 μg g^{-1} concentration of indoxacarb for 72 h **(A,B,C,D)**. DEPC-Diet as a control (Indox-UNSEL population) without exposure to indoxacarb **(E)**. Similarly, the effect of dsCYP321A7+dsCYP6AE43, dsCYP321A7, dsCYP6AE43 and dsRED on the midguts physiology of *S. frugiperda* larvae (Indox-SEL population) after feeding on dsRNAs, or the dsRED as a control for 24 h followed by exposure to diet supplemented with LC_{20}: 6.84 μg g^{-1} concentration of indoxacarb for 72 h **(F,G,H,I)**. DEPC-Diet as a control (Indox-UNSEL population) without exposure to indoxacarb **(J)**.

et al., 2017). Taken together with the present results, this indicated that indoxacarb resistance in FAW is a more complex mechanism than initially considered. The phylogenetic tree (**Supplementary Figure S3A**) demonstrates that *CYP6AE43* and *CYP321A7* belong to the *CYP6AE* subfamily (*CYP3* clan of insect P450s). P450s from the CYP6AE subfamily of insect P450s have been shown in a number of studies to play an important role in the development of insecticide resistance (Hu et al., 2017; Shi et al., 2018), this study was focused on *CYP6AE43* and *CYP321A7*. The amino acid sequences of *CYP6AE43* and *CYP321A7* contain various shared conserved motifs including heme-binding predicted substrate recognition sites, suggesting that the enzyme is functional. These results are in line with previous findings (Guo et al., 2015; Hou et al., 2021).

To further explore if the indoxacarb-induced genes *CYP321A7* and *CYP6AE43* are involved in indoxacarb detoxification, we fed specific *dsCYP321A7* and *dsCYP6AE43 S. fugiperda* larvae to silence target genes and then analyzed phenotypic effects. Greater larval mortality was observed in the resistant populations of FAW after feeding on dsRNAs-fed (*CYP321A7* and *CYP6AE43*) followed by the exposure of an LC_{20} concentration of indoxacarb as compared to dsRED and Diet-DEPC as a control (**Figure 5A–C**). Similar findings have been seen previously by Naqqash *et al.* (2020) and Bai-Zhong *et al.* (2020) who reported that the subfamilies of the CYP321, CYP6, and CYP9 of P450 genes could be induced by insecticides. Similarly, we found that downregulation of P450 genes significantly reduced the larval developmental time, larval growth and larval weight following feeding on the dsRNAs-supplemented diet with subsequent indoxacarb exposure. Naqqash *et al.* (2020) and Zhao *et al.* (2016) also documented that the larval growth and development was significantly reduced in *H. armigera* and *Leptinotarsa decemlineata* due to dsRNAs feeding. Studies continue to reveal the dynamic role P450s play in the regulation of growth and the development of insecticide resistance in various insects. Therefore, it is understood that the downregulation of these genes via RNAi could result in higher mortality across various insect species (Zhang et al., 2013; Jin et al., 2015; Zhao et al., 2016; Bai-Zhong et al., 2020; Hafeez et al., 2020). Knocking down of P450 genes increased larval mortality, reduced developmental duration, and increased insecticide susceptibility, indicating the role of P450 genes in larval growth, development, and sensitivity to indoxacarb. Physiological and biochemical studies have shown that P450 enzymes are vital to in insect hormone metabolism pathways but details of the molecular processes remain unknown (Iga and Kataoka, 2012). The growth of FAW larvae was hindered after downregulation of *CYP321A7* and *CYP6AE43* by RNAi, but how these P450 genes regulate this process requires further study.

CONCLUSION

It was shown that the droplet feeding of dsRNAs (*CYP321A7* and *CYP6AE43*) via artificial diet significantly increased mortality rates of indoxacarb-resistant larvae. Shorter larval developmental time was detected in the dsRNAs-exposed larvae of FAW. Similarly, larval weight was also reduced in the dsRNAs-exposed resistant population. To our knowledge, this is the first time an indoxacarb-resistant FAW population was used to evaluate the effects of different dsRNA on larval mortality, growth, and insecticide susceptibility. Our results elucidate some of the effects of the RNAi technique and the function of specific genes. The application of dsRNA may offer a route to reduce the development of resistance in FAW against various insecticides in the field. This paves the route for further study into the suppression of resistance in fall armyworm and various other important agricultural insect pests.

DATA AVAILABILITY STATEMENT

The original contributions presented in the study are included in the article/**Supplementary Material**, further inquiries can be directed to the corresponding authors.

AUTHOR CONTRIBUTIONS

All authors contributed to the data collection, analysis and interpretation of the data, drafting, and revising the manuscript, and approved the fifinal version of the manuscript. The original study design was made by MH, XL and YL and discussed with the other authors and approved the manuscript.

FUNDING

This work was supported by the Key R&D Program of Zhejiang Province (2020C02003), the Shanghai Innovation Project for Agricultural Promotion (2019N3- 9), and the Joint Agricultural Project between Pinghu County and Zhejiang Academy of Agricultural Sciences (PH20190002). Project funded by China National Postdoctoral Science foundation (2020M681921) and the Primary Research & Development Plan of Lishui (No. 2021ZDYF10).

SUPPLEMENTARY MATERIAL

The Supplementary Material for this article can be found online at: https://www.frontiersin.org/articles/10.3389/fphys.2022.884447/full#supplementary-material.

REFERENCES

Ahmad, M., Sayyed, A. H., Saleem, M. A., and Ahmad, M. (2008). Evidence for Field Evolved Resistance to Newer Insecticides in *Spodoptera Litura* (Lepidoptera: Noctuidae) from Pakistan. *Crop Prot.* 27, 1367–1372. doi:10.1016/j.cropro.2008.05.003

Aktar, W., Sengupta, D., and Chowdhury, A. (2009). Impact of Pesticides Use in Agriculture: Their Benefits and Hazards. *Interdiscip. Toxicol.* 2, 1–12. doi:10.2478/v10102-009-0001-7

Alves, A. P., Allgeier, W. J., and Siegfried, B. D. (2008). Effects of the Synergist S,S,S-tributyl Phosphorotrithioate on Indoxacarb Toxicity and Metabolism in the European Corn Borer, Ostrinia Nubilalis (Hübner). *Pestic. Biochem. Physiol.* 90, 26–30. doi:10.1016/j.pestbp.2007.07.005

Arain, M. S., Shakeel, M., Elzaki, M. E. A., Farooq, M., Hafeez, M., Shahid, M. R., et al. (2018). Association of Detoxification Enzymes with Butene-Fipronil in Larvae and Adults of *Drosophila melanogaster*. *Environ. Sci. Pollut. Res.* 25, 10006–10013. doi:10.1007/s11356-018-1202-4

Bai-Zhong, Z., Xu, S., Cong-Ai, Z., Liu-Yang, L., Ya-She, L., Xing, G., et al. (2020). Silencing of Cytochrome P450 in *Spodoptera Frugiperda* (Lepidoptera: Noctuidae) by RNA Interference Enhances Susceptibility to Chlorantraniliprole. *J. Insect Sci.* 20, 1–7. doi:10.1093/jisesa/ieaa047

Bautista, M. A. M., Miyata, T., Miura, K., and Tanaka, T. (2009). RNA Interference-Mediated Knockdown of a Cytochrome P450, CYP6BG1, from the Diamondback Moth, *Plutella Xylostella*, Reduces Larval Resistance to Permethrin. *Insect Biochem. Mol. Biol.* 39, 38–46. doi:10.1016/j.ibmb.2008.09.005

Bennett, M., Deikman, J., Hendrix, B., and Iandolino, A. (2020). Barriers to Efficient Foliar Uptake of dsRNA and Molecular Barriers to dsRNA Activity in Plant Cells. *Front. Plant Sci.* 11, 816. doi:10.3389/fpls.2020.00816

Boaventura, D., Bolzan, A., Padovez, F. E., Okuma, D. M., Omoto, C., and Nauen, R. (2020). Detection of a Ryanodine Receptor Target-site Mutation in Diamide Insecticide Resistant Fall Armyworm, Spodoptera Frugiperda. *Pest Manag. Sci.* 76, 47–54. doi:10.1002/ps.5505

Bradford, M. M. (1976). A Rapid and Sensitive Method for the Quantitation of Microgram Quantities of Protein Utilizing the Principle of Protein-Dye Binding. *Anal. Biochem.* 72, 248–254. doi:10.1016/0003-2697(76)90527-3

Burtet, L. M., Bernardi, O., Melo, A. A., Pes, M. P., Strahl, T. T., and Guedes, J. V. (2017). Managing Fall Armyworm, *Spodoptera Frugiperda* (Lepidoptera: Noctuidae), with Bt maize and Insecticides in Southern Brazil. *Pest Manag. Sci.* 73, 2569–2577. doi:10.1002/ps.4660

Bustin, S. A., Benes, V., Garson, J. A., Hellemans, J., Huggett, J., Kubista, M., et al. (2009). The MIQE Guidelines: Minimum Information for Publication of Quantitative Real-Time PCR Experiments. *Clin. Chem.* 55 (4), 611–622. doi:10.1373/clinchem.2008.112797

Chen, C., Han, P., Yan, W., Wang, S., Shi, X., Zhou, X., et al. (2018). Uptake of Quercetin Reduces Larval Sensitivity to Lambda-Cyhalothrin in *Helicoverpa Armigera*. *J. Pest Sci.* 91, 919–926. doi:10.1007/s10340-017-0933-1

Chen, X., Head, G. P., Price, P., Kerns, D. L., Rice, M. E., Huang, F., et al. (2019). Fitness Costs of Vip3A Resistance in *Spodoptera Frugiperda* on Different Hosts. *Pest Manag. Sci.* 75, 1074–1080. doi:10.1002/ps.5218

Cordova, D., Benner, E. A., Sacher, M. D., Rauh, J. J., Sopa, J. S., Lahm, G. P., et al. (2006). Anthranilic Diamides: A New Class of Insecticides with a Novel Mode of Action, Ryanodine Receptor Activation. *Pestic. Biochem. Physiol.* 84, 196–214. doi:10.1016/j.pestbp.2005.07.005

Davis, C. C. (1993). Environmental Concerns about Pesticide Use in Philippine Agriculture. *Sci. Total Environ.* 134, 293–306. doi:10.1016/S0048-9697(05)80030-0

Day, R., Abrahams, P., Bateman, M., Beale, T., Clottey, V., and Cock, M. (2017). Fall Armyworm: Impacts and Implications for Africa. *Outlooks Pest Manag* 28, 196–201. doi:10.1564/v28_oct_02

Desneux, N., Decourtye, A., and Delpuech, J. (2007). The Sublethal Effects of Pesticides on Beneficial Arthropods.. *Annu Rev Entomol 52:81* 52, 81–106. doi:10.1146/annurev.ento.52.110405.091440

Ehrlich, P. R., and Raven, P. H. (1964). Butterflies and Plants: A Study in Coevolution. *Evolution* 18, 586–608. doi:10.2307/240621210.1111/j.1558-5646.1964.tb01674.x

Elzaki, M., Miah, M., and Han, Z. (2017). Buprofezin Is Metabolized by CYP353D1v2, a Cytochrome P450 Associated with Imidacloprid Resistance in *Laodelphax Striatellus*. *Ijms* 18, 2564. doi:10.3390/ijms18122564

Feyereisen, R. (2006b). Evolution of Insect P450. *Biochem. Soc. Trans.* 34, 1252–1255. doi:10.1042/BST0341252

Feyereisen, R. (2006a). Evolution of Insect P450. *Biochem. Soc. Trans.* 34, 1252–1255. doi:10.1042/BST0341252

Feyereisen, R. (2012). Insect CYP Genes and P450 Enzymes. *Insect Mol. Biol. Biochem.*, 236–316. doi:10.1016/B978-0-12-384747-8.10008-X

Ginting, S., Zarkani, A., and Hadi Wibowo, R. (2020). *New invasive pest,* Spodoptera frugiperda *(J. e. smith) (lepidoptera: Noctuidae) attacking corn in bengkulu*. indonesia: Serangga 25, 105–117.

Giraudo, M., Hilliou, F., Fricaux, T., Audant, P., Feyereisen, R., and Le Goff, G. (2015). Cytochrome P450s from the Fall Armyworm (*Spodoptera Frugiperda*): Responses to Plant Allelochemicals and Pesticides. *Insect Mol. Biol.* 24, 115–128. doi:10.1111/imb.12140

Goergen, G., Kumar, P. L., Sankung, S. B., Togola, A., and Tamò, M. (2016). First Report of Outbreaks of the Fall Armyworm *Spodoptera Frugiperda* (J E Smith) (Lepidoptera, Noctuidae), a New Alien Invasive Pest in West and Central Africa. *PLoS One* 11, e0165632. doi:10.1371/journal.pone.0165632

Gul, H., Ullah, F., and Hafeez, M. (2021). Sublethal Concentrations of Clothianidin Affect Fecundity and Key Demographic Parameters of the Chive Maggot, Bradysia Odoriphaga.. *Ecotoxicology* 30, 1150–1160. doi:10.1007/s1064602102446x

Guo, Y., Zhang, X., Wu, H., Yu, R., Zhang, J., Zhu, K. Y., et al. (2015). Identification and Functional Analysis of a Cytochrome P450 Gene CYP9AQ2 Involved in Deltamethrin Detoxification from *Locusta migratoria*. *Pestic. Biochem. Physiol.* 122, 1–7. doi:10.1016/j.pestbp.2015.01.003

Gupta, G. P., Rani, S., Birah, A., and Raghuraman, M. (2005). Improved Artificial Diet for Mass Rearing of the Tobacco Caterpillar, *Spodoptera Litura* (Lepidoptera: Noctuidae). *Int. J. Tropical. Insect. Sci.* 25, 55–58. doi:10.1079/IJT200551

Gutiérrez-Moreno, R., Mota-Sanchez, D., Blanco, C. A., Whalon, M. E., Terán-Santofimio, H., Rodriguez-Maciel, J. C., et al. (2019). Field-Evolved Resistance

of the Fall Armyworm (Lepidoptera: Noctuidae) to Synthetic Insecticides in Puerto Rico and Mexico. *J. Econ. Entomol.* 112, 792–802. doi:10.1093/jee/toy372

Hafeez, M., Liu, S., Jan, S., Ali, B., Shahid, M., Fernández-Grandon, G. M., et al. (2019a). Gossypol-induced Fitness Gain and Increased Resistance to Deltamethrin in Beet armyworm,Spodoptera exigua(Hübner). *Pest Manag. Sci.* 75, 683–693. doi:10.1002/ps.5165

Hafeez, M., Liu, S., Jan, S., Gulzar, A., Fernández-Grandon, G. M., Qasim, M., et al. (2019b). Enhanced Effects of Dietary Tannic Acid with Chlorantraniliprole on Life Table Parameters and Nutritional Physiology of Spodoptera Exigua (Hübner). *Pestic. Biochem. Physiol.* 155, 108–118. doi:10.1016/j.pestbp.2019.01.012

Hafeez, M., Liu, S., Jan, S., Shi, L., Fernández-Grandon, G. M., Gulzar, A., et al. (2019c). Knock-Down of Gossypol-Inducing Cytochrome P450 Genes Reduced Deltamethrin Sensitivity in Spodoptera Exigua (Hübner). *Ijms* 20, 2248. doi:10.3390/ijms20092248

Hafeez, M., Jan, S., and Nawaz, M. (2019d). Sub Lethal Effects of Lufenuron Exposure on Spotted Bollworm Earias Vittella (Fab): Key Biological Traits and Detoxification Enzymes Activity. *Environ Sci Pollut Res* 26, 14300–14312. doi:10.1007/s11356019046558

Hafeez, M., Liu, S., and Jan, S. (2019e). Gossypol-Induced Fitness Gain and Increased Resistance to Deltamethrin in Beet Armyworm, Spodoptera Exigua (Hübner). *Pest Manag Sci* 76, 683–693. doi:10.1002/ps.5165

Hafeez, M., Liu, S., Yousaf, H. K., Jan, S., Wang, R.-L., Fernández-Grandon, G. M., et al. (2020). RNA Interference-Mediated Knockdown of a Cytochrome P450 Gene Enhanced the Toxicity of α-cypermethrin in Xanthotoxin-Fed Larvae of Spodoptera Exigua (Hübner). *Pestic. Biochem. Physiol.* 162, 6–14. doi:10.1016/j.pestbp.2019.07.003

Hafez, A. M., Mota-Sanchez, D., Hollingworth, R. M., Vandervoort, C., and Wise, J. C. (2020). Metabolic Mechanisms of Indoxacarb Resistance in Field Populations of *Choristoneura Rosaceana* (Harris) (Lepidoptera: Tortricidae). *Pestic. Biochem. Physiol.* 168, 104636. doi:10.1016/j.pestbp.2020.104636

Hou, W.-T., Staehelin, C., Elzaki, M. E. A., Hafeez, M., Luo, Y.-S., and Wang, R.-L. (2021). Functional Analysis of CYP6AE68, a Cytochrome P450 Gene Associated with Indoxacarb Resistance in *Spodoptera Litura* (Lepidoptera: Noctuidae). *Pestic. Biochem. Physiol.* 178, 104946. doi:10.1016/j.pestbp.2021.10494610.1016/j.pestbp.2021.104946

Hu, B., Zhang, S. H., Ren, M. M., Tian, X. R., Wei, Q., Mburu, D. K., et al. (2017). The Expression of *Spodoptera Exigua* P450 and UGT Genes: Tissue Specificity and Response to Insecticides. *Insect Sci.* 26, 199–216. doi:10.1111/1744-7917.12538

Hu, B., Zhang, S. H., Ren, M. M., Tian, X. R., Wei, Q., Mburu, D. K., et al. (2019). The Expression of *Spodoptera Exigua* P450 and UGT Genes: Tissue Specificity and Response to Insecticides. *Insect Sci.* 26, 199–216. doi:10.1111/1744-7917.12538

Iftikhar, A., Hafeez, F., Hafeez, M., Farooq, M., Asif Aziz, M., Sohaib, M., et al. (2020). Sublethal Effects of a Juvenile Hormone Analog, Pyriproxyfen on Demographic Parameters of Non-target Predator, *Hippodamia convergens* Guerin-Meneville (Coleoptera: Coccinellidae). *Ecotoxicology* 29, 1017–1028. doi:10.1007/s10646-020-02159-7

Iga, M., and Kataoka, H. (2012). Recent Studies on Insect Hormone Metabolic Pathways Mediated by Cytochrome P450 Enzymes. *Biol. Pharm. Bull.* 35, 838–843. doi:10.1248/bpb.35.838

Jan, S., Liu, S., Hafeez, M., Zhang, X., Dawar, F. U., Guo, J., et al. (2017). Isolation and Functional Identification of Three Cuticle Protein Genes during Metamorphosis of the Beet Armyworm, Spodoptera Exigua. *Sci. Rep.* 7, 16061. doi:10.1038/s41598-017-16435-w

Jin, S., Singh, N. D., Li, L., Zhang, X., and Daniell, H. (2015). Engineered Chloroplast dsRNA Silences Cytochrome P450 Monooxygenase , V -ATPase and Chitin Synthase Genes in the Insect Gut and Disrupts Helicoverpa Armigera Larval Development and Pupation. *Plant Biotechnol. J.* 13, 435–446. doi:10.1111/pbi.12355

Li, T., and Liu, N. (2017). Regulation of P450-Mediated Permethrin Resistance in *Culex quinquefasciatus* by the GPCR/Gαs/AC/cAMP/PKA Signaling cascade. *Biochem. Biophys. Rep.* 12, 12–19. doi:10.1016/j.bbrep.2017.08.010

Li, X. J., Wu, M. F., Ma, J., Gao, B. Y., Wu, Q. L., Chen, A. D., et al. (2020). Prediction of Migratory Routes of the Invasive Fall Armyworm in Eastern China Using a Trajectory Analytical Approach. *Pest Manag. Sci.* 76, 454–463. doi:10.1002/ps.5530

Li, X., Schuler, M. A., and Berenbaum, M. R. (2007). Molecular Mechanisms of Metabolic Resistance to Synthetic and Natural Xenobiotics. *Annu. Rev. Entomol.* 52, 231–253. doi:10.1146/annurev.ento.51.110104.151104

Lim, Z. X., Robinson, K. E., Jain, R. G., Sharath Chandra, G., Asokan, R., Asgari, S., et al. (2016). Diet-delivered RNAi in *Helicoverpa Armigera* - Progresses and Challenges. *J. Insect Physiol.* 85, 86–93. doi:10.1016/j.jinsphys.2015.11.005

Liu, X. N., Liang, P., Gao, X. W., and Shi, X. Y. (2006). Induction of the Cytochrome P450 Activity by Plant Allelochemicals in the Cotton Bollworm, *Helicoverpa Armigera* (Hubner). *Pestic. Biochem. Physiol.* 84, 127–134.

Liu, Y., Qi, M., Chi, Y., and Wuriyanghan, H. (2016). De Novo Assembly of the Transcriptome for Oriental ArmywormMythimna separata(Lepidoptera: Noctuidae) and Analysis on Insecticide Resistance-Related Genes. *J. Insect Sci.* 16, 92. doi:10.1093/jisesa/iew079

Livak, K. J., and Schmittgen, T. D. (2001). Analysis of Relative Gene Expression Data Using Real-Time Quantitative PCR and the 2−ΔΔCT Method. *Methods* 25, 402–408. doi:10.1006/meth.2001.1262

Lu, K., Cheng, Y., Li, W., Li, Y., Zeng, R., and Song, Y. (2020). Activation of CncC Pathway by ROS Burst Regulates Cytochrome P450 CYP6AB12 Responsible for λ-cyhalothrin Tolerance in Spodoptera Litura. *J. Hazard. Mater.* 387, 121698. doi:10.1016/j.jhazmat.2019.121698

Mallet, J. (1989). The Evolution of Insecticide Resistance: Have the Insects Won? *Trends Ecol. Evol.* 4, 336–340. doi:10.1016/0169-5347(89)90088-8

McCann, S. F., Annis, G. D., Shapiro, R., Piotrowski, D. W., Lahm, G. P., Long, J. K., et al. (2001). The Discovery of Indoxacarb: Oxadiazines as a New Class of Pyrazoline-type Insecticides. *Pest Manag. Sci.* 57, 153–164. doi:10.1002/1526-4998(200102)57:2<153::aid-ps288>3.0.co;2-o

Mello, C. C., and Conte, D. (2004). Revealing the World of RNA Interference. *Nature* 431, 338–342. doi:10.1038/nature02872

Monnerat, R., Martins, E., Macedo, C., Queiroz, P., Praça, L., Soares, C. M., et al. (2015). Evidence of Field-Evolved Resistance of *Spodoptera Frugiperda* to Bt Corn Expressing Cry1F in Brazil that Is Still Sensitive to Modified Bt Toxins. *PLoS One* 10, e0119544. doi:10.1371/journal.pone.0119544

Montezano, D. G., Specht, A., Sosa-Gómez, D. R., Roque-Specht, V. F., Sousa-Silva, J. C., Paula-Moraes, S. V., et al. (2018). Host Plants ofSpodoptera frugiperda(Lepidoptera: Noctuidae) in the Americas. *Afr. Entomol.* 26, 286–300. doi:10.4001/003.026.0286

Moores, G. D., Philippou, D., Borzatta, V., Trincia, P., Jewess, P., Gunning, R., et al. (2009). An Analogue of Piperonyl Butoxide Facilitates the Characterisation of Metabolic Resistance. *Pest Manag. Sci.* 65, 150–154. doi:10.1002/ps.1661

Naqqash, M. N., Gökçe, A., Aksoy, E., and Bakhsh, A. (2020). Downregulation of Imidacloprid Resistant Genes Alters the Biological Parameters in Colorado Potato Beetle, *Leptinotarsa decemlineata* Say (Chrysomelidae: Coleoptera). *Chemosphere* 240, 124857. doi:10.1016/j.chemosphere.2019.124857

Nascimento, A. R. B. d., Fresia, P., Cônsoli, F. L., and Omoto, C. (2015). Comparative Transcriptome Analysis of Lufenuron-Resistant and Susceptible Strains of *Spodoptera Frugiperda* (Lepidoptera: Noctuidae). *BMC Genomics* 16, 985. doi:10.1186/s12864-015-2183-z

Nawaz, M., Hafeez, M., Mabubu, J. I., Dawar, F. U., Li, X., Khan, M. M., et al. (2018). Transcriptomic Analysis of Differentially Expressed Genes and Related Pathways in *Harmonia axyridis* after Sulfoxaflor Exposure. *Int. J. Biol. Macromolecules* 119, 157–165. doi:10.1016/j.ijbiomac.2018.07.032

Nehare, S., Moharil, M. P., Ghodki, B. S., Lande, G. K., Bisane, K. D., Thakare, A. S., et al. (2010). Biochemical Analysis and Synergistic Suppression of Indoxacarb Resistance in Plutella Xylostella L. *J. Asia-Pacific Entomol.* 13, 91–95. doi:10.1016/j.aspen.2009.12.002

Riveron, J. M., Irving, H., Ndula, M., Barnes, K. G., Ibrahim, S. S., Paine, M. J. I., et al. (2013). Directionally Selected Cytochrome P450 Alleles Are Driving the Spread of Pyrethroid Resistance in the Major Malaria Vector Anopheles Funestus. *Proc. Natl. Acad. Sci. U.S.A.* 110, 252–257. doi:10.1073/pnas.1216705110

Robertson, J. L., and Preisler, H. K. (1992). *Pesticide Bioassays with Arthropods*. Boca Raton, FL: CRC Press, CRC.

Scott, J. G. (1999a). Cytochromes P450 and Insecticide Resistance. *Insect Biochem. Mol. Biol.* doi:10.1016/S0965-1748(99)00038-7

Scott, J. G. (1999b). Cytochromes P450 and Insecticide Resistance. *Insect Biochem. Mol. Biol.* 29, 757–777. doi:10.1016/S0965-1748(99)00038-7

Shi, Y., Wang, H., Liu, Z., Wu, S., Yang, Y., Feyereisen, R., et al. (2018). Phylogenetic and Functional Characterization of Ten P450 Genes from the CYP6AE Subfamily of *Helicoverpa Armigera* Involved in Xenobiotic Metabolism. *Insect Biochem. Mol. Biol.* 93, 79–91. doi:10.1016/j.ibmb.2017.12.006

Sun, Z., Shi, Q., Li, Q., Wang, R., Xu, C., Wang, H., et al. (2019). Identification of a Cytochrome P450 CYP6AB60 Gene Associated with Tolerance to Multi-Plant Allelochemicals from a Polyphagous Caterpillar Tobacco Cutworm (*Spodoptera Litura*). *Pestic. Biochem. Physiol.* 154, 60–66. doi:10.1016/j.pestbp.2018.12.006

Tang, B., Cheng, Y., Li, Y., Li, W., Ma, Y., Zhou, Q., et al. (2020). Adipokinetic Hormone Enhances CarE -mediated Chlorpyrifos Resistance in the Brown Planthopper, Nilaparvata Lugens. *Insect Mol. Biol.* 29, 511–522. doi:10.1111/imb.1265910.1111/imb.12659

Thompson, G. D., and Dutton, B. (2003). Insecticide Resistance Action Committee (IRAC). *Pest Outlook* 14, 146. doi:10.1039/b308501p

Ullah, F., Gul, H., and Desneux, N. (2019). Imidacloprid Induced Hormesis Effects on Demographic Traits of the Melon Aphid, Aphis Gossypii. *Entomolgen* 39, 325–337. doi:10.1127/entomologia/2019/0892

Ullah, F., Gul, H., Tariq, K., Murtaza, M., Ali, A., Desneux, N., et al. (2021). Expression changes of cytochrome P450 genes at low lethal and sublethal concentrations of acetamiprid in melon aphid, Aphis gossypii January 2021. Conference: International Conference on Smart Plant Protection At: Institute of Plant Protection, MNS University of Agriculture, Multan SPP-IPM-104

Ullah, F., Gul, H., Tariq, K., Desneux, N., Gao, X., and Song, D. (2020a). Functional analysis of cytochrome P450 genes linked with acetamiprid resistance in melon aphid, Aphis gossypii. *Pestic. Biochem. Physiol* 170, 104687. doi:10.1016/j.pestbp.2020.104687

Ullah, F., Gul, H., Yousaf, H. K., Xiu, W., Qian, D., and Gao, X. (2020b). Author Correction: Impact of low lethal concentrations of buprofezin on biological traits and expression profile of chitin synthase 1 gene (CHS1) in melon aphid, Aphis gossypii. *Sci. Rep.* 9 (1), 12291. doi:10.1038/s41598-020-74318-z

van Asperen, K. (1962). A Study of Housefly Esterases by Means of a Sensitive Colorimetric Method. *J. Insect Physiol.* 8, 401–416. doi:10.1016/0022-1910(62)90074-4

Vontas, J. G., Small, G. J., and Hemingway, J. (2000). Comparison of Esterase Gene Amplification, Gene Expression and Esterase Activity in Insecticide Susceptible and Resistant Strains of the Brown Planthopper, Nilaparvata Lugens (Stal). *Insect Mol. Biol.* 9, 655–660. doi:10.1046/j.1365-2583.2000.00228.x

Wang, K., Zhao, J., Han, Z., and Chen, M. (2022). Comparative Transcriptome and RNA Interference Reveal CYP6DC1 and CYP380C47 Related to Lambda-Cyhalothrin Resistance in Rhopalosiphum Padi. *Pestic. Biochem. Physiol.* 183, 105088. doi:10.1016/j.pestbp.2022.105088

Wang, R.-L., Zhu-Salzman, K., Baerson, S. R., Xin, X.-W., Li, J., Su, Y.-J., et al. (2017). Identification of a Novel Cytochrome P450 CYP321B1 Gene from Tobacco Cutworm (*Spodoptera Litura*) and RNA Interference to Evaluate its Role in Commonly Used Insecticides. *Insect Sci.* 24, 235–247. doi:10.1111/1744-7917.12315

Wang, X., Chen, Y., Gong, C., Yao, X., Jiang, C., and Yang, Q. (2018a). Molecular Identification of Four Novel Cytochrome P450 Genes Related to the Development of Resistance of *Spodoptera Exigua* (Lepidoptera: Noctuidae) to Chlorantraniliprole. *Pest Manag. Sci.* 74, 1938–1952. doi:10.1002/ps.4898

Wang, X., Huang, Q., Hao, Q., Ran, S., Wu, Y., Cui, P., et al. (2018b). Insecticide Resistance and Enhanced Cytochrome P450 Monooxygenase Activity in Field Populations of *Spodoptera Litura* from Sichuan, China. *Crop Prot.* 106, 110–116. doi:10.1016/j.cropro.2017.12.020

Wang, X., Khakame, S. K., Ye, C., Yang, Y., and Wu, Y. (2013). Characterisation of Field-Evolved Resistance to Chlorantraniliprole in the Diamondback moth,Plutella Xylostella, from China. *Pest Manag. Sci.* 69, 661–665. doi:10.1002/ps.3422

Wang, X., Lou, L., and Su, J. (2019). Prevalence and Stability of Insecticide Resistances in Field Population of Spodoptera Litura (Lepidoptera: Noctuidae) from Huizhou, Guangdong Province, China. *J. Asia-Pacific Entomol.* 22, 728–732. doi:10.1016/j.aspen.2019.05.009

Wang, X., Xiang, X., Yu, H., Liu, S., Yin, Y., Cui, P., et al. (2018c). Monitoring and Biochemical Characterization of Beta-Cypermethrin Resistance in *Spodoptera Exigua* (Lepidoptera: Noctuidae) in Sichuan Province, China. *Pestic. Biochem. Physiol.* 146, 71–79. doi:10.1016/j.pestbp.2018.02.008

Wee, C. W., Lee, S. F., Robin, C., and Heckel, D. G. (2008). Identification of Candidate Genes for Fenvalerate Resistance inHelicoverpa Armigerausing cDNA-AFLP. *Insect Mol. Biol.* 17, 351–360. doi:10.1111/j.1365-2583.2008.00809.x

Wing, K. D., Sacher, M., Kagaya, Y., Tsurubuchi, Y., Mulderig, L., Connair, M., et al. (2000). Bioactivation and Mode of Action of the Oxadiazine Indoxacarb in Insects. *Crop Prot.* 19, 537–545. doi:10.1016/S0261-2194(00)00070-3

Wu, S., Yang, Y., Yuan, G., Campbell, P. M., Teese, M. G., Russell, R. J., et al. (2011). Overexpressed Esterases in a Fenvalerate Resistant Strain of the Cotton Bollworm, *Helicoverpa Armigera*. *Insect Biochem. Mol. Biol.* 41, 14–21. doi:10.1016/j.ibmb.2010.09.007

Xiao, Y., Liu, K., Zhang, D., Gong, L., He, F., Soberón, M., et al. (2016). Resistance to Bacillus Thuringiensis Mediated by an ABC Transporter Mutation Increases Susceptibility to Toxins from Other Bacteria in an Invasive Insect. *Plos Pathog.* 12, e1005450. doi:10.1371/journal.ppat.1005450

Xu, J., Su, X., Bonizzoni, M., Zhong, D., Li, Y., Zhou, G., et al. (2018). Comparative Transcriptome Analysis and RNA Interference Reveal CYP6A8 and SNPs Related to Pyrethroid Resistance in *Aedes albopictus*. *Plos Negl. Trop. Dis.* 12, e0006828. doi:10.1371/journal.pntd.0006828

Yang, X., Deng, S., Wei, X., Yang, J., Zhao, Q., Yin, C., et al. (2020). MAPK-directed Activation of the Whitefly Transcription Factor CREB Leads to P450-Mediated Imidacloprid Resistance. *Proc. Natl. Acad. Sci. U.S.A.* 117, 10246–10253. doi:10.1073/pnas.1913603117

Zhang, D.-d., Xiao, X. U., Xu, Y., Yang, W. U., Wu, Q.-l., and Wu, K.-m. (2021). Insecticide Resistance Monitoring for the Invasive Populations of Fall Armyworm, *Spodoptera Frugiperda* in China. *J. Integr. Agric.* 20, 783–791. doi:10.1016/S2095-3119(20)63392-5

Zhang, J., Khan, S. A., Heckel, D. G., and Bock, R. (2017). Next-Generation Insect-Resistant Plants: RNAi-Mediated Crop Protection. *Trends Biotechnol.* 35, 871–882. doi:10.1016/j.tibtech.2017.04.009

Zhang, L., Liu, B., Zheng, W., Liu, C., Zhang, D., Zhao, S., et al. (2020). Genetic Structure and Insecticide Resistance Characteristics of Fall Armyworm Populations Invading China. *Mol. Ecol. Resour.* 20, 1682–1696. doi:10.1111/1755-0998.13219

Zhang, X., Liu, X., Ma, J., and Zhao, J. (2013). Silencing of Cytochrome P450 CYP6B6 Gene of Cotton Bollworm (*Helicoverpa Armigera*) by RNAi. *Bull. Entomol. Res.* 103, 584–591. doi:10.1017/S0007485313000151

Zhao, C., Tang, T., Feng, X., and Qiu, L. (2014). Cloning and Characterisation of NADPH-dependent Cytochrome P450 Reductase Gene in the Cotton bollworm,Helicoverpa Armigera. *Pest Manag. Sci.* 70, 130–139. doi:10.1002/ps.3538

Zhao, J., Liu, N., Ma, J., Huang, L., and Liu, X. (2016). Effect of Silencing CYP6B6 of *Helicoverpa Armigera* (Lepidoptera: Noctuidae) on its Growth, Development, and Insecticide Tolerance. *J. Econ. Entomol.* 109, 2506–2516. doi:10.1093/jee/tow181

Zhao, P., Xue, H., Zhu, X., Wang, L., Zhang, K., Li, D., et al. (2022). Silencing of Cytochrome P450 Gene CYP321A1 Effects Tannin Detoxification and Metabolism in *Spodoptera Litura*. *Int. J. Biol. Macromolecules* 194, 895–902. doi:10.1016/j.ijbiomac.2021.11.144

Zhao, Y.-X., Huang, J.-M., Ni, H., Guo, D., Yang, F.-X., Wang, X., et al. (2020). Susceptibility of Fall Armyworm, Spodoptera Frugiperda (J.E. Smith), to Eight Insecticides in China, with Special Reference to Lambda-Cyhalothrin. *Pestic. Biochem. Physiol.* 168, 104623. doi:10.1016/j.pestbp.2020.104623

Conflict of Interest: The authors declare that the research was conducted in the absence of any commercial or financial relationships that could be construed as a potential conflict of interest.

Publisher's Note: All claims expressed in this article are solely those of the authors and do not necessarily represent those of their affiliated organizations, or those of the publisher, the editors and the reviewers. Any product that may be evaluated in this article, or claim that may be made by its manufacturer, is not guaranteed or endorsed by the publisher.

frontiers | Frontiers in Physiology

ORIGINAL RESEARCH
published: 15 June 2022
doi: 10.3389/fphys.2022.879216

Physiological Responses of the Firefly *Pyrocoelia analis* (Coleoptera: Lampyridae) to an Environmental Residue From Chemical Pesticide Imidacloprid

Yi-zhe Wang[1], *Cheng-quan Cao*[2] *and Dun Wang*[1]*

[1]State Key Laboratory of Crop Stress Biology for Arid Areas, Northwest A&F University, Yangling, China, [2]College of Life Science, Leshan Normal University, Leshan, China

Imidacloprid, a neonicotinoid insecticide, is widely applied to control insect pests across a broad spectrum. Though the impact of residues from this chemical pesticide on non-target organisms in the field has been reported, it was not well characterized across a wide range of ecosystems, especially for some species considered as environmental indicators that live in forests. The effects of sublethal dose of imidacloprid on firefly, *Pyrocoelia analis*, were analyzed physiologically and biochemically in this study to better understand the impact of chemical pesticide application on environmental indicators such as fireflies. After imidacloprid treatment, the midgut tissues of the larva presented an abnormal morphology featured as atrophy of fat body cells, shrinking cells, and the destruction of a midgut structure. The activities of antioxidant enzymes, superoxide dismutase, catalase, and peroxidase were noticeably increased during early exposure to sublethal imidacloprid and then decreased at later stages. The malondialdehyde content significantly increased after 12 h of exposure to imidacloprid compared with the control. Similarly, the enzyme activities of polyphenol oxidase and acetylcholinesterase were increased after the imidacloprid treatment and then decreased at the later stage. In summary, a sublethal dose of imidacloprid caused destructive change in the tissue structure, and this damage was followed by an excessive reactive oxygen species that could not be eliminated by antioxidant enzymes. Our results indicated that the residues of imidacloprid might cause severe toxicity to non-target insects in the environment even far away from the agro-ecosystem where the chemicals were applied.

Keywords: Pyrocoelia analis, imidacloprid, toxicology, antioxidant enzyme activity, tissue structure

OPEN ACCESS

Edited by:
Ran Wang,
Beijing Academy of Agricultural and Forestry Sciences, China

Reviewed by:
Youssef Dewer,
Agricultural Research Center, Egypt
Lin Jin,
Nanjing Agricultural University, China

***Correspondence:**
Dun Wang
wanghande@nwsuaf.edu.cn
dunwang@foxmail.com

Specialty section:
This article was submitted to Invertebrate Physiology, a section of the journal Frontiers in Physiology

Received: *19 February 2022*
Accepted: *09 May 2022*
Published: *15 June 2022*

Citation:
Wang Y-z, Cao C-q and Wang D (2022) Physiological Responses of the Firefly Pyrocoelia analis (Coleoptera: Lampyridae) to an Environmental Residue From Chemical Pesticide Imidacloprid. Front. Physiol. 13:879216. doi: 10.3389/fphys.2022.879216

INTRODUCTION

Since imidacloprid [1-(6-chloro-3-pyridylmethyl)-N-nitroimidazolidin-2-ylideneamine] was launched in 1991 by Bayer, it has become one of the most widely used neonicotinoid insecticides with a market share of more than 25% of global pesticide sales due to its high efficiency and broad spectrum (Bass et al., 2015; Kohl et al., 2019). Since its introduction, environmental problems caused by the widespread use of imidacloprid have become increasingly prominent (Morrissey et al., 2015; Pietrzak et al., 2020; Thompson et al., 2020). Several studies have

documented that these neonicotinoids persist in the environment for a long time and the contents of neonicotinoid pesticides in different farmlands were all present at the ng/g level (Li et al., 2018; Thompson et al., 2020). Imidacloprid can competitively bind to nicotinic acetylcholine receptors (nAChRs), and the postsynaptic nAChRs are blocked irreversibly, causing the continuous conduction of nerve impulses and thus producing lethal effects (Matsuda et al., 2001; Cartereau et al., 2021). Apart from acting on target organisms, imidacloprid can be dispersed in other non-target organisms and accumulate in the environment by different types of applications (Cloyd and Bethke, 2011; Goulson, 2013; Sharma et al., 2019; Singh and Leppanen, 2020). Most of the residuals are nonbiodegradable and toxic, and several studies have documented that imidacloprid can persist in the environment for a long time (Brunet et al., 2004; Flores-Cespedes et al., 2012) and the contents of neonicotinoid pesticides in different farmlands are present at the ng g^{-1} level (Li et al., 2018; Thompson et al., 2020).

In previous studies, the impact of imidacloprid on non-target species has been investigated, and we know that imidacloprid leads to changes in physiological and biochemical parameters (Vohra et al., 2014; Siregar et al., 2021), Seifert and Stollberg (2005) performed interactions of imidacloprid with the nAChRs of embryonic frog muscle cells and found that imidacloprid induces the contraction of embryonic frog muscle at doses as low as 3.3×10^{-7} M. Xia et al. (2016) found that the cysts of the loach tests were disorganized and the interstitial tissue was increased when the loach was exposed to imidacloprid. Moreover, the low dose of imidacloprid resulted in marked irregularities and fragmentation of midgut cells in earthworms (Dittbrenner et al., 2011). The exposure to imidacloprid led to changes in the biochemical parameters of the Pacific white shrimp *Litopenaeus vannamei*, which caused oxidative stress, retarded growth, and immune and tissue damage (Fu et al., 2022). Pervez and Manzoor (2020) found that physiological and behavioral functions for normal foraging and colony maintenance were modified in honeybees (*Apis mellifera*) exposed to 1.25, 2.5, and 5 mg L^{-1} imidacloprid, respectively.

Exposures to low concentrations of imidacloprid have been reported to change the physiological responses of organisms (Zhang et al., 2014). Moreover, the AChE activity, antioxidant enzyme activities, and MDA contents were considered as the significant biomarkers to investigate the influence of pollutants (Deng et al., 2021; Guo et al., 2022). Under the stress of imidacloprid, the acetylcholinesterase in the synapse cannot metabolize imidacloprid in the postsynaptic nAChRs, and this caused continuous nerve impulses and induced oxidative stress (Jepson et al., 2006; Janner et al., 2021). Reactive oxygen species (ROS) can be produced in living organisms, but excessive ROS can also result in oxidative stress and lipid peroxidation. Malondialdehyde (MDA) is the end product of lipid peroxidation caused by ROS, and the MDA level may also indicate the level of ROS (Chen J. et al., 2015). To protect cells from oxidative stress, some antioxidant and detoxifying enzymes scavenge the overproduced ROS, such as superoxide dismutase (SOD), catalase (CAT), peroxidase (POD), and polyphenol oxidase (PPO) (Maity et al., 2008; Chen et al., 2018). Thus, the toxic effects of the pesticide on organisms can be indicated by the level of MDA and enzymatic activities.

The firefly is an important species and is considered to be an environmental indicator, has ornamental value, and is also useful to control pests, such as slugs and snails (Ohba, 2005; Fang et al., 2013; Fu and Benno Meyer-Rochow, 2013; Osozawa et al., 2015; Guo, 2017; Sato, 2019). *Pyrocoelia analis* belongs to the order Coleoptera, family Lampyridae (Fu, 2014) and is a common local firefly in most mountain regions of west China. Fireflies are very sensitive to pollution and insecticides (Pearsons et al., 2021) and fireflies have been used as ecological indicators due to their diverse luminescence and flashing behaviors (Fu et al., 2017; Zhang et al., 2019; Zhang et al., 2021). Over the past decades, wild firefly populations have declined globally, and some species were even threatened with extinction (Fu et al., 2017; Chatragadda, 2020; Lewis et al., 2020; Mbugua et al., 2020; Pearsons et al., 2021), and pesticide use was considered as one of the most serious threats to fireflies (Lewis et al., 2020). However, fewer studies have investigated the influence of chemical pesticides on fireflies at very low doses in the environment. In this study, we examined the toxicity of imidacloprid to fireflies, the detoxifying enzyme activity, antioxidant activity, and histological sections were analyzed to understand the effects of sub-lethal dose of imidacloprid on *Pyrocoelia analis*. This study reported the physiological response of imidacloprid to *Pyrocoelia analis*, and we provide a fundamental understanding for the physiological response of fireflies to chemical pesticides.

MATERIALS AND METHODS

Chemicals

Imidacloprid (≥95.5% purity) was purchased from Shandong Sino-agri United Biotechnology Co., Ltd, China. The other chemicals used in the experiment were of analytical grade and were purchased from Tiancheng Chemical Company in Yangling (Shannxi, China).

Insects

All the larvae of one firefly species, *Pyrocoelia analis*, were from the Firefly Breeding Base in Hainan, China. The larvae of the firefly were domesticated for 2 weeks in an insect rearing room (26 ± 1°C, 70% relative humidity and a 12:12 light/dark cycle) in a laboratory and were fed with a snail species that was collected at the Northwest A&F University. After acclimation, some of the third instars larvae were selected and moved to transparent plastic boxes (30 cm × 20 cm × 10 cm) after comparing them with larval developmental parameters available from previous growth experiments. Every transparent plastic box had 60 larvae and the bottom of the box was covered by a moist filter paper.

Determination of Sublethal Concentration

We dissolve imidacloprid with acetone, and diluted it with water at different concentrations (0.025, 0.05, 0.1, 0.2, and 0.4 mg/L). To determine the sublethal concentration of imidacloprid in larvae of *P. analis*, different imidacloprid concentrations were sprayed on the third instar larvae. Three replicates of 30 larvae from each replicate were used for each treatment and a solvent group without

imidacloprid was used as a control. The mortality was recorded after 0, 3, 6, 12, 24, 48, and 72 h. The calculation of the toxicity regression equation and LC_{10} was based on corrected mortality.

Experimental Design

According to the result from the determination of sublethal concentrations, the concentration of 1 mg/L was set in the experiment. Larvae were placed in each transparent plastic box with a filter paper, and the imidacloprid of 1 mg/L concentration was sprayed on the larvae until the filter paper was moist (to make the humidity in the box at 75%). The pesticide treatment group was all tested with triple replicates of 100 larvae in each replicate. All the experiments were maintained under laboratory conditions at 26 ± 1°C under a 12:12 light/dark cycle for 3 days. After the application of imidacloprid, the larvae were collected at the 0, 3, 6, 12, 24, 48, and 72 h for observation of poisoning symptoms, histopathological studies, analysis in enzyme activities (SOD, POD, PPO, CAT and AChE activities), and MDA assays.

Recording of Poisoning Symptoms

The larvae of *P. analis* collected at 0h, 3h, 6h, 12h, 24h, 48h, and 72 h were observed for post-pesticide treatment for the recording of poisoning symptoms. The recording of symptoms was conducted immediately after collection. During this observation, we recorded the curling degree of the larvae, the retraction position of the head, and the illuminator characteristics. The larvae were then photographed in a bright field and dark field, respectively.

Histological Examination

The larvae were collected in a 10 ml tube at different times compared to the control group and treatment group, and placed in a 4% paraformaldehyde solution over 24 h. Then, the samples were dehydrated in ascending grades of alcohol, cleared in xylene, and embedded in paraffin wax (75% alcohol 1H, 85% alcohol 1h, 95% alcohol 1h, 95% alcohol 1H, 95% alcohol 1H, anhydrous ethanol I 1h, anhydrous ethanol II 1H, xylene 1h, xylene 1H, wax I 1 h, and wax II 1H). The samples soaked in wax were embedded in the embedding machine. After cooling in a −20° freezer, the wax blocks were removed from the embedding frame after solidification and trimmed. Approximately 3 μm thin sections were cut on a rotatory microtome (RM 2016, Leica Germany). The ribbons with tissues were stretched and fixed to a clean albumenized glass slide and warmed to 60°C. These glass slides were, then, placed in an incubator overnight for stretching and the removal of bubbles. The slices were sequentially placed in xylene I for 8 min, xylene II for 8 min, anhydrous ethanol I for 6 min, anhydrous ethanol II for 6 min, 95% alcohol for 6 min, 85% alcohol for 6 min, 75% alcohol for 5 min, and rinsed with running water for 5 min. Then, the slices were stained with Harris hematoxylin for 3–8 min and rinsed with running water to remove the excess fuel. After that, the samples were differentiated with 1% hydrochloric acid alcohol for a few seconds and rinsed with tap water. The sections were then stained in eosin staining solution for 1–3 min, they were dehydrated in ascending grades of alcohol (75% alcohol 30s, 85% alcohol 30s, 95% alcohol I 1min, 95% alcohol II 2 min, anhydrous ethanol I 5 min, and anhydrous ethanol II 5 min), cleared in xylene (xylene I 5 min and xylene II 7 min), and covered with neutral gum. The slides were photographed and examined under a microscope (Ds-fi3, High-definition Color Microscope Camera—Nikon Japan).

Enzyme Activity and MDA Assays

The larvae of *P. analis* were collected at 0, 3, 6, 12, 24, 48, and 72 h post-pesticide treatment and then were frozen in the −80°C freezer. Three biological replicates were frozen at each time point. Once the sample collection was completed, each replicate was weighed and then put into 2 ml tubes with a steel bead and were grinded to a powder state using the Mixer Mill MM 400 (Retsh GmbH, Germany). Then, we added 0.05 M phosphate-buffered saline (PBS) to the tube and mixed it well. The homogenate was centrifuged at 2000 r/min at 4°C for 10 min and the supernatant was used for the measurement of the MDA content, enzyme activities, and protein concentrations. The protein concentration was measured using the method of Bradford (1976). All experimental steps were carried out in accordance with the kit instructions. All the kits used for the enzyme activity tests and MDA contents were purchased from the Jiancheng Bioengineering Institute (Nanjing, China). The results of these enzymatic assays were given in units of enzymatic activity per milligram of protein (U/mg prot), and the MDA content was defined as a nanomole TBA reactive substance per milligram protein (nmol/mg prot). The enzyme activity was the average of the three biological replicates.

Statistical Analysis

All statistics were conducted by SPSS software (SPSS 26.0). Parametric tests were preceded by tests to evaluate the homogeneity of variances. Differences between the treatment and controls regarding enzyme activity and MDA content were determined using the independent-samples *t*-test. A one-way analysis of variance (ANOVA) followed by a LSD multiple comparison test was used to analyze the enzyme activity and MDA content of each group at different times after exposures to imidacloprid, and the significant differences between the groups were compared. Data are expressed as the mean ± standard error (SE). $p < 0.05$ was regarded as statistically significant, and $p < 0.01$ was considered as statistically very significant.

RESULTS

Toxicity of Imidacloprid Against *P. analis*

Under laboratory conditions, imidacloprid is highly toxic to third-instar larvae of *P. analis*. The toxicity regression equation (72 h) was y = -2.123 + 7.892x with a fiducial limit of 95%, and the chi-squared test of goodness of fit for this equation was 1.302. The imidacloprid sublethal concentration LC_{10} was calculated as 0.1 mg/L through the toxicity regression equation, and the fiducial limit of 95% was 0.056—0.144 mg/L.

Poisoning Symptoms and Luminant Characters

The larvae of *P. analis* showed hyperactivity and began moving quickly at the beginning of exposure to imidacloprid. The poisoning symptoms were observed in larvae of *P. analis* when

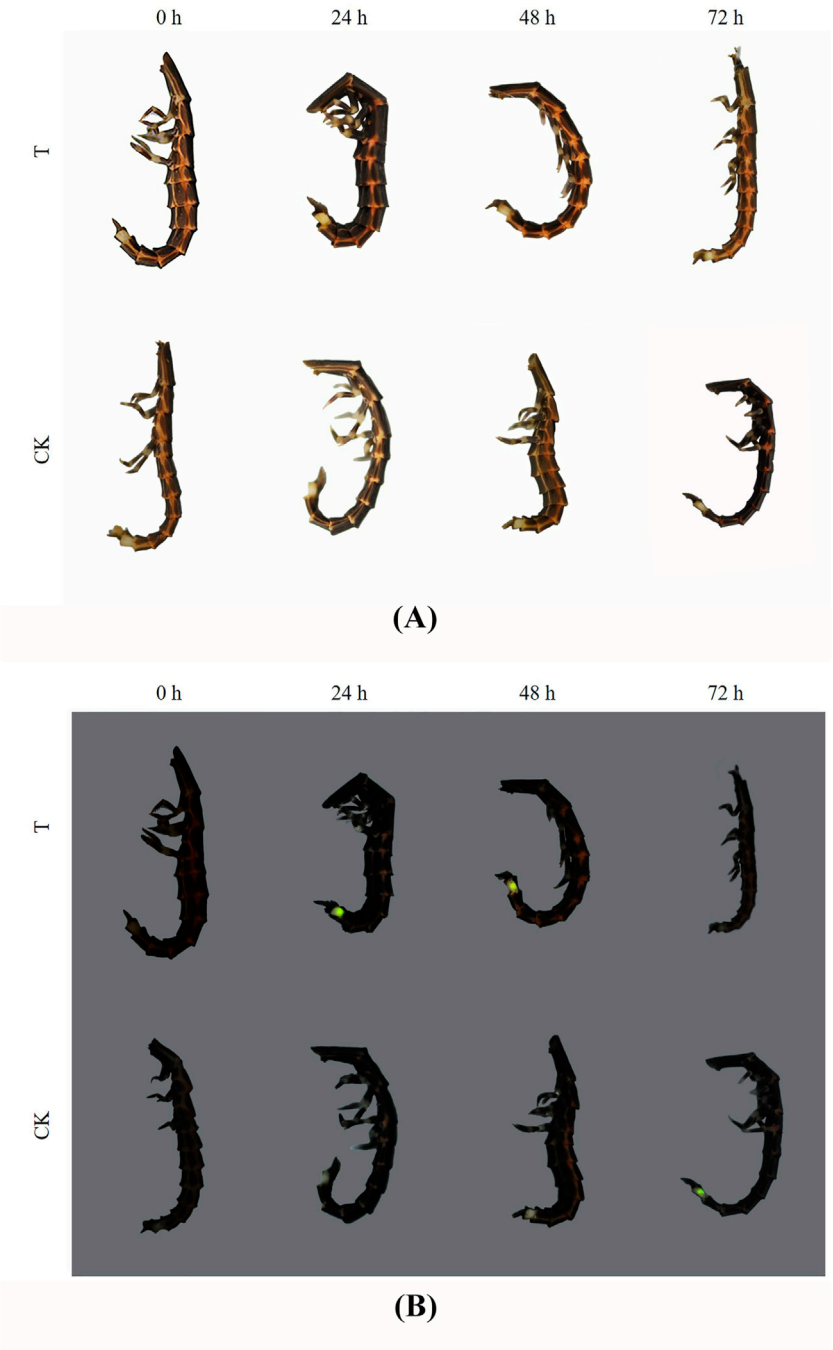

FIGURE 1 | Poisoning symptoms and luminant characters of *P. analis* at different times. **(A)** Photo in the bright field **(B)**. Photo in the darkfield. T: the treated group, CK: the control group.

exposed to imidacloprid after 6 h (**Figure 1**). The heads of the larvae were bent toward the inside of the thorax and the bodies were twisted into a 3D-shape, accompanied with intermittently trembling. After 24 h post-treatment, the larvae laid on their side and the heads of these insects were almost at right angles to the prothorax. Their legs were constantly shaking, and the illuminators began to emit luminescence continuously after responding to gentle stimulation. However, the control group did not respond to gentle stimulation. This persistent glow phenomenon was observed from 12 to 48 h after treatment and the luminous brightness gradually decreased with the increased exposure time to imidacloprid. After 72 h, the head of the larva protruded from the prothorax, and the antennae and legs convulsed continually, then the insects regurgitated gastric juice and the illuminator no longer glowed.

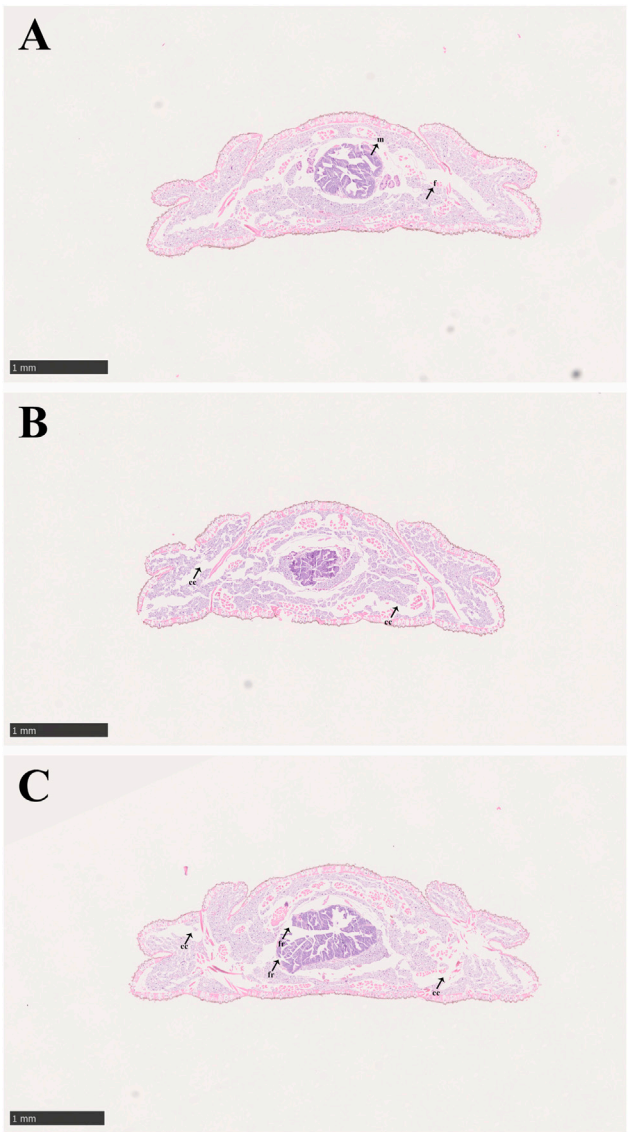

FIGURE 2 | Midgut structure of *P. analis.* **(A)** Control group, **(B)** after 48 h of imidacloprid exposure, **(C)** after 72 h of imidacloprid exposure. m, midgut cell; f, normal fat body; cc, cellular compartmentation; fr, fragmentation of the midgut.

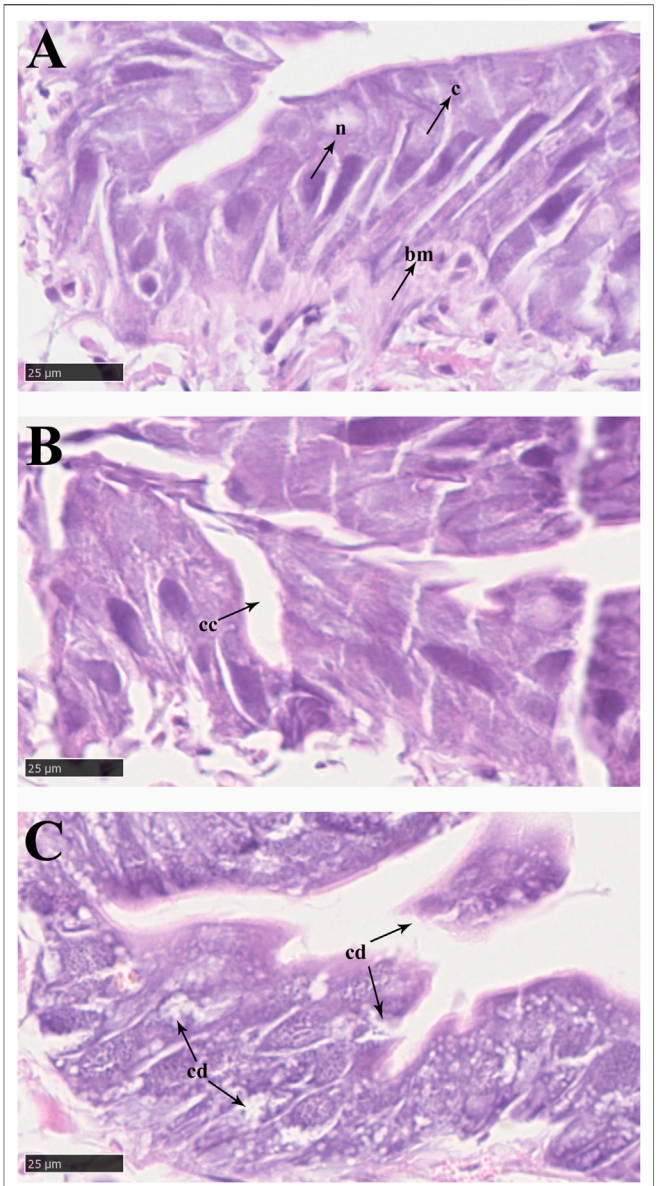

FIGURE 3 | Epithelial cells in the midgut of *P. analis.* **(A)** Control group. **(B)** After 48 h of imidacloprid exposure. **(C)** After 72 h of imidacloprid exposure. bm, basement membrane; c, cytoplasm; n, nucleus; cc, cellular compartmentation; cd, cell debris.

Tissue Histological Profiles

The condition of the midgut tissue deteriorated with increasing imidacloprid exposure time (**Figure 2**). In the control group, the tissues of midgut in larvae of *P. analis* were normal and the structure of the midgut was complete. The cells of the tissues were clear, and the adipocytes around the midgut were normal and tightly arranged (**Figure 2A**). However, the larger gap between the cells was observed in the midgut and adipose tissue during the treatment after 48 h of exposure (**Figure 2B**). With increasing imidacloprid exposure time, we observed shrinking cells, fragmentation of the midgut, and the increased occurrence of intercellular spaces (**Figure 2C**).

In the control groups, the shapes of midgut epithelial cells were neatly arranged and dense, and the nuclei were clearly visible (**Figure 3A**). With increasing exposure time to imidacloprid, the cell structure was unclear, increased cellular compartmentation and irregularity of nuclei shape also arose in midgut tissue after 48 h (**Figure 3B**). Furthermore, after 72 h of imidacloprid exposure, the degradation of the cellular compartmentation was observed in midgut tissue, many midgut cells were destroyed, and there was some cell debris in the lumen (**Figure 3C**). Moreover, the atrophy of fat body cells was also observed after 48 h post-exposure and the shrinking cells fragmented after 72 h of exposure (**Figure 4**).

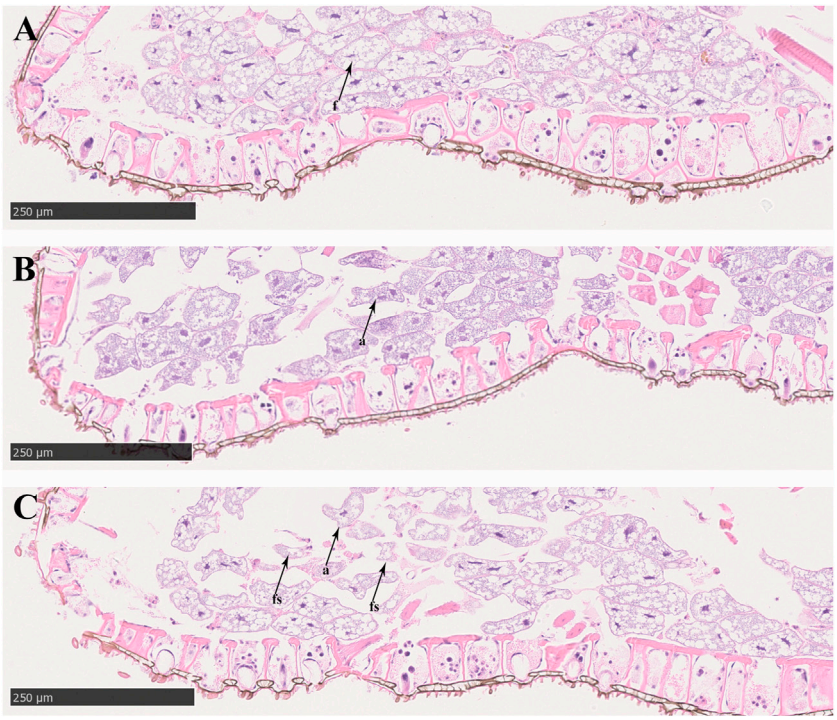

FIGURE 4 | Fat body cell of *P. analis*. **(A)** Control group, **(B)** after 48 h of imidacloprid exposure, **(C)** after 72 h of imidacloprid exposure. f, normal fat body cell; a, atrophy of fat body cell; fs, the fragmented shrinking cell.

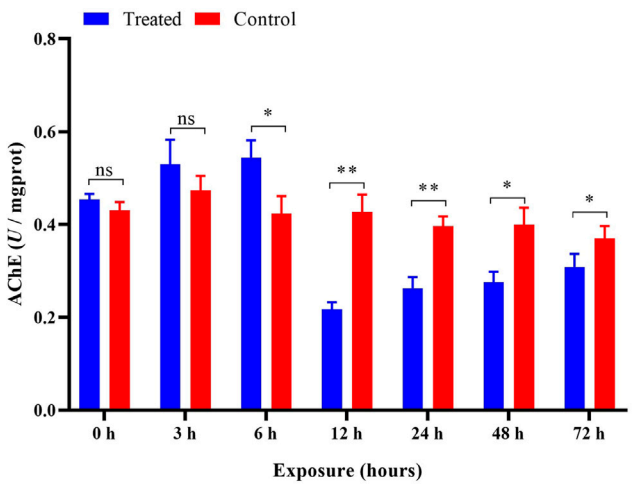

FIGURE 5 | Effects of imidacloprid on the AChE activity of *P. analis*. Each bar represents the mean of three replicates, and the error bars represent the standard deviation (SD). Significant values (*$p < 0.05$, **$p < 0.01$) refer to the difference between exposed samples and the controls.

AChE Activity

Compared with the control, no significant ($p > 0.05$) changes were observed in AChE activity during the 0 h and after 3 h of pesticide exposure. However, after exposure to imidacloprid at 6 h, the activity of AChE was significantly ($p < 0.05$) higher than that of the control group, reaching approximately 129% of the value in the control, and they were significantly inhibited at 12, 24, 48, and 72 h of exposure (**Figure 5**). Univariate analysis (ANOVA) revealed significant influences of different duration ($p < 0.05$) on the activity of AChE (**Table 1**), and AChE activity gradually increased over time and then was significantly inhibited after 12 h in exposed imidacloprid (**Figure 5** and **Table 1**).

Antioxidant Enzyme Activity

The activity of SOD was significantly increased ($p < 0.05$ and $p < 0.01$) after 3–24 h and then was inhibited ($p < 0.05$) after 48 h of exposure compared to the control (**Figure 6A**). The ANOVA revealed significant influences of different duration ($p < 0.05$) on the activity of SOD, and the SOD activity in treatments was increased significantly ($p < 0.05$) with increasing exposure time during 3–24 h (**Table 1**), indicating that the duration of exposure played a crucial role in affecting the activity of SOD in *P. analis*.

Compared with the control, a significant increase in the CAT activity was observed in the *P. analis* larvae after imidacloprid exposure from 6 to 24 h ($p < 0.01$), while the CAT activity was inhibited significantly ($p < 0.01$) after 72 h of exposure (**Figure 6B**). The results of the ANOVA showed the significant influences of different duration ($p < 0.05$) on the activity of CAT, the trend of CAT activity increased first and then decreased, while the peak occurred at 24 h after imidacloprid exposure (**Table 1**).

TABLE 1 | Effects of imidacloprid on antioxidant enzymes, detoxifying enzymes, and malondialdehyde content of *P. analis*. larvae.

(h)	SOD (U/mg protein)	CAT (U/mg protein)	POD (U/mg protein)	PPO (U/mg protein)	AChE (U/mg protein)	MDA (nmol/mg protein)
0	20.367 ± 0.568 d	11.900 ± 0.153 e	2.730 ± 0.090 c	5.920 ± 0.407 b	14.133 ± 0.633 c	0.144 ± 0.002 d
3	23.524 ± 0.640 c	12.733 ± 0.067 e	3.219 ± 0.125 b	8.064 ± 0.306 a	16.853 ± 0.480 b	0.144 ± 0.002 d
6	25.087 ± 0.581 c	14.947 ± 0.260 cd	3.697 ± 0.102 a	7.273 ± 0.425 a	18.567 ± 0.691 a	0.159 ± 0.009 c
12	27.527 ± 0.709 b	16.567 ± 0.338 b	2.412 ± 0.173 c	5.211 ± 0.074 b	16.467 ± 0.437 b	0.192 ± 0.004 b
24	31.098 ± 1.849 a	18.567 ± 0.491 a	2.055 ± 0.044 d	3.665 ± 0.236 c	14.347 ± 0.558 c	0.152 ± 0.006 cd
48	19.740 ± 0.896 d	15.187 ± 0.238 c	2.044 ± 0.072 d	3.955 ± 0.068 c	12.700 ± 0.666 cd	0.227 ± 0.004 a
72	19.984 ± 0.661 d	14.200 ± 0.173 d	1.708 ± 0.072 e	2.406 ± 0.249 d	11.233 ± 0.633 d	0.237 ± 0.001 a

Data are expressed as mean ± SE of three replicates. Different letters (a, b, c, d, and e) indicate statistical differences between groups at the $p < 0.05$ *level at the same column.*

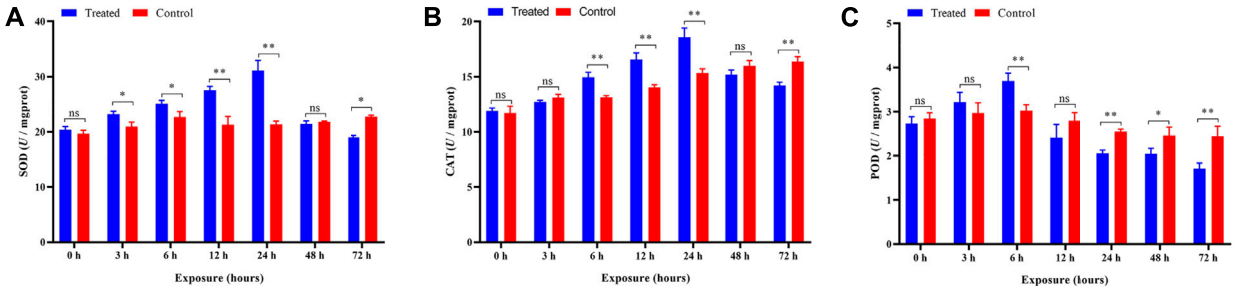

FIGURE 6 | Effects of imidacloprid on the antioxidant activity of *P. analis*. Each bar represents the mean of three replicates, and the error bars represent the standard deviation (SD). Significant values (*$p < 0.05$, **$p < 0.01$) refer to the difference between exposed samples and the controls. **(A)** Effects of imidacloprid on the SOD activity of *P. analis*. **(B)** Effects of imidacloprid on the CAT activity of *P. analis*. **(C)** Effects of imidacloprid on the POD activity of *P. analis*.

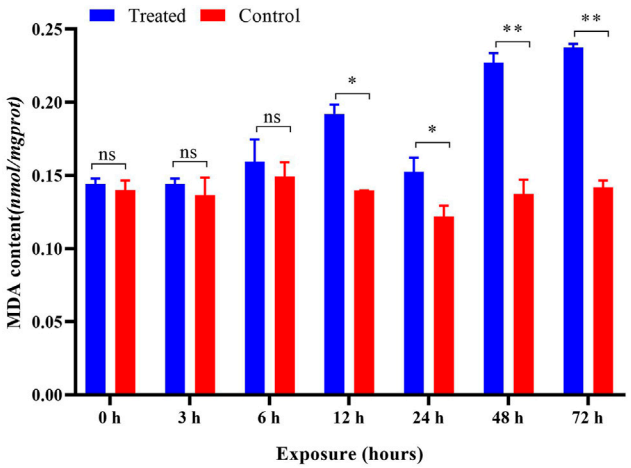

FIGURE 7 | Effects of imidacloprid on the MDA content of *P. analis*. Each bar represents the mean of three replicates, and the error bars represent the standard deviation (SD). Significant values (*$p < 0.05$, **$p < 0.01$) refer to the difference between exposed samples and the controls.

The activity of the POD was significantly elevated in larvae of *P. analis* exposed to imidacloprid after 6 h of treatment. However, the activity of the POD was significantly lower than that of the control after 24 h, 48, and 72 h (**Figure 6C**). The results of the ANOVA showed that the significant ($p < 0.05$) variation of POD activity in *P. analis* was observed with the increase of exposure time to imidacloprid, with POD activity increasing at first and then decreasing, and the peak occurred after 6 h (**Table 1**).

After imidacloprid exposure, the content of MDA was significantly higher than that of the control after 6 h of exposure (**Figure 7**). The results of the ANOVA showed that different duration ($p < 0.05$) played a crucial role in affecting the content of MDA induced by imidacloprid (**Table 1**). With increasing exposure time, the content of MDA was increased significantly in the treatments from 6 to 12 h, decreased from 12 to 24 h, and then increased from 24 to 48 h. There was no significant difference after imidacloprid exposure between 48 and 72 h ($p < 0.05$) (**Table 1**).

Detoxifying Enzyme Activity

After imidacloprid exposure, the PPO activity was significantly higher ($p < 0.05$) than that of the control after 3 h of exposure. In addition, there was a significant decrease in PPO activity in the treatment groups after 12 h indicating an inhibition of the PPO activity (**Figure 8**). Our ANOVA revealed significant influences of different duration ($p < 0.05$) on the activity of PPO, and the trend of PPO activity variation was similar to that of POD activities in *P. analis* larvae infected with imidacloprid; however, the peak value appeared at 3 h, which was 3 h earlier than the changes of POD activities (**Table 1**).

DISCUSSION

Fireflies are an ideal environmental indicator species for pollution and insecticides due to their susceptibility to pesticides and

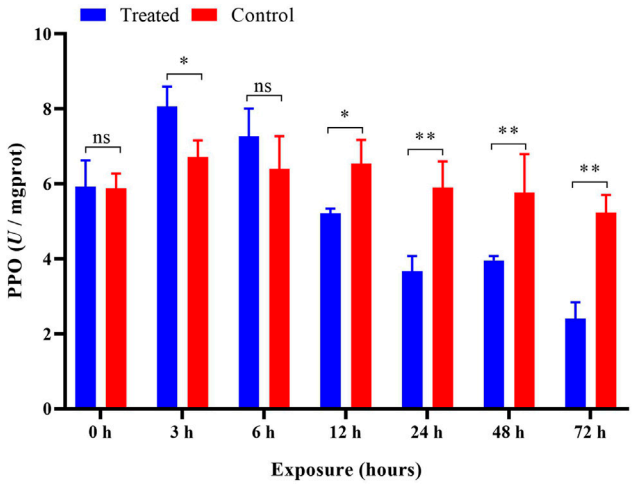

FIGURE 8 | Effects of imidacloprid on the PPO activity of *P. analis*. Each bar represents the mean of three replicates, and the error bars represent the standard deviation (SD). Significant values (*$p < 0.05$, **$p < 0.01$) refer to the difference between exposed samples and the controls.

flashing behaviors (Lewis et al., 2020; Colares et al., 2021; Pearsons et al., 2021; Zhang et al., 2021). Thus, our study investigated the physiological and histological changes in response to imidacloprid and characterized their luminant characters following the imidacloprid exposure. The imidacloprid exposure concentration used in the present study also represented the residual concentrations of imidacloprid in the environment in some regions (0.1 mg/L to over 0.32 mg/L) (Van Dijk et al., 2013; Chen M. et al., 2015; Li et al., 2018). The larvae of *P. analis* exposed to a dose of 0.1 mg/L imidacloprid showed an obvious toxic response within 6 h of exposure, however, only a few died within 72 h. Pearsons et al. (2021) also obtained a similar result after measuring the toxic response and mortality of Eastern North American fireflies when exposed to clothianidin.

In our study, persistent luminescence in the larvae of *P. analis* was observed after 12 h of exposure to imidacloprid. This phenomenon could be related to imidacloprid binding to the nAChRs, which caused the continuous conduction of nerve impulses (Topal et al., 2017; Cartereau et al., 2021). However, some studies reported that bioluminescence could be an auxiliary oxygen detoxifying mechanism in fireflies (Barros and Bechara, 1998; Dubuisson et al., 2004). Bioluminescence is a reaction that requires oxygen (Lambrechts et al., 2014), and reactive oxygen species and superoxide played crucial roles in bioluminescence (Luo and Liu, 2015). Studies have shown a link between bioluminescence and oxygen-free radical metabolism (Richter, 1977; Timmins et al., 2001; Nazari et al., 2013), moreover, antioxidant enzymes and luciferase could cooperate to minimize the oxidative stress (Barros and Bechara, 2001). Therefore, in our study, the persistent luminescence of larvae was likely caused by an excess reactive oxygen species in their body. The first significant increase in the MDA content was detected at 12 h after the imidacloprid exposure, and this coincided with the start of the continuous glow. The level of MDA at 48 h was significantly lower than that at 24 h after exposure to imidacloprid. According to Barros and Bechara (1998), the decline in the MDA content was caused by bioluminescence and antioxidant enzymes that cooperated to minimize the oxidative stress. With increasing exposure time in the treatment, gradual dimming to the extinction of luminescence from larvae was observed over 48–72 h. This could be due to damage to the biological system caused by excess ROS (Toyokuni, 1999; Juan et al., 2021).

In our study, there were significant impairment in midgut cells and fat body cells after 48 and 72 h of imidacloprid exposure. Overall, the observed histological profiles in the fat body cells and midgut tissue included the different shapes of cells and the level of cytoplasmic homogeneity. These changes may be caused by excess ROS in the organisms as organisms can produce excessive ROS under the stimulation of imidacloprid (Janner et al., 2021). The increased levels of ROS lead to oxidative stress, gastrointestinal damage (Xiao et al., 2006), lipid peroxidation, and cell damage (Davalli et al., 2018). Thus, significant oxidative damage was observed in the tissues and cells in our study while ROS in eukaryotic cells is commonly produced during cellular respiration (Juan et al., 2021. In previous studies, similar damage was also reported in honeybees (*Apis mellifera* L.) after 72 h of pesticide exposure (Pervez and Manzoor, 2020). Dittbrenner et al. (2011) showed that there was significant damage to the midgut tissue in *Eisenia fetida* for all imidacloprid exposure times (1, 7, and 14 days). Moreover, cell membranes are sensitive to radical damage due to the presence of polyunsaturated fatty acids. Lipid peroxidation occurs when ROS contacts with membrane phospholipids. Lipid peroxidation causes changes in the membrane structure, damaging the integrity of cells, and imposing oxidative stress resulting in apoptosis (Yadav et al., 2019). This result was also reflected in the morphological changes of fat body cells in this study.

The enzyme AChE catalyzes the hydrolysis of acetycholine, and it is involved in important functions such as biological nerve function regulation and muscle movement (Hemingway et al., 2004). Previous reviews have demonstrated that AChE is induced by exposure to the sublethal doses of neonicotinoids, and it can be used as a biological indicator to identify pesticide residues in terrestrial and freshwater aquatic systems (Fulton and Key, 2001; Moreira et al., 2001; Yadav et al., 2009). In the present study, the activity of AChE was significantly increased at 6 h compared with the control after imidacloprid exposure. The increase in AChE activity may be attributed to the imidacloprid binding to the insect nicotinic receptor (Li et al., 2017). However, compared with the control after imidacloprid exposure, the activity of AChE was markedly inhibited from 12 to 72 h. The inhibitory effects indicated that sublethal imidacloprid could cause harmful damage to the biochemical metabolism of *P. analis*. Li et al. (2017) also obtained a similar result after measuring the AChE activity of *Apis mellifera* and *Apis cerana* when exposed to imidacloprid at different times. During exposure to imidacloprid, AChE activity increased from 0–to 6 h and then decreased after 12–72 h in our study. This phenomenon is mainly related to the morphology of AChE in larvae and the induction of

imidacloprid metabolites on target enzymes (Suchail et al., 2001; Tomalski et al., 2010). The key point of AChE active variation in the present study corresponds with the half-life of imidacloprid (5 h) in bees (Suchail et al., 2004). Therefore, the variation of AChE activity may be associated with the half-life of imidacloprid. The result was consistent with the report of Jin et al. (2015), who found that the sublethal imidacloprid could make the activity of AChE in *Apis mellifera* rise and then fall within 24 h. We feel the effect of imidacloprid on AChE in *P. analis* should be subjected to further investigation.

Previous reviews have demonstrated that pesticides induced oxidative stress leading to the generation of free radicals which caused lipid peroxidation (El-Gendy et al., 2010). The antioxidant enzymes play a vital role in defending against free radicals in organisms and they are the first line to prevent the damage of ROS to the biological system (Rodriguez et al., 2004; Hong et al., 2020). In the antioxidant system of the insects, the functions of SOD, CAT, and POD are to remove excess oxygen free radicals and maintain the redox balance (Felton and Summers, 1995; Wang et al., 2020). Some reviews have reported that slight oxidative stress can induce these antioxidant enzymes (Zhang et al., 2013; Zhang et al., 2014). However, severe oxidative stress can damage the metabolic mechanism of biological systems, causing the inhibition of these enzymes (Siddique et al., 2007; Zhang et al., 2014; Wang et al., 2016; Li et al., 2017; Jameel et al., 2019).

In this present study, we tested the activity of four antioxidant enzymes (SOD, CAT, and POD) in *P. analis* at different times after exposure to imidacloprid. SOD can remove the superoxide (O_2^-) to H_2O_2 and protect the cells from oxidant damage. The results presented have shown that the activity of SOD was significantly increased after 3–24 h of exposure to imidacloprid. This phenomenon indicated that sublethal imidacloprid could induce the biosynthesis of SOD in *P. analis* in the early stages of exposure to pesticides. This result was consistent with the report of Yucel and Kayis (2019), who found that imidacloprid could increase the SOD activity in *Galleria mellonella* L. However, with increasing exposure time, the activity of SOD was significantly decreased from the peak, and SOD activity was inhibited compared with the control after 72 h of exposure. This result indicated that overt oxidative stress had occurred and SOD fails to scavenge the overproduction of ROS. According to Wang et al. (2016), the main reason for the decline in SOD was the excess O_2^- which inhibited the synthesis of SOD. Ge et al. (2015) showed that the trend of SOD activity variation was due to the metabolism of imidacloprid over time. Siddique et al. (2007) reported that the excessive ROS could render protective mechanisms of the cell ineffectively and inactivate the SOD.

SOD can catalyze the conversion of O_2 to H_2O_2 further detoxified by CAT and POD. CAT is an important antioxidant enzyme, which can scavenge H_2O_2 to H_2O and O_2 (Koivula et al., 2011). In the present study, the trend of CAT activity variation was similar to the SOD activity in *P. analis* larvae infected with imidacloprid. This phenomenon could be explained by the synergistic effect of SOD and CAT (Zhang et al., 2013). With the antioxidant reaction of SOD, the content of H_2O_2 increased, to maintain the balance of hydroxyl radicals (-OH) in the organism, and the activity of CAT also increased accordingly (Ge et al., 2015). Moreover, compared with the control, we observed a sharp decline in SOD and CAT activities at 48 h as compared to 24 h and the CAT activity was inhibited significantly ($p < 0.01$) at 72 h in the treatments. These results could be attributed to enzyme synthesis, inactivation, or assembly of its subunit modification caused by ROS (Verma and Dubey, 2003; Batista-Silva et al., 2019; Jameel et al., 2019). Wang et al. (2016) reported that CAT could be inhibited even under the stress of low-concentration imidacloprid for a long time.

POD is the enzyme that catalyzes the oxidation of substrates with hydrogen peroxide as an electron acceptor. It mainly exists in the peroxisome of the carrier, and it has the dual effect of eliminating the toxicity of hydrogen peroxide and phenols, amines, aldehydes, and benzene (Sunde and Hoekstra, 1980). In the present study, the POD activity was increased at first from 0 to 6 h, although the difference was not significant at 3 h compared with the control, and then decreased from 6 to 72 h. This variation showed that at the beginning of imidacloprid exposure, the POD activity was activated, but the POD activity gradually decreased with the extension of the exposure time. The result was consistent with the report of Zhang et al. (2014), who found that a relatively low concentration of imidacloprid could increase the activity of POD in *Eisenia fetida* over short-term exposures. Zhang et al. (2013) also obtained a similar result after measuring the POD activity of *E. fetida* after exposure to fomesafen at different times.

MDA is the end product of lipid peroxidation, and the MDA level may also indicate the level of ROS (Chen J. et al., 2015) and the extent of cell tissue trauma (Zhang et al., 2013). In the present study, the content of MDA did not change after exposure to imidacloprid at 0, 3, and 6 h. However, it was significantly increased after 12–72 h of exposure as compared to the control. A possible reason for this observation is connected to the ROS content and antioxidant enzyme activity (Wu and Liu, 2012; Wang et al., 2016). At the beginning of exposure to imidacloprid, stimulation of pesticides increased the activity of antioxidant enzymes in organisms (Zhang et al., 2014; Li et al., 2017). However, with the extension of the exposure time, the MDA content in organisms increased gradually due to the accumulation of ROS (Balieira et al., 2018). The increase in the MDA content showed that lipid peroxidation could be caused by sublethal imidacloprid in *P. analis*. Many studies have shown that membrane lipid peroxidation is caused by ROS and this induced many negative effects (Bhattacharyya and Datta, 2001; Schaffazick et al., 2005; Balint et al., 2021). The results of the present study also confirm this point and our results also indicate that MDA has an obvious indicating effect in *P. analis* even under the stress of low concentrations of imidacloprid.

PPO is a copper-containing oxidase that oxidizes monohydric and dihydric phenols to quinones (Zhang and Sun, 2021). PPO is a crucial enzyme for melanin synthesis in insects and usually exists in insect hemolymph in the form of zymogen (Lu et al., 2014). It is activated and hydrolyzed by specific serine protease cascade to generate active PPO, which plays an important role in

insect immune responses (Jiang et al., 1998; Xu et al., 2020; Ma et al., 2010). This enzyme could be an indicator for assessing the toxicity of pesticide residues (Lu et al., 2014). Magierowicz et al. (2020) reported that *Tanacetwn vulgare* essential oil significantly increased the PPO activity in larvae of *Acrobasis advenella* (Lepidoptera: Pyralidae). Ma et al. (2010) showed that cantharidin could significantly inhibit the activity of PPO in the fifth instar larvae of *Mythimna separata*. The results of the present study show that the activity of PPO increased at first and then decreased after imidacloprid exposure. This result was consistent with the report of Li et al. (2017), who found that PPO activity in *Apis mellifera* increased first and then gradually decreased with prolonged time after exposure to sublethal doses of imidacloprid. The PPO is an important immune protein in insects and mediates humoral immunity (Fan et al., 2016). In the present study, we found sublethal imidacloprid inhibited the activity of PPO significantly over 12 h. The inhibition could cause insects to be more susceptible to infection by bacteria (Zhao et al., 2007), fungi (Yassine et al., 2012; Dubovskiy et al., 2013), and some other microorganisms (Binggeli et al., 2014).

The impacts of pesticides on insect fitness have been extensively studied, and some pesticides reduced the fitness of bee larvae of both *Apis mellifera* and *Apis cerana* (He et al., 2022). Even sublethal imidacloprid can affect foraging and colony fitness in *Monomorium antarcticum* and *Linepithema humile* (Barbieri et al., 2013). In particular, neonicotinoid insecticides may reduce the fitness by impairing sperm and hypopharyngeal glands (Minnameyer et al., 2021). As imidacloprid used in our study is a member of the neonicotinoid group, it caused toxicity to firefly larvae implying that imidacloprid might reduce the fitness of firefly even at a very low dose.

Previous studies found that the fitness of the insect could be affected by the antioxidant enzyme activity (Dhivya et al., 2018), and a reduction in antioxidant enzyme activity was accompanied by a decrease in insect fitness (Slos et al., 2009; Xie et al., 2015; Cai et al., 2018). The possible reason for a reduction in fitness was impaired digestion and absorption caused by the released free radicals when the antioxidant enzyme activity was reduced (Rahimi et al., 2018). Similarly, we found that the antioxidant enzyme activity of *Pyrocoelia analis* was inhibited significantly after the treatment of low dose imidacloprid. These results implied that residues of imidacloprid in the environment affect the fitness of fireflies.

As a widely used chemical pesticide in a range of agro-ecosystem, imidaclorpid residues could be easily spread throughout the whole ecosystems. Although there were many species in the agro-ecosystem affected by the imidacloprid residues that we previously discussed, very few studies have focused on the effects of this chemical on remote regions and other ecosystems. This study characterized the toxicology of a sub-lethal dose of imidacloprid for fireflies that inhabit a forest ecosystem. The very low dose of imidacloprid caused irreversible physiological changes to the fireflies and overt toxicity implying that the chemical pesticide residues affected the whole ecosystem and not only the agroecosystem where it was applied. This potential threat to ecosystem health has not been seriously addressed by the region's agricultural administration or by farmers.

DATA AVAILABILITY STATEMENT

The original contributions presented in the study are included in the article/Supplementary Material; further inquiries can be directed to the corresponding author.

AUTHOR CONTRIBUTIONS

DW conceived the project and provided laboratory condition and funding. YZW and CQC raised and maintained the insects. YZW conducted the experiments, data collection, and software analysis. YZW performed data analysis and wrote the original draft of the manuscript. DW performed writing—review and editing of the manuscript. All authors read the manuscript and approved the submitted version.

FUNDING

This study was supported by a grant of the Shaanxi Key Project of Science and Technology (2020zdzx03-03-02).

ACKNOWLEDGMENTS

The authors thank Ken Smith from the University of Arizona for his editing of the scientific writing. They thank Chao Tong from Chongsheng Biotechnology Co., Ltd., in Sichuan Province for the help in insect rearing and managing. They also thank Yun Meng from the Institute of Entomology, Northwest A&F University, for her assistance in laboratory tests.

REFERENCES

Balieira, K. V. B., Mazzo, M., Bizerra, P. F. V., Guimarães, A. R., Nicodemo, D., and Mingatto, F. E. (2018). Imidacloprid-induced Oxidative Stress in Honey Bees and the Antioxidant Action of Caffeine. *Apidologie* 49, 562–572. doi:10.1007/s13592-018-0583-1

Bálint, B., Balogh, K., Mézes, M., and Szabó, B. (2021). Differences in the Effects of Sodium Selenate and Sodium Selenite on the Mortality, Reproduction, Lipid Peroxidation and Glutathione Redox Status of Folsomia candida Willem 1902 (Collembola). *Eur. J. Soil Biol.* 107, 103361. doi:10.1016/j.ejsobi.2021.103361

Barbieri, R. F., Lester, P. J., Miller, A. S., and Ryan, K. G. (2013). A Neurotoxic Pesticide Changes the Outcome of Aggressive Interactions between Native and Invasive Ants. *Proc. R. Soc. B* 280, 20132157. doi:10.1098/rspb.2013.2157

Barros, M. P., and Bechara, E. J. H. (1998). Bioluminescence as a Possible Auxiliary Oxygen Detoxifying Mechanism in Elaterid Larvae. *Free Radic. Biol. Med.* 24, 767–777. doi:10.1016/s0891-5849(97)00335-3

Barros, M. P., and Bechara, E. J. H. (2001). Daily Variations of Antioxidant Enzyme and Luciferase Activities in the Luminescent Click-Beetle Pyrearinus Termitilluminans: Cooperation against Oxygen Toxicity. *Insect Biochem. Mol. Biol.* 31, 393–400. doi:10.1016/s0965-1748(00)00132-6

Bass, C., Denholm, I., Williamson, M. S., and Nauen, R. (2015). The Global Status of Insect Resistance to Neonicotinoid Insecticides. *Pesticide Biochem. Physiology* 121, 78–87. doi:10.1016/j.pestbp.2015.04.004

Batista-Silva, W., Heinemann, B., Rugen, N., Nunes-Nesi, A., Araújo, W. L., Braun, H. P., et al. (2019). The Role of Amino Acid Metabolism during Abiotic Stress Release. *Plant Cell. Environ.* 42, 1630–1644. doi:10.1111/pce.13518

Bhattacharyya, J., and Datta, A. G. (2001). Studies on the Effects of Lipopolysaccharide on Lipid Peroxidation of Erythrocyte and its Reversal by Mannitol and Glycerol. *J. Physiol. Pharmacol.* 52, 145–152.

Binggeli, O., Neyen, C., Poidevin, M., and Lemaitre, B. (2014). Prophenoloxidase Activation Is Required for Survival to Microbial Infections in Drosophila. *PLoS Pathog.* 10, e1004067. doi:10.1371/journal.ppat.1004067

Brunet, J.-L., Maresca, M., Fantini, J., and Belzunces, L. P. (2004). Human Intestinal Absorption of Imidacloprid with Caco-2 Cells as Enterocyte Model. *Toxicol. Appl. Pharmacol.* 194, 1–9. doi:10.1016/j.taap.2003.08.018

Cai, Q., Wang, J.-J., Shao, W., Ying, S.-H., and Feng, M.-G. (2018). Rtt109-dependent Histone H3 K56 Acetylation and Gene Activity Are Essential for the Biological Control Potential of Beauveria Bassiana. *Pest. Manag. Sci.* 74, 2626–2635. doi:10.1002/ps.5054

Cartereau, A., Taillebois, E., Le Questel, J.-Y., and Thany, S. H. (2021). Mode of Action of Neonicotinoid Insecticides Imidacloprid and Thiacloprid to the Cockroach Pameα7 Nicotinic Acetylcholine Receptor. *Ijms* 22, 9880. doi:10.3390/ijms22189880

Chatragadda, R. (2020). Decline of Luminous Firefly Abscondita Chinensis Population in Barrankula, Andhra Pradesh, India. *Int. J. Trop. Insect Sci.* 40, 461–465. doi:10.1007/s42690-019-00078-7

Chen, C., Hu, W., Zhang, R., Jiang, A., and Liu, C. (2018). Effects of Hydrogen Sulfide on the Surface Whitening and Physiological Responses of Fresh-Cut Carrots. *J. Sci. Food Agric.* 98, 4726–4732. doi:10.1002/jsfa.9007

Chen, J., Zeng, L., Xia, T., Li, S., Yan, T., Wu, S., et al. (2015). Toward a Biomarker of Oxidative Stress: a Fluorescent Probe for Exogenous and Endogenous Malondialdehyde in Living Cells. *Anal. Chem.* 87, 8052–8056. doi:10.1021/acs.analchem.5b02032

Chen, M., Yi, Q., Hong, J., Zhang, L., Lin, K., and Yuan, D. (2015). Simultaneous Determination of 32 Antibiotics and 12 Pesticides in Sediment Using Ultrasonic-Assisted Extraction and High Performance Liquid Chromatography-Tandem Mass Spectrometry. *Anal. Methods* 7, 1896–1905. doi:10.1039/c4ay02895c

Cloyd, R. A., and Bethke, J. A. (2011). Impact of Neonicotinoid Insecticides on Natural Enemies in Greenhouse and Interiorscape Environments. *Pest. Manag. Sci.* 67, 3–9. doi:10.1002/ps.2015

Colares, C., Roza, A. S., Mermudes, J. R. M., Silveira, L. F. L., Khattar, G., Mayhew, P. J., et al. (2021). Elevational Specialization and the Monitoring of the Effects of Climate Change in Insects: Beetles in a Brazilian Rainforest Mountain. *Ecol. Indic.* 120, 106888. doi:10.1016/j.ecolind.2020.106888

Davalli, P., Marverti, G., Lauriola, A., and D'Arca, D. (2018). Targeting Oxidatively Induced DNA Damage Response in Cancer: Opportunities for Novel Cancer Therapies. *Oxidative Med. Cell. Longev.* 2018, 1–21. doi:10.1155/2018/2389523

Deng, S., Wu, Y., Duan, H., Cavanagh, J.-A. E., Wang, X., Qiu, J., et al. (2021). Toxicity Assessment of Earthworm Exposed to Arsenate Using Oxidative Stress and Burrowing Behavior Responses and an Integrated Biomarker Index. *Sci. Total Environ.* 800, 149479. doi:10.1016/j.scitotenv.2021.149479

Dhivya, K., Vengateswari, G., Arunthirumeni, M., Karthi, S., Senthil-Nathan, S., and Shivakumar, M. S. (2018). Bioprospecting of Prosopis Juliflora (Sw.) DC Seed Pod Extract Effect on Antioxidant and Immune System of Spodoptera Litura (Lepidoptera: Noctuidae). *Physiological Mol. Plant Pathology* 101, 45–53. doi:10.1016/j.pmpp.2017.09.003

Dittbrenner, N., Schmitt, H., Capowiez, Y., and Triebskorn, R. (2011). Sensitivity of *Eisenia fetida* in Comparison to Aporrectodea Caliginosa and Lumbricus Terrestris after Imidacloprid Exposure. Body Mass Change and Histopathology. *J. Soils Sediments* 11, 1000–1010. doi:10.1007/s11368-011-0397-5

Dubovskiy, I. M., Whitten, M. M. A., Kryukov, V. Y., Yaroslavtseva, O. N., Grizanova, E. V., Greig, C., et al. (2013). More Than a Colour Change: Insect Melanism, Disease Resistance and Fecundity. *Proc. R. Soc. B* 280, 20130584. doi:10.1098/rspb.2013.0584

Dubuisson, M. n., Marchand, C. c., and Rees, J.-F. (2004). Fire?y Luciferin as Antioxidant and Light Emitter: the Evolution of Insect Bioluminescence. *Luminescence* 19, 339–344. doi:10.1002/bio.789

El-Gendy, K. S., Aly, N. M., Mahmoud, F. H., Kenawy, A., and El-Sebae, A. K. H. (2010). The Role of Vitamin C as Antioxidant in Protection of Oxidative Stress Induced by Imidacloprid. *Food Chem. Toxicol.* 48, 215–221. doi:10.1016/j.fct.2009.10.003

Fan, S. L., Guan, J. M., Yang, B., Lu, A. R., Ling, E. J., and Song, H. S. (2016). Recent Achievements on the Insect Important Innate Immunity Protein Prophenoloxidase. *Chin. Bull. Life Sci.* 28, 70–76. doi:10.13376/j.cbls/2016009

Fang, L., Yang, J.-W., Wang, J.-L., Zhu, J.-Q., and Fu, X.-H. (2013). Preliminary Investigation of Predation of the Snail Bradybaena Ravida by Larvae of the Firefly Pyrocoelia Pectoralis. *Chin. J. Appl. Entomology* 50, 197–202. doi:10.7679/j.issn.2095-1353.2013.025

Felton, G. W., and Summers, C. B. (1995). Antioxidant Systems in Insects. *Arch. Insect Biochem. Physiol.* 29, 187–197. doi:10.1002/arch.940290208

Flores-Céspedes, F., Figueredo-Flores, C. I., Daza-Fernández, I., Vidal-Peña, F., Villafranca-Sánchez, M., and Fernández-Pérez, M. (2012). Preparation and Characterization of Imidacloprid Lignin-Polyethylene Glycol Matrices Coated with Ethylcellulose. *J. Agric. Food Chem.* 60, 1042–1051. doi:10.1021/jf2037483

Fu, X., and Benno Meyer-Rochow, V. (2013). Larvae of the Firefly Pyrocoelia Pectoralis (Coleoptera: Lampyridae) as Possible Biological Agents to Control the Land Snail Bradybaena Ravida. *Biol. Control* 65, 176–183. doi:10.1016/j.biocontrol.2013.02.005

Fu, X. H. (2014). *Chinese Firefly Ecological Guide*. Beijing: The Commercial Press.

Fu, X., Li, J., Tian, Y., Quan, W., Zhang, S., Liu, Q., et al. (2017). Long-read Sequence Assembly of the Firefly Pyrocoelia Pectoralis Genome. *Gigascience* 6, 1–7. doi:10.1093/gigascience/gix112

Fu, Z., Han, F., Huang, K., Zhang, J., Qin, J. G., Chen, L., et al. (2022). Impact of Imidacloprid Exposure on the Biochemical Responses, Transcriptome, Gut Microbiota and Growth Performance of the Pacific White Shrimp Litopenaeus Vannamei. *J. Hazard. Mater.* 424, 127513. doi:10.1016/j.jhazmat.2021.127513

Fulton, M. H., and Key, P. B. (2001). Acetylcholinesterase Inhibition in Estuarine Fish and Invertebrates as an Indicator of Organophosphorus Insecticide Exposure and Effects. *Environ. Toxicol. Chem.* 20, 37–45. doi:10.1002/etc.5620200104

Ge, W., Yan, S., Wang, J., Zhu, L., Chen, A., and Wang, J. (2015). Oxidative Stress and DNA Damage Induced by Imidacloprid in Zebrafish (*Danio rerio*). *J. Agric. Food Chem.* 63, 1856–1862. doi:10.1021/jf504895h

Goulson, D. (2013). REVIEW: An Overview of the Environmental Risks Posed by Neonicotinoid Insecticides. *J. Appl. Ecol.* 50, 977–987. doi:10.1111/1365-2664.12111

Guo, C., Lv, S., Liu, Y., and Li, Y. (2022). Biomarkers for the Adverse Effects on Respiratory System Health Associated with Atmospheric Particulate Matter Exposure. *J. Hazard. Mater.* 421, 126760. doi:10.1016/j.jhazmat.2021.126760

Guo, Q. (2017). "Studies on Biology and Predacious Function of *Pyrocoelia Analis* (Fabricius)," master's thesis. Guizhou: University of Guizhou.

He, Q., Yang, Q., Liu, Q., Hu, Z., Gao, Q., Dong, Y., et al. (2022). The Effects of Beta-cypermethrin, Chlorbenzuron, Chlorothalonil, and Pendimethalin on *Apis mellifera* Ligustica and *Apis cerana* Cerana Larvae Reared *In Vitro*. *Pest Manag. Sci.* 78, 1407–1416. doi:10.1002/ps.6757

Hemingway, J., Hawkes, N. J., McCarroll, L., and Ranson, H. (2004). The Molecular Basis of Insecticide Resistance in Mosquitoes. *Insect Biochem. Mol. Biol.* 34, 653–665. doi:10.1016/j.ibmb.2004.03.018

Hong, Y., Huang, Y., Wu, S., Yang, X., Dong, Y., Xu, D., et al. (2020). Effects of Imidacloprid on the Oxidative Stress, Detoxification and Gut Microbiota of Chinese Mitten Crab, Eriocheir Sinensis. *Sci. Total Environ.* 729, 138276. doi:10.1016/j.scitotenv.2020.138276

Jameel, M., Alam, M. F., Younus, H., Jamal, K., and Siddique, H. R. (2019). Hazardous Sub-cellular Effects of Fipronil Directly Influence the Organismal Parameters of Spodoptera Litura. *Ecotoxicol. Environ. Saf.* 172, 216–224. doi:10.1016/j.ecoenv.2019.01.076

Janner, D. E., Gomes, N. S., Poetini, M. R., Poleto, K. H., Musachio, E. A. S., de Almeida, F. P., et al. (2021). Oxidative Stress and Decreased Dopamine Levels Induced by Imidacloprid Exposure Cause Behavioral Changes in a Neurodevelopmental Disorder Model in *Drosophila melanogaster*. *Neurotoxicology* 85, 79–89. doi:10.1016/j.neuro.2021.05.006

Jepson, J. E. C., Brown, L. A., and Sattelle, D. B. (2006). The Actions of the Neonicotinoid Imidacloprid on Cholinergic Neurons of *Drosophila melanogaster*. *Invert. Neurosci.* 6, 33–40. doi:10.1007/s10158-005-0013-8

Jiang, H., Wang, Y., and Kanost, M. R. (1998). Pro-phenol Oxidase Activating Proteinase from an Insect, Manduca Sexta: A Bacteria-Inducible Protein Similar to Drosophila Easter. *Proc. Natl. Acad. Sci. U.S.A.* 95, 12220–12225. doi:10.1073/pnas.95.21.12220

Jin, S. X., Meng, L. F., and Diao, Q. Y. (2015). Effect of Sublethal Doses of Imidacloprid on Acetylcholinesterase Activity in *Apis mellifera*. *Chin. J. Appl. Entomology* 52, 315–323. doi:10.14378/kacs.2015.52.52.3

Juan, C. A., Pérez de la Lastra, J. M., Plou, F. J., and Pérez-Lebeña, E. (2021). The Chemistry of Reactive Oxygen Species (ROS) Revisited: Outlining Their Role in Biological Macromolecules (DNA, Lipids and Proteins) and Induced Pathologies. *Ijms* 22, 4642. doi:10.3390/ijms22094642

Kohl, K. L., Harrell, L. K., Mudge, J. F., Subbiah, S., Kasumba, J., Osma, E., et al. (2019). Tracking Neonicotinoids Following Their Use as Cotton Seed Treatments. *Peerj* 7, e6805. doi:10.7717/peerj.6805

Koivula, M. J., Kanerva, M., Salminen, J.-P., Nikinmaa, M., and Eeva, T. (2011). Metal Pollution Indirectly Increases Oxidative Stress in Great Tit (*Parus major*) Nestlings. *Environ. Res.* 111, 362–370. doi:10.1016/j.envres.2011.01.005

Lambrechts, D., Roeffaers, M., Goossens, K., Hofkens, J., Van de Putte, T., Schrooten, J., et al. (2014). A Causal Relation between Bioluminescence and Oxygen to Quantify the Cell Niche. *Plos One* 9, e97572. doi:10.1371/journal.pone.0097572

Lewis, S. M., Wong, C. H., Owens, A. C. S., Fallon, C., Jepsen, S., Thancharoen, A., et al. (2020). A Global Perspective on Firefly Extinction Threats. *Bioscience* 70, 157–167. doi:10.1093/biosci/biz157

Li, T. T., Zheng, S. S., Wang, J., Zhao, Y. H., and Li, C. (2018). A Review on Occurence and Transformation Behaviors of Neonicotinoid Pesticides. *Asian J. Ecotoxicol.* 13, 9–21.

Li, Z., Li, M., He, J., Zhao, X., Chaimanee, V., Huang, W.-F., et al. (2017). Differential Physiological Effects of Neonicotinoid Insecticides on Honey Bees: A Comparison between *Apis mellifera* and *Apis cerana*. *Pesticide Biochem. Physiology* 140, 1–8. doi:10.1016/j.pestbp.2017.06.010

Lu, A., Zhang, Q., Zhang, J., Yang, B., Wu, K., Xie, W., et al. (2014). Insect Prophenoloxidase: the View beyond Immunity. *Front. Physiol.* 5, 252. doi:10.3389/fphys.2014.00252

Luo, Y., and Liu, Y. (2015). Role of Superoxide in Bioluminescence. *Chem. J. Chin. Universities-Chinese* 36, 24–33. doi:10.7503/cjcu20140804

Ma, Y., Liu, R. R., Ma, Z. Q., and Zhang, Y. L. (2010). Effects of Cantharidin on for Metabolizing Enzymes and PPO in *Mythimna separata* (Walker) (Lepidoptera: Noctuidae). *Acta Entomol. Sin.* 53, 870–875. (in Chinese). doi:10.16380/j.kcxb.2010.08.010

Magierowicz, K., Górska-Drabik, E., and Sempruch, C. (2020). The Effect of Tanacetum Vulgare Essential Oil and its Main Components on Some Ecological and Physiological Parameters of Acrobasis Advenella (Zinck.) (Lepidoptera: Pyralidae). *Pesticide Biochem. Physiology* 162, 105–112. doi:10.1016/j.pestbp.2019.09.008

Maity, S., Roy, S., Chaudhury, S., and Bhattacharya, S. (2008). Antioxidant Responses of the Earthworm Lampito Mauritii Exposed to Pb and Zn Contaminated Soil. *Environ. Pollut.* 151, 1–7. doi:10.1016/j.envpol.2007.03.005

Matsuda, K., Buckingham, S. D., Kleier, D., Rauh, J. J., Grauso, M., and Sattelle, D. B. (2001). Neonicotinoids: Insecticides Acting on Insect Nicotinic Acetylcholine Receptors. *Trends Pharmacol. Sci.* 22, 573–580. doi:10.1016/s0165-6147(00)01820-4

Mbugua, S. W., Wong, C. H., and Ratnayeke, S. (2020). Effects of Artificial Light on the Larvae of the Firefly Lamprigera Sp. In an Urban City Park, Peninsular Malaysia. *J. Asia-Pacific Entomology* 23, 82–85. doi:10.1016/j.aspen.2019.10.005

Minnameyer, A., Strobl, V., Bruckner, S., Camenzind, D. W., Van Oystaeyen, A., Wäckers, F., et al. (2021). Eusocial Insect Declines: Insecticide Impairs Sperm and Feeding Glands in Bumblebees. *Sci. Total Environ.* 785, 146955. doi:10.1016/j.scitotenv.2021.146955

Moreira, S. M., Coimbra, J., and Guilhermino, L. (2001). Acetylcholinesterase of LmK. Hemolymph: A Suitable Environmental Biomarker. *Bull. Environ. Contam. Toxicol.* 67, 0470–0475. doi:10.1007/s00128-001-0147-2

Morrissey, C. A., Mineau, P., Devries, J. H., Sanchez-Bayo, F., Liess, M., Cavallaro, M. C., et al. (2015). Neonicotinoid Contamination of Global Surface Waters and Associated Risk to Aquatic Invertebrates: A Review. *Environ. Int.* 74, 291–303. doi:10.1016/j.envint.2014.10.024

Nazari, M., Hosseinkhani, S., and Hassani, L. (2013). Step-wise Addition of Disulfide Bridge in Firefly Luciferase Controls Color Shift through a Flexible Loop: a Thermodynamic Perspective. *Photochem. Photobiol. Sci.* 12, 298–308. doi:10.1039/c2pp25140j

Ohba, N. (2005). "Feeding Habits of the Larvae of Pyrocoelia Abdominalis and P. Atripennis (Coleoptera: Lampyridae) to the Land Snail, Acusta Despecta," in *Science Report of the Yokosuka City Museum*, 1–19.

Osozawa, S., Oba, Y., Kwon, H.-Y., and Wakabayashi, J. (2015). Vicariance ofPyrocoeliafireflies (Coleoptera: Lampyridae) in the Ryukyu Islands, Japan. *Biol. J. Linn. Soc.* 116, 412–422. doi:10.1111/bij.12595

Pearsons, K. A., Lower, S. E., and Tooker, J. F. (2021). Toxicity of Clothianidin to Common Eastern North American Fireflies. *PeerJ* 9, e12495. doi:10.7717/peerj.12495

Pervez, M., and Manzoor, F. (2020). A Study on Lethal Doses of Various Pesticides on Honeybees (*Apis mellifera* L.) - a Laboratory Trial. *Physiol. Entomol.* 46, 34–44. doi:10.1111/phen.12338

Pietrzak, D., Kania, J., Kmiecik, E., Malina, G., and Wątor, K. (2020). Fate of Selected Neonicotinoid Insecticides in Soil-Water Systems: Current State of the Art and Knowledge Gaps. *Chemosphere* 255, 126981. doi:10.1016/j.chemosphere.2020.126981

Rahimi, V., Hajizadeh, J., Zibaee, A., and Sendi, J. J. (2018). Effect of Polygonum Persicaria (Polygonales: Polygonaceae) Extracted Agglutinin on Life Table and Antioxidant Responses in Helicoverpa Armigera (Lepidoptera: Noctuidae) Larvae. *J. Econ. Entomology* 111, 662–671. doi:10.1093/jee/toy006

Richter, C. (1977). Inhibition of Firefly Bioluminescence by Scavengers of Singlet Oxygen, Superoxide Radicals and Hydroxyl Radicals. *Experientia* 33, 860–862. doi:10.1007/bf01951244

Rodriguez, C., Mayo, J. C., Sainz, R. M., Antolin, I., Herrera, F., Martin, V., et al. (2004). Regulation of Antioxidant Enzymes: a Significant Role for Melatonin. *J. Pineal Res.* 36, 1–9. doi:10.1046/j.1600-079X.2003.00092.x

Sato, N. (2019). Prey-tracking Behavior and Prey Preferences in a Tree-Climbing Firefly. *Peerj* 7, e8080. doi:10.7717/peerj.8080

Schaffazick, S. R., Pohlmann, A. R., de Cordova, C. A. S., Creczynski-Pasa, T. B., and Guterres, S. S. (2005). Protective Properties of Melatonin-Loaded Nanoparticles against Lipid Peroxidation. *Int. J. Pharm.* 289, 209–213. doi:10.1016/j.ijpharm.2004.11.003

Seifert, J., and Stollberg, J. (2005). Antagonism of a Neonicotinoid Insecticide Imidacloprid at Neuromuscular Receptors. *Environ. Toxicol. Pharmacol.* 20, 18–21. doi:10.1016/j.etap.2004.09.011

Sharma, A., Kumar, V., Shahzad, B., Tanveer, M., Sidhu, G. P. S., Handa, N., et al. (2019). Worldwide Pesticide Usage and its Impacts on Ecosystem. *SN Appl. Sci.* 1, 1446. doi:10.1007/s42452-019-1485-1

Siddique, H. R., Gupta, S. C., Mitra, K., Murthy, R. C., Saxena, D. K., and Chowdhuri, D. K. (2007). Induction of Biochemical Stress Markers and Apoptosis in Transgenic *Drosophila melanogaster* against Complex Chemical Mixtures: Role of Reactive Oxygen Species. *Chemico-Biological Interact.* 169, 171–188. doi:10.1016/j.cbi.2007.06.035

Singh, A., and Leppanen, C. (2020). Known Target and Nontarget Effects of the Novel Neonicotinoid Cycloxaprid to Arthropods: A Systematic Review. *Integr. Environ. Assess. Manag.* 16, 831–840. doi:10.1002/ieam.4305

Siregar, P., Suryanto, M. E., Chen, K. H.-C., Huang, J.-C., Chen, H.-M., Kurnia, K. A., et al. (2021). Exploiting the Freshwater Shrimp Neocaridina Denticulata as Aquatic Invertebrate Model to Evaluate Nontargeted Pesticide Induced Toxicity by Investigating Physiologic and Biochemical Parameters. *Antioxidants* 10, 391. doi:10.3390/antiox10030391

Slos, S., De Meester, L., and Stoks, R. (2009). Food Level and Sex Shape Predator-Induced Physiological Stress: Immune Defence and Antioxidant Defence. *Oecologia* 161, 461–467. doi:10.1007/s00442-009-1401-2

Suchail, S., Debrauwer, L., and Belzunces, L. P. (2004). Metabolism of Imidacloprid inApis Mellifera. *Pest. Manag. Sci.* 60, 291–296. doi:10.1002/ps.772

Suchail, S., Guez, D., and Belzunces, L. P. (2001). Discrepancy between Acute and Chronic Toxicity Induced by Imidacloprid and its Metabolites inApis Mellifera. *Environ. Toxicol. Chem.* 20, 2482–2486. doi:10.1002/etc.5620201113

Sunde, R. A., and Hoekstra, W. G. (1980). Structure, Synthesis and Function of Glutathione Peroxidase. *Nutr. Rev.* 38, 265–273. doi:10.1111/j.1753-4887.1980.tb05957.x

Thompson, D. A., Lehmler, H.-J., Kolpin, D. W., Hladik, M. L., Vargo, J. D., Schilling, K. E., et al. (2020). A Critical Review on the Potential Impacts of Neonicotinoid Insecticide Use: Current Knowledge of Environmental Fate, Toxicity, and Implications for Human Health. *Environ. Sci. Process. Impacts* 22, 1315–1346. doi:10.1039/c9em00586b

Timmins, G. S., Jackson, S. K., and Swartz, H. M. (2001). The Evolution of Bioluminescent Oxygen Consumption as an Ancient Oxygen Detoxification Mechanism. *J. Mol. Evol.* 52, 321–332. doi:10.1007/s002390010162

Tomalski, M., Leimkuehler, W., Schal, C., and Vargo, E. L. (2010). Metabolism of Imidacloprid in Workers of Reticulitermes Flavipes (Isoptera: Rhinotermitidae). *Ann. Entomological Soc. Am.* 103, 84–95. doi:10.1603/008.103.011110.1093/aesa/103.1.84

Topal, A., Alak, G., Ozkaraca, M., Yeltekin, A. C., Comaklı, S., Acıl, G., et al. (2017). Neurotoxic Responses in Brain Tissues of Rainbow Trout Exposed to Imidacloprid Pesticide: Assessment of 8-Hydroxy-2-Deoxyguanosine Activity, Oxidative Stress and Acetylcholinesterase Activity. *Chemosphere* 175, 186–191. doi:10.1016/j.chemosphere.2017.02.047

Toyokuni, S. (1999). Reactive Oxygen Species-induced Molecular Damage and its Application in Pathology. *Pathol. Int.* 49, 91–102. doi:10.1046/j.1440-1827.1999.00829.x

Van Dijk, T. C., Van Staalduinen, M. A., and Van der Sluijs, J. P. (2013). Macro-Invertebrate Decline in Surface Water Polluted with Imidacloprid. *Plos One* 8, e62374. doi:10.1371/journal.pone.0062374

Verma, S., and Dubey, R. S. (2003). Lead Toxicity Induces Lipid Peroxidation and Alters the Activities of Antioxidant Enzymes in Growing Rice Plants. *Plant Sci.* 164, 645–655. doi:10.1016/s0168-9452(03)00022-0

Vohra, P., Khera, K. S., and Sangha, G. K. (2014). Physiological, Biochemical and Histological Alterations Induced by Administration of Imidacloprid in Female Albino Rats. *Pesticide Biochem. Physiology* 110, 50–56. doi:10.1016/j.pestbp.2014.02.007

Wang, J., Wang, J., Wang, G., Zhu, L., and Wang, J. (2016). DNA Damage and Oxidative Stress Induced by Imidacloprid Exposure in the Earthworm *Eisenia fetida*. *Chemosphere* 144, 510–517. doi:10.1016/j.chemosphere.2015.09.004

Wang, W., Gao, C., Ren, L., and Luo, Y. (2020). The Effect of Longwave Ultraviolet Light Radiation on Dendrolimus Tabulaeformis Antioxidant and Detoxifying Enzymes. *Insects* 11, 1. doi:10.3390/insects11010001

Wu, H.-D., and Liu, Q.-Z. (2012). Antioxidative Responses inGalleria Mellonellalarvae Infected with the Entomopathogenic nematodeHeterorhabditissp.Beicherriana. *Biocontrol Sci. Technol.* 22, 601–606. doi:10.1080/09583157.2012.670803

Xia, X., Xia, X., Huo, W., Dong, H., Zhang, L., and Chang, Z. (2016). Toxic Effects of Imidacloprid on Adult Loach (*Misgurnus anguillicaudatus*). *Environ. Toxicol. Pharmacol.* 45, 132–139. doi:10.1016/j.etap.2016.05.030

Xiao, N., Jing, B., Ge, F., and Liu, X. (2006). The Fate of Herbicide Acetochlor and its Toxicity to *Eisenia fetida* under Laboratory Conditions. *Chemosphere* 62, 1366–1373. doi:10.1016/j.chemosphere.2005.07.043

Xie, J., De Clercq, P., Pan, C., Li, H., Zhang, Y., and Pang, H. (2015). Physiological Effects of Compensatory Growth during the Larval Stage of the Ladybird, *Cryptolaemus montrouzieri*. *J. Insect Physiology* 83, 37–42. doi:10.1016/j.jinsphys.2015.11.001

Xu, D., Yang, X., Wang, Y., and Sun, L. (2020). Cascading Mechanism Triggering the Activation of Polyphenol Oxidase Zymogen in Shrimp Litopenaeus Vannamei after Postmortem and the Correlation with Melanosis Development. *Food Bioprocess Technol.* 13, 1131–1145. doi:10.1007/s11947-020-02435-8

Yadav, A., Gopesh, A., Pandey, R. S., Rai, D. K., and Sharma, B. (2009). Acetylcholinesterase: a Potential Biochemical Indicator for Biomonitoring of Fertilizer Industry Effluent Toxicity in Freshwater Teleost, Channa Striatus. *Ecotoxicology* 18, 325–333. doi:10.1007/s10646-008-0286-x

Yadav, D. K., Kumar, S., Choi, E.-H., Chaudhary, S., and Kim, M.-H. (2019). Molecular Dynamic Simulations of Oxidized Skin Lipid Bilayer and Permeability of Reactive Oxygen Species. *Sci. Rep.* 9, 4496. doi:10.1038/s41598-019-40913-y

Yassine, H., Kamareddine, L., and Osta, M. A. (2012). The Mosquito Melanization Response Is Implicated in Defense against the Entomopathogenic Fungus Beauveria Bassiana. *PLoS Pathog.* 8, e1003029. doi:10.1371/journal.ppat.1003029

Yucel, M. S., and Kayis, T. (2019). Imidacloprid Induced Alterations in Oxidative Stress, Biochemical, Genotoxic, and Immunotoxic Biomarkers in Non-mammalian Model organismGalleria mellonellaL. (Lepidoptera: Pyralidae). *J. Environ. Sci. Health, Part B.* 54, 27–34. doi:10.1080/03601234.2018.1530545

Zhang, J., and Sun, X. (2021). Recent Advances in Polyphenol Oxidase-Mediated Plant Stress Responses. *Phytochemistry* 181, 112588. doi:10.1016/j.phytochem.2020.112588

Zhang, Q.-L., Guo, J., Deng, X.-Y., Wang, F., Chen, J.-Y., and Lin, L.-B. (2019). Comparative Transcriptomic Analysis Provides Insights into the Response to the Benzo(a)pyrene Stress in Aquatic Firefly (Luciola Leii). *Sci. Total Environ.* 661, 226–234. doi:10.1016/j.scitotenv.2019.01.156

Zhang, Q.-L., Jiang, Y.-H., Dong, Z.-X., Li, H.-W., and Lin, L.-B. (2021). Exposure to Benzo[a]pyrene Triggers Distinct Patterns of microRNA Transcriptional Profiles in Aquatic Firefly Aquatica Wuhana (Coleoptera: Lampyridae). *J. Hazard. Mater.* 401, 123409. doi:10.1016/j.jhazmat.2020.123409

Zhang, Q., Zhang, B., and Wang, C. (2014). Ecotoxicological Effects on the Earthworm *Eisenia fetida* Following Exposure to Soil Contaminated with Imidacloprid. *Environ. Sci. Pollut. Res.* 21, 12345–12353. doi:10.1007/s11356-014-3178-z

Zhang, Q., Zhu, L., Wang, J., Xie, H., Wang, J., Han, Y., et al. (2013). Oxidative Stress and Lipid Peroxidation in the Earthworm *Eisenia fetida* Induced by Low Doses of Fomesafen. *Environ. Sci. Pollut. Res.* 20, 201–208. doi:10.1007/s11356-012-0962-5

Zhao, P., Li, J., Wang, Y., and Jiang, H. (2007). Broad-spectrum Antimicrobial Activity of the Reactive Compounds Generated *In Vitro* by Manduca Sexta Phenoloxidase. *Insect Biochem. Mol. Biol.* 37, 952–959. doi:10.1016/j.ibmb.2007.05.001

Conflict of Interest: The authors declare that the research was conducted in the absence of any commercial or financial relationships that could be construed as a potential conflict of interest.

Publisher's Note: All claims expressed in this article are solely those of the authors and do not necessarily represent those of their affiliated organizations, or those of the publisher, the editors, and the reviewers. Any product that may be evaluated in this article, or claim that may be made by its manufacturer, is not guaranteed or endorsed by the publisher.

Advantages of publishing in Frontiers

OPEN ACCESS
Articles are free to read for greatest visibility and readership

FAST PUBLICATION
Around 90 days from submission to decision

HIGH QUALITY PEER-REVIEW
Rigorous, collaborative, and constructive peer-review

TRANSPARENT PEER-REVIEW
Editors and reviewers acknowledged by name on published articles

Frontiers
Avenue du Tribunal-Fédéral 34
1005 Lausanne | Switzerland

Visit us: www.frontiersin.org
Contact us: frontiersin.org/about/contact

REPRODUCIBILITY OF RESEARCH
Support open data and methods to enhance research reproducibility

DIGITAL PUBLISHING
Articles designed for optimal readership across devices

FOLLOW US
@frontiersin

IMPACT METRICS
Advanced article metrics track visibility across digital media

EXTENSIVE PROMOTION
Marketing and promotion of impactful research

LOOP RESEARCH NETWORK
Our network increases your article's readership